Plasma cell differentiation in the B-cell malignancy Waldenström Macroglobulinemia

Jennifer Kate Shrimpton

Submitted in accordance with the requirements for the degree of
Doctor of Philosophy

The University of Leeds
Faculty of Medicine and Health

July 2019

The candidate confirms that the work submitted is her own and that appropriate credit has been given where reference has been made to the work of others.

This copy has been supplied on the understanding that it is copyright material and that no quotation from the thesis may be published without proper acknowledgement.

The right of Jennifer Kate Shrimpton to be identified as Author of this work has been asserted by her in accordance with the Copyright, Designs and Patents Act 1988.

Acknowledgements

My sincere thanks go first and foremost to my supervisors Dr Gina Doody, Professor Reuben Tooze and Dr Roger Owen. Thank you for providing me with the opportunity to undertake this research and for your guidance and expertise throughout the project. I am very grateful for your generosity in sharing both your time and knowledge and for fostering a great environment to work in.

I would like to take this opportunity to acknowledge WMUK and the WM patients and their families, without whom this project would not have been possible. Thanks also to Dr Ruth de Tute for her assistance in acquiring patient samples.

Huge thanks go to everyone within the lab group - I feel so lucky to have spent the last four years in the company of such a lovely bunch of people. A special thank you goes to Sophie Stephenson, who has always been incredibly generous with her time and practical expertise - and for making everything better with her wonderful baked goodies!

I am grateful to Michelle Campbell for her patience and advice on all matters flow cytometry, including the skilful wrangling of both machines and analysis programs. Thanks also go to Matthew Care for his expert analysis of the RNA sequencing data and for patiently explaining some of the complexities of bioinformatics.

Big hugs to Emily, Charlotte and Nicole who have become great friends and provided invaluable moral support, particularly when things didn't quite go according to plan!

Finally, I would like to say a huge thank you to my mum Carolyn, who has been such an incredible source of support throughout my PhD and without whom this would not have been possible.

Abstract

Waldenström macroglobulinemia (WM) is unique amongst B-cell malignancies in that the neoplastic cells retain the capacity to undergo plasma cell differentiation. This gives rise to a clonal neoplasm encompassing the spectrum of differentiation and as such presents a challenge to model and treat effectively. Therefore, the feasibility of using an *in vitro* culture system to model the differentiation of primary WM B-cells derived from patient samples was examined and their response to different stimuli characterised. Subsequent to T-dependent activation, WM B-cells successfully differentiate and generate plasma cells with an equivalent immunophenotype and lifespan to that of healthy B-cells, and do so more efficiently than B-cells derived from patients with splenic marginal zone lymphoma, which shares a related aetiology to WM. Unlike healthy cells or those derived from other B-cell neoplasms, however, WM B-cells generate a novel population of plasma cells that do not express CD38 and their appearance is strongly linked to the characteristic MYD88^{L265P} mutation.

The virtually ubiquitous presence of MYD88^{L265P}, coupled with reports suggesting that TLR signalling is required for the survival of MYD88-mutated cells prompted investigation into the response of WM cells to stimuli mimicking a T-independent immune response. Whilst WM B-cells remain receptive to TLR stimulation, they fail to differentiate in response to a combination of TLR7 agonism and BCR ligation and demonstrate a profound apoptotic response that is in stark contrast to their healthy counterparts. This unexpected response is not as a result of a secreted factor acting *in trans* or due to the upregulation of Fas or its ligand within the WM population. Indeed, RNA sequencing identifies substantial disruption of multiple essential pathways within these cells subsequent to TLR stimulation, but no significant differences in the expression of either pro-apoptotic or survival genes. The data presented here suggest that WM cells rely on additional support from the bone marrow microenvironment for their survival and that ligation of TLR7 and the BCR without an additional signal such as CD40L are insufficient to sustain the WM population.

Table of contents

List of figures

List of tables

Chapter 1 - Introduction

1.1   B-cell mediated immunity

The immune system is critically important in defence against pathogens and functions as an immunosurveillance mechanism, enabling the distinction of neoplastic cells from healthy ones. B-cells are essential for combatting pathogens; mature cells are primed to release high affinity antibodies, they also form the core of our immunological "memory". Upon antigen binding and receipt of a second activation signal, B-cells undergo differentiation generating a population of both long and short-lived antibody-secreting plasma cells (figure 1.1). Short-lived plasma cells are transient but long-lived plasma cells may persist for many years, serving to maintain humoral immunity (Slifka *et al.*, 1998). The role of B-cells in the anti-tumour response is less well-defined. Whilst the production of specific antibodies against tumours mediates antibody-dependent cellular cytotoxicity, cytokine release by B-cells after a tumour has become established results in an immunosuppressive effect and can enhance tumour progression (Inoue *et al.*, 2006). B-cells themselves can become oncogenic when mutations occur, resulting in the dysregulation of survival and proliferative pathways.
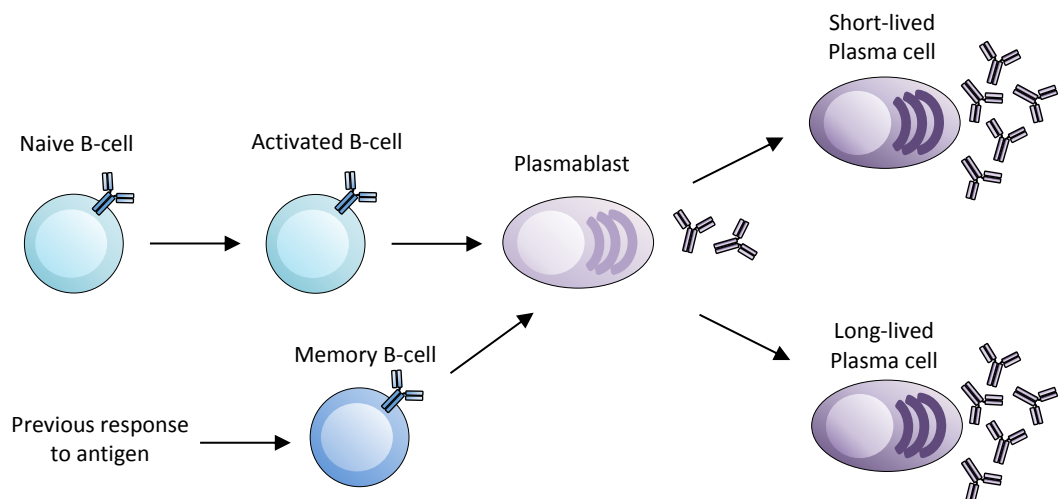
Figure 1.1 B-cell differentiation to plasma cell effectors. Antigen binding initiates signalling cascades that result in the proliferation and differentiation of naïve B-cells, resulting in the production of both long and short-lived plasma cells. Upon repeated challenge by an antigen, memory B-cells respond by generating plasma cell populations.

1.1.1 Plasma cell differentiation

The differentiation of B-cells into plasma cells is accompanied by distinct changes in the expression of multiple cell surface markers. Five of these markers are particularly informative for defining B-cell subsets and assessing the progress of differentiation; CD19, CD20, CD27, CD38 and CD138 (figure 1.2).

Naive B-cell	Activated B-cell	Plasmablast	Plasma cell
$CD19^+$	$CD19^{++}$	$CD19^+$	$CD19^{+/-}$
$CD20^{++}$	$CD20^{++}$	$CD20^-$	$CD20^-$
$CD38^{-/lo}$	$CD38^{lo}$	$CD38^+$	$CD38^{++}$
$CD138^-$	$CD138^-$	$CD138^-$	$CD138^+$
$CD27^-$ (naïve)	$CD27^{-/+}$	$CD27^+$	$CD27^+$
$CD27^+$ (memory)			
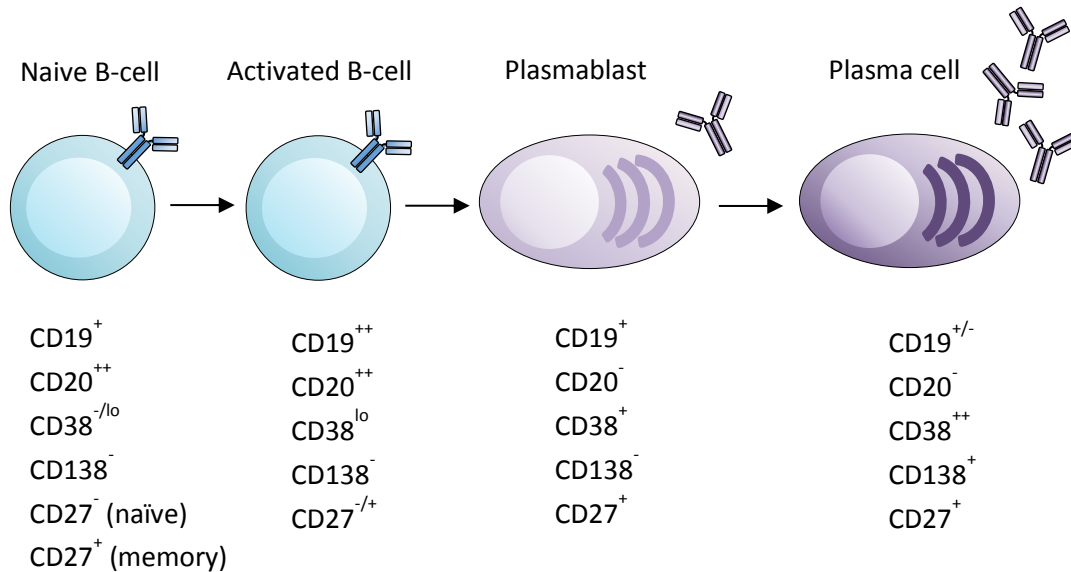
Figure 1.2 Immunophenotypic changes that accompany plasma cell differentiation. CD20 downregulation is accompanied by the upregulation of CD27 and sequential increase of first CD38 and CD138 as B-cells progress to terminally-differentiated plasma cells.

CD19 is ubiquitously expressed on B-cells throughout their development and thus serves as a lineage marker (Nadler *et al.*, 1983; Anderson *et al.*, 1984). It functions as a co-receptor for the B-cell receptor (BCR), decreasing the signal threshold required for antigen receptor-dependent stimulation and functioning as a signalling adaptor (Carter and Fearon, 1992; Fearon *et al.*, 2000). Activation of CD19 results in phosphorylation of the cytoplasmic tail of the protein, enabling recruitment of PI3K and the initiation of downstream signalling (Tuveson *et al.*, 1993; Sato *et al.*, 1997; Otero *et al.*, 2001). Whilst plasma cells were thought to retain CD19 expression, recent publications have identified the presence of a $CD19^-$ plasma cell fraction (Mei *et al.*, 2015; Arumugakani *et al.*, 2017; Brynjolfsson *et al.*, 2017).

B-cells express CD20 during the majority of their development until it is downregulated during plasma cell differentiation (Stashenko *et al.*, 1980). CD20 has diverse functions, including

regulation of differentiation and cell cycle progression and involvement in calcium signalling (Deans *et al.*, 1993; Tedder *et al.*, 1985; Tedder and Engel, 1994).

The expression of the CD27 receptor is commonly used to distinguish naïve and memory B-cell subsets, with it being absent in the former and present on the latter (Maurer *et al.*, 1992; Agematsu *et al.*, 1997). Surface expression of CD27 increases during differentiation, with plasma cells strongly expressing this marker (Jung *et al.*, 2000). Indeed, interaction of CD27 with its ligand, CD70 promotes plasma cell differentiation and augments immunoglobulin synthesis (Agematsu *et al.*, 1995; Nagumo and Agematsu, 1998; Nagumo *et al.*, 1998). CD27 signalling can also activate the canonical and non-canonical NF-κB pathways (Yamamoto *et al.*, 1998).

Many cells from the lymphoid and myeloid lineages express CD38, including monocytes and macrophages, NK cells and both T- and B-cells (Alessio *et al.*, 1990; Banchereau and Rousset, 1992). CD38 is expressed at various stages of B-cell development; being present on pro- and pre-B-cells before being downregulated in mature B-cells and finally upregulated subsequent to B-cell activation as the cells become plasmablasts (Stashenko *et al.*, 1981; Banchereau and Rousset, 1992; Galibert *et al.*, 1996). CD38 functions as an ADP-ribose hydrolase, catalysing the conversion of NAD^+ and $NADP^+$ to cyclic ADP-ribose (cADPR) which plays an essential role in the regulation of intracellular Ca^{2+} (Howard *et al.*, 1993; Zocchi *et al.*, 1998; Moreno-García *et al.*, 2005). It is also involved in both cell adhesion and signal transduction although the molecular mechanism for the latter has yet to be fully elucidated (Lund *et al.*, 1998; Moreno-García *et al.*, 2005; Malavasi *et al.*, 2008).

During plasma cell differentiation, the expression of CD38 and CD138 are sequentially upregulated, with plasmablasts expressing CD38 and plasma cells defined by the additional expression of CD138 (O'connell *et al.*, 2004). CD138, also known as Syndecan-1, is a transmembrane heparan sulfate proteoglycan and a member of the syndecan proteoglycan family (Bernfield *et al.*, 1992). CD138 mediates plasma cell adhesion to the bone marrow stroma and appears to enhance their survival (Ridley *et al.*, 1993; McCarron *et al.*, 2017). Investigation of the role of CD138 in multiple myeloma has demonstrated that it interacts with many components within the bone marrow microenvironment, including growth factors, cytokines and chemokines (Derksen *et al.*, 2002; Yang *et al.*, 2002; Khotskaya *et al.*, 2009; Reijmers *et al.*, 2010).

Plasma cell differentiation requires the repression of the B-cell transcriptional programme and the coordinated induction of a host of transcription factors responsible for the generation and maintenance of antibody secreting cells. Regulation of this process is achieved through antagonism of transcription factors that maintain cellular identity (figure 1.3).
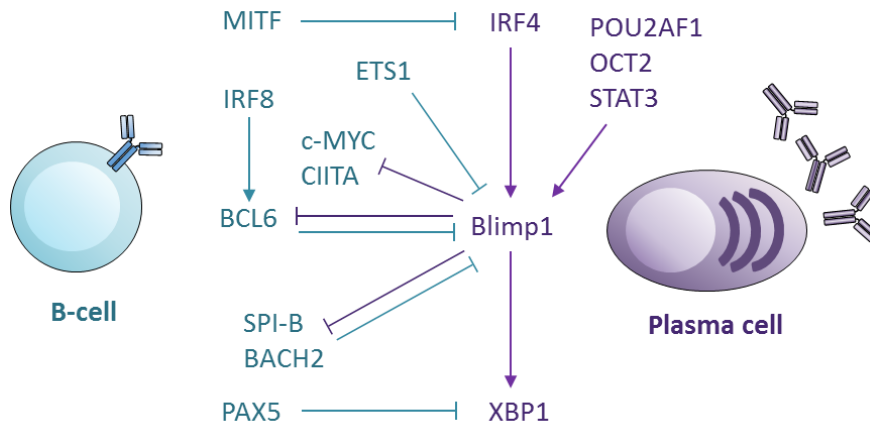
Figure 1.3 The interaction between key transcription factors involved in the regulation of plasma cell differentiation. B-cells express multiple transcription factors that serve to commit and preserve their cellular identity. These include PAX5, BCL6 and SPI-B, which have an antagonistic relationship with many of the transcription factors essential for terminal differentiation. Following B-cell activation, genes such as *IRF4* and the master regulator of plasma cell differentiation, *PRDM1* which encodes BLIMP-1, are upregulated. These, in turn, repress the genes responsible for maintaining the B-cell transcriptional programme. Transcription factors involved in maintaining B-cell identity are coloured blue, whilst those that drive plasma cell differentiation are denoted in purple. Activation or repression are indicated by arrows or bars respectively.

An essential component of the B-cell programme is the transcription factor PAX5 (paired box protein 5). Expression of PAX5 is both critical to commit haematopoietic progenitors to adopt a B-cell fate and to preserve their identity subsequent to this commitment (Nutt *et al.*, 1999; Horcher *et al.*, 2001; Cobaleda *et al.*, 2007). PAX5 regulates the expression of B-cell transcription factors BACH2, IRF8 and SPI-B whilst repressing the essential regulator of plasma cells, BLIMP-1 (Usui *et al.*, 1997; Schebesta *et al.*, 2007; Pridans *et al.*, 2008). In addition to its control of B-cell fate, PAX5 is also involved in the regulation of BCR signalling, promoting VDJ recombination of the immunoglobulin heavy chain (Nutt *et al.*, 1997; Fuxa *et al.*, 2004). It activates genes encoding CD79a, involved in signal transduction, the BCR co-receptor CD19 and the BCR signalling adaptor BLNK (Kozmik *et al.*, 1992; Fitzsimmons *et al.*, 1996; Nutt *et al.*, 1998; Schebesta *et al.*, 2002).

The transcriptional repressor BCL6 was identified as essential for the formation of germinal centres (Dent *et al.*, 1997; Fukuda *et al.*, 1997; Bihui *et al.*, 1997). BCL6 suppresses plasma cell differentiation by repressing the effects of BLIMP-1 (Reljic *et al.*, 2000; Shaffer *et al.*, 2000). BCL6 expression is supported by IRF8, but repressed by BLIMP-1 and IRF4 (Cimmino *et al.*, 2008; Carotta *et al.*, 2014).

Several members of the ETS family of transcription factors are involved in maintaining B-cell identity. SPI-B is one such factor, expressed only within lymphoid cells (Ray *et al.*, 1992; Su *et al.*, 1996). Whilst SPI-B is not required to initiate the formation of germinal centres, its expression is responsible for their maintenance, which collapse in its absence (Su *et al.*, 1997). It is also involved in BCR signal transduction and has an antagonistic relationship with BLIMP-1 (Garrett-Sinha *et al.*, 1999; Shaffer *et al.*, 2002). Another ETS family member, ETS1 negatively regulates plasma cell differentiation via the repression of BLIMP-1 (John *et al.*, 2008).

BLIMP-1 (B lymphocyte-induced maturation protein 1), encoded by *PRDM1* (PR domain containing 1) has been termed the master regulator of B-cell differentiation and is essential for the generation of terminally differentiated plasma cells (Shapiro-Shelef *et al.*, 2003). It functions as a transcriptional repressor, suppressing multiple genes responsible for maintaining the B-cell programme, such as MYC, PAX5 and SPI-B (Lin *et al.*, 1997; Shaffer *et al.*, 2002; Lin *et al.*, 2002). Whilst BLIMP-1 is critical for plasma cell generation, the initiation of B-cell differentiation is able to occur in its absence (Kallies *et al.*, 2007). Engagement of CD40 on the surface of B-cells during interactions with helper T-cells over the course of an immune response demonstrates synergism with the binding of T-cell derived IL-21 in upregulating BLIMP-1 and promoting terminal differentiation (Ding *et al.*, 2013).

Whilst the regulatory capacity of BLIMP-1 is most well characterised in the context of plasma cell differentiation, it has multiple additional functions within B-cells. BLIMP-1 exerts transcriptional control over antigen presentation by MHC classes I and II, regulating MHC expression in response to IFN-γ (Tooze *et al.*, 2006; Doody *et al.*, 2007). A regulatory role for BLIMP-1 has also been identified in B-cell malignancies. Mutations in BLIMP-1 are common in activated B-cell diffuse large B-cell lymphoma (ABC DLBCL), demonstrating that it acts as a tumour suppressor (Pasqualucci *et al.*, 2006; Mandelbaum *et al.*, 2010; Lohr *et al.*, 2014).

IRF4 is required for both B-cell and plasma cell processes, playing an essential role in germinal centre formation and class switch recombination whilst also regulating plasma cell differentiation (Klein *et al.*, 2006; Sciammas *et al.*, 2006). The outcome of IRF4 regulation occurs according to the concentration of its expression, with low levels activating BCL6 and activation-induced cytidine deaminase (AID) and eliciting a germinal centre response (Sciammas *et al.*, 2006). Levels of IRF4 above a certain threshold shifts its binding to different motifs, resulting in BLIMP-1 activation and suppression of BCL6 (Ochiai *et al.*, 2013).

Plasma cell differentiation is accompanied by the acquisition of Ig secretory capacity. Due to their immense secretory burden, plasma cells are sensitive to ER stress and may initiate the unfolded protein response (UPR) if a build-up of unfolded proteins occurs (Yoshida *et al.*, 2001;

Lee *et al.*, 2002; Todd *et al.*, 2009). The UPR aims to resolve the issue of protein accumulation within the ER by a combination of decreased protein synthesis and upregulation of chaperones that promote protein folding (Harding *et al.*, 2000; Yoshida *et al.*, 2000; Todd *et al.*, 2008). Prior to plasma cell differentiation, XBP1 is suppressed by PAX5, but decreasing levels of PAX5 enable it to become activated (Reimold *et al.*, 1996). Models of XBP1 deficiency demonstrate that it is not required to generate plasma cells (Todd *et al.*, 2009; Taubenheim *et al.*, 2012). However, XBP1 is induced in plasma cells in response to ER stress and activates the UPR (Reimold *et al.*, 2001; Yoshida *et al.*, 2001; Calfon *et al.*, 2002; Lee *et al.*, 2002). XBP1 is thus key for plasma cell function by facilitating immunoglobulin secretion via ER remodelling and the processing of immunoglobulin (Schaffer et al., 2004).

1.2   T-cell dependent and T-independent immune response

The response of B-cells can be divided into two categories – those that require T-cell help and those that do not. These are classified as T-dependent (TD) and T-independent (TI) responses, respectively (figure 1.4). TD responses are generally elicited by protein antigens and require either cognate interaction from follicular helper T-cells (T_{FH}) or natural killer T follicular helper cells (NKT_{FH}) (Vinuesa and Chang, 2013). T_{FH} interaction is particularly important for the production of long-lived plasma cells and memory cells. TI responses, on the other hand, involve receipt of costimulatory signals from other sources. These include Toll-like receptor (TLR) activation by bacterial motifs, extensive BCR crosslinking by polysaccharides from capsular bacteria or interaction with neutrophil B-helper cells (N_{BH}) (Puga *et al.*, 2012). In general, TI activation results in a more rapid response.
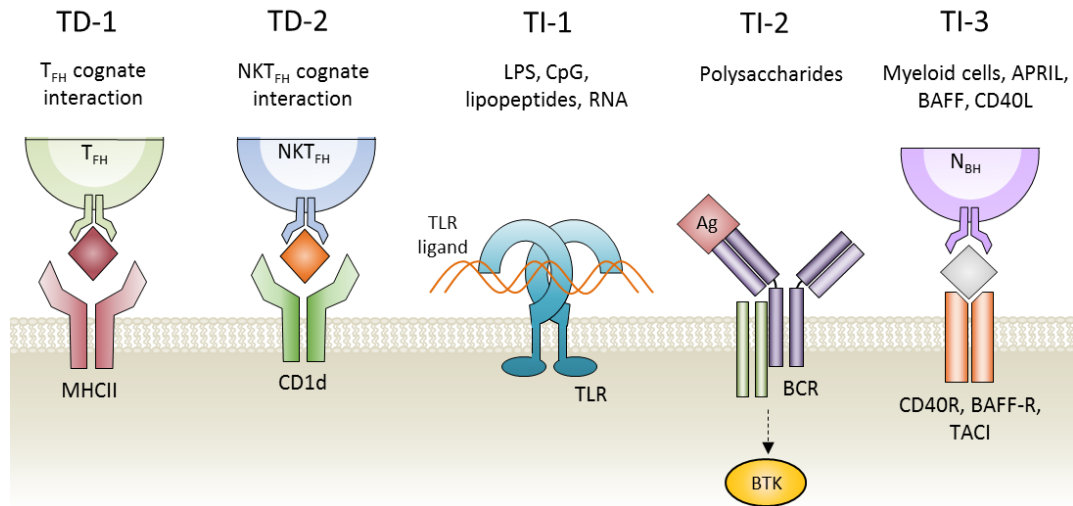
Figure 1.4 Classes of T-dependent and T-independent immune responses. During the classical TD-1 response to a proteinaceous antigen, T_{FH} provide the second activation signal. The response elicited by glycolipids (TD-2) involves B-cell interaction with NKT_{FH} cells. TLR ligation is the source of the additional signal in the TI-1 response, whereas the repetitive epitopes of encapsulated bacteria crosslink the BCR and the signal is transduced by BTK (Bruton's tyrosine kinase) in TI-2 responses. Interaction with N_{BH} cells and soluble factors such as BAFF and APRIL elicit the TI-3 response

1.3 T-cell dependent response

When an antigen binds the B-cell receptor (BCR), it induces activation and proliferation of the B-cell. Subsequently the antigen is processed and presented to T_{FH} cells in a complex with MHC-II (Liu *et al.*, 1991). This complex binds to the T-cell receptor and induces the T_{FH} cell to express CD40L and various cytokines such as IL-4 (Breitfeld *et al.*, 2000; Schaerli *et al.*, 2000). The interaction between CD40 and CD40L delivers a potent activation signal to the B-cell. The T-cell dependent response is a two-step process. The first step is rapid - the activated B-cells proliferate, may undergo class switch recombination (CSR) and differentiate into short-lived plasmablasts (MacLennan *et al.*, 2003). This occurs outside of lymphoid follicles and is known as the extrafollicular response. These cells produce antibodies of moderate affinity but they do not persist. Some B-cells will, however, take part in the second step of the TD response. These cells re-enter the lymphoid follicle and form a germinal centre (GC) whereby they undergo somatic hypermutation (SHM) and CSR.

CSR and SHM require activation-induced cytidine deaminase (AID or *AICDA*) and its expression is tightly regulated (Muramatsu *et al.*, 2000). One of the signalling cascades instigated by the TD response is the transcription factor nuclear factor-kappa B (NF-κB) pathway. NF-κB plays a pivotal role in both processes as its subunits bind the promotor and enhancers of the *AICDA* gene and induce transcription (figure 1.5) (Victora and Nussenzweig, 2012).
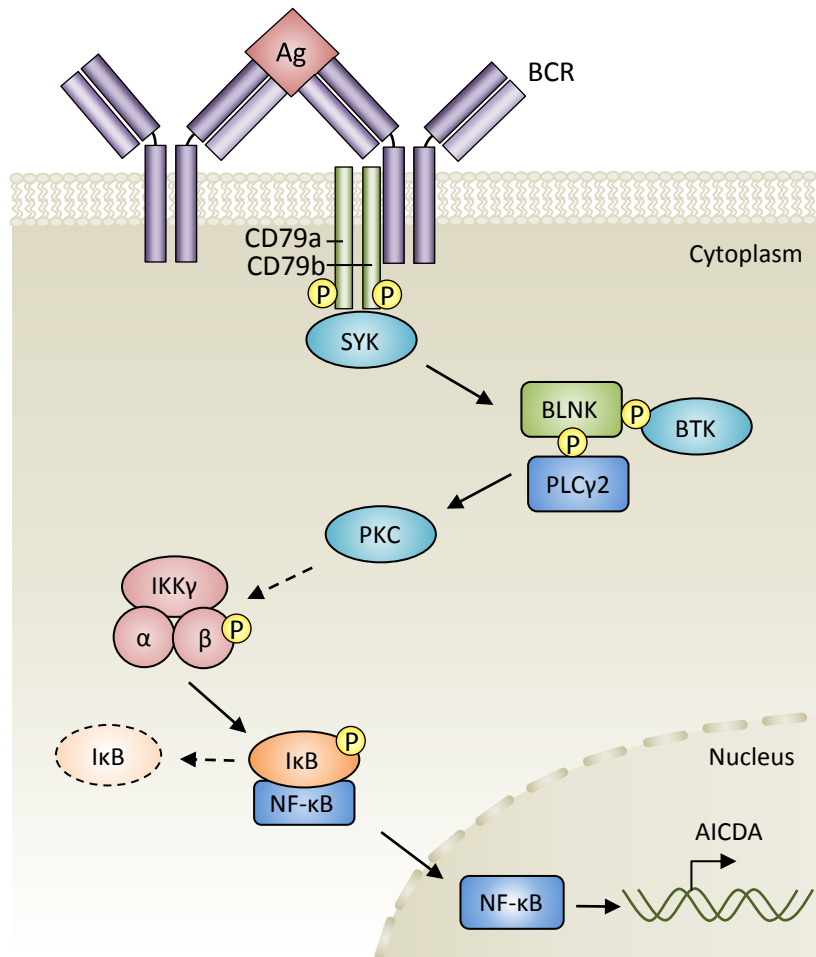
Figure 1.5 BCR signalling activates the NF-κB pathway. The BCR is composed of surface transmembrane immunoglobulin molecules and associated CD79a/CD79b (Igα/Igβ) heterodimers. When the mIg is bound by an antigen, aggregation of receptors occurs and CD79a/CD79b are phosphorylated. This results in the activation of multiple signalling cascades through the recruitment of Src family kinases such as LYN, tyrosine kinases such as SYK and enzymes, including PLCγ2. The complex of multiple proteins including BLNK, BTK and PLCγ2 is known as the signalosome. PLCγ2 is a fundamental effector for downstream signalling, it facilitates activation of PKC which ultimately results in IKK-mediated IκB degradation and release of NF-κB. SYK – spleen tyrosine kinase, BLNK – B-cell linker protein, BTK – Brutons tyrosine kinase, PLCγ2 – phospholipase C-gamma 2, IKK – inhibitor of kappa-B kinase, IκB – inhibitor of kappa-B.

The GC microenvironment facilitates the clonal expansion, affinity-based selection and maturation of B-cells. The resultant terminally-differentiated plasma cells produce large quantities of high-affinity antibodies and memory B-cells are primed to respond quickly to repeated infection (Allen *et al.*, 2007). During CSR and SHM, double stranded DNA breaks are formed and repaired and point mutations occur. This, when combined with the highly proliferative nature of germinal centre B-cells, means that the GC often becomes the source of B-cell malignancies (figure 1.6).
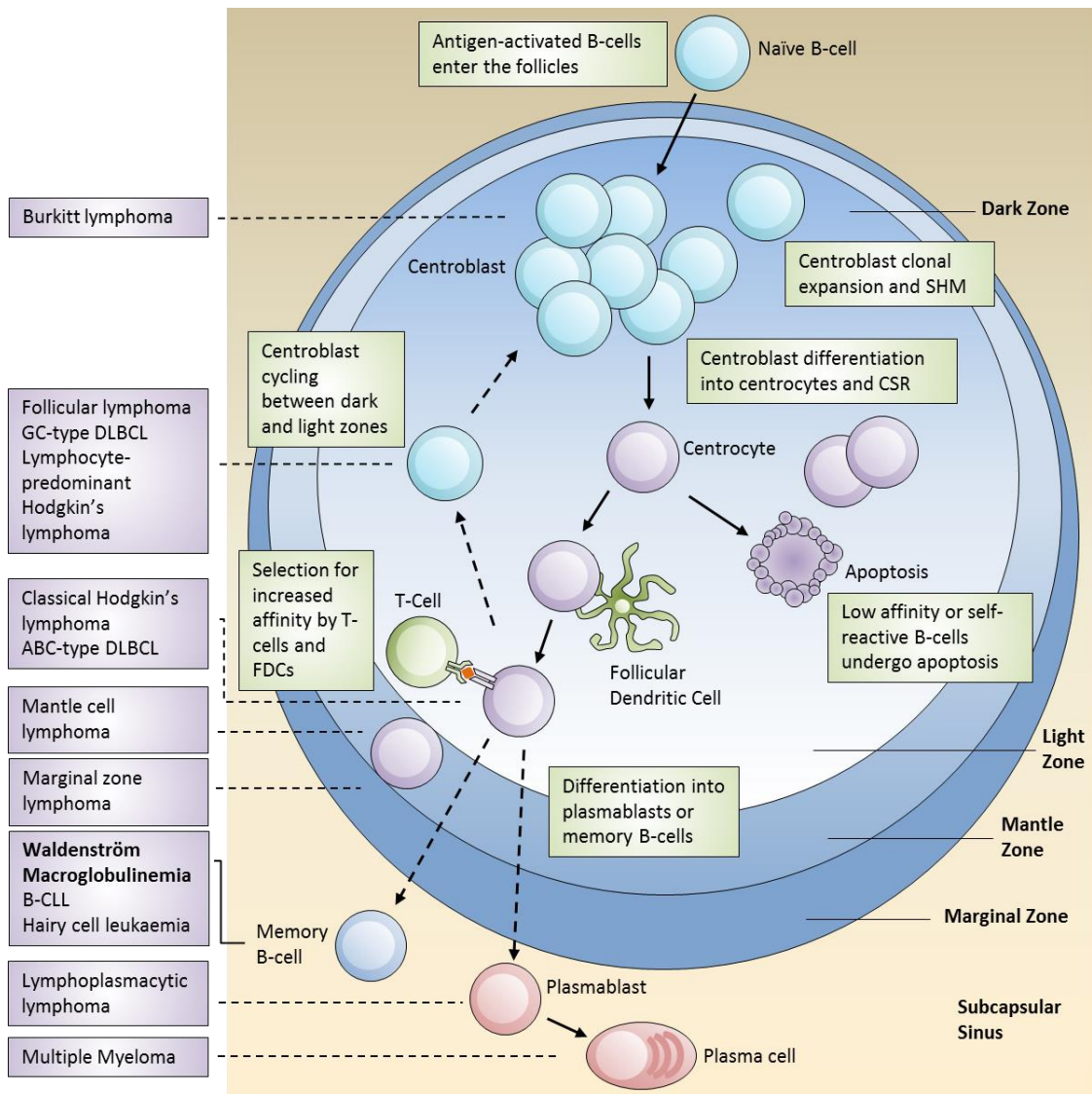
Figure 1.6 B-cell germinal centre development and cell of origin for several B-cell neoplasms. In the dark zone, the centroblasts proliferate and undergo somatic hypermutation (SHM) which generates clonal diversity. SHM increases the B-cell repertoire through mutation of the variable region of the antibody and facilitates increased antigen affinity. CSR enables the generation of different isotypes and involves the deletion of segments of the antibody heavy chain locus, followed by non-homologous end joining to repair the break and re-join the variable and constant regions. Centroblasts differentiate and migrate to the light zone where they interact with follicular dendritic cells (FDCs) and follicular helper T-cells (T_{FH}) and undergo class switch recombination (CSR). The centrocytes undergo apoptosis unless their antibody affinity is sufficient to confer a selection advantage and they are rescued by the T_{FH} or FDCs. Centrocytes displaying self-reactivity undergo apoptosis. Centroblast-centrocyte cycling enables unselected cells to improve their affinity. Selected centrocytes exit the GC and differentiate into plasma cells or memory B-cells. B-cell malignancies and their proposed normal counterparts are indicated on the left-hand side. Adapted from: (Vinuesa *et al.*, 2009; Kuppers, 2005)

Different neoplasms arise depending on their cellular origin and mutational status. Waldenström macroglobulinemia (WM) is a rare, non-Hodgkin lymphoma that develops from memory B-cells (Kriangkum *et al.*, 2004b).

1.4   Waldenström macroglobulinemia

Jan Gosta Waldenström was a Swedish clinician who, in 1944, first described two patients that presented with symptoms of a distinct neoplasm that would come to bear his name (Waldenström, 1944). Both patients suffered from various symptoms, including lymphadenopathy, thrombocytopenia, oronasal bleeding and accumulation of lymphoid cells within the bone marrow but without bone pain, which is classically associated with multiple myeloma (Niscola *et al.*, 2010; Terpos *et al.*, 2014). He noted that the bone marrow infiltrate consisted of B-cells rather than plasma cells, which he again contrasted to multiple myeloma. In addition to these symptoms, the patients exhibited abnormally high serum viscosity and one demonstrated evidence of cryoglobulinemia. Waldenström identified large quantities of globulin with a high molecular weight which he astutely attributed to be macroglobulins rather than aggregates of multiple small proteins.

Waldenström pioneered the concept of monoclonal versus polyclonal gammopathies. He identified patients that did not show evidence of malignancy but possessed a narrow band of hypergammaglobulinemia following serum protein electrophoresis as having a benign monoclonal gammopathy, now most commonly referred to as monoclonal gammopathy of undetermined significance. Whereas he discerned broad band hypergammaglobulinemia as a polyclonal gammopathy (Waldenstrom, 1961). The distinction between monoclonal and polyclonal gammopathies is particularly important because the former is the precursor to B-cell malignancy, whilst polyclonal gammopathies most commonly originate from inflammatory responses rather than a neoplastic cause (Dispenzieri *et al.*, 2001).

WM is characterised by the infiltration and accumulation of clonal B-lymphocytes in the bone marrow, which give rise to neoplastic plasma cells that secrete monoclonal IgM paraprotein (Owen *et al.*, 2003). The uniform ability of WM B-cells to undergo plasma cell differentiation is unique amongst B-cell malignancies as cells from other neoplasms are either halted at a particular stage of differentiation, such as the activated B-cell-like stage in ABC DLBCL or only retain a limited capacity for differentiation such as marginal zone lymphoma (Alizadeh *et al.*, 2000; Van Huyen *et al.*, 2000; Owen *et al.*, 2003; Dufresne *et al.*, 2010). WM may occur as smouldering or symptomatic disease. Alternately, if a patient presents with an abnormal level of IgM, but no bone marrow infiltration and are symptom-free they are classified as having IgM

MGUS, an IgM monoclonal gammopathy of undetermined significance. A patient with IgM MGUS or smouldering WM is at significant risk of developing symptomatic WM, with a progression rate to WM of approximately 2% per year (Kyle *et al.*, 2003).

Initially, investigation into the molecular pathogenesis of WM revealed the recurrent somatic mutation of the myeloid differentiation primary response gene (MYD88), on the short arm of chromosome 3 (Treon *et al.*, 2012). The MYD88 mutation is a single base transition from CTG to CCG, resulting in an amino acid substitution from leucine to proline at position 265. MYD88 is an adaptor protein for the TLR family and is important for NF-κB activation (Medzhitov *et al.*, 1998). A second recurrent mutation was also discovered, the CXCR4-WHIM-like mutation – CXCR4^{S338X} which results in protein truncation (Treon *et al.*, 2012; Hunter *et al.*, 2014).

MYD88^{L265P} was identified as the most common mutation in WM, present in 91% of patients (Treon *et al.*, 2012). It was also observed to occur at a much lower level in IgM MGUS, suggesting that MYD88^{L265P} may be critical for the progression of disease. Further investigation by allele specific oligonucleotide PCR concurred with these findings, noting that the MYD88 mutation was highly prevalent among patients with WM (Xu *et al.*, 2013). However, the increased sensitivity of the technique revealed that the MYD88^{L256P} mutation was present in far more patients (in excess of 50%) with IgM MGUS than was previously reported. The importance of MYD88 mutation in WM is clear, but its presence alone does not fully explain the transformation of IgM MGUS to malignant disease.

The mechanism of transformation from smouldering WM or IgM MGUS to WM has yet to be fully elucidated. Paiva *et al.* (2014) reported that 12% of IgM MGUS patients had a population of clonal B-cells that were found to progressively accumulate, as the disease transformed into symptomatic WM (Paiva *et al.*, 2014). In addition to the accumulation of clonal B-cells, they increasingly displayed the same signature phenotype as WM clonal B-cells (CD22^{low}CD25^{+}CD27^{+}IgM^{+}).

Subsequently, the same group used multidimensional flow cytometry to increase the sensitivity of their characterisation of the phenotypes of the clonal B-cells in each of the three disease groups (Paiva *et al.*, 2015). A comparison of the disease stages revealed that whilst patients with WM and IgM MGUS possessed molecularly and phenotypically similar clonal B-cell populations, the mutations present in symptomatic WM occurred less frequently in patients with IgM MGUS. Analysis of the gene expression profiles of WM and IgM MGUS revealed that they possess high levels of similarity (Chng *et al.*, 2006).

The identification of MYD88^{L265P} and its prevalence implies that WM cell survival results from constitutive activation of the NF-κB pathway. NF-κB activation is one of the many downstream

effects of BCR stimulation, but this does not require MYD88. Therefore, this indicates that an alternate pathway must be involved in WM pathogenesis such as the TLR or BAFF-R pathways (Treon *et al.*, 2012).

1.5   MYD88 in B-cell responses

Whilst MYD88 is not required in the T-cell dependent response, B-cell differentiation can be induced in a manner independent of T-cell interaction and elicits antibody production and limited CSR (Rawlings *et al.*, 2012). Whilst the antibodies produced in a T-cell independent (TI) immune response are generally of lower affinity than those produced from plasma cells that have undergone the germinal centre reaction, it nevertheless enables B-cells to rapidly mount a defence against invading pathogens and generates some long-lived plasma cells (Fairfax *et al.*, 2008). A TI response can be initiated in several ways, such as when B-cells activated by antigens receive additional signals from TLRs, but may also occur independently of TLR ligation, following binding of multivalent antigens (Obukhanych and Nussenzweig, 2006).

1.5.1   Toll-like receptors

TLRs are present on many cells within the immune system, particularly B-cells, plasmacytoid dendritic cells and macrophages (Takeda and Akira, 2005). TLRs may be located either on the surface of cells such as TLR 1, 2 and 4 or localised within endosomes (TLRs 7, 8 and 9) and bind their ligands which are usually highly evolutionarily conserved bacterial motifs, such as LPS or CpG (Akira and Takeda, 2004). Currently, 11 human TLRs have been reported, but TLR11 appears to be non-functional due to the presence of a stop codon within the gene resulting in protein truncation (Zhang *et al.*, 2004). The TLRs may be divided into three groups based on their ligands: TLRs 1, 2, 4 and 6 recognise lipids and lipopeptides, nucleic acids serve as the ligands for TLRs 3, 7, 8 and 9 and TLR5 recognises proteins (Takeuchi *et al.*, 1999; Alexopoulou *et al.*, 2001; Hayashi *et al.*, 2001; Takeuchi *et al.*, 2001; Takeuchi *et al.*, 2002). The ligand of TLR10 remains unknown but it has been reported to undergo homodimerisation and is also able to heterodimerise with TLRs 1 and 2 (Hasan *et al.*, 2005). The TLRs that have been characterised in humans and their associated ligands are summarised in table 1.1.

Table 1.1 Human toll-like receptors and their ligands

TLR	Ligand	Location	Heterodimer
1	Triacyl lipopeptides	Surface	TLR 2
2	Peptidoglycan, lipopeptides, lipoproteins, zymosan	Surface	TLR1, TLR6
3	Double-stranded RNA	Endosomal	-
4	Lipopolysaccaride	Surface	-
5	Flagellin	Surface	-
6	Diacyl lipopeptides	Surface	TLR2
7	Single-stranded RNA	Endosomal	-
8	Single-stranded RNA	Endosomal	-
9	Unmethylated deoxycytidyl-phosphate-deoxyguanosine (CpG) motifs	Endosomal	-
10	Unknown	Surface	TLR 1, TLR 2
11	(Non-functional)	Endosomal	-

Mature human B-cells express TLRs 1, 6, 7, 9 and 10, with low or negligible expression of TLRs 3, 5 and 8 (Hornung *et al.*, 2002; Bernasconi *et al.*, 2003; Bourke *et al.*, 2003). In stark contrast to murine B-cells, human B-cells lack TLR4 and thus are unable to be activated by LPS (Bernasconi *et al.*, 2003). Naïve and memory B-cells have their own distinct TLR expression patterns; whilst naïve B-cells have been shown to express only low levels or TLRs 6, 7, 9 and 10, memory cells express these receptors at much higher levels, conferring additional sensitivity to TLR activation (Bernasconi *et al.,* 2003).

The requirement of a second signal subsequent to BCR ligation, such as that provided by TLRs, acts to maintain immunological tolerance to self-ligands that may otherwise elicit an aberrant response (Fulcher and Basten, 1997; Vos *et al.*, 2000; Pone *et al.*, 2010). TLR stimulation induces signalling cascades, ultimately resulting in the activation of the canonical NF-κB pathway, translocation of NF-κB to the nucleus and gene expression for cell survival and proliferation. All members of the TLR family except TLR 3 signal through MYD88 and thus it plays a critical role in signal transduction for the TI response (figure 1.7) (Takeda and Akira, 2005).
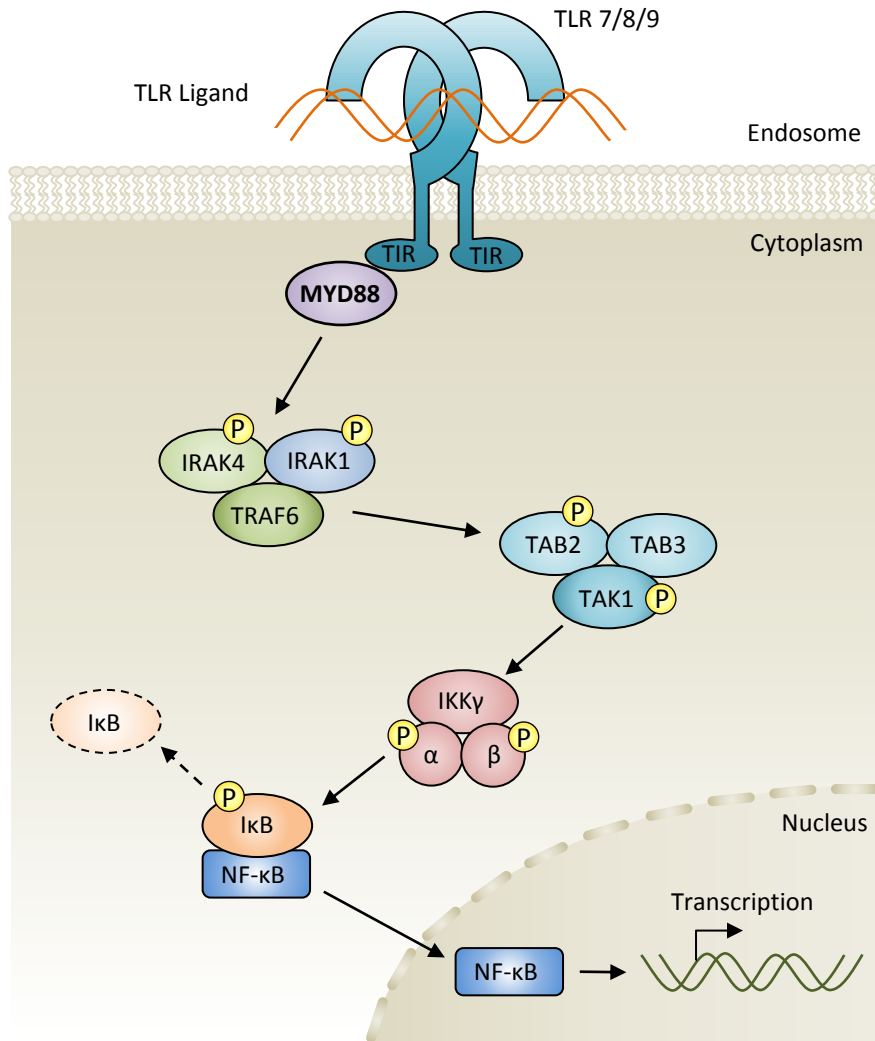
Figure 1.7 MYD88 is essential for the T-cell independent TLR signalling pathway. TLR signalling pathways are initiated upon ligand binding and this induces dimerisation of the receptors, resulting in interactions between their intracellular TIR (Toll-interleukin-1 receptor) domains. This facilitates the recruitment of the adaptor protein MYD88 which binds via its corresponding TIR domain. MYD88 oligomerises and subsequently forms a complex with the serine/threonine kinase IRAK4 which in turn undergoes autophosphorylation and in addition phosphorylates IRAK1. IRAK1 subsequently activates TRAF6, leading to the recruitment of the TAK1-TAB2-TAK3 and IKKα-IKKβ-IKKγ complexes and the resultant phosphorylation of IKKα and IKKβ. IκB is phosphorylated by IKKα and IKKβ and consequently it is degraded. Degradation of IκB enables the nuclear translocation of NF-κB which results in gene expression. IRAK1/4 – interleukin-1 receptor-associated kinase, TRAF6 – TNF Receptor-Associated Factor 6, TAK - transforming growth factor-β-activated kinase 1, TAB2/3 – TAK1 binding protein.

MYD88^{L265P} is also a common mutation in activated B-cell type diffuse large B-cell lymphoma (ABC DLBCL) and occurs in B-cell chronic lymphocytic leukaemia (B-CLL) (Ngo *et al.*, 2011; Jimenez *et al.*, 2013). In each case, constitutive NF-κB signalling promotes oncogenic cell survival. Ngo *et al.*, identified MYD88^{L265P} as a gain-of-function mutation resulting in the

constitutive signalling. Knockdown of MYD88 in ABC DLBCL cell lines by shRNA resulted in improved cell killing when used in combination with shRNAs against CARD11 or CD79b. This suggests that the BCR and TLR signalling pathways function in a non-redundant manner.

1.6   MYD88 mutation in WM

1.6.1   Structure of MYD88

MYD88 contains three functional domains; a death domain located at its N-terminus, followed by an intermediate domain and, at its C-terminus, a TIR domain (Hardiman *et al.*, 1996) (figure 1.8). The death domain adopts a conformation of six antiparallel α-helices and is crucial for MYD88 interaction with the death domains of IRAK1 and 4. This interaction brings the kinase domain of IRAK4 into close proximity with IRAK1, which enables its phosphorylation (Burns *et al.*, 2003).

The TIR domain is important for upstream signal transduction; the TIR of TLRs interacts with the corresponding MYD88 TIR domain and enables MYD88 to recruit IRAK4 (Watters *et al.*, 2007) . The structure of the MYD88 TIR domain is similar to other members of the TLR/IL-1R superfamily, comprising of five β-sheets (βA-βE) connected by surface-exposed loops to four α-helices (αA-αC and αE) (Ohnishi *et al.*, 2009).
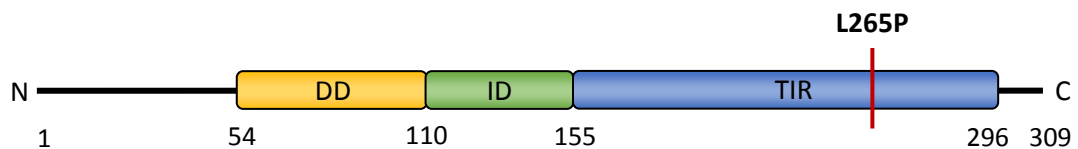
Figure 1.8 Representation of the domain structure of MYD88. DD – death domain, ID – intermediate domain, TIR – Toll-interleukin-1 receptor domain. The location of the L265P mutation is shown. Numbers denote amino acids.

Upon TLR stimulation, MYD88 undergoes oligomerisation and this facilitates interaction with the IRAKs. The resulting complex has been termed the Myddosome and is important for the downstream activation of NF-κB (Gay *et al.*, 2011). MYD88-TLR TIR-TIR interactions are believed to initiate the formation of the Myddosome (Loiarro *et al.*, 2005) . The L265P mutation occurs at a highly conserved residue situated in the hydrophobic core of the protein and forms part of the TIR βD β-sheet. This mutation increases the propensity of MYD88 to oligomerise and form spontaneous Myddosomes without the requirement of TLR signalling (Loiarro *et al.*, 2013).

MYD88^{L265P} enhances oligomerisation with both mutant and WT MYD88 and the strength of these interactions is significantly increased compared to the interaction between two WT domains (Loiarro *et al.*, 2005). This ultimately results in apoptotic resistance via the constitutive activation of the NF-κB pathway. WM B-cells possessing MYD88^{L265P} therefore have a survival advantage over their WT counterparts.

1.6.2   Mechanism of MYD88 signalling

Engagement of TLRs with their cognate ligand induces dimerization of the receptor, facilitating the recruitment of MYD88 and initiating the formation of the oligomeric Myddosome complex (Jin and Lee, 2008). Subsequent recruitment of IRAK-4 to the complex is mediated by a peptide sequence spanning the intermediate and death domain (Motshwene *et al.*, 2009). Jannssens et al., identified a splice variant of MYD88 lacking the ID, which they have termed MYD88s (Janssens *et al.*, 2003). MYD88s is unable to recruit IRAK-4 to the Myddosome, highlighting the importance for the ID in its assembly (Janssens *et al.*, 2003).

Dimerisation of IRAK-4 is critical to facilitate *trans*-autophosphorylation, whereby the activation loop of one kinase is brought in close proximity to its neighbour, enabling phosphate exchange (Motshwene *et al.*, 2009; Vollmer *et al.*, 2017). IRAK-4 subsequently activates IRAK-1 by phosphorylation, which appears to be promoted by MYD88 (Li and Verma, 2002). IRAK-1 interacts with TRAF6 via its C-terminal enabling the translocation of TRAF6 from the membrane to the cytosol in a phosphorylation-dependent manner and activation of downstream NF-κB signalling (Qian *et al.*, 2001).

Unusually, IRAK-1 signalling is negatively regulated by its own activity as a kinase (Kollewe *et al.*, 2004; Noubir *et al.*, 2004). Activation of IRAK-1 by IRAK-4 results in hyper-autophosphorylation. Extensive phosphorylation of IRAK-1 results in its dissociation from the protein signalling complex, whereby it is subsequently ubiquitinated and degraded by the proteasome (figure 1.9) (Kollewe *et al.*, 2004; Noubir *et al.*, 2004).
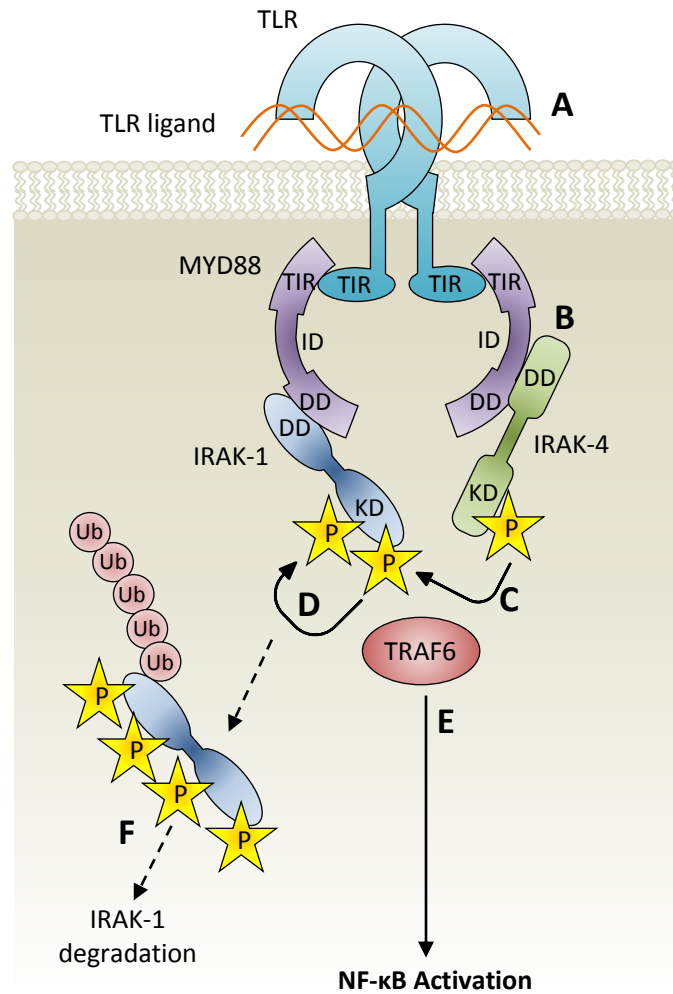
Figure 1.9 Mechanism of MYD88 signalling following TLR ligation. A) Ligand binds to TLR, induces TLR dimerisation. MYD88 interacts with the TIR domain of TLR. B) MYD88 binds with IRAK-4 via a peptide sequence spanning the ID and DD. C) The KD domains of IRAK-1 and -4 are brought within close proximity and this enables the phosphorylation of IRAK-1 by IRAK-4. D) Phosphorylation of IRAK-1 induces further autophosphorylation. E) Thereafter it interacts with TRAF6, initiating the pathway leading to nuclear translocation of NF-κB. Multiple phosphorylations of IRAK-1 eventually destabilise its interaction with the Myddosome. F) Following the dissociation of IRAK-1 from the Myddosome complex, it undergoes ubiquitination and degradation. TIR - Toll/interleukin-1 receptor homology domain, ID - Intermediary domain, DD - Death domain, KD - Kinase domain. Adapted from Jannssens *et al*., 2003.

Control of this pathway may occur in a variety of ways, with one example being the regulation of adaptor molecules, such as the ubiquitination of IRAK-1. The alternately spliced MYD88s is able to inhibit MYD88 signalling by dimerising with the full-length MYD88, but the activation signal is not propagated further due to its inability to activate IRAK-4 (Janssens *et al.*, 2003). A member of the TIR superfamily, ST2, binds to MYD88 via its TIR domain and thus prevents its

interaction with TLRs (Brint *et al.*, 2004). As with MYD88, inhibitory splice variants of the IRAKs also occur and function in a similar manner (Hardy and O'Neill, 2004; Rao *et al.*, 2005).

In addition to the regulation of components within the TLR signalling pathway, regulation of TLR signalling may be achieved via their location, particularly for the endosomal TLRs (Miggin and O'Neill, 2006). These TLRs recognise elements of bacterial DNA and RNA and have the potential for the recognition of self-ligands, thus their sequestration within endosomal compartments prevents them from coming into contact with these molecules (Barton *et al.*, 2006). Expression of TLRs can also be regulated via anti-inflammatory cytokines and the TLRs themselves may be degraded (Chuang and Ulevitch, 2004; McCartney-Francis *et al.*, 2004).

1.6.3   The Myddosome

The Myddosome is an oligomeric complex that acts like a scaffold, facilitating the recruitment of the IRAK-family kinases to potentiate the TLR signal. The crystal structure of the Myddosome was first determined by Lin and colleagues (Lin *et al.*, 2010). It forms a left-handed helical structure by the association of the death domains of MYD88, IRAK-4 and IRAK-1 or IRAK-2 in a sequential process. Based on their findings and the structure of other DD-containing complexes, they proposed a 6:4:4 MYD88:IRAK-4:IRAK-1 stoichiometry (Park *et al.*, 2007; Lin *et al.*, 2010). Each molecule within the complex has, at most, six partner death domains within its immediate locale, giving rise to a hexagonal pattern (Lin *et al.*, 2010).

Subsequently, Motschwene et al., demonstrated that stoichiometries of 7:4 or 8:4 were the most likely to form (Motshwene *et al.*, 2009). They speculate that 7:4 Myddosomes may be able to interact with 8:4 complexes, enabling the formation of scaffolds of alternating 7:4 and 8:4 Myddosomes (figure 1.10).
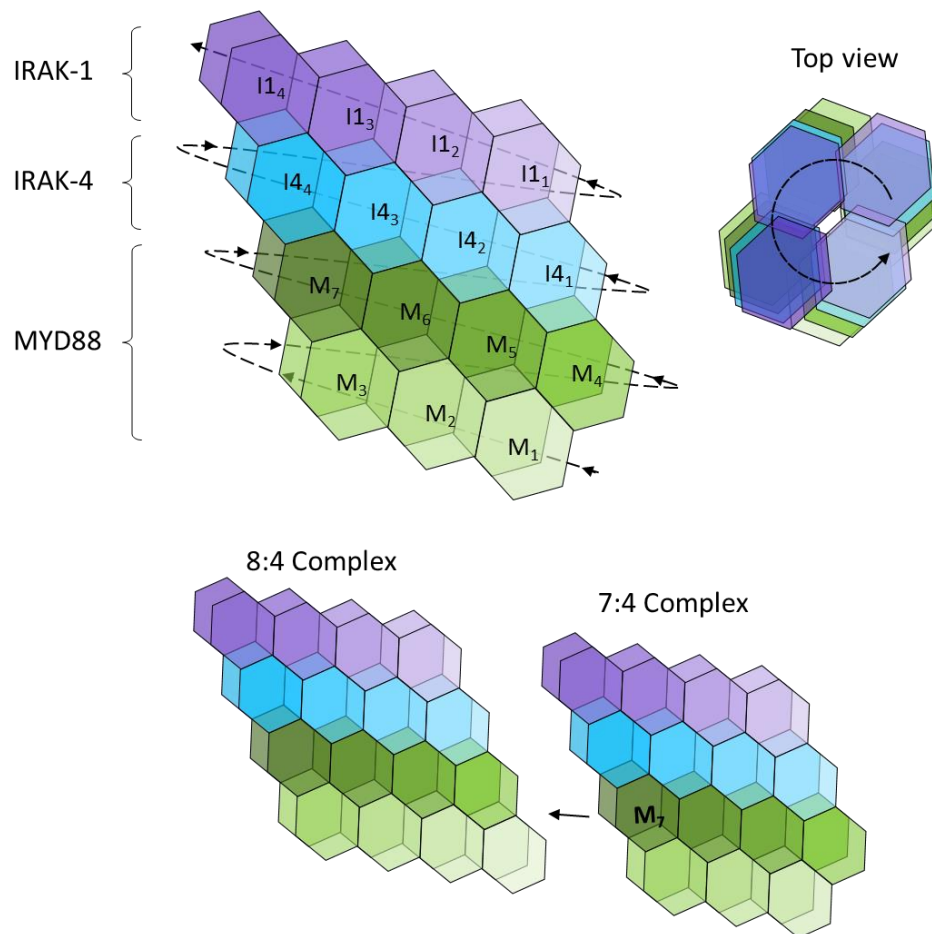
Figure 1.10 Tertiary structure of the Myddosome. Each layer of the helix consists of 4 DD molecules and is constructed sequentially. MYD88 molecules are depicted in shades of green, IRAK-4 - blue, IRAK-1 - purple. A planar view is illustrated on the right, demonstrating a hollow in the centre of the complex. The putative association of alternating 7:4 and 8:4 Myddosomes has been suggested to occur via the 7th MYD88 molecule in the 7:4 complex (Motschwene *et al.*, 2009).

The first stage in Myddosome assembly is the homodimerisation of MYD88, facilitated by the interaction between the TIR domains (Li *et al.*, 2005; Loiarro *et al.*, 2005). The MYD88[L265P] mutation can initiate the formation of the Myddosome without the prior requirement of TLR ligation (Ngo *et al.*, 2011; Treon *et al.*, 2012). Moreover, MYD88[L265P] interacts most strongly with wild-type MYD88 molecules, thus requiring only a limited number of mutant moieties for multiple complexes to form (Avbelj *et al.*, 2014).

1.6.4   Canonical and non-canonical NF-κB signalling pathways

Signalling through TLRs and subsequent Myddosome formation has been established to elicit NF-κB pathway activation (Kawai and Akira, 2007). There are two distinct branches of the NF-κB signalling axis, the canonical and non-canonical pathways. Aberrant activation of the canonical arm of the NF-κB pathway by MYD88^{L265P} is central to the pathogenesis of WM (Treon *et al.*, 2012). However, under normal conditions, multiple receptors on B-cells are able to initiate canonical NF-κB signalling, including the BCR and TLRs (figure 1.10). Ligation of these receptors results in phosphorylation of IKKβ and activation of the trimeric IκB kinase complex. This complex is composed of a regulatory IKKγ subunit and catalytically active IKKα and β subunits. This in turn phosphorylates the inhibitor of κB (IκB), resulting in its ubiquitination and subsequent proteasomal degradation. IκB degradation releases dimers of canonical NF-κB family members such as p50-p65 (RELA) leaving them free to translocate to the nucleus and initiate transcription. Canonical NF-κB signalling is usually characterised as swift but transient whereas non-canonical NF-κB activation is slower but more persistent.

In contrast to the canonical pathway, non-canonical signalling is mediated through NIK (NF-κB-inducing kinase. Activation of NIK, for example by CD40, first results in IKKα phosphorylation, which itself phosphorylates the C-terminal of p100. This results in the degradation of the C-terminal end of the protein and the generation of p52. The RelB-p52 dimer is then able to undergo nuclear translocation (figure 1.11).
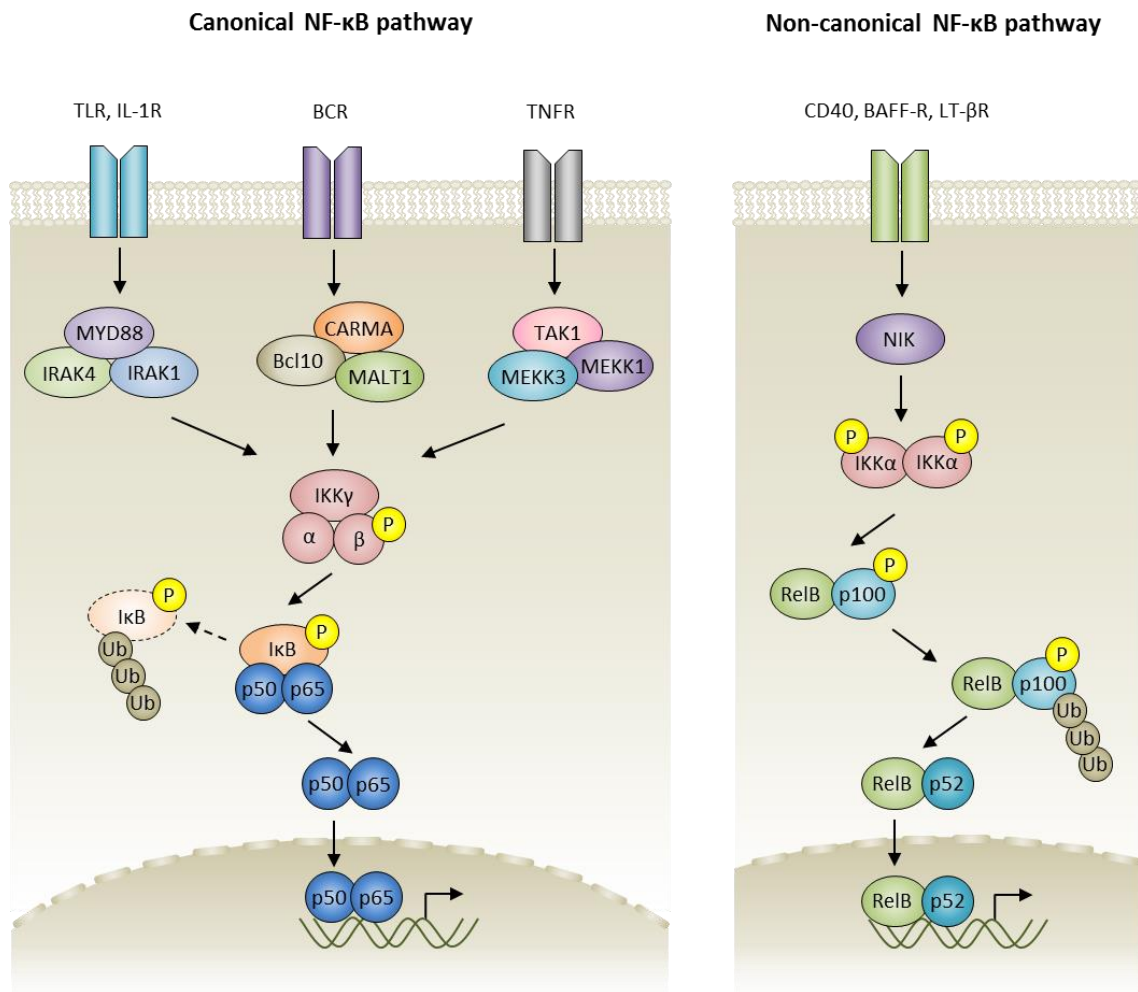
Figure 1.11 Activation of canonical and non-canonical NF-κB signalling in B-cells. Upon the initiation of canonical NF-κB signalling, phosphorylation activates the IκB kinase complex which, in turn, phosphorylates IκB (inhibitor of κB), targeting it for ubiquitination and proteasomal degradation. This process releases the p50-p65 dimer for nuclear translocation. Non-canonical signalling is achieved through the processing of the p100 subunit. NIK (NF-κB-inducing kinase) activation results the sequential phosphorylation of IKKα and then the C-terminal of p100, which is degraded. This enables RelB-p52 to move to the nucleus.

Whilst the focus of WM is on the canonical pathway, non-canonical signalling may also be important to WM cells due to their residence within the bone marrow. Neighbouring cells located within the bone marrow microenvironment provide several different sources of ligands that activate the non-canonical NF-κB pathway within the neoplastic clone. These include the production of BAFF by monocytes and the provision of CD40 signalling by mast cells and T-cells (Morrison *et al.*, 2005; Elsawa *et al.*, 2006; Ho *et al.*, 2008). The combination of mutations occurring within WM cells thus facilitates improved survival over their wild-type counterparts through constitutive activation of the canonical NF-κB pathway but also localises these cells to

a permissive environment which provides supplemental signals to support neoplastic growth and survival.

1.7 CXCR4 signalling

Following the discovery of MYD88^{L265P}, mutations in CXCR4 were identified as the second most prevalent in WM (Hunter *et al.*, 2014). CXCR4 is the cognate receptor for the chemokine SDF-1 (stromal cell derived factor-1), which is also known as CXCL12 (Bleul *et al.*, 1996). SDF-1 is expressed on the stromal and endothelial cells of the bone marrow and facilitates homing of lymphocytes to the niche via a chemotactic gradient (Bleul *et al.*, 1996). The association of CXCR4 expression and the infiltration of neoplastic cells to the bone marrow was first identified by two groups in CLL (Burger *et al.*, 1999; Möhle *et al.*, 2000). In a similar manner, the CXCR4/SDF-1 axis is key to the homing of WM cells to the bone marrow and their subsequent adhesion to endothelial and stromal cells within the niche (Ngo *et al.*, 2008).

Control of CXCR4 signalling is normally exerted by internalisation of the receptor, resulting in desensitisation (Haribabu *et al.*, 1997; Signoret *et al.*, 1997). Following activation, the intracellular domain of CXCR4 is rapidly phosphorylated by GRK, this enables binding of β-arrestin which ultimately results in attenuation of G-protein activation and internalisation of the receptor (Cheng *et al.*, 2000). Mutations to CXCR4 within WM are restricted to the intracellular cytoplasmic tail of the protein (Poulain *et al.*, 2016). The most predominant mutation, CXCR4^{S338X}, is often referred to as CXCR4^{WHIM} as it was originally identified in patients with WHIM syndrome (Hernandez *et al.*, 2003). These mutations prevent the internalisation of the receptor, resulting in aberrant activation of a multitude of downstream signalling cascades (figure 1.12).

CXCR4 signalling is mediated by heterotrimeric G-proteins. Ligand binding triggers conformational changes within the Gα subunit, enabling the release of the trimer from CXCR4 and subsequent disassociation of this subunit and the Gβ/Gγ dimer. The function of CXCR4 is altered depending on the stage of lymphopoiesis, enabling egress of mature B-cells from the bone marrow before enabling plasma cells to return to the niche (Honczarenko *et al.*, 1999; Glodek *et al.*, 2003; Palmesino *et al.*, 2006). The PI3K pathway is particularly important for lymphocyte chemotaxis (Ganju *et al.*, 1998; Helbig *et al.*, 2003; Kukreja *et al.*, 2005). This pathway has been found to be constitutively active in WM, aiding the infiltration of the neoplastic clone within the bone marrow (Leleu *et al.*, 2007).
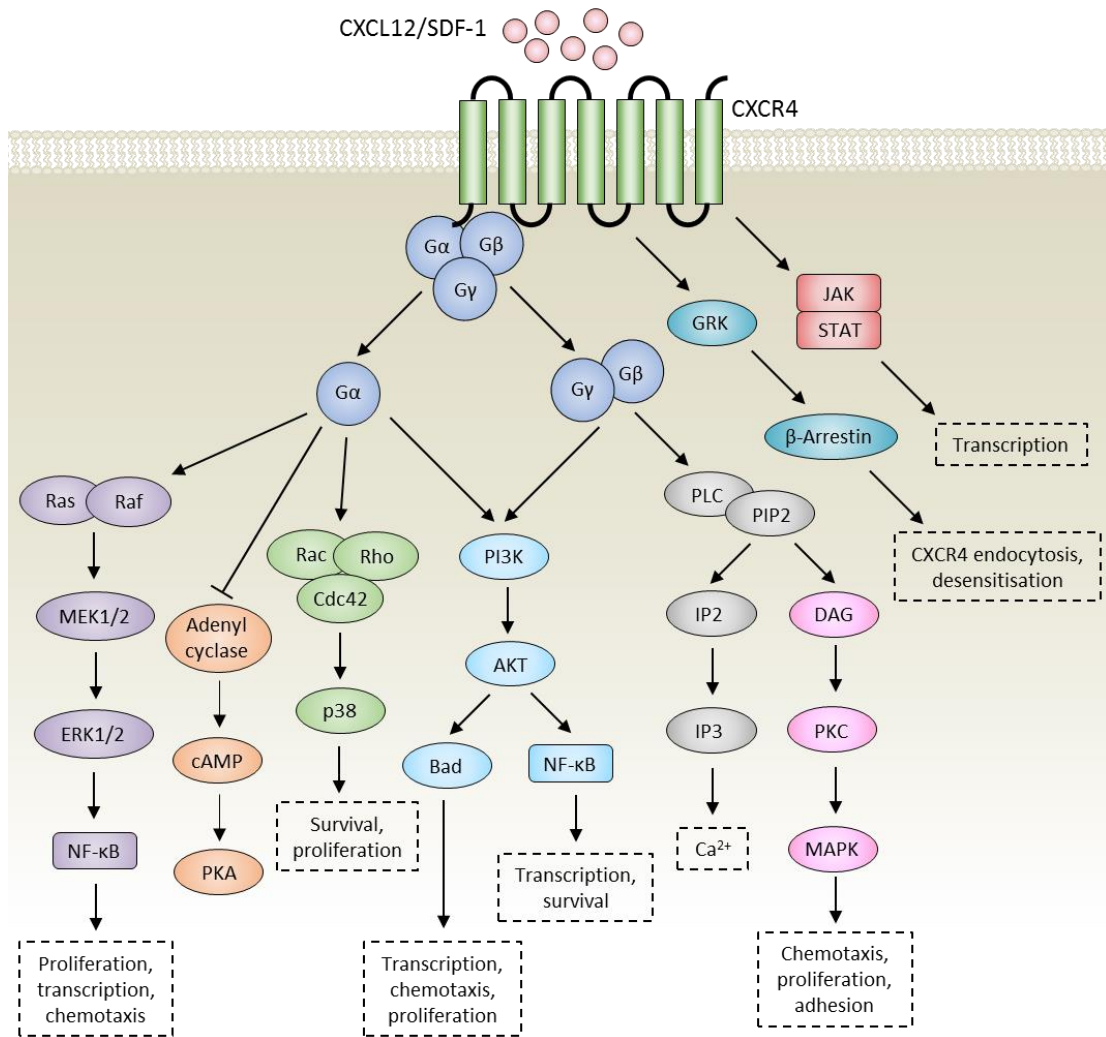
Figure 1.12 Divergent signalling cascades activated by CXCR4 ligation. The CXCR4/SDF-1 axis activates multiple downstream processes including chemotaxis, cell proliferation and survival, gene transcription and calcium release. cAMP - cyclic adenosine monophosphate; PKA - protein kinase A; JAK - Janus kinase; STAT - signal transducer and activator of transcription; Cdc42 - cell division control protein 42 homolog; Rac - Ras-related C3 botulinum toxin substrate; Rho - Ras homolog gene family; GRK – G-protein-coupled receptor kinase; FOXO - Forkhead box protein; PIP2 - phosphatidylinositol bisphosphate; PLC - phospholipase C; PKC - protein kinase C; Ras - Rat sarcoma protein family; IP3 - inositol 1,4,5 trisphosphate; PI3K - phosphoinositide-3 kinase; ERK1/2 - extracellular regulated kinase 1/2.

CXCR4 stimulation can also result in the activation of NF-κB via several diverging signalling pathways, facilitating survival and transcription. In WM, CXCR4 signalling results in the upregulation of the adhesion molecule VLA-4, mediating adhesion to stromal cells and contributing to chemotherapy resistance (Ngo *et al.*, 2008).

1.8   Treatment of WM

The ubiquitous expression of CD20 on B-cells up to the plasmablast stage originally led to the use and recommendation of Rituximab as a standard of care in WM (Dimopoulos *et al.*, 2007). Rituximab is a monoclonal CD20 antibody and has been commonly used as a first line of treatment in WM (Dimopoulos *et al.*, 2007; Buske *et al.*, 2013; Dimopoulos *et al.*, 2014). It is generally well tolerated by patients and does not damage stem cells, a key factor in treatment selection if an autologous stem cell transplant is being considered as salvage therapy (Treon *et al.*, 2001; Gertz *et al.*, 2004; Kyriakou *et al.*, 2014). A common complication for patients when on Rituximab is a paradoxical increase in IgM levels within the serum, termed "IgM flare" which may require plasmapheresis to prevent hyperviscosity, but is otherwise manageable (Treon *et al.*, 2004; Treon *et al.*, 2005).

The efficacy of Rituximab as a single agent prompted trials of its use in combination with other drugs such as alkylators and purine analogues (Treon *et al.*, 2006; Dimopoulos *et al.*, 2007; Tedeschi *et al.*, 2012; Kastritis *et al.*, 2015; Souchet *et al.*, 2016). Two common combination regimes are Rituximab and Bendamustine and R-CHOP (Rituximab plus cyclophosphamide, doxorubicin, vincristine, and prednisone) (Rummel *et al.*, 2005; Treon *et al.*, 2011; Rummel *et al.*, 2013; Tedeschi *et al.*, 2015). Combination therapies which include Rituximab have now become the current standard of care for the treatment of WM (Owen *et al.*, 2014).

One of the drugs that has recently demonstrated efficacy in treating WM is Ibrutinib (Yang *et al.*, 2013) (Treon *et al.*, 2015). Ibrutinib is a selective inhibitor of Bruton's tyrosine kinase (BTK). The first evidence of the interaction between MYD88 and BTK was provided by Jefferies and colleagues, who observed co-immunoprecipitation of MYD88 with endogenous BTK following the overexpression of MYD88 in HEK293 cells (Jefferies *et al.*, 2003). They also demonstrated that BTK interacts with the TIR domain of TLRs (Jefferies *et al.,* 2003). Subsequently, co-immunoprecipitation of MYD88 and BTK in macrophages stimulated with LPS provided additional evidence of this interaction and thus a link between BTK and TLR signalling (Liu *et al.*, 2011). Furthermore, the interaction between these two proteins was also identified in human neutrophils (Krupa *et al.*, 2013). Investigation into the effects of MYD88^{L265P} within WM cell lines revealed that it enhanced BTK activity, thus providing a rationale for BTK inhibition (Yang *et al.*, 2013). BTK is involved in both the BCR and TLR signalling pathways and has previously been shown to be effective at killing ABC DLBCL with chronic active BCR signalling (Wilson *et al.*, 2015). Ibrutinib elicits a similar response in WM cells (Treon *et al.*, 2015), highlighting the importance of MYD88^{L265P}/NF-κB induced survival and therefore targeting this pathway is key for effective therapy (figure 1.13).
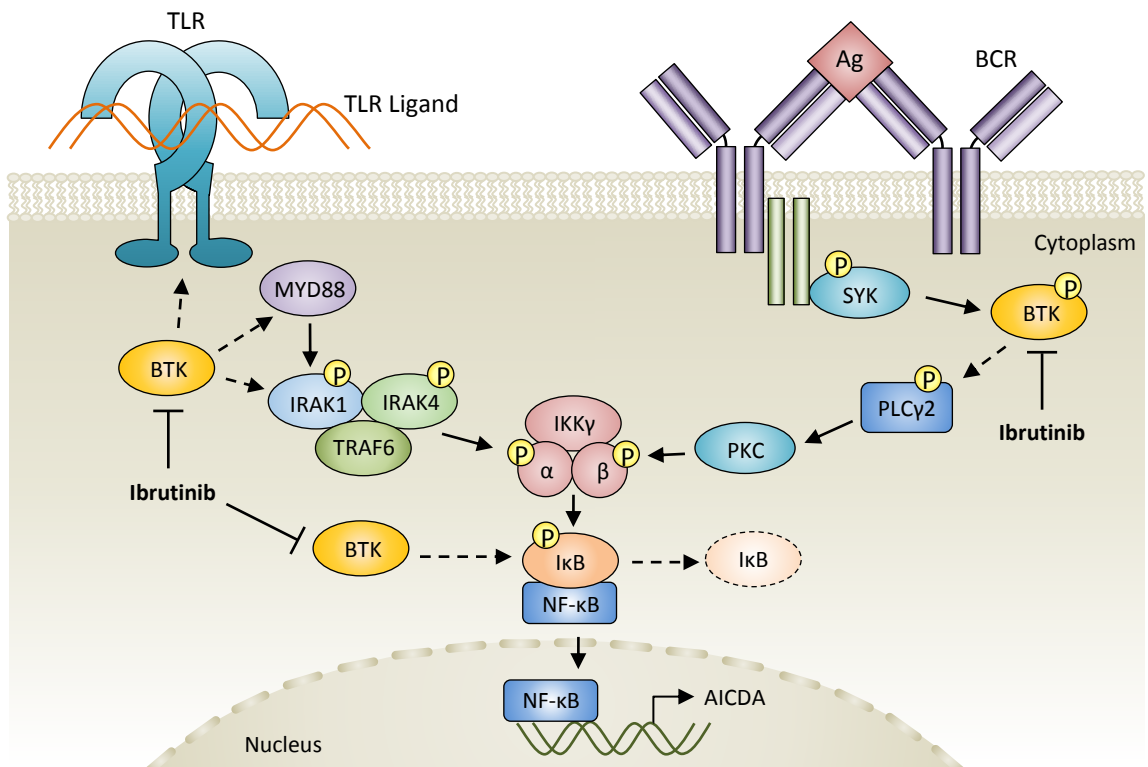
Figure 1.13 Involvement of BTK in the TLR and BCR signalling pathways. BTK is able to interact with multiple components of the TLR pathway, including the TLR TIR domain, MYD88, IRAK1 and IκB (Jefferies *et al.,* 2003). In WM, MYD88^{L265P} complexes with BTK upon TLR stimulation and this results in BTK phosphorylation (Yang et al., 2013). BTK is constitutively activated and phosphorylates IκB, releasing NF-κB. In the BCR pathway, BTK phosphorylates PLCγ2, which, in turn cleaves phosphatidylinositol-4, 5-bisphosphate (PIP$_2$). This results in the generation of inositol triphosphate (IP$_3$) and diacylglycerol (DAG). DAG interacts with PKC and this activates the NF-κB pathway whilst IP$_3$ is critical for intracellular Ca^{2+} release and thus BCR signal transduction.

A clinical trial of combination therapy of Ibrutinib and Rituximab in both treatment naïve and relapsed/refractory patients has recently been completed (Dimopoulos *et al.*, 2018). Results from this trial indicate that progression-free survival is significantly increased in patients receiving Ibrutinib-Rituximab compared to those receiving Rituximab and a placebo, regardless of their previous treatment status (Dimopoulos *et al.*, 2018). Due to the heterogeneity of the B-cell state within WM and the variety of mutations that may be present, a multi-faceted approach appears to provide the best outcome for patients.

WM treatment has thus far focussed on the B-cell component of the disease, presenting an opportunity to improve patient outcomes with the inclusion of a more plasma-cell specific therapy. One such example is the trial of the CD38 monoclonal antibody Daratumumab.

Daratumumab has previously demonstrated efficacy in MM and CD38$^+$ CLL (de Weers *et al.*, 2011; Lokhorst *et al.*, 2015; Usmani *et al.*, 2016; Matas-Céspedes *et al.*, 2017). Investigation of the efficacy of Daratumumab in treating WM has been undertaken using WM cell lines and suggests that it may be effective (Paulus *et al.*, 2016; Paulus *et al.*, 2017b; Paulus *et al.*, 2018). A phase II trial evaluating a combination of Daratumumab plus Ibrutinib is currently being conducted in WM patients (A study of Daratumumab in patients with relapsed or refractory Waldenström Macroglobulinemia. Trial number NCT03187262). A greater understanding of WM aetiology will help to inform future treatment.

1.9   Aims and objectives

Our group has previously published a novel technique for the *in vitro* differentiation of B-cells that is able to generate long-lived plasma cells (Cocco *et al.*, 2012). B-cells derived from peripheral blood or bone marrow are isolated and stimulated with a ligand such as CD40L and antibody to the BCR. The activated B-cells are cultured with cytokines to initially support viability and then conditions are sequentially altered to drive differentiation. Stromal cell support is provided to mimic the plasma cell niche and this enables long-term culture of plasma cells.

This is the first time a detailed investigation will be conducted into the differentiation of WM B-cells using this *in vitro* differentiation method. It will enable the characterisation of B-cell immunophenotype by flow cytometry and will permit quantification of cellular proliferation as differentiation occurs.

1.9.1   Preliminary results

Initial results indicated that some WM cells are able to differentiate when they are stimulated with CD40L but others are resistant to differentiation (data generated by Dr J. Sinfield). In addition, when WM cells were stimulated with R848 (Resiquimod), a selective synthetic agonist for TLR7/8, WM cells appeared to die rather than proliferate (figure 1.14).
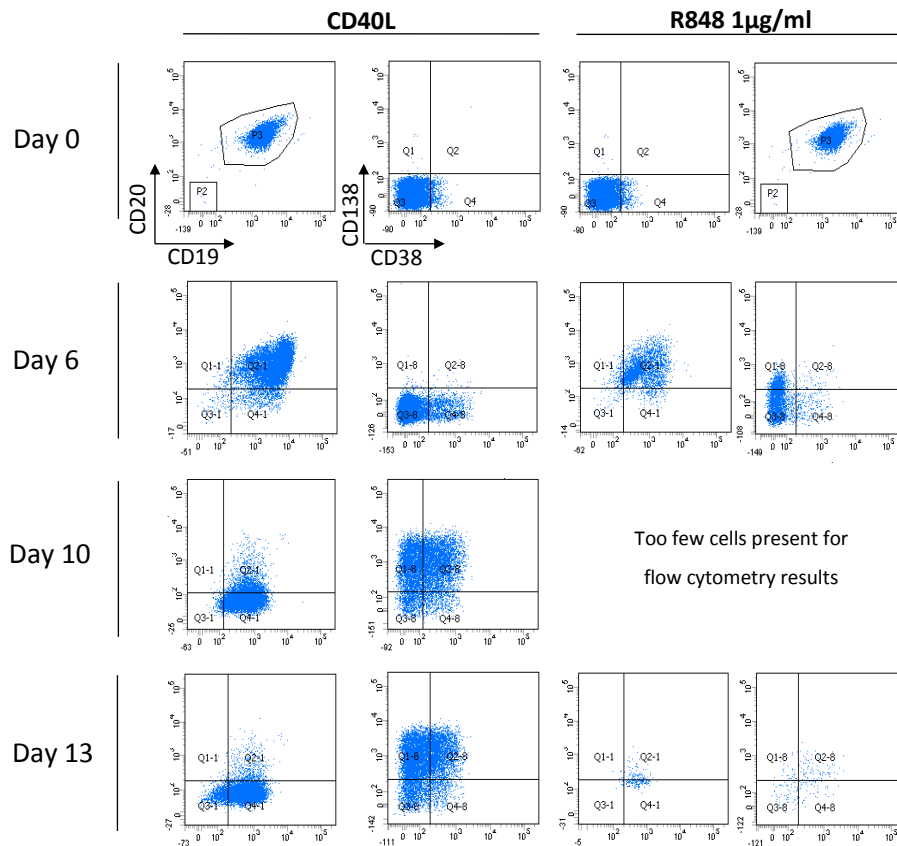
Figure 1.14 Immunophenotype of WM B-cells differentiated with CD40L or R848 stimulation. B-cells were isolated from the BM of a WM patient and stimulated with either CD40L + F(ab')$_2$ anti-IgG/M or 1µg/ml R848 + F(ab')$_2$ anti-IgG/M. Whilst the cells stimulated with CD40L differentiated, a population was resistant and retained an undifferentiated phenotype (CD19$^+$CD20$^+$CD38$^-$CD138$^-$). Meanwhile, cells stimulated with 1µg/ml R848 declined sharply in number, to an extent that a phenotype for day 10 could not be obtained (data generated by Dr J. Sinfield).

1.9.1.1   Hypotheses

1) Following activation with stimuli that mimics a T-dependent immune response, primary WM B-cells will be able to undergo differentiation and generate a population of long-lived plasma cells within the *in vitro* culture system.

The impact of MYD88 activation on WM B-cell differentiation will be assessed using the *in vitro* model. The response of healthy primary B-cells isolated from peripheral blood will be established to provide a control differentiation profile. The ability of WM cells to differentiate in response to the same stimuli will be evaluated, including cell phenotype, viability and number and compared to healthy controls. The longevity of the WM plasma cell population will also be assessed, to confirm that they persist in culture long-term.

2) WM cells require an intact TLR signalling pathway and will generate long-lived plasma cells in response to stimuli mimicking a T-independent immune response.

The necessity for TLR signalling for the survival of for MYD88^{L265P}-mutated WM cells has been postulated by two groups but has not been investigated in primary human cells (Lim *et al.*, 2013; Wang *et al.*, 2014). Preliminary data from the *in vitro* culture system has indicated that this is not the case and that additional activation of the MYD88 pathway – in addition to prior constitutive signalling - initiated by TLR7-R848 ligand binding has a detrimental effect on WM B-cell survival. Therefore the response of WM cells to TLR activation will be investigated further to determine their requirement for this signalling pathway.

3) WM B-cells will be able to generate a population of plasma cells more efficiently than cells derived from patients with other B-cell malignancies.

The ability of neoplastic B-cells to retain their capacity to differentiate into plasma cells is not exclusive to WM. B-cells from other malignancies often exhibit some level of plasmacytic differentiation, such as that which occurs in marginal zone lymphoma and B-cell chronic lymphocytic leukaemia. However, unlike WM in which the capacity for differentiation is retained throughout the B-cell population, the proportion of cells within other malignancies which remain able to initiate a differentiation response and the degree to which they are able to differentiate is highly variable. The differentiation profile of primary cells isolated from the bone marrow of patients with B-cell neoplasms that are not WM will therefore be characterised. This will enable phenotypic comparison to both WM and healthy cells and facilitate assessment of the extent to which differentiation is compromised in a proportion of the population.

1.9.1.2   Project aims

- Assess the feasibility of using the in vitro system to model plasma cell differentiation in primary WM cells.
- Analyse the impact of MYD88^{L265P} mutation on WM B-cell differentiation and survival in response to stimuli mimicking a T-dependent or T-independent immune response.
- Characterise the response of primary B-cells derived from other B-cell neoplasms to these different types of stimuli and compare them to WM and healthy cells.
- Investigate the aberrant response of WM cells as postulated by the preliminary data.
- Analyse and compare gene expression between healthy and WM differentiating cells, particularly the expression of transcription factors and cell cycle regulators to gain further insight into WM B-cell differentiation.

Chapter 2 - Methods

2.1 *In vitro* generation of long-lived plasma cells

2.1.1 Donors and clinical samples

Peripheral blood was obtained from healthy donors with their informed consent. Patient bone marrow aspirates and peripheral blood provided by the haematological malignancy diagnostic service (HMDS) Leeds, were from anonymous donors, derived from surplus clinical samples . Approval for the study was granted by the Leeds (East) NHS Research Ethics Committee, REC reference number 07/Q1206/47.

2.1.2 Isolation of PBMCs

50ml peripheral blood obtained from healthy donors was mixed with an equal volume of sterile phosphate buffered saline (PBS) at room temperature. 34ml of the blood/PBS mix was layered on top of 17ml Lymphoprep (Allere Ltd.). Samples of peripheral blood or bone marrow from WM patients were. When working with small quantities of patient samples, peripheral blood or bone marrow was mixed with sterile room temperature (RT) PBS to a volume of 8ml and layered on to 4ml Lymphoprep. The blood/lymphoprep was centrifuged at 2400rpm for 20 minutes at RT (acceleration 5, brake 0). All centrifugation was carried out with a 5810 R bench top centrifuge (Eppendorf). The lymphocyte layer was removed and divided between two 50ml falcon tubes containing 10ml cold PBS. The volume was made up to 50ml with cold PBS, then the peripheral blood mononuclear cells (PBMCs) were centrifuged at 1800rpm for 15 minutes at 4°C. The cells were combined into one tube, washed with 50ml cold PBS and centrifuged at 1500rpm for 10 minutes at 4°C. This was repeated, then the PBS was removed and the cells washed with 15ml ice-cold MACS buffer - 2.5ml MACS BSA stock solution, 47.5ml autoMACS rinsing solution (Miltenyi Biotec). The cells were counted using a haemocytometer before being centrifuged at 1500rpm for 10 minutes at 4°C. The cell pellet was stored on ice.

Suppliers and details of general tissue culture materials and reagents are provided in table 2.7.

2.2 Protocols used to isolate B-cells

Four different protocols were used to isolate either total B-cells or memory and naïve B-cell fractions (table 2.1).

Table 2.1 B-cell isolation protocols

	A	**B**	**C**	**D**
Name	Basic isolation (Negative selection)	Alternate total B-cell isolation (CD20$^+$ selection)	Naïve and memory separation	FACS sort (6-way cell sort)
Methods section	2.2.1	2.2.2	2.2.3	2.3
Description	Magnetic separation with memory B-cell isolation kit (Miltenyi Biotec)	CD3/CD56 depletion followed by CD20$^+$ positive selection	Magnetic separation with memory B-cell isolation kit (Miltenyi Biotec) followed by CD23$^+$ positive selection	Cells stained with CD3, CD15, CD19, CD23, CD38 and CD64 to identify and separate the B-cell fraction from PBMCs
Output	Unlabelled total B-cells	CD20$^+$ labelled total B-cells	CD23$^+$ naïve B-cells, unlabelled memory B-cells	CD19$^+$ CD23$^+$ CD38$^{-/+}$ Naïve B-cells, CD19$^+$ CD23$^-$ CD38$^{-/+}$ memory B-cells

2.2.1 Basic total B-cell isolation (negative selection, protocol A)

2.2.1.1 Isolation of B-cells with memory B-cell kit

The following protocol was used for B-cell selection with a memory B-cell isolation kit (Miltenyi Biotec) for a total quantity of 1 x 10^8 cells or fewer. Where the PBMC yield exceeded 1 x 10^8, all quantities of reagents were doubled.

The PBMC pellet was resuspended in 400µl of cold MACS buffer. 100µl B-cell Biotin-Antibody Cocktail was added and the mixture incubated for 20 minutes 4°C. Subsequently, 300µl cold MACS buffer and 200µl Anti-Biotin Microbeads were added, mixed, and then incubated for 20-30 minutes at 4°C. 10ml cold MACS buffer was added and the cells centrifuged for 10 minutes at 1500rpm 4°C. The cell pellet was resuspended in 1ml cold MACS buffer.

2.2.1.2 Magnetic separation of cells

In order to negatively select for memory and naïve B-cells, an LD Column (Miltenyi Biotec) was placed in the magnetic field of a suitable MACS separator and rinsed with 2ml of cold MACS buffer. The cell suspension was applied to the column and the unlabelled cells that passed through were collected in a fresh tube. The column was washed twice with 1ml of cold MACS buffer and the effluent collected in the same tube. To further increase B-cell purity, cells were

applied to a second LD column, washed twice with 1ml of cold MACS buffer and the unlabelled cells collected in a fresh tube (protocol A+). The cells were counted and resuspended in Iscove's Modified Dulbecco's Medium (IMDM) (Gibco) + 10% heat-inactivated fetal bovine serum (HIFBS) (Gibco) at 5 x 10^5 cells/ml.

2.2.2 Alternate total B-cell isolation (CD20$^+$ selection, protocol B)

2.2.2.1 CD3/CD56 depletion

After isolation of naïve and memory B-cells, their purity was increased further with additional magnetic separation using anti-CD3 and CD56 microbeads.

The cell number was determined using a haemocytometer and the cell suspension centrifuged at 300 × g for 10 minutes. The cell pellet was resuspended in 80 µl MACS buffer /10^7 cells. 20µl each of anti-CD3 and CD56 MicroBeads (Miltenyi) were added per 10^7 cells, mixed and incubated for 15 minutes at 4°C. Cells were washed by adding 1–2ml MACS buffer /10^7 cells and centrifuged at 300 × g for 10 minutes. The resulting pellet was resuspended in 500µl MACS buffer.

An MS Column (Miltenyi Biotec) was placed in the magnetic field of a suitable MACS separator and rinsed with 500µl cold MACS buffer. The cell suspension was applied to the column and the cells that passed through were collected in a fresh tube. The column was washed twice with 3 × 500µl of cold MACS buffer and the effluent collected in the same tube. The cells were counted and resuspended in IMDM + 10% FBS at 5 x 10^5 cells/ml.

2.2.2.2 Isolation of B-cells by CD20 selection

PBMCs were isolated and depleted for CD3/CD56 positive cells as described previously. Depletion was performed with LD Columns (Miltenyi) when cell numbers exceeded the capacity of MS columns (Up to 10^7 magnetically labelled cells from up to 2×10^8 cells). Subsequently, the cell number was determined using a haemocytometer and the cell suspension centrifuged at 300 × g for 10 minutes. The cell pellet was resuspended in 80µl MACS buffer /10^7 cells. 20µl each of anti-CD20 MicroBeads (Miltenyi) were added per 10^7 cells, mixed and incubated for 15 minutes at 4°C. Cells were washed by adding 1–2ml MACS buffer /10^7 cells and centrifuged at 300 × g for 10 minutes. The resulting pellet was resuspended in 500µl MACS buffer. The cell suspension was applied to MS columns and the flow-through discarded. The MS columns were flushed with 1ml cold MACS buffer and the effluent collected in a fresh tube. The CD20$^+$ cells were counted and resuspended in IMDM + 10% FBS at 5 x 10^5 cells/ml.

A **B**

Basic B-cell isolation method (Negative selection)

Incubate PBMCs with Miltenyi B-cell antibody cocktail

↓

Depletion on LD column

Non B-cell fraction remains on column ◄--- and is discarded

↓

Unlabelled B-cell fraction

↓

Cells used for differentiation

Alternate B-cell isolation method (CD20⁺ selection)

Incubate PBMCs with CD3/CD56 antibodies

↓

Depletion on LD column ---► CD3⁺ CD56⁺ cells remain on column and are discarded

↓

Incubate with CD20 antibody

↓

Selection on MS column #1 ⌐ Column flushed and CD20⁺ cells put onto a fresh MS column

CD20⁻ flow through discarded ◄

Selection on MS column #2 ◄

CD20⁻ flow through discarded ◄ Column flushed

CD20⁺ cells used for differentiation ◄

Figure 2.1 Scheme of total B-cell isolation protocols. PBMCs were isolated as per methods section 2.1.2. The basic isolation method (A) uses a memory B-cell isolation kit (Miltenyi Biotec) methods sections 2.1.3.1 and 2.1.3.2. The alternate method (B) positively selects for CD20⁺ cells subsequent to a CD3/CD56 depletion step (sections 2.1.4.1 and 2.1.4.2).

2.2.3 Isolation of naïve and memory B-cell subsets (protocol C)

PBMCs were isolated and depletion of non-B-cells was performed with a Miltenyi memory B-cell isolation kit. The unlabelled total B-cell fraction was incubated with 10µl CD23, 90µl MACS buffer per 10^7 cells for 20 min at 4°C. The cells were washed then incubated with 20µl Microbeads, 80µl MACS buffer per 10^7 cells for 15 min 4°C. Cells were washed by adding 1–2ml MACS buffer /10^7 cells and centrifuged at 300 × g for 10 minutes. The resulting pellet was resuspended in 500µl MACS buffer. The cell suspension was applied to an MS column and the flow through collected contained unlabelled CD23⁻ memory B-cells. The columns were flushed and the CD23⁺ naïve cell fraction was collected. To increase the purity of the CD23⁻ memory fraction, the suspension was applied to a second MS column and the CD23⁻ flow through collected in a fresh tube.

2.3 B-cell isolation by fluorescence-activated cell sorting (FACS) (protocol D)

2.3.1 Red Cell Lysis

A fresh solution of 160mM ammonium chloride was prepared and filter-sterilised. 10ml ammonium chloride was added per 2ml whole blood and incubated at 37°C for 5-10 minutes. The lysate was centrifuged for 3 minutes at 2000rpm. Cell pellets were combined and washed twice with 50ml MACS buffer. The cell pellet was resuspended in 10ml MACS buffer + 1% DNaseI (Ambion) and the cells counted using a haemocytometer. The cells were centrifuged at 300 x g for 10 minutes at 4°C, the supernatant discarded and PBMCs stored on ice prior to staining.

2.3.2 Staining cells for sorting

The cells were resuspended in blocking buffer (1x10^7 cells/100µl blocking buffer) and incubated for 15 minutes at 4°C. The cells were stained with the appropriate antibodies for 20-30 minutes at 4°C with light excluded. 10ml MACS buffer + 1% DNaseI was added and the cells passed through a 70µm cell sieve (Falcon). The suspension was centrifuged at 300 x g for 10 minutes at 4°C and the cells resuspended at 2.5-5.0 x 10^7 cells/ml in MACS buffer + DNaseI. Following sorting, the cell fractions were collected in sterile Eppendorf tubes or FACS tubes 1-2ml RPMI (+ 10% FBS + 1% Penicillin/Streptomycin) for monocytes, granulocytes and T-cells and IMDM (+ 10% FBS + 1% Penicillin/Streptomycin) for B-cells.

Table 2.2 Antibodies used for FACS 6-way sort

Antibody	Fluorophore	Volume per 10^7 cells	Supplier
CD3	VioGreen	2µl	Miltenyi
CD15	FITC	2µl	Miltenyi
CD19	PE	2µl	Miltenyi
CD23	APC	2µl	BD Biosciences
CD38	PE-Cy7	1µl	BD Biosciences
CD64	VioBlue	2µl	Miltenyi

2.3.3 Gating strategy for flow cytometry 6-way sort

The gating strategy used for the 6-way sort is as follows:
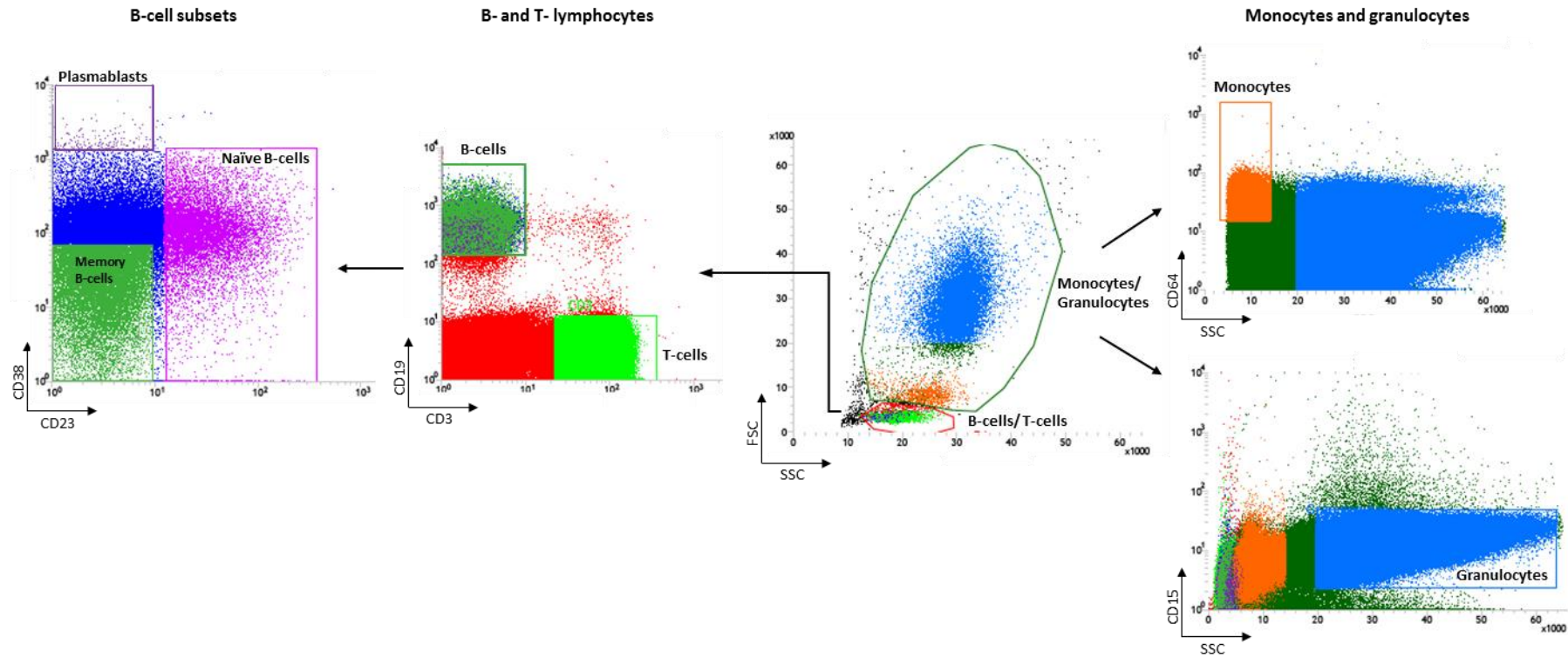
Figure 2.2 Gating strategy for 6-way cell sort. Cells were initially gated on their size according to forward and side scatter and divided into two groups. The monocytes and granulocytes were distinguished by their higher expression of CD64 or CD15, respectively. T-cells were separated from B-cells by their expression of CD3. The CD19^{+} B-cells were subdivided into naïve, memory and plasmablasts by their expression of CD23 and CD38: naïve B-cells CD19^{+}CD23^{+}, memory B-cells CD19^{+}CD23^{-} and plasmablasts CD19^{+}CD23^{-}CD38^{++}.

2.4   *In vitro* B-cell differentiation – tissue culture

2.4.1   Preparation of CD40L-L fibroblasts

In preparation for B-cell differentiation (where necessary), murine fibroblasts transfected with human CD40L (CD40L-L cells) were plated 24 hours in advance. CD40L-L cells were irradiated in advance at 50Gy for 50 minutes in a gamma irradiator (NDT) and stored at -80°C. An aliquot of 1×10^6 pre-irradiated CD40L-L cells was thawed and added to 10ml room temperature IMDM media + 10% HIFBS then centrifuged at 1500rpm for 5 minutes. CD40L-L cells were resuspended in 12ml fresh IMDM + 10% HIFBS and 0.5ml plated per well of a 24-well plate (~40,000 cells/ well) and incubated overnight at 37°C + 5% CO_2 (Sanyo).

2.4.2   Preparation of M2-10B4 stromal cells

M2-10B4 murine bone marrow stromal cells were cultured in RPMI 1640 (Sigma) + 10% HIFBS (37°C + 5% CO_2) and passaged twice weekly. To prepare M2-10B4 cells for co-culture with differentiating B-cells, they were irradiated when they had reached confluency of ~80% at 57Gy for 57 minutes on day 5 of the B-cell differentiation. The cells were washed and plated at 1×10^6 cells / 24-well plate (0.5ml media / well) and the plates incubated overnight at 37°C + 5% CO_2.

2.4.3   Conditions used during B-cell differentiation

B-cells were cultured with IMDM + 10% HIFBS supplemented with 1 x TxHybridoMax hybridoma growth supplement, 1 x Lipid Mixture 1, chemically defined and 1 x MEM amino acids solution (table 2.3). The culture conditions for various stages of differentiation are as follows:

Day 0-3: B-cells were cultured in 24-well plates at 2.5×10^5 cells/ml in IMDM + 10% HIFBS + supplements with the addition of hIL-2 (20 U/ml), hIL-21 (50 ng/ml) and F(ab')$_2$ goat anti-human IgM and IgG (10µg/ml). B-cells were stimulated by the TLR 7/8 agonist R848, TLR9 agonist CpG ODN 2006 or gamma-irradiated CD40L-L cells (1×10^6/plate) (table 2.3).

Day 3-6: B-cells were reseeded at 1×10^5/ml in T-25 or T-50 tissue culture flasks in IMDM + 10% HIFBS + supplements with the addition of hIL-2 (20 U/ml) and hIL-21 (50 ng/ml). If cultured with CD40L-L cells on day 0, B-cells were removed by gently pipette mixing before reseeding.

Day 6-9: When using Transwell cell culture inserts, cells were seeded at 1.5 or 3×10^5/well into the upper chamber of 24 or 12 well plate with Transwell inserts respectively in IMDM + 10% HIFBS + supplements with the addition of hIL-6 (10 ng/ml), IhL-21 (50 ng/ml), IFN-α (100 U/ml. The lower chamber of the plate was seeded with gamma-irradiated M2-10B4 cells (4.16 × 10^4/well and 8.33× 10^4/well for 24 and 12 well plates, respectively). When Transwells were not used, cells were resuspended at 5×10^5 cells/ml and cultured in 96-well round-bottomed plates at 200μl/well.

Day 9: Cells were re-fed by replacing half of the media with the same media as day 6.

Day 13 onwards: hIL-21 was withdrawn from the media + supplements + hIL6 + IFN-α. Cells were re-fed every 3-4 days by replacing half of the volume of media - from the lower chamber if Transwells were used - with fresh media + supplements + day 13 cytokines.

2.4.4   Reagents used during *in vitro* B-cell differentiations

Table 2.3 Table of cytokines and other reagents used during an *in vitro* differentiation

Name	Company	Cat no.
hIL-2	Roche	11147528001
hIL-6	PeproTech	200-06
hIL-21	PeproTech	500-P191
IFN-α	Sigma/PeproTech	SRP4596
Goat anti-human F(ab')₂ (anti-IgM & IgG)	Jackson ImmunoResearch	109-006-127
R848 (Resiquimod)	Invivogen	144875-48-9
CpG ODN 2006	Invivogen	tlrl-2006
HybridoMax hybridoma growth supplement	Gentaur	TX-HYB
Lipid Mixture 1 chemically defined	Sigma	L0288
MEM Amino Acids Solution	Sigma	M5550

B-cell activation by co-culture with CD40L-L
cells or addition of TLR agonist

Day 0

B-cells

CD40L-L cell layer

+ F(ab')$_2$ anti-IgG/M +
IL-2 + IL-21

Day 3

Activated B-cells

+ IL-2 + IL-21 + Supplements

B-cells seeded into transwell plates or
96 well round-bottomed plates

Day 6

Plasmablasts

M2-10B4 cell layer

+ IL-21 + IL-6 + IFNα +
Supplements

Day 13

Plasma Cells

M2-10B4 cell layer

+ IL-6 + IFNα + Supplements

Figure 2.3 Diagrammatic representation of the conditions used throughout an *in vitro* B-cell differentiation. Isolated B-cells are activated by either CD40L or a TLR agonist, paired with antibody to the BCR. Activated B-cells are removed from the stimuli at day 3 before being placed into Transwells with stromal support or 96-well plates at day 6. Cytokines are added sequentially as indicated and the media supplemented with 1 x TxHybridoMax hybridoma growth supplement, 1 x Lipid Mixture 1, chemically defined and 1 x MEM amino acids solution from day 3 or the differentiation.

2.5   Flow Cytometry

2.5.1   Flow cytometry

Flow cytometry was performed using a LSRII 3 laser (BD Biosciences) or CytoFLEX S (Beckman Coulter). Analysis was performed using FACSDiva v8.0.0 (BD Biosciences) or FlowJo v10 (Treestar).

2.5.2   Immunophenotype analysis

Where possible, at least 10,000 live cell events were recorded. Fluorescence minus one (FMO) or matched isotype controls were used. FMO controls consisted of the experimental cells stained with all the fluorophores minus one fluorophore. Cells were washed with 1ml FACS buffer before being blocked with 25µl 2x blocking buffer at 4°C for 15min. Blocking buffer contained hIgG (Sigma) and normal mouse serum (Sigma). The cells were subsequently incubated with the immunophenotyping antibody mix (table 2.4) at 4°C for 30min. Cells were washed with 1ml FACS buffer and resuspended in 300µl FACS buffer.

Table 2.4 Antibodies used for immunophenotype analysis.

Antibody	Fluorophore	Clone	Vol/10^7	Supplier	Cat no.	Isotype
CD19	PE	HIB19	2µl	Miltenyi	130-091-247	IgG1κ
CD20	e450	2H7	2µl	eBioscience	48-0209-42	IgG2bk
CD27	FITC	M-T271	2.5µl	BD Biosciences	555440	IgG1κ
CD38	PE-Cy7	HB-7	0.5µl	BD Biosciences	335825	IgG1κ
CD138	APC	44F9	2µl	Miltenyi	130-091-250	IgG1κ

The antibodies for CD19 and CD27 were exchanged for Fas and FasL to assess their expression during the course of B-cell differentiation.

Table 2.5 Antibodies used for Fas and FasL analysis.

Antibody	Fluorophore	Clone	Vol/10^7	Supplier	Cat no.	Isotype
Fas - CD95	FITC	NOK-1	10 µl	Miltenyi	130-092-415	IgG1κ
FasL - CD178	PE	DX2	10 µl	Miltenyi	130-096-456	IgG1κ

2.5.3   Gating strategy for flow cytometry

The gating strategy used throughout for flow cytometry is as follows:
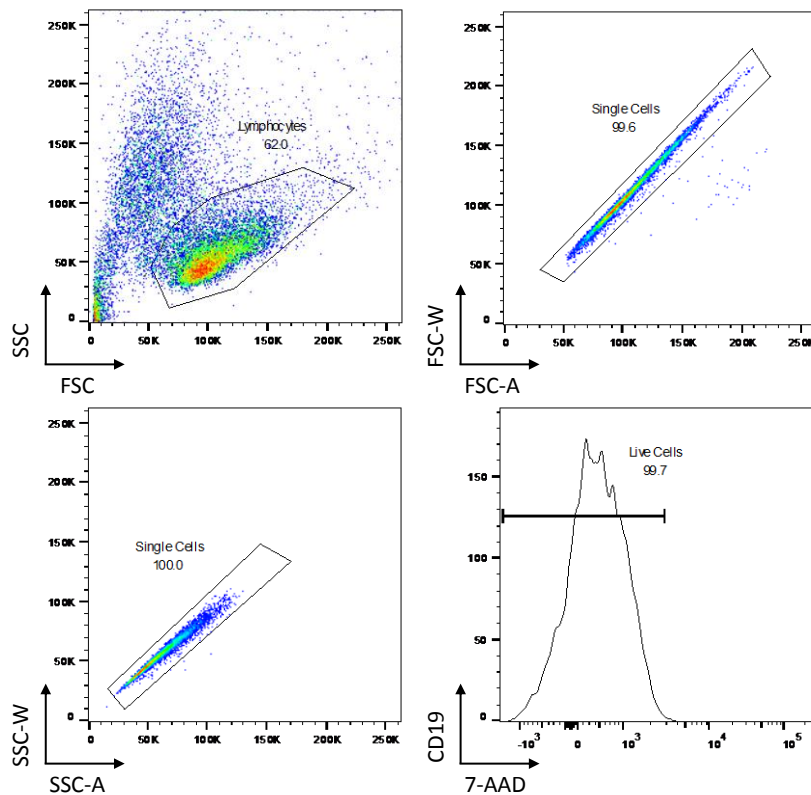
Figure 2.4 Gating strategy for immunophenotype analysis. B-lymphocytes were gated firstly on their forward vs. side scatter characteristics. Doublets were excluded for both forward and side scatter by plotting area against width. Live-dead discrimination was based upon staining with 7-AAD against the B-cell marker CD19.

2.5.4   Cell number quantitation

CountBright Absolute counting beads (Invitrogen) were used to quantify cell number. Cells from multiple wells were pooled to minimise well to well variation. CountBright beads were vortexed for 30 seconds prior to use. 50µl of counting beads were added to either 300µl undiluted cells or, if less than 300µl cells were available, cells were diluted to a total volume of 300µl and the original volume of cells used was recorded. 1,000 bead events were collected and the number of live cells recorded. The following calculation was performed to determine cell number:

Calculation of cell concentration: (A/B) x (C/D) = concentration of sample as cells/µl

Where: A = number of cell events B = number of bead events C = assigned bead count of the lot (beads/50 µl) D = volume of sample (µl)

2.5.5 Intracellular staining

Cells were washed with 1ml PBS then resuspended in 1ml PBS at 1x10^6 cells/ml. In order to assess viability, Zombie Aqua or Zombie UV dyes (BioLegend) were used. 1µl reconstituted fluorescent reactive dye was added and samples incubated at RT for 30min in the dark. 25µl blocking buffer was added and incubated on ice for 15min. The surface stain antibodies were added and samples incubated for 30 min on ice. The cells were washed with1ml PBS and fixed in 100µl 1x Foxp3 fixation/permeabilisation solution (eBioscience) and incubated in the dark at RT for 20min. Cells were washed with 1x permeabilisation buffer and resuspended in permeabilisation buffer with the intracellular antibodies and incubated in the dark at RT for 30min. The cells were washed with 1x permeabilisation buffer then resuspended in FACS buffer.

2.5.6 TLR quantification and immunophenotype analysis

The panel of antibodies provided in table 2.6 were used to assess TLR7-9 expression on B-cells isolated from peripheral blood or bone marrow or on cell lines. Cells were stained with antibodies to the surface markers before being fixed and permeabilised and stained with the intracellular antibodies (section 2.5.5).

Table 2.6 Antibodies used for TLR quantification.

Fluorochrome	Antigen	Location	Source	Clone	Cat no.	Vol/10^6
BV421	CD25	Surface	BD Biosciences	M-A251	562442	1µl
BV510	LAIR1	Surface	BD Biosciences	DX26	744558	5µl
FITC	TLR8	Intra	R&D Systems	935166	IC8999G	1µl
PE	TLR7	Intra	R&D Systems	533707	IC5875P	10µl
PerCP-Cy5.5	CD19	Surface	BD Biosciences	SJ25C1	332780	5µl
PE-Cy7	CD27	Surface	BD Biosciences	M-T271	560609	1µl
APC	TLR9	Intra	BD Pharmingen	eB72-1665	560428	20µl
APC-H7	CD20	Surface	BD Biosciences	L27	641414	5µl

2.6 Visualisation and further analysis of flow cytometry data

viSNE and SPADE analysis was performed using the cloud based platform Cytobank (Cytobank, Inc.). Prior to analysis, raw flow cytometry data files were amalgamated using an FCS file concatenation tool. Files were grouped based on sample origin (healthy, WM samples, other lymphoproliferative disorder samples etc.), the type of stimulation used to activated the B-cells (CD40L vs R848) and the time point the flow cytometry data was collected (day 0, day 6, day 13

etc.) - closely related time points from day 13 onwards (+/- 48 hours) were grouped together for clarity. The concatenated data was then gated to exclude doublets and to ensure that only live cells were analysed.

2.6.1 viSNE analysis

viSNE (visualisation of t-Distributed Stochastic Neighbour Embedding) maps were generated with the following parameters. The channels selected for visualisation were CD19, CD20, CD27, CD38 and CD138. Proportional sampling of the concatenated data was used for downsampling. Analysis was performed using the default t-SNE parameters but with perplexity = 50 and 5000 iterations.

Proportional rather than equal sampling was used because the number of events within each concatenated file was highly variable between time points and different groups and this prevented the exclusion of files that had few events. Runs were performed with an identical random seed to optimise the clustering. A test analysis was performed with 100,000 events, (perplexity = 30, 1000 iterations and theta = 0.5) but the separation and resolution of the maps were poor so the final analyses were performed with 500,000 events (perplexity = 50, 5000 iterations, theta = 0.5).

2.6.2 SPADE analysis

Clustering analysis of the viSNE output was then performed using SPADE (**S**panning-Tree **P**rogression **A**nalysis of **D**ensity-normalized **E**vents). The default analysis parameters were retained and downsampling was not performed in order to include all of the events within this analysis. Clusters of nodes were then labelled manually according to the phenotype.

2.7 Supernatant experiments

Tissue culture supernatant (TCSN) was taken from *in vitro* differentiation experiments at day 3 and 6, centrifuged at 1500rpm for 5min and frozen prior to use. TCSN was diluted with the addition of IMDM + 10% HIFBS. A second differentiation was performed and the TCSN was added at day 3 when the cells were resuspended in day 3 media conditions to give a final concentration of either 1:10 or 1:100 of the total volume.

2.8   Dose response experiments

Cells from cell lines were resuspended at 2.5×10^5/ml. R848 was added at a concentration of 10µg/ml, 1µg/ml or 0.1µg/ml or CpG was added at concentrations of 20µg/ml, 2µg/ml or 0.2µg/ml with or without the addition of F(ab')$_2$ anti-IgG/M. 1ml of this was plated per well of a 24-well plate. After 72h cell number was determined by flow cytometry using CountBright Absolute counting beads and viability by Annexin V/7-AAD staining.

2.8.1   Assessment of viability by Annexin V/7-AAD staining

Cells were harvested from each well and washed with 2ml 1x PBS. Cells were subsequently washed with 1ml 1x binding buffer. 100µl of staining mix – 5µl Annexin V + 95µl 1x binding buffer (BioLegend) – was added per sample and cells were incubated for 15 minutes at RT in the dark. The cells were washed with 1ml 1x binding buffer, resuspended in 200ul binding buffer and 5µl 7-AAD (BD Biosciences) added per sample. Samples were analysed immediately by flow cytometry. Apoptotic cells were identified as Annexin V positive, 7-AAD negative and late stage apoptosis was identified as Annexin V positive, 7-AAD positive.

2.9   Tissue culture

2.9.1   Cell lines

All cells were cultured at 37°C and 5% CO_2. Cell lines were cultured until they reached approximately 80% confluence before passaging.

WM cell lines: BCWM.1, MWCL.1 (cells courtesy of Dr Steven Ansell, Mayo Clinic, USA) were grown in RPMI-1640 + 10% HIFBS.

ABC DLBCL cell lines: OCI-Ly3 was grown in RPMI-1640 + 10% HIFBS and OCI-Ly10 in IMDM + 10% HIFBS + 2-ME.

2.9.2 Tissue culture materials and reagents

Table 2.7 Materials and reagents used in tissue culture

Product	Company	Cat no.
12-well flat-bottomed plates	Corning	CLS3513
24-well flat-bottomed plates	Corning	CLS3527
96-well round-bottomed plates	Corning	CLS3799
Transwell inserts, clear polyester membrane, 0.4µm pore	Corning	CLS3470
RPMI-1640 medium	Sigma	R8758
IMDM, supplemented with Glutamax	Gibco	31980-022
Fetal Bovine Serum, South America origin	Gibco	10500-64
Fetal Bovine Serum, "Gold"	PAA	A15-151
Penicillin-Streptomycin	Sigma	P4333
2-Mercaptoethanol	Sigma	M6250
Lymphoprep	Alere	1116508
CountBright Absolute counting beads	Invitrogen	C36950
Memory B-cell isolation kit, human	Miltenyi	130-093-546
autoMACS rinsing solution	Miltenyi	130-091-222
MACS BSA stock solution	Miltenyi	130-091-376
5ml round-bottomed polystyrene tubes	Falcon	10186360
5ml round-bottomed polypropylene tubes	Falcon	10654411
PBS tablets	Sigma	P4417
Annexin V	BioLegend	640992
7-AAD (PerCP-Cy5)	BD Biosciences	559925
Foxp3/Transcription factor fixation staining buffer set	eBioscience	00-5523-00

2.10   PCR

2.10.1 RNA isolation

Cells were centrifuged at 2000rpm for 5min at RT, the supernatant discarded and the pellet resuspended in 800µl TRIzol (Thermofisher). 160µl of chloroform was added to the samples, they were thoroughly shaken to mix and incubated for 2-3 minutes at room temperature. Samples were centrifuged at 12,000 x g for 15 minutes at 4°C and the upper aqueous phase removed to a fresh tube.

10µg RNase-free glycogen was added to the aqueous phase to improve precipitation. RNA was precipitated by adding 400µl 100% isopropanol to the aqueous phase, incubating at room temperature for 10 minutes and then centrifuging the mix at 12,000 x g for 10 minutes at 4°C. The supernatant was removed and discarded and the RNA pellet washed with 800µl 75% ethanol. Samples were vortexed, then centrifuged at 7,500 x g for 5 minutes at 4°C. The supernatant was discarded and the pellet air-dried for 5-10 minutes. Pellets were resuspended in 44µl RNase-free water, then incubated at 55°C for 10 minutes.

2.10.2 DNAse I treatment of RNA

5µl of 10x buffer and 1µl DNAse I (DNA Free, Ambion) was added to each RNA sample and then incubated at 37°C for 20 minutes. 5µl DNAse I inactivation reagent was added and the RNA concentration within 1µl of sample measured on an ND-1000 NanoDrop Spectrophotometer (Thermo Fisher Scientific).

2.10.3 cDNA synthesis

1µg RNA was used for cDNA synthesis, however when the RNA concentration was low and more than 5µl was required for 1µg, the volume of mixes 1 and 2 used were doubled (Table 2.6).

Table 2.8 cDNA synthesis master mixes.

Mix 1		Mix 2	
Reagent	**Supplier**	**Reagent**	**Supplier**
1µl Oligo dT	Invitrogen	4µl 5x cDNA synthesis buffer	Invitrogen
1µl dNTPs	Invitrogen	2µl DTT	Sigma
3µl Nuclease-free dH$_2$O	Ambion	2µl MgCl$_2$	Applied Biosystems
-	-	1µl RNAse Out	Invitrogen
-	-	0.25µl Reverse transcriptase (SSII)	Invitrogen
-	-	0.75µl Nuclease-free dH$_2$O	Ambion
Total volume - 5µl	-	Total volume - 10µl	-

5µl RNA was mixed with 5µl Mix 1 and incubated at 65°C for 5 minutes. The sample was placed on ice for 1 minute before adding 10µl Mix 2. It was then incubated at 42°C for 50 minutes and then incubated at 70°C for 15 minutes. Subsequently the mixture was chilled on ice, 1µl RNAseH (Invitrogen) added and then the mixture was incubated at 37°C for 20 minutes.

2.10.4 Conventional PCR

100ng cDNA was used for PCR. The master mix and PCR conditions are indicated in tables 2.7 and 2.8.

Table 2.9 Composition of PCR master mix.

Reagent	Volume	Supplier
10x buffer	2.5µl	Applied Biosystems
10mM dNTPs	0.5µl	Invitrogen
10µM Forward Primer	0.5µl	Sigma
10µM Reverse Primer	0.5µl	Sigma
25mM MgCl$_2$	1.5µl	Applied Biosystems
DMSO	1.25µl	Sigma
AmpliTaq Gold	0.125µl	Applied Biosystems
DNA	100ng	-
Nuclease-free dH$_2$O	To 25µl	Ambion

Table 2.10 PCR conditions.

PCR cycle conditions

94°C	10 minutes	
94°C	30 seconds	
60°C	30 seconds	x 36 cycles
72°C	1 minute	
72°C	7 minutes	
15°C	Hold	

PCR products were then run on either a 1% or 3% agarose gel (see section 2.10.5).

Table 2.11 PCR primers.

Primer	Sequence (5'-3')
MYD88 variant determination Forward Primer	AGTTGTGTGTGTCTGACCGC
MYD88 variant determination Reverse Primer	GAGACAACCACCACCATCCG
Amplification of MYD88 var.1 only Forward primer	CGAAAAGAGGTTGGCTAGAAGG
Amplification of MYD88 var.1 only Reverse primer	GGCGAGTCCAGAACCAAGATT
GAPDH (GAPD728) Forward Primer	TGGACCTGACCTGCCGTCTA
GAPDH (GAPD970) Reverse Primer	CCTGTTGCTGTAGCCCAAATTC

2.10.5 Agarose gel electrophoresis and extraction

Gels were prepared to the percentage required by melting agarose (Sigma) in 1x TBE buffer and adding one drop of Ethidium bromide per 50ml gel. Gels were run at voltages between 100-150V. Bands were visualised on a UV transilluminator before being excised. A QIAquick gel extraction kit (Qiagen) was used for gel extraction and purification according to the manufacturer's instructions. DNA was eluted in 35µl elution buffer.

2.10.6 DNA sequencing

Samples were sent to Source Bioscience for Sanger sequencing and chromatograms viewed with Chromas Lite (Technelysium Ltd).

2.11   RNA sequencing

RNA samples were quantified with a Qubit HS RNA assay kit (Thermo Fisher Scientific) and the quality was assessed by RNA HS assay using the TapeStation system (Agilent). Sequencing libraries were generated by using a TruSeq Stranded Total RNA Human/Mouse/Rat kit (Illumina) according to the manufacturer's protocol. Library performance was checked on the TapeStation followed by picogreen quantification. Equimolar pooling was performed across all the libraries and the final pool was sequenced on a NextSeq 500 platform (Illumina) using 75-bp single-end sequencing.

The fastq files were assessed for initial quality using FastQC v0.11.8, trimmed for adapter sequences using TrimGalore v0.6.0 and aligned to GRCh38.p12 (Gencode release 28) with STAR aligner (v2.6.0c) using twopassMode (Dobin *et al.*, 2013). Transcript abundance was estimated using RSEM v1.3.0 and imported into R v3.5.1 using txImport v1.10.1 and then processed using DESeq2 v1.22.2 (Development Core Team, 2008; Li and Dewey, 2011; Love *et al.*, 2014; Soneson *et al.*, 2015). Using DESeq2 rLog transformed data, exploratory analysis of biological replicates was carried out using correlation heatmaps and MDS (all genes) and PCA (500 most variant genes). Differential gene expression was determined using DESeq2, quality visualised using MA plots and shrinkage of log fold estimated using the apeglm method (Zhu *et al.*, 2018). rLog transformed data was exported for downstream visualisations using the GENE-E package v3.0.21. These analyses were performed by Dr M. Care.

Genes with adjusted p-values of less than 0.01 were considered significant. Significantly differentially expressed genes were input into the DAVID functional annotation tool (LHRI). Read data was visualised using the Integrative Genomics Viewer (Broad Institute).

Table 2.12 Resources used during bioinformatic analysis.

Program	Version	Link to resource
FastQC	v0.11.8	https://www.bioinformatics.babraham.ac.uk/projects/fastqc/
TrimGalore	v0.6.0	https://www.bioinformatics.babraham.ac.uk/projects/trim_galore/
GENE-E	v3.0.21	https://software.broadinstitute.org/GENE-E/
DAVID	v6.8	https://david.ncifcrf.gov/summary.jsp
IGV	v2.5.x	https://software.broadinstitute.org/software/igv/

Chapter 3 – Differentiation responses to T-dependent activation

3.1 Introduction

Initially, the differentiation profile of healthy B-cells in response to stimulation with CD40L and F(ab')$_2$ anti-IgG/M was established. This includes immunophenotype analysis of the cells at each key stage of differentiation in addition to cell counts to provide a baseline for future comparison to patient samples. The effect of removing either the CD40L or F(ab')$_2$ anti-IgG/M component from the differentiation was then further interrogated to determine the response of healthy B-cells to each of these stimuli in isolation. Subsequently, it was important to determine whether the *in vitro* system would enable WM cells to differentiate into plasma cells – a key facet of WM pathology *in vivo* that is not recapitulated in current work with cell lines. Therefore the response of B-cells derived from WM patients was characterised and compared to the response of healthy cells under the same conditions.

3.2 Response of healthy cells during *in vitro* B-cell differentiations with CD40L stimulation

In order to establish the profile of cell proliferation, viability and immunophenotype throughout their differentiation in the *in vitro* system, total B-cells were isolated from the peripheral blood of a healthy donor and cultured with CD40L + F(ab')$_2$ anti-IgG/M stimulation according to the method developed by Cocco *et al*., 2012 (methods section 2.1).

CD40L is a co-stimulatory molecule found on a range of cells including activated T-cells, granulocytes, dendritic cells and macrophages. Arguably the most important interaction between CD40L and its receptor on B-cells occurs during T-cell dependent immune responses where it is critical to induce B-cell class switching, proliferation, antibody secretion and the formation of germinal centres. CD40L-L cells - murine fibroblasts transfected with human CD40L - were therefore used to provide stimulation to the B-cells by co-culturing them as described in methods section 2.1.10.

M2-10B4 cells are a murine bone marrow stromal cell line and were added to the culture conditions at day 6 to support long-term B-cell survival as they provide an array of soluble factors similar to those found in the stromal niche that plasma cells occupy. Whilst culture with M2-10B4 cells improves plasma cell viability, it does not affect cell phenotype during differentiation

(Cocco *et al.*, 2012). Samples were taken for analysis by flow cytometry at time points corresponding to key phenotypic stages of B-cell differentiation.

The response of the B-cells in the *in vitro* system should closely resemble that of B-cells *in vivo*. Following isolation from peripheral blood, day 0 B-cells are undifferentiated and remain quiescent until they receive stimulation. They should express high levels of CD19 and CD20, with positivity for CD27 denoting the memory B-cell compartment. At this stage, there is expected to be a range of expression of CD38, but all cells should be negative for the plasma cell marker CD138. By day 6 the B-cells should have differentiated to the plasmablast stage and express $CD19^+ CD20^- CD38^+ CD138^- CD27^+$. During the subsequent week, a large proportion of cells will acquire the plasma cell phenotype ($CD19^+ CD20^- CD38^+ CD138^+ CD27^+$) and virtually all remaining cells are expected to have fully differentiated into plasma cells by day 20. Thereafter, the phenotype of the cells should remain unchanged. The immunophenotype of cells from a healthy donor at each stage of differentiation in the *in vitro* system is displayed in figure 3.1 (details of antibodies used for immunophenotype analysis are provided in methods section table 2.4).

In this example, the purity of B-cells as indicated by their co-expression of CD19 and CD20 following isolation by magnetic separation was greater than 99%. The distribution of CD38 expression was variable, with two thirds of cells possessing this marker and the rest with low or no expression. In this sample, the proportion of naïve to memory B-cells was 45%:55%. Following T-dependent stimulation with CD40L and F(ab')$_2$ anti-IgG/M, the cells initiate the differentiation response and have generated plasmablasts by day 6, evidenced by their downregulation of the B-cell marker CD20 and upregulation of CD38 and CD27. The distribution of cells at day 13 consists of a mixed population of plasmablasts and plasma cells, with some cells having progressed further than others. For these cells, the expression of CD20 has continued to decline and levels of CD19 have also decreased slightly. Virtually all cells have become $CD38^+$ with 65.7% of those now possessing dual expression of CD38 and CD138, denoting their plasma cell status. The upregulation of CD27 is almost complete, with 94% of cells expressing this marker. By day 22, more than 90% of the remaining cells in culture have become plasma cells, with almost all of these having completely lost CD20 expression. The proportion of plasma cells subsequently increases to almost 100% and these fully differentiated cells are maintained for the duration of the culture.
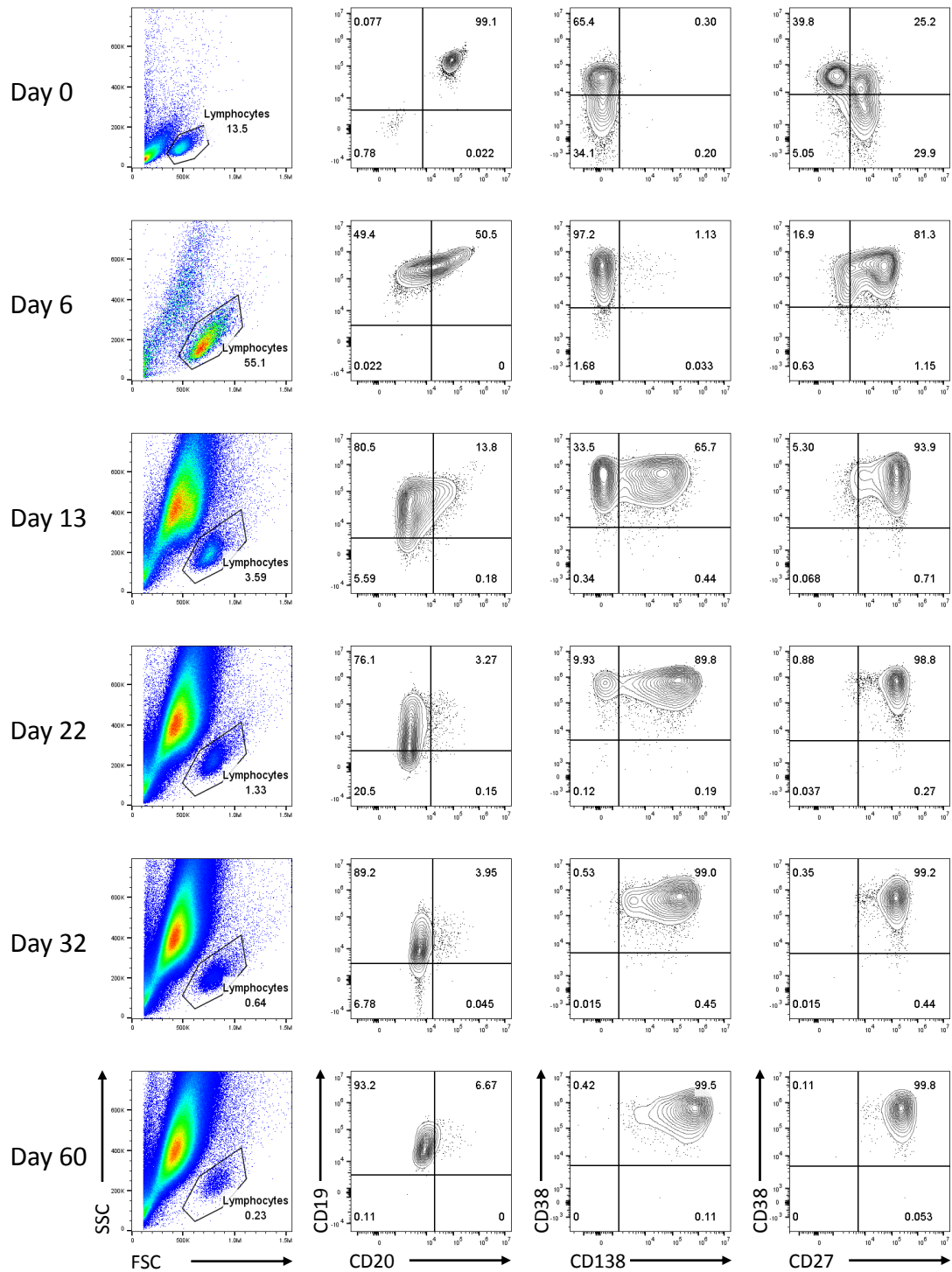
Figure 3.1 A representative example of the immunophenotype of healthy cells between day 0 and 60 of an *in vitro* differentiation. Total B-cells were derived from the peripheral blood of a healthy donor (isolation protocol A) and stimulated with CD40L + F(ab')$_2$ anti-IgG/M at day 0. Live cells were distinguished by their exclusion of 7-AAD staining and were assessed by flow cytometry for surface markers at the indicated time points. The percentage of cells expressing each marker are indicated within individual quadrants.

Activation of B-cells during an immune response *in vivo* via a T-dependent manner results in extensive proliferation in order to generate sufficient numbers of effector cells to combat the infection. Cell survival is tightly regulated in order to prevent an excessive response and autoimmunity, therefore only a small number of highly specific memory cells and long-lived plasma cells persist upon resolution of the immune response. The cells thus begin in a quiescent state before activation, stimulation results in rapid proliferation and differentiation and subsequently the long-lived cells must return from a highly proliferative active state to a quiescent one. To assess this response in the *in vitro* system, cell number was quantified between day 0 and 6 with a haemocytometer and thereafter by flow cytometry with CountBright absolute counting beads. The accompanying cell counts for the differentiation depicted in figure 3.1 are displayed in figure 3.2.
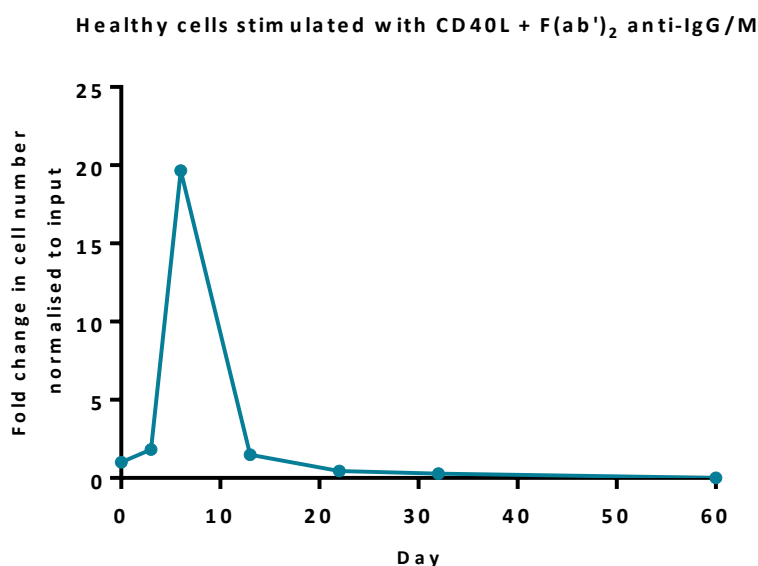
Figure 3.2 The fold change in cell number during the course of an *in vitro* differentiation mirrors the observed phenotype. Total B-cells were derived from the peripheral blood of a healthy donor and stimulated with CD40L + F(ab')$_2$ anti-IgG/M. Cell number per ml was recorded at each time point and then normalised relative to the number of input B-cells at day 0 to determine the fold change at each stage.

The number of cells for this donor increased slightly by day 3 as the cells became activated. This was followed by a 19-fold increase between days 3 and 6 as the activated B-cells undergo extensive proliferation and become plasmablasts. A rapid decline in cell number occurred by day 13, corresponding to the acquisition of the plasma cell phenotype, following which cell numbers declined slightly, but the plasma cell population was largely maintained long-term.

3.2.1   Reproducibility and intra- and inter-donor variation

The proportion of memory and naïve B-cells isolated from each donor can vary considerably depending when samples were taken. This was observed seasonally and also if the donor had recently suffered from an infection. Unless otherwise stated, differentiation experiments were performed with total B-cells so reproducibility between these controls are crucial. In order to address the reproducibility of the system, two independent differentiations were performed on total B-cells derived from the PB of the same donor taken several months apart.

The flow cytometry results from both of these differentiations are shown in figure 3.3. The immunophenotype of the cells at each stage are very similar to one another and are also comparable to the phenotypes depicted in figure 3.1, in which the cells were isolated from a different donor. In each of the three differentiations, the proportion of plasmablasts at day 6 is approximately 90% and the proportion of plasma cells at day 20 is also at least 90%.

Despite the variation that can occur between samples, the *in vitro* system demonstrates robust reproducibility of phenotypes obtained during differentiations between different donors or independent samples taken from the same donor following stimulation with CD40L + F(ab')$_2$ anti-IgG/M.
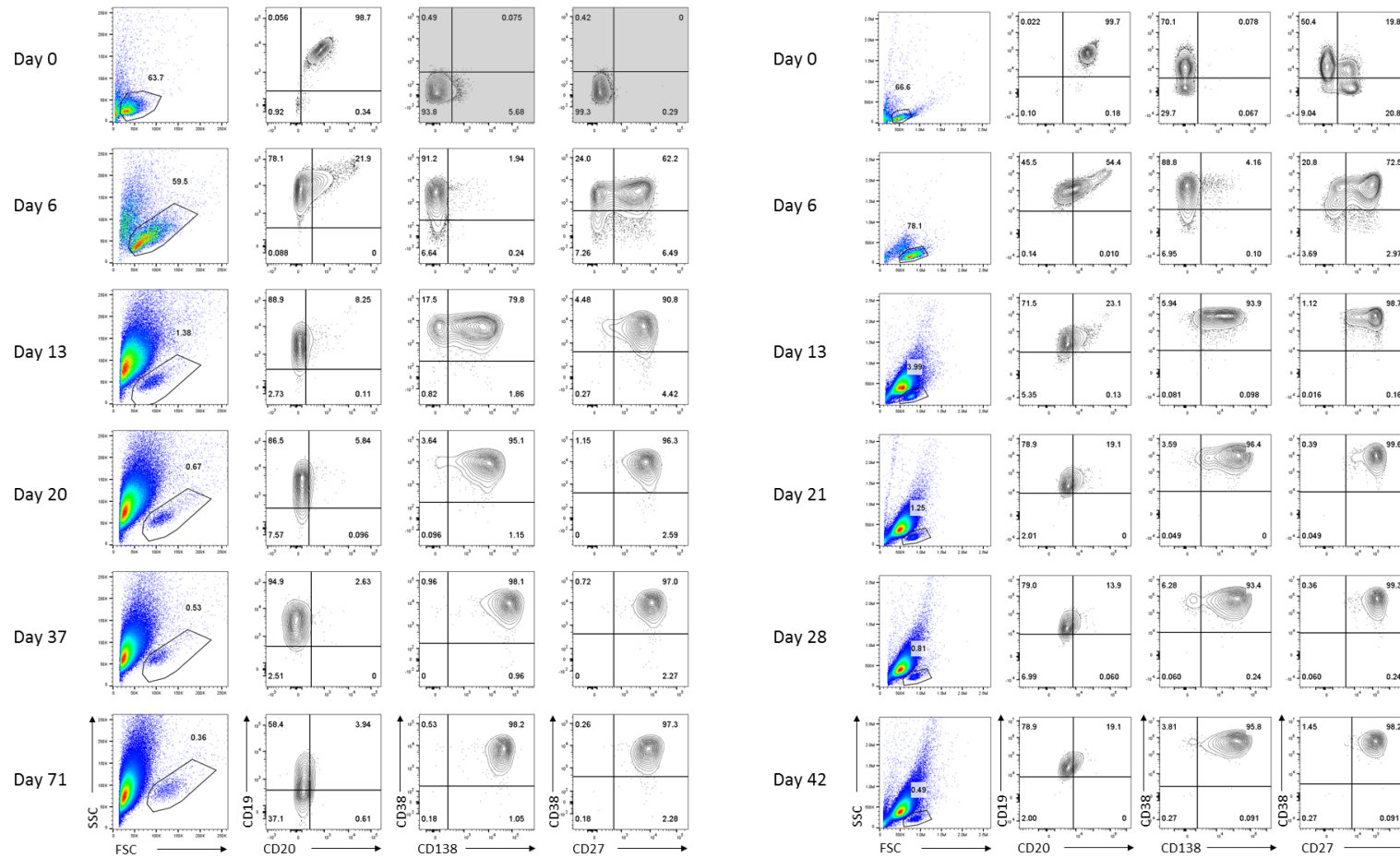
Figure 3.3 The immunophenotype of cells from independent differentiations is highly reproducible. B-cells were derived from the peripheral blood of a healthy donor on two separate occasions (isolation protocol A) and stimulated with CD40L + F(ab')$_2$. The cells were assessed by flow cytometry for the surface markers CD19, CD20, CD38, CD138 and CD27 at the indicated time points. Percentages are indicated within individual quadrants. Note: the flow cytometer voltage setting for CD38 and CD27 at day 0 on the left hand side had not been optimised and thus the distribution of naïve and memory cells cannot be determined for this time point so have been greyed out.

3.3 The differentiation profile of healthy B-cells stimulated with CD40L

B-cell differentiation in response to T-dependent stimuli is characterised by extensive proliferation, followed by a contraction in cell number upon resolution of the immune response. The *in vitro* system replicates these stages and this can be seen by cell counts recorded at each stage of differentiation. The change in cell number throughout differentiations from multiple independent experiments is shown in figure 3.4. Some differentiations did not have sufficient numbers of cells initially to support long-term culture after a proportion of cells were used at each time point for analysis so these have been excluded. Only differentiations that were in culture for at least 20 days have been included.
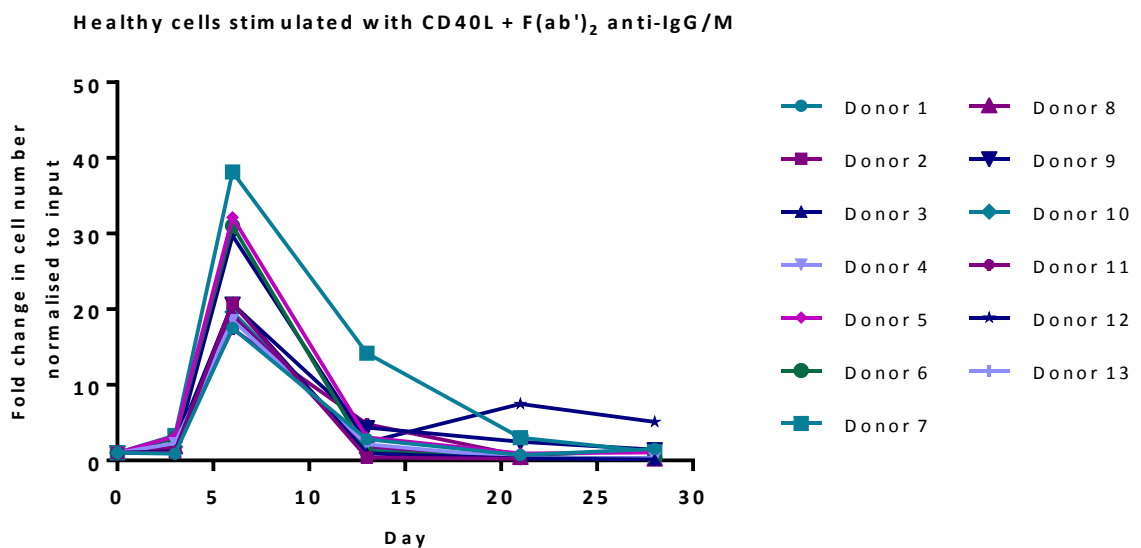
Figure 3.4 Healthy B-cells display a similar and reproducible change in cell number upon activation with stimuli mimicking a T-dependent immune response. B-cells derived from the peripheral blood of healthy donors (isolation protocol A or B) were stimulated with CD40L and F(ab')$_2$ anti-IgG/M. Cell number at each time point was determined by manual counts between days 0-6 and then by flow cytometry thereafter with CountBright Absolute counting beads (see methods section 2.5.4). The cell number at each point was normalised to the number of "input" cells for that specific donor obtained at day 0.

In each case, cell number remains fairly constant or increases slightly between day 0 and day 3 as the cells become activated, followed by an expansion of between 15-40-fold as the activated B-cells proliferate and differentiate into plasmablasts. Subsequently, the number of cells sharply

declines to levels roughly equivalent to the initial number of input cells. Cell number thereafter remains broadly stable as the plasma cells generated persist long-term. A slight deterioration in plasma cell number is expected as cultures are maintained for such extended amounts of time. The bone marrow is a multifaceted niche with a milieu of cytokines and stromal cells that support the long-term survival of plasma cells residing within this environment. Whilst the *in vitro* system endeavours to recreate the complexity of the BM microenvironment with as few components as possible, there are inevitably aspects of this niche that are not modelled here.

The profile of cell surface marker expression during differentiations is illustrated in figure 3.5. All B-cells possess high levels of CD19 and CD20 at day 0 following purification from PB. Whilst levels of CD19 are expected to remain relatively constant, it was occasionally observed that a number of plasma cells generated following CD40L stimulation downregulated CD19 at the latter time points and this can be seen in the top left graph. The expression of CD20 in all instances declines between day 0 and day 6, with expression falling to below 20% for the majority of donors by days 13-15 and decreasing further thereafter. The expression of CD38 is quite variable in the isolated cells initially, but by day 13, virtually all cells from all donors have upregulated its expression. The subsequent increase in expression of CD138 after levels of CD38 have risen is demonstrated in the middle-right graph, with little change between day 0 and 6 when the cells have become plasmablasts and then a large increase in the percentage of CD138$^+$ cells by day 13-15 when over 50% of cells have become plasma cells. The proportion of plasma cells increases at each subsequent time point. The proportion of memory B-cells varies between donors and his can be seen in the bottom graph. However, for all donors, expression of CD27 rises by day 6 and by day 13, almost 100% of cells express this marker.
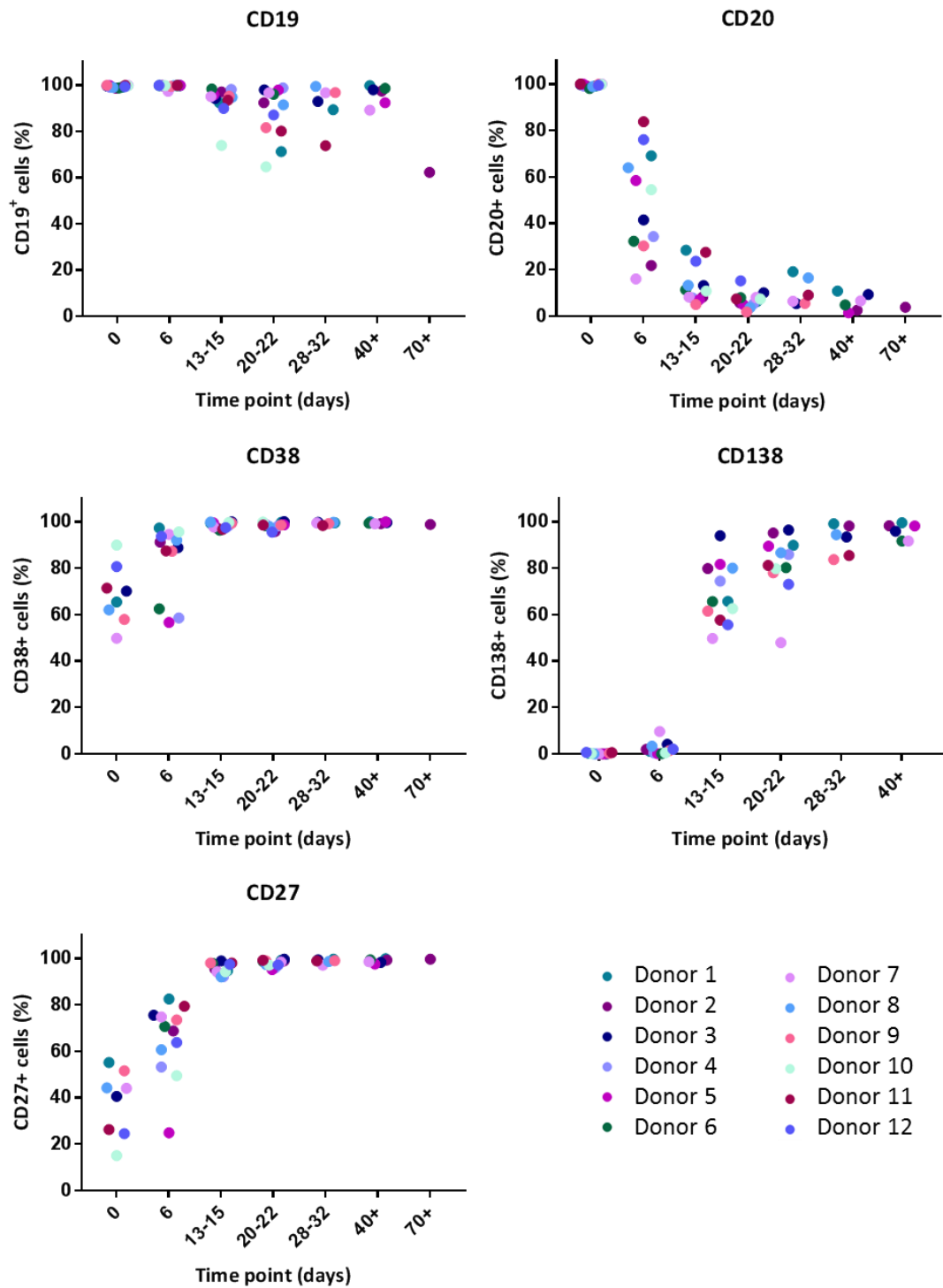
Figure 3.5 Scatter plot profiles for the expression of each CD marker assayed in multiple differentiations with healthy B-cells. B-cells derived from the peripheral blood of healthy donors (isolation protocol A or B) were stimulated with CD40L and F(ab')$_2$ anti-IgG/M. Each scatter plot displays the percentage of live cells expressing the stated CD marker as determined at each time point via flow cytometry. Data from comparable intervals were grouped together for clarity. Each independent differentiation is represented by a different colour.

The profile of cell surface marker expression and change in cell number during *in vitro* differentiations closely resembles the changes B-cells undergo *in vivo*. All healthy samples successfully generated plasma cells given sufficient numbers of input cells and do so by day 20. The phenotype at the later time points – those past day 13 – of the differentiations are very similar, regardless of the initial proportion of naïve and memory B-cells, which can vary widely between each donor.

3.4   The effect of CD40L or F(ab')$_2$ anti-IgG/M omission on B-cell phenotype and number

In order to respond to T-dependent antigens, B-cells require T-cell assistance, therefore activation of B-cells in this manner requires a combination of signals from both the BCR and CD40 as well as additional secondary signals such as T-cell provided cytokines. The response of B-cells to dual signals from these sources has been defined in the previous section, but the individual contribution of CD40L-L cells or F(ab')$_2$ anti-IgG/M alone within the *in vitro* culture system has not been addressed. Therefore, to determine the impact of each of these components on the cell number and phenotype of the B-cells, differentiations were performed omitting these stimuli in turn.

3.4.1   Omission of F(ab')$_2$ anti-IgG/M from the culture system

In order to determine whether the omission of F(ab')$_2$ anti-IgG/M had an effect on B-cell differentiation with CD40L stimulation, cells were cultured with and without F(ab')$_2$ anti-IgG/M and with CD40L-L cells until day 3. No other culture conditions were altered and the temporal changes in cytokines remained the same. In this instance, cells had been sorted by FACS instead of being isolated by magnetic separation. B-cells were separated based on their expression of CD27, the presence or absence of which denoted their memory or naïve phenotype, respectively, and each was cultured separately. The phenotype of each condition is displayed in figure 3.6. Unfortunately, the memory cells cultured with F(ab')$_2$ anti-IgG/M did not proliferate between days 3 and 6 and therefore numbers were insufficient for further immunophenotype analysis.
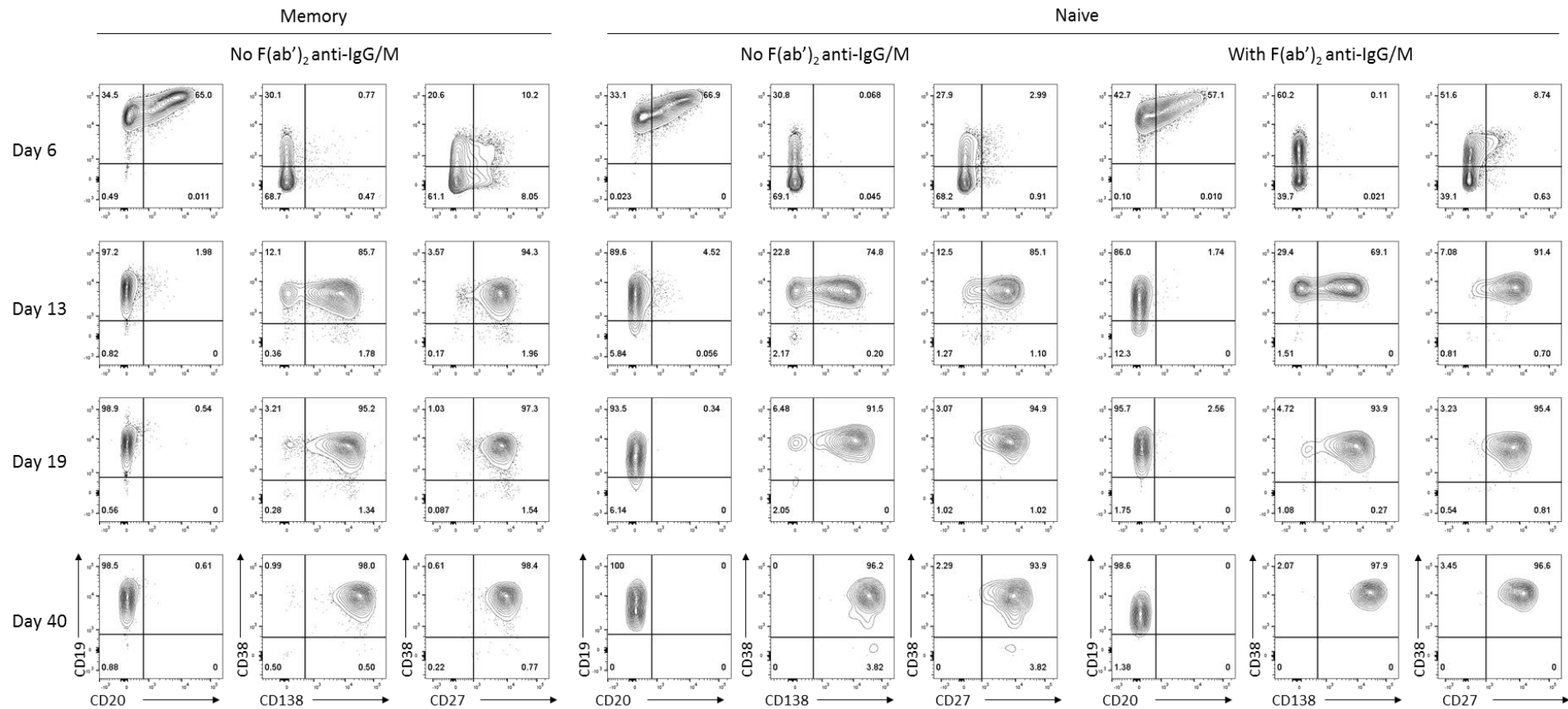
Figure 3.6 The immunophenotype of differentiating cells at early time points is altered with the removal of F(ab')$_2$ anti-IgG/M stimulation. B-cells were derived from the peripheral blood of a healthy donor and sorted by flow cytometry into naïve and memory fractions (isolation protocol D, details of antibodies used for 6-way sort are provided in methods section table 2.2). These were stimulated with CD40L with or without the addition of F(ab')$_2$ anti-IgG/M and assessed by flow cytometry for surface markers at the indicated time points. Percentages are indicated within individual quadrants.

At day 6, B-cells derived from naïve cells and cultured without F(ab')$_2$ anti-IgG/M had the highest expression of CD20, with a noticeable population of CD19^{++} CD20^{++} cells. This population is not present when the naïve cells are stimulated with CD40L and F(ab')$_2$. The memory cells cultured in the absence of F(ab')$_2$ consisted of a population of cells that had downregulated CD20 but, similar to the naïve cells, also had a population of cells that retain high expression of both CD19 and CD20. Whilst the comparison to memory cells with CD40L and F(ab')$_2$ anti-IgG/M cannot be made here, if this result is instead compared to the immunophenotype obtained for total B-cells, the CD19^{++}CD20^{++} population does not occur, suggesting that the lack of F(ab')$_2$ anti-IgG/M in this case is delaying loss of CD20 in these cells. The naïve cells activated with the dual stimulation possessed twice the proportion of CD38^{+} cells compared to those without F(ab')$_2$ anti-IgG/M, supporting a conclusion that its absence results in a delay to differentiation. The removal of F(ab')$_2$ anti-IgG/M from the culture system also results in a delay to the upregulation of CD27 in the naïve fraction.

The differences in phenotype between the two naïve conditions are almost completely lost by day 13 of the differentiation. In addition, the naïve phenotypes have become more similar at this time point to the memory phenotype, but the memory fraction has generated a higher proportion of plasma cells. From day 20 onwards the phenotypes of each condition are nearly indistinguishable from one another. In summary, differentiating B-cells without F(ab')$_2$ anti-IgG/M appears to delay their progression to plasmablasts, but thereafter has little effect on the generation of plasma cells. Memory B-cells are more efficient at generating plasma cells than their naïve counterparts even without this key signal. Interestingly, in the absence of F(ab')$_2$ anti-IgG/M, the differences in phenotype for both of these subsets is less profound than expected, indicating the importance of the dual signal for the memory response.

The fold change in cell number of the memory and naïve fractions for this donor are displayed in figure 3.7.
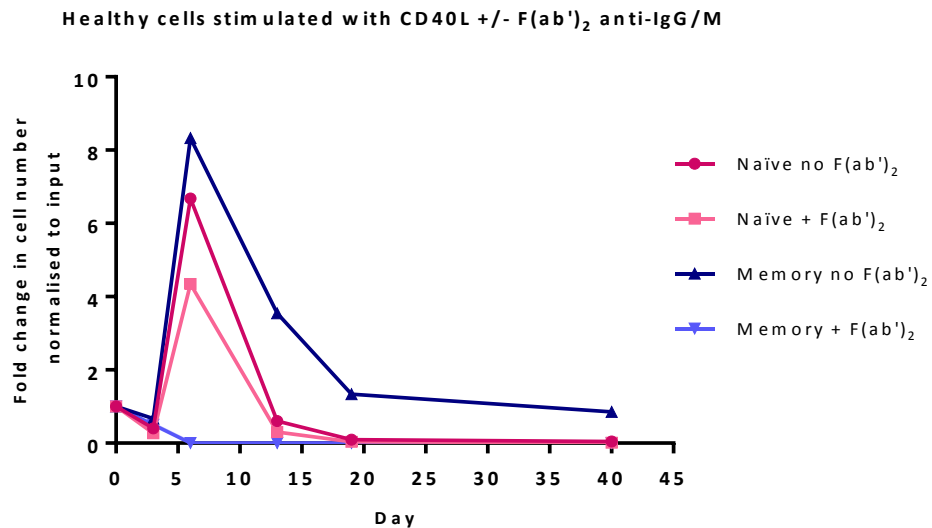
Figure 3.7 Number of cells cultured with CD40L and with or without the addition of F(ab')$_2$ anti-IgG/M. Cells derived from the peripheral blood of a healthy donor were sorted by FACS into memory and naïve phenotypes (isolation protocol D) and cultured separately with CD40L with or without F(ab')$_2$ anti-IgG/M. Cell number at each time point was determined by flow cytometry. The cell number at each point was normalised to the number of "input" cells obtained at day 0.

Cell numbers decreased in all conditions between days 0 and 3. This does not normally occur in differentiations with healthy cells and is likely as a result of the stress the cells undergo during the cell sorting process. However, between days 3 and 6, even without the additional F(ab')$_2$ stimulation, both subsets were able to proliferate. Due to the initial drop in numbers, the fold change between day 3 and day 6 for the naïve without F(ab')$_2$ anti-IgG/M, naïve + F(ab')$_2$ anti-IgG/M and memory without F(ab')$_2$ anti-IgG/M was 16.7, 16.3 and 12.6-fold, respectively. Surprisingly, there was very little difference between the fold change increase between these time points for the naïve cells, when one would expect the dual stimulation to result in more proliferation. The memory fraction generated a greater number of cells at day 6 when compared to the input cell number than the naïve cells due to the enhanced survival of these cells over their naïve counterparts. Unfortunately, the memory-derived cells cultured with F(ab')$_2$ anti-IgG/M did not survive. For all remaining conditions, cell numbers declined between days 6 and 13 but a greater proportion of memory-derived plasma cells survived compared to their naïve-derived counterparts, which was as expected. The long-term survival of plasma cells generated from the memory fraction was superior to those from the naïve fraction.

Whilst a delay in differentiation at day 6 occurs when the cells do not receive both signals, the proliferation of the naïve-derived cells when F(ab')$_2$ anti-IgG/M was omitted from the culture was almost the same as when it was present, possibly as a result of the delay in differentiation

that was observed by phenotype analysis. The cells remain in the activated B-cell stage which is more highly proliferative for longer, thus generating a greater number of progeny. A similar delay was observed in early differentiation for memory cells without F(ab')$_2$ and its removal also appears to decrease proliferation but it does not affect the survival of plasma cells.

3.4.2 Stimulation of B-cells with F(ab')$_2$ anti-IgG/M only

B-cell activation can occur in the absence of CD40L, namely during T-independent immune responses. In the case of the *in vitro* system, it was unclear as to the extent of survival and differentiation of B-cells in the absence of these signals. Therefore, a reciprocal experiment to the one previously demonstrated was performed to understand the impact of CD40L omission on total B-cells. The phenotype of the cells obtained in this experiment are shown in figure 3.8.
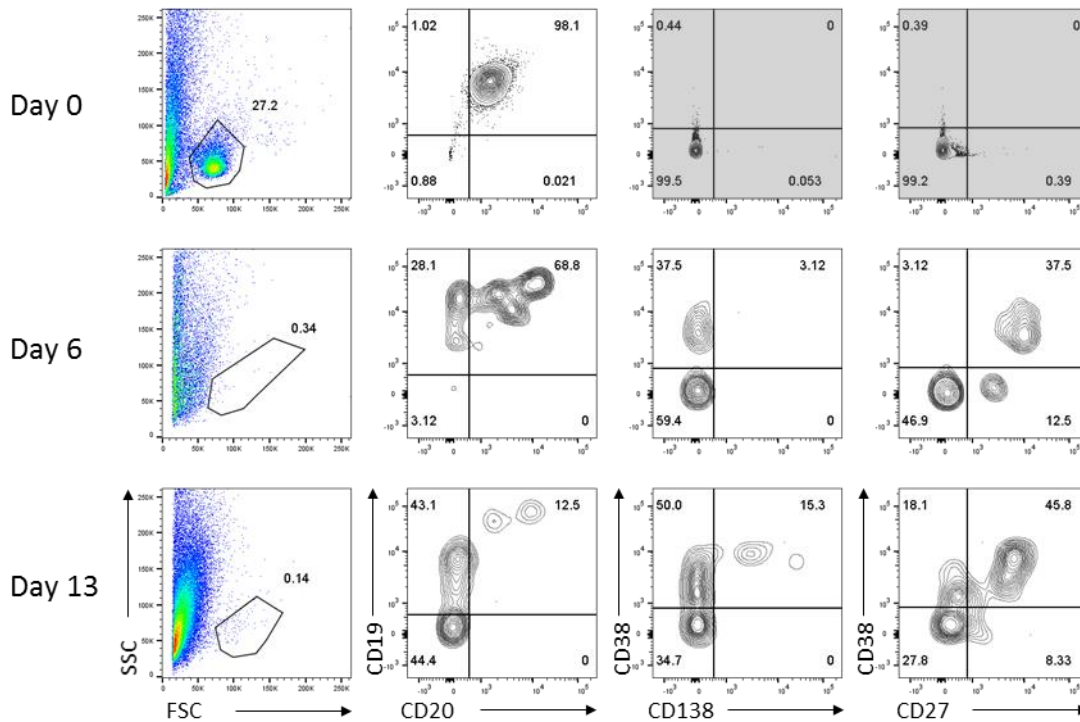
Figure 3.8 Absence of a CD40L signal results in severely impaired differentiation. B-cells were derived from the peripheral blood of a healthy donor (isolation protocol A). The cells were stimulated with F(ab')$_2$ anti-IgG/M alone and assessed by flow cytometry for surface markers at the indicated time points. Percentages are indicated within individual quadrants. Note: the flow cytometer voltage setting for CD38 and CD27 at day 0 had not been optimised and thus the expression of these markers cannot be determined for this time point - these plots have been greyed out.

B-cell purity of viable cells was greater than 98% initially but there are so few surviving cells at the subsequent time points that a phenotype cannot be accurately determined. Interestingly, of the remaining cells at day 13, expression of CD20 appears to have decreased and there is some evidence of a population of CD38$^+$ cells. The paucity of surviving cells however, makes any conclusions regarding their phenotype unreliable, particularly cells which are on the verge of apoptosis as is the case here. The positivity for the markers depicted may simply be as a result of autofluorescence. Cell survival under these conditions was extremely poor and the fold change in cell number is depicted in figure 3.9.

Healthy cells stimulated with only F(ab')$_2$ anti-IgG/M
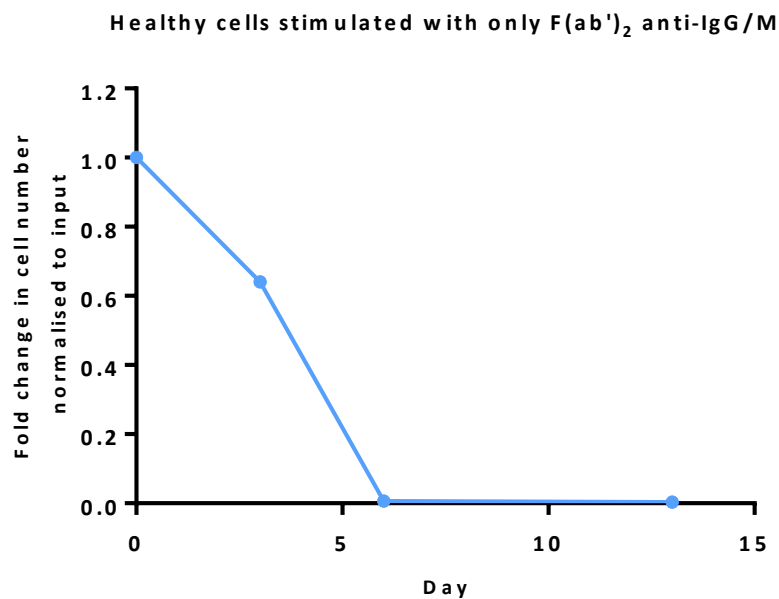
Figure 3.9 Number of cells following stimulation with F(ab')$_2$ anti-IgG/M only. Cells derived from the peripheral blood of a healthy donor were stimulated with F(ab')$_2$ anti-IgG/M only. Cell number at each time point was determined by flow cytometry. The cell number at each point was normalised to the number of "input" cells obtained at day 0.

The number of cells in culture falls substantially between day 0 and 3 and decreases to virtually zero thereafter. A very small number of cells persist to day 13 but there are no viable cells after this time point. Control of B-cell survival is exerted through Fas-dependent apoptosis, which is crucial to maintain immunological tolerance. CD40 receptor engagement prevents B-cell death by upregulating the anti-apoptotic proteins Bcl-2 and cFLIP. B-cells can also be rescued from cell death via other mechanisms such as ligation of TLRs or IL-4R, but in this case, none of these additional signals are present. The results from this differentiation illustrate the consequences when B-cells do not receive sufficient survival signals to overcome Fas-mediated apoptosis.

3.5   Response of WM B-cells to CD40L stimulation

Following the characterisation of the response of healthy cells, it was imperative to ascertain whether WM B-cells would also respond to CD40L stimulation and what if any, are the differences between patient samples and healthy controls. The ability of neoplastic B-cells to differentiate is critical to the pathogenesis of WM. However, constitutive activation of the NF-κB pathway endowed by the $MYD88^{L265P}$ mutation is thought to be independent of stimulation by CD40L and BCR ligation. Despite this, there is evidence for a level of chronic active BCR signalling within WM (Argyropoulos *et al.*, 2016; Munshi *et al.*, 2017). Whilst the mutational burden on the BCR cascade is much lower, with an occurrence of approximately 15%, compared to the virtually ubiquitous $MYD88^{L265P}$ mutation and largely confined to CD79A and B, it nevertheless may influence the response of WM B-cells to these stimuli. Signalling via both T-dependent and T-independent means converges on NF-κB, so activation with CD40L + $F(ab')_2$ anti-IgG/M may synergise with the constitutive signalling to produce a more profound response.

WM diagnostic flow cytometry results are summarised in table 3.1 below. Three samples were previously frozen and the corresponding data could not be obtained.

Table 3.1 WM diagnostic flow cytometry results. Cells have been left blank if the data were not reported. Data was collected at HMDS Leeds and provided by Dr R. de Tute.

Sample	Neoplastic %	Kappa	Lambda	CD19	CD20	CD5	CD10	CD305	CD23	CD200	ROR1	CD43	CD79b	CD81	CD31	CD39	CD49d	CD103	CD11	CD25	CD22	CD38	CD95
WM1	frozen sample - no diagnostic flow cytometry data available																						
WM2	4.4	n	y	+	+	-	-	-															
WM3	3.4	y	n	++	++	+/-	-	-	-	+/-	+/-	+	++	++	++	++	+	-	-	+	+	+	+
WM4	60	y	n	++	+	+	-	+	+	+	-	-	+	+	+	++	+	-	-	+	+		
WM5	>90	y	n	++	++	+/-	-	-	-	-	-	+/-	++	++	++	+	++	-	-	+/-			
WM6	54	n	y	+	++	-	-		+/-	-	+	-	++	+	++	++	+	-	+/-	++			
WM7	82			++	+/-	-	-		-	+	-	-	+/-	+	++	+	+	-	-	+			
WM8	frozen sample - no diagnostic flow cytometry data available																						
WM9	frozen sample - no diagnostic flow cytometry data available																						
WM10	89	y	n	++	++	+	-		+/-	+	-	+	++	++	++	+	+	-	-	++			
WM11	90	y	n	+	++	-	-		-	+	-	-	++	+	++	++	+	-	-	+			
WM12	40	y	n	++	++	+/-	-	-	-	+/-	-	+/-	++	++	++	++	++	-	-	+	+	++	+
WM13	45	n	y	++	+	-	-		+/-	+	-	+/-	++	+	+	+	+	-	-	+			
WM14	>90	y	n	++	++	+/-	-		-	-	-	+/-	++	+	+	++	+	-	-	++			

3.5.1 WM cells differentiate following stimulation with CD40L

Whilst the immunophenotype of WM cells *in vivo* at the B-cell and plasma cell stages has been well documented, whether the cells possess the same phenotype as healthy cells as they progress through each stage of differentiation has not been previously investigated (San Miguel *et al.*, 2003; Konoplev *et al.*, 2005; Toma *et al.*, 2007; Paiva *et al.*, 2013). Whether the clonal cells can be distinguished and if they differentiate concurrently to the fraction of healthy cells in the sample is another question to address. Initially, WM B-cells derived from samples of patient bone marrow were assessed to determine whether they remained able to differentiate into plasma cells when stimulated with CD40L + F(ab')$_2$ anti-IgG/M. Several different profiles of differentiation were obtained, the first of which is illustrated below in figure 3.10. In this example, the phenotype of the cells throughout the differentiation closely resembles a healthy differentiation.
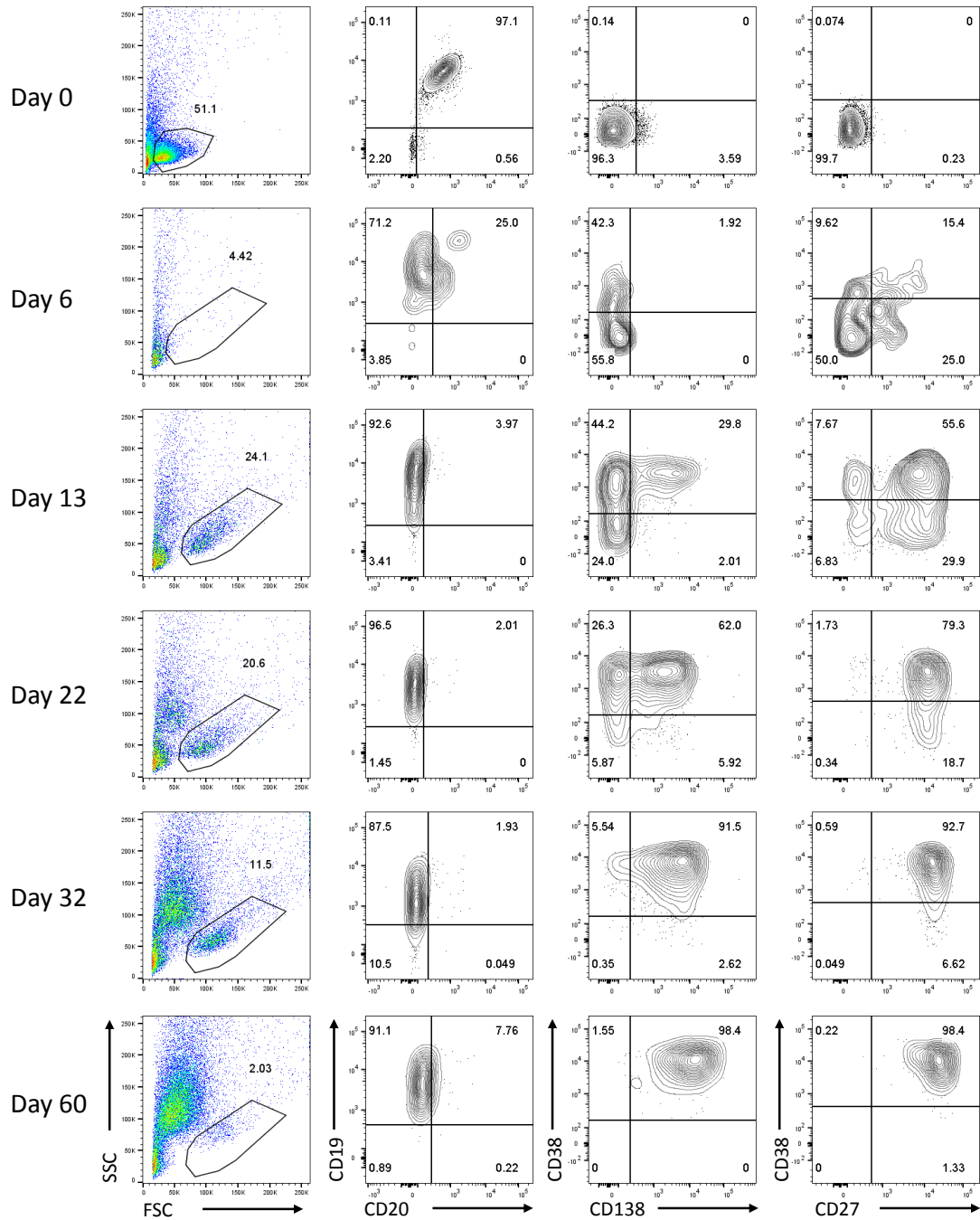
Figure 3.10 Example of WM cells that differentiate with a "normal" phenotype. B-cells were isolated from the bone marrow of a patient with WM (isolation protocol A). The cells were activated with CD40L + F(ab')$_2$ anti-IgG/M and the immunophenotype assayed by flow cytometry at each time point. Percentages are shown for each quadrant.

In this sample, the number of cells at day 6 was low, affecting the quality of the flow data, but the cells have begun to show evidence of differentiation, with a loss of CD20 and an increase in the levels of CD38 expression. By day 13, more than 90% of cells have lost CD20 expression. The proportion of cells that have upregulated CD38 has increased to just under 75%, with one third

of these having differentiated into plasma cells. Increase in CD27 expression has risen from 40% to 80% during this period between day 6 and day 10. The proportion of fully differentiated plasma cells increases at each subsequent time point and these cells are maintained long term. This sample confirms that stimulation with CD40L can, at least in some cases, result in complete differentiation and the generation of plasma cells from WM B-cells.

3.5.2   Summary of WM differentiations stimulated with CD40L

It has been established that WM B-cells are able to generate plasma cells that are phenotypically equivalent to healthy PCs. It was then essential to repeat the *in vitro* differentiations with additional patient samples to assemble a more representative overview of responses to this type of stimulation. The following section compares the number of cells and phenotypes obtained during differentiations with 8 WM samples to those with B-cells from healthy donors.

The overall response of most WM samples (figure 3.11) shares a similar profile of proliferation to healthy controls, with an expansion in cell number occurring between day 3 and 6 of the differentiation, followed by a substantial decrease in cell number to day 14 and subsequently cell numbers reaching a plateau at approximately day 20. However, the amplitude of the increase to cell number during the proliferative phase is considerably lower than that which occurs in differentiations with healthy cells. Healthy differentiations average a 20-30 fold increase to cell number whereas WM cells are only able to expand 4-fold. The fold change in cell number depicted in figure 3.11 (top) between days 3 and 6 for samples WM5, 7 and 9 is underrepresented because of a decrease in cell number that occurred between day 0 and 3 for each of these samples. Similarly, this also decreases the average fold change for the WM samples in the bottom graph of figure 3.11. The decrease in cell number between day 0 and 3 is a phenomenon that affected patient samples to a much greater extent than samples derived from healthy donors. The average fold change in cell number between day 0 and 3 for healthy donors was 2, with cell numbers decreasing between these two time points in only 1/13 samples. In contrast, the average fold change in cell number between day 0 and 3 for WM samples was 0.7 and cell numbers decreasing in 5/6 instances. It is likely due to the greater delay that occurred between when the sample of bone marrow was taken to when the B-cells were isolated than occurred for samples of PB from healthy donors, thus in some cases affecting the viability of the WM B-cells. For WM5, 7 and 9, whilst a drop in cell number occurred by day 3, each was able to proliferate to a comparable level to the WM samples that did not experience a decrease in number. However, the expansion in cell number even when this is taken into account is still lower than for healthy cells. This was unexpected, since one would anticipate that neoplastic cells would be more inclined towards proliferation and have a survival advantage over

their healthy counterparts. Samples WM1 and WM2 did not proliferate between days 3 and 6 as expected, but similar numbers of plasma cells were present at the later time points as cell numbers for these samples did not drop as sharply.
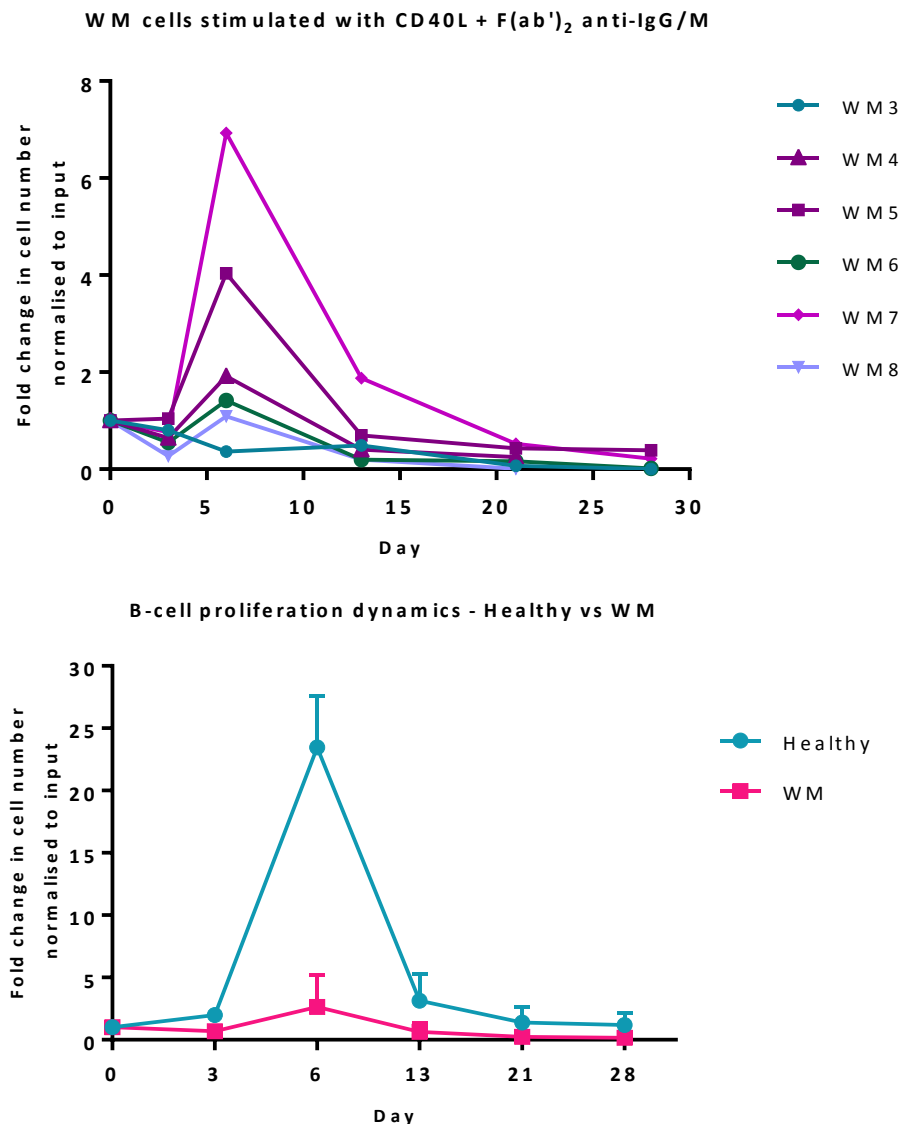
Figure 3.11 WM B-cells display a range of cell number profiles following activation with stimuli mimicking a T-dependent immune response. (Top) B-cells derived from the bone marrow of patients diagnosed with WM (isolation protocol B) were stimulated with CD40L and F(ab')$_2$ anti-IgG/M. Cell number at each time point was determined by manual counts for days 3 and 6 and then by flow cytometry thereafter. The cell number at each point was normalised to the number of "input" cells for that specific patient obtained at day 0. (Bottom) A comparison of the average proliferation dynamics of healthy and WM patient-derived B-cells over the course of differentiation. Healthy n = 13, WM n = 6, error bars - 95% confidence interval.

Whilst some samples taken from WM patients were nearly indistinguishable from healthy samples in terms of phenotype following activation, overall there was a far greater range of

responses to CD40L stimuli than was observed in healthy controls. This is illustrated in figure 3.12. The only marker to remain constant is the ubiquitous B-cell maker CD19, which is maintained throughout the differentiations as expected. Initially, expression of CD20 is invariant, but whilst it decreases by day 6 for all samples, the range of expression between different samples is considerable at over 80%. Thereafter, the variability in levels of CD20 are maintained, with some samples showing the expected trend of loss of CD20 as the differentiation progresses (WM1 and 6), but others (WM3, 7 and 8) retaining high CD20 expression throughout. Levels of CD38 at day 0 were extremely variable between samples, with several samples negative for the presence of any CD38 and one sample with 100% CD38 positivity. The common trend for these samples was to demonstrate increasing levels of CD38 throughout the differentiation, but there was still a large variety in expression levels, contrasting with the homogenous high levels of CD38 expressed in healthy cells from day 6 onwards. Expression of CD138 too, followed the expected overall trend to increase as plasma cells were generated, but again, there was considerable differences between samples, very unlike the healthy controls. Levels of CD138 were also delayed in WM cells compared to their healthy counterparts. The expression levels of CD27 are more similar to the controls than some of the other markers, with upregulation of this marker in almost all cells by days 13-15, after which it is maintained.
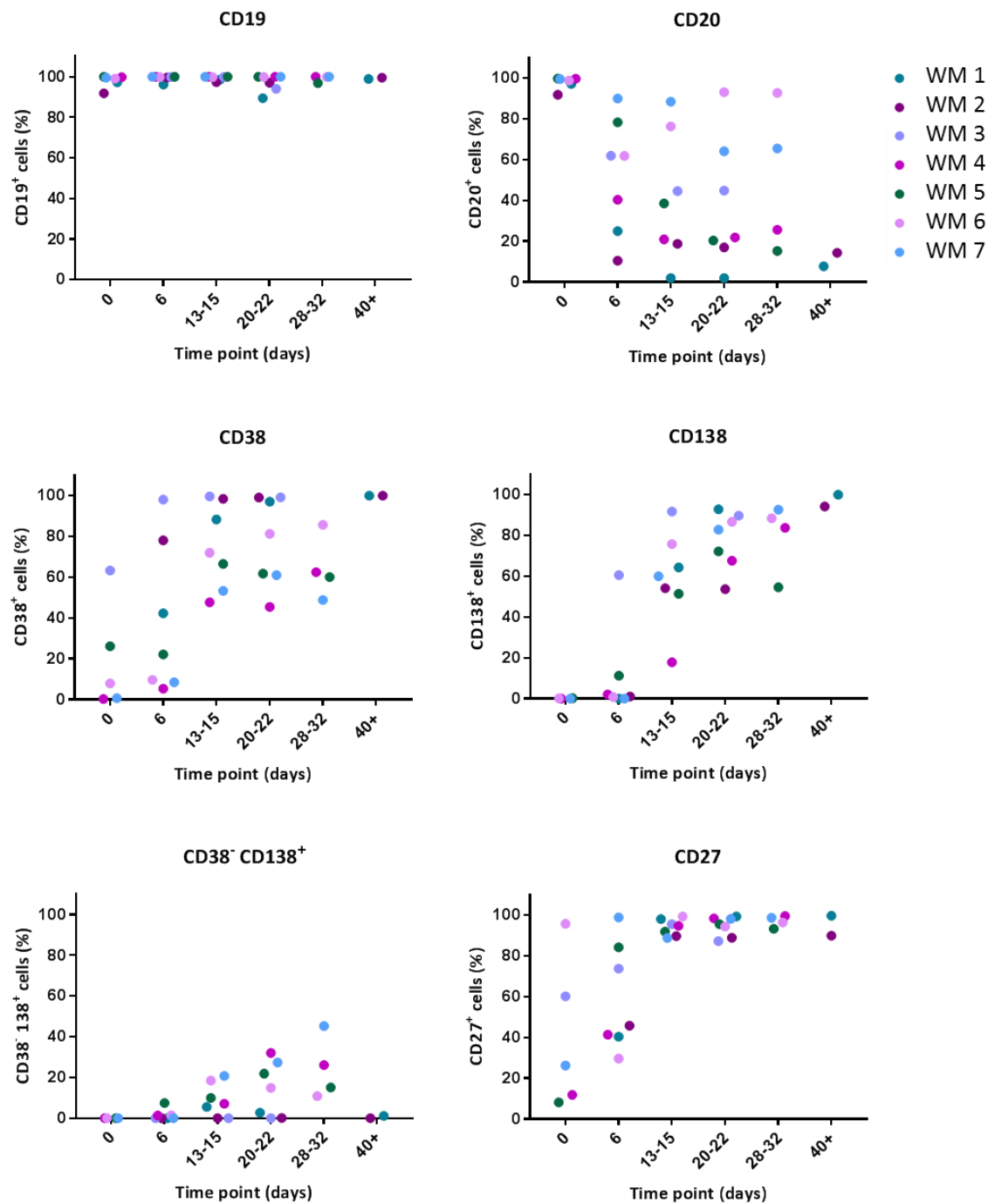
Figure 3.12 Scatter plot profiles for the expression of each CD marker assayed in multiple differentiations with B-cells isolated from WM patients. B-cells derived from the bone marrow of WM patients (isolation protocol B) were stimulated with CD40L and F(ab')$_2$ anti-IgG/M. Each scatter plot displays the percentage of live cells expressing the stated CD marker as determined at each time point via flow cytometry. The lower left plot depicts the percentage of cells that expressed CD138 but without CD38 expression. Data from comparable intervals were grouped together for clarity. Each independent differentiation is represented by a different colour.

A comparison of the average expression of the variable CD markers between healthy and WM samples subsequent to CD40L simulation is provided in figure 3.13.
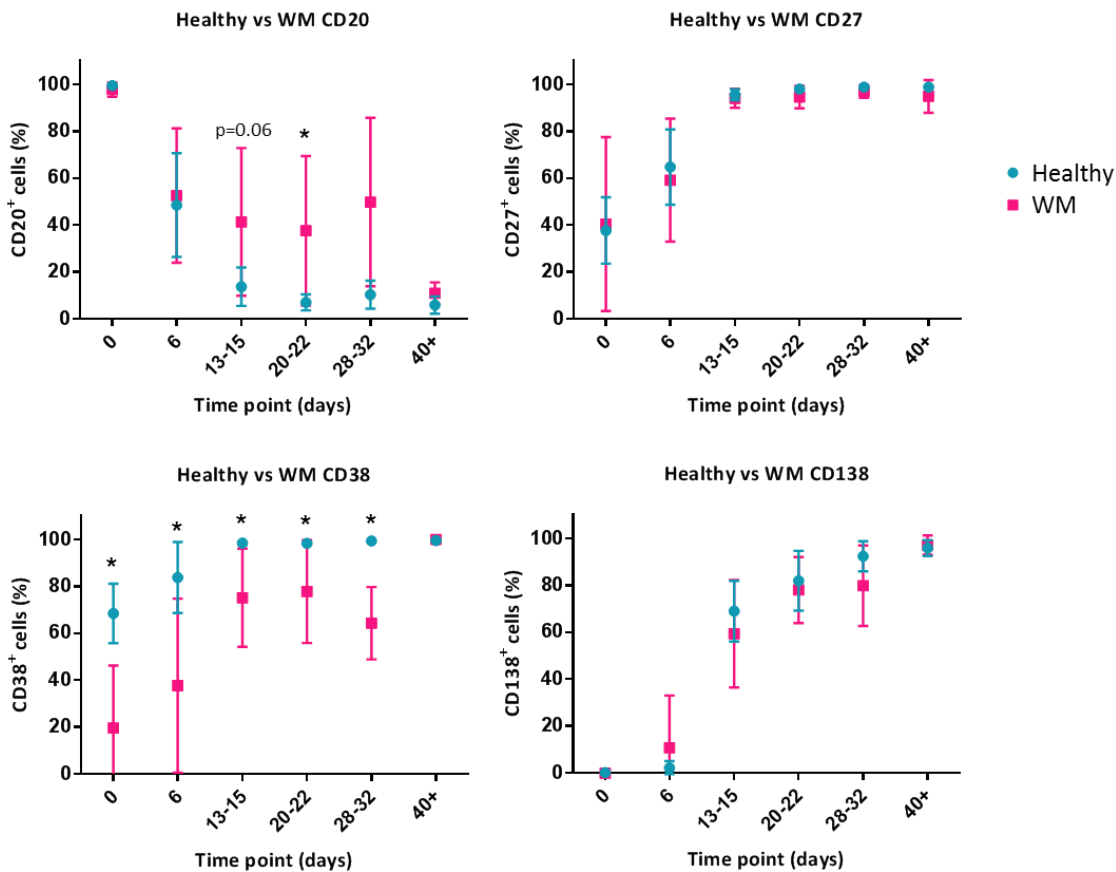
Figure 3.13 Comparison of the average expression of immunophenotypic markers between healthy and WM cells subsequent to CD40L + F(ab')₂ anti-IgG/M stimulation. B-cells derived from the bone marrow of patients diagnosed with WM or peripheral blood of healthy donors (isolation protocol A+ or B) were stimulated with CD40L and F(ab')₂ anti-IgG/M. Each plot displays an average of the percentage of live cells expressing the stated CD marker as determined at each time point via flow cytometry (healthy n = 12, WM n = 7). Values for WM expression significantly different from healthy samples are indicated – (*, p < 0.05, t-test with Welch's correction). Error bars represent S.D.

WM cells demonstrate significantly higher levels of CD20 expression and significantly lower expression levels of CD38 than cells derived from healthy donors. Whilst the expression of CD27 is highly variable in WM samples at day 0, there is no significant difference between the average expression in WM to that of the healthy samples. There was also no significant difference in average CD138 expression. The most intriguing result and a factor which partly explains the large amount of variation in CD38 expression is the presence in some samples of a population of cells that possess CD138 without any expression of CD38 (figure 3.12, lower left plot). This population does not occur in differentiations with healthy cells and will be discussed further.

3.5.3 Alternate plasmablast-like phenotype observation

There is far more variability in WM differentiations than occurred with healthy controls but the phenotypes observed during differentiations with WM patient-derived cells can be broadly divided into two categories. Whilst some WM samples differentiate with phenotypes similar to healthy cells as previously discussed, others differentiate in an unconventional way, with a population of $CD38^-$ $CD138^+$ plasmablast-like intermediates generated. The full immunophenotype of one such differentiation is displayed in figure 3.14.
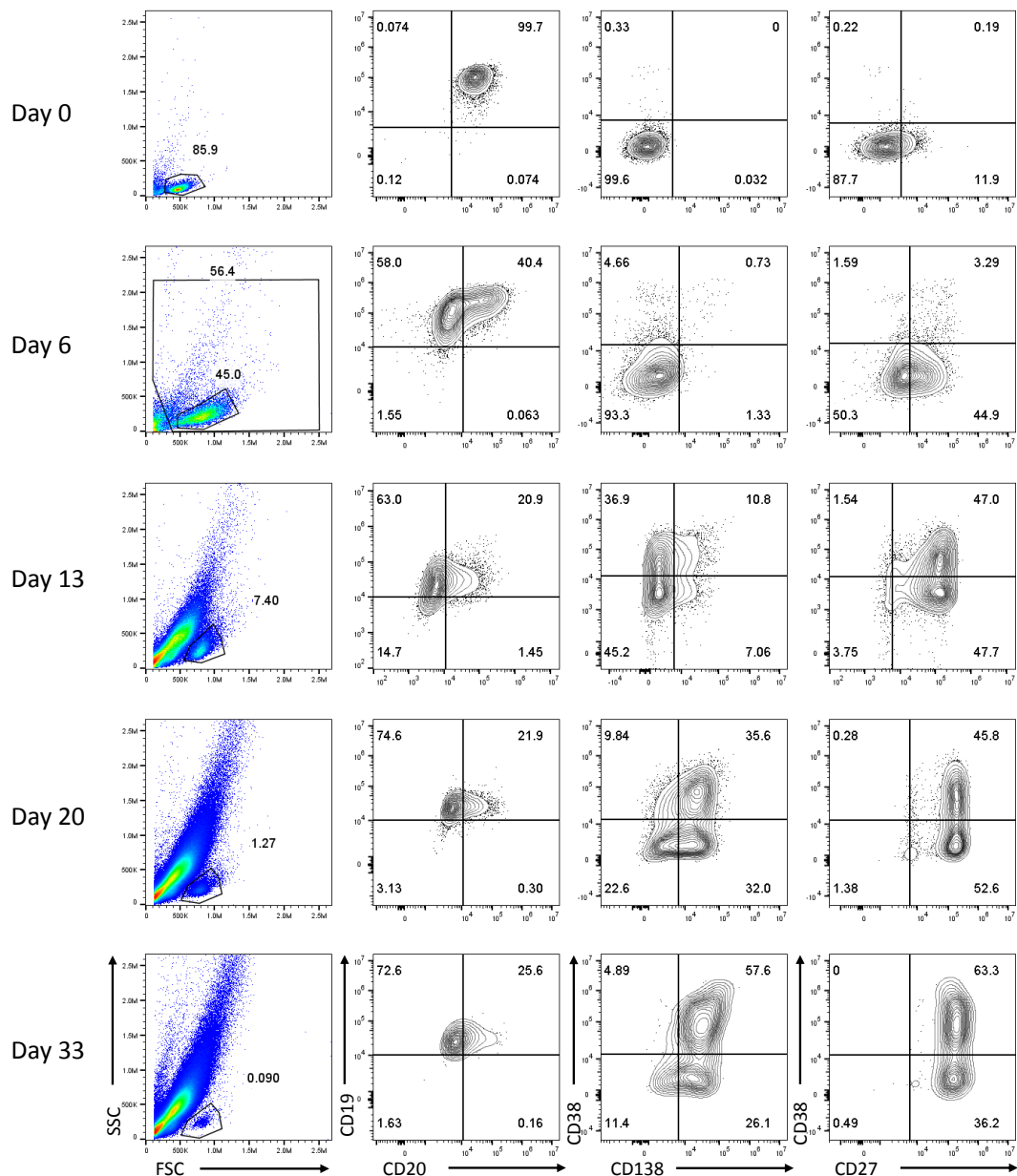
Figure 3.14 A population of cells expressing CD138 in the absence of CD38 frequently occurs during differentiations with WM B-cells. B-cells were derived from the BM from a patient with WM and stimulated with CD40L and F(ab')$_2$ anti-IgG/M. Cells were stained for the surface markers CD19, CD20, CD38, CD138 and CD27 and assayed by flow cytometry at each indicated time point.

The B-cells derived from the bone marrow of this patient were almost exclusively CD38$^-$ and expressed only low levels of CD27. At day 6, there is some evidence of differentiation, with downregulation of CD20 and upregulation of CD27. Whilst a limited number of cells (approximately 5%) have increased expression of CD38 and just under 1% have also upregulated CD138, the proportion of CD38$^+$ plasmablasts is considerably lower than that which occurs with healthy cells. The level of expression of CD138 is also approximately 10-fold lower than is seen for healthy cells. There also appears to be a small fraction of cells that have severely impaired differentiation, retaining CD20 expression, failing to upregulate either CD38 or CD138, but expressing CD27.

The most striking deviation in phenotype when compared to healthy cells emerges at day 13, whereby, in addition to a population of plasmablasts (CD38$^+$ CD138$^-$) and plasma cells (CD38$^+$ CD138$^+$), there is a "third" phenotypically distinct population which upregulated CD138 in the absence of CD38 expression. The proportion of these unusual plasmablast-alternate cells increases to approximately one third of the total population by day 20 and remains present until at least day 38. Overall, the generation of plasma cells is delayed, with a decrease in the fraction of cells that are CD38$^+$ CD138$^-$ - 9.8% to 4.9% and a decrease in the CD38$^-$ CD138$^+$ fraction – 32-26.1%. This suggests that the CD38$^-$ CD138$^+$ fraction represents an alternate intermediate phenotypic step and that some of these cells do indeed upregulate CD38 eventually. The expression of CD markers in the CD38$^-$ CD138$^+$ population is provided in figure 3.14.
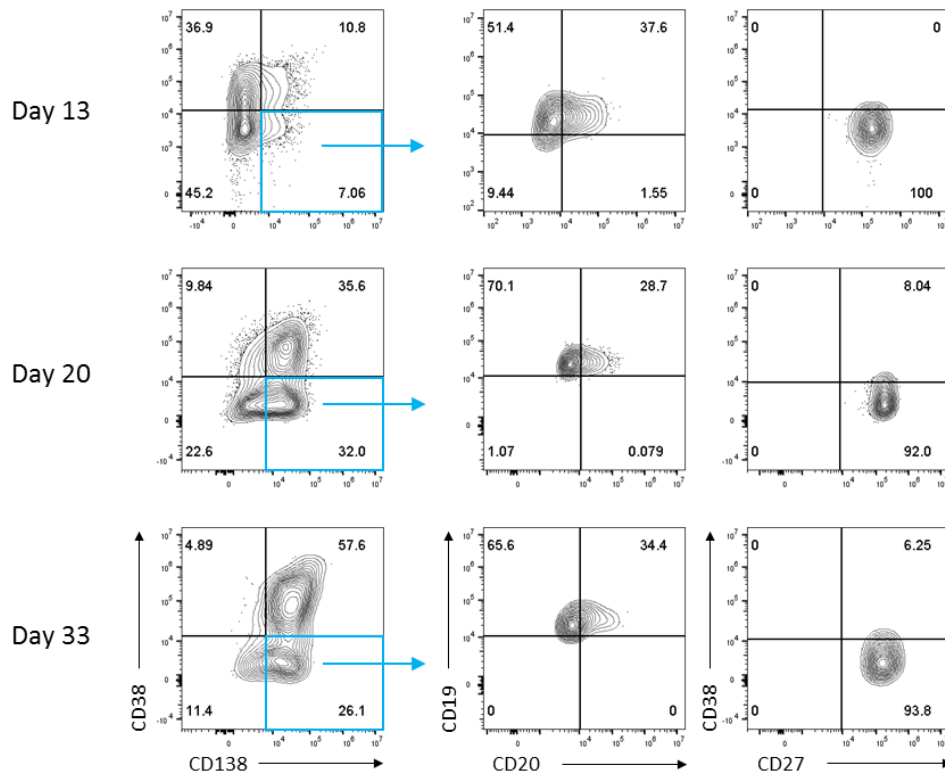
Figure 3.15 Expression of additional CD markers on CD38⁻ CD138⁺ WM fraction. WM B-cells were stimulated with CD40L + F(ab')₂ anti-IgG/M and assessed by flow cytometry for surface markers at the indicated time points. The cell surface marker expression for the CD38⁻ CD138⁺ quadrant is displayed on the right. Percentages are indicated within individual quadrants.

The proportion of cells expressing CD20 is slightly higher in this fraction when compared to the complete population of cells. These cells also express high levels of CD27.

The unusual phenotype of CD38⁻ CD138⁺ cells occurred in 4 of 9 (44%) WM differentiations with CD40L + F(ab')₂ anti-IgG/M taken to at least day 13. A selection of examples of this phenotype are illustrated in figure 3.15. In each case, the generation of day 6 plasmablasts is delayed compared to healthy controls and the CD38⁻ CD138⁺ cells do not emerge until day 13. In each of these three differentiations, this population of cells remains present for at least 14 days subsequent to day 13. Similarly to the phenotype depicted in figure 3.13, loss of CD20 is incomplete, with a notable proportion of cells failing to downregulate this marker even by the final time point. The upregulation of CD27 is unperturbed in these differentiations but the overall level of CD138 expression in the WM plasma cells is again lower than for plasma cells generated from healthy B-cells.
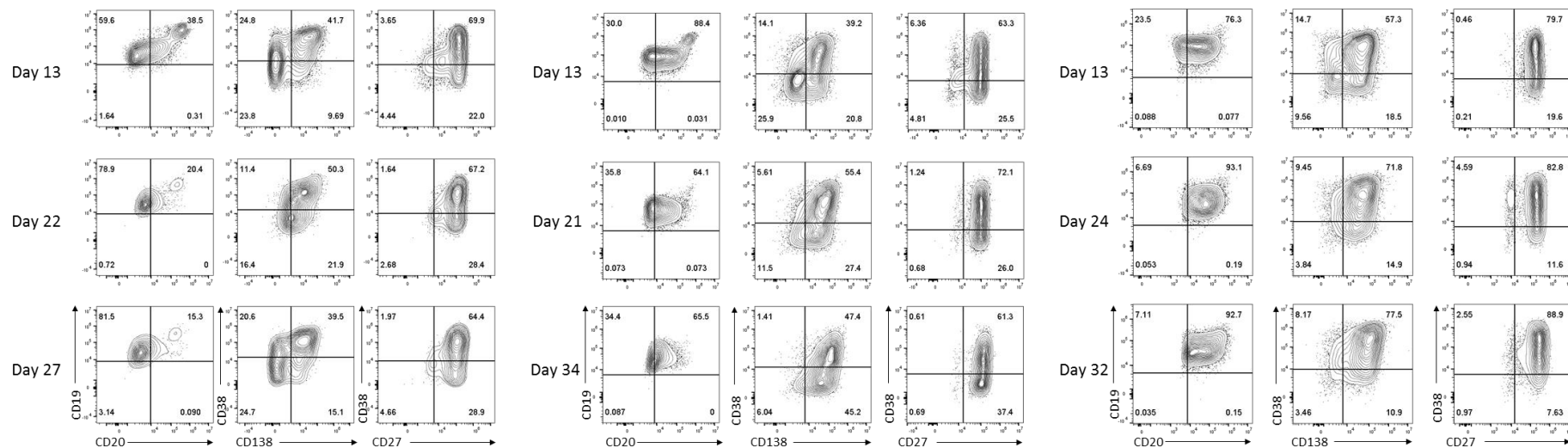
Figure 3.16 Additional examples of the CD38⁻ CD138⁺ population from three further WM differentiations with CD40L. B-cells were isolated from the BM of three independent patients with WM (isolation protocol B) and stimulated with CD40L + F(ab')₂ anti-IgG/M at day 0. The immunophenotype was determined at the indicated time points by flow cytometry. Percentages of cells within each quadrant are indicated.

The CD38⁻ CD138⁺ fraction generated in each case possesses the same distribution of the other markers as the rest of the population. The presence of these cells has not previously been reported in the WM literature and warrants additional investigation.

3.5.4   Immunophenotype comparison between WM differentiations that generated alternate plasmablasts and those that did not

The unexpected emergence of this phenotypically distinct population raised a number of questions as to its origins and whether there were further deviations in phenotype from either healthy differentiation or, indeed, those with other WM cells. To address these questions, the immunophenotype of the WM differentiations that generated the alternate plasmablasts was examined further and compared with the other WM differentiations that did not generate this unusual population to see if there were additional differences between them and to try to determine if the generation of this alternate cell population could be predicted from the phenotype obtained at earlier time points.

The expression of cell surface markers in figure 3.16 have been separated into those differentiations that did not generate CD38⁻ CD138⁺ cells and those that did. Levels of CD20 are highly variable in each group of differentiations, but are higher from day 6 onwards in those differentiations which generated the alternate plasmablasts. Interestingly, expression of CD38 initially appears to be at a much lower level in those cells that went on to generate the alternate PB phenotype than those that did not. In addition to this, there is very little increase in the proportion of cells expressing CD38 between day 0 and day 6 in samples which went on to generate the CD38⁻ CD138⁺ population. The proportion of cells that have upregulated CD138 at each stage does not vary widely between the two variations of differentiations. The upregulation of CD27 is not significantly different between the two either.

From this selection of markers, the expression of CD38 in WM samples appears to serve as the best predictor for the generation of CD38⁻ CD138⁺ cells. WM samples which initially consist of cells with low levels of CD38 and also possibly lower CD27 expression, which do not increase expression of CD38 between day 0 and day 6 appear much more likely to differentiate with the alternate plasmablast-like intermediate.
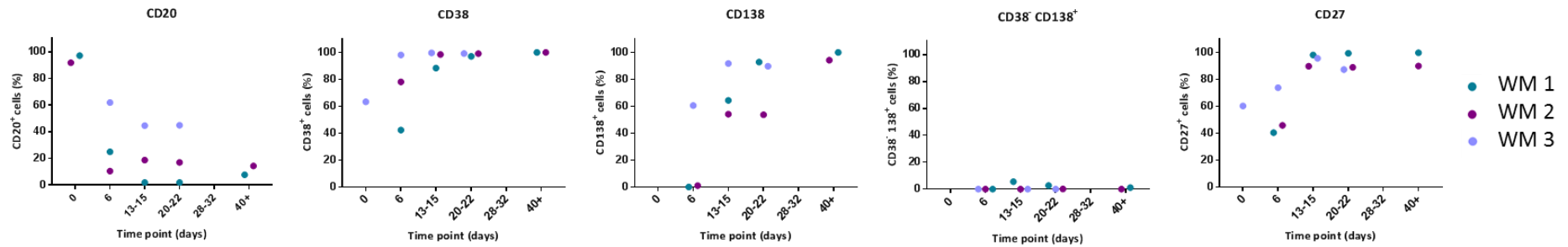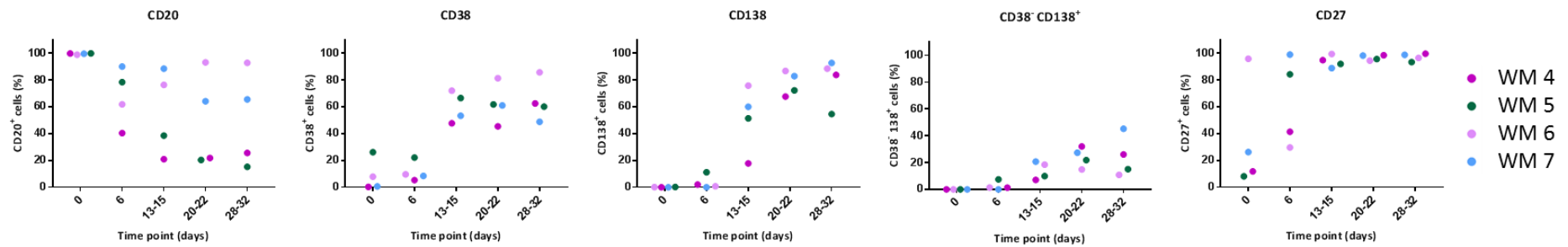
Figure 3.17 Scatter plot profiles for the expression of each CD marker in differentiations with WM cells divided into those which generated CD38⁻CD138⁺ cells and those that did not. B-cells derived from the bone marrow of WM patients (isolation protocol A or B) were stimulated with CD40L and F(ab')₂ anti-IgG/M. Each scatter plot displays the percentage of live cells expressing the stated CD marker as determined at each time point via flow cytometry. The top set of plots display data from differentiations that did not generate the alternate plasmablast-like phenotype (CD38⁻ CD138⁺) and the bottom set represents those differentiations that did generate these cells. The fourth plot depicts the percentage of cells that expressed CD138 but without CD38 expression. Data from comparable intervals were grouped together for clarity. Each independent differentiation is represented by a different colour and the colours used to denote each patient are consistent with figure 3.12.

3.6   Discussion

The response of healthy B-cells to stimuli mimicking a T-dependent immune response was initially investigated. Healthy cells derived from multiple donors demonstrated uniform phenotypes following stimulation with CD40L that corresponded to the established stages of differentiation *in vivo* (figure 3.5). The B-cells became activated between day 0 and 3, with cell numbers remaining largely unchanged during this time (figure 3.4). Subsequently, the cells underwent high levels of proliferation and this coincided with upregulation of the plasmablast marker CD38. A population of plasma cells were generated by day 13 of the differentiation in all samples, accompanied by a contraction in cell numbers (figures 3.4 and 3.5). The population of plasma cells was maintained indefinitely until elective termination of the cultures.

Omission of each of the activation stimuli from differentiations with healthy cells were performed in turn. Results from these experiments demonstrate that B-cells were not reliant on the F(ab')$_2$ anti-IgG/M signal for differentiation and survival, but its absence delayed differentiation as evidenced by the phenotype of these cells at early time points (figure 3.6). B-cells that did not receive CD40 stimulation were completely unable to survive (figure 3.9). Removal of CD40L underscores how vital this stimulation is to initiate differentiation and overcome apoptotic signals.

Subsequently, the response of B-cells isolated from WM patients to CD40L stimulation was characterised. WM cells rely on the constitutive activation of the NF-κB signalling pathway conferred by the MYD88^{L265P} mutation for their survival. MYD88 functions as an adaptor for the majority of toll-like receptors which recognise a wide variety of pathogen associated molecular patterns and are critically involved in the T-independent immune response. Whilst both the T-dependent and T-independent signalling pathways converge on NF-κB activation, the capacity of WM cells to respond to isolated CD40L stimuli and BCR ligation had not previously been assessed. The *in vitro* differentiation system enabled the phenotypic response of WM cells each key time point to be characterised.

WM B-cells do indeed successfully generate a population of plasma cells that express CD38$^+$ CD138$^+$ CD27$^+$ following stimulation with CD40L + F(ab')$_2$ anti-IgG/M, recapitulating the differentiation response of the neoplastic cells *in vivo* (figure 3.12). However, there are considerable differences between the phenotypic profile and cell number of the WM samples compared to their healthy counterparts.

Surprisingly, WM B-cells did not proliferate to the same extent as was observed in the healthy controls (figure 3.11). This was unexpected, as the MYD88^{L265P} mutation should confer a

competitive advantage and it is also thought that chronic active BCR signalling has a role to play in WM. The requirement for intact BCR signalling in WM was first postulated in 2001 by Ciric and colleages (Ciric *et al.*, 2001). Analysis of the immunoglobulin heavy chain present on the surface of WM clones indicated that mutations preserved sIgM structure and hence functional capacity of the BCR in WM cells. The occurrence of mutations associated with the BCR signalling cascade have been documented, though they appear to be restricted to CD79A and CD79B (Poulain *et al.*, 2013; Varettoni *et al.*, 2013). However the frequency of this incidence is low, at approximately 15% of WM cases. Despite this, there is evidence for chronic active BCR signalling within WM (Argyropoulos *et al.*, 2016; Munshi *et al.*, 2017).

Argyropoulos et al., analysed WM BCR signalling by phosphoflow cytometry and observed elevated basal levels of phosphorylation amongst BCR-related proteins in WM samples (Argyropoulos *et al.*, 2016). Subsequently, they established phosphorylation profiles for neoplastic versus healthy B-cells for six components downstream of the BCR comprising of pSFK, pSYK, pBLNK, pPLCγ2, pERK and pAKT. Interestingly, their data also stratified WM patients via their phosphoprofiles into those which were more similar to healthy cells, corresponding to a more indolent clinical phenotype, and those that deviated more substantially from the controls. It would be most interesting if the WM cells that differentiated with a phenotype that was closely matched that of healthy cells described here was analogous to the "healthy-like group" defined in that study.

Despite WM cells being postulated to originate for a memory B-cell precursor, levels of CD27 observed in many WM samples here was lower than expected (figure 3.12). The data presented here concur with the findings of Kriangkum and colleagues, who performed clonotypic analysis on populations of CD20$^+$ CD27$^-$ and CD20$^+$ CD27$^+$ WM cells derived from BM and PB (Kriangkum *et al.*, 2004a). The frequency of CD27$^-$ neoplastic cells was higher than those expressing CD27, indicating that CD27 does not distinguish the WM clone. In accordance with this, Sahota and colleagues proposed a model whereby WM cells derive from CD27$^+$ memory B-cells but shed CD27 as the disease progresses (Sahota *et al.*, 2009). Upregulation of CD27 appeared unaffected during WM differentiations, with the proportion of cells expressing this marker at each stage closely mirroring that of the healthy cohort (figure 3.13).

A subset of WM differentiations displayed significant impairment to CD20 downregulation (figures 3.12 and 3.13). The CXCR4/SDF-1 signalling axis is crucial for B-cell homing to the bone marrow and plays an important role in CD20 regulation (Burger and Kipps, 2006; Pavlasova *et al.*, 2015). Somatic mutations in CXCR4 are common in WM and invariable co-occur with MYD88^{L265P} (Hunter *et al.*, 2014). Whilst a direct connection between CXCR4 mutation status and dysregulation of CD20 loss cannot be made here due to the unavailability of CXCR4 mutation

status amongst the patients studied, it remains plausible that samples with increased retention of CD20 may comprise those that possess this mutation. The detection of elevated levels of CD20 in WM differentiations is also in accordance with Kriangkum et al., (2004) who observed increased expression of CD20 in WM patients with active disease.

Perhaps the starkest deviation from the normal immunophenotype observed throughout the differentiations was the generation of a population of WM cells expressing CD138 without prior upregulation of CD38 (figure 3.14). This unusual population arises between day 6 and day 13 when the cells are transitioning from plasmablasts to plasma cells. The time at which these cells appear initially suggests that the $CD38^-$ $CD138^+$ population may be an as yet undescribed plasmablast-like intermediate. WM plasmablasts have not been well characterised but a population of cells that shares this phenotype has been observed during diagnostic flow cytometry on bone marrow aspirates (Dr. R. de Tute personal communication). The presence of this population is maintained in each sample for at least 14 days and thus well into the time period where only plasma cells should remain (figure 3.12). The proportion of these cells in a few cases diminishes slightly as time progresses and further investigation is required in order to determine whether these cells ever increase CD38 expression and become phenotypically "normal" plasma cells at some point down the line. The appearance of these cells could have potential ramifications for treatment. Trials of CD38 antibodies such as Daratumumab have commenced in recent years and may soon comprise part of the WM treatment regime, paired with the CD20 monoclonal antibody Rituximab (A Study of Daratumumab in Patients with Relapsed or Refractory Waldenström Macroglobulinemia. Trial number: NCT03187262). The absence of both CD38 and CD20 on this population of cells will render this combination of antibodies ineffective a leave a residual population of neoplastic cells unchecked in these patients.

The most successful differentiation experiments have a prerequisite on quality samples, with sufficient quantities of B-cells and adequate viability. This was not an issue for healthy samples derived from peripheral blood as isolation of B-cells could be performed immediately subsequent to when the sample was taken. However, BM sample quality was highly heterogeneous, affecting the number of cells obtained during the isolation process and having a prolonged impact on viability. This has considerable repercussions at the latter stage of differentiation, because such a high proportion of cells die between day 6 and day 14. In order for high quality data to be obtained at beyond this point, there is a reliance on having low levels of cell death in the early stages and high levels of proliferation when the cells become activated to generate sufficient numbers of plasmablasts at day 6 such that even though a large proportion of cells perish in the subsequent week, there are enough plasma cells for further analysis. It

should be noted that the paucity of cells from some WM samples precluded the analysis of all time points and the rarity of this neoplasm resulted in fewer complete data sets than for healthy samples.

Chapter 4 – Differentiation responses to T-independent activation

4.1   Introduction

The differentiation profiles for both healthy and WM B-cells in response to CD40L stimulation have been established. However, B-cell activation can also occur by other means such as cross-linking of the BCR by polyvalent antigen or ligation of pattern recognition receptors such as toll-like receptors (Mosier *et al.*, 1977; Mond *et al.*, 1995). In WM B-cells, the MYD88^{L265P} mutation initiates the same signalling cascade that is elicited by TLR ligation as it lies directly downstream of nearly all the TLRs (Medzhitov *et al.*, 1998; Akira and Takeda, 2004). Research has identified a prior requirement for TLR signalling in MYD88^{L265P} cell lines and murine B-cells (Lim *et al.*, 2013; Wang *et al.*, 2014). The *in vitro* differentiation system enables further investigation of these findings in primary human cells. Thus, it is important to determine the response of healthy cells to TLR ligation and to identify if it differs from a T-dependent response. This, combined with the characterisation of WM responses to TLR stimulation, will enable comparisons to be made between normal and neoplastic B-cells and also between the two types of immune response.

In order to mimic a T-independent response, B-cells were activated with a combination of the synthetic TLR7/8 agonist, Resimiquod (R848), and antibody to the BCR. Inclusion of F(ab')$_2$ anti-IgG/M serves to cross-link the BCR, an essential step in initiating differentiation, without co-ligation of the inhibitory Fc receptor FcYRIIB (Ono *et al.*, 1996). Dual activation of the BCR and TLRs have been shown to elicit a synergistic response, whilst also functioning to prevent B-cell tolerance to TLR signalling (Poovassery *et al.*, 2009; Pone *et al.*, 2012; Kuraoka *et al.*, 2017). Prior to assessing the response of WM cells, the differentiation characteristics of healthy B-cells in response to stimulation with R848 + F(ab')$_2$ anti-IgG/M were examined. This included the effects of reagent carryover and dose response evaluation in order to refine the culture protocol for this type of stimulation and to determine the optimal concentration of R848. As with CD40L differentiations, the effect of F(ab')$_2$ anti-IgG/M removal on phenotype and cell number was also examined. Subsequently, the effect of R848 + F(ab')$_2$ anti-IgG/M stimulation was examined in WM primary B-cells.

4.2   Response of healthy cells to R848 stimulation

Whilst stimulation of B-cells with CD40L mimics a T-cell dependent immune response, B-cell activation can also occur via a T-cell independent pathway. This response can be initiated when

Toll-like receptors are bound by their ligands and provide the second activation signal. In murine models, stimulation of TLR4 with LPS is classically used to activate B-cells (Sultzer, 1968; Poltorak *et al.*, 1998; Hoshino *et al.*, 1999). However, unlike their murine counterparts, human mature B-cells do not express TLR4, rendering this stimulation ineffective (Muzio *et al.*, 2000; Hornung *et al.*, 2002; Zarember and Godowski, 2002). Human B-cells express a range of other TLRs, including TLR7, 8 and 9 which are located within endosomes (Lee *et al.*, 2003; Heil *et al.*, 2004; Nishiya and DeFranco, 2004). The synthetic TLR7/8 agonist R848 was therefore used to stimulate the B-cells, replacing the CD40L-L expressing fibroblasts, with the continued addition of a constant amount of F(ab')$_2$ anti-IgG/M. Preliminary differentiation experiments with healthy B-cells taken to day 13 were conducted with three concentrations of R848 – 10, 1 and 0.1µg/ml. Representative results from one donor are depicted in figure 4.1.
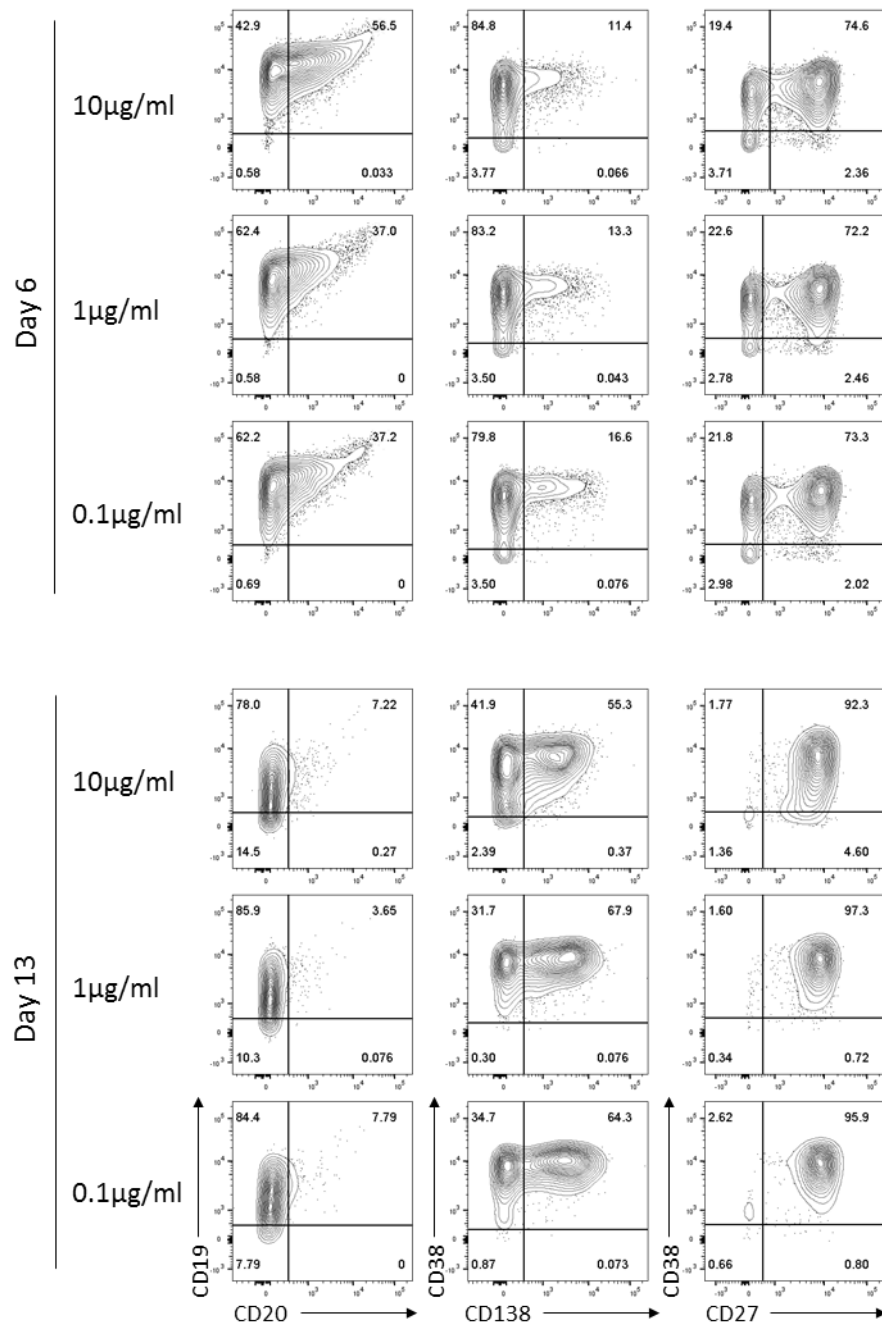
Figure 4.1 The concentration of R848 used for B-cell activation affects the phenotype. B-cells were derived from the peripheral blood of a healthy donor (isolation protocol A) and stimulated with three concentrations of R848 - 10, 1 or 0.1μg/ml + F(ab')$_2$ anti-IgG/M. Data are representative of three independent experiments. The cells were assessed by flow cytometry for the surface markers CD19, CD20, CD38, CD138 and CD27 at the indicated time points. Percentages are indicated within individual quadrants.

The B-cells display dose-dependent changes in phenotype. Cells stimulated with 0.1μg/ml R848 had progressed to a more differentiated phenotype at day 6, with those stimulated with 10μg/ml R848 displaying the least differentiated phenotype – with the highest proportion of

cells retaining CD20 and lowest proportion of CD38$^+$ CD138$^+$ cells amongst the three conditions. The proportion of viable B-cells was also affected by the concentration of R848, with 53.6% viable cells at 10μg/ml, 42.7% at 1μg/ml and 33.9% at 0.1μg/ml (data not shown).

Interestingly, the impact of R848 concentration on how rapidly the cells differentiate remains at day 13, but the pattern is no longer dose-dependent. The cells which were activated with the highest concentration of R848 continue to phenotypically lag behind their counterparts that received lower levels of R848 stimulation. However, the B-cells which have progressed furthest are those which were stimulated with 1μg/ml R848 – with the greatest proportion of plasma cells and lowest proportion of cells retaining CD20.

Whilst the initial B-cell purity following isolation was >95%, a population of non-B-cells expanded between day 6 and 13. These cells are occasionally observed in CD40L cultures when B-cell purity at day 0 falls below approximately 95% and comprise of T- or NK-cells. Addition of R848 to the culture appeared to favour the expansion of these cells compared to differentiations performed with CD40L. In order to minimise the occurrence these cells, the isolation protocol was adapted to be more stringent, with an additional separation step using a fresh LD magnetic column to increase B-cell purity further (isolation protocol A+).

4.2.1   Investigation of R848 carryover

A delay in differentiation was observed for B-cells cultured with the highest concentration of R848. During the process of a differentiation, the media is removed and replaced at day 3 to prevent persistent activation. In the case of differentiations with CD40L-L expressing fibroblasts, the CD40 signal ceases when the B-cells are removed from contact. However, since the R848 is a soluble factor, it is possible that quantities of R848 might persist after removal of the day 0 media. Whilst the activated B-cells are resuspended in fresh media at day 3, there is potential for some carryover of R848, particularly for the highest concentration. Considering that B-cells were able to respond to levels of R848 100 times lower than the maximum concentration tested, any persistent R848 may subsequently have a significant knock-on effect on the differentiation. It was noted by Arpin and colleagues that B-cells cultured in the continued presence of CD40L were unable to differentiate into plasma cells (Arpin *et al.*, 1995). Similarly, prolonged TLR signalling results in tolerance, rendering the cells unresponsive to this type of stimulation in order to regulate autoimmunity (Poovassery *et al.*, 2009; Kuraoka *et al.*, 2017). Whilst such an extreme effect does not appear to be the case here, it was nevertheless important to ensure that the R848 did not remain in the culture and affect the phenotype of the cells. To determine whether carryover of R848 was affecting differentiation and to optimise the protocol in an attempt to minimise the potential remaining levels of R848, cells cultured with 10μg/ml R848

underwent an additional wash with 10ml fresh media before being resuspended with day 3 media (figure 4.2).

The difference in phenotype for differentiations with and without the media wash are most pronounced for the highest concentration of R848 as expected. The cells treated with 10μg/ml R848 that were not washed at day 3 displayed a considerable delay in differentiation. At this concentration, the proportion of cells retaining CD20 at day 6 without the wash was almost double that of those with the wash and the percentage of plasma cells was over four times lower at only 2.8% compared to 12.1% subsequent to a media wash (figure 4.2). This illustrates the considerable impact that continued TLR stimulation has on differentiation. The phenotype at day 6 for 0.1μg/ml R848 with and without the media wash was virtually identical. This indicates that at this concentration, any carryover of R848 is negligible and has no effect on cell phenotype.
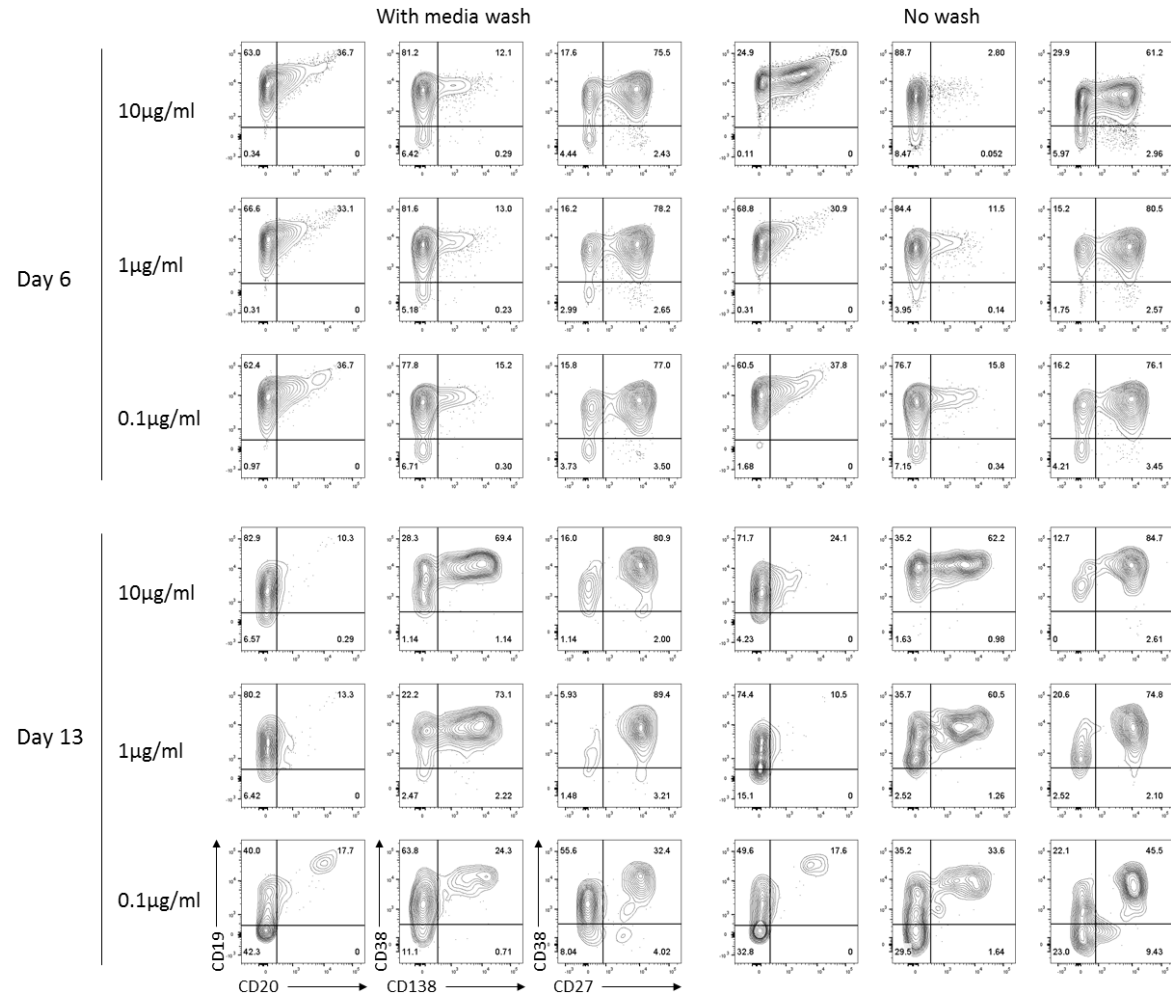
Figure 4.2 The immunophenotype of differentiating cells with and without a media wash at day 3. B-cells were derived from the peripheral blood of a healthy donor (isolation protocol A+) and stimulated with either 10, 1 or 0.1µg/ml R848 + F(ab')$_2$ anti-IgG/M. The media was replaced as usual on day 3 either with or without an additional wash with 10ml fresh media. Cells from a non-B-cell fraction that expanded after day 6 (CD19$^-$ CD20$^-$) are apparent in the lower right quadrants of the 0.1µg/ml R848 day 13 plots.

The phenotype of the cells with the media wash at day 6 was very consistent between the three concentrations of R848 used. Phenotypic differences between the three conditions were very subtle, with the proportion of cells expressing each marker varied by less than 5% at day 6. The trend of higher levels of R848 delaying differentiation is no longer clearly evident, however the proportion of plasma cells does appear to be inversely dose-dependent, with the lowest concentration of R848 generating the greatest proportion of CD38$^+$ CD138$^+$ cells at day 6.

Cell survival was poor at day 13, this was due to a population of non-B-cells that again expanded between day 6 and day 13, negatively affecting the number of B-cells as the differentiation progressed. The expansion of a non-B-cell fraction at later time points within the culture system has previously been investigated (work performed by Dr G. Arumugakani). The identity of this population was found to consist of NK-cells or T-cells that were not removed during the B-cell isolation process. In order to increase the purity of the isolated B-cell fraction and eliminate the appearance of the T- or NK-cells cells from the culture, an additional depletion step using CD3 and CD56 microbeads was subsequently incorporated into the B-cell isolation procedure.

Interestingly, the cells which were stimulated with 1µg/ml R848 have produced the highest proportion of plasma cells, though the phenotype of the cells stimulated with 0.1µg/ml R848 has been skewed due to the presence of the non-B-cell fraction. It is clear that prolonged exposure of B-cells to small quantities of R848 is sufficient to affect the phenotype of the cells. In order to prevent the carryover of R848 from affecting future differentiations, the 10ml media wash at day 3 was incorporated as standard for all concentrations of R848 used.

4.2.2   R848 dose response

Having established that prolonged exposure to R848 does have an impact on cell phenotype, the protocol was optimised to prevent this and to minimise the occurrence of non-B-cells by increasing the stringency of the isolation procedure. It was now possible to determine the effect of R848 dose response on phenotype and cell number, without the results becoming skewed by persistent stimulation with residual R848. A differentiation was performed with the cells from a healthy donor, stimulated with three concentrations of R848, as before, but in this instance, the protocol included an additional CD3/CD56 depletion and day 3 media wash (figure 4.3).
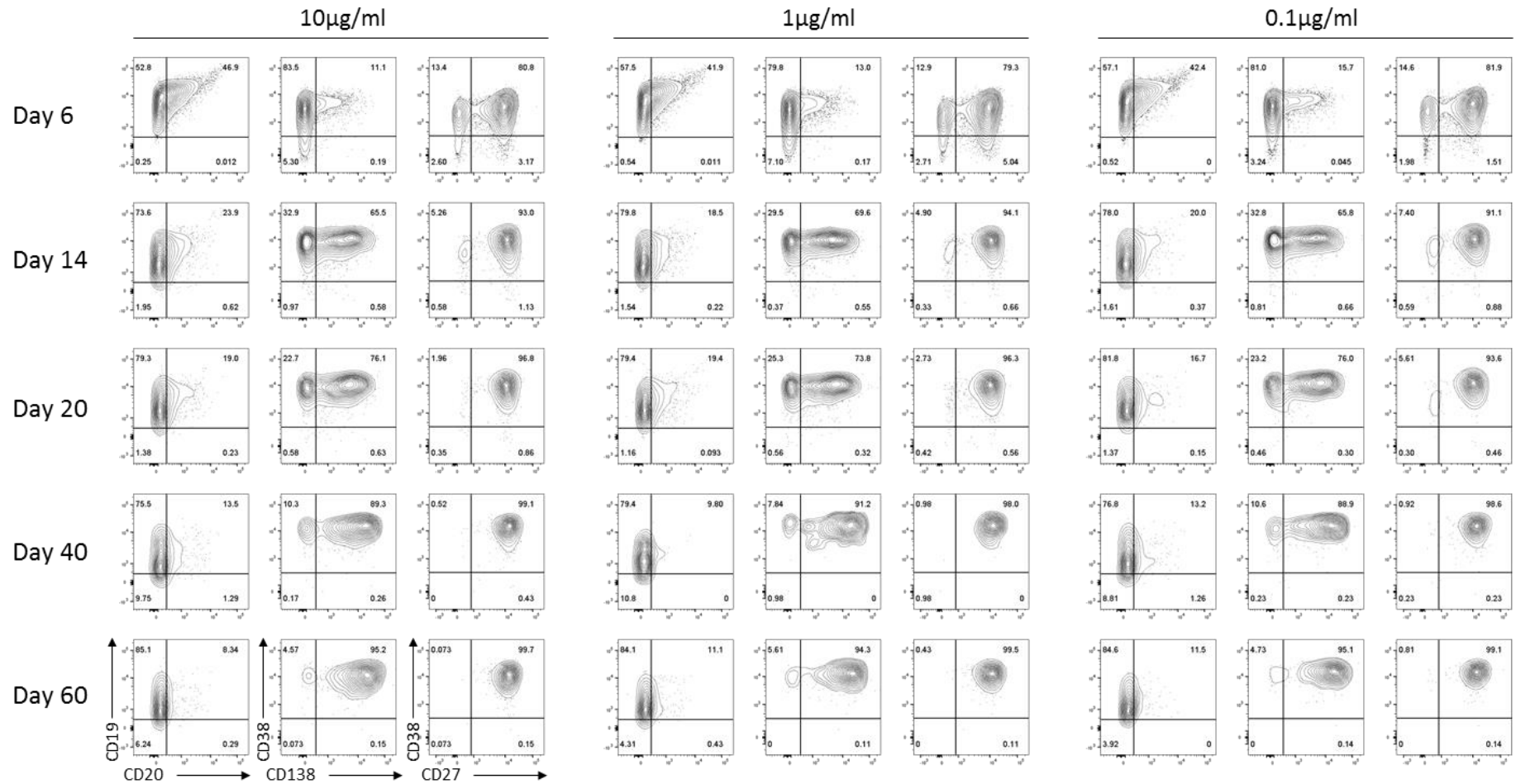
Figure 4.3 Differentiation of B-cells from a healthy donor with three concentrations of R848. B-cells were derived from the peripheral blood of a healthy donor (isolation protocol A+), with CD3/CD56 depletion and stimulated with either 10, 1 or 0.1µg/ml R848 + F(ab')₂ anti-IgG/M. Cells were washed with 10ml fresh media at day 3. The phenotype was assessed by flow cytometry for surface markers at the indicated time points. Percentages are indicated within individual quadrants.

The improved isolation of B-cells in this instance resulted in increased purity and prevented the expansion of a $CD19^-$ $CD20^-$ non-B-cell fraction, enabling the cells to be maintained until elective termination of the culture. B-cells from all conditions were successfully able to generate populations of long-lived plasma cells. Once again, at day 6 the proportion of $CD38^+$ $CD138^+$ cells was inversely correlated to the concentration of R848 used to stimulate the cells but did not quite reach the threshold for significance (Pearson's correlation coefficient r = -0.993, p = 0.0755, R^2 = 0.986, n = 5). This trend was not reflected in the expression of the other markers. The differences in phenotype between the three conditions are no longer apparent from day 14 onwards.

The fold change number of cells at each time point is displayed in figure 4.4.
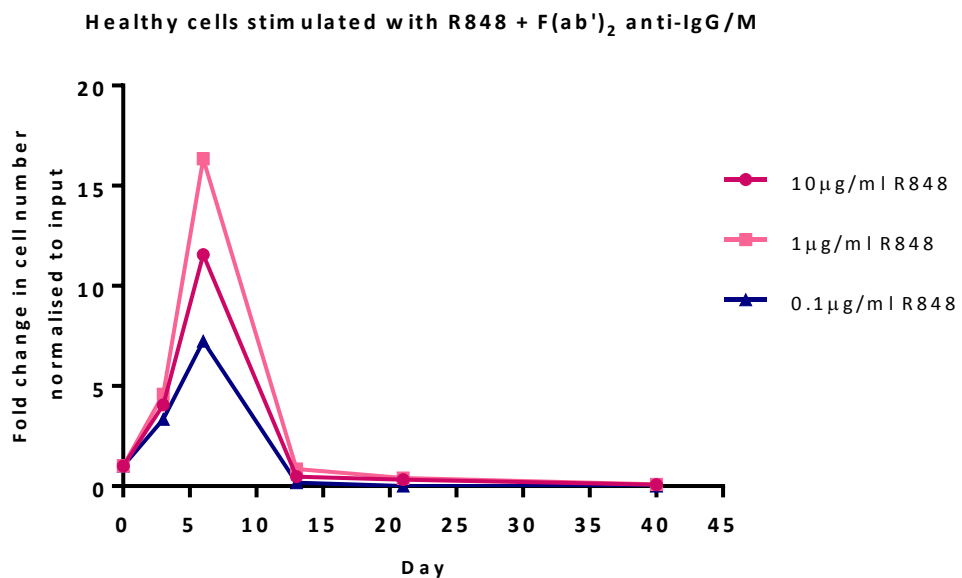
Figure 4.4 Stimulation of healthy B-cells with different concentrations of R848 results in different levels of fold-change for each condition. B-cells derived from the peripheral blood of a healthy donor (isolation protocol A+), with CD3/CD56 depletion, were stimulated with 10, 1 or 0.1µg/ml R848 and F(ab')$_2$ anti-IgG/M. Cell number at each time point was determined by manual counts between days 0-6 and then by flow cytometry thereafter. The cell number at each point was normalised to the number of "input" cells for that specific donor obtained at day 0.

The profile of proliferation recapitulates the response of B-cells *in vivo* and is comparable with the profile seen in cells stimulated with CD40L. In contrast to the phenotypes observed at day 6, the fold change in cell number was not correlated with the concentration of R848 used. B-cells which were activated with 1µg/ml R848 exhibited greater levels of proliferation between

day 0 and 3 and subsequently between day 3 and day 6 of the differentiation than cells stimulated with the other concentrations of R848.

The results from this differentiation were used to establish the concentration of R848 to be used in future differentiations. An important factor determining the quality of the flow cytometry results and other downstream analysis during *in vitro* differentiations is the number of cells available, particularly for late time points following the contraction in cell number after day 6. Cells which were stimulated with 1μg/ml R848 displayed the greatest fold increase in number and survived slightly better than the cells from the other two conditions. This, in combination with the intermediate phenotype observed at day 6, indicated that 1μg/ml R848 would be the optimal concentration of the three to use for future differentiations.

4.2.3   Removal of F(ab')$_2$ anti-IgG/M from the culture system

In previous differentiations, a cross-linking F(ab')$_2$ anti-IgG/M was used at day 0 because of its importance in instigating B-cell maturation(Ono *et al.*, 1996). F(ab')$_2$ fragment antibodies retain two antibody-binding portions linked by the hinge region, whilst a large proportion of the Fc region is removed. The removal of the constant region eliminates co-ligation to the Fc receptor FcγRIIB, which is known to inhibit BCR signalling (Ono *et al.*, 1996). F(ab')$_2$ is used to cross-link the BCR, resulting in receptor aggregation and providing the initial activating signal responsible for B-cell proliferation and differentiation.

The effect of F(ab')$_2$ anti-IgG/M on B-cell phenotype and cell number throughout differentiations with B-cells activated with CD40L was limited. However, the strength of the CD40L stimulation appears to elicit a much greater proliferative response from the B-cells than that which occurs following R848 stimulation. Co-stimulation of both the BCR and TLRs has been shown to demonstrate synergism in the production of autoantibodies and the activation of the naïve B-cell subset (Leadbetter *et al.*, 2002; Rui *et al.*, 2003; Viglianti *et al.*, 2003). Therefore, F(ab')$_2$ anti-IgG/M may play a bigger role when the cells are stimulated with R848. To determine the impact of F(ab')$_2$ anti-IgG/M in combination with TLR stimulation, B-cells were stimulated with R848 both with and without the addition of F(ab')$_2$ anti-IgG/M at day 0. Three concentrations of R848 were used to establish whether more extensive TLR ligation nullified the effects of removing F(ab')$_2$ anti-IgG/M (figure 4.5).

.
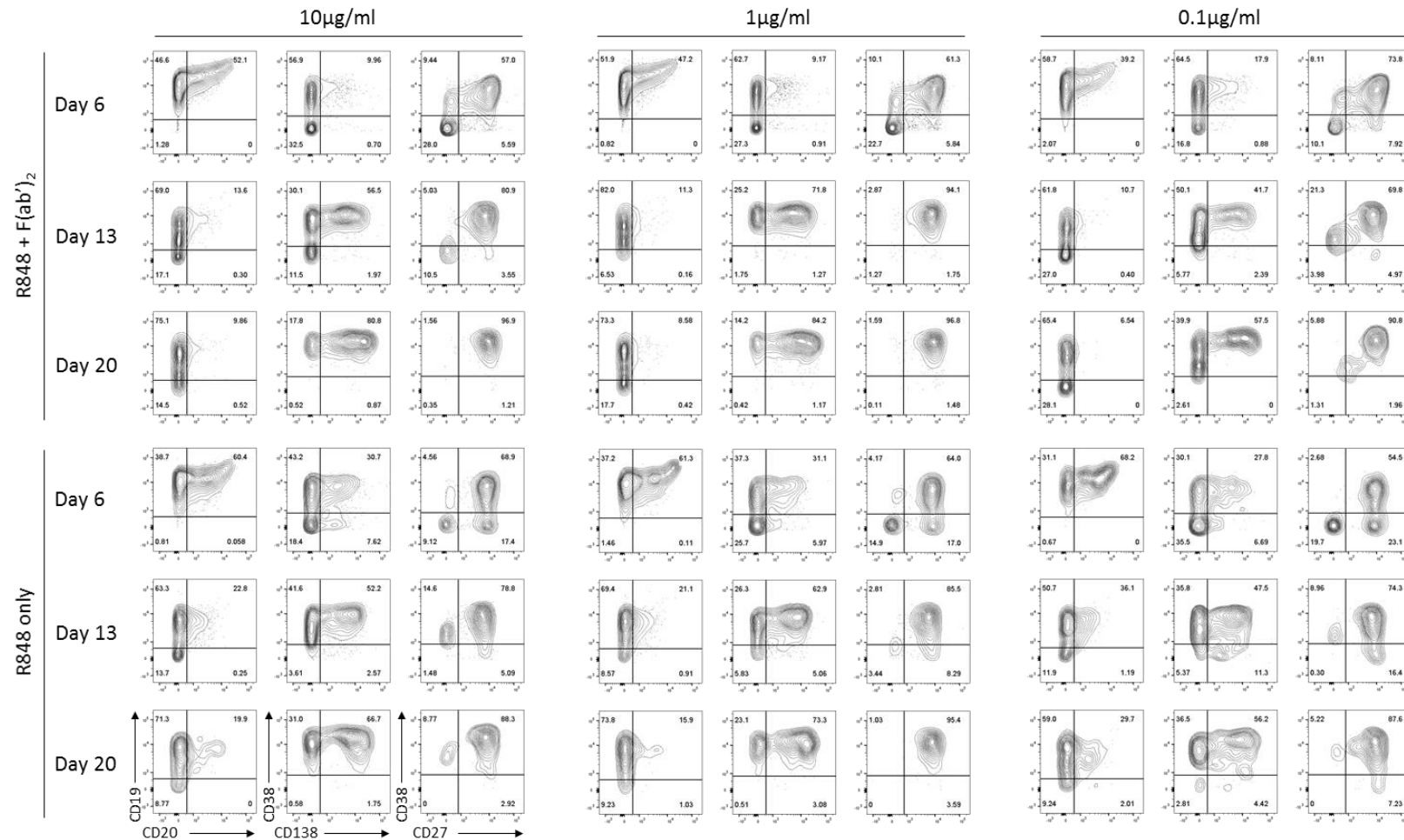
Figure 4.5 Immunophenotype of cells cultured with three different concentrations of R848, both with and without the addition of F(ab')₂ anti-IgG/M. B-cells were isolated from the peripheral blood of a healthy donor (isolation protocol A+), with CD3/CD56 depletion, and stimulated with 10, 1 or 0.1µg/ml R848 with or without the addition of F(ab')₂ anti-IgG/M. The phenotype was assessed by flow cytometry for surface markers at the indicated time points. Percentages are indicated within individual quadrants.

Omission of F(ab')$_2$ anti-IgG/M resulted in delayed B-cell differentiation compared to cells cultured with the addition of F(ab')$_2$ anti-IgG/M. At day 6, a distinct population of cells expressing very high levels of CD19 and CD20 was observed for B-cells that had been cultured without F(ab')$_2$ anti-IgG/M but it was absent when the cells received stimulation with F(ab')$_2$ anti-IgG/M. The CD19^{++} CD20^{++} cell populations were back-gated to analyse their expression of CD38 and CD138. They displayed an undifferentiated B-cell phenotype, with cells expressing low levels of CD38 and CD138. The proportion of the CD19^{++} CD20^{++} population compared to those that had downregulated CD20 appeared to be inversely dose dependent, with the greatest prevalence occurring in cells treated with 0.1µg/ml R848 and becoming less apparent at the higher concentrations of R848. This fraction is largely lost between day 6 and 13, as the cells become more differentiated, although a greater proportion of cells still retain CD20 expression when F(ab')$_2$ anti-IgG/M was absent. Cells stimulated with 10µg/ml or 1µg/ml R848 without F(ab')$_2$ anti-IgG/M continued to phenotypically lag behind their counterparts at day 20, with each generating a smaller proportion of plasma cells. However, the proportion of plasma cells was very similar for the lowest concentration of R848, both with and without the addition of F(ab')$_2$ anti-IgG/M. These results demonstrate that receipt of both stimulatory signals is of greater importance here than was observed following CD40L stimulation.

This differentiation was performed before the B-cell isolation procedure was optimised to minimise the expansion of any non-B-cell fraction. Stimulation with R848 again appeared to result in the preferential expansion of this population and, accordingly, it had detrimental consequences for B-cell survival. In order to determine if this effect was reproducible and if the impact on B-cell phenotype persisted after day 20, B-cells from a different healthy donor were cultured with 1µg/ml R848 and F(ab')$_2$ anti-IgG/M, or 1µg/ml R848 alone. The phenotypes were analysed by flow cytometry to day 40 of the culture and are displayed in figure 4.6.
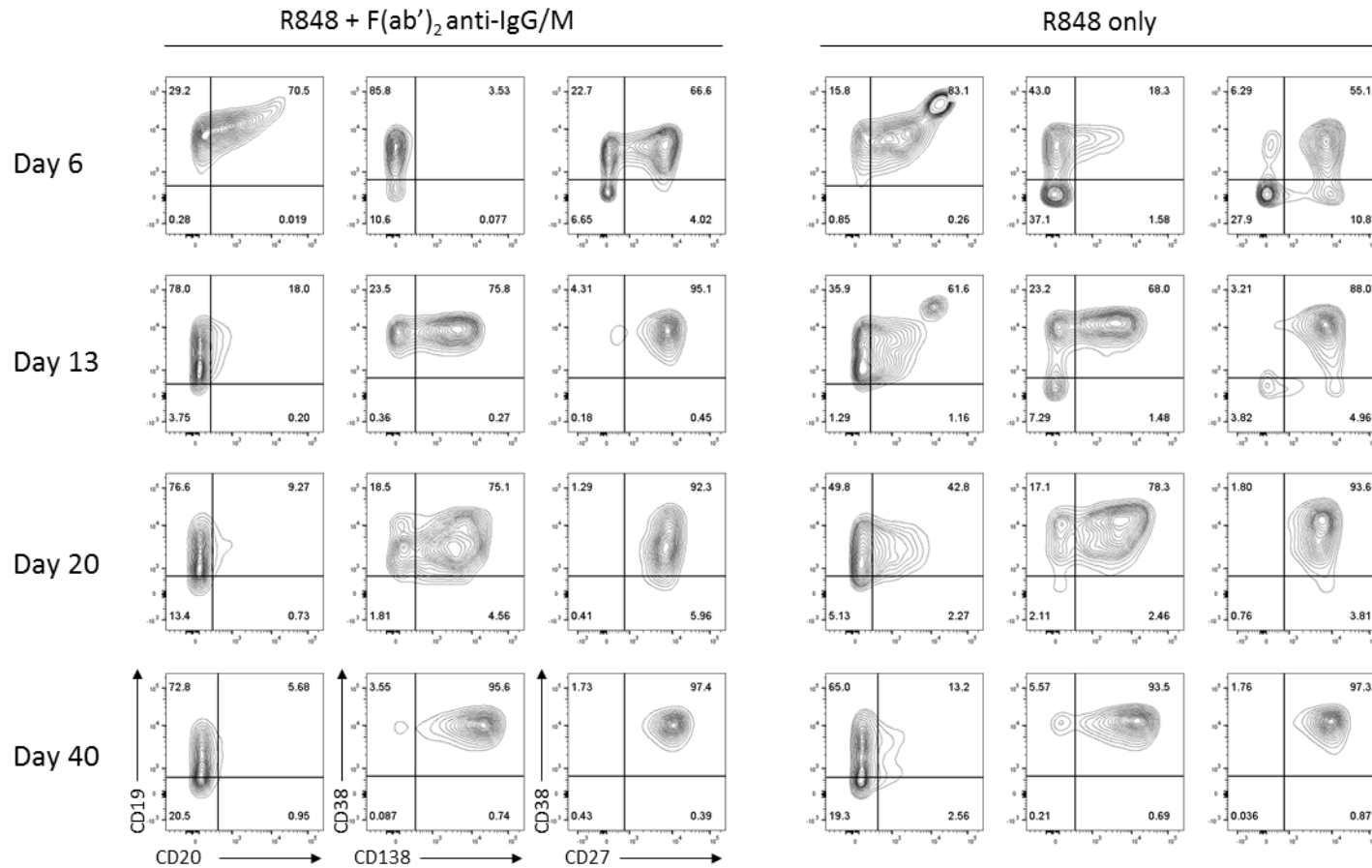
Figure 4.6 Differentiation of B-cells from a healthy donor with R848 stimulation, with or without the addition of F(ab')₂ anti-IgG/M. B-cells were isolated from the peripheral blood of a healthy donor (isolation protocol A+), with CD3/CD56 depletion and stimulated with 1µg/ml R848 with or without F(ab')₂ anti-IgG/M. Cells were washed at day 3 with 10ml fresh media. The phenotype was assessed by flow cytometry for surface markers at the indicated time points. Percentages are indicated within individual quadrants.

As before, omission of F(ab')$_2$ anti-IgG/M resulted distinct phenotypic differences between cells from the two conditions. A population of CD19^{++} CD20^{++} cells is once again present at day 6 of the differentiation when cells are cultured with R848 alone and it persists to day 13. Loss of CD20 appears to be impaired when the cells do not receive F(ab')$_2$ anti-IgG/M stimulation, with a considerable proportion of cells retaining CD20 expression at day 20 and to a lesser extent day 40 following omission of F(ab')$_2$ anti-IgG/M. Interestingly, B-cells that were cultured with R848 alone generated a population of plasma cells at day 6, whereas the B-cells that had received stimulation from both sources did not. This effect was also observed during dose response experiments, with cells stimulated with lower concentrations of R848 generating a greater proportion of CD38$^+$ CD138$^+$ cells at day 6 (figure 4.3). It appears therefore that a fraction of B-cells are particularly sensitive to low levels of stimulation and are primed to respond with increased alacrity, but this response is mitigated when the cells receive stimulation above a certain threshold. B-cells that were stimulated with both R848 and F(ab')$_2$ anti-IgG/M possessed a greater proportion of plasma cells at day 13, overtaking those that were cultured with R848 alone. Subsequently, differences in the proportion of plasma cells between the two conditions were lost and the expression of CD38, CD138 and CD27 was very similar. The fold change in cell number at each time point are presented in figure 4.7.

Healthy cells stimulated with 1µg/ml R848 +/- F(ab')$_2$ anti-IgG/M
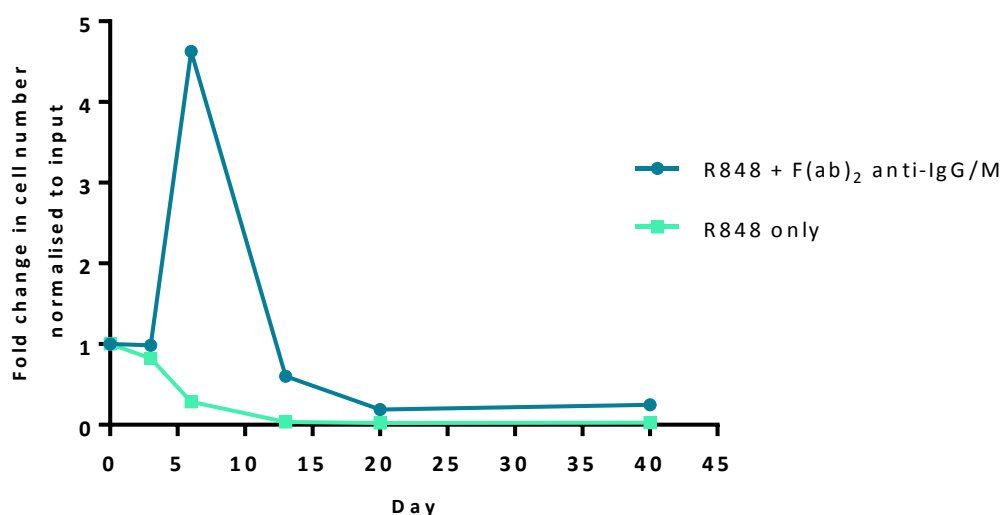
Figure 4.7 B-cells demonstrated no fold change increase in number following stimulation with R848 without the addition of F(ab')$_2$ anti-IgG/M. B-cells derived from the peripheral blood of a healthy donor (isolation protocol A+), with CD3/CD56 depletion were stimulated with 1µg/ml R848 +/- F(ab')$_2$ anti-IgG/M at day 0. Cells were washed at day 3 with 10ml fresh media. Cell number at each time point was determined by manual counts between days 0-6 and then by flow cytometry thereafter. The cell number at each point was normalised to the number of "input" cells for that specific donor obtained at day 0.

The variances in phenotype observed were accompanied by substantially different proliferative profiles. Cells stimulated with both R848 and F(ab')$_2$ anti-IgG/M demonstrated the classic profile, with steady cell numbers between day 0 and day 3, followed by an increase to day 6, a steep decline between day 6 and day 13 and then numbers stabilising to a plateau. However, cells activated with R848 alone declined in number at each successive time point. This is somewhat at odds with the phenotype – considering the increased proportion of plasma cells in this condition at day 6, it might be expected that the cells would have undergone a burst of proliferation but this does not appear to be reflected in the cell number. However, it may be that the cells underwent high levels of proliferation and subsequently died within a very short timeframe, such that the cell numbers at these early time points more closely resemble the latter stages of previous differentiations. The addition of F(ab')$_2$ anti-IgG/M to cells being stimulated with R848 thus alters the phenotype of the cells, slows the rate of differentiation and results in a greater population of cells at day 6.

4.3 The differentiation profile of healthy B-cells stimulated with R848

As with CD40L stimulations, it was important to collate data for multiple differentiations to establish an overall phenotypic and cell number profile for the cells following stimulation with R848. The cell numbers for nine independent differentiations that were cultured to day 28 are displayed in figure 4.8.

Healthy cells stimulated with R848 + F(ab')₂ anti-IgG/M
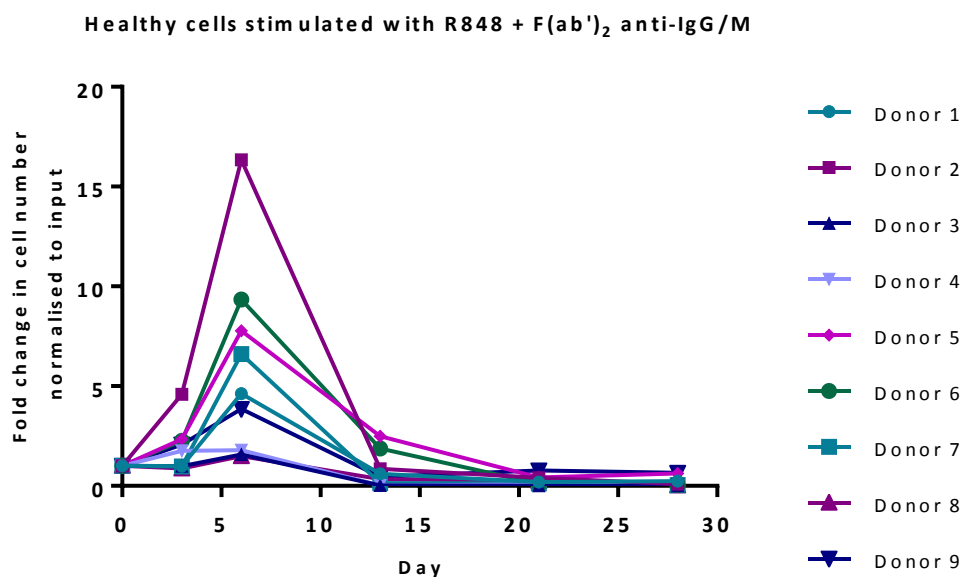
Figure 4.8 Healthy B-cells display a range change in cell number upon activation with stimuli mimicking a T-independent immune response. B-cells derived from the peripheral blood of healthy donors (isolation protocol A+ or B) were stimulated with 1µg/ml R848 and F(ab')₂ anti-IgG/M. Cells were washed at day 3 with 10ml fresh media. The cell number at each time point was determined by manual counts between days 0-6 and then by flow cytometry thereafter. The cell number at each point was normalised to the number of "input" cells for that specific donor obtained at day 0.

There was a more varied cell number profile for differentiations with R848 than was seen in differentiations with CD40L stimulation. In 6 of the 9 donors, similar to CD40L, cell numbers remained broadly the same or increased between day 0 and 3, followed by an increase in number to day 6. Donors 3 and 8 display a roughly equivalent overall profile, but the expansion in number is only twofold. The cells from donor 4 behaved differently, with an increase in cell number by day 3 but no further increase by day 6. The number of viable cells in culture subsequently fell for all donors and thereafter decreased slightly before reaching a plateau.

The profile of cell surface marker expression is depicted in figure 4.9. Despite greater variability in the amplitude of the B-cell proliferative response when cultured with R848 stimulation, each donor displayed a high level of phenotypic consistency across all of the differentiations. Downregulation of CD20 has commenced in all samples by day 6, and expression falls below 40% of the population after day 13, with the loss of this marker continuing as the differentiations progress. The upregulation of CD38 is extremely consistent across each independent differentiation, with approximately 90% of cells expressing this marker by day 6 and this rises to virtually all cells at the subsequent time point. The range of CD138 expression is slightly more variable for the donors between day 6 and day 20, but all follow the same pattern of

upregulation and only plasma cells remain at the latter time points. The upregulation of CD27 is very uniform and concurrent with the increase in CD38 levels.
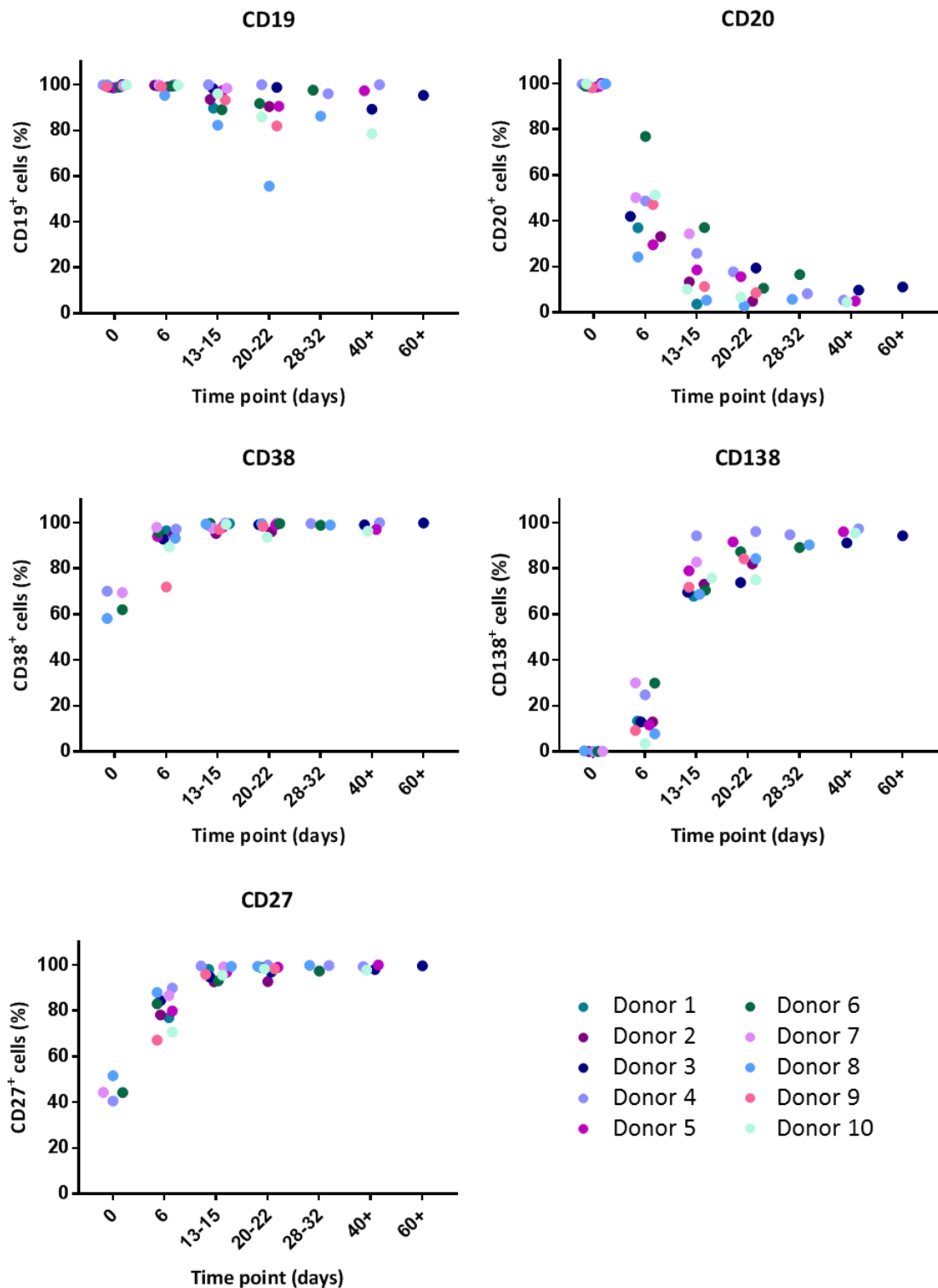
Figure 4.9 Scatter plot profiles for the expression of each CD marker assayed in multiple differentiations with healthy B-cells. B-cells derived from the peripheral blood of healthy donors were stimulated with 1μg/ml R848 and F(ab')$_2$ anti-IgG/M. Each scatter plot displays the percentage of live cells expressing the stated CD marker as determined at each time point via flow cytometry. Data from comparable intervals were grouped together for clarity. Each independent differentiation is represented by a different colour.

4.4 Comparison of responses to R848 with CD40L in healthy cells

Differences between stimulation with CD40L and R848 are clearly apparent during *in vitro* differentiations. In order to make a direct comparison of the response of B-cells to each of these stimuli, independent experiments with three different donors were performed, activating the isolated B-cells with either 1μg/ml R848 + F(ab')$_2$ anti-IgG/M or CD40L + F(ab')$_2$ anti-IgG/M. The cell numbers obtained for each condition are represented below in figure 4.10.

Healthy cells stimulated with CD40L vs R848
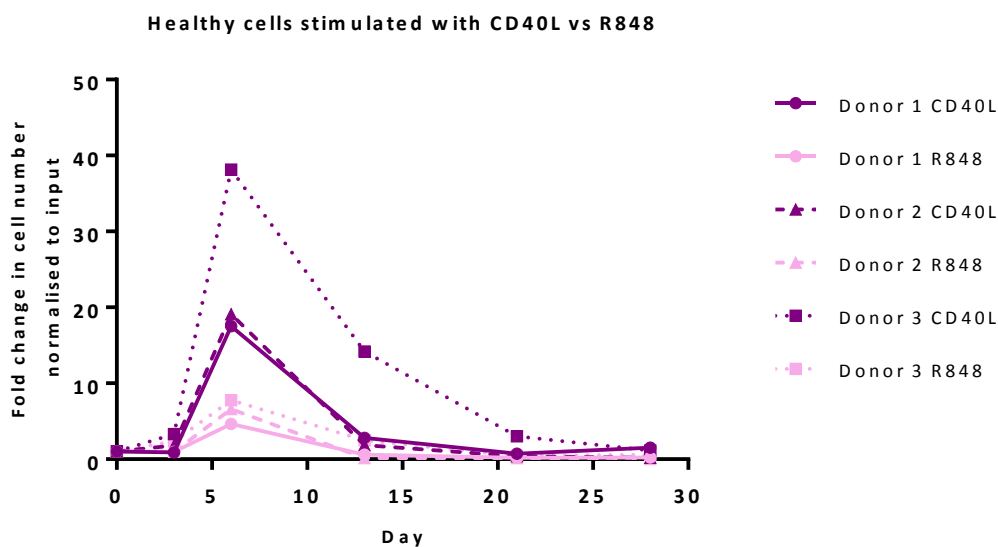
Figure 4.10 The amplitude of the proliferative response of healthy B-cells to R848 stimulation is considerably lower than for CD40L stimulation. B-cells derived from the peripheral blood of three independent healthy donors (isolation protocol B) were stimulated with either 1μg/ml R848 or CD40L and F(ab')$_2$ anti-IgG/M at day 0. Cells were washed at day 3 with 10ml fresh media. Cell number at each time point was determined by manual counts between days 0-6 and then by flow cytometry thereafter. The cell number at each point was normalised to the number of "input" cells for that specific donor obtained at day 0.

A stark contrast in the amplitude of proliferation was observed for each of the three donors. Cell numbers for both conditions increased between day 0 and 3, with a slightly higher average increase of 3.3-fold for CD40L stimulated cells compared to a 2.3-fold increase for those stimulated with R848. Subsequently, numbers increased in both conditions, but the observed increase for cells in the CD40L condition was almost 4x greater than that of cells stimulated by R848 - with an average of 24.9-fold increase for cells stimulated with CD40L and a 6.3-fold increase for those stimulated with R848. The difference between the amplitude of proliferation

that occurs from day 3-6 between the two types of stimulation are significant (unpaired Welch's t-test p = 0.0011).

Subsequent to day 6, there was a decline in cell numbers for both conditions before numbers stabilised thereafter. At day 28, cells which were stimulated with CD40L had generated on average 0.95 plasma cells per input cell and those stimulated with R848 had generated an average of 0.38 - a difference of 2.5-fold.

A representative phenotype from donor 1 is depicted in figure 4.11. The phenotype of the cells at each time point from each condition are presented side by side. In comparison to CD40L stimulation, B-cells activated with R848 generate a population of plasma cells more rapidly, with 24.8% of cells expressing both CD38 and CD138 at day 6 compared to 4.16% of CD40L-stimulated cells. The increase in CD27 expression is also more rapid, with >90% of R848-stimulated cells expressing this marker compared to 76.5% for those activated with CD40L. However, by day 13 of the differentiation, the phenotypic differences between the two conditions are no longer present.

At day 13, in both conditions, levels of CD20 expression have declined and the proportion of $CD38^+$ $CD138^+$ cells has increased to >90% of the total population, with virtually all cells having upregulated CD27 expression. The plasma cell population subsequently increases to >95% and is maintained in both conditions. Despite the variation in proliferation, both types of stimulation generate phenotypically identical plasma cells.
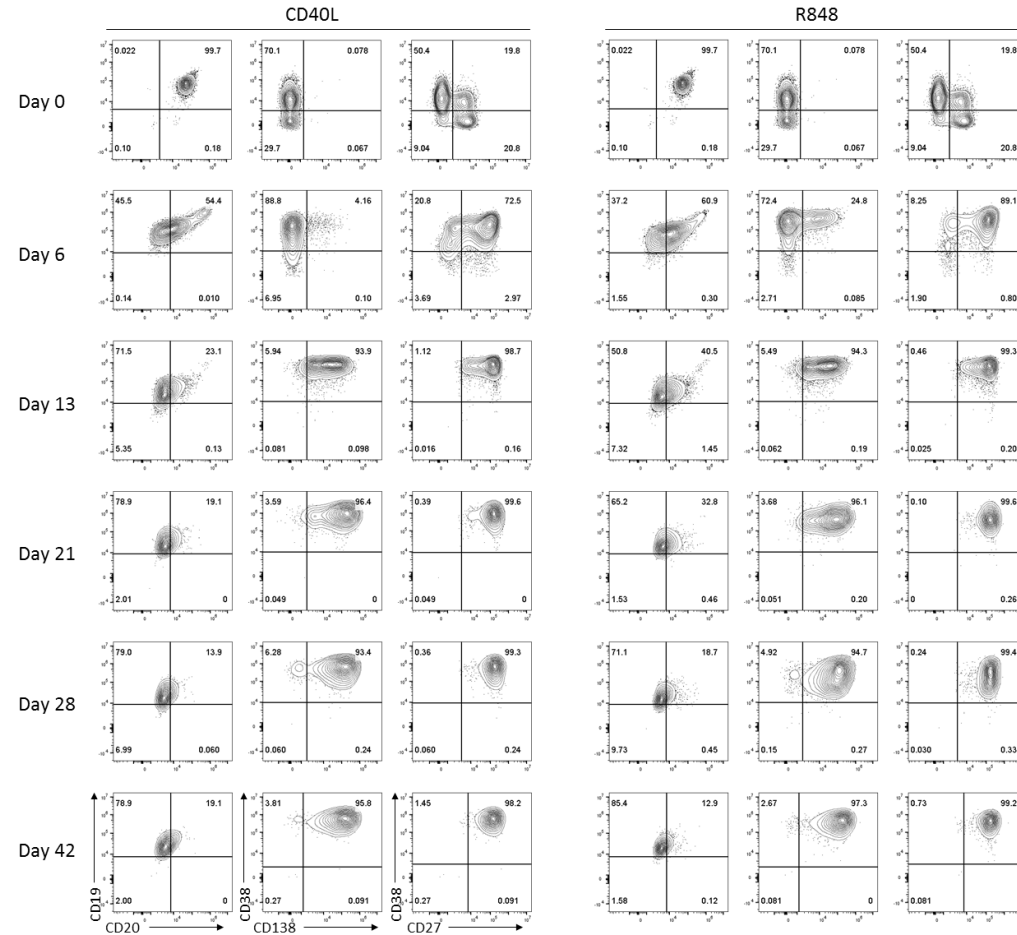
Figure 4.11 Differentiation of B-cells from a healthy donor with either CD40L or R848 stimulation. B-cells were isolated from the peripheral blood of a healthy donor (isolation protocol B) and stimulated with either CD40L or 1μg/ml R848 + F(ab')$_2$ anti-IgG/M. Cells were washed at day 3 with 10ml fresh media. The phenotype was assessed by flow cytometry for surface markers at the indicated time points. Percentages are indicated within individual quadrants. Gates were adjusted to compensate for increased background autofluorescence as the differentiation progresses. Representative phenotype from donor 1 (figure 4.10).

There are likely to be several factors contributing to the decreased proliferative response of B-cells following R848 stimulation. One is that memory B-cells expand preferentially in response to TLR ligation compared to their naïve counterparts (Bernasconi *et al.*, 2002; Bernasconi *et al.*, 2003). Memory cells comprise a smaller fraction of the total B-cell population (for example the donor in figure 4.3 has approximately 40% using CD27 as a marker of memory) and whilst they proliferate following TLR ligation, stimulation with CD40L + F(ab')$_2$ anti-IgG/M results in proliferation within both compartments and thus a greater contribution to the total number of day 6 cells generated. In addition to this, the stimulation provided by the CD40L-L cells constitutes an extremely potent activation signal. In contrast, the activation signals delivered through TLR7 appear to be more moderate.

Furthermore, activation with R848 generates a population of plasma cells more quickly than CD40L stimulation. Plasma cells exit the cell cycle, transitioning from the highly proliferative plasmablast stage and return to a state of quiescence. In the differentiation presented in figure 4.11, the pool of proliferating cells at day 6 has been reduced by 20% compared to the population of cells in the CD40L condition, implying that these cells will have stopped undergoing division before this time point and thus were not contributing additional numbers to the total population at day 6.

4.5   Response of WM B-cells to R848 stimulation

The rationale for investigation of the effects of TLR stimulation on WM B-cell differentiation stems from research conducted by Wang et al., and the Staudt group, both of which indicate that the MYD88^{L265P} mutation does not act independently to induce B-cell proliferation but instead requires signals from TLRs (Lim *et al.*, 2013; Wang *et al.*, 2014). These studies were not performed in primary human cells, but rather ABC DLBCL cell lines or murine B-cells transduced with the MYD88^{L265P} mutation, so the effect in WM primary cells has yet to be investigated. In order to address this, B-cells derived from the peripheral blood or bone marrow of patients diagnosed with WM were stimulated with 1µg/ml R848 + F(ab')$_2$ anti-IgG/M. The cell numbers obtained for these differentiations are displayed in figure 4.12.

WM cells stimulated with R848 + F(ab')$_2$ anti-IgG/M
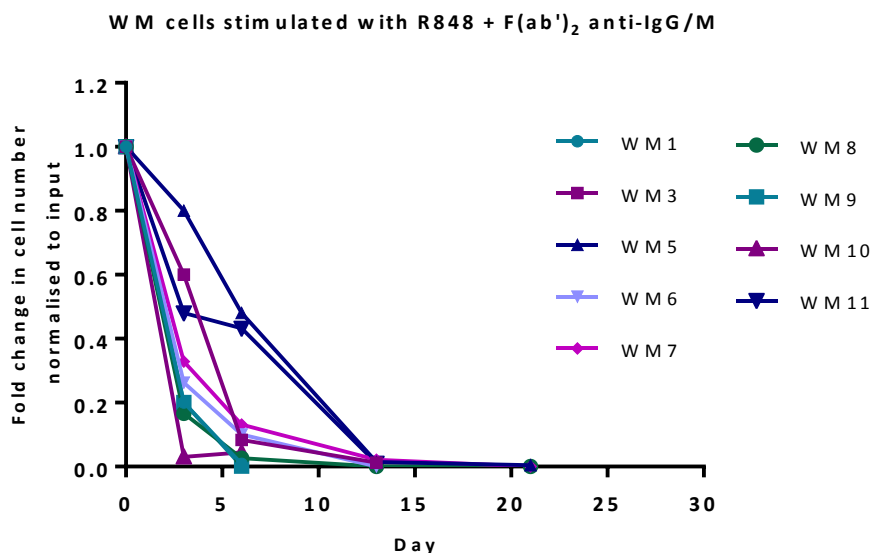
Figure 4.12 The number of WM cells rapidly declines subsequent to activation with stimuli mimicking a T-independent immune response. B-cells derived from the bone marrow of patients diagnosed with WM (isolation protocol B) were stimulated with 1μg/ml R848 and F(ab')$_2$ anti-IgG/M. Cells were washed at day 3 with 10ml fresh media. The cell number at each time point was determined by manual counts between days 0-6 and then by flow cytometry thereafter. The cell number at each point was normalised to the number of "input" cells for that specific patient obtained at day 0.

Most unexpectedly, WM cell numbers decreased for all samples at each successive time point, with the number of viable cells in culture falling to zero in most cases by day 13 of the differentiation. The most acute decrease in cell number occurred between day 0 and day 3 for all but two of the samples. A decrease in cell number between these time points was observed previously in patient samples stimulated with CD40L, but the proliferative phase between days 3 and 6 remained intact for these cells despite the initial drop in number. This is not the case for WM samples stimulated with R848, as no proliferation was observed in these samples and cell numbers continue to fall.

WM cells stimulated with R848 also displayed an impaired ability to differentiate. An example of the drastic differences in phenotype observed is provided in figure 4.13. A differentiation was performed with WM B-cells stimulated concurrently with either CD40L + F(ab')$_2$ anti-IgG/M or 1μg/ml R848 + F(ab')$_2$ anti-IgG/M. WM cells in receipt of CD40L stimulation successfully generated a population of long-lived plasma cells whereas cells stimulated with R848 were wholly unable to respond. These cells retained an undifferentiated phenotype, failing to lose expression of CD20 and failing upregulate CD38, CD138 or CD27.
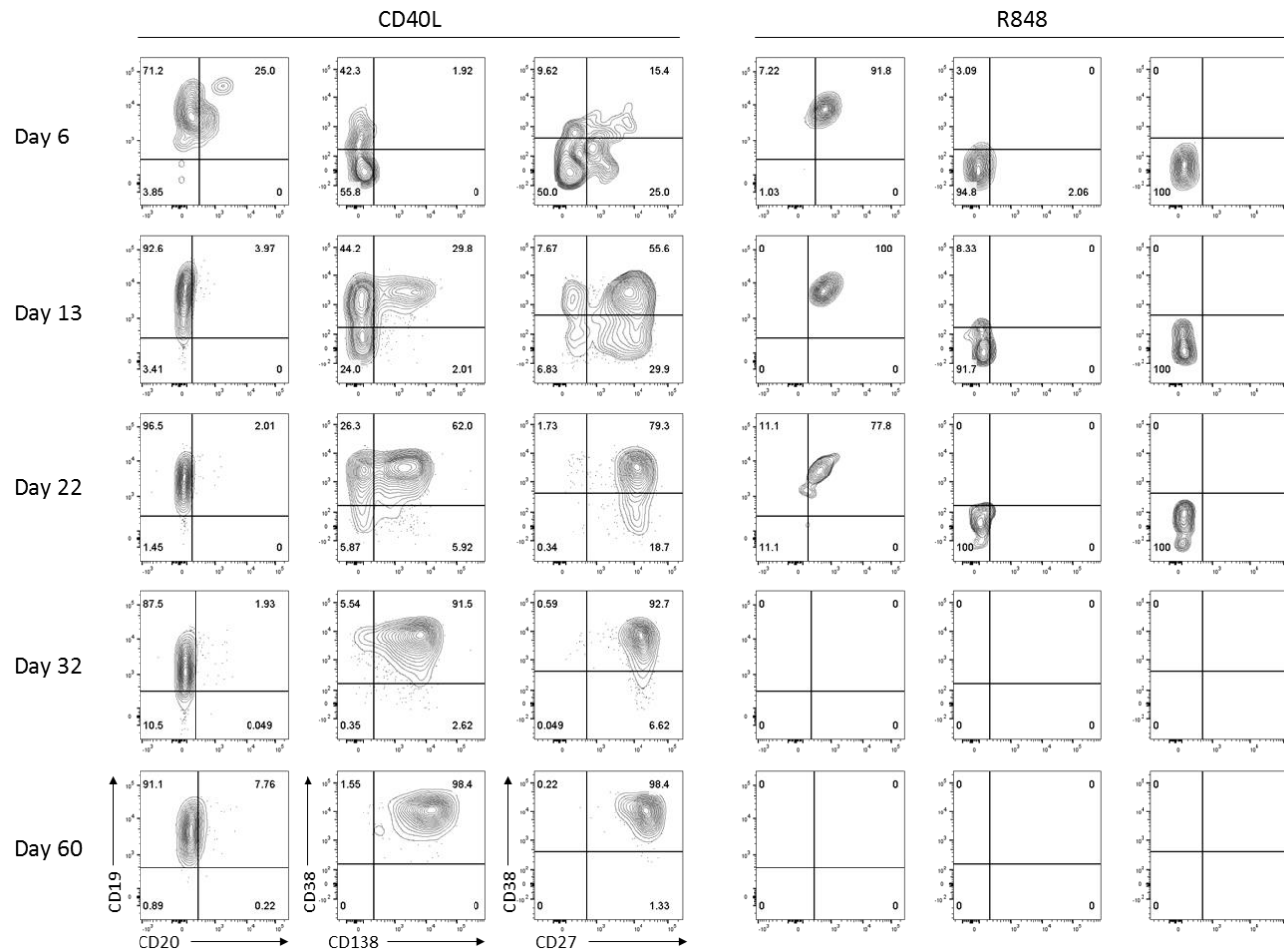
Figure 4.13 B-cells derived from a WM patient are able to differentiate into plasma cells following CD40L stimulation but are completely unable to respond to R848 stimulation.
B-cells were isolated from the bone marrow of a patient diagnosed with WM (isolation protocol B) and stimulated with either CD40L or 1μg/ml R848 + F(ab')$_2$ anti-IgG/M. The phenotype was assessed by flow cytometry for surface markers at the indicated time points. Percentages are indicated within individual quadrants.

Whilst the cells from this example demonstrated a complete inability to differentiate, a range of phenotypes were observed for WM cells stimulated with R848 + F(ab')$_2$ anti-IgG/M. Figure 4.14 illustrates the phenotypic profiles for 12 independent differentiations with WM samples.
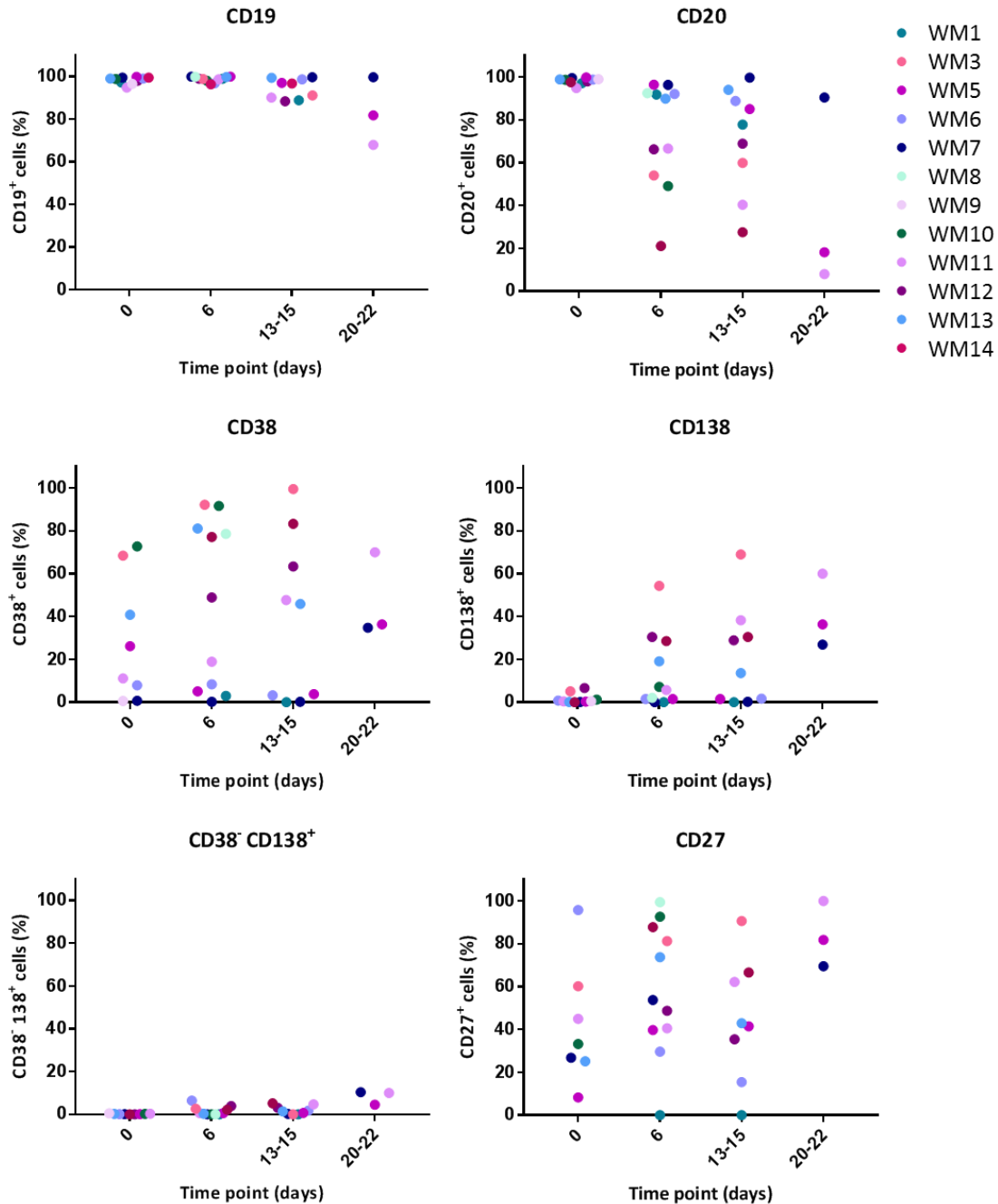
Figure 4.14 Scatter plot profiles for the expression of each CD marker assayed in multiple differentiations with WM B-cells. B-cells derived from the bone marrow of patients diagnosed with WM were stimulated with 1μg/ml R848 and F(ab')$_2$ anti-IgG/M. Each scatter plot displays the percentage of live cells expressing the stated CD marker as determined at each time point via flow cytometry. Data from comparable intervals were grouped together for clarity. Each independent differentiation is represented by a different colour.

The WM cells did not remain viable past days 13-15 for all but three of the differentiations and in several samples the cells did not persist past day 6. This therefore resulted in limited phenotypic data for some of these experiments.

From day 6 onwards, expression of CD20 was highly variable between all samples. In 5 of the 12 samples, expression of this marker decreased to 70% or below of the total population between day 0 and 6. The proportion of cells retaining expression of this marker for these five samples decreased further in some instances, but in others it did not. For the other 7 samples, high levels of CD20 expression (greater than 70% of the total population) were maintained to days 13-15. The WM cells exhibited a wide range of CD38 expression at day 0 and this variability continues across each time point. There is no discernible trend of increasing CD38 expression amongst the samples as the differentiations progressed, as would normally be expected, although the proportion of $CD38^+$ cells does increase in some samples, for example WM7.

Five samples generated a population of $CD38^+$ $CD138^+$ plasma cells comprising at least one quarter of the total surviving population at either days 13-15 or days 20-22 of the differentiation. The remaining WM cells either completely failed to upregulate this marker, or displayed only low levels of CD138 acquisition. Unlike WM cells that were stimulated with CD40L + F(ab')$_2$, there does not appear to be a population of $CD38^-$ $CD138^+$ cells. As with CD38, expression of CD27 varied considerably, with levels increasing in some samples and decreasing in others as the differentiation progressed.

A comparison of the immunophenotypic markers between WM and healthy cells subsequent to 1µg/ml R848 stimulation illustrates the different responses to this type of stimuli (figure 4.15). The expression of CD38 is significantly lower in the WM cells for each time point assayed ($p = <$ 0.05, t-test with Welch's correction). In addition to decreased levels of CD38 expression, WM cells demonstrate an impairment to plasma cell differentiation, expressing significantly lower levels of CD138 from day 13, by which time approximately 70% of healthy cells express this marker. The lack of a significant difference between the WM and healthy cells for CD20 and CD27 expression at day 20-22 may be explained by the survival of the non-neoplastic fraction of B-cells in the WM samples, contributing to a phenotype that more closely resembles that of the healthy cells.
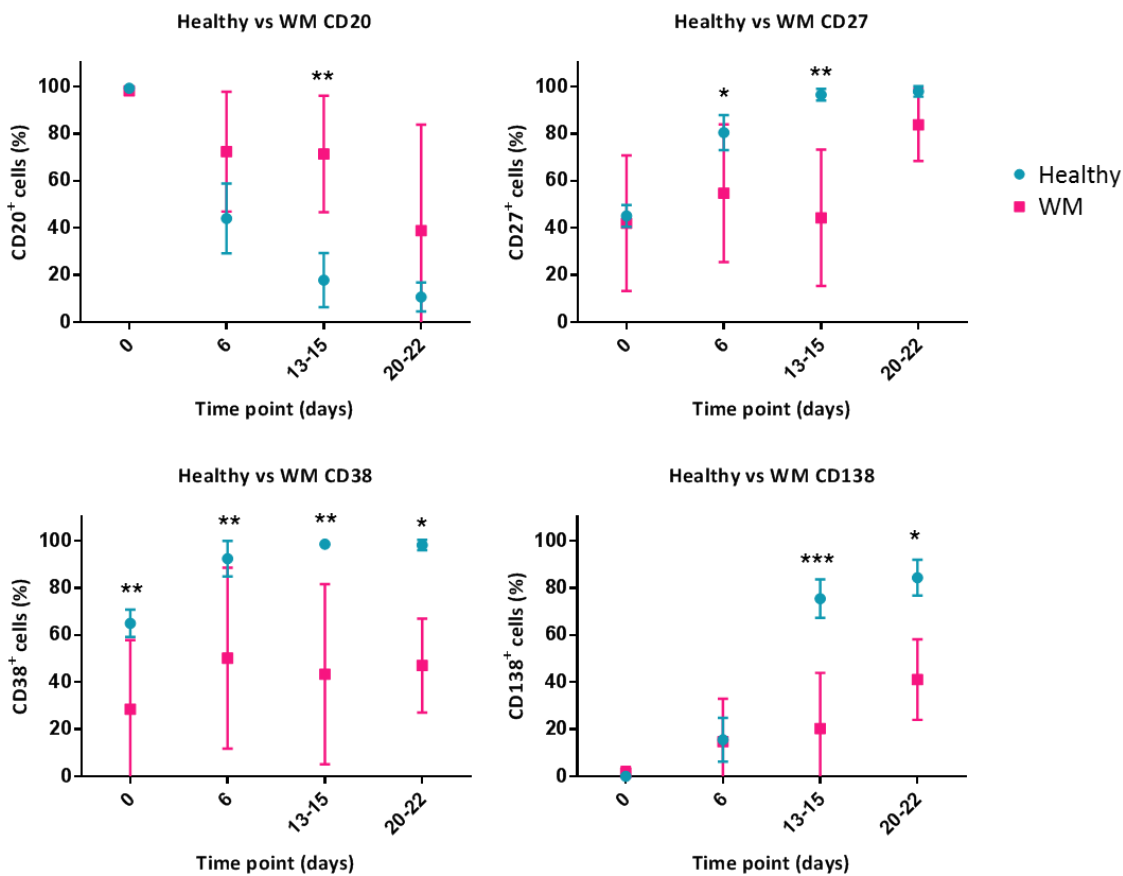
Figure 4.15 Comparison of the average expression of immunophenotypic markers between healthy and WM cells subsequent to 1µg/ml R848 + F(ab')$_2$ anti-IgG/M stimulation. B-cells derived from the bone marrow of patients diagnosed with WM or peripheral blood of healthy donor (isolation protocol B) were stimulated with 1µg/ml R848 and F(ab')$_2$ anti-IgG/M. Cells were washed with 10ml fresh media at day 3. Each plot displays an average of the percentage of live cells expressing the stated CD marker as determined at each time point via flow cytometry (healthy n = 9, WM n = 12). Values for WM expression significantly different from healthy samples are indicated – (*, $p < 0.05$, **, $p < 0.001$, ***, $p < 0.001$, t-test with Welch's correction). Error bars represent S.D.

There appeared to be a distinction between samples that were able to generate a population of plasma cells and those that were unable to do so. Therefore, the data from WM differentiations was stratified into two groups - those which generated a proportion of plasma cells that comprised at least 25% of the viable population during the course of the differentiation and those that were unable to do this. A comparison of the fold change in cell number is presented in figure 4.15 and the associated scatter plot profiles in figure 4.16.

WM cells stimulated with R848 + F(ab')$_2$ anti-IgG/M
(unable to generate plasma cells)

WM cells stimulated with R848 + F(ab')$_2$ anti-IgG/M
(generated plasma cells)
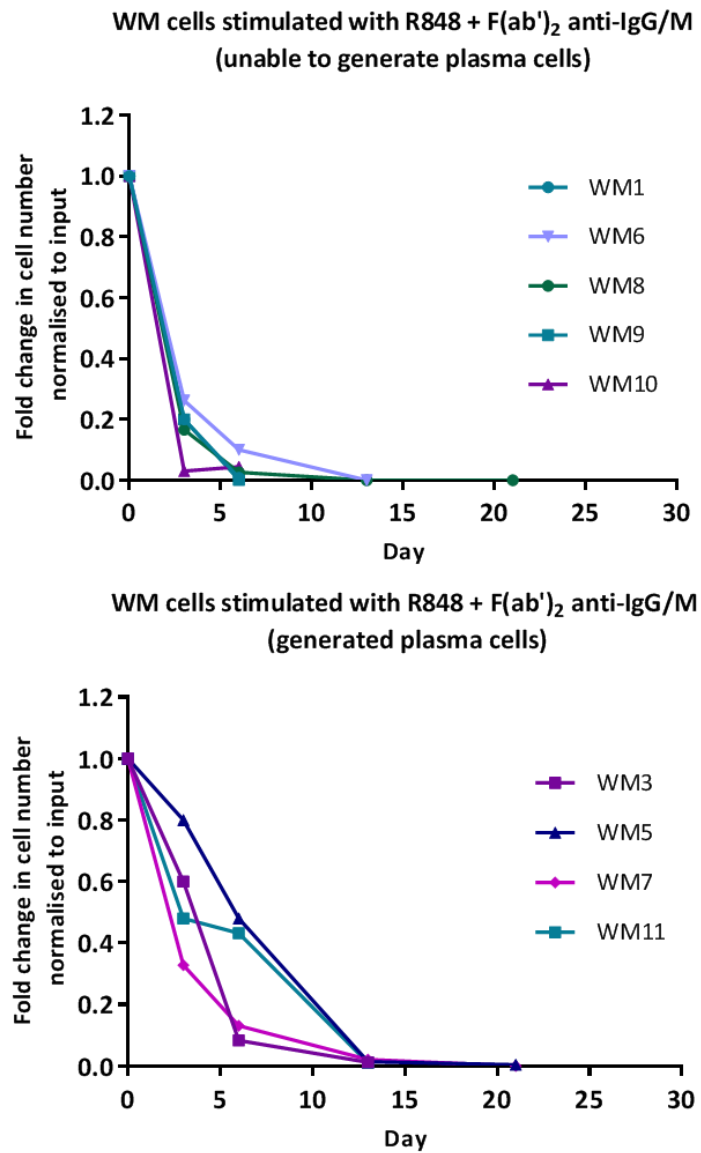
Figure 4.16 WM cell number declines more rapidly in samples unable to generate plasma cells. B-cells derived from the bone marrow of patients diagnosed with WM (isolation protocol B) were stimulated with 1µg/ml R848 and F(ab')$_2$ anti-IgG/M. Cells were washed with 10ml fresh media at day 3. The cell number at each point was normalised to the number of "input" cells for that specific patient obtained at day 0. Patient numbers correspond to those in figure 4.14 and 4.17.

It appears that the cell number in samples that are unable to generate plasma cells falls more steeply between day 0 and 3 than for samples which are able to differentiate into plasma cells. The fold change difference between the two groups at both day 3 and day 6 is significant (unpaired Students t-test $p = 0.006$, $p = 0.031$). This raises several possibilities; either the samples which were unable to respond contained a greater proportion of WM cells, perhaps these samples possess intrinsically lower levels of TLR7/8 or it may be that the signalling pathway is further perturbed in these samples in comparison to the rest of the patient cohort.
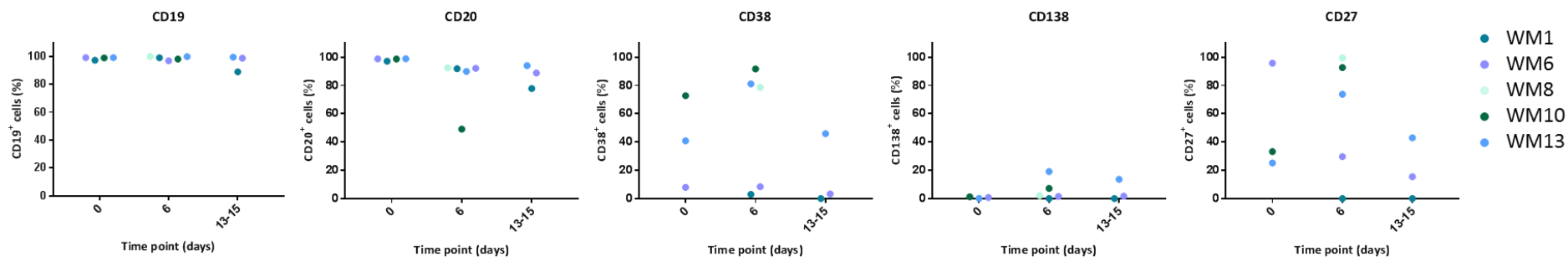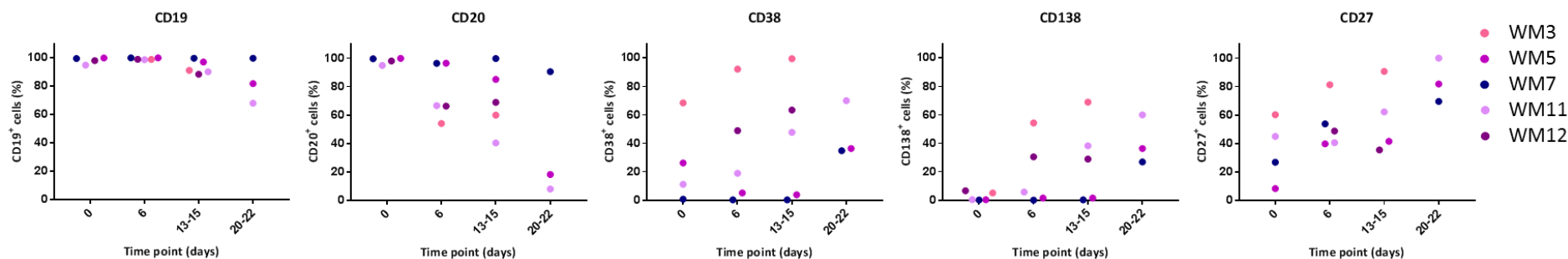
Figure 4.17 Scatter plot profiles for the expression of each CD marker in differentiations with WM cells divided into those which generated plasma cells and those that did not. B-cells derived from the bone marrow of WM patients were stimulated with 1µg/ml R848 and F(ab')$_2$ anti-IgG/M. Each scatter plot displays the percentage of live cells expressing the stated CD marker as determined at each time point via flow cytometry. The top set of plots display data from differentiations that produced fewer than 25% plasma cells and the bottom set represents those differentiations that generated plasma cells comprising >25% of the total population. Data from comparable intervals were grouped together for clarity. Each independent differentiation is represented by a different colour and the colours used to denote each patient are consistent with figure 3.

4.5.1 Differential response of individual populations within the total isolated WM B-cells

On several occasions, WM cells stimulated with 1µg/ml R848 + F(ab')$_2$ anti-IgG/M generated two phenotypically distinct populations that corresponded to differences in FSC and SSC characteristics, an example of which is illustrated in figure 4.18. These two diverging phenotypes appear to denote a fraction of B-cells that are able to differentiate (upper plots) and a second which does not (lower plots). The phenotype of the cells in the upper plots alters in a manner consistent with differentiation of these cells, with decreasing CD20 expression and increasing CD38, CD138 and CD27 levels from day 3 to day 14, in addition to a larger cell size. Whereas the cells that remain distinctly smaller on the FSC/SSC biaxial plots retain a B-cell-like phenotype (CD20$^+$ CD38^{low} CD138$^-$ CD27$^-$) for the entire time course. This phenomenon was not observed when WM cells were stimulated with CD40L + F(ab')$_2$ anti-IgG/M.

It is possible that the cells which retain the capacity to differentiate in response to stimulation with R848 are the un-mutated fraction as the total B-cells are not entirely comprised of the WM clone in each case. Since the WM and healthy cells are normally indistinguishable from each other by the surface markers assayed by flow cytometry in these experiments, the phenotype obtained comprises features from both populations. The WM cells were able to differentiate subsequent to CD40L + F(ab')$_2$ anti-IgG/M stimulation and thus any differences between the neoplastic and healthy cells would have been masked. However, if the WM cells do not proceed with differentiation but the healthy cells are able to do so, a similar divergence in phenotype would be expected to occur as seen here.
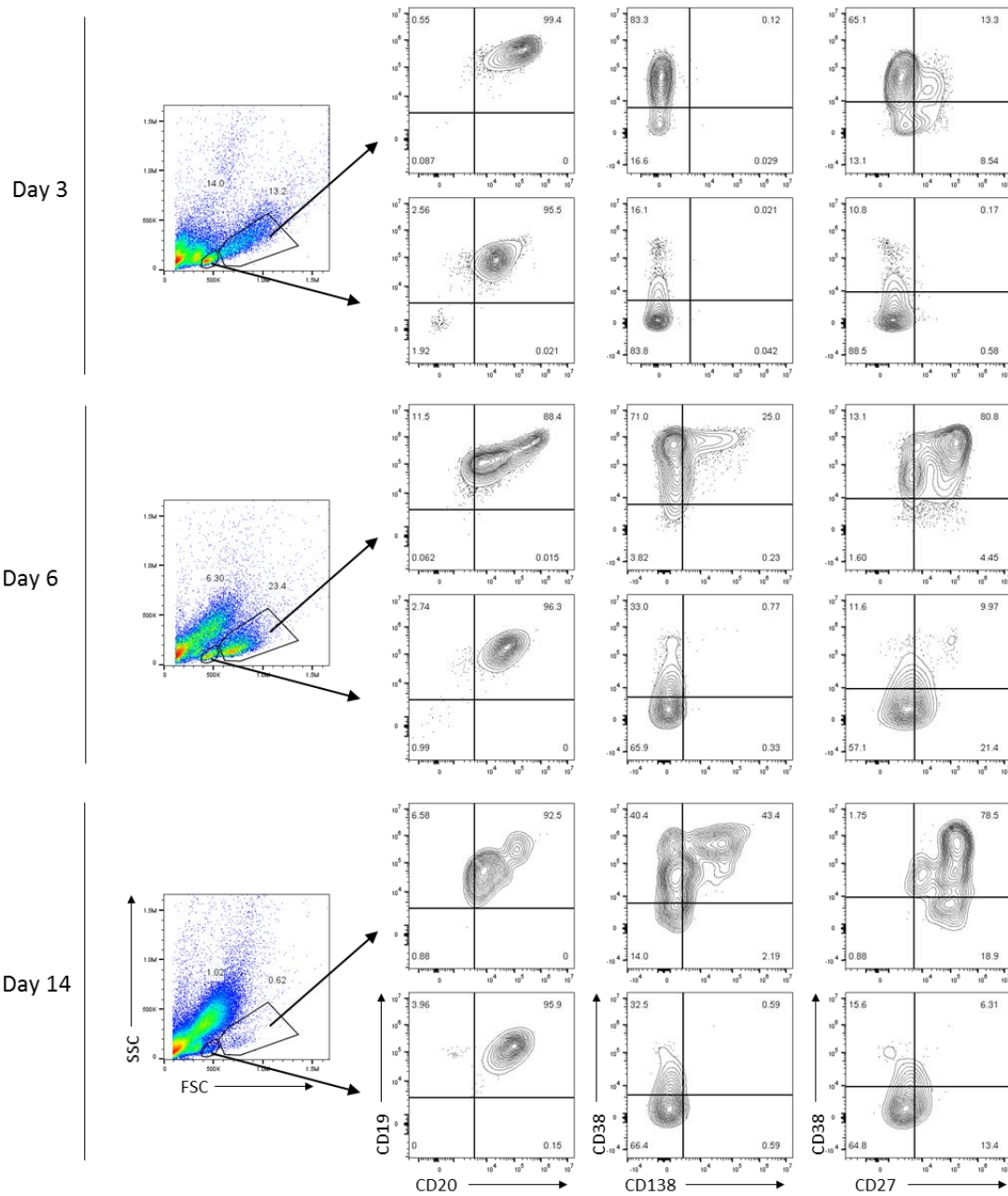
Figure 4.18 WM B-cells activated with R848 generate phenotypically distinct populations that can be discriminated based on FSC and SSC characteristics. B-cells were isolated from the bone marrow of a patient diagnosed with WM and stimulated with 1µg/ml R848 + F(ab')$_2$ anti-IgG/M. Populations were gated on FSC and SSC, with the phenotype of the larger subset presented on the top and that of the smaller subset on the bottom for each time point. Percentages are indicated within individual quadrants.

In summary, primary B-cells isolated from the bone marrow of WM patients demonstrate a profound impairment in plasma differentiation and survival subsequent to stimulation with the TLR7/8 agonist R848 + F(ab')$_2$ anti-IgG/M compared to B-cells derived from the peripheral blood of healthy donors. Whilst B-cells from healthy donors were successfully able to generate a population of long-lived plasma cells by day 13, WM B-cells produced only a small proportion of

plasma cells and in some instances, completely failed to differentiate (table 4.1). Concurrently, cell numbers fell and there was a deficiency in proliferation which normally occurs between days 3 and 6 in healthy samples.

Table 4.1 Comparison of the capacity of WM cells to proliferate and generate plasma cells subsequent to either CD40L or R848 stimulation. Only differentiations with phenotypic data up to at least day 13 have been included.

Patient	CD40L stimulation			R848 stimulation		
	Proliferation	Plasmablasts	Plasma Cells	Proliferation	Plasmablasts	Plasma Cells
1	-	-	-	No	No	No
3	No	Yes	Yes	No	Yes	Yes
4	Yes	Yes	Yes	-	-	-
5	Yes	Yes	Yes	No	Limited	Limited
6	Yes	Yes	Yes	No	Yes	No
7	Yes	Yes	Yes	No	Limited	Limited
8	Yes	Yes	Yes	No	Yes	No
9	Yes	Yes	Yes	No	No	No
10	-	-	-	No	Yes	No
11	-	-	-	No	Yes	Yes
12	-	-	-	*	Yes	Limited
13	-	-	-	*	No	No

* - Too few cells for accurate cell counts to be obtained

4.6   Discussion

Expression of TLRs on human B-cells is variable, with the memory B-cell fraction possessing intrinsically higher levels of TLRs, including TLR7, than the naïve subset (Hornung *et al.*, 2002; Bernasconi *et al.*, 2003). As a consequence, stimulation with a TLR agonist favours the expansion of the memory B-cell compartment (Bernasconi *et al.*, 2002). This accounts for a substantial proportion of the variability observed between the response to R848 and CD40L stimulations. *In vivo*, memory cells are primed to respond with increased alacrity to reinfection and thus the secondary immune response results in pathogen clearance more swiftly (Ahmed and Gray, 1996; Tangye *et al.*, 2003). Activation with R848 in the *in vitro* system results in the production of plasma cells more rapidly than with CD40L stimulation, recapitulating the *in vivo* response (figure 4.9).

Somewhat less expected was the significantly lower fold-change increase in cell number observed between days 3 and 6 of the differentiation following TLR stimulation versus that

which was observed following CD40L stimulation (figure 4.8). Memory B-cells initiate division earlier in response to stimulation and generate a greater number of cells (Tangye *et al.*, 2003). Thus one would anticipate that R848 stimulation might result in similar levels of proliferation overall due to preferential activation of the memory subset and their capacity to proliferate, even with reduced proliferation of the naïve population in response to this type of stimuli, but this was not the case. There are several factors that may contribute to this observation. Firstly, the proliferative response of the memory fraction to R848 stimulation may indeed be greater than the response to CD40L stimulation, but since they comprise approximately 20-40% of the total B-cell population, the resulting cell numbers compared to the total input would remain less unless a certain threshold of proliferation was passed (Morbach *et al.*, 2010). The *in vitro* culture system was optimised to generate the greatest number of viable cells following CD40L stimulation (Cocco *et al.*, 2012). The CD40L-L cells used to mimic a T-dependent response provide a powerful stimulation, surplus to that which is required for successful B-cell activation and both memory and naïve cells are more equally responsive so it is perhaps not surprising that the amplitude of proliferation across the differentiations with R848 stimulation are lower. It was noted by Simchoni and Cunningham-Rundles that stimulation with CD40L and IL-21 resulted in the proliferation of practically all cells within the memory and naïve subsets, whereas stimulation via TLR7 or TLR9 only induced proliferation in a smaller fraction of IgM^+ $CD27^+$ cells (Simchoni and Cunningham-Rundles, 2015). In addition to this, phenotypic R848 stimulation generates a population of plasma cells more rapidly than occurs subsequent to CD40L stimulation. The differentiation of this population removes them from the pool of proliferating cells, limiting their contribution to the overall number.

The total number of plasma cells generated compared to the input cells in a direct comparison between the two types of stimuli was lower after R848 stimulation (figure 4.10). But, in the same manner as those produced from CD40L stimulation, the plasma cells that were generated with R848 could be maintained for several months and thus are similarly long-lived.

Synergistic co-operation between BCR and TLR stimulation is well established (Coutinho *et al.*, 1974; Leadbetter *et al.*, 2002). Upregulation of TLR9 in the naïve B-cell subset was observed by Bernasconi et al., in response to BCR ligation, but it was not required by memory cells (Bernasconi *et al.*, 2003). This may explain why addition of F(ab')$_2$ anti-IgG/M has a greater impact when cells are stimulated with R848 compared to CD40L. The synergistic effect of BCR and TLR7 co-stimulation was observed here when F(ab')$_2$ anti-IgG/M was removed from the culture system and the cells were stimulated with R848 only. This resulted in a population of cells that retained a non-differentiated phenotype for an extended period of time (figure 4.5). The proportion of these unresponsive cells increased for the lower concentrations of R848,

implying that dual stimulation is vital to increase the sensitivity of cells to TLR ligation that would otherwise fail to initiate a differentiation response. Primary B-cells do not normally survive *in vitro* in an undifferentiated state and thus these cells must have been supported by a combination of TLR signalling and the cytokine milieu within the culture system to persist for a protracted period. However, these cells were eventually lost from the culture, either because the intrinsic apoptotic signals overcame the pro-survival signals or because the cells were ultimately able to differentiate, although the former appears more likely.

Due to the fact that the R848 is soluble, rather than provided by cell-cell contact as with the CD40L stimulation, the potential for carryover of residual compound is considerably greater. Three concentrations of R848 were tested and it became clear that prolonged TLR stimulation affected the phenotype of the cells, resulting in a delay in differentiation in a similar manner as occurs when B-cells receive continued CD40L stimulation (figure 4.1) (Randall *et al.*, 1998; Upadhyay *et al.*, 2014). This response appears to reflect a mechanism for TLR tolerance, whereby cells become unresponsive to additional TLR signals following exposure to chronic TLR stimulation (Poovassery *et al.*, 2009). An additional wash of the cells with 10ml fresh media at day 3 was sufficient to prevent this response from occurring (figure 4.2). Interestingly, B-cells exposed to the lowest concentration of R848 generated the greatest proportion of CD38$^+$ CD138$^+$ plasma cells by day 6 of the differentiation. This suggests that a small portion of B-cells, presumably from the memory fraction, are particularly sensitive to low levels of stimulation and demonstrate an enhanced response compared to the rest of the population.

Despite the phenotypic differences that occur during the early portion of the differentiations between the two types of stimulation, the divergence in phenotype is minimal from day 13 onwards. Ultimately, stimulation of healthy B-cells with R848, as with CD40L generates phenotypically identical plasma cells that comprise most, if not all, of the total population by day 20 of the differentiation and these cells can be maintained in culture long-term.

The most striking but unanticipated result presented in this chapter was the impaired response of WM B-cells to stimulation with R848 (figures 4.12 and 4.13). The initial reason to examine that effect of TLR stimulation on WM B-cells originated from the results presented by Lim *et al.* suggesting that MYD88^{L265P} cells still require TLR signals for proliferation and survival (Lim *et al.*, 2013). They demonstrated that MYD88^{L265P} binds constitutively to both TLR7 and TLR9 and that silencing of the TLR7/9 genes suppressed activation of the NF-κB pathway within the MYD88^{L265P} expressing ABC DLBCL cell lines OCI-Ly3 and OCI-Ly10 and promoted apoptosis, but had no effect on the MYD88^{WT} GCB cell line SU-DHL-6. Depletion of proteins responsible for the trafficking of TLR7 and TLR9 to endosome also proved to be lethal. In addition to this, they also assessed the

effect of a TLR9 suppressing inhibitory oligonucleotide, which abrogated NF-κB signalling and resulted in decreased survival of the ABC DLBCL cell lines.

Subsequently, data was published by Wang *et al.* that appeared to support the findings of Lim *et al.* (Wang *et al.*, 2014). They investigated the effect of the MYD88^{L265P} mutation by retrovirally transducing mutated *Myd88* alleles into activated murine B-cells that had previously been exposed to antigens. These cells were either cultured *in vitro* or adoptively transferred to Rag1 deficient mice. In the absence of B-cell mitogens, the MYD88^{L265P} bearing cells underwent multiple rounds of spontaneous proliferation. However, the MYD88^{L265P} population was not self-sustaining and the proliferation was limited by a negative feedback loop via the induction of TNFAIP3. In order to determine whether TLR signalling was a prerequisite for survival, they treated the cells with chloroquine, a compound which prevents endosomal acidification and proteolytic cleavage of TLR7 and 9 which is essential for their activation (Park *et al.*, 2008) and this, in turn, inhibited proliferation as did mutation of the TLR trafficking protein Unc93b1. Taken together, the results from these investigations indicate that signals via the TLR 7 and 9 signalling pathways must remain intact and are a prerequisite for the sustained proliferation and survival that is characteristic of MYD88^{L265P} B-cells *in vivo*. Thus, one might expect WM cells to demonstrate an enhanced response to TLR stimulation, with a combination of the intrinsic activation NF-κB via MYD88^{L265P} and additional *in vitro* ligation of this receptor with R848 + F(ab')$_2$ anti-IgG/M.

In contrast to this, when primary B-cells isolated from patients with WM were stimulated with 1µg/ml R848, they demonstrated both impaired survival and differentiation (figures 4.12 and 4.13). Cell numbers fell sharply between day 0 and 3 and continued to decline further thereafter. Whilst a decrease in number for WM cells was often observed when they were activated with CD40L, the cells were subsequently able to proliferate and cell numbers recovered between day 3 and day 6. Paired with the inability of the cells to survive subsequent to stimulation with R848 was a profound defect in the generation of plasma cells. Whilst activation with CD40L resulted in the generation of plasma cells in each sample by day 13-15, stimulation with R848 elicited the production of fewer plasma cells or in some cases none at all (figure 4.14).

In several instances, WM cells persisted with an undifferentiated B-cell phenotype in addition to a fraction of cells that were able to respond phenotypically (figure 4.18). It is possible that these WM cells are refractory to differentiation as they are already receiving the downstream signals normally initiated from TLR ligation but as a consequence of the MYD88^{L265P} mutation and are thus unresponsive when additional stimuli are provided. Whilst it is not possible to determine whether the fraction of WM cells that are able to respond to TLR7 ligation correspond to the proportion of non-neoplastic cells from the flow cytometry analysis presented here, this

remains a feasible explanation for the difference between the proportion of cells able to initiate the differentiation program and those that cannot.

The reasons underlying the negative effect of TLR7 signalling on WM cells are less clear but there are several possible explanations for the lack of survival of WM cells following R848 stimulation. It is possible that the WM B-cells are incapable of receiving the TLR signal, either due to the absence of TLR7 or an uncoupling of the signalling pathway. Without pro-survival signals provided by the binding of a cognate antigen or stimulation via TLRs, B-cells are programed to undergo apoptosis and a similar situation may be occurring here. Alternatively, it may be that the tonic survival signals provided by the constitutive activation of the NF-kB pathway are normally sufficient to endow enhanced survival of WM cells over their healthy counterparts, but that additional TLR signalling above this threshold triggers the activation of a negative feedback loop such as TNFAIP3, resulting in lethality.

Another hypothesis is that WM cells undergo T-cell independent activation induced cell death following TLR7 activation. Cells participating in the immune response are tightly regulated to prevent autoimmunity and limit inflammatory damage after pathogen clearance. During T-cell dependent responses, Fas expression on activated B-cells is upregulated, priming them for sensitivity to FasL-mediated apoptosis (Schattner *et al.*, 1995). R848 and F(ab')$_2$ anti-IgG/M stimulation may also result in the upregulation of surface expression of Fas, priming the WM cells for susceptibility to apoptosis. In addition, WM cells secrete BAFF which upon binding to TACI enhances the expression of Fas and FasL (Elsawa *et al.*, 2006; Figgett *et al.*, 2013). Binding of FasL may therefore initiate a profound pro-apoptotic signal which is able to overcome inhibitory signalling from BCR ligation and ultimately results in WM cell death. These will be investigated further in later chapters in an effort to further understand the response of WM cells to this type of stimulation.

The results presented here do not concur with the findings of Lim *et al*., 2013 or Wang *et al*., 2014 regarding the requirement of TLR signalling, but do corroborate with the more recent publication by Wang and colleagues (Wang *et al.*, 2016). They observed amplified levels of accumulation of MYD88^{L265P} transduced plasmablasts within the spleens of mice bearing a mutation to Unc93b1 following adoptive transfer. Unc93b1 is essential for trafficking of the TLRs to the endosomes and hence the TLR3, 7, 8 and 9 signalling pathways are abrogated in its absence (Kim *et al.*, 2008). Similarly, enhanced accumulation of MYD88^{L265P} plasmablasts also occurred subsequent to TLR9 deficiency. Following this line of thought, if the abolition of endosomal TLR signalling results in increased numbers of MYD88 mutated plasmablasts, it suggests that it is advantageous for these cells to be refractory to TLR ligation and one would

anticipate that the consequences of additional stimulation via the endosomal TLRs would have a detrimental impact on the MYD88^{L265P} cells and this is indeed the case.

Chapter 5 - Differentiation responses in other lymphoproliferative disorders and Schnitzler syndrome

5.1   Introduction

The preceding chapters have established the differentiation phenotype and cell number profile of WM and healthy B-cells following activation with stimuli mimicking either a T-dependent or a T-independent immune response. In order to determine whether the response of WM cells is unique or shares characteristics with other neoplasms, differentiations with B-cells from a selection of other lymphoproliferative disorders (LPDs) were performed to provide further comparison with WM cells. In particular, cells from individuals with splenic marginal zone lymphoma (SMZL) were examined as these patients present with similar symptoms to WM and they possesses related aetiologies. B-cells derived from bone marrow, peripheral blood or splenic samples were activated with CD40L + F(ab')$_2$ anti-IgG/M or R848 + F(ab')$_2$ anti-IgG/M and the response of the cells was assessed by flow cytometry.

In addition to this, the effect of these two types of stimulation on Schnitzler syndrome B-cells was also investigated. Schnitzler syndrome is a rare autoinflammatory condition and shares clinical features with WM such as monoclonal IgM gammopathy as well as involvement of the MYD88 signalling pathway in pathogenesis (Lim *et al.*, 2002). Individuals with Schnitzler syndrome are particularly prone to developing Waldenström's macroglobulinemia and thus may represent an intermediate between healthy controls and WM samples.

5.2   Differential diagnosis of WM

The differential diagnosis of WM is particularly difficult before information regarding the MYD88 mutation status is obtained and immunophenotyping is performed. Several patient samples were obtained that were expected to be WM but were later confirmed otherwise by diagnostic flow cytometry and detection of MYD88 mutation status by allele-specific oligonucleotide PCR (ASO PCR). These samples largely consisted of splenic marginal zone lymphoma with an IgM paraprotein, with one incidence each of mantle cell lymphoma and B-cell chronic lymphocytic leukaemia. In addition to the occurrence of IgM paraprotein, the presentation of patients with WM and SMZL can be similar, with incidences of splenomegaly, mucosal bleeding and cold agglutinin disease occurring in both cases (Thieblemont *et al.*, 2002; Owen *et al.*, 2003). The

similarities in these neoplasms provide an opportunity to examine the distinctiveness of the WM B-cell response within the *in vitro* system.

5.2.1   Marginal zone lymphoma

Three subtypes of MZL are recognised: nodal, extranodal and splenic (Norris and Stone, 2008). Since the majority of the additional LPD samples were from SMZL, they will be the main focus of this section, but the results from the other two neoplasms – one sample each of mantle cell lymphoma and B-cell CLL - will also be included in later analysis. Therefore the group as a whole will be termed "other LPDs" and the response of the subset of SMZL cells will be highlighted if they are of particular interest. SMZL is a rare, indolent lymphoma with splenic, bone marrow and PB involvement (Molina *et al.*, 2011). Low levels of monoclonal Ig, most commonly IgM, occur in approximately one third of patients affected (Matutes *et al.*, 2007; Traverse-Glehen *et al.*, 2011). The neoplastic cells consist of B-cells and activated B-cells located in the marginal zone which infiltrate the white pulp of the spleen, commonly resulting in splenomegaly (Thieblemont *et al.*, 2002). In addition, cells resembling centrocytes erode the mantle zone and invade the germinal centres, further disrupting the architecture of the spleen. The cell of origin in SMZL is postulated to be a marginal zone memory B-cell that has previously encountered antigen (Tierens *et al.*, 2003; Stamatopoulos *et al.*, 2004; Zibellini *et al.*, 2010).

Dysregulation of NF-κB signalling plays a key role in SMZL pathogenesis, with approximately one third of SMZL patients possessing mutations in NF-κB regulators within both the canonical and non-canonical pathways, including *IKBKB*, *TRAF3* and *MAP3K14 (Rossi et al., 2011).* Inactivating mutations in the transcription factor KLF are also common (20-40%), resulting in aberrant NF-κB activation by preventing its suppression (Clipson *et al.*, 2014; Piva *et al.*, 2014; Parry *et al.*, 2015). Whilst deregulated NF-κB signalling is a common feature of both SMZL and WM aetiology, the frequency of the MYD88[L265P] mutation in SMZL is low, with an incidence of approximately 6%-15% (Yan *et al.*, 2012; Varettoni *et al.*, 2013; Martinez-Lopez *et al.*, 2015).

The capacity to differentiate into plasma cells appears to be conserved in a large proportion of SMZL cases, with observations in the literature ranging from 21-74% (Mollejo *et al.*, 1995; Hammer *et al.*, 1996; Van Huyen *et al.*, 2000; Dufresne *et al.*, 2010). It is expected therefore that there will be varying degrees of differentiation amongst these samples following stimulation in the *in vitro* system.

5.3   Differentiation profiles from non-WM lymphoproliferative disorders

Having established the response of WM B-cells to stimulation with CD40L, the next key question to address was how the responses of B-cells derived from patients with other lymphoproliferative disorders compared. B-cells were isolated from each sample and stimulated with CD40L + F(ab')$_2$ anti-IgG/M as described previously. A summary of clinical information for these patients is provided in table 3.2 accompanied by the capacity of B-cells from each sample to generate plasmablasts or plasma cells after culture within the *in vitro* system. All samples were negative for the MYD88^{L265P} mutation as determined by ASO PCR. Several samples were bone marrow aspirates (table 5.1), similar to the type of samples used from WM patients. In differentiations performed with WM BM samples, it appeared that if there was an extended amount of time between when the sample was collected and when an *in vitro* experiment was initiated, cell viability was negatively impacted. Additional samples that have been prepared and stored in the same manner provide further reference as to the effects on cell survival and differentiation of both the sample source (bone marrow vs. blood) and the delay between sample collection and initiation of the differentiation experiment.

Table 5.1 Clinical data and differentiation capability of B-cells isolated from LPD patients with CD40L + F(ab')$_2$ anti-IgG/M stimulation. PB, peripheral blood. BM, bone marrow.

Patient	Sample type	Diagnosis	Culture length (days)	Plasmablasts	Plasma Cells
1	Spleen	SMZL	0-6	Yes	No
2	PB	SMZL	0-28	No	No
3	BM	Mantle cell	0-13	Yes	Yes
5	BM	SMZL	0-15	Yes	Limited
5	PB	SMZL	0-15	Yes	Yes
6	PB	SMZL	0-28	Yes	Yes
7	BM	SMZL	0-28	Yes	Limited
8	BM	B-cell CLL	0-28	Yes	Yes
9	BM	SMZL	0-6	Yes	No

The phenotypic profiles for each of these differentiations is depicted in figure 5.1.
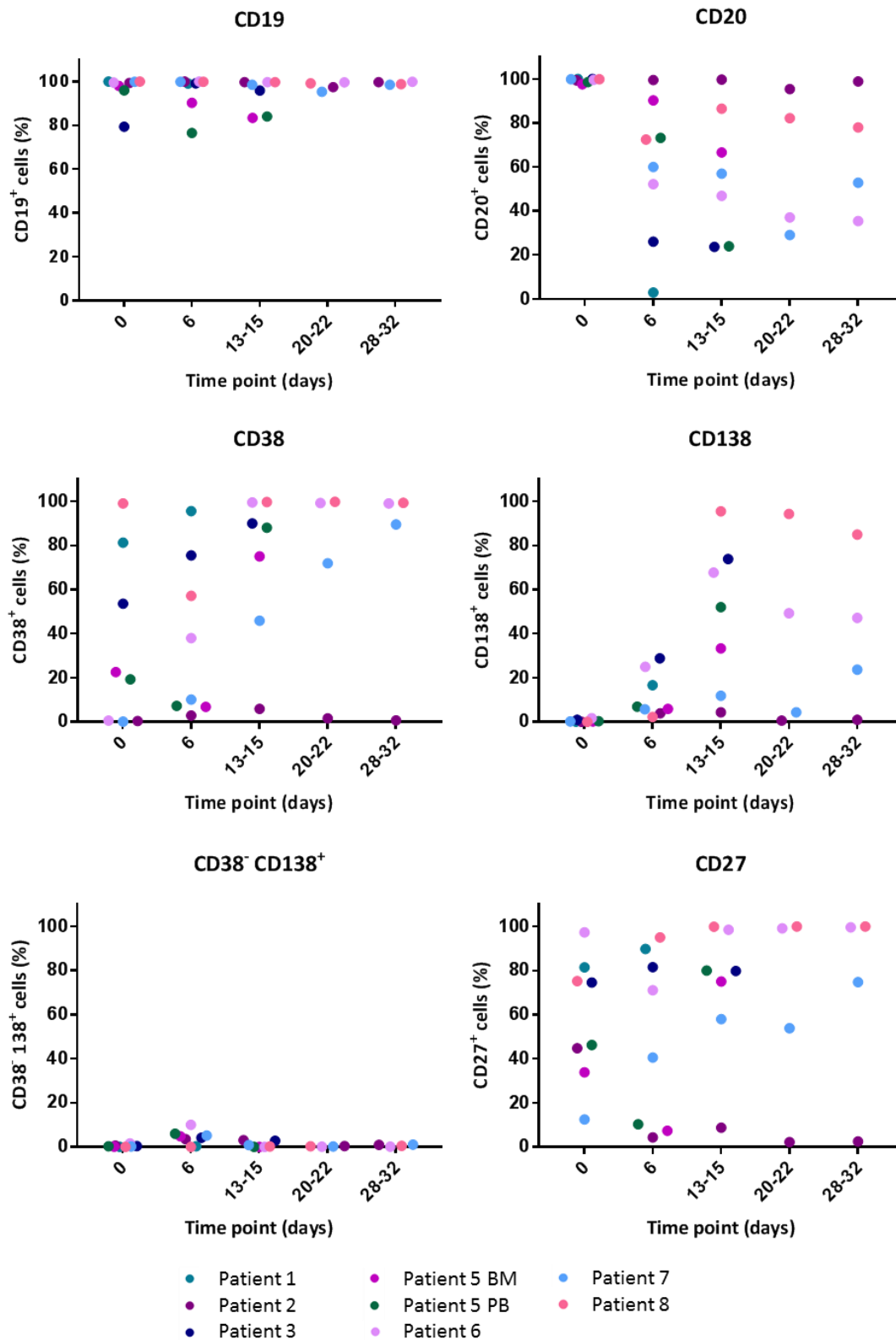
Figure 5.1 Scatter plot profiles for the expression of each CD marker assayed in multiple differentiations with B-cells isolated from patients with LPDs. B-cells derived from the bone marrow, PB or spleen of patients with various LPDs (isolation protocol B) were stimulated with CD40L and F(ab')$_2$ anti-IgG/M. Each scatter plot displays the percentage of live cells expressing the stated CD marker as determined at each time point via flow cytometry. Data from comparable intervals were grouped together for clarity. Each independent differentiation is represented by a different colour.

The expression of each marker, with the exception of CD19, was highly variable between the samples, as was the extent to which they were able to differentiate. For example, the cells derived from a peripheral blood sample from patient 2, denoted in purple in the scatter plots, were completely unable to differentiate. These cells retained the B-cell phenotype throughout the entire culture period, with an absence of upregulation of CD38, CD138 or CD27. In contrast, B-cells from patient 8 were able to differentiate successfully following CD40L + F(ab')$_2$ anti-IgG/M stimulation, generating a population of plasma cells by days 13-15. The samples from patient 5 consisted of a matched bone marrow and peripheral blood sample. Unfortunately, the cells from this patient were no longer viable after day 13. However, assessment of the phenotype at the three time points shown indicates that cells from both samples were able to differentiate. Interestingly, B-cells from the peripheral blood displayed a more differentiated phenotype at day 13, with fewer than 30% of cells retaining CD20 expression compared to almost 70% in cells derived the bone marrow and 20% more cells expressing CD138 at this time point. The difference in phenotype may reflect an increased disease burden within the bone marrow compared to the peripheral blood. A very small proportion of CD38$^-$ CD138$^+$ cells appear to be present at day 6 in some samples but this is due to a greater spread of negative expression in these samples at this time point compared to the healthy controls and isotypes used determine the gates on the biaxial plots and not evidence of a true CD38$^-$ CD138$^+$ population. Subsequently, there is no evidence that any of these samples generate CD38$^-$ CD138$^+$ cells.

The LPDs do share some phenotypic features with the WM cells subsequent to stimulation with CD40L + F(ab')$_2$ anti-IgG/M. The pattern of CD20 retention in the cells is very similar in both WM and the other LPDs, with a broad range of expression throughout the time course, with some samples demonstrating downregulation of this marker and others retaining it. Expression of CD38 is also comparable between the LPDs and WM, with expression increasing in general, although patient 2 was completely unable to upregulate this marker, CD138 or CD27. The similarity in CD38 expression across the various neoplasms is in part due to the proportion of WM cells that acquire the alternate plasmablast-like phenotype of CD38$^-$ CD138$^+$. If one omits these samples when examining overall CD38 expression, then the other WM samples upregulate CD38 more swiftly and to a greater extent than the LPDs do. The generation of plasma cells and expression of CD138 is considerably less consistent between the WM and LPD samples, with all WM samples increasing expression of this marker, but a more mixed response of the LPD subset, with samples from patients 6 and 8 generating considerably more plasma cells than the other LPD samples. The expression of CD27 is more highly variable in the LPD group, again with a large range of expression, whereas the WM cells uniformly upregulated this marker to >90% between day 6 and day 13 of the differentiation.

Figure 5.2 displays the fold change in cell number for 8 of the 9 differentiations. The number of B-cells isolated from the samples of BM and PB from patient 5 were very low so accurate counts could not be determined.

O ther LPDs stim ulated w ith CD40L + F(ab')$_2$ an ti-IgG/M
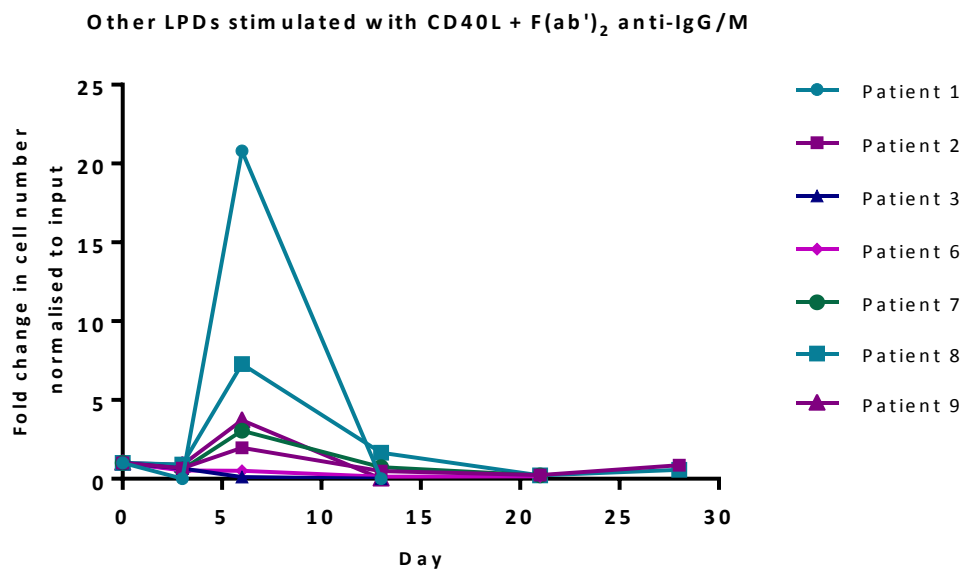
Figure 5.2 The change in cell number following B-cell activation with stimuli mimicking a T-dependent immune response in samples derived from patients with LPDs is highly variable. B-cells derived from either the peripheral blood, bone marrow or spleen of patients with LPDs that were not WM (isolation protocol B) were stimulated with CD40L and F(ab')$_2$ anti-IgG/M. Cell number at each time point was determined by manual counts for days 3 and 6 and then by flow cytometry thereafter. The cell number at each point was normalised to the number of "input" cells for that specific patient obtained at day 0. Patient numbers are consistent with figure 5.1.

The proliferative response of the LPD-derived B-cells did not necessarily match their capacity to differentiate. B-cells from patients 3 and 6 were successfully able to generate successive populations of plasmablasts and plasma cells, but the plasmablast transition was not accompanied by an increase in cell number as is observed for both healthy and WM cells. Other samples such as that of patients 1, 7 and 8 demonstrated a cell number profile which more closely resembles that of healthy cells, with an increase in cell number between days 3 and 6 followed by a sharp decline thereafter. Due to the decrease in numbers from day 0 to day 3, the fold change in number of cells for patient 1 between days 3 and 6 was approximately 60-fold – considerably greater than that which was observed in healthy cells. Surprisingly, despite the extensive proliferation, all the cells subsequently died between day 6 and day 13. This could be

due to exhaustion of the cells after undergoing such an intense period of proliferation or may indicate a reliance on IL-2, which is removed from the culture from day 6 onwards.

A decrease in cell number was observed in all samples, which consisted of bone marrow, peripheral blood and one splenic sample, between days 0 and 3. This corresponds to the results observed in differentiations with WM samples. The difference in the average fold change in cell number at day 3 between the WM and LPD samples was not significant, but the difference between the healthy samples and either the WM or LPD samples at this time point was highly significant in both instances (adjusted p-value for multiple t-tests $p < 0.005$). Whilst this effect cannot be solely attributed to the differing methods of sample collection and storage, it seems likely that it is a major contributing factor at this early time point. These data indicate that the delay between sample acquisition and differentiation does have a knock-on effect on the numbers of viable cells and that efforts should be made to minimise the length of time samples are in storage to optimise results.

In summary, differentiations performed on B-cells derived from patients with an assortment of LPDs that were not WM generate a wide variety of phenotypes, ranging from the complete absence of differentiation to samples which generate populations of plasma cells within a comparable time scale to healthy cells. When compared to the phenotypes and cell numbers observed here, WM B-cells are considerably more proficient at generating plasma cells, and these cells are sustained for longer and with greater numbers during *in vitro* culture, in line with their capability *in vivo*. The capacity of B-cells from several of the LPD patients to differentiate is clearly compromised, mirroring the impairment of these neoplasms *in vivo* (Van Huyen *et al.*, 2000; Swerdlow *et al.*, 2016). The inability of patient B-cells to undergo differentiation underscores that B-cells placed into the *in vitro* culture system are not able to spontaneously overcome inherent defects resulting from neoplastic transformation, despite being provided with stimulation and an environment conducive to differentiation. No evidence of a $CD38^-$ $CD138^+$ population akin to that of the WM samples was observed in any of the differentiations with LPD B-cells, indicating that the plasmablast-like intermediate phenotype may be restricted to WM cells.

5.4   Response of LPD B-cells to TLR7 stimulation

Where possible, concurrent differentiations were performed with both CD40L + F(ab')$_2$ anti-IgG/M (figure 5.2) and R848 + F(ab')$_2$ anti-IgG/M for the LPD B-cells to enable direct comparison between both types of stimulation. The normalised fold change in cell numbers for R848-stimulated cells are depicted in figure 5.3.
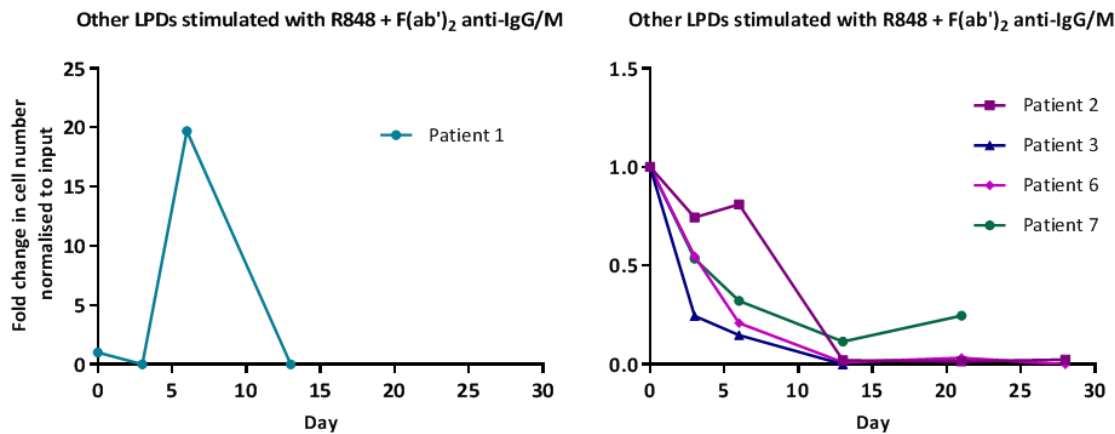
Figure 5.3 B-cells from LPDs display variable fold-changes in cell number upon activation with R848. B-cells derived from the bone marrow, peripheral blood or splenic samples of patients with diagnosed LPDs (isolation protocol B) were stimulated with 1µg/ml R848 and F(ab')$_2$ anti-IgG/M. Cells were washed with 10ml fresh media at day 3. The cell number at each time point was determined by manual counts between days 0-6 and then by flow cytometry thereafter. The cell number at each point was normalised to the number of "input" cells for that specific individual obtained at day 0.

The response of B-cells from the LPDs to R848 stimulation was highly variable but can broadly be divided as above, with only the cells from patient 1 demonstrating a substantial proliferative response. The most common response, occurring in three of the six samples was a decrease in cell number at each subsequent time point in a similar manner to that which was observed for WM cells, with slightly different dynamics observed for patients 2 and 7. Data from patient 1 were excluded from the statistical analysis of the fold change profiles due to the considerable deviation in proliferation dynamics to the other LPD samples. The average fold change in number for the remaining five LPDs was used to compare with the averages obtained for the WM samples as a whole and when the WM samples had been stratified into two groups based on their capacity to generate plasma cells as per chapter 2. Whilst the profile of the LPDs is not significantly different compared to the entire group of WM samples or the subset that demonstrated some differentiation following R848 stimulation, it was statistically significant compared to the fold change that occurred in WM samples that were unable to differentiate at day 3 and at day 6 ($p < 0.01$ and $p < 0.05$ respectively, two-tailed unpaired t-test with Welch's correction). This suggests that whilst LPDs in general may respond poorly to TLR7 stimulation, approximately half of the WM samples demonstrate a considerably worse response in terms of cell number and survival.

It would thus appear that the response of WM cells is actually very similar to other LPDs following R848 stimulation. However, when the response of the two worst responding LPDs –

LPD patient 3 and 6 – to R848 are examined further and compared to their matched CD40L-stimulated counterparts, a different picture emerges. The cell number profiles for these two LPDs subsequent to stimulation with either CD40L or 1µg/ml R848 + F(ab')$_2$ anti-IgG/M are shown in figure 5.4 with two WM samples for comparison.
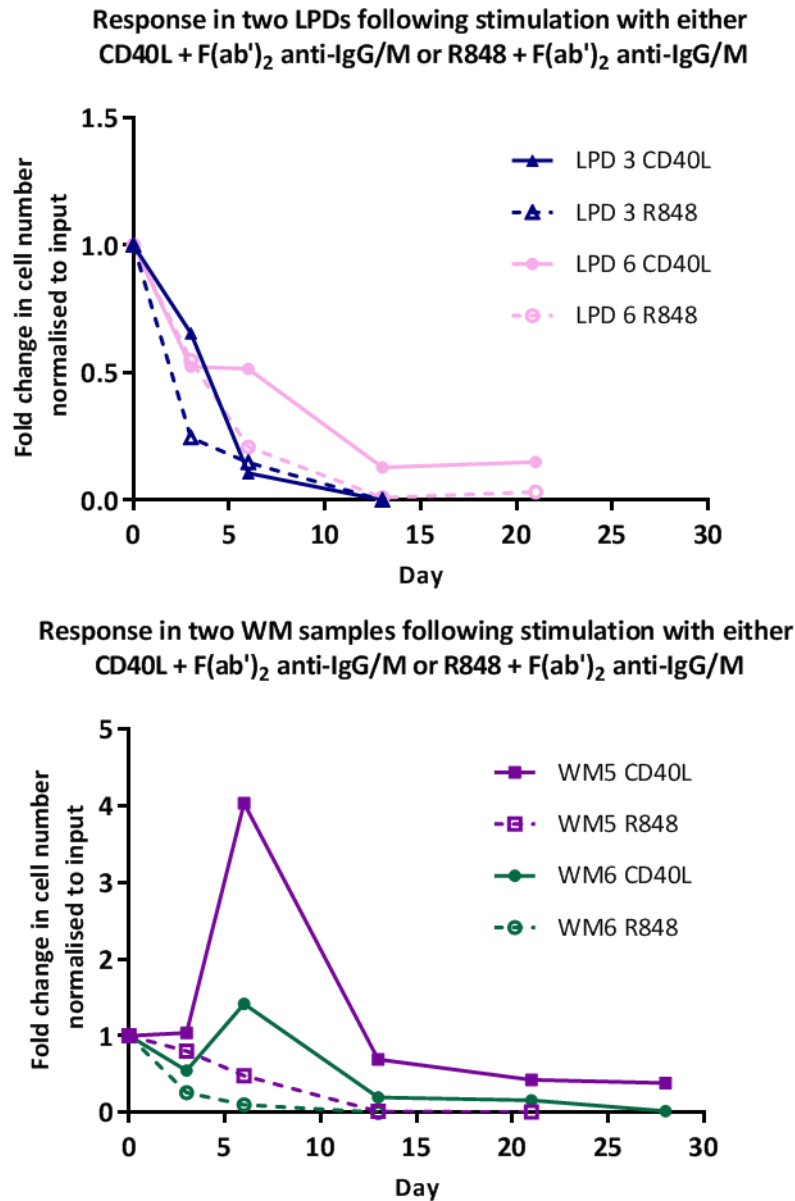
Figure 5.4 WM cells display distinct fold-change profiles subsequent to each type of stimulation whereas the poorly responding LPDs do not. B-cells derived from the bone marrow or peripheral blood of patients with diagnosed LPDs (top) or WM (bottom) were stimulated concurrently with either CD40L or 1µg/ml R848 and F(ab')$_2$ anti-IgG/M (isolation protocol B). Cells were washed with 10ml fresh media at day 3. The cell number at each time point was determined by manual counts between days 0-6 and then by flow cytometry thereafter. The cell number at each point was normalised to the number of "input" cells for that specific individual obtained at day 0.

This demonstrates that, in fact, these LPD samples responded very poorly in terms of proliferation to both types of stimulation. In contrast, the WM cells successfully responded to CD40L stimulation, with a peak in proliferation coinciding with transition to the plasmablast stage but B-cells differentiated simultaneously showed a severely impaired response following R848 stimulation.

The corresponding phenotypes obtained at each time point are displayed in figure 5.5. There are no general trends that can be applied to all of the samples as they behave quite differently from one another. However, only B-cells from one sample – that from patient 6 – were successfully able to generate plasma cells. This is in contrast to the phenotypes obtained when the cells were stimulated with CD40L, in which all but one sample exhibited some ability to generate plasma cells. There is some evidence of differentiation in the sample from patient 7, with decreasing CD20 expression and increasing CD38 and CD27 levels, however these B-cells are unable to generate plasma cells, with virtually no CD138 expression by the latest time point assayed.
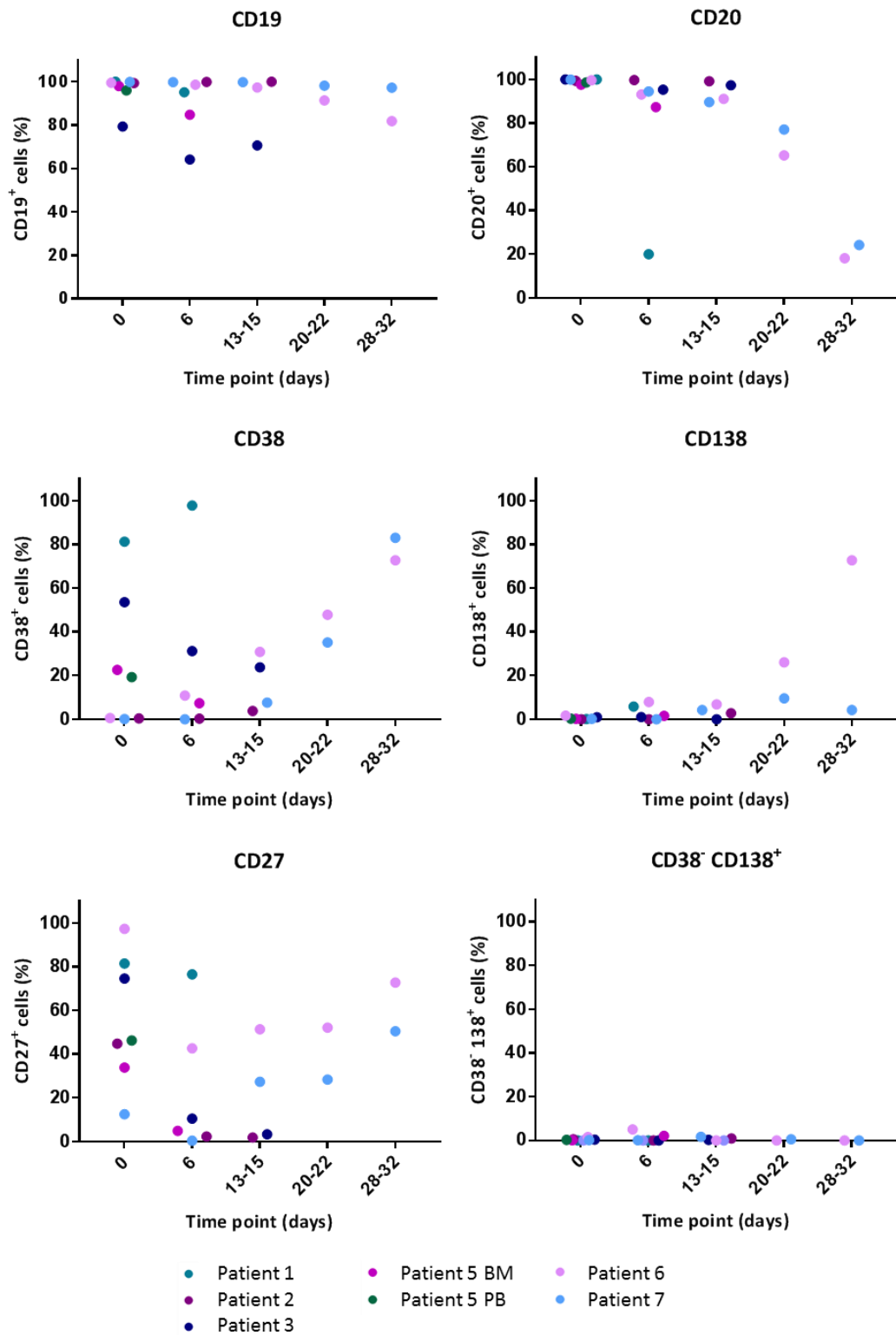
Figure 5.5 Scatter plot profiles for the expression of each CD marker assayed in multiple differentiations with B-cells from various LPDs. B-cells derived from the bone marrow, peripheral blood or splenic samples of patients with LPDs were stimulated with 1μg/ml R848 and F(ab')$_2$ anti-IgG/M (isolation protocol B). Cells were washed with 10ml fresh media at day 3. Each scatter plot displays the percentage of live cells expressing the stated CD marker as determined at each time point via flow cytometry. Data from comparable intervals were grouped together for clarity. Each independent differentiation is represented by a different colour and the colours are consistent with figure 5.1.

The various differentiation capabilities of the LPD B-cells subsequent to the two types of stimulation are summarised in table 5.2.

Table 5.2 Comparison of the capacity of B-cells derived from multiple LPDs to generate plasmablasts and plasma cells subsequent to either CD40L or R848 stimulation.

Patient	Diagnosis	CD40L stimulation		R848 stimulation	
		Plasmablasts	Plasma Cells	Plasmablasts	Plasma Cells
1	SMZL	Yes	No	Yes	No
2	SMZL	No	No	No	No
3	Mantle cell	Yes	Yes	No	No
5	SMZL	Yes	Limited	No	No
5	SMZL	Yes	Yes	No	No
6	SMZL	Yes	Yes	Yes	Yes
7	SMZL	Yes	Limited	Yes	No

In 3/7 samples, the ability of the B-cells to differentiate is matched following activation with both types of stimuli. However, in the other 4 samples, the capacity for differentiation is diminished when cells receive R848 stimulation compared to when they receive CD40L stimulation. This is most striking for patents 3 and 5 which are able to generate both plasmablasts and plasma cells when CD40L stimulation is provided but are incapable of responding to R848 stimulation.

In summary, the LPD samples, with the exception of patient 1, displayed a weaker proliferative response to stimulation with R848 + F(ab')$_2$ anti-IgG/M in comparison to that which was observed following CD40L + F(ab')$_2$ anti-IgG/M stimulation. In addition, samples capable of generating plasma cells following activation with CD40L were, in general, less able to do so subsequent to TLR7 stimulation. The variable capacity for plasma cell differentiation amongst these samples within the *in vitro* system is in line with the spectrum of differentiation observed *in vivo*. Despite the fold-change profiles initially appearing similar between WM and the other LPDs, direct comparison of the proliferation of these samples following both types of stimulation reveals that the highly divergent response of WM B-cells to these stimuli is unique.

5.5   Schnitzler syndrome

Schnitzler syndrome (SchS) is a rare disorder characterized by chronic urticaria, bone and joint pain and monoclonal IgM gammopathy (Lipsker, 2010). Individuals with Schnitzler syndrome are more prone to developing lymphoproliferative disorders than the general population, with the development of Waldenström's macroglobulinemia being the most common occurrence (Lim *et al.*, 2002; de Koning, 2014). Schnitzler's syndrome patients demonstrate a good response to IL-1 pathway blockade with anakinra (Cascavilla *et al.*, 2010). The IL-1R pathway interestingly also employs MYD88 in signal transduction, suggesting a potential common thread between IgM gammopathy and clinical response (Janssens and Beyaert, 2002). Given the presence of IgM paraprotein, the possibility that some of these patients may harbour the MYD88^{L265P} mutation within the B-cell fraction therefore presented an attractive opportunity to further examine the effect of MYD88 on B-cell differentiation and to compare the phenotypic profile of Schnitzler syndrome B-cells throughout the differentiation to that which was observed for WM cells. Patient data for the three SchS individuals is summarised in table 5.3.

Table 5.3 Clinical data for Schnitzler syndrome patients.

	SchS 1	SchS 2	SchS 3
Sex	Female	Female	Male
Age at symptom onset (years)	Mid 50s	59	43
CRP mg/l	-	75.2	110
Hb g/dl	-	119	100
IgM g/l reference range: 0.4-3.0 g/l	-	5	6
Bone marrow histology	-	MZL	MGUS
Duration of anakinra treatment (months)	-	45	27
Response to anakinra	-	Complete	Complete
Clonal progression requiring chemotherapy?	-	No	No
Mutations identified by Sanger sequencing	-	*MYD88*^{L265P}	*MYD88*^{L265P}
Mutations identified by ASO-PCR	-	*MYD88*^{L265P}	*MYD88*^{L265P}

MYD88^{L265P} mutations were identified in the PBMCs of two of the three patients, but its presence within the B-cell lineage cannot be inferred from this result.

5.5.1 Response of Schnitzler syndrome B-cells to stimulation with CD40L + F(ab')$_2$ anti-IgG/M

Figure 5.6 displays the phenotypic profiles for four differentiations with SchS B-cells, consisting of samples from three unique patients and one independent repeat performed on a fresh sample of peripheral blood taken several months after the initial sample. Interestingly, the proportion of memory B-cells appear to be lower in SchS samples than in healthy controls, with fewer than 10% CD27$^+$ cells at day 0. Interestingly, Lower levels of CD27 expression than expected were also observed in the WM samples. This may reflect a difference in the origins of the memory populations present in both WM and SchS patients compared with healthy individuals (Bagnara *et al.*, 2015). An alternate explanation for the downregulation of CD27 in these individuals is that it has been lost via a process of shedding from the cell surface over time (Ho *et al.*, 2008; Braggio *et al.*, 2012).

The general profile of cell surface marker expression across the samples is normal, with all samples cultured for at least 13 days generating plasma cells. In each case, loss of CD20 is accompanied by successive upregulation of first CD38 and then CD138 and the acquisition of CD27 as the cells progress from the plasmablast to the plasma cell stage. However, one sample possesses a notable departure in phenotype from healthy cells - SchS 3. Intriguingly, SchS 3 cells generated a population of CD38$^-$ CD138$^+$ cells by day 13 of the differentiation, identical to the plasmablast-like cells that often occur in differentiations with cells derived from WM patients.
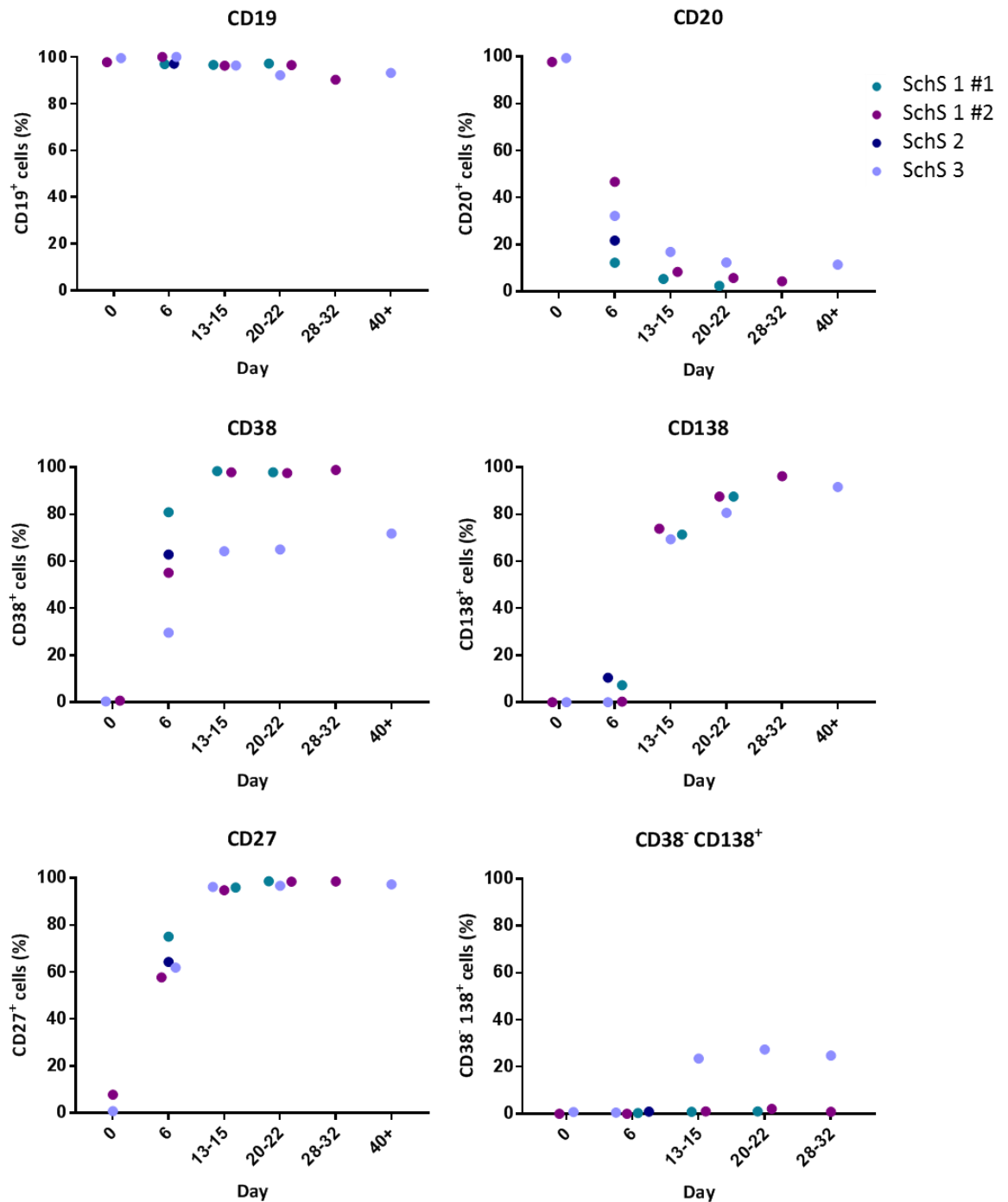
Figure 5.6 Scatter plot profiles for the expression of each CD marker assayed in multiple differentiations with Schnitzler syndrome B-cells. B-cells derived from the peripheral blood of patients with SchS were stimulated with CD40L and F(ab')$_2$ anti-IgG/M (isolation protocol B). Each scatter plot displays the percentage of live cells expressing the stated CD marker as determined at each time point via flow cytometry. Data from comparable intervals were grouped together for clarity. Each independent differentiation is represented by a different colour.

The corresponding fold change in cell number for each of these differentiations is shown in figure 5.7.

Schnitzler syndrome B-cells stimulated with CD40L + F(ab')$_2$ anti-IgG/M
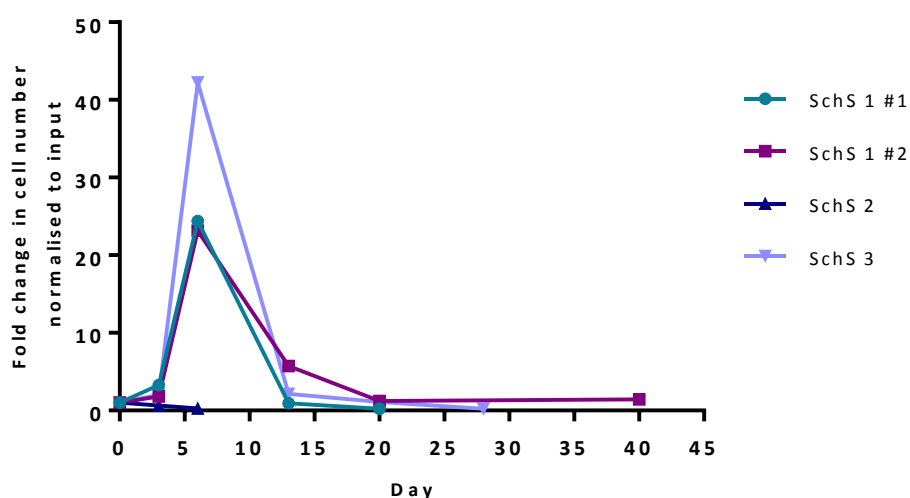
Figure 5.7 The change in cell number following B-cell activation with stimuli mimicking a T-dependent immune response in samples derived from Schnitzler syndrome patients. B-cells derived from the peripheral blood of SchS patients (isolation protocol B) were stimulated with CD40L and F(ab')$_2$ anti-IgG/M. Cell number at each time point was determined by manual counts for days 3 and 6 and then by flow cytometry thereafter. The cell number at each point was normalised to the number of "input" cells for that specific individual obtained at day 0.

The profiles again are mostly comparable to healthy cells, with the exception of SchS 2. B-cells from the PB of SchS 2 were isolated by flow sort. Whilst the phenotype of the cells was unaffected, there was a negative impact on the viability caused by the shear stress, resulting in too few cells to continue this experiment to the later time points.

5.5.2   Observation of WM alternate plasmablast phenotype in differentiations with SchS B-cells

By far the most interesting result from differentiations with SchS B-cells is the observation of the alternate plasmablast-like phenotype in one sample. As has been previously demonstrated, the other LPDs that were analysed did not display this unusual phenotype, so it is striking that PB from a patient with SchS should do so. The presence of this population does, however, tie in with the abnormal bone marrow histology, indicating the presence of monoclonal gammopathy of undetermined significance and the presence of MYD88^{L265P} detected by PCR. Figure 5.8 depicts the full phenotype of cells from this differentiation and a second differentiation with SchS B-cells that possess a "normal" phenotype for comparison.
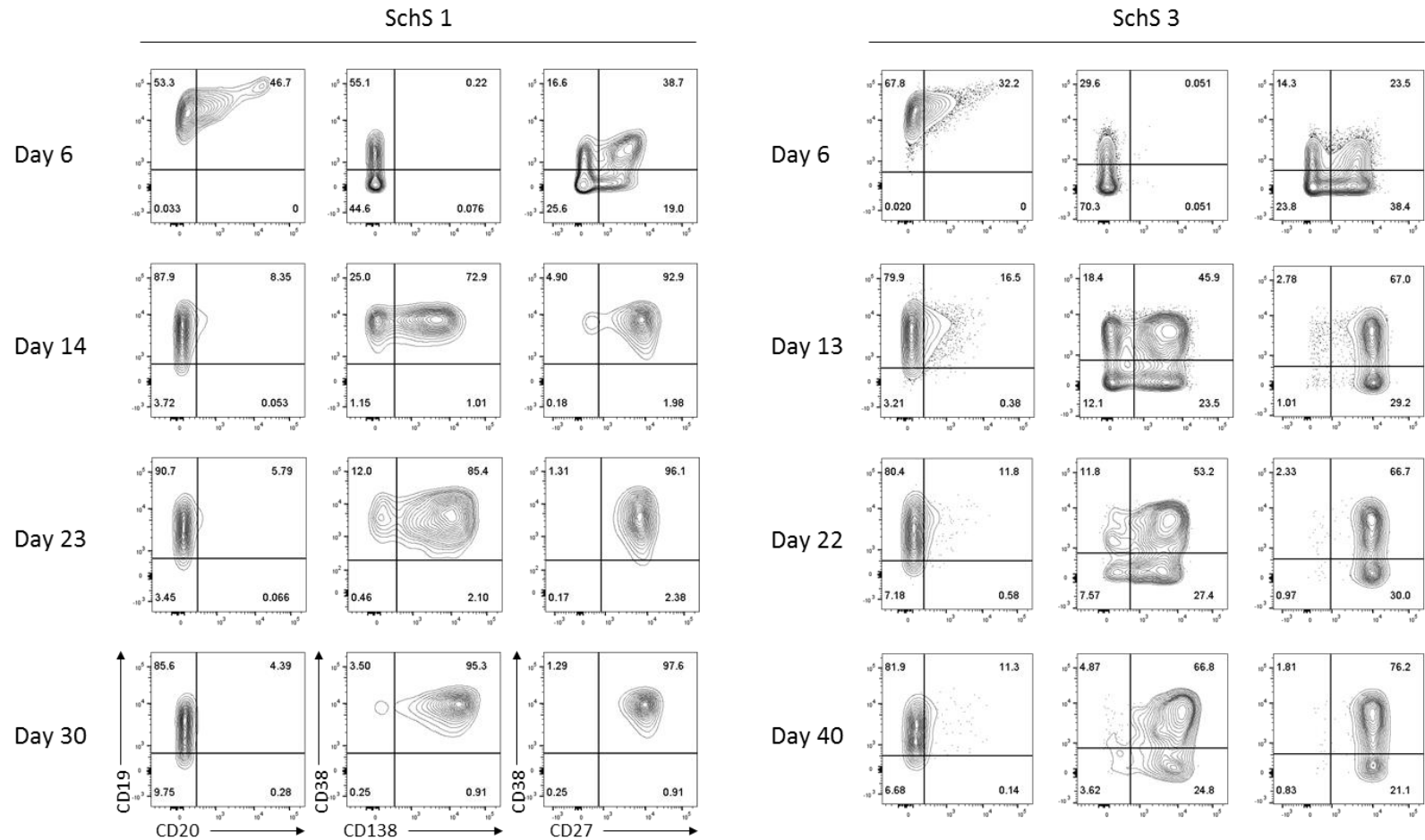
Figure 5.8 Example of differentiations with Schnitzler's B-cells that differentiate with a normal phenotype (left) and WM-like phenotype (right). B-cells were isolated from the peripheral blood of patients with Schnitzler syndrome (isolation protocol B). The cells were activated with CD40L + F(ab')$_2$ anti-IgG/M and the immunophenotype assayed by flow cytometry at each time point. Percentages are displayed for each quadrant.

This distinctive population emerges within the same time frame as CD38$^-$ CD138$^+$ WM cells. The precursors which generate this plasmablast-like population are indistinguishable from their counterparts in the preceding flow analysis, which differentiate normally. As with WM samples, this population is maintained for several weeks in the culture. By day 40, all cells have upregulated CD138, but the division between those that have upregulated CD38 and those cells that are unable to do so remains apparent. The downregulation of CD20 in this sample seems unaffected, unlike the WM samples, where CD20 downregulation is often delayed. The upregulation of CD27 is unperturbed, as with the WM samples. To confirm that the CD38$^-$ CD138$^+$ cells could not be distinguished from the rest of the population by the expression of any other marker within the experiment, the full phenotype of this subset is displayed in figure 5.9.
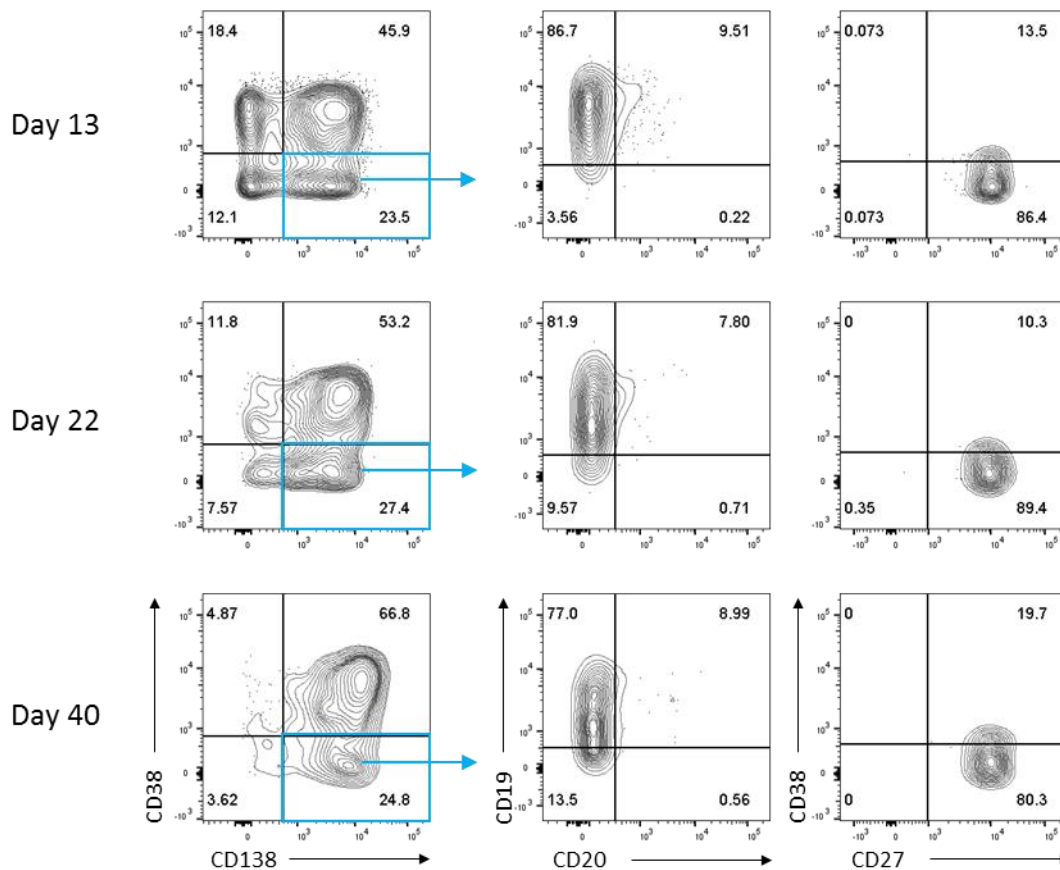
Figure 5.9 Full phenotype of SchS alternate plasmablast-like cells. The expression of CD19, CD20 and CD27 for the CD38$^-$ CD138$^+$ population (blue quadrant) for each time point indicated are shown on the right. Percentages are displayed for each quadrant.

There is no difference in the expression of the other markers in these cells and they otherwise appear to differentiate in a normal manner. Overall, the phenotype of the SchS sample that

generated the alternate plasmablasts appears to be an intermediate between that of a healthy control and a WM differentiation, generating CD38⁻ CD138⁺ cells but without an impediment to CD20 downregulation.

PCR analysis had been performed on peripheral blood mononuclear cells and demonstrated the presence of the MYD88^{L265P} mutation (S. Savic, personal communication). To confirm that this mutation was present within the B-cell population, RNA was taken from cells at day 6 of the differentiation. Sequencing analysis revealed that both patients possessed both wild-type and mutant forms of MYD88 (figure 5.10).
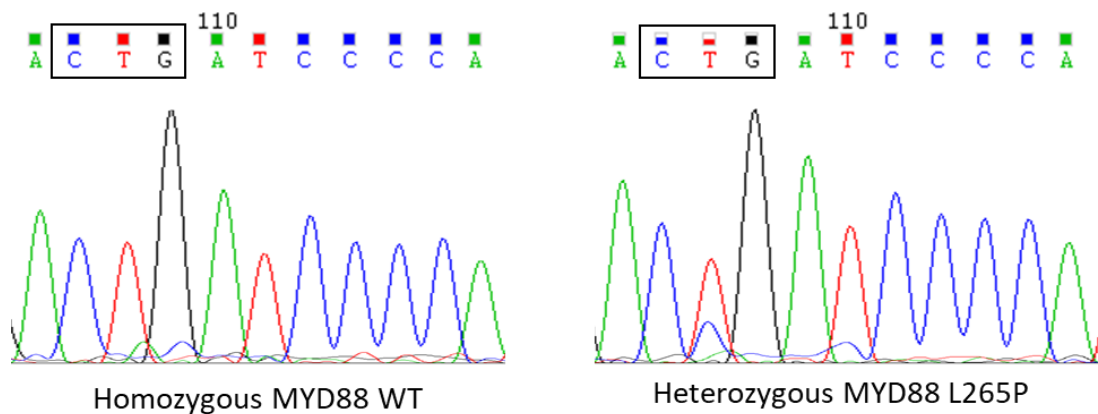
Figure 5.10 B-cells from patients with Schnitzler syndrome possessed both wild-type and mutant forms of MYD88. Representative sequencing trace from a MYD88 PCR performed on SchS cells taken at day 6 of the differentiation. The trace on the left is homozygous for wild type MYD88 – a leucine present at position 365 (CTG), whilst the trace on the left demonstrates heterozygosity at this base, with an additional peak for cytosine beneath the tyrosine peak.

B-cells isolated from SchS patients were able to differentiate into plasma cells and demonstrated comparable proliferation dynamics to healthy cells. Despite the similarities between Schnitzler syndrome and WM, the appearance of the CD38⁻ CD138⁺ population was still completely unexpected. Sequencing of SchS 3 day 6 cells from this differentiation revealed that they possessed the MYD88^{L265P} mutation, reinforcing the link between MYD88 mutation and this unusual phenotype.

5.6   The effect of R848 stimulation on SchS B-cells

Schnitzler syndrome B-cells shared phenotypic and proliferative features with both healthy and WM B-cells in differentiations following activation with CD40L + F(ab')$_2$ anti-IgG/M. Since the reaction of WM cells to TLR7 stimulation in comparison to healthy controls was so markedly different, the response of Schnitzler's B-cells was investigated in order to determine if they behaved in the same way. A graph depicting the fold-change in number for B-cells derived from two SchS patients is presented in figure 5.11. The initial sample from patient SchS 3 was sorted by flow cytometry. As with the CD40L stimulation, the sorting process resulted in a detrimental effect on cell viability, with a substantial loss of cells occurring between day 0 and day 3. When B-cells from the peripheral blood of patient SchS 3 were isolated by magnetic separation, a considerably greater amplitude of proliferation is observed compared to the input cell number as the viable population is preserved during the initial phase of the differentiation.
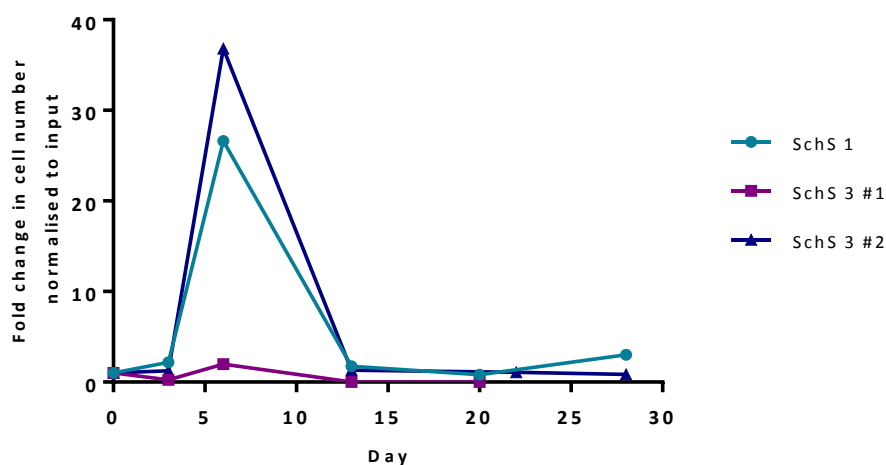
Figure 5.11 The change in cell number following B-cell activation with stimuli mimicking a T-independent immune response in samples derived from Schnitzler syndrome patients. B-cells derived from the peripheral blood of SchS patients were stimulated with 1µg/ml R848 + F(ab')$_2$ anti-IgG/M. Cell number at each time point was determined by manual counts for days 3 and 6 and then by flow cytometry thereafter. The cell number at each point was normalised to the number of "input" cells for that specific individual obtained at day 0.

The amplitude of the fold change increase between day 3 and 6 for SchS 1 and SchS 3 #2 is considerably greater than the average fold change observed in healthy cells in response to this type of stimuli. In both cases, it is also greater than that which was observed following parallel

experiments with CD40L stimulation. SchS 1 cells expanded 7.49-fold subsequent to activation with CD40L + F(ab')$_2$ anti-IgG/M and 12.17-fold following activation with 1μg/ml R848 + F(ab')$_2$ anti-IgG/M and similarly SchS 3 cells increased 20.87-fold with CD40L and 29.5-fold with R848. The proliferation of healthy cells was always greater subsequent to CD40L stimulation in comparison to R848 stimulation so the reversal of responsiveness in SchS cells is notable.

The phenotypic profiles for these differentiations are summarised in figure 5.12. Spontaneous transformation of B-cells, most likely due to reactivation of latent EBV was occasionally observed during *in vitro* differentiations. When this occurs, high levels of proliferation are induced in this fraction and the phenotype of the population becomes skewed away from terminally-differentiated plasma cells and back towards a less differentiated B-cell phenotype. The SchS samples were particularly prone to transformation subsequent to activation with R848. An initial sign of this phenomenon is the increase in cell number observed between day 20 and day 28 for the SchS 1 sample shown in figure 5.11. Due to this effect, the phenotypes of the SchS samples have not been included past day 20-22 as they are no longer informative as to the proportion of plasma cells in the population, even though the cells remained viable and in culture past this point.
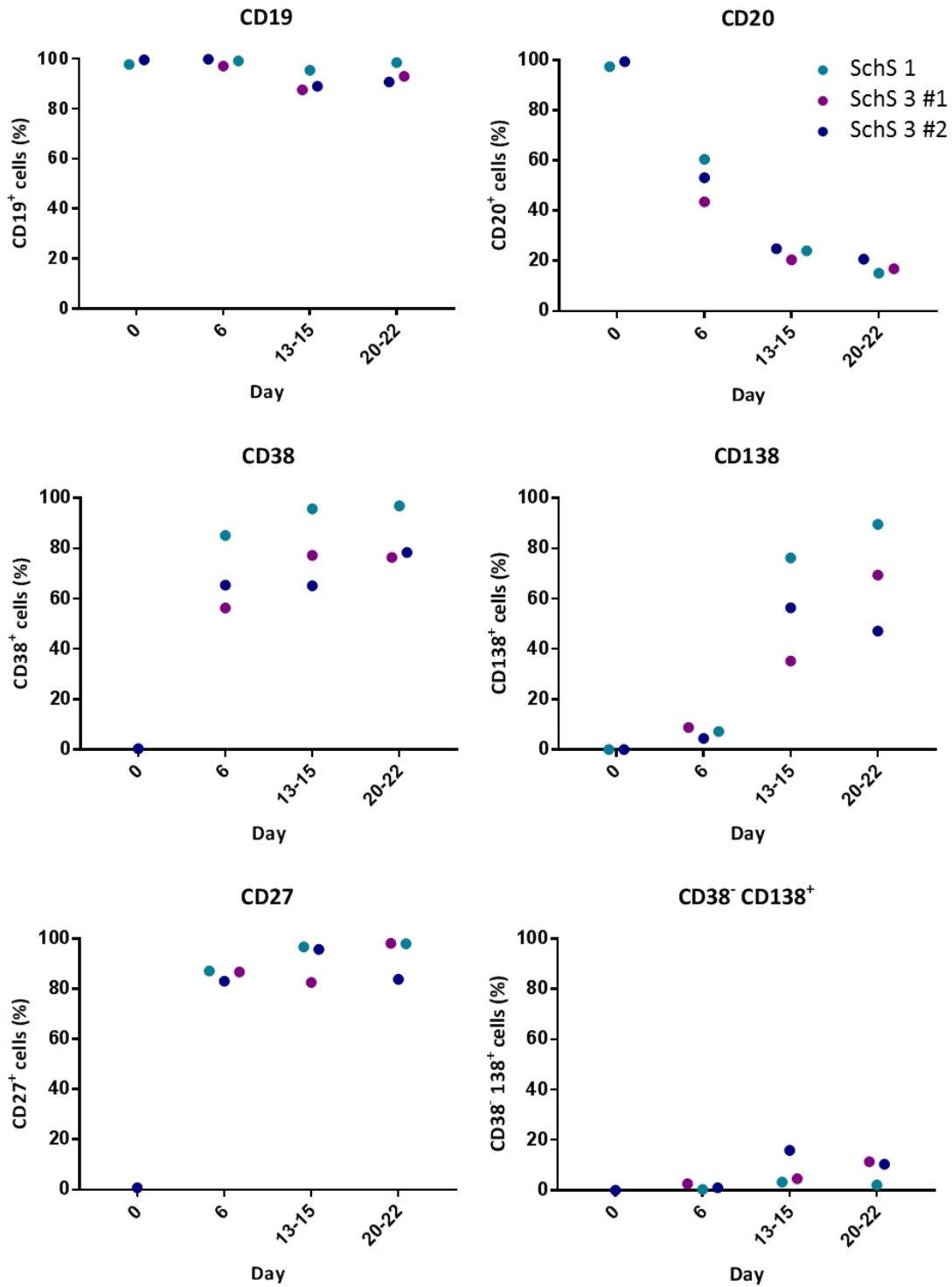
Figure 5.12 Scatter plot profiles for the expression of each CD marker assayed in multiple differentiations with Schnitzler syndrome B-cells. B-cells derived from the peripheral blood of patients with SchS were stimulated with 1µg/ml R848 and F(ab')$_2$ anti-IgG/M (isolation protocol B). Cells were washed with 10ml fresh media at day 3. Each scatter plot displays the percentage of live cells expressing the stated CD marker as determined at each time point via flow cytometry. Data from comparable intervals were grouped together for clarity. Each independent differentiation is represented by a different colour.

SchS cells are able to differentiate in response to TLR7 ligation, generating a population of plasma cells in each case. It does appear, however, that the generation of plasma cells subsequent to activation with R848 is less efficient than occurs when the SchS cells are stimulated with CD40L, with a smaller proportion of cells acquiring CD138 expression. Expression of the other surface markers is generally comparable between the two conditions and follows the expected pattern, although upregulation of CD27 is more rapid in R848-stimulated cells, with 85.6% of the total population expressing this marker at day 6 compared to. 64.7% in CD40L-stimulated cells at the same time point.

Once again, B-cells derived from patient SchS 3 generated a population of CD38$^-$ CD138$^+$ cells by day 13-15. An independent repeat was performed with B-cells isolated from a new sample of PB from this patient. This, in turn, also generated a CD38$^-$ CD138$^+$ fraction although there was a slightly lower overall proportion.

It is clear that the B-cells derived from these patients share phenotypic features with both healthy and WM cells. Results from experiments with healthy cells demonstrated that removal of F(ab')$_2$ anti-IgG/M from the culture had a substantial effect on the phenotype and proliferation of the differentiating cells. Since performing this experiment with WM cells was very difficult due to the paucity of cells and their death subsequent to stimulation with R848, the effect of omission of F(ab')$_2$ anti-IgG/M from the culture was examined in the SchS cells.

B-cells from patient SchS 1 stimulated with R848 and F(ab')$_2$ anti-IgG/M differentiated with a phenotype that is indistinguishable from healthy cells (figure 5.13). Removal of F(ab')$_2$ anti-IgG/M results in a population of CD19^{++} CD20^{++} cells which do not express CD38, CD138 or CD27. This population is analogous to that which occurs in differentiations with healthy cells when F(ab')$_2$ anti-IgG/M is omitted. These cells remain present at day 13, before they are lost by day 22. In healthy cells, the effect of F(ab')$_2$ anti-IgG/M removal on cell phenotype was negligible from day 20 onwards, with the majority of cells displaying a CD38$^+$CD138$^+$ phenotype (figure 4.6). In contrast, SchS B-cells cultured with only R848 stimulation display a considerable difference in phenotype at day 22. Omission of F(ab')$_2$ anti-IgG/M delays the generation of plasma cells by approximately 50%, suggesting that dual receptor engagement may be more important for plasma cell generation in SchS B-cells.
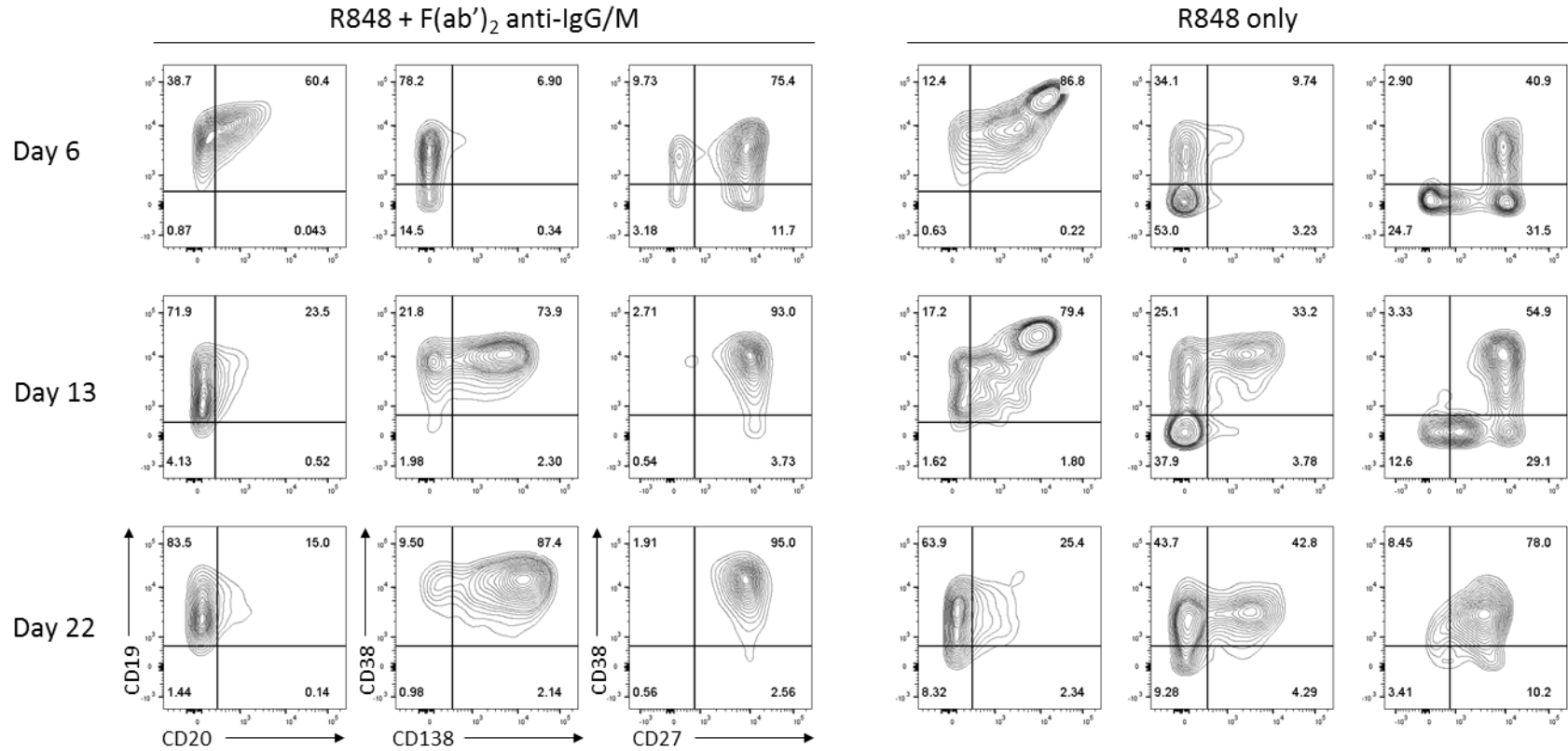
Figure 5.13 SchS B-cells which differentiate with a normal phenotype also demonstrate the same phenotypic response as healthy B-cells when F(ab')₂ anti-IgG/M is omitted.

B-cells were isolated from the peripheral blood of a patient with Schnitzler syndrome (patient SchS 1) (isolation protocol B). The cells were activated with 1µg/ml R848 +/- F(ab')₂ anti-IgG/M and the immunophenotype assayed by flow cytometry at each time point. Cells were washed with 10ml fresh media at day 3. Percentages are displayed for each quadrant.

Interestingly, Schnitzler syndrome B-cells display similar proliferation dynamics both with and without the presence of F(ab')$_2$ anti-IgG/M, although the amplitude of proliferation between days 3 and 6 is considerably reduced (figure 5.14).
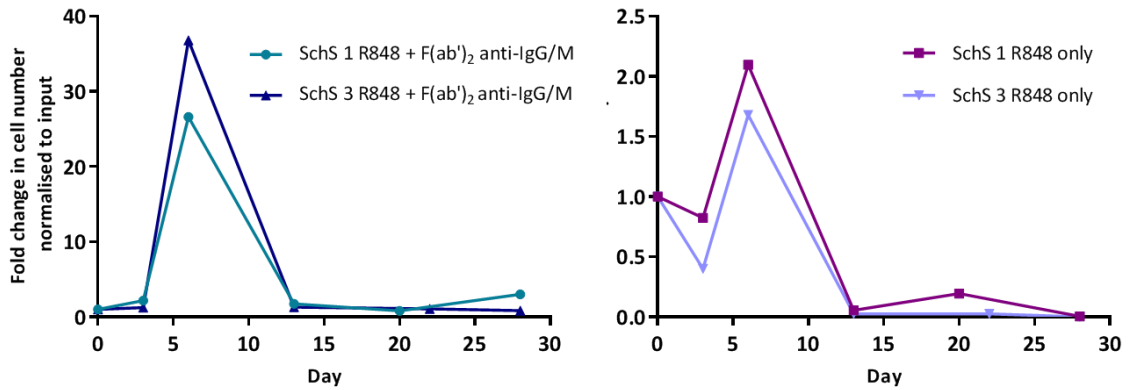
Figure 5.14 SchS B-cells display similar proliferation dynamics but a decrease in the amplitude of the response when F(ab')$_2$ anti-IgG/M is omitted from the culture. B-cells derived from the peripheral blood of two Schnitzler's syndrome patients (isolation protocol B) were stimulated with 1µg/ml R848 + F(ab')$_2$ anti-IgG/M (left) or 1µg/ml R848 alone (right). Cells were washed with 10ml fresh media at day 3. The cell number at each time point was determined by manual counts between days 0-6 and then by flow cytometry thereafter. The cell number at each point was normalised to the number of "input" cells for that specific individual obtained at day 0.

The fall in cell number observed between day 0 and day 3 may be as a consequence of a decreased proportion of B-cells that are able to respond to this weaker activation stimuli, perhaps due to variances in innate TLR7 expression. In the absence of BCR crosslinking, survival signals are diminished and unable to overcome the intrinsic pro-apoptotic program, resulting in cell death. Despite this, proliferation occurred in both samples from day 3 to day 6, unlike healthy cells, in which numbers reduced at each successive time point. This appears to support a hypothesis that SchS B-cells, or at least a proportion of them, are hyperresponsive to TLR stimulation and are able to proliferate to a much greater extent than their healthy counterparts. Accordingly, the hyperresponsive cells may correspond to a CD27$^-$ memory compartment, thus explaining the apparent deficiency in the total memory fraction (Bagnara *et al.*, 2015).

A comparison of the phenotypes obtained for B-cells isolated from patient SchS 3 following stimulation with R848, with and without F(ab')$_2$ anti-IgG/M are shown in figure 5.15.
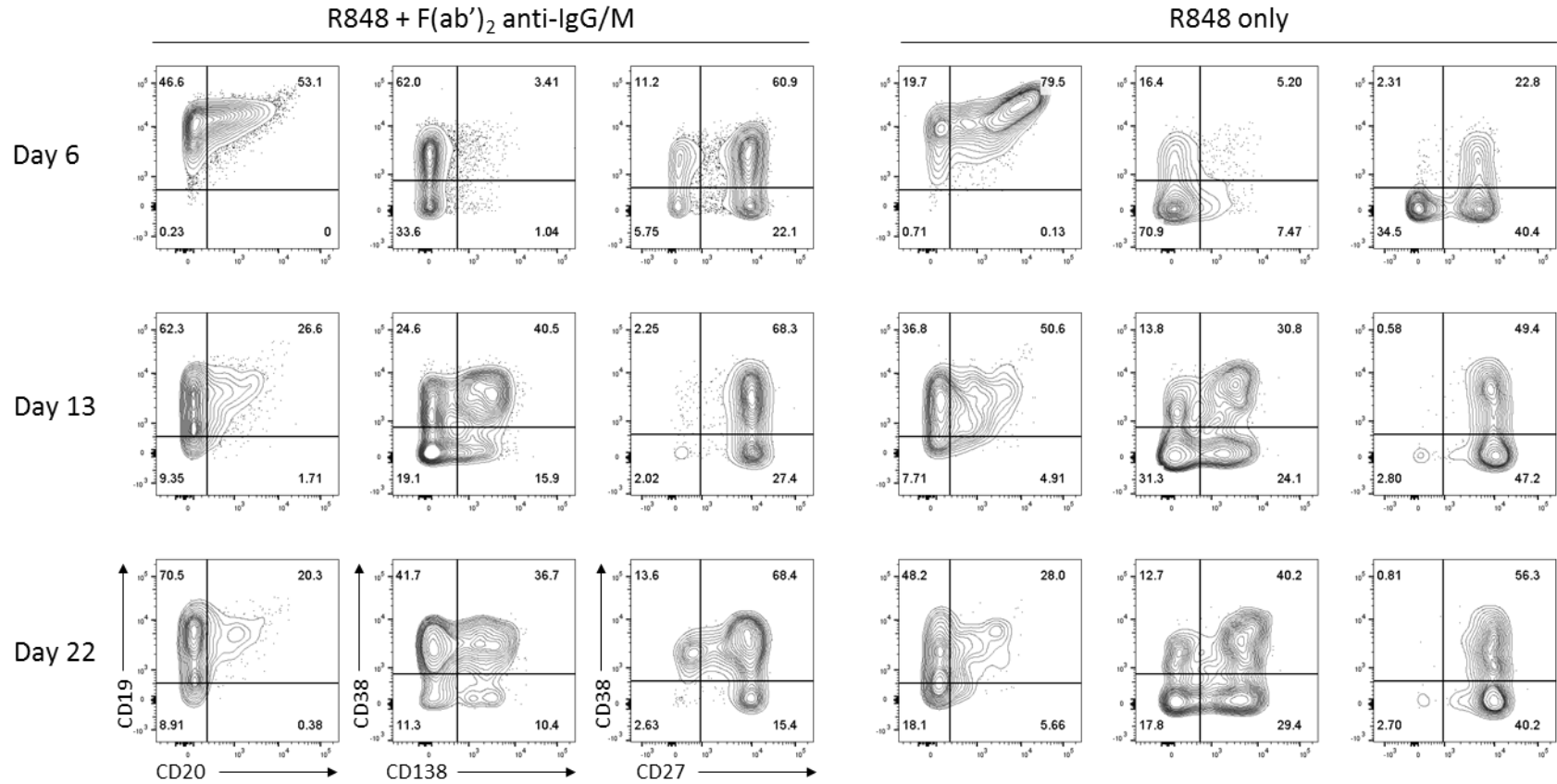
Figure 5.15 Stimulation of SchS B-cells with R848 in the absence of BCR crosslinking generates a greater proportion of CD38$^-$ CD138$^+$ cells. B-cells were isolated from the peripheral blood of a patient with Schnitzler syndrome (SchS 3) (isolation protocol B). The cells were activated with 1μg/ml R848 +/- F(ab')$_2$ anti-IgG/M and the immunophenotype assayed by flow cytometry at each time point. Cells were washed with 10ml fresh media at day 3. Percentages are displayed for each quadrant.

In both conditions, a population of CD38$^-$ CD138$^+$ cells arose. However, it emerged earlier and comprised a greater proportion of the total population when the cells are stimulated with R848 in the absence of F(ab')$_2$ anti-IgG/M. The proportion of CD38$^-$ CD138$^+$ cells increases at each successive time point when the cells were activated with R848 alone, whereas it diminishes between day 13 and day 22 following dual TLR/BCR stimulation. The population of CD38$^-$ CD138$^+$ cells were back-gated to examine the expression of the other markers in this subset (figure 5.16).
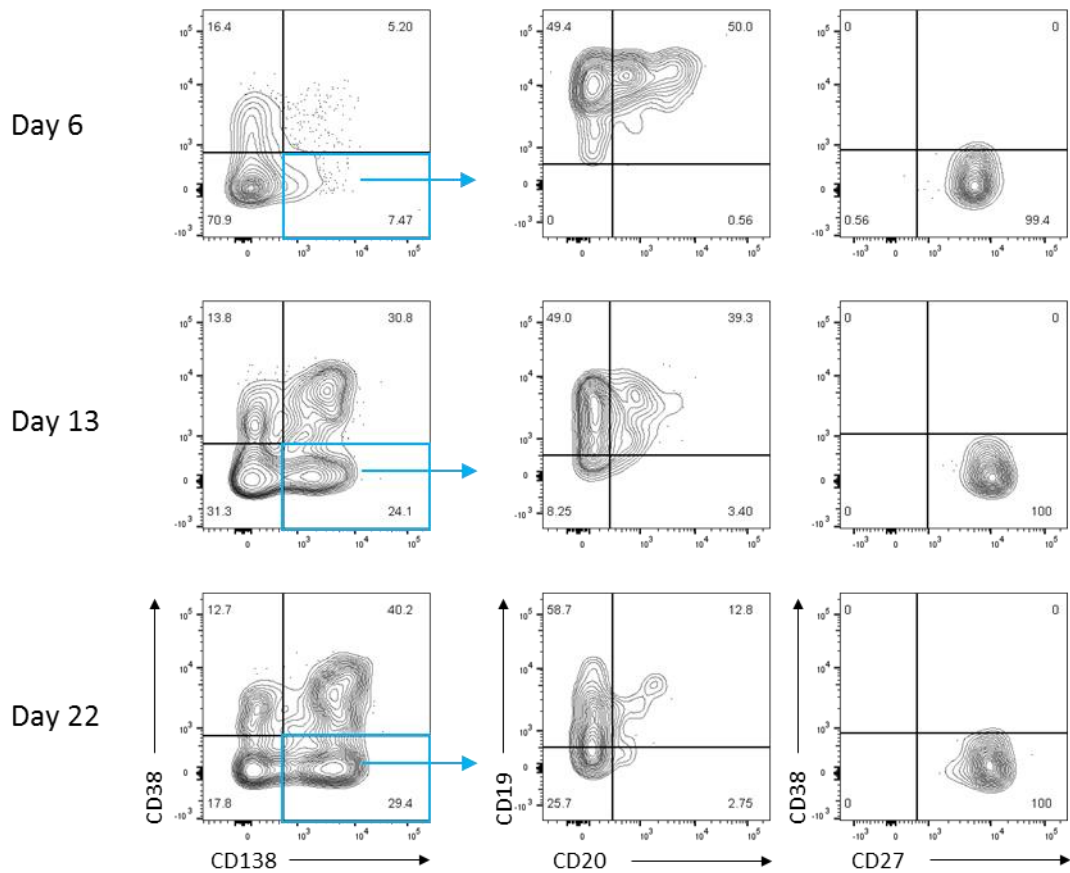
Figure 5.16 Expression of additional markers on alternate plasmablast-like population generated subsequent to stimulation with 1μg/ml R848 only. The expression of CD19, CD20 and CD27 for the CD38$^-$ CD138$^+$ population (blue quadrant) for each time point indicated are shown on the right. Percentages are displayed for each quadrant.

The CD38$^-$ CD138$^+$ population appears otherwise normal in the expression of the other markers assayed. This subset exhibits more rapid differentiation than the population as a whole, with a smaller proportion of CD20$^+$ cells at each successive time point compared to the population as a whole (figure 5.15). In addition to this, all CD38$^-$ CD138$^+$ cells have upregulated CD27 compared to ~60% by day 6 of differentiation.

The lack of BCR ligation in this sample clearly favours the generation of the alternate plasmablast phenotype over stimulation of both TLR7 and the BCR. Moreover, this unusual population emerges earlier following R848 stimulation in comparison to CD40L stimulation and this is accelerated further with the removal of F(ab')$_2$ anti-IgG/M. Activation with CD40L + F(ab')$_2$ anti-IgG/M resulted in a greater proportion of CD38$^-$ CD138$^+$ cells than R848 + F(ab')$_2$ anti-IgG/M, but omission of F(ab')$_2$ anti-IgG/M lead to the highest overall proportion of these cells (Table 5.4).

Table 5.4 Proportion of CD38$^-$ CD138$^+$ cells generated following stimulation of SchS-derived B-cells with three different combinations of activating stimuli. SchS cells were stimulated with conditions mimicking T-dependent stimulation (CD40L + F(ab')$_2$ anti-IgG/M), T-independent stimulation (R848 + F(ab')$_2$ anti-IgG/M) or TLR stimulation alone (R848 only). The proportion of CD38$^-$ CD138$^+$ cells within the total population at each time point was assessed by flow cytometry.

<div align="center">

Proportion of CD38$^-$ CD138$^+$ cells (%)

</div>

Day	CD40L + F(ab')$_2$ anti-IgG/M	1µg/ml R848 + F(ab')$_2$ anti-IgG/M	1µg/ml R848 only
6	0.0	1.0	7.5
13	23.5	15.9	24.1
22	27.4	10.4	29.4

B-cells derived from patients with Schnitzler syndrome are able to successfully differentiate into plasma cells following stimulation with CD40L + F(ab')$_2$ anti-IgG/M. Despite all samples possessing the MYD88^{L265P} mutation, confirmed within the B-cell lineage in SchS 3, SchS B-cells do not suffer a detriment to survival subsequent to stimulation with 1µg/ml R848 + F(ab')$_2$ anti-IgG/M like WM B-cells. In fact, SchS B-cells appear to be hyperresponsive to this stimulus, demonstrating a greater fold-change increase in cell number between day 3 and 6 of the differentiation.

B-cells derived from patient SchS3 are particularly remarkable. This sample shares phenotypic characteristics unique to WM samples, generating a CD38$^-$ CD138$^+$ population following both T-dependent and T-independent stimulations. However, in stark contrast to WM B-cells, these B-cells do not die subsequent to R848 stimulation and can even generate plasma cells without additional BCR ligation. Since both samples possess the MYD88^{L265P} mutation it appears that a different feature of WM cells is responsible for the cell death.

5.7 Discovery of a novel MYD88 mutation in Schnitzler syndrome B-cells

Further examination of the *MYD88* sequence data revealed that both SchS patient 2 and 3 possessed an additional mutation at amino acid position 256. As with MYD88[L265P], this mutation is a single base transition from cytosine to tyrosine, CTC → CCC, resulting in an amino acid substitution of leucine to proline. The MYD88[L256P] mutation was not present in any of the six WM samples analysed or any of the cells lines tested, which included the WM cell lines BCWM.1 and MWCL.1 (data not shown) and the ABC DLBCL cell lines OCI-Ly3 and OCI-Ly-10 (figure 5.17). The lack of a MYD88[L256P] mutation in SchS 1 does not necessarily mean that this patient does not possess it. In a similar manner to the MYD88[L265P] mutation in WM, this mutation may occur within a proportion of the SchS B-cell population and as such is not identified here as the sequencing of this sample was only performed once.
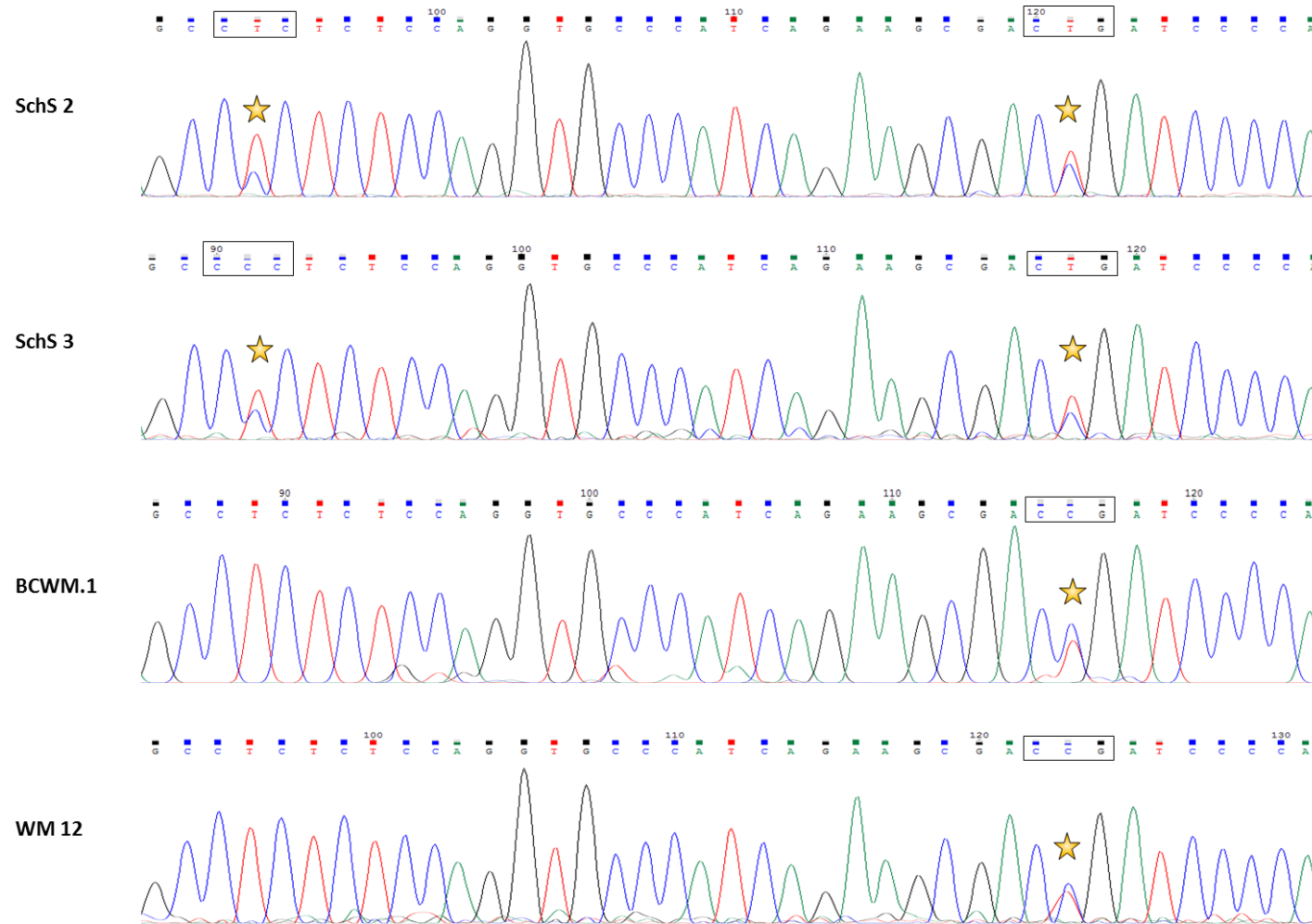
Figure 5.17 Schnitzler syndrome B-cells possess a novel MYD88 mutation, MYD88[L256P]. Sequencing traces from a *MYD88* PCR performed on SchS cells, the WM cell line BCWM.1 and WM patient 12. The location of MYD88[L265P] and MYD88[L265P] are starred. SchS and WM samples were taken at day 6 of the differentiation.

5.7.1 Effect of the L256P mutation on the structure of MYD88

To assess the impact of this mutation on the conformation of the protein, the modelling tool SWISS-MODEL was used (Schwede *et al.*, 2003). The tertiary structure of MYD88 is shown in figure 5.18, with the location of MYD88[L256P] and its impact on the local protein structure.
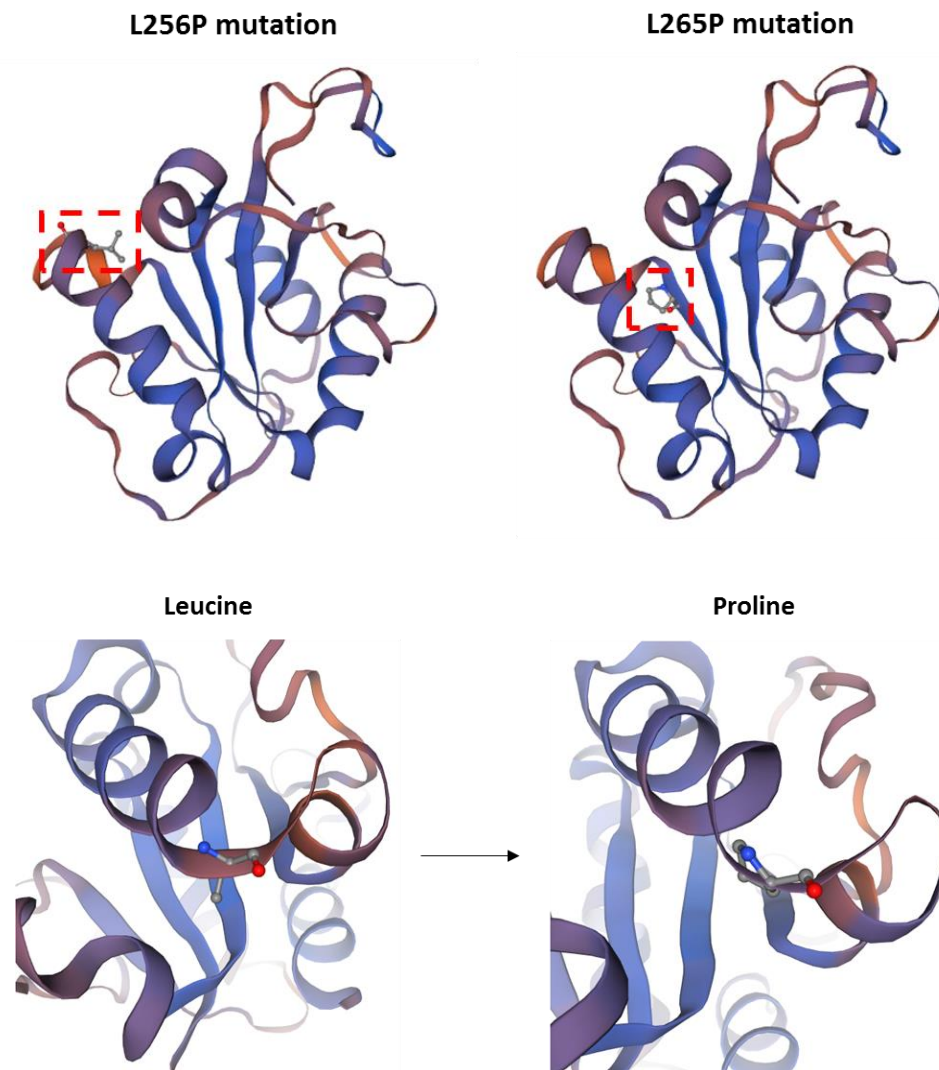
Figure 5.18 Location of L256P within the structure of MYD88. (Top) Ribbon diagrams demonstrating the location of the L256P residue within the 3D structure of MYD88. A comparison of the location of MYD88[L265P] is provided on the right. (Bottom) Visualisation of the structure from a different angle demonstrates a slight rotation to the α-helix induced by the L256P mutation but the region is otherwise undisturbed.

The L256P mutation is present in the αC region of the protein, within the TIR domain, in a loop just prior to the β-sheet that contains leucine 265. Since the nomenclature of these mutations

is so similar, the L256P mutation will hereafter be referred to as MYD88^{SchS} for clarity. Lymphoma-associated MYD88 mutations rarely disrupt the conformation of the TIR domain due to its stability, but rather influence the interaction between the proteins (Avbelj *et al.*, 2014). As with the L265P mutation, MYD88^{SchS} has very little effect on the tertiary structure of the protein and one would anticipate that the integrity of the TIR domain would be unaffected by this mutation. Interestingly however, MYD88^{SchS} lies on the proposed axis of dimerisation (figure 5.19), suggesting that it may alter protein-protein interactions (Bovijn *et al.*, 2013).
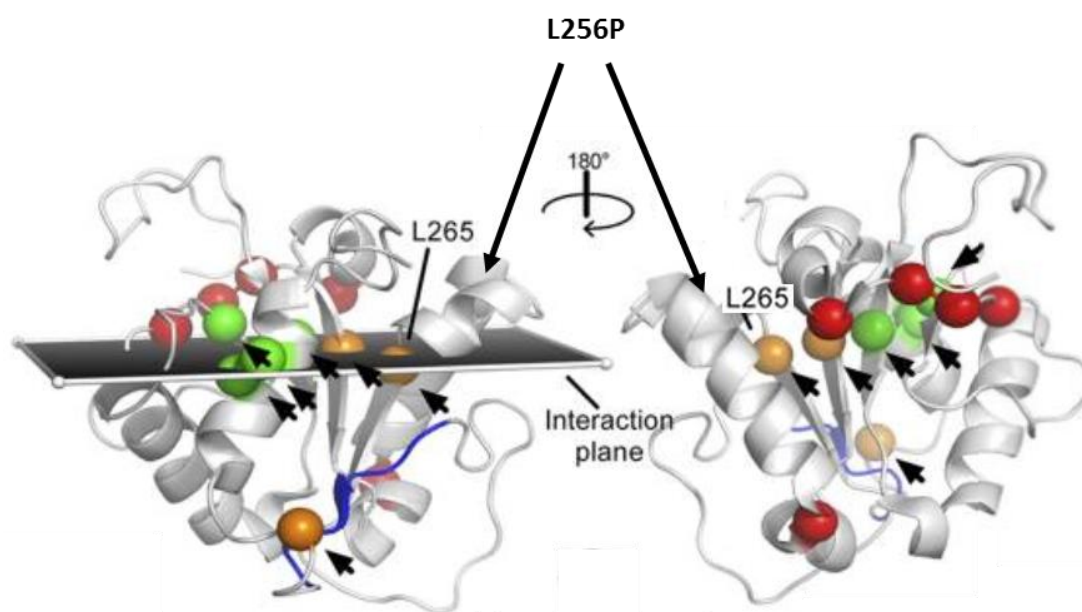
Figure 5.19 MYD88^{SchS} lies on the interaction plane between MYD88 moieties. Cancer-associated mutations modelled by Avbelj and colleagues map to hub locations (orange) or lie on the interaction plane (red). The MYD88^{SchS} mutation is located on this axis as indicated. Arrows designate areas of interaction. Residues indicated in green are interfacing hubs for which mutations have not been documented thus far and the blue section denotes a region with reduced flexibility following MYD88 mutation. Adapted from Avbelj *et al*., 2014.

Whilst any conclusions are tentative, MYD88^{SchS} may increase the propensity of the protein to undergo oligomerisation in a similar manner to MYD88^{L265P}, resulting in Myddosome formation and potentiation of NF-κB signalling. It is possible that the combination of both MYD88 mutations increases this further. Additional investigation of the incidence of this mutation in SchS patients is warranted to determine its frequency. Assessment of NF-κB activation would provide insight as to its effect and may provide an explanation for the proliferation observed during *in vitro* differentiations.

5.8   Discussion

Multiple samples were obtained over the course of the project from patients that were subsequently diagnosed with an LPD that was not WM. This represented an opportunity not only to compare the response of WM cells to those from other B-cell lymphoproliferative disorders but they also provided additional controls for the way in which patient samples are stored versus that of healthy samples and the knock-on effect that results. Seven of the nine LPD samples were from patients that has been diagnosed with SMZL with an IgM paraprotein (table 5.1). These samples share both clinical features with WM and similar molecular pathology, with dysregulation of NF-κB a common feature of both neoplasms (Arcaini *et al.*, 2016). The incidence of MYD88^{L265P} within SMZL is infrequent (Varettoni *et al.*, 2013) and thus enables comparison of highly related aetiologies on this differentiation of B-cells within the *in vitro* system. Of note however, was a suspected MYD88^{L265P} mutation in one SMZL sample.

In all LPD samples, a greater proportion of cells died following the initial isolation and the assessment of cell number three days later than occurred in healthy samples (figure 5.2). Similar levels of viability and a reduction in cell number were also observed in differentiations with BM samples from WM patients. This was a common feature of all clinical samples, indicating that the increased time the samples are stored as whole blood or bone marrow in sample collection tubes negatively impacts the viability of the cells although it does not appear to affect the phenotype. Whilst these additional samples enabled phenotypic comparison to the WM differentiations, they also confirmed that the decrease in cell numbers seen in the initial stages of WM differentiations can most likely be attributed to the treatment of the samples in general rather than an inherent feature of the WM B-cells.

The results of stimulating multiple types of LPDs with CD40L + F(ab')$_2$ anti-IgG/M revealed an array of phenotypes which were unsurprisingly more highly variable compared to the group of WM samples (figure 5.1). The LPD B-cells displayed a range of abilities to generate plasma cells, in keeping with the variable capacity of the neoplasms to differentiate *in vivo* (Young *et al.*, 2006; Ribera-Cortada *et al.*, 2015; Swerdlow *et al.*, 2016).

Compared to the LPDs, WM B-cells were more effective at generating plasma cells in response to stimulation with CD40L + F(ab')$_2$ anti-IgG/M, upregulating CD38 more rapidly and generating a greater proportion of plasma cells. B-cells from several of the LPD samples demonstrated impaired differentiation, with one sample completely unable to differentiate, in accordance with the inability of these cells to differentiate *in vivo* (figure 5.1) (Van Huyen *et al.*, 2000). These results verify that B-cells possessing an inherent defect in their ability to differentiate do not

spontaneously acquire the capacity to do so under the *in vitro* conditions, despite being placed within an environment highly conducive to differentiation. Despite the high incidence of NF-κB dysregulation in SMZL cells, the examples here did not generate a CD38$^-$ CD138$^+$ plasmablast-like population, suggesting this unusual subset of cells is not a general feature of neoplastic B-cells (figure 5.1).

Initially, it appeared that the proliferation dynamics observed in WM cells was common to other LPD samples (figure 5.2). However, on further investigation, those LPD samples which most closely matched the cell death seen in the WM samples responded equally poorly to both CD40L and R848 stimulation (figures 5.3 and 5.4), unlike the WM cells which are able to proliferate and differentiate in response to CD40L but suffer impaired differentiation and survival subsequent to R848 stimulation. Whilst the prevalence of MYD88^{L265P} within SMZL as a whole is low, it would be very interesting to compare the differentiation profiles of MYD88 mutated SMZL samples with WM B-cells. In the same context, one might hypothesise that MYD88^{WT} WM samples would behave differently due to the absence of the mutation and this presents a very interesting line of enquiry.

B-cells derived from patients with Schnitzler syndrome presented an excellent opportunity to examine the response of potentially MYD88^{L265P} mutated B-cells in a non-WM background. Patients with SchS are at an increased risk of neoplastic transformation, with approximately 20% progressing to WM (de Koning, 2014). Each patient possessed the MYD88^{L265P} mutation within either the lymphoid or myeloid lineages or both as demonstrated by Sanger sequencing and ASO-PCR (S. Savic, personal communication). Whilst the phenotype of the differentiating B-cells from two of the patients was relatively normal, the third patient generated a population of CD38$^-$ CD138$^+$ cells, which seem to be a hallmark of WM within the *in vitro* system (figures 5.6 and 5.8). This patient possessed evidence of MGUS within the bone marrow and whilst this has not currently progressed, it is interesting to speculate that perhaps patient SchS 3 is at a higher risk of further neoplastic B-cell transformation to WM due to the irregularities observed in the phenotype during differentiation experiments. Whilst SchS and WM share several commonalities, the presence of a large fraction of CD38$^-$ CD138$^+$ cells during a differentiation in one of the three SchS patients is particularly striking. The detection of MYD88^{L265P} within B-cells collected during the differentiation presented here appears to confirm the relationship between this mutation and this unusual phenotype and suggests this patient may be at a particular risk of developing WM in the future (figure 5.10).

It has been demonstrated in mouse models that the presence of MYD88^{L265P} alone is insufficient to cause WM (Knittel *et al.*, 2016). As demonstrated in this and previous chapters, the presence of MYD88^{L265P} does not guarantee that B-cells will generate the alternate plasmablast-like

phenotype. MYD88[L265P] was confirmed in all samples with WM and two of the SchS samples and yet the appearance of this population during differentiations that reached at least day 20 was 50% in both instances – 4/8 in WM and 1/2 in SchS. Thus, additional factors must contribute to the emergence of these distinctive cells.

As with healthy cells, a proportion of SchS cells are able to respond rapidly to TLR stimulation alone, generating a small population of plasma cells by day 6. At this time point, the proportion of CD38$^-$ CD138$^+$ cells outnumbers those with the conventional plasma cell phenotype. It would appear, therefore, that the CD38$^-$ CD138$^+$ precursors are particularly TLR7 sensitive and able to initiate differentiation more quickly. The favouring of the CD38$^-$ CD138$^+$ fraction in SchS cells following stimulation with R848 in the absence of BCR ligation by F(ab')$_2$ anti-IgG/M suggests that additional activation of the BCR signalling cascade may suppress the generation of this aberrant population when both the BCR and TLR7 are ligated concomitantly. It is possible that stimulation with CD40L without F(ab')$_2$ anti-IgG/M would generate a greater proportion of these cells but this has not been investigated.

This effect may help to explain why the alternate plasmablast-like population does not emerge when WM B-cells are stimulated with 1μg/ml R848 and F(ab')$_2$ anti-IgG/M. It is possible that the WM cells that would normally constitute the precursors for the CD38$^-$ CD138$^+$ alternate plasmablasts are particularly sensitive to TLR signalling. Thus, they are most profoundly affected by stimulation of TLR7, resulting in apoptosis either from over-activation or conversely a lack of pro-survival signalling. In addition to this, dual receptor engagement of TLR7 and the BCR dampens the emergence of this distinctive population and therefore it is absent when WM B-cells are stimulated with R848.

The proliferative response of healthy cells to stimulation with R848 was weaker than that which was observed following CD40L stimulation. In contrast, SchS B-cells appear to be hyperresponsive to TLR7 stimulation, with concomitant BCR and TLR7 stimulation resulting in enhanced proliferation compared to activation with CD40L (figure 5.11). This is intriguing, especially in the light of the profoundly impaired survival and differentiation of WM B-cells when they are exposed to this type of stimulation. SchS B-cells also demonstrated an improved proliferative response to TLR7 stimulation alone, although dual receptor ligation certainly has a synergistic effect on the proliferation of SchS cells (figure 5.14).

The response of SchS B-cells appears to fit in well with the data generated by Lim *et al*., and Wang et al (Lim *et al.*, 2013; Wang *et al.*, 2014). A situation may be occurring in SchS B-cells whereby the tolerance to self-ligands is broken due to MYD88[L265P] and thus stimulation via the TLR/IL-1R superfamily increases the proliferation of the MYD88-mutated cell fraction and

induces the differentiation of this population, resulting in inflammation and increased levels of IgM paraprotein.

The identification of a novel MYD88 mutation within SchS B-cells may also shed some light on the differential response of these cells in comparison to WM. The MYD88^{SchS} mutation shares similarities with MYD88^{L265P}, being located with the TIR domain and falling within the interaction plane (Bovijn *et al.*, 2013; Avbelj *et al.*, 2014). Whilst the possibility that the MYD88^{SchS} mutation has no impact on oligomerisation and Myddosome formation remains, the results from these *in vitro* differentiations in combination with the literature regarding MYD88 protein structure do suggest a potential effect. The aetiology of Schnitzler syndrome remains largely unknown, thus investigation into the incidence of this mutation and characterisation of its effects are required as it may contribute to SchS pathology.

Differentiations with samples from other LPDs that are not WM have established that these neoplastic B-cells behave differently to both healthy cells, as expected, but also exhibit a different profile to WM. In contrast, B-cells from a patient with Schnitzler syndrome demonstrated remarkable phenotypic similarities to WM cells, indicating that the MYD88^{L265P} mutation is a factor contributing to the departure in phenotype from healthy controls observed for both WM and SchS. The differences in the proliferative response of SchS B-cells to WM B-cells might represent the more simplistic mutational landscape of a pre-malignant condition compared to that of full-blown WM and the additional abnormalities that accompany neoplastic transformation.

Chapter 6 – Further analysis and visualisation of flow cytometry data

6.1   viSNE analysis

6.1.1   viSNE introduction

A large quantity of flow cytometry data was generated throughout the course of the project to assess the phenotype of the differentiating cells at multiple time points. However, displaying an accurate representation of numerous data sets in a condensed format presented a challenge. To supplement previous analysis and to encompass the global differences between differentiations with WM-derived cells and differentiations with healthy cells, an algorithm called viSNE (visualisation of t-Distributed Stochastic Neighbour Embedding) was used in order to display the data and identify populations and trends that become apparent when multiple data sets are analysed simultaneously (Kotecha *et al.*, 2010). An important aspect of viSNE analysis is that the algorithm considers all of the phenotypic markers that have been selected for use simultaneously and thus enables the relationships between populations of cells within complex data to be visually packaged into a biaxial plot. In order to perform this analysis, the cloud-based platform Cytobank was used (Kotecha *et al.*, 2010).

Hinton and Roweis initially developed a method for organising high dimensional data in a two-dimensional space, with an aim to preserve the greatest extent of the structure of this complex, nonlinear data than is possible with principle component analysis (Hinton and Roweis, 2003). They called this technique stochastic neighbour embedding (SNE). Several years later, a modification of this algorithm was developed and published by van der Maaten and Hinton, improving the cost function - an estimate of how the model is performing - and was easier to optimise (Maaten and Hinton, 2008). This version used a Student-t distribution rather than a Gaussian distribution so it was designated t-SNE.

Application of this algorithm to mass cytometry data was first described by Amir *et al*., 2013 (Amir *et al.*, 2013). In order to readily visualise their high dimensional single cell data, they developed viSNE (visualisation of t-Distributed Stochastic Neighbour Embedding). Subsequently, a variant of this algorithm based on the Barnes-Hut approximation was developed by Laurens van der Maaten, which enabled the analysis to be performed more rapidly whilst using less memory (Van Der Maaten, 2014). Cytobank uses this version of the algorithm, termed the Barnes-Hut implementation.

6.1.2 viSNE workflow

Raw flow cytometry fcs files were concatenated using an fcs concatenation tool downloaded from cytobank.org. Initially, flow cytometry data was acquired on an LSRII 3-laser, but a year into the project this machine was retired and replaced with a CytoFLEX S flow cytometer. The settings parameters between the two machines are different as the CytoFLEX S is able to record over a much greater range. These differences preclude the concatenation of fcs files recorded on the two cytometers because the populations of cells occupy different positions on the axes. This resulted in some groups containing fewer samples than were able to be included in previous analysis which did not require this level of compatibility. Samples were concatenated based on their origin, the type of stimulation they received and the time point the phenotype was assessed, summarised in table 6.1. The number of concatenated samples that comprise each group are indicated.

Table 6.1 Sample groups used in viSNE analysis.

Time point	Stimulation	Sample Group					
		Healthy	WM	SMZL	Other LPDs	SMZL + Other	All LPDs
Day 0		n=11	n=12	n=7	n=2	n=9	n=21
Day 6	CD40L	n=11	n=8	n=7	n=2	n=9	n=17
	R848	n=6	n=9	n=7	n=2	n=9	n=18
Day 13-15	CD40L	n=11	n=6	n=6	n=2	n=8	n=14
	R848	n=7	n=6	n=6	n=2	n=8	n=14
Day 20-22	CD40L	n=8	n=4	n=3	n=2	n=5	n=19
	R848	n=4	-	n=2	n=1*	n=3	n=4**
Day 28+	CD40L	n=6	n=4	n=3	n=1*	n=4	n=8
	R848	n=4	-	-	-	-	-

*viSNE analysis was not performed when there was only one sample, but these were included within the all LPDs group.

**This condition contains the same set of samples as SMZL + Other LPDs as no WM cells survive to this time point.

The viSNE algorithm generates a random seed each time an analysis is performed which influences the initial point at which the plot is populated and thus the locations of the clusters that are generated. Due to the stochastic nature of the algorithm and the variable number of

events within each concatenated data file, pairwise analysis of multiple different data sets results in viSNE plots that look different each time. Therefore, two diverging analysis workflows were performed to facilitate global comparisons between all of the amalgamated samples and another to evaluate specific variations between two of the selected groups.

In order to compare all of the data together, a viSNE analysis was performed on all 6 groups of concatenated data. Including all of these groups within one analysis enables plots to be generated where the clusters are located in the same positions in each case. This in turn enables differences to be more easily identified. In order to examine the relationship between the populations of cells generated in each group more closely, an additional step was performed whereby SPADE plots were generated from the initial viSNE results. The scheme for this analysis is illustrated in figure 6.1.

Expression of each of the markers - CD19, CD20, CD38, CD138, and CD27 - are informative and thus will contribute to the separation of populations as calculated by the algorithm so all were included within the analysis.

Raw flow cytometry data files

Concatenate data into groups based on origin + time point + type of stimulation

Healthy	WM	SMZL	Other LPDs	SMZL + Other LPDs	WM + SMZL + Other LPDs
- Day 0	- Day 0	- Day 0	- Day 0	- Day 0	- Day 0
- Day 6 CD40L	- Day 6 CD40L	- Day 6 CD40L	- Day 6 CD40L	- Day 6 CD40L	- Day 6 CD40L
- Day 6 R848	- Day 6 R848	- Day 6 R848	- Day 6 R848	- Day 6 R848	- Day 6 R848
- etc.	- etc.	- etc.	- etc.	- etc.	- etc.

Gate concatenated files to ensure only live cells are included in the analysis

Select files to be used for viSNE analysis and clustering channels (CD19, CD20, CD38, CD138, CD27)

Comparison between all groups

- Healthy
- WM
- SMZL
- Other LPDs
- SMZL + Other LPDs
- All LPDs (WM + SMZL + Other)

Pairwise comparison

e.g. Healthy vs WM

Generate SPADE plots from viSNE results

Figure 6.1 Scheme for viSNE and SPADE analysis.

viSNE plots each individual cell in a two-dimensional space based upon the level of expression of each marker enabling visualisation of complex data. The expression of each surface marker is presented on a rainbow scale, with dark blue indicating no expression and dark red indicating the highest expression. Each column represents a different marker, with an accompanying scale for each. Populations of cells expressing similar levels of each marker are clustered together. The progress of differentiation can therefore be tracked from B-cell to plasma cell via the colour change and overall shape on each subsequent plot. By concatenating the raw flow cytometry data for multiple differentiations, this analysis can provide an overview of these data sets an enable patterns to more easily be seen.

6.1.3 Analysis of CD40L stimulated cells

The viSNE plots for healthy differentiations are shown in figure 6.2. It should be noted that viSNE is normally used to cluster cells from multiple lineages, for example from PBMCs, whereas here it is being applied to differentiating B-cells only. This results in maps that do not appear quite like traditional viSNE maps such as those from Amir *et al.*, with separate clearly defined clusters, but rather these bivariate plots display a gradual shift in marker expression as occurs during B-cell differentiation (Amir *et al.*, 2013).

 The distribution of B-cells at day 0 illustrates how the algorithm separates the cells based upon varying expression of the markers assessed. The naïve B-cell fraction falls mostly within a large dark blue cluster distinguished on the CD27 plot. Using this location as a starting point, is can be observed that a proportion of these cells possess higher levels of CD38 expression than their counterparts and that this coincides with the highest levels of CD20 expression. Memory cells are identified within the CD27 plot by their increased expression of CD27 and are thus coloured as either green or yellow. They share high levels of CD20 but relatively lower CD38 expression. At day 6, the location of the cells within the space has shifted, as has the expression of the cell surface markers. The plasmablasts are located centrally, with increased expression of CD38 and CD27 and loss of CD20. As the cells become terminally differentiated plasma cells and acquire CD138, they converge at the very bottom of the plots.

For healthy cells, this analysis highlights several things of note. The population of CD19 negative plasma cells that are sometimes generated (Halliley *et al.*, 2015; Arumugakani *et al.*, 2017) can be seen from days 13-15 onwards as a small cluster at the southern tip of the plots, most easily distinguished in the CD19 column. Despite the CD19 negativity of these cells, they possess high levels of CD38, CD138 and CD27. Interestingly, the algorithm continues to display a wide range of colours when the cells are clustered by expression of CD138 from day 21 onwards, indicating

a range of expression of this marker. This is unexpected because the cells present at these time points are almost exclusively plasma cells and the expression of CD138 appears largely invariant when this data is displayed as a traditional biaxial contour plot, so one would anticipate a relatively homogenous red tone akin to the CD38 clustering. This subtle difference that normally cannot be distinguished may delineate the short and long-lived plasma cells but requires further investigation.
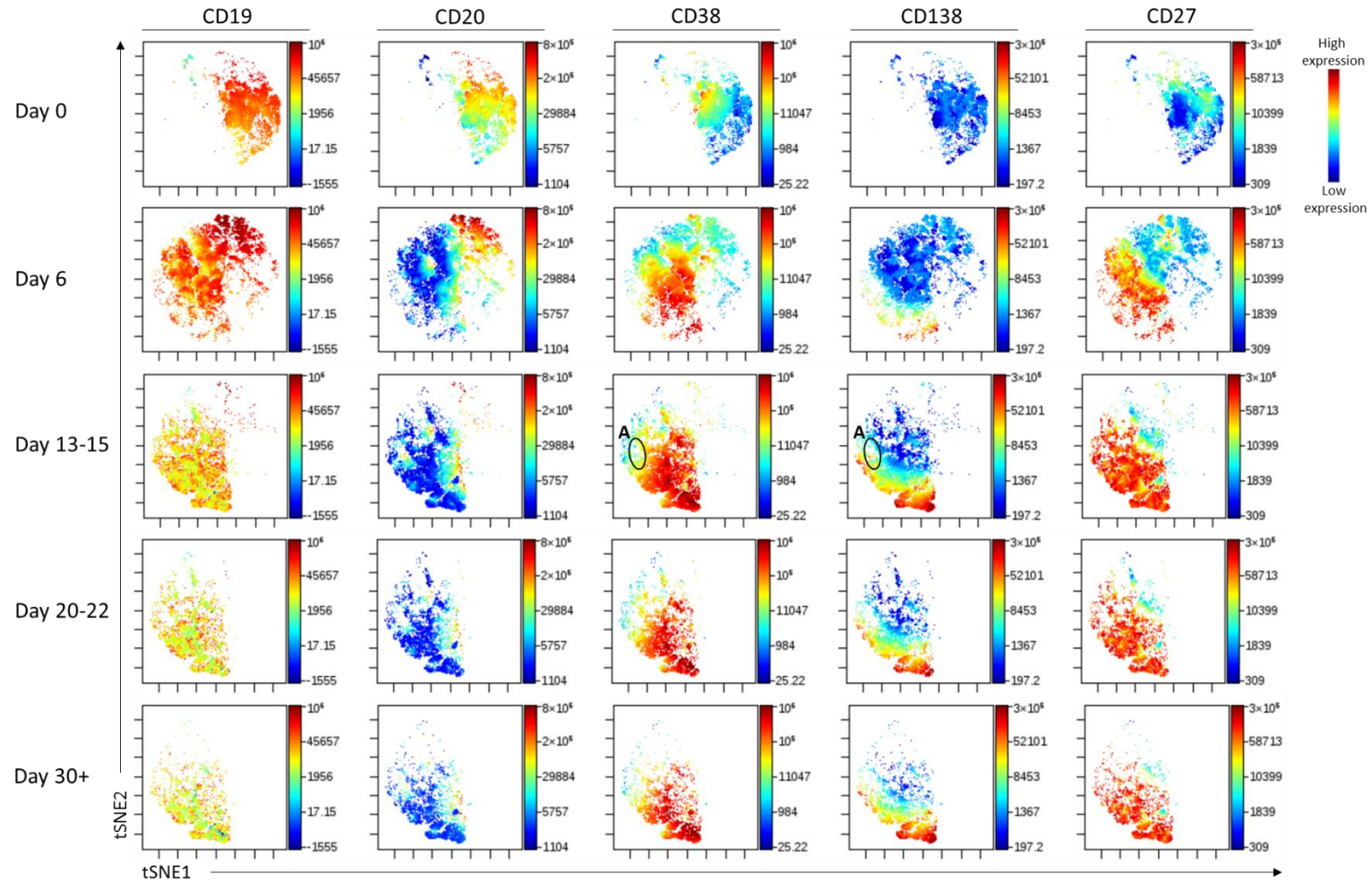
Figure 6.2 viSNE plots of healthy CD40L-stimulated cells. B-cells were stimulated at day 0 with CD40L + F(ab')$_2$ anti-IgG/M. viSNE plots created from concatenated raw flow cytometry data where similar time points have been grouped together for clarity. Each column has been coloured using the marker indicated. A – Absence of CD38$^-$ CD138$^+$ cells.

An equivalent summary of differentiating WM cells is depicted in figure 6.3. In this case, the plots depicting the B-cells at day 0 appear quite similar to the healthy plots, but thereafter they diverge substantially. These viSNE plots illustrate the heterogeneity of the response of WM cells compared to healthy B-cells by displaying them as a continuum across the space, rather than the more discrete location of the healthy cells within the lower left quadrant from day 13 onwards. The lower efficiency of plasma cell generation by these cells is highlighted by the decreased proportion of cells located at the southern tip of the plots, which conversely are densely populated in the viSNE plots for healthy cells. The delay in the loss of CD20 for many of the WM cells can be seen in several red clusters that persist throughout the differentiation within the CD20 column – population A – as well as a more diffuse group present at the top right. The locations of these clusters demonstrate that there is a fraction of cells which are less responsive to CD40L stimulation and remain in a pre-plasmablast like stage – those in the top right – whilst the other CD20$^+$ cells are more closely related to plasmablasts or plasma cells, despite their inability to downregulate this marker.

The CD38$^-$ CD138$^+$ population of plasmablast-like cells in WM differentiations can be identified as a cluster in the CD138 column from day 13 onwards on the left hand side of the plots and has been circled (B). At the corresponding location on the viSNE maps of healthy controls, cells falling within the boundaries of this cluster are almost completely absent. Interestingly, a very small population can be seen in the healthy plots at day 13 (figure 6.2, cluster A), but with a slightly different phenotype of CD20$^+$, CD138^{low} and a lower expression of CD38 than the other plasmablasts at this time point. However in this instance this cluster appears to represent a group of cells that have not upregulated as quickly as the rest of the population, as this population substantially diminishes between days 15-20 as the differentiation progresses and the remaining cells increase CD38 and CD138 expression in line with the recognised CD38$^+$ CD138$^+$ plasma cell phenotype. It is nevertheless intriguing that the WM CD38$^-$ CD138$^+$ precursor may have a counterpart in healthy samples but they exhibit a divergent response to CD40L stimulation.
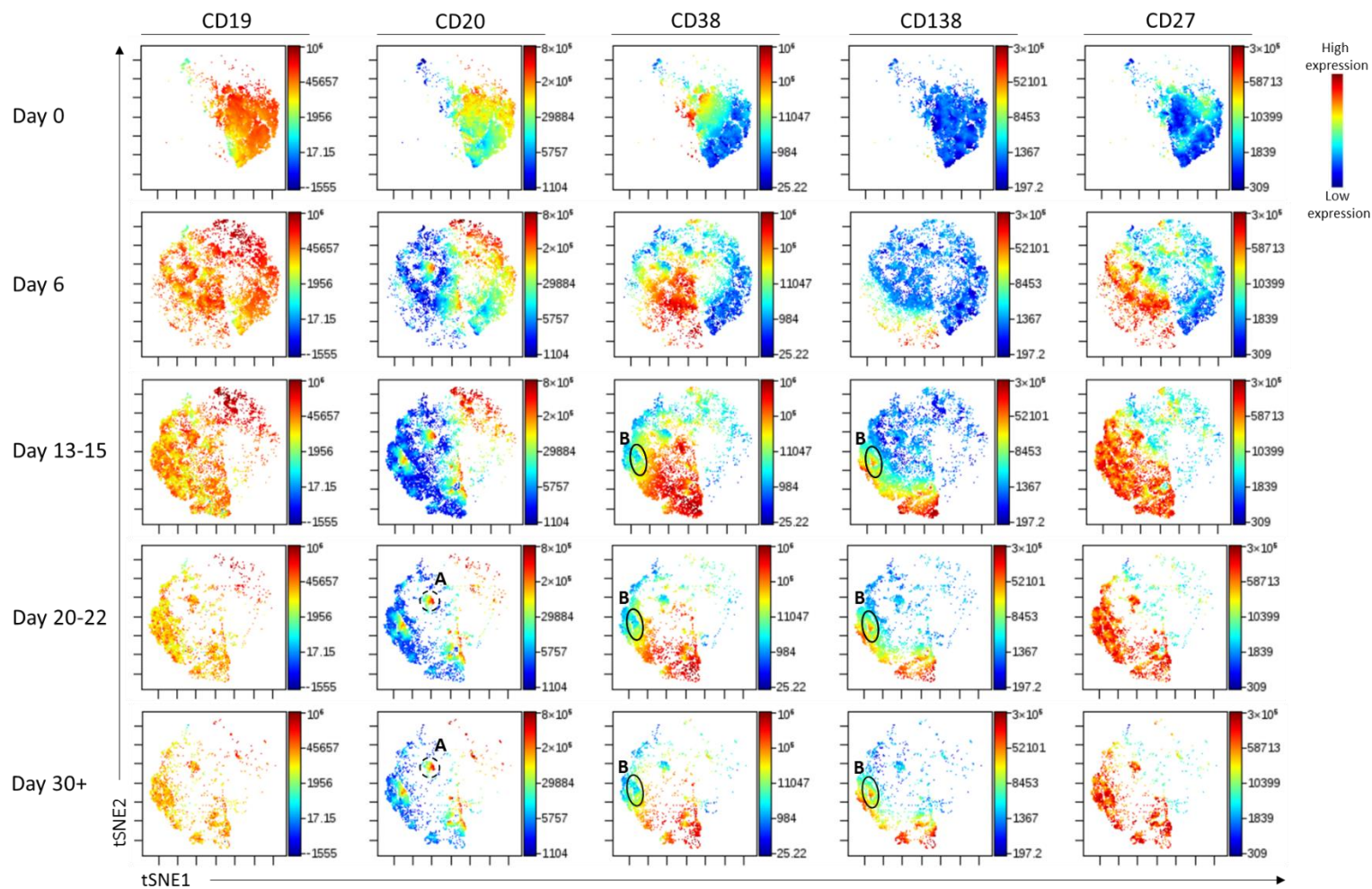
Figure 6.3 viSNE plots of CD40L-stimulated WM differentiations. B-cells derived from WM patients were stimulated with CD40L + F(ab')$_2$ anti-IgG/M. Clusters of particular interest are circled . A – Persistent CD20^{hi}population, B – CD38- CD138+ population.

B-cells derived from the bone marrow of patients with SMZL were differentiated in order to determine if the phenotypes observed in WM cells were representative of B-cell neoplasms in general or if WM cells demonstrated a unique profile. A group of concatenated samples from SMZL differentiations were included in this analysis in order to further investigate the relatedness of WM cells to this neoplasm. The viSNE maps of SMZL B-cells are different to both healthy and WM B-cells as one might expect (figure 6.4). The most noticeable aspect of this difference is the absence of a cluster which, in healthy and WM B-cells, denotes $CD19^+$ $CD20^+$ $CD27^-$ naïve B-cells with low to medium expression of CD38 (figure 6.4, cluster A). CD38 has been found to be variably expressed in SMZL, with early investigations by Mollejo *et al.,* and Wu *et al.,* indicating the SMZL cells were negative for this marker, but more recent phenotypic analysis confirms CD38 expression in some patients (Mollejo *et al.*, 1995; Wu *et al.*, 1996; Algara *et al.*, 2002; Kost *et al.*, 2008).

The location of the SMZL cells within the viSNE plots from subsequent time points fall somewhere between the healthy and WM cells. In a similar manner to the WM cells, the SMZL cells form a sweep across the biaxial plots with cells that are unable to respond correctly to CD40L stimulation continuing to be present in the upper right quadrant even at the later time points. These cells express high levels of CD20, intermediate levels of CD38 and low levels of CD138, this in combination with their location, suggesting that they are quite similar to the healthy day 6 plasmablasts but that they are unable to proceed further with differentiation. The location that corresponds to the WM $CD38^+$ $CD138^-$ population is completely devoid of cells, emphasising the highly distinct nature of this population to WM (figure 6.4, cluster B). The SMZL viSNE plots share a cluster of $CD27^{low}$ plasma cells with the healthy samples, but that cluster is much less populated within the WM plots.

Another cluster that is more prominent in the SMZL plots is a group of persistent $CD20^-$ $CD38^+$ plasmablasts located at the centre of the viSNE maps which have been circled with a dashed line on the day 30+ CD38 and CD138 plots (figure 6.4, cluster C). It appears that a fraction of SMZL B-cells are able to differentiate to this stage but suffer a defect that prevents them from progressing further. Plasmablasts occupying this location occur in the healthy and WM viSNE maps at day 6 and 13-15, but these populations subsequently diminish and are either able to complete differentiation or do not survive to the later time points, unlike the SMZL cells.
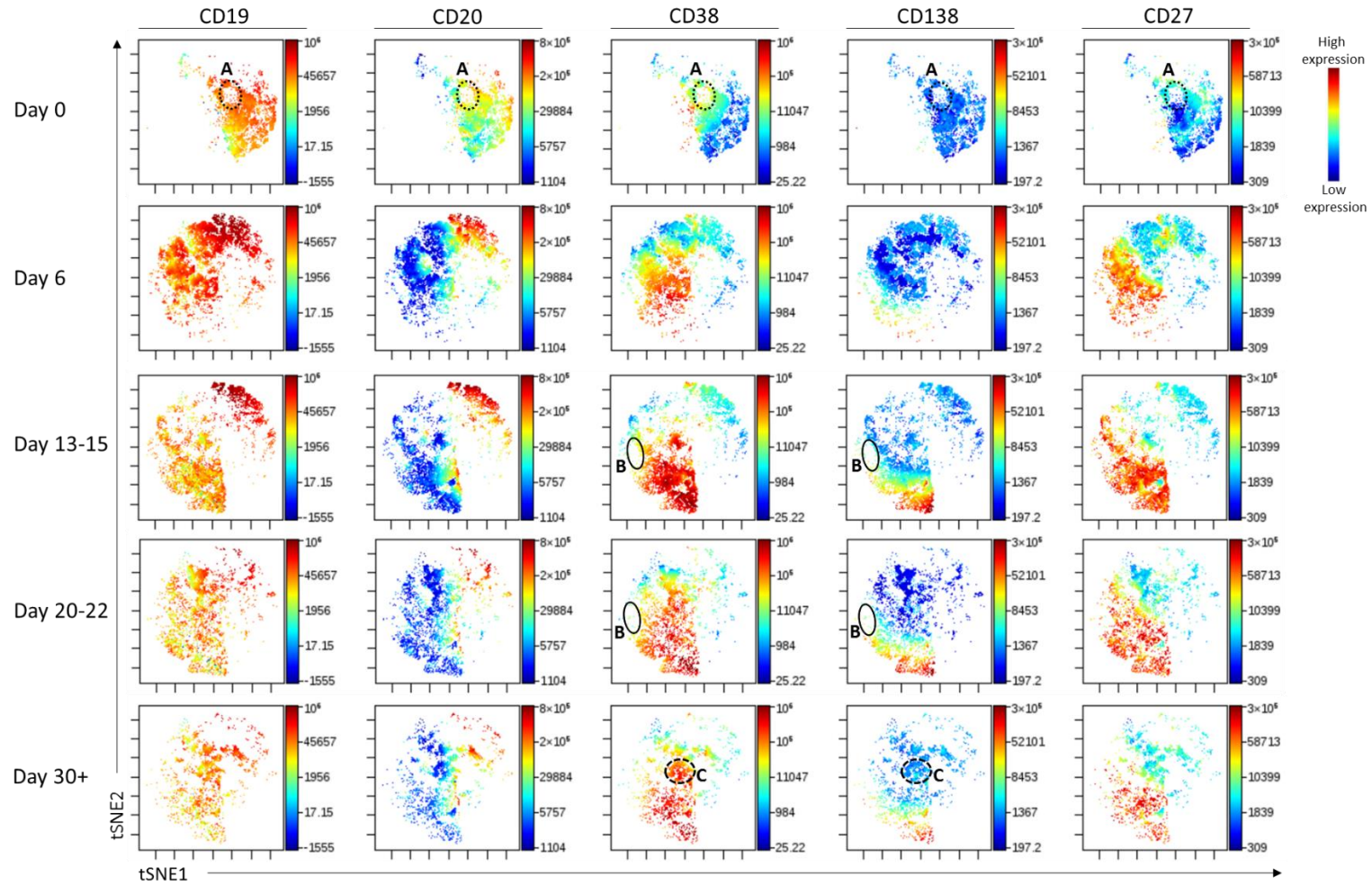
Figure 6.4 viSNE plots of CD40L-stimulated SMZL differentiations. B-cells derived from SMZL patients were stimulated with CD40L + F(ab')$_2$ anti-IgG/M. Clusters of particular interest are circled. A – Absence of CD19$^+$ CD20$^+$ CD27$^-$ CD38^{low} cluster, B – Absence of CD38$^-$ CD138$^+$ population., C – Persistent plasmablasts.

A group comprising of concatenated data from all non-healthy samples was also created in order to visualise the profile in comparison to healthy controls and to determine whether the distinctive clusters observed in each individual LPD group are still present following amalgamation of the samples. This set of data includes WM, SMZL and samples from two other LPDs. The viSNE maps of this concatenated data is presented in figure 6.5. The proportion of B-cells that are unable to successfully respond to CD40L stimulation is most evident in this merged data. The location of the healthy differentiating cells shifts completely from one side of the plots to the other as B-cells become plasma cells, but the in case of the LPD samples, a large fraction of cells remain in their initial position throughout the entire time course, retaining a B-cell phenotype. Compared to healthy cells, there is much less downregulation of CD19 by the LPD cells.

Several clusters of CD20$^+$ plasmablasts and plasma cells that were identified in the WM group remain prominent within this larger set of samples. In addition, the distinctive WM CD38$^-$ CD138$^+$ fraction is not masked by the concatenation of multiple different LPDs together (figure 6.5, cluster A). A feature of SMZL B-cells is lost in this combined data – the lack of a CD38$^+$ CD27$^-$ naïve B-cell fraction is evident within the SMZL group but due to the presence of these cells in the other LPDs, this distinction is now absent. This underscores that whilst a combinatorial LPD group provides a useful method of comparison to healthy cells, pairwise differences between groups should be evaluated in order to establish the full picture.

Thus, following stimulation with CD40L + F(ab')$_2$ anti-IgG/M, B-cells derived from healthy cells clearly behave in a distinct manner to cells derived from patients with LPDs as evidenced by the viSNE plots. Moreover, B-cells from patients grouped by their LPD share the same characteristics within their respective groups but are different when compared to another LPD.
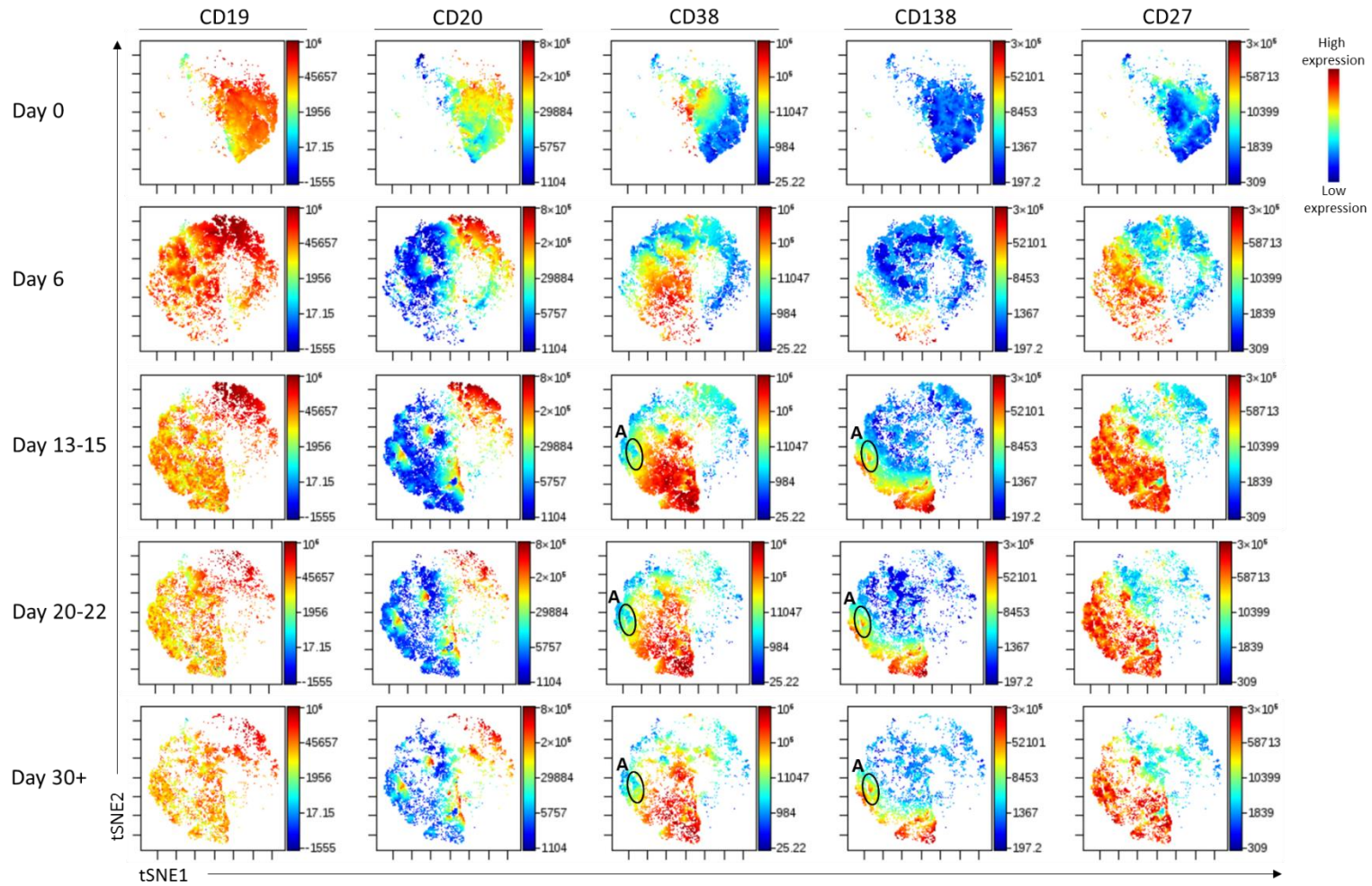
Figure 6.5 viSNE plots of CD40L-stimulated LPD cells. LPD B-cells were stimulated with CD40L + F(ab')$_2$ anti-IgG/M at day 0. Plots were created from concatenated data from multiple LPDs. Clusters of particular interest are circled. A – CD38$^-$ CD138$^+$ plasmablast-like.

6.1.4   Analysis of R848 stimulated cells

The differentiation data was divided based on the stimulation that the cells received, enabling comparison between viSNE plots for each type of stimuli. viSNE plots for healthy cells stimulated with 1µg/ml R848 + F(ab')$_2$ anti-IgG/M are displayed in figure 6.6. By day 6, B-cells stimulated with R848 have progressed further though the differentiation process, with a greater proportion of cells having downregulated CD20, more extensive CD38 expression, paired with increased CD27 levels and a greater proportion of cells expressing CD138 than occurs following stimulation with CD40L. This results in the upper right quadrant of the plots being less populated in figure 6.6 compared to figure 6.2. The spatial arrangement of the populated clusters is very similar between the two conditions. A cluster of CD27^{low} plasmablasts is evident in the viSNE maps for both types of stimuli.

From day 20 onwards, the overall arrangement of clusters is virtually identical, and the expression of cell surface markers is very similar between the two types of stimulation. Whilst both conditions generate populations that consists almost exclusively of plasma cells by day 20, a delay in differentiation at the latter time points can be seen in the viSNE plots that is not observed from examining the biaxial flow data. In fact, the day 20-22 R848 plots look most similar to day 30+ in CD40L, suggesting that the difference between the two types of stimuli is present for longer than initially thought.

CD19$^-$ plasma cells are generated earlier and in greater quantities when the cells were stimulated with R848. The location of the R848-plasma cells is more compact at the bottom of the biaxial plots compared to CD40L-plasma cells which form a slight sweep across a larger area. This indicates that plasma cells generated from R848 stimulation are more closely related.

The location of the WM CD38$^-$ CD138$^+$ fraction has been circled to demonstrate the absence of healthy cells falling within this boundary (figure 6.6, cluster A).
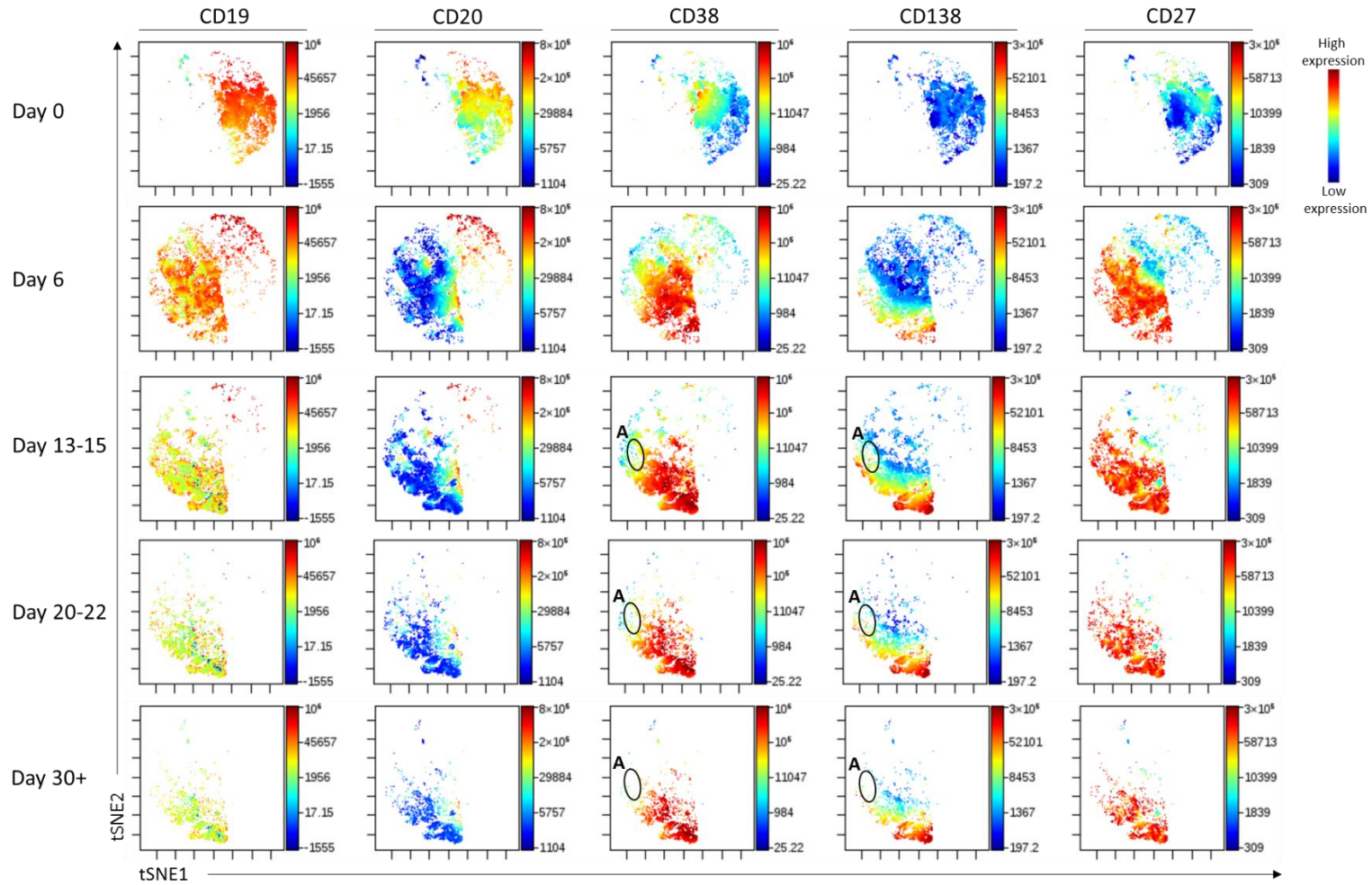
Figure 6.6 viSNE plots of R848-stimulated healthy differentiations. Cells were stimulated with 1µg/ml R848 + F(ab')$_2$ anti-IgG/M. Clusters of interest are circled. A – Absence of CD38$^-$ CD138$^+$ population.

Data from chapter 4 established that WM B-cells die following stimulation with 1µg/ml R848 + F(ab')$_2$ anti-IgG/M (figure 4.12). After day 13-15 of these differentiations, there were too few cells to generate meaningful viSNE maps so only data up to day 13-15 is displayed (figure 6.7). As one might expect, the spatial arrangement of WM clusters at day 6 for both types of stimuli share similarities and appear more closely related to one another than if they are compared to healthy cells stimulated with R848. However, there are several differences of note between the viSNE plots of WM cells stimulated with R848 compared to those that received CD40L stimulation. The R848-stimulated WM cells are much less efficient at generating plasma cells than their CD40L-stimulated counterparts and this is illustrated here by the lower density of cells at the southern point of the plots. The two clusters of CD20$^+$ plasmablasts that are generated at day 6 subsequent to CD40L stimulation (figure 6.7, cluster A) are almost completely absent at this time point when the WM cells are stimulated with R848 and these diminish further from day 6 to day 13-15.

A particularly prominent feature of the R848 plots at day 13-15 is the presence of a large portion of cells located on the on the lower right hand side of the bivariate plots which are particularly recalcitrant to differentiation. This cluster is much more conspicuous in the R848-stimulated cells but this population is also evident in the differentiations with CD40L. There is very little phenotypic progression of the WM cells cultured with R848 between day 6 and days 13-15, in fact the population becomes more skewed towards a greater proportion of cells that have been unable to respond, whereas those from the CD40L condition have begun to migrate to the upper left of the plots as they acquire a more differentiated phenotype. Whilst the CD40L plots consist of a smooth continuum of populations, there appears to be a divide in R848 plots, almost directly down the middle, separating the population of cells that are unable to differentiate and those which have been able to respond and have generated a small population of plasma cells. Since an intermediate population is not present, this feature may denote the proportion of non-neoplastic cells within the culture, as they display a phenotype which is much more similar to that of the healthy cells following stimulation with R848. There are clearly few cells as the differentiation progresses, but there is no evidence of the CD38$^-$ CD138$^+$ population at day 13-15 (figure 6.7, cluster B).
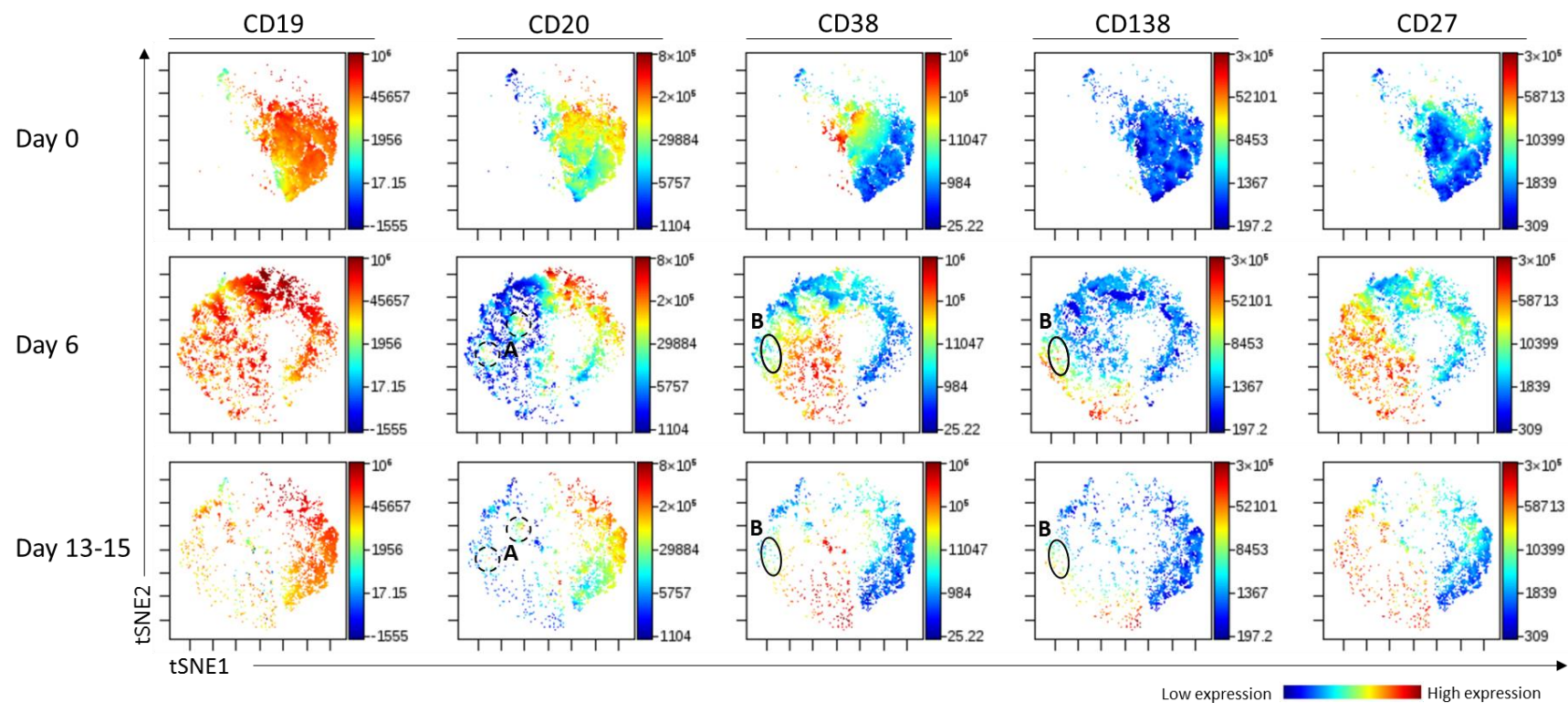
Figure 6.7 viSNE plots of R848-stimulated WM differentiations. Cells were stimulated with 1µg/ml R848 + F(ab')$_2$ anti-IgG/M. Clusters of interest are circled. A – Absence of persistent CD20^{hi} fraction observed in differentiations with WM samples. B – Absence of CD38$^-$ CD138$^+$ population.
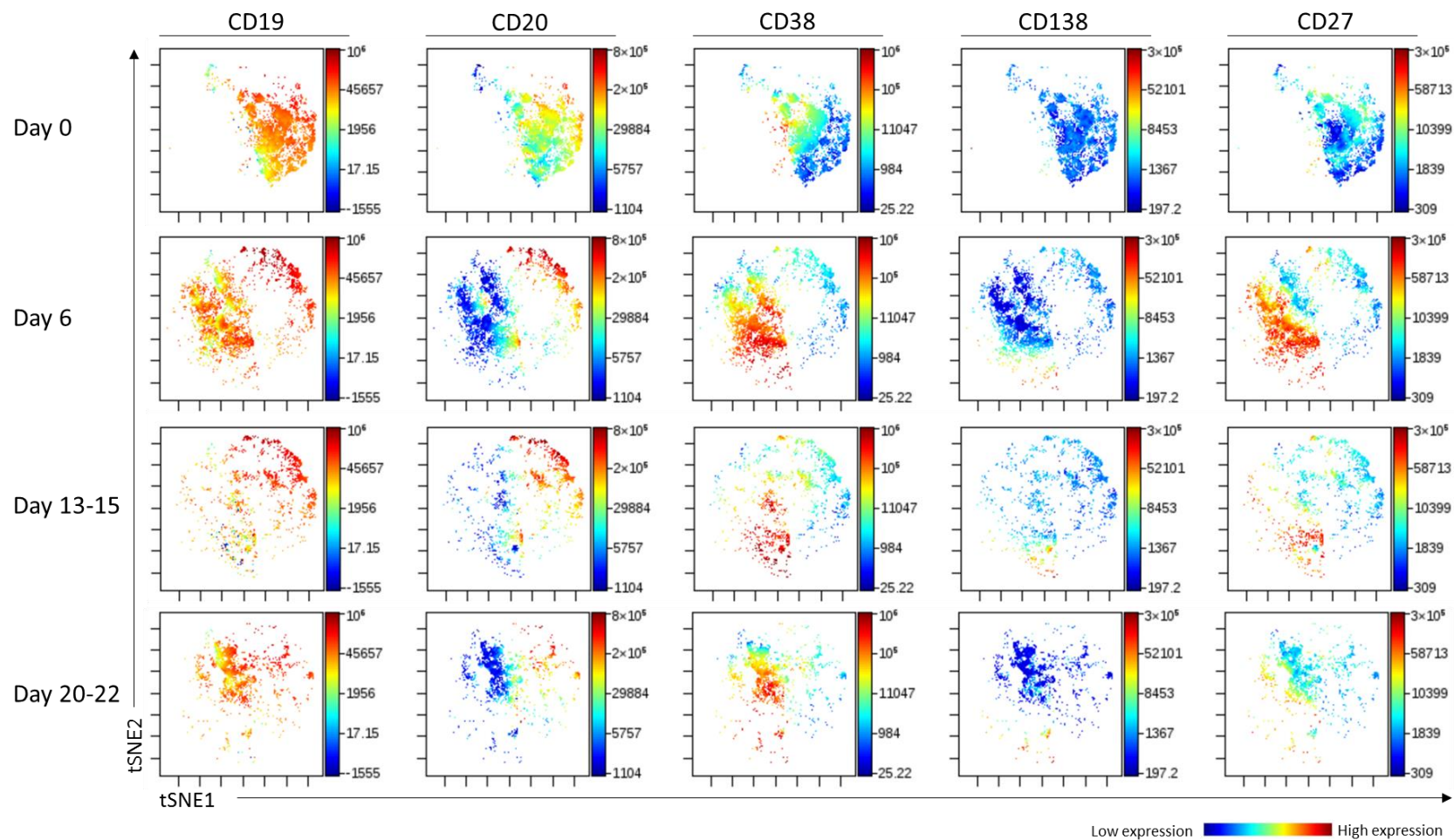
Figure 6.8 viSNE plots of R848-stimulated SMZL differentiations. B-cells derived from SMZL patients were stimulated with 1µg/ml R848 + F(ab')$_2$ anti-IgG/M.

Figure 6.8 displays the viSNE plots generated from SMZL samples stimulated with R848. A decrease in the number of SMZL cells surviving subsequent to R848 stimulation compared with CD40L is evident, but there were sufficient numbers to produce an informative viSNE plot for day 20-22. Interestingly, whilst cell survival is considerably better in this group compared to the WM samples, plasma cell differentiation is more substantially impaired.

In a similar manner to SMZL B-cells stimulated with CD40L, the SMZL cells activated with R848 generate a significant proportion of plasmablasts that persist to day 20-22 without progressing any further. The location of the clusters at the 13-15 and day 20-22 time points are different, favouring the plasmablast fraction at the later time point rather than the plasma cell fraction as would be expected. This may be due to the data being sampled from a pool of 2 at day 20-22 rather than a pool of 6 for the previous plots and thus a skewing of the populations towards a sample with high levels of plasmablasts at this time point. However, this does highlight that a clear subset of SMZL cells are able to differentiate into plasmablasts and survive long-term but are incapable of terminal differentiation.

The proportion of cells that appear to be incapable of differentiating is an obvious commonality shared between both the SMZL and WM groups that does not occur in healthy differentiating cells. Whilst this fraction increases considerably in WM cells following R848 stimulation compared with CD40L stimulation, it appears that the proportion of unresponsive cells in the SMZL samples is similar across both types of stimulation.

Data from all LPD samples stimulated with 1μg/ml R848 + F(ab')$_2$ anti-IgG/M were combined in figure 6.9 as for the CD40L stimulation. Since the WM cells died before day 20 of the differentiation, only this first three time points containing amalgamated data from all groups are shown. The large sweep of cells makes it clear that there is certainly a general impairment to differentiation following R848 stimulation compared to healthy cells. It is evident from this data that the characteristic WM CD38$^-$ CD138$^+$ fraction is not generated by any of the samples here and is limited to WM cells stimulated with CD40L.
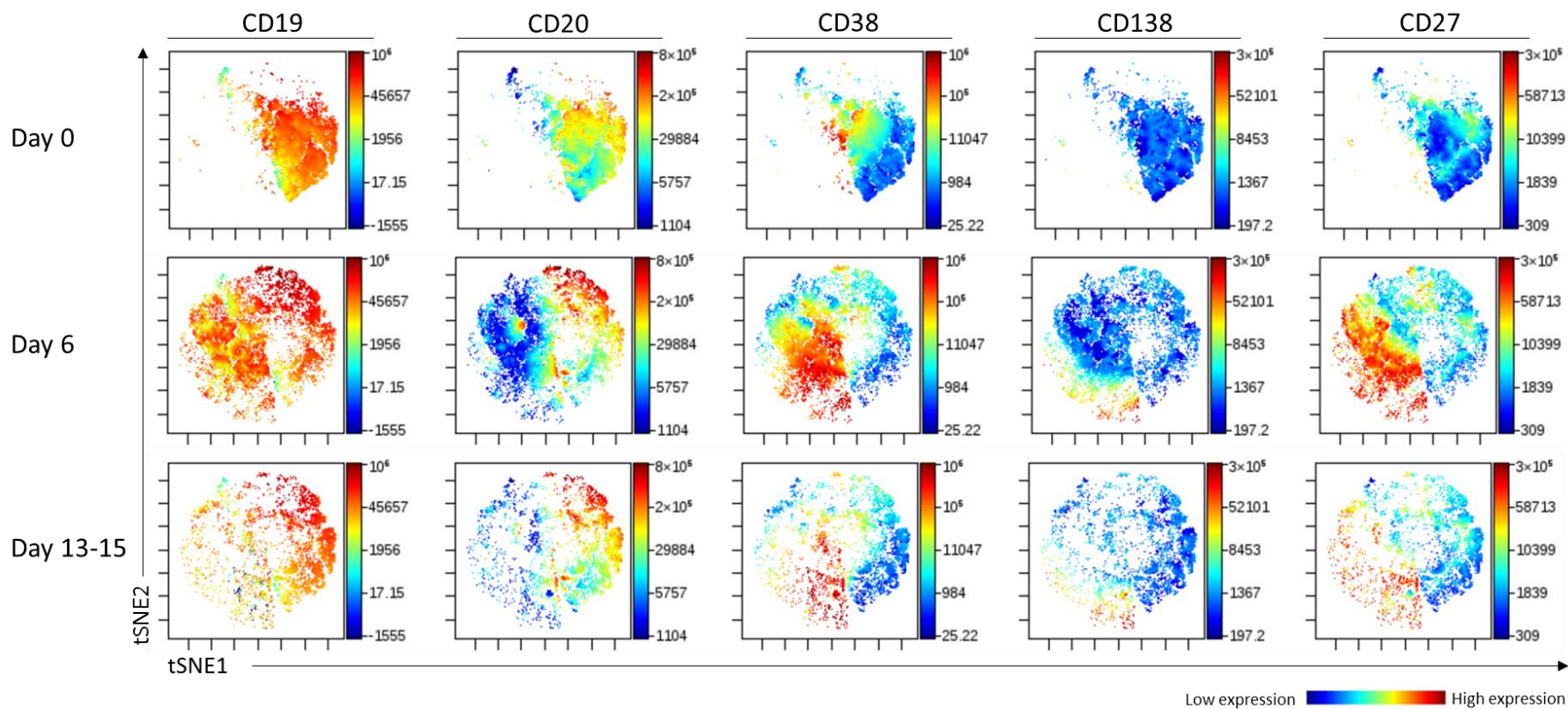
Figure 6.9 viSNE plots of R848-stimulated LPD B-cells. Cells were stimulated with 1µg/ml R848 + F(ab')₂ anti-IgG/M. Plots were created from concatenated data from multiple LPDs and contain WM, SMZL and samples from two other LPDs.

6.2 SPADE on viSNE

6.2.1 SPADE introduction

The previous analysis enabled global comparisons to be made, but to further interrogate the data and examine the relationships between the different populations of cells generated during the differentiations, an algorithm called SPADE was used as an automated method to categorise groups in order to generate clusters that correspond to the viSNE plots shown previously. SPADE (**s**panning-tree **p**rogression **a**nalysis of **d**ensity-normalized **e**vents) is a clustering algorithm that enables visualisation of populations within multidimensional flow cytometry data by representing them within a tree (Qiu *et al.*, 2011). The location of the clusters within the plot cannot be used to infer relatedness, but rather this can be determined by the connections between the different clusters, termed edges. The fewer the number of edges from one cluster to another, the more similar they are.

Populations of cells are denoted as clusters or nodes of differing size depending on the number of cells they represent and each node is linked to the other most closely related nodes by one or more edges. The colour of any given node illustrates the expression of a marker by that population of cells. In this case, as with the viSNE analysis, blue represents low or no expression and red represents the highest expression. The SPADE algorithm, like viSNE, is unbiased and thus allows identification of populations in an objective manner.

A small section of a SPADE tree is depicted in figure 6.10, demonstrating how populations can be discriminated, in this case the memory and naïve B-cell fraction by using CD27 expression.
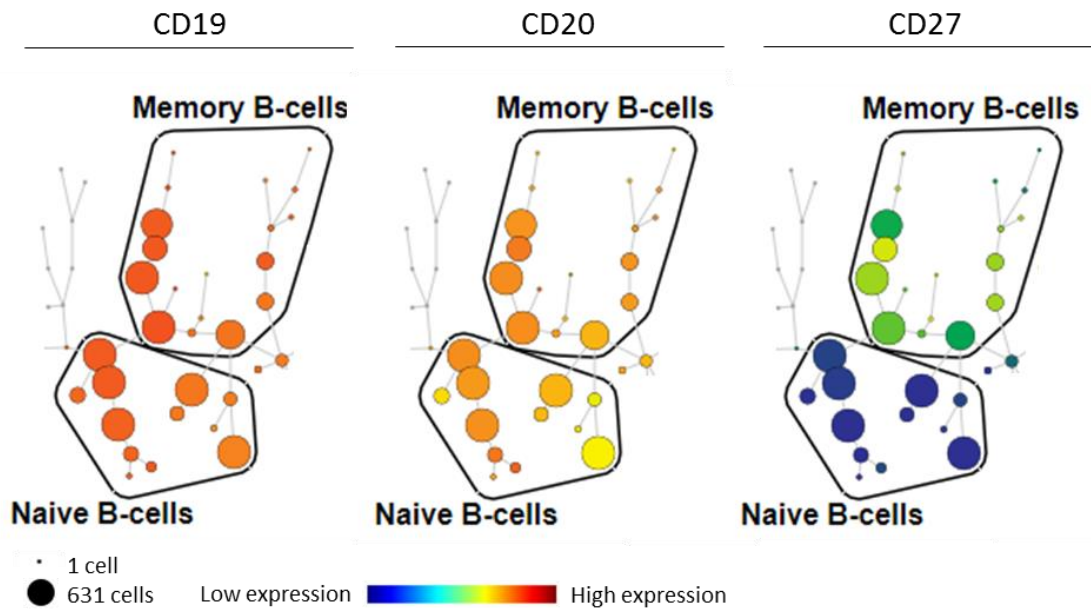
Figure 6.10 Section of a SPADE plot containing the naïve and memory B-cell fractions. The tree was constructed from concatenated flow data for day 0 B-cells isolated from healthy donors. Cells have been clustered using the marker indicated.

Since SPADE plots only display the expression of one marker at a time, consolidating clusters together based on a shared phenotype facilitates comparison between plots. This is not performed by the algorithm, rather they must be established by whomever is analysing the output. For the data presented here, several groups were initially determined based on populations of cells which matched the recognised phenotype for each stage of differentiation – B-cells (both the memory and naïve fraction), plasmablasts and plasma cells – by their expression of CD19, CD20, CD27, CD38 and CD138. Labelling of the nodes was performed first for the concatenated healthy samples so any deviations from this could be identified in the patient samples. Subsequently, collections of related nodes that did not fall within the pre-established groups but that shared the same phenotype as each other were identified and named appropriately depending on their distinguishing features.

The temporal and spatial movement of B-cell populations during a healthy differentiation is illustrated in the selection of SPADE plots in figure 6.11. CD38 was chosen to colour these plots as the expression of this marker increases over the course of the differentiation.
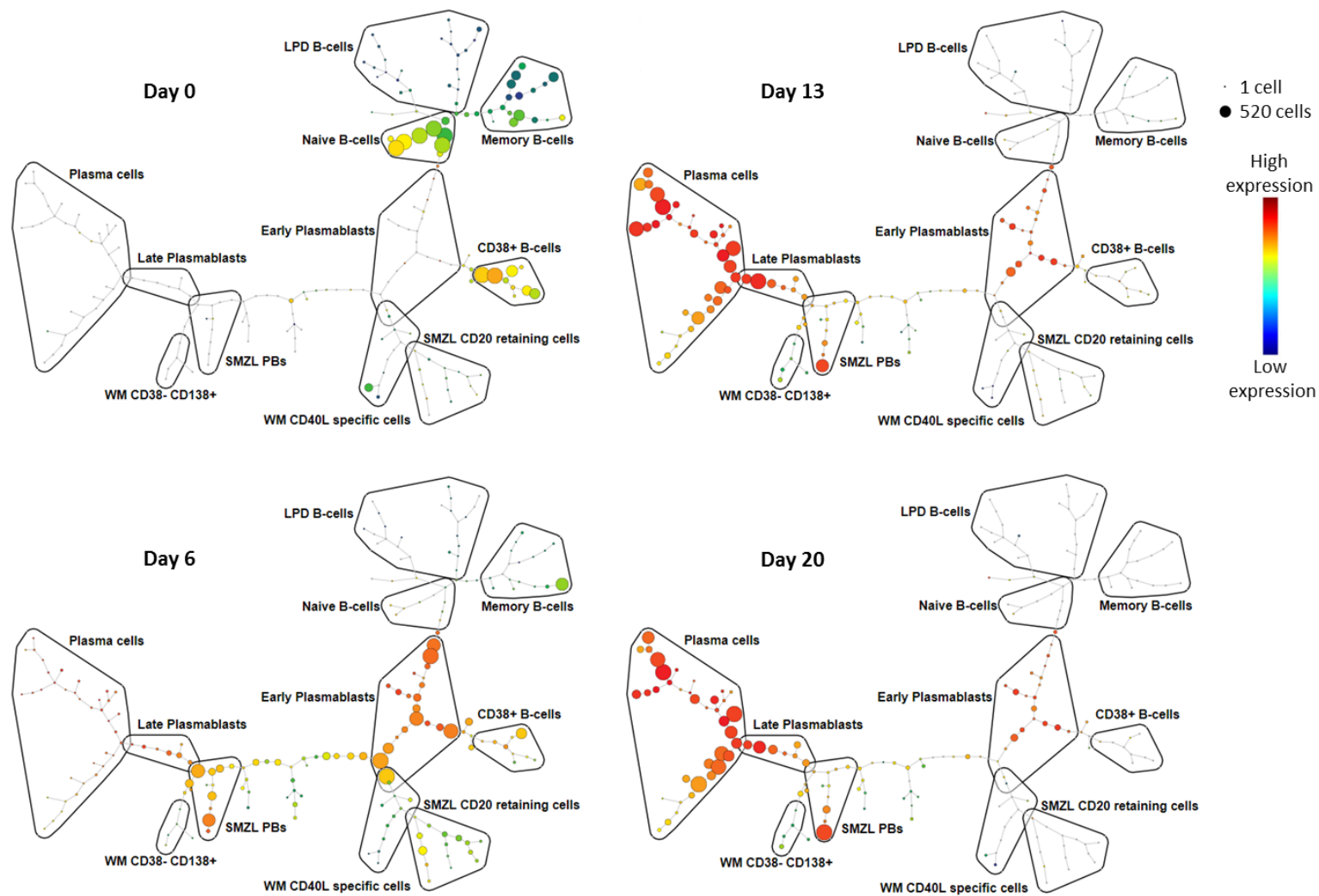
Figure 6.11 SPADE plots depicting changes in the B-cell population during an *in vitro* differentiation. B-cells isolated from healthy donors were stimulated with CD40L and F(ab')₂ anti-IgG/M. Plots were constructed from concatenated flow data at each time point indicated. Expression intensity is indicated by colour – blue to red = low to high.

At day 0, the only populated branches are those that contain the memory and naïve B-cell fractions and a branch containing B-cells that express higher levels of CD38 than the rest of the population. By day 6, the number of cells within the B-cell nodes has depleted as the cells have become plasmablasts. Consequently, most of the population of cells now lie within a section that has been designated early plasmablasts and the upregulation of CD38 expression is demonstrated by the change of colour from green to yellow or orange. From day 13 onwards, the majority of the cells have become plasma cells and have shifted accordingly, although some plasmablasts persist, which have been termed late plasmablasts.

Using this method, the presence of unusual populations can be confirmed in a non-biased manner. To demonstrate this, SPADE analysis was performed using only the samples from the healthy group. A population of CD19- plasma cells that sometimes occurs at the late stages of an *in vitro* differentiation are clearly defined by their location at the tip of a branch of the plots shown in figure 6.12.
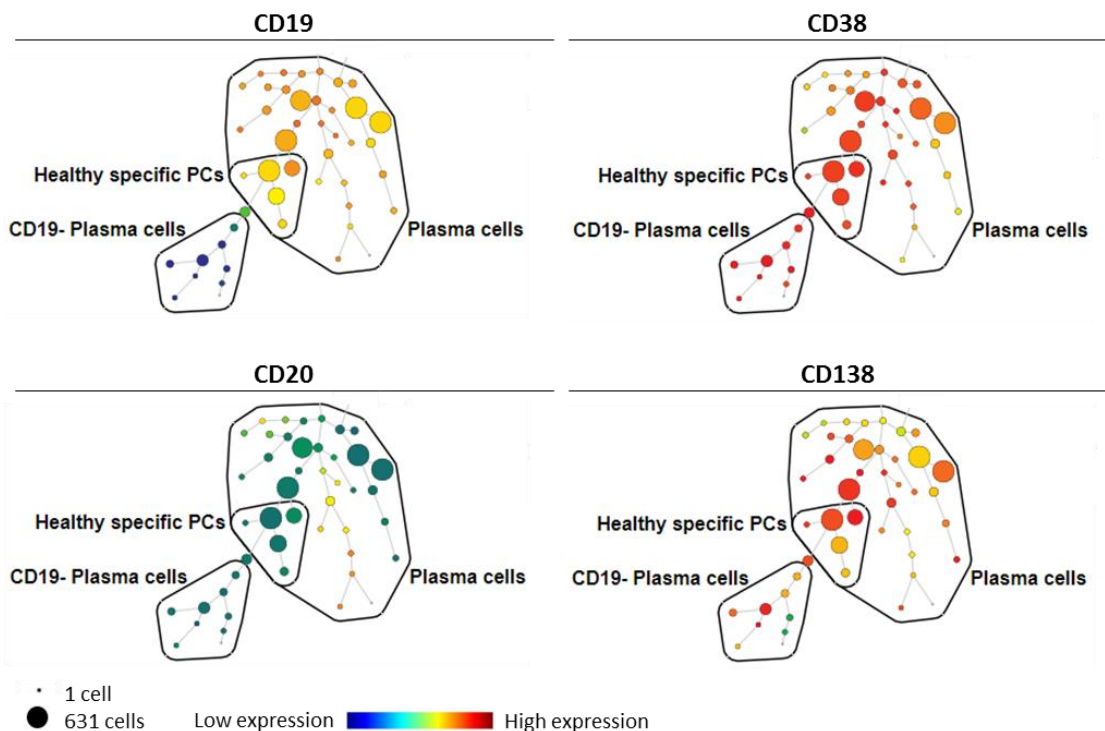
Figure 6.12 Section of a SPADE plot illustrating the phenotype and separation of the CD19- plasma cells from the CD19+ plasma cell fraction. The tree was constructed from concatenated flow data for day 30+ B-cells isolated from healthy donors stimulated with CD40L and F(ab')2 anti-IgG/M. Cells have been clustered using the marker indicated. The intensity of expression is indicated by colour – blue = low/no expression, red = high expression.

6.2.2   Comparison of CD40L and R848 stimulations in healthy cells

The phenotype of healthy differentiating cells following stimulation with either CD40L + F(ab')$_2$ anti-IgG/M or 1µg/ml R848 + F(ab')$_2$ anti-IgG/M are comparable to each other when compared on biaxial flow plots. SPADE analysis provides additional insight as to the relationship between the populations generated by both types of stimuli.

The similarity in the phenotypes of healthy cells stimulated with either CD40L or R848 is demonstrated in figure 6.13. However, visualisation of the data in this manner enables some differences to be distinguished that are not normally discernible by analysing regular flow cytometry contour plots. The greatest divergence between the plots occurs at day 6 of the differentiation, as would be expected by the differences observed from the raw data. B-cells stimulated with CD40L + F(ab')$_2$ anti-IgG/M generated populations that are spread across multiple branches within the early plasmablast segment of the tree, whereas those stimulated with R848 are located within only a few edges of one another and are thus more closely related. This is most interesting as it appears to reflect the findings that certain subsets of B-cells are more responsive to TLR stimulation, hence the more homogeneous location of the populations within the tree whilst activation with CD40L elicits a response from a broader proportion of the cells and thus there are a greater variety of plasmablasts (Bernasconi *et al.*, 2003; Capolunghi *et al.*, 2008; Simchoni and Cunningham-Rundles, 2015).

The increased rapidity of the B-cell response to R848 + F(ab')$_2$ anti-IgG/M stimulation can also be seen at day 6, where the nodes within the plasma cell section have begun to be populated by cells in the R848 condition but not yet by those stimulated with CD40L. Thereafter, the distribution of the populations across the plasma cell nodes is very similar between both types of stimulation, but with a greater proportion of CD138^{++} plasma cells generated by stimulation with R848 at day 20.
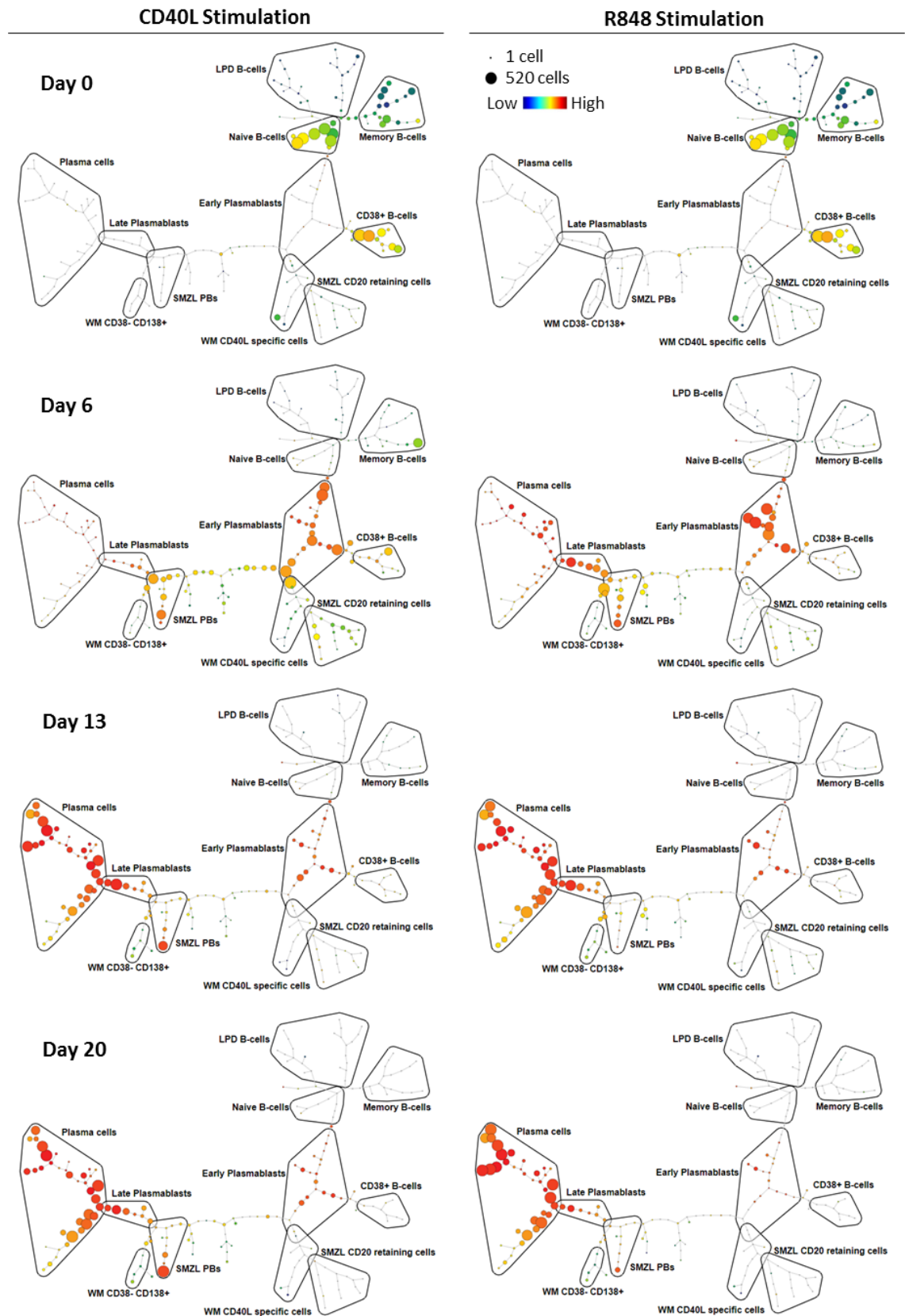
Figure 6.13 SPADE plots depicting changes in the B-cell population during an *in vitro* differentiation. B-cells were isolated from healthy donors and stimulated with CD40L or 1µg/ml R848 and F(ab')₂ anti-IgG/M. Plots are coloured according to CD38 expression.

6.2.3   Differences between healthy and WM differentiations

Figure 6.14 depicts SPADE plots constructed from WM concatenated flow data at day 13 of differentiation, with the intensity of expression of CD38 and CD138 indicated. The equivalent plots of concatenated healthy cells at this time point is shown on the left for comparison. In the upper healthy SPADE tree, all nodes are orange or red, denoting high levels of CD38 in all cells and the lower tree illustrates the separation of the plasmablasts and plasma cells by CD138 expression. However, in the CD38 WM tree, a distinct collection of green nodes can be seen at the tip of the top leftmost branches, denoting a population that is completely absent in the healthy data. These CD38 low cells have a comparable level of CD138 expression to the WM cells that fall within the "classic" plasma cell group delineated by the healthy cells and are thus the peculiar $CD38^-$ $CD138^+$ fraction. The WM cells in general exhibit lower levels of CD38 and CD138 expression than their healthy counterparts. The most closely related healthy cells to these $CD38^-$ $CD138^+$ cells lie further up the branch and are located within the plasmablast group, suggesting that the $CD38^-$ $CD138^+$ cells are more similar to healthy plasmablasts than plasma cells.
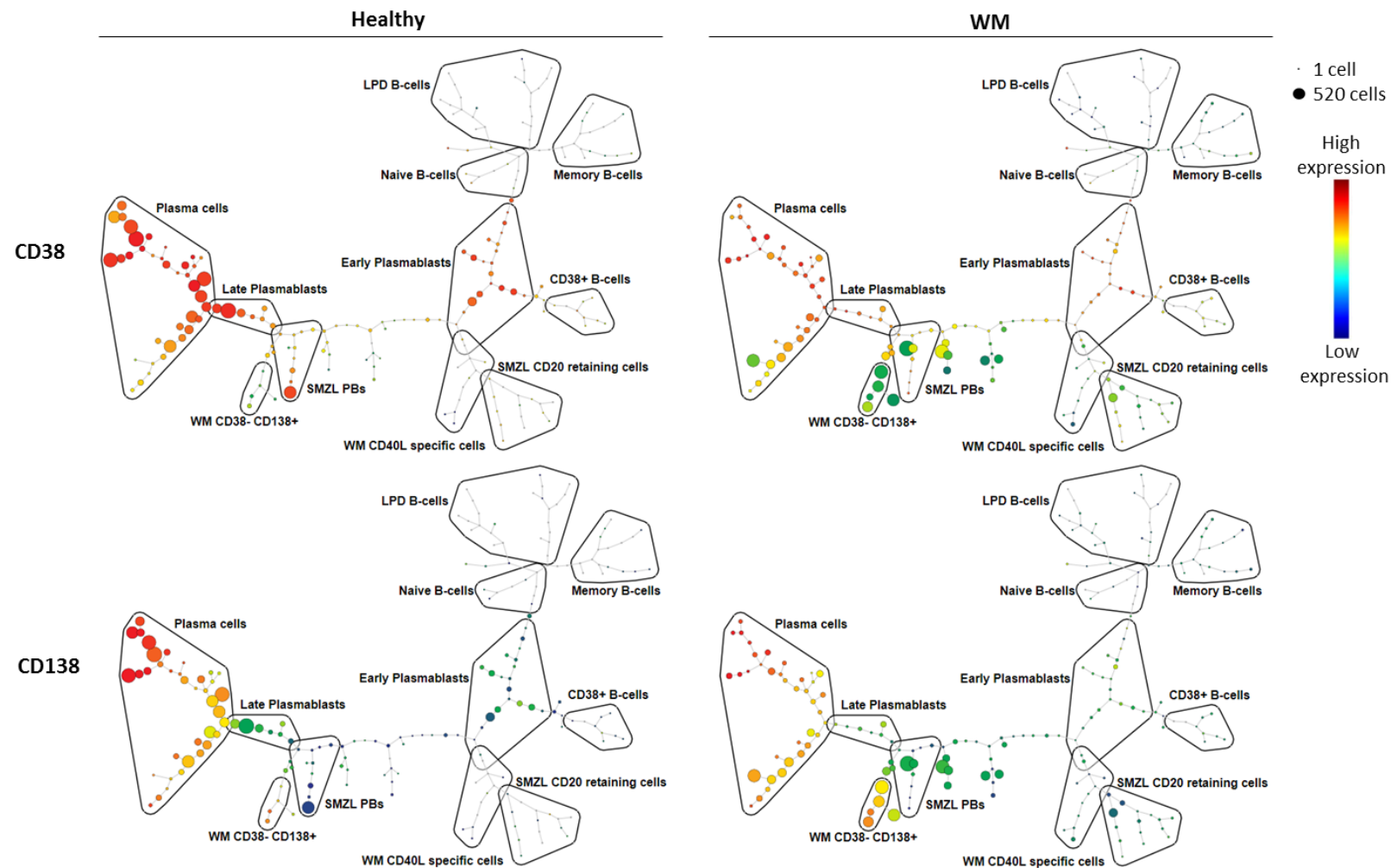
Figure 6.14 SPADE plots depicting the CD38⁻ CD138⁺ WM population and spatial differences between heathy cells and WM cells at day 13. The cells in each case were stimulated with CD40L and F(ab')$_2$ anti-IgG/M at day 0. Plots are coloured according to the markers indicated.

The failure of WM cells to respond to TLR7 stimulation was completely unexpected. A comparison of healthy and WM cells at day 13 of the differentiation following stimulation with R848 + F(ab')$_2$ anti-IgG/M is shown in figure 6.15. Four markers are shown to demonstrate the lack of differentiation in the WM cells. Virtually all nodes in the WM SPADE plots lie on the right hand side, which is normally only populated at day 0 by undifferentiated B-cells. In contrast, almost all of the healthy cells have become plasma cells at this time point and shifted to the bottom left of the trees. The phenotype across the spread of WM nodes is very similar, the cells have retained CD20 expression and failed to increase the expression of CD38, CD138 and CD27.

Whilst the memory and naïve B-cells from healthy donors are all located within the designated sections, there is a large group of WM specific B-cells which are closely related, but clearly divergent, illustrating a difference that was not visible from the raw flow data. The most closely related healthy counterpart to WM cells has been postulated to be memory B-cells. Whilst expression of CD27 is lower in the WM cells than was expected, it is intriguing that there are multiple populated nodes within the memory B-cell portion at this time point whilst there are no cells within the naïve group.

These analyses confirm that there is considerable divergence in the way WM cells differentiate in response to CD40L stimulation when compared to healthy controls. They concur with initial results extrapolated from individual flow data and make it considerably easier to visualise the changes across these data sets during differentiations. The fact that analysis via viSNE and SPADE highlight unusual populations such the CD38$^-$ CD138$^+$ WM population and the CD19$^-$ plasma cells is very encouraging.
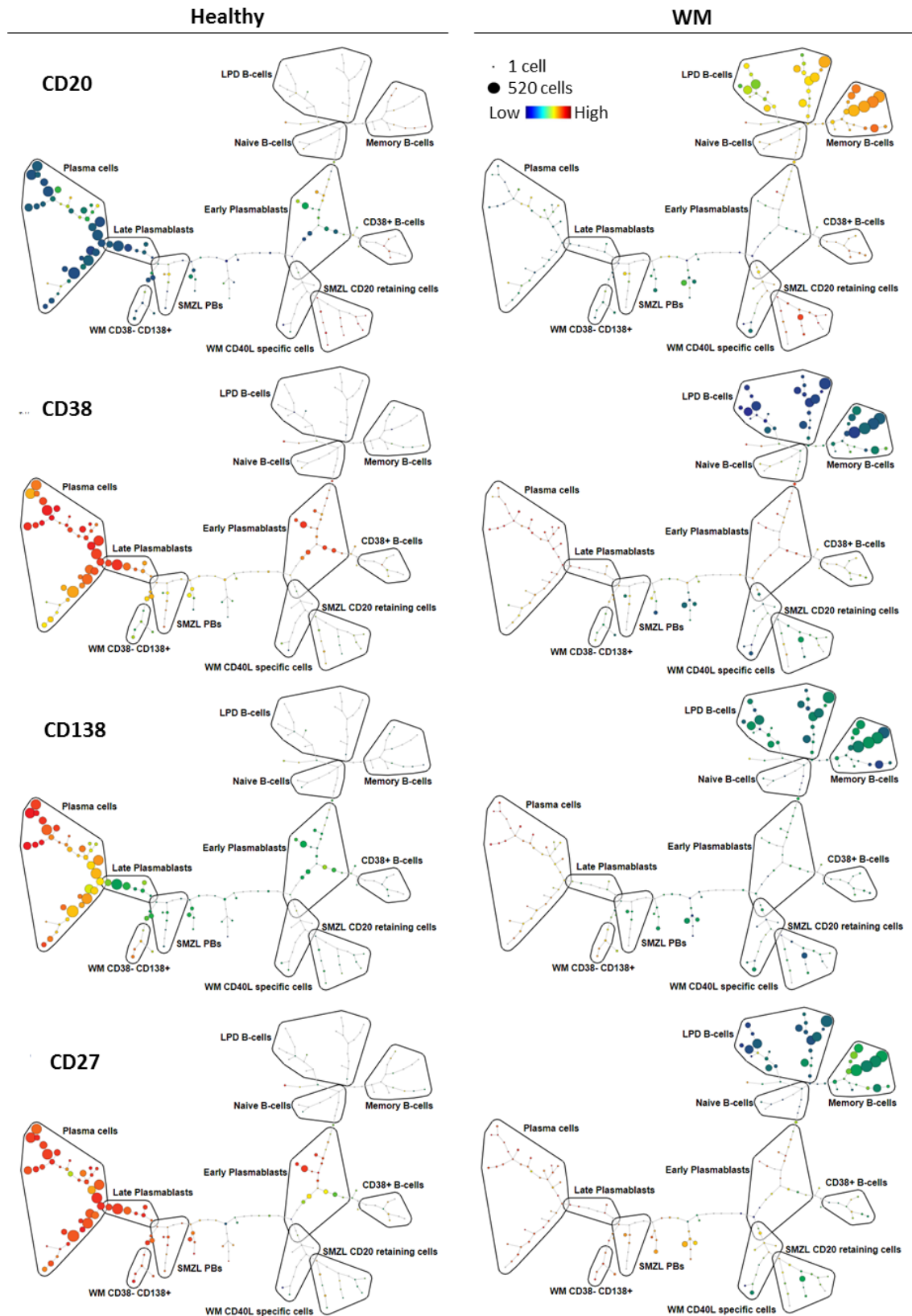
Figure 6.15 SPADE plots comparing populations from WM or healthy cells at day 13 of *in vitro* differentiation. The cells were stimulated with 1μg/ml R848 and F(ab')$_2$ anti-IgG/M. Plots are coloured according to the markers indicated.

6.2.4   Comparison of SMZL differentiations to healthy and WM

The viSNE maps for day 0 B-cells from each group were more similar than expected, however SPADE reveals more detail regarding the relationships between the different populations of cells. A section of the SPADE plots are presented in figure 6.16, with the intensity of expression for the markers CD27 and CD38 shown. Each group possesses a unique spread of nodes across the trees.   The healthy cells are located on three branches, but the populated nodes are clustered tightly together, implying that within these clusters, the cell are homogenous and highly related. The distribution of populated nodes within the SMZL and WM samples are distinct from both the healthy group and from each other. The SMZL B-cells are less homogenous than the healthy cells, and the overlap between the most populous nodes with the healthy cells is quite low. A large proportion of the SMZL cells lie at the intersection between the naïve and memory B-cells, distinguishing them from the healthy and WM groups. The WM plot possesses the most diverse set of cells, with populated nodes across many of the branches. Some of the cells fall within the B-cell fractions defined by the healthy controls but a large proportion of naïve cells lie within the top two branches which are only populated by B-cells from the LPDs and were defined thus. The proportion of neoplastic cells within the WM samples varied more highly than in the SMZL group and this may contribute to the range of populations observed here.

The viSNE plots demonstrated that SMZL group lacked a cluster of CD38^{+} B-cells that was present in both the WM and healthy groups. This can been seen here, with much lower expression of CD38 in the SMZL fraction compared to both the WM and healthy cells.
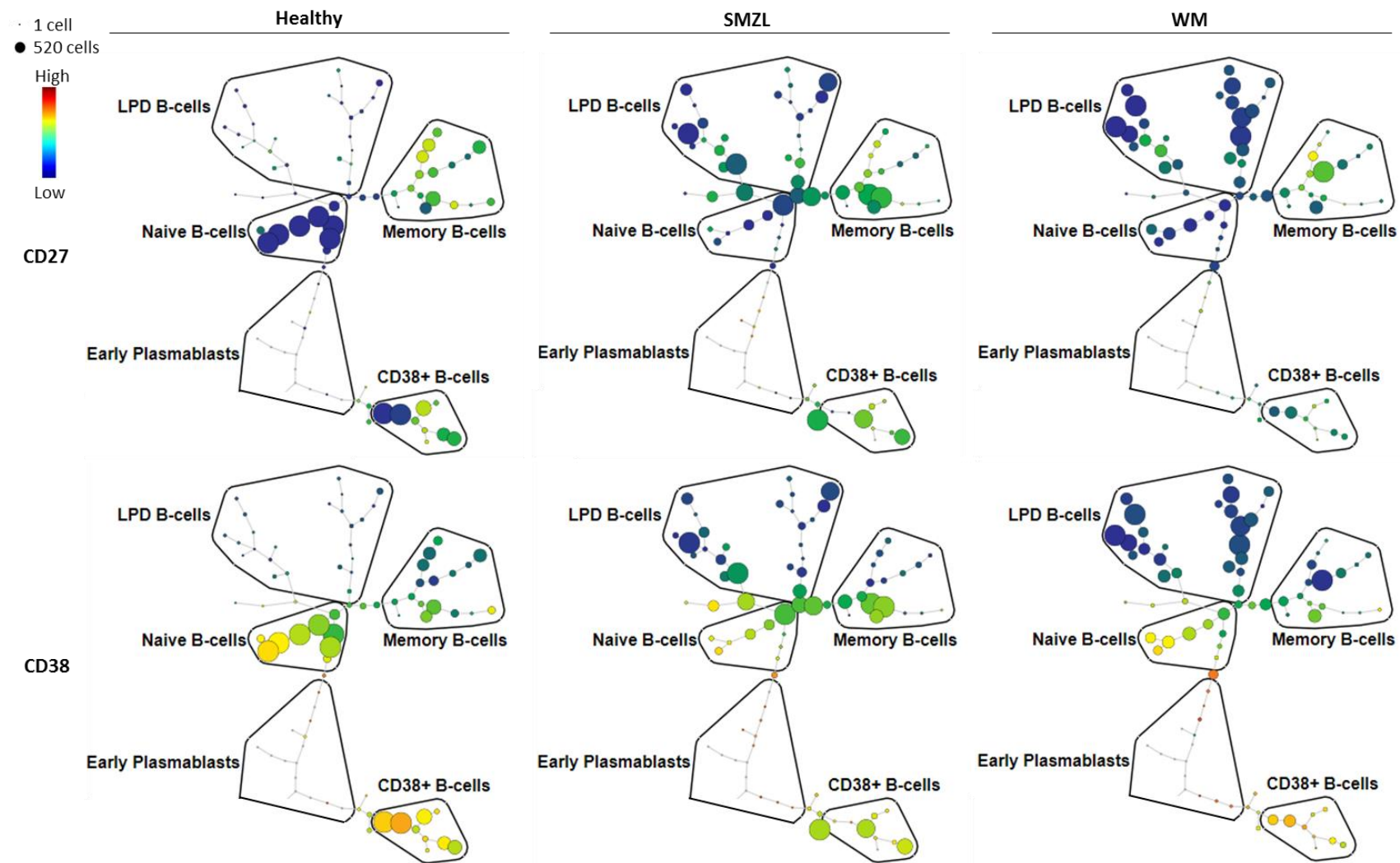
Figure 6.16 SPADE plots comparing B-cell populations from healthy, SMZL or WM cells at day 0 of *in vitro* differentiation.

6.2.5   Differentiations WM and SMZL B-cells generate distinct populations

Differences in the viSNE maps for both WM and SMZL cells are apparent and SPADE enables the relatedness of the cells to be interrogated (figure 6.17). At day 6, virtually all of the WM cells are located in a highly related branch which has been termed WM CD40L specific cells due to this extreme aggregation. In contrast, the SMZL cells are more spread across the plot. There is some overlap between the SMZL cells that fall within the WM CD40L group and a small proportion of WM cells that lie within the SMZL CD20 retaining group. These clusters are highly related and are not populated in the SPADE trees for healthy cells, suggesting that the dysregulation to the plasma cell program in these cells, whilst caused by alternate mechanisms, results in phenotypically related populations of transitional pre-plasmablast cells. The SMZL B-cells have upregulated CD38 more rapidly in a proportion of the total population than the WM cells. These SMZL plasmablasts are more closely related to the late plasmablasts which emerge in healthy differentiations at day 13 than the clusters B-cells or early plasmablasts but are distinct from the location of the healthy cells.

By day 13, the SMZL population is split between a large fraction of plasma cells and two smaller fractions – CD20 retaining cells that are unable to progress further and a fraction of cells which overlap with the early plasmablast segment. The WM cells have also shifted so they broadly fall within the defined plasma cell section, but favour the lower fork, with lower levels of CD38 and CD138 than the SMZL plasma cells. The SMZL differentiation does not generate any $CD38^-$ $CD138^+$ cells and this branch is bare.

Interestingly, at the final time point, the plasma cell proportion of the SMZL population has diminished and a population of cells with a plasmablast phenotype predominate. A similar effect was observed in the viSNE plots for SMZL cells stimulated with R848 but there is no obvious change in the CD40L viSNE. This result may be as a consequence of fewer samples being amalgamated at the later time points (n=6 at day 13 and n=3 at day 20) and a preferential skew away from the plasma cells or may reflect the inability of these cells to produce long-lived plasma cells and thus the population generated at day 13 have not survived. The SMZL samples appear to generate a population of plasma cells but WM cells generate a greater proportion of long-lived plasma cells.
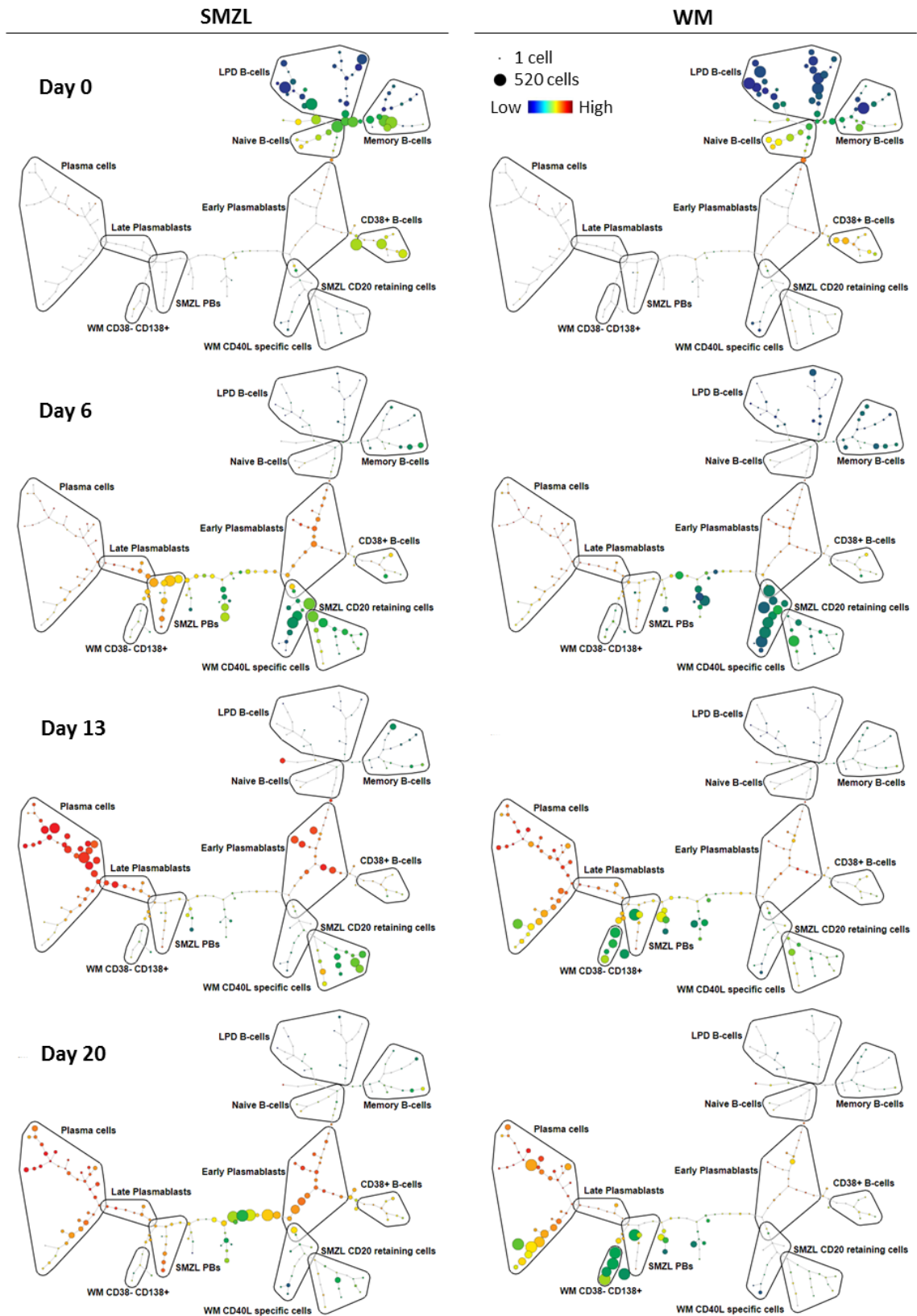
Figure 6.17 SPADE plots comparing B-cell differentiation between SMZL and WM cells. B-cells were isolated from SMZL or WM bone marrow and stimulated with CD40L and F(ab')$_2$ anti-IgG/M. Plots are coloured according to CD38 expression.

The differential responses of B-cells from both of these LPDs is at its most apparent when SPADE plots are compared for B-cells subsequent to stimulation with R848 (figure 6.18). A large proportion of the WM cells are completely unable to respond and fail to initiate plasma cell differentiation. Some cells, do however respond, populating the nodes within the early plasmablast and late plasmablast sections. Between day 0 and 6, the cells within the naïve portion of the tree are lost, indicating that it is potentially these cells that are the ones that retain the ability to respond and become plasmablasts. These naïve B-cells may comprise the non-neoplastic fraction of cells, explaining their capability of response to TLR7 stimulation. This also supports evidence that WM cells are most closely related to healthy memory cells (Sahota *et al.*, 2009; García-Sanz *et al.*, 2016). Additionally, the surviving cells at day 13 are enriched for those falling within the memory fraction, suggesting that they have a survival advantage to the rest of the population.

SMZL cells, on the other hand, do respond at least partially to R848 stimulation. Almost all the B-cell nodes become depopulated between day 0 and 6, implying that most of the SMZL cells are able to initiate some form of differentiation program in response to the stimuli and those that do not are unable to survive. The populations of SMZL cells at day 6 of the differentiation overlap considerably with the healthy cells at this time point, although there is a prevalence of SMZL plasmablasts that are much less prominent in the healthy control group. The difference between the day 6 and day 13 SPADE trees is very noticeable, with the cells appearing to have reverted to a less differentiated state between these two time points albeit with a small fraction of cells that are potentially non neoplastic progressing to the plasma cell stage. There was only one fewer sample in the day 13 concatenated data (n=6) than the day 6 data (n=7) so skewing of the results by a predominating sample is unlikely. In the same manner as when the cells were stimulated with CD40L, the SMZL plasmablast fraction is lost after day 6 suggesting that there is a block in the differentiation program of these cells and that they are unable to survive. The SPADE plot for the day 20 SMZL population generated following activation with R848 is very similar when compared with the equivalent plot for the CD40L stimulated cells. The surviving cells are related to healthy early plasmablasts but are distinct from the healthy populations.
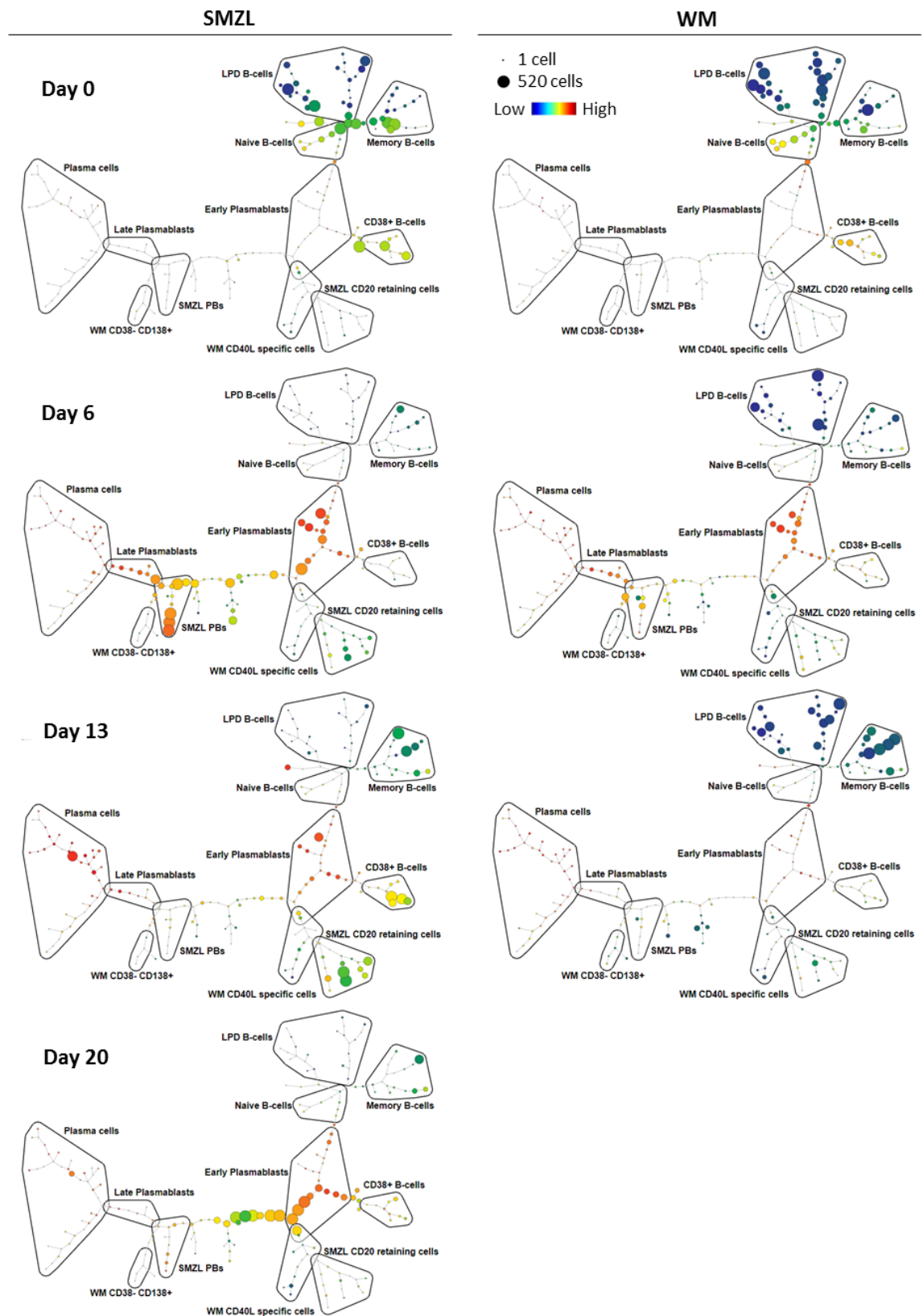
Figure 6.18 SPADE plots comparing B-cell differentiation between SMZL and WM cells. B-cells were isolated from SMZL or WM bone marrow and stimulated with 1µg/ml R848 + F(ab')$_2$ anti-IgG/M. Plots are coloured according to CD38 expression.

6.2.6   Overview of healthy cells vs all LPDs

The responses of all of the LPD samples to the two types of stimulation at day 13 of the differentiation in comparison to healthy cells are summarised in figure 6.19. Whilst differences are observed in the healthy group at day 6 of the differentiation, the final result following either stimulation is almost identical from day 13 onwards. The overlap of the populated nodes between the healthy cells with either stimulation is extensive, this is in contrast to the LPDs, which diverge not only from the healthy plots but also substantially differ between the different stimulations.

The SPADE plots for the LPD cells in the CD40L condition are more similar to their healthy counterparts than the R848 plots. Whilst LPD B-cells do generate plasmablasts and plasma cells after CD40L stimulation that correspond to the healthy populations, a considerable proportion of LPD cells diverge from this. The unusual populations of cells generated by the dysregulation of B-cell differentiation in these cells can be identified as discrete groups of nodes which separate WM and SMZL cells from both healthy cells and each other.

The profound inability of WM cells to respond correctly to TLR7 stimulation predominates in the R848 plots, with the SMZL plasmablasts generated earlier in the time course unable to survive to this time point.
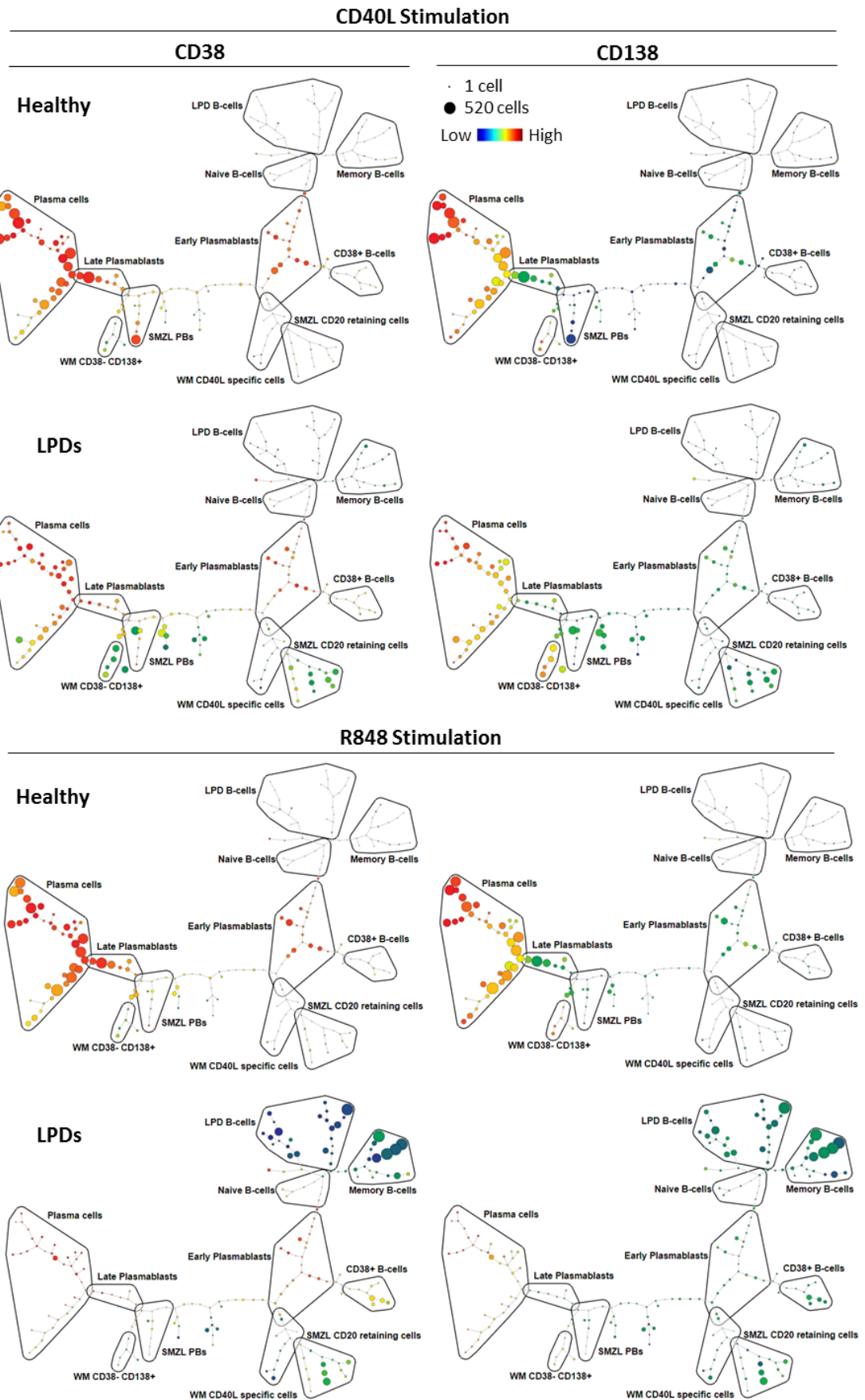
Figure 6.19 SPADE plots comparing B-cell differentiation between healthy and LPDs. Plots depict cells at day 13 of differentiation and are coloured according to the expression of the markers indicated.

6.3 Discussion

These analyses provide additional insight into the differentiation of healthy B-cell and B-cells derived from patients with LPDs. Performing viSNE on groups of concatenated raw flow cytometry data enable large numbers of samples to be compared simultaneously without loss of high dimensional data (table 6.1 and figure 6.1). The data represented here depict a slightly unconventional use of viSNE as the samples include only B-cells. This analysis has limitations, particularly with regards to clustering non-discrete populations such as this, but has still proven to be highly informative. A similar comparison with a more extensive panel would be very interesting - inclusion of additional cell surface markers commonly used in diagnostic flow cytometry would enable the algorithms to more easily distinguish neoplastic cells from their healthy counterparts and improve the clustering. A comparison with a greater variety of LPDs and a greater number of samples within the groups would likely result in clearer distinctions between the different groups. However, the detection of unusual phenotypic fractions such as the WM CD38$^-$ CD138$^+$ cells in an unsupervised, unbiased manner independently confirms their existence within the larger population as a whole and supports the conclusions drawn from the raw data.

A feature common to both types of stimulation are a subset of cells that are unable to respond to stimulation and retain the B-cell phenotype throughout the course of the differentiation, suggesting that these cells are completely refractory to both T-dependent and T-independent stimulation (figure 6.18). However, this fraction of cells is considerably smaller in the SMZL group than in the WM group and the overall proportion that remain unresponsive is roughly equivalent in both the CD40L and R848 conditions (figures 6.17 and 6.18). In the case of the WM cells, the unresponsive fraction comprises a much greater proportion of the total population when the cells have been stimulated with R848, suggesting that some cells are selectively responsive and able to correctly initiate differentiation following CD40L stimulation but are unable to do so when they are given R848 stimulation (figure 6.14 and 6.15). This itself is surprising, given the ubiquitous reliance of these cells on the constitutive activation of the NF-κB signalling pathway via MYD88^{L265P}, but perhaps ties in with the observed cell death in WM cells following R848 stimulation.

Data from the group of concatenated SMZL cells demonstrates that they are able to generate plasma cells but their capacity to do so is considerably less than WM cells (figure 6.17). This is consistent with what occurs *in vivo*, where differentiation among SMZL cells is limited but does occur (Mollejo *et al.*, 1995; Hammer *et al.*, 1996; Van Huyen *et al.*, 2000; Dufresne *et al.*, 2010).

These results also identify a block in differentiation for a large proportion of these cells at the plasmablast or pre-plasmablast stage.

The results inferred from the phenotypes of individual samples in previous chapters were supported by analysis via viSNE and SPADE. Both methods demonstrate differences in the flow cytometry data between healthy cells and WM cells throughout the differentiation. They also provide further insight into the data such has the potential for a similar population of alternate plasmablast-like cells to exist in healthy samples (figure 6.2). It is interesting to speculate that an equivalent precursor of the $CD38^-$ $CD138^+$ cells may occur in healthy samples due to the results from viSNE analysis. For these individuals, this population of plasmablasts appear to have a slightly delayed response to stimulation compared to the rest of the population, rather than an inability to upregulate CD38 and generate phenotypically normal plasma cells. However, when using SPADE on viSNE, the $CD38^-$ $CD138^+$ cells appear more closely equivalent to healthy plasma cells (figure 6.14). It is thus currently unclear as to whether this population of cells represents a true intermediate stage in plasma cell differentiation or is actually the "end point" and denotes a subset of phenotypically distinct plasma cells.

The results presented here emphasise the uniqueness of the B-cell differentiation profile for each group presented here. There is not only a "healthy" and "disease" set of phenotypes and relationships but rather each group possesses characteristics that these unbiased and unsupervised algorithms identify even when a group contains a mixture of different LPDs.

Chapter 7 – Investigation of the WM B-cell response to TLR7 ligation

7.1   Introduction

In order to determine the reason for the unexpected response of WM cells to R848 stimulation, several different avenues were explored. WM cells most closely resemble the memory B-cell fraction and thus far, differentiations were performed with total healthy B-cells. It is possible that a response similar to that of the WM cells may occur in memory cells derived from healthy donors. Therefore, memory and naïve B-cell fractions were isolated from the PB of healthy donors and stimulated with R848. The reaction of each subset was examined to determine if there is a difference in phenotype and cell number between the two and whether the memory subset shared any characteristics with the WM response to this type of stimulation.

Subsequently, the response of WM and ABC DLBCL cell lines possessing the MYD88^{L265P} mutation to TLR agonists was assessed in order to determine whether simply the presence of MYD88^{L265P} confers susceptibility to apoptosis when the cells are cultured with these compounds. The impact of the addition of a combination of TLR agonists and F(ab')$_2$ anti-IgG/M to WM cell lines was also investigated to more closely replicate the stimuli used in the *in vitro* culture system.

Another potential explanation for the response of WM cells is that stimulation with R848 may trigger the secretion of a factor that is detrimental to cell survival. To determine if this is the case, supernatant was taken from differentiations performed with WM or healthy cells, stimulated either with R848 + F(ab')$_2$ anti-IgG/M or CD40L + F(ab')$_2$ anti-IgG/M and added to subsequent differentiations with healthy or neoplastic B-cells which were monitored for cell number, viability and phenotypic changes.

The humoral immune response is subject to control by activation-induced cell death; a process by which B-cells undergo apoptosis following ligation of the Fas receptor by its ligand FasL, thus constraining a potentially damaging response. Therefore, the presence of Fas and FasL on differentiating cells was investigated to assess whether WM cells stimulated with R848 upregulated their expression to a greater extent than control cells. In addition to this, the expression of endosomal TLR receptors on B-cells isolated from the bone marrow of patients with WM and other LPDs was evaluated and compared to that of healthy cells derived from the peripheral blood or bone marrow.

The possibility that the effect of R848 on phenotypic response and cell number could be ameliorated in WM cells with the introduction of CD40L stimulation in addition to R848 + F(ab')$_2$

anti-IgG/M was investigated. Samples of WM and healthy cells taken at day 6 of differentiation were also analysed by RNA-sequencing to identify differentially expressed genes between the both groups and the two alternate types of stimulation.

7.2   The response of memory and naïve B-cell subsets to TLR stimulation

Since WM cells more closely resemble memory B-cells than naïve B-cells (Sahota *et al.*, 2002; Kriangkum *et al.*, 2004b), confirmation that memory B-cells are able to respond to TLR7 stimulation correctly within the *in vitro* system was necessary in order to determine that the observations in WM cells do not arise from a general impairment in memory cells to differentiate in response to R848 stimulation. Therefore, B-cells were isolated from the peripheral blood of two healthy donors and separated into naïve and memory fractions. These two subsets were concurrently stimulated with 1µg/ml R848 + F(ab')$_2$ anti-IgG/M.

The fold change in cell number recorded over the course of the culture is shown in figure 7.1. At day 3, the naïve fraction from both donors did not increase in number, but in contrast, the memory cells had doubled in number. By day 6, in both instances, the memory fraction had proliferated to a much greater extent than the naïve fraction. Whilst the naïve cells from donor 1 expanded in number, the corresponding subset from donor 2 did not exhibit any increase in number. Between day 6 and 13, cell numbers decreased in all conditions, but more cells persisted in the memory fractions for both donors. There were substantially fewer naïve cells by day 20 of the differentiation and as such there were not enough to generate meaningful phenotypic data at the later time points. In contrast, the memory fractions produced a greater number of plasma cells that persisted until the culture was terminated.
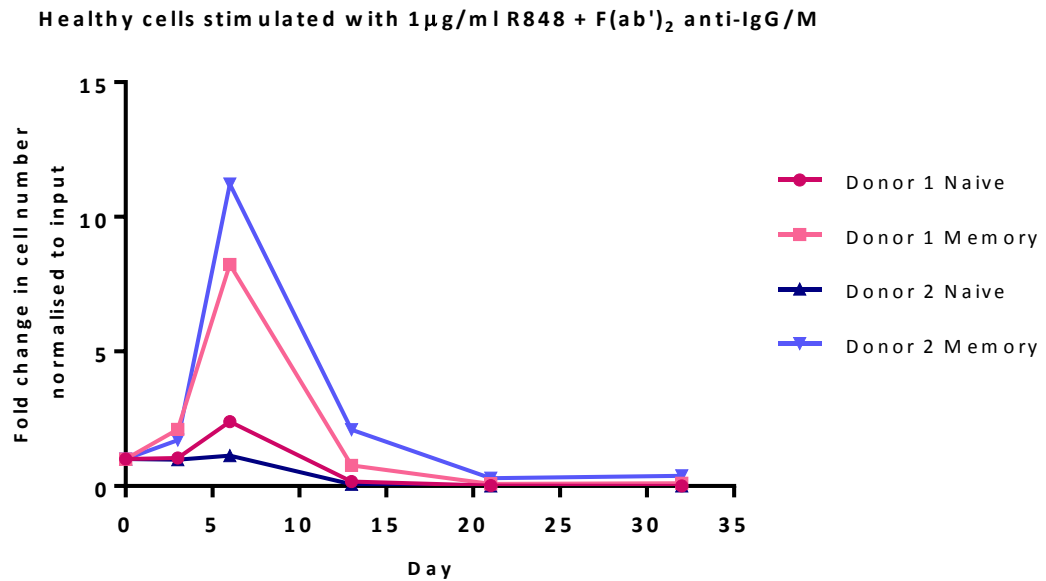
Figure 7.1 Memory B-cells demonstrate enhanced proliferation and survival in response to TLR7 stimulation. Naïve and memory B-cells derived from the peripheral blood of healthy donors (isolation protocol C) were stimulated with 1µg/ml R848 and F(ab')$_2$ anti-IgG/M. Cells were washed at day 3. Cell number at each time point was determined by manual counts between days 0-6 and then by flow cytometry thereafter. The cell number at each point was normalised to the number of "input" cells for that specific donor obtained at day 0.

Whilst the proliferative response and total number of cells generated by each of the two B-cell subsets was very different, the phenotype at day 6 is remarkably consistent (figure 7.2). The parity continued throughout the differentiation, with no significant difference in phenotype between naïve and memory cells at any of the time points examined. The only minor difference between the two groups is that the memory fraction from both donors had a slightly greater spread of CD38 expression from day 13 onwards, compared to a more consistent expression within the naïve subset. Both fractions generated a high proportion of plasma cells by day 13, despite the limited proliferative response of the naïve cells.

Overall, the memory fraction from both donors was better able to respond to R848, with a greater number of long-lived plasma cells generated than from the naïve subset. This is consistent with the published literature, whereby memory B-cells have been shown to proliferate preferentially in response to TLR agonism (Simchoni and Cunningham-Rundles, 2015). These results demonstrate that the aberrant response of WM cells to activation with R848 + F(ab')$_2$ anti-IgG/M in the *in vitro* system is not due to an inherent defect in the response of memory cell compartment to this type of stimuli. The strength of the memory response to TLR7 ligation makes the deficient reaction of WM cells perhaps even more surprising.
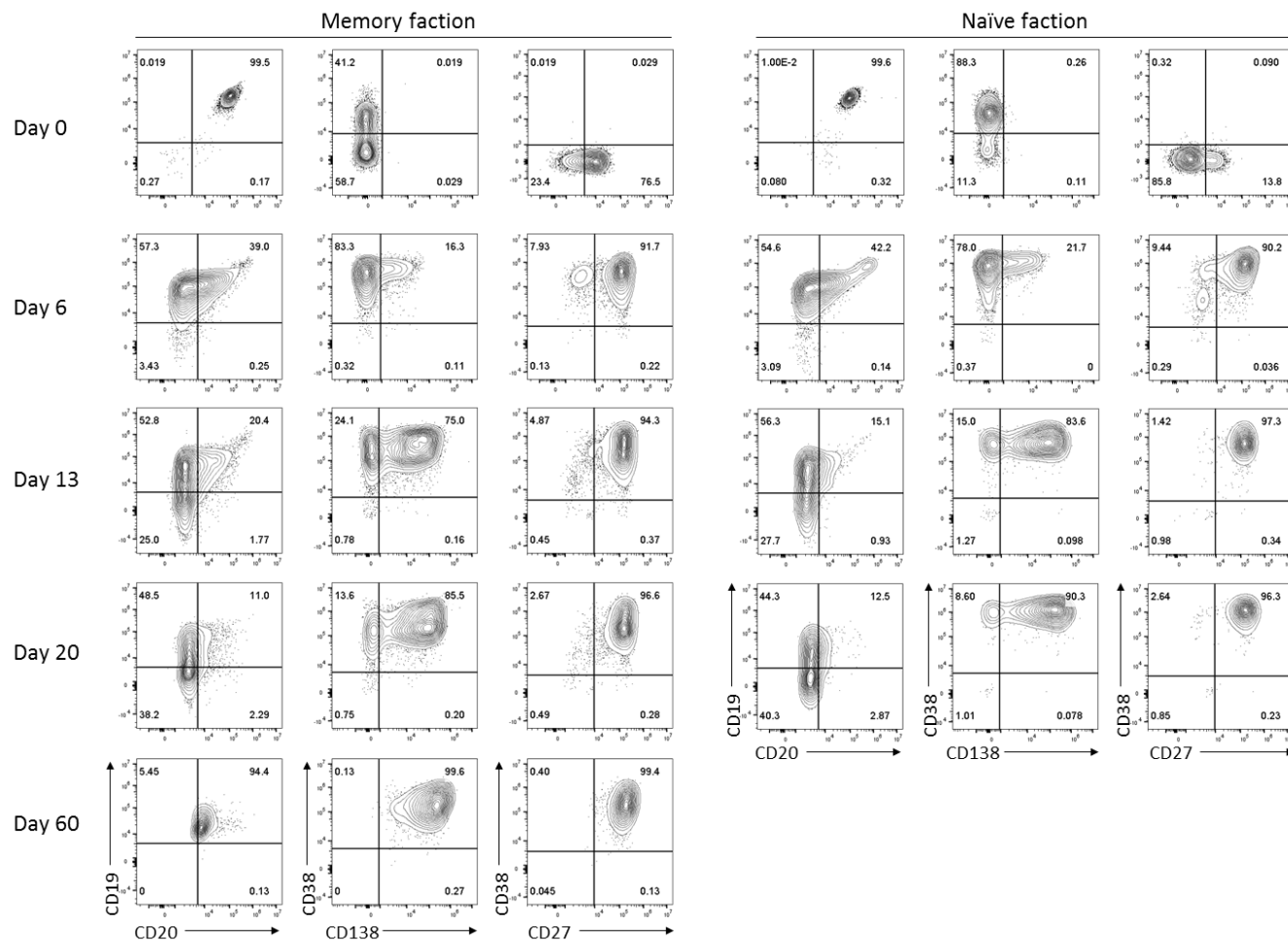
Figure 7.2 The phenotype of memory and naïve B-cell subsets in response to TLR7 stimulation. A representative phenotype from one donor is shown (n =2). B-cells were derived from the peripheral blood of healthy donors and stimulated with 1µg/ml R848 + F(ab')₂ anti-IgG/M. The phenotype was assessed by flow cytometry for surface markers at the indicated time points. Percentages are indicated within individual quadrants.

7.3   Dose response of MYD88^{L265P} cell lines to TLR agonists

The MYD88^{L265P} mutation appears to be tightly linked with the aberrant response of WM B-cells to activation with R848 so the reaction of cell lines possessing this mutation to TLR ligation was characterised. Two WM cell lines were examined, MWCL.1 and BCWM.1, both of which are heterozygous for MYD88^{L265P} (Treon *et al.*, 2012). Additionally, two ABC DLBCL cell lines were also selected for investigation; OCI-Ly10 which is homozygous for the MYD88^{L265P} mutation and OCI-Ly3 which is homozygous for MYD88^{L265P} (Ngo *et al.*, 2011). Three different concentrations of R848 were added to the culture media, with or without F(ab')$_2$ anti-IgG/M. The cells were cultured for 72 hours and then the number and viability were analysed by flow cytometry.

7.3.1   TLR7/8 agonist R848

There was no effect in terms of either cell number or viability on the addition of R848 with or without F(ab')$_2$ anti-IgG/M on either of the WM cell lines or OCI-Ly3 (figure 7.3). The only significant differences occurred for the OCI-Ly10 cell line, in which R848 concentrations of 10μg/ml and 1μg/ml increased the total cell number compared to the control but did not significantly increase the viability of these cells.
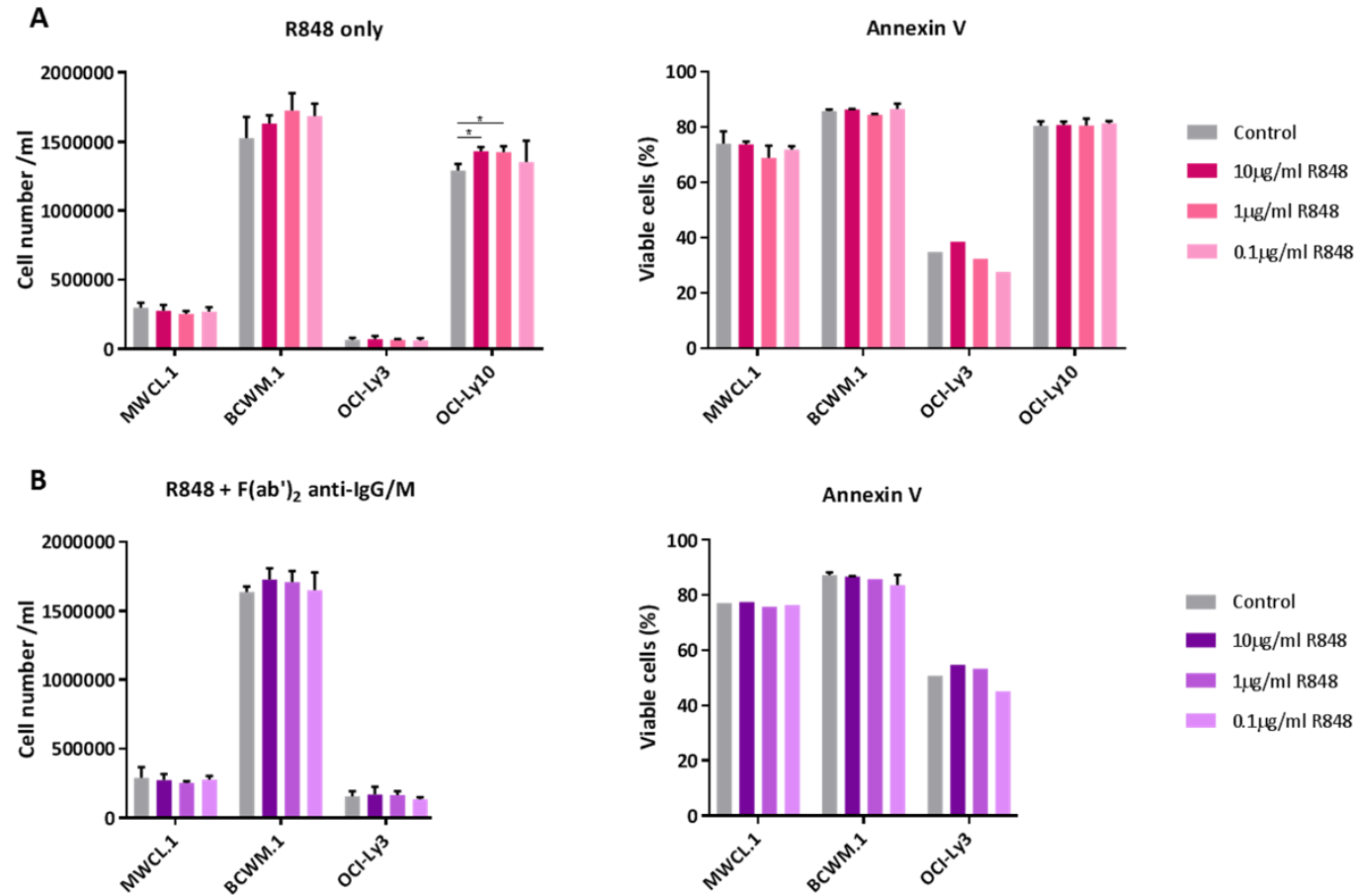
Figure 7.3 Dose response of WM and ABC DLBCL cell lines following the addition of three concentrations of the TLR7/8 agonist R848 alone (A) or with F(ab')₂ anti-IgG/M (B). Cell lines were seeded in 96-well plates at 2 x 10^5 cells/well and treated with 10, 1 or 0.1µg/ml R848. After 72 hours, cell number was quantified on a flow cytometer using CountBright beads. Cell number/ml is depicted (left) with corresponding graph of cell viability (right) as measured by Annexin V/ 7-AAD staining. Control cells were seeded at the same density, but in media alone. Values significantly different from the control are indicated – (*, $p < 0.05$, t-test with Welch's correction). Error bars represent S.D (n = 3).

7.3.2 TLR9 agonist CpG ODN 2006

Of the other endosomal TLRs, TLR9 is highly expressed on B-cells, so the reaction of the MYD88-mutated cell lines to a TLR9 agonist was also investigated (Hornung *et al.*, 2002; Dasari *et al.*, 2005; Månsson *et al.*, 2006). As with TLR7, TLR9 is located within endosomes but recognises unmethylated CpG DNA instead of ss-RNA (Hemmi *et al.*, 2000; Hemmi *et al.*, 2002; Heil *et al.*, 2004). Three classes of CpG have been identified, each of which demonstrates differing activity in PBMCs (Vollmer *et al.*, 2003). CpG oligodeoxynucleotide (ODN) 2006 was chosen as it belongs to the class B ODNs, which are potent activators of B-cells (Vollmer *et al.*, 2003). The concentrations to be tested were determined from the working concentration and published literature (Reid *et al.*, 2005; Sivori *et al.*, 2006).

A significant increase in cell number was observed for MWCL.1 with the highest concentration of CpG tested, but it was not accompanied with an increase in cell viability (figure 7.4). This was replicated with the addition of F(ab')$_2$ anti-IgG/M. A significant increase in number was also observed for BCWM.1, but this time only with the lowest concentration of agonist. However this was not observed when a combination of CpG and F(ab')$_2$ anti-IgG/M were used. As with MWCL.1, the viability was unaffected in both conditions.

The highest concentration of CpG significantly increased the number of OCI-Ly10 cells compared to the control, but the viability remained the same for all conditions tested. Whilst there was no impact of the addition of CpG to the number of OCI-Ly3 cells, the highest dose had a negative impact on the viability. This cell line did not proliferate very much in the 3 days in either condition, so the decrease in viability may just be a reflection of the high proportion of apoptosis occurring intrinsically within the culture.

Whilst a statistically significant decrease in viability was observed for OCI-Ly3, the addition of CpG resulted in significant increases to cell number in the other three cell lines and thus it does not appear that this result reflects the general trend. These findings, in combination with the R848 results, confirm that the presence of MYD88^{L265P} alone does not confer susceptibility to cell death following ligation of either TLR7 or TLR9.
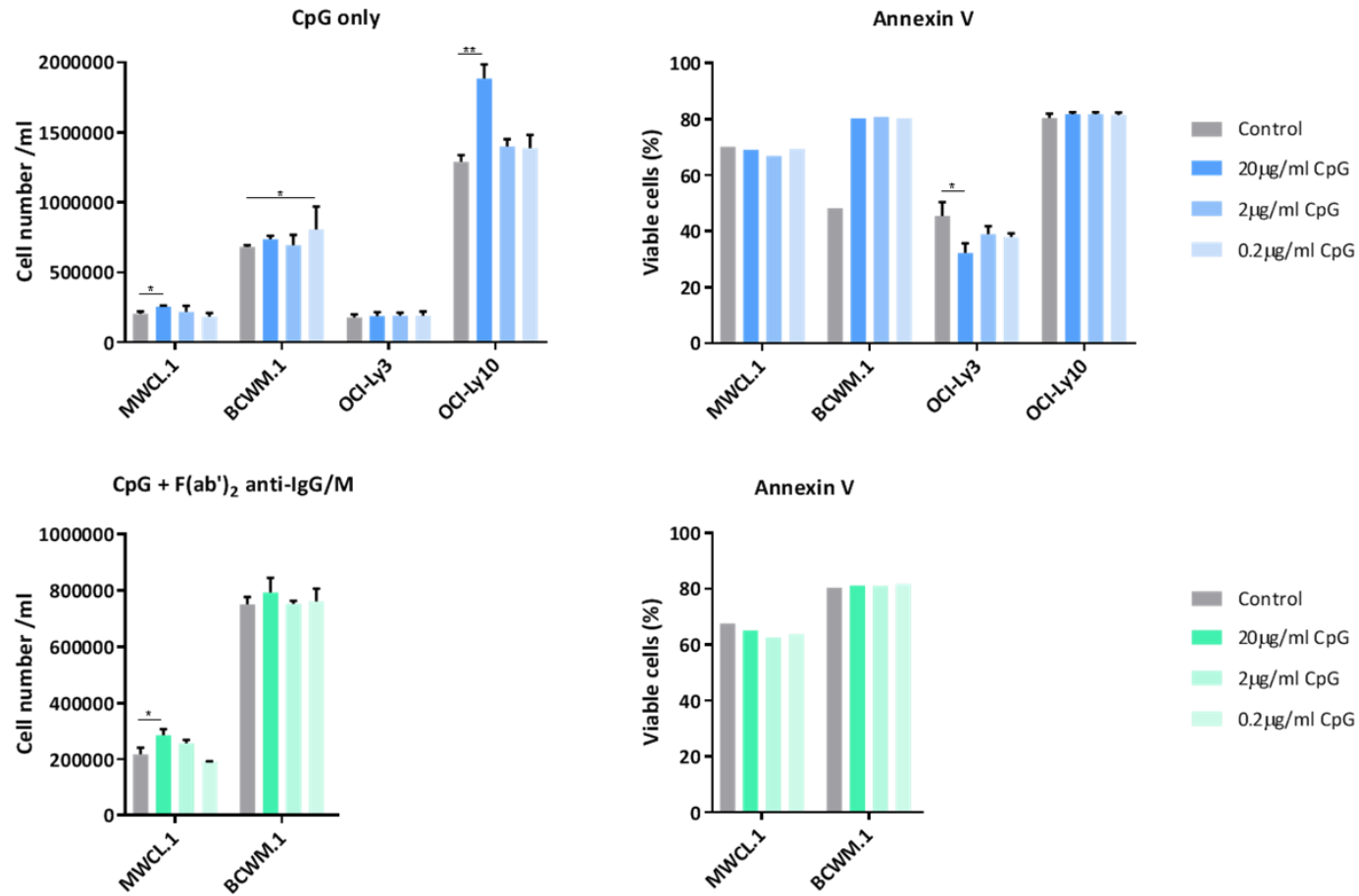
Figure 7.4 Dose response of WM and ABC DLBCL cell lines following the addition of three concentrations of the TLR9 agonist CpG ODN 2006 alone (A) or with F(ab')₂ anti-IgG/M (B). Cell lines were seeded in 96-well plates at 2×10^5 cells/well and treated with 20, 2 or 0.2µg/ml CpG. After 72 hours, cell number was quantified on a flow cytometer. Cell number/ml is depicted (left) with corresponding graph of cell viability (right) as measured by Annexin V/ 7-AAD staining. Control cells were seeded at the same density, but in media alone. Values significantly different from the control are indicated – (*, $p < 0.05$; **, $p < 0.01$, t-test with Welch's correction). Error bars represent S.D ($n = 3$).

7.4   Application of supernatant taken from differentiating WM B-cells to subsequent *in vitro* differentiations

In the context of ABC-DLBCL cell lines, the presence of MYD88[L265P] confers increased activation of both NF-κB and JAK-STAT3 leading to the autocrine production of IL-10, IL-6 and IFNβ that are thought to provide survival signals to the lymphoma cells (Ngo *et al.*, 2011). In contrast, exposure of chronic lymphocytic leukaemia (CLL) B-cells to a TLR9 agonist triggers apoptosis following autocrine production of IL-10 and activation of STAT1 (Liang *et al.*, 2010). Following phosphorylation, STAT1 induces pro-apoptotic genes such as caspases, TRAIL (TNF-related apoptosis-inducing ligand) and FasL. Since the addition of R848 did not adversely affect the proliferation of the MYD88 L265P-expressing cell lines, it is plausible that, in WM patient-derived B-cells, stimulation with R848 may be causing these cells to secrete a factor that results in killing *in–trans* as observed for CLL.

7.4.1   The effect of WM supernatant on healthy differentiating cells

The impact of WM supernatant (S/N) on differentiating B-cells was initially investigated with cells derived from healthy donors. Supernatant taken from differentiations with WM cells that had been stimulated with either CD40L or R848 + F(ab')$_2$ anti-IgG/M was applied to healthy differentiating B-cells at day 3, after they had been activated with either CD40L or R848. The healthy cells were resuspended in the day 3 differentiation conditions at 1 x 10^5/ml and 200μl added per well of a 96-well plate. The supernatant was subsequently added at concentrations of either 1:10 or 1:100. After 72 hours, the number of cells, viability and phenotype was determined by flow cytometry. A scheme for the supernatant experiments is depicted in figure 7.5.
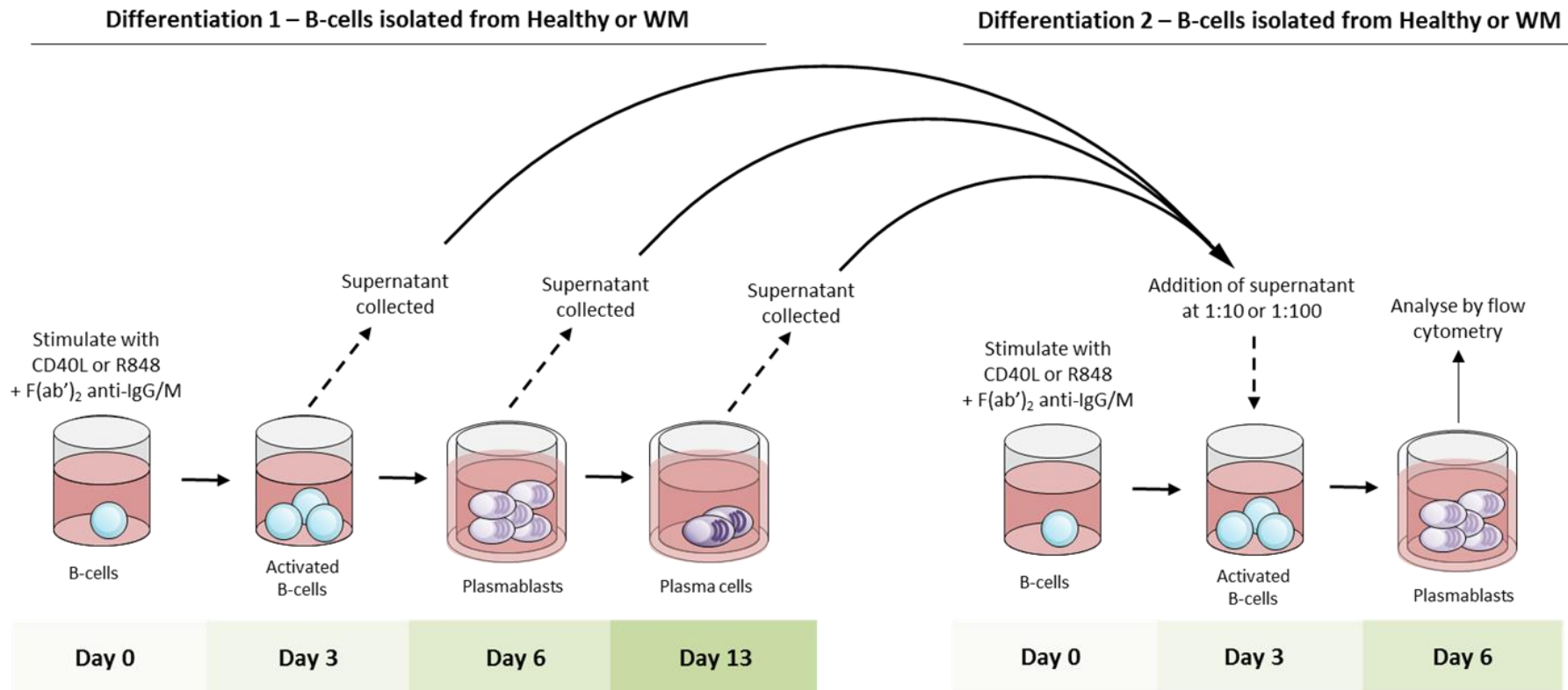
Figure 7.5 Scheme for supernatant experiments. Two independent *in vitro* differentiation experiments were performed, the first to generate the supernatant and the second to assess the effect on cell number, viability and phenotype. B-cells were isolated from WM patient BM or PB from healthy donors and stimulated with either CD40L + F(ab')$_2$ anti-IgG/M or 1µg/ml R848 + F(ab')$_2$ anti-IgG/M. Supernatants were collected at day 3, day 6 and/or day 13 from these differentiations. Subsequently, supernatants were added at a concentration of 1:10 or 1:100 to a second independent differentiation with B-cells derived from healthy or WM patients at day 3, following activation with CD40L + F(ab')$_2$ anti-IgG/M or 1µg/ml R848 + F(ab')$_2$ anti-IgG/M. The cells were analysed by flow cytometry 72 hours later to assess their phenotype and viability.

Supernatants from 5 independent WM differentiations that were concurrently stimulated with either CD40L + F(ab')$_2$ anti-IgG/M or 1µg/ml R848 + F(ab')$_2$ anti-IgG/M were tested. The details of which are provided in table 7.1. Control wells were cultured in the same conditions, stimulated with either CD40L or 1µg/ml R848 + F(ab')$_2$ anti-IgG/M but did not include the addition of supernatant. Supernatant taken from day 6 of a differentiation with healthy cells stimulated with R848 was also tested to assess whether there was a difference between the supernatant taken from cells with high levels of viability following this type of stimulation compared to the WM population which consists of almost entirely non-viable cells at this time point.

Table 7.1 Details of supernatants used.

Sample	Day harvested	Stimuli
Healthy	6	R848
WM 1	3	CD40L
WM 1	3	R848
WM 2	3	CD40L
WM 2	3	R848
WM 3	6	CD40L
WM 3	6	R848
WM 4	6	CD40L
WM 4	6	R848
WM 5	13	CD40L
WM 5	13	R848

The results for the first healthy donor are shown in figure 7.6.
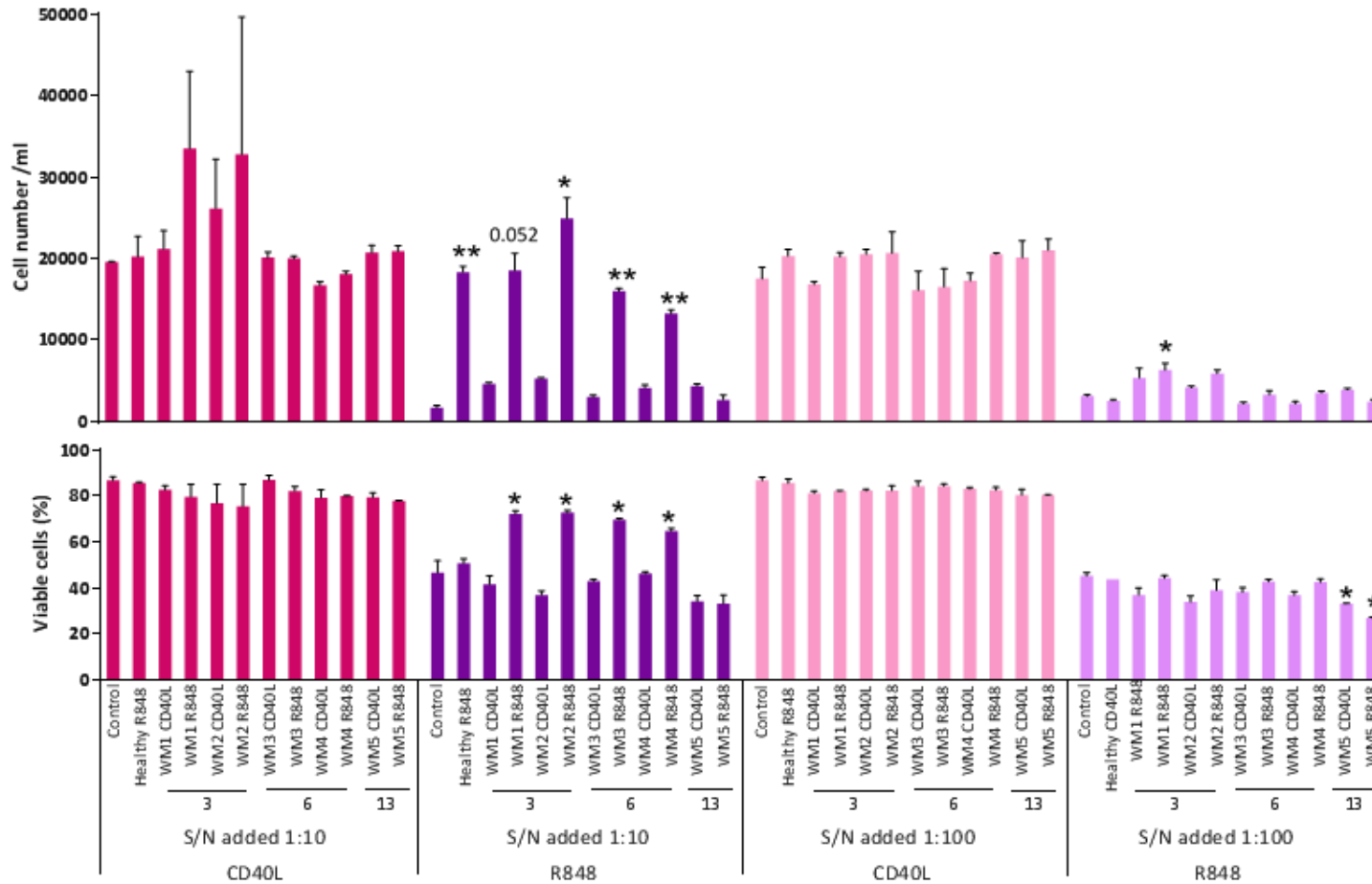
Figure 7.6 Supernatant from WM B-cells stimulated with 1µg/ml R848 + F(ab')₂ to healthy differentiating cells which have also been stimulated with 1µg/ml R848 + F(ab')₂ results in significantly increased cell numbers and viability. S/N added at a dilution of either 1:10 or 1:100 to healthy cells stimulated with either CD40L or R848. Top – cell numbers determined by flow cytometry using CountBright beads, bottom - viability as measured by percentage 7-AAD negative cells. Statistical analysis by Student's t-test with Welch's correction *, p < 0.05; ** p < 0.01. Results significantly different from the controls for each condition are indicated. Data are in duplicate with error bars denoting S.D.

There was no significant effect of the addition of any of the supernatants to the healthy cells stimulated with CD40L + F(ab')$_2$ anti-IgG/M at dilutions of either 1:10 or 1:100. The day 3 supernatants from the WM cells activated with R848 may potentially increase the cell number although the variance of these values was very high so it is not significant here. There was no significant effect on cell viability in any of the conditions. However, when the healthy cells were initially stimulated with R848 + F(ab')$_2$ anti-IgG/M, there was a significant effect of the addition of supernatant from WM cells which were activated with R848. Instead of having a detrimental effect on cell numbers and viability, supernatant from WM differentiations at both day 3 and day 6 increased cell numbers significantly, accompanied by a significant increase to viability.

A potentially confounding factor in these results is the effect of R848 carryover. The supernatant derived from R848-stimulated WM differentiations at day 3 will contain some R848. However, the effect should be minimal as the supernatants were diluted by 10-fold when added to the fresh media that the healthy cells were resuspended in at day 3. Additionally, it has been previously shown that carryover of 0.1µg/ml R848 had a negligible effect on cell number and phenotype. Interestingly, there is also a significant increase in cell number after the addition of healthy supernatant from cells stimulated with R848 but this is not accompanied by an increase in viability. There is no residual R848 subsequent to day 3, so this supports a conclusion that these cells are secreting factors supporting cell proliferation. Therefore, whilst the potential for carryover of R848 from day 3 samples cannot be eliminated completely and thus may contribute to any increase in proliferation observed following the addition of this supernatant, it seems likely that the effect observed here is genuine. The WM supernatant taken at day 6 also results in a significant increase to cell number in these samples, accompanied by a significant increase in viability from approximately 45% to 65-70%. Supernatant taken at this time point of the differentiation should pose no risk of R848 carryover so this would appear to be due to an effect of some sort of secreted factor from the WM cells that is being induced following R848 stimulation.

The effect on cell number was considerably reduced when the concentration of supernatant was decreased to 1:100, as would be expected if the cells were secreting factors acting in-trans. Nevertheless, the pattern of increased cell number and viability with WM R848 supernatant can still be observed in the healthy cells following stimulation with R848 + F(ab')$_2$ anti-IgG/M, although in most instances it is not significant. It would appear that this concentration of supernatant lies just over the threshold where an observable effect can occur.

Whilst the cell number was unaffected, the viability of the cells was negatively affected by the addition of the WM day 13 supernatant. Whilst cells in the earlier stages of differentiation release factors that foster survival and proliferation, the population that exists at day 13 largely

consists of plasma cells, which will have altered there secretome accordingly. Moreover, a large proportion of cell death occurs subsequent to day 6, likely accompanied by the release of apoptotic factors into the harvested media which may account for this result.

The phenotype was assessed for cells that had the higher concentration of supernatant added as this had a greater effect on the cell number and viability. The results are presented in figure 7.7. The limited effect of the addition of the supernatants to the healthy cells stimulated with CD40L + F(ab')$_2$ anti-IgG/M is reflected in only very subtle differences surface marker expression. Expression of CD20 was bi-modal in cells which received CD40L-stimulated supernatant, whereas the proportion of CD20^{++} cells is reduced with the R848-stimulated supernatant, indicating that the cells have proceeded further in the differentiation. There were subtle effects of the supernatant on CD38 expression, with the day 6 supernatants increasing the average MFI to 366 compared to the day 3 supernatant average of 248.5. Examination of the matched supernatant pairs shows no difference in phenotype between the two types of stimulation and that the changes observed in the healthy phenotype appear to be as a result from the particular time point the supernatant was taken at.

The healthy cells stimulated with R848 + F(ab')$_2$ anti-IgG/M have progressed slightly further in differentiation, having downregulated CD20 and upregulated CD38, CD138 and CD27 to a greater extent than their CD40L-stimulated counterparts. In line with the more profound impact of the supernatant on cell number and overall viability, considerably greater effects of the supernatant on the cell phenotype was also observed. The addition of R848-stimulated WM supernatant resulted in a considerably less differentiated phenotype. These cells retained higher levels of CD20 expression and a reduced proportion had upregulated CD38 and CD138. Interestingly, whilst addition of healthy supernatant resulted in a significant increase to cell number, there is almost no change in the phenotype, just a slightly tighter spread of CD38 expression. As for the CD40L-stimulated healthy cells, addition of day 13 WM supernatant had no effect on the phenotype.
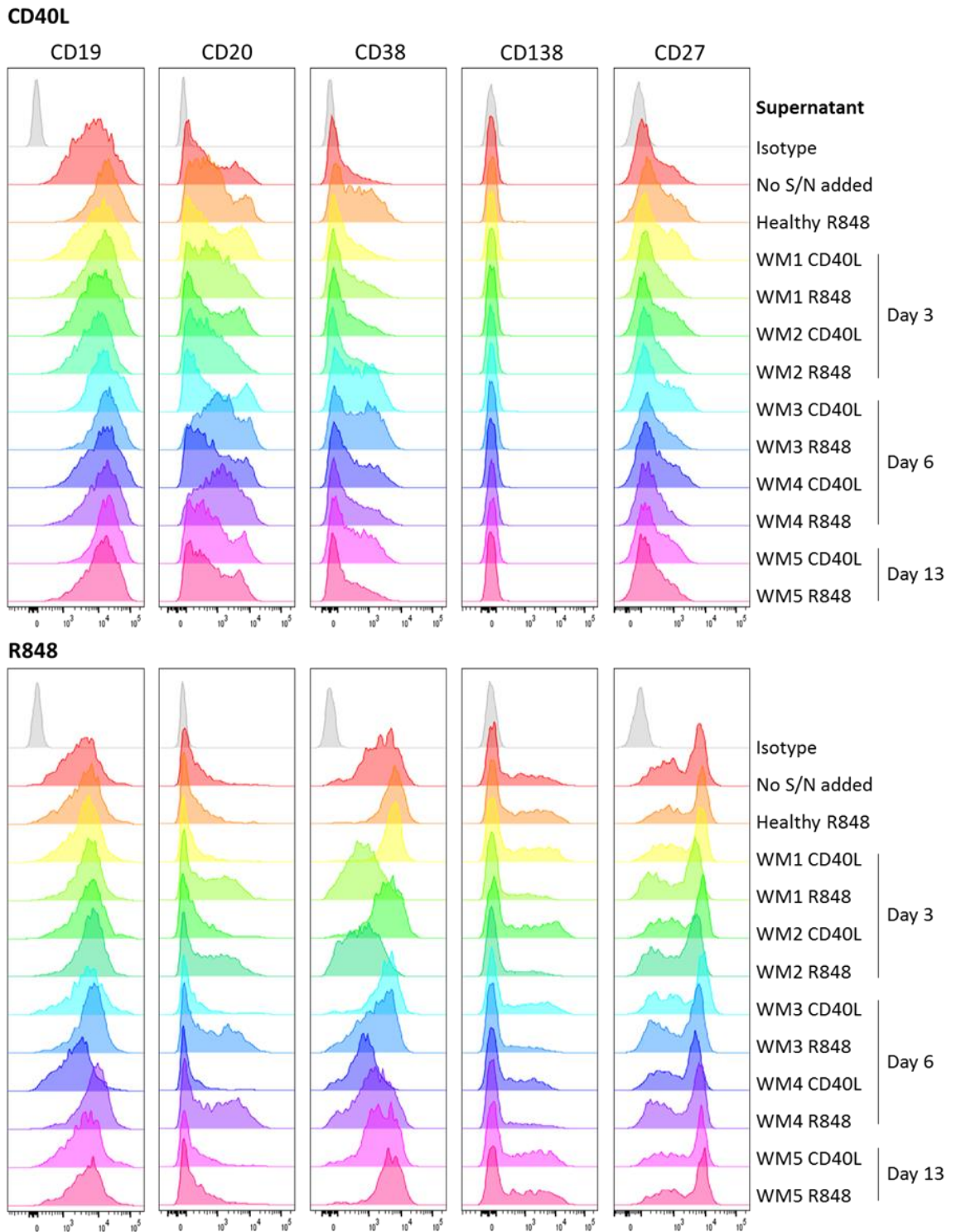
Figure 7.7 The phenotype of healthy differentiating cells is affected by the addition of WM supernatant. Histograms for the expression of each of the five cell surface markers on healthy differentiating cells corresponding to that of the donor in figure 7.6. Supernatant was added at a dilution of 1:10 at day 3 of the differentiation and the phenotype assayed by flow cytometry at day 6. Top – cells stimulated with CD40L + F(ab')$_2$ anti-IgG/M, bottom - 1µg/ml R848 + F(ab')$_2$ anti-IgG/M (isolation protocol B, 10ml media wash at day 3). The identity of the supernatants used are displayed on the right.

The results obtained from a second differentiation with B-cells derived from a different healthy donor are very comparable (figure 7.8). Once again, there was no significant effect on cell number or viability when the supernatant was added to the healthy cells stimulated with CD40L + F(ab')$_2$ anti-IgG/M at either concentration. However, supernatant from WM cells activated with R848 taken at either day 3 or day 6 of the differentiation, significantly increased the cell numbers, matched in three of the four instances by a substantial increase in viability. Addition of WM1 CD40L-stimulated supernatant increased the viability but had no significant impact on the cell number. The impact of the reduced concentration of supernatant was more modest, with small but significant increases in number for three of the R848 supernatant and a similar small increase with the WM1 CD40L supernatant. The viability of the cells was only significantly increased for the WM1 R848 supernatant taken at day 3.
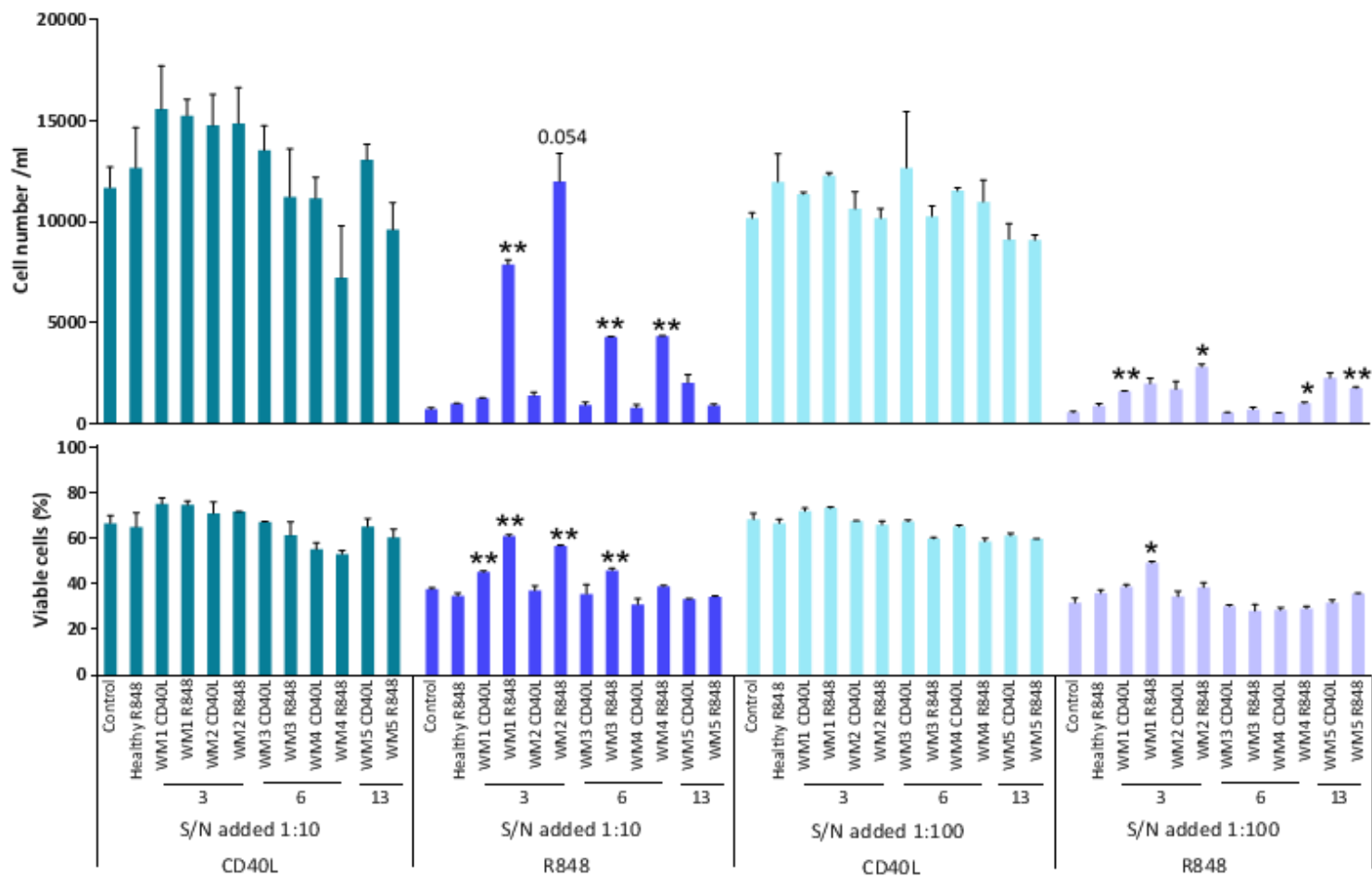
Figure 7.8 Addition of supernatant derived from WM B-cells stimulated with 1µg/ml R848 + F(ab')₂ to healthy cells from a second donor which have also been stimulated with 1µg/ml R848 + F(ab')₂ results in significantly increased cell numbers and viability. S/N added at a dilution of 1:10 or 1:100 to healthy cells stimulated with either CD40L or R848. Top – cell numbers determined by flow cytometry using CountBright beads, bottom - viability as measured by percentage 7-AAD negative cells. Statistical analysis by Student's t-test with Welch's correction *, p < 0.05; ** p < 0.01. Results significantly different from the controls for each condition are indicated. Error bars denote S.D (n = 2).

The phenotypes of the cells are also very similar to that of the first healthy donor (figure 7.9). In cells that were stimulated with CD40L + F(ab')$_2$ anti-IgG/M, there is a small effect on the expression of CD20 following the addition of the WM R848-stimulated supernatant, with a reduction in the proportion of CD20^{++} cells and a slight decrease in the shoulder of the CD27 histograms. The expression of the other markers is otherwise consistent across the conditions.

As with the first donor, a substantial change in the phenotype of the R848-stimulated cells is seen following the addition of the R848 supernatants. In the same manner as the previous donor, cells from this individual display a less-differentiated phenotype following the addition of the WM R848 supernatant. The effect on the phenotype of the supernatants taken at day 6 is less profound for this donor, but an increase in the MFI for CD38 and a decrease for CD20 occurs compared to the CD40L-stimulated supernatant.

In summary, the addition of supernatant derived from R848-stimulated WM cells at either day 3 or 6 of the differentiation resulted in a marked increase to cell numbers for R848-stimulated healthy cells. A similar but less pronounced effect appears to occur upon the application of WM supernatant from cells stimulated with R848 to healthy cells that had been stimulated with CD40L + F(ab')$_2$ anti-IgG/M. This was somewhat surprising, given that all cells isolated from WM patients die subsequent to R848 stimulation, despite the WM clone comprising a variable proportion of the samples.

In general, the supernatants harvested at day 3 of the differentiation result in an increase to the cell number, accompanied by an increase in overall viability. The extent to which the cell numbers are increased are greater than can be explained solely by the increase to viability, thus, the day 3 supernatant must support proliferation. This is accompanied by a less differentiated phenotype, suggesting that the factors within the supernatant delay differentiation, enabling the cells to remain in a proliferative state for longer and supporting their viability. During an immune response, secretion of factors by the B-cell population to supplement an environment conducive to cellular proliferation and survival would seem to be advantageous for an efficacious response, so this result is not unexpected.
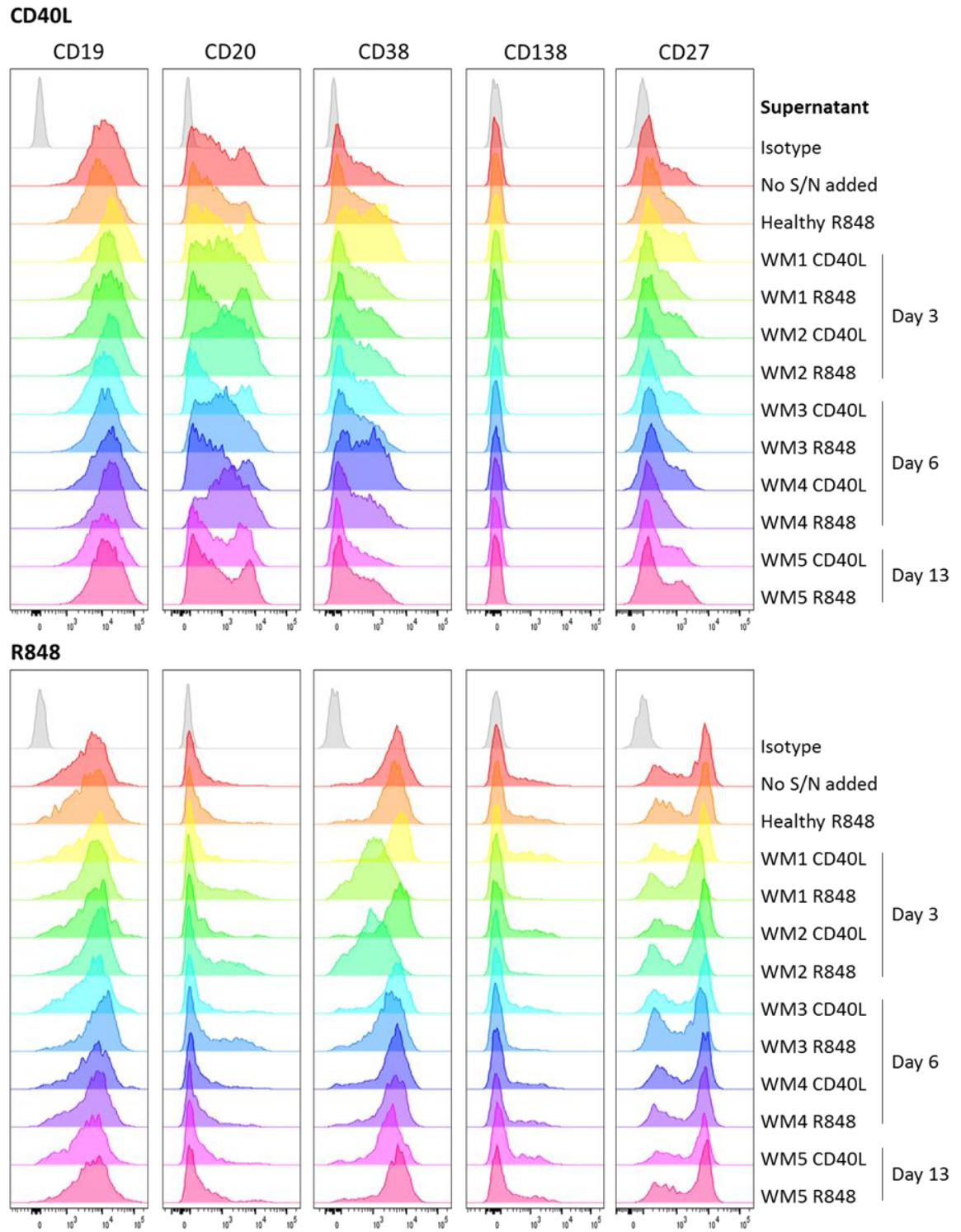
Figure 7.9 Addition of WM supernatant affects the phenotype of healthy cells stimulated with R848 more profoundly than those stimulated with CD40L. Histograms for the expression of each of the five cell surface markers on healthy differentiating cells corresponding to that of the donor in figure 7.8. Supernatant was added at a dilution of 1:10 at day 3 of the differentiation and the phenotype assayed by flow cytometry at day 6. Top – cells stimulated with CD40L + F(ab')$_2$ anti-IgG/M, bottom - 1µg/ml R848 + F(ab')$_2$ anti-IgG/M. The identity of the supernatants used are displayed on the right.

The supernatant taken at day 6 also increased cell number and viability, but to a lesser extent than the day 3 supernatant and the impact on the phenotype was also reduced. In a similar manner to the day 3 secretome, it would seem likely that these cells would also secrete pro-survival factors to support the differentiating population. However, delaying differentiation into effector cells is perhaps less beneficial as the response progresses, once a pool of plasmablasts has been established and thus the phenotype of the cells here is comparable to the CD40L-stimulated cohort.

It should be noted that supernatant collected at day 3 from R848-stimulated cells will still contain R848. The results of experiments described in previous chapters have shown that persistent R848 stimulation results in additional proliferation of the cells and delays differentiation. This is remedied by the inclusion of an additional wash step with fresh media to dilute the R848 to levels that have no effect on the continuing culture, but in this case the day 3 supernatant was collected with any R848 still present and undiluted. However, the increase to healthy cell numbers was also observed after the addition of WM supernatant taken at day 6, at which time the cells will have been washed and thus any carryover of R848 will have been eliminated. This indicates that whilst there could be some effect of R848 carryover at day 3, there is a genuine effect of secreted factors from WM cells stimulated with R848 that would normally increase proliferation instead of resulting in cell death.

The effect of supernatants derived from WM cells on healthy CD40L-stimulated cells was limited. One explanation for this lies with the difference in strength of the signal provided by the CD40L-L cells versus that of the R848. The CD40L-L cells provide a powerful activation signal that seems to mask the effects of the supernatant. In contrast, the intensity of the R848 stimulation is diminished in comparison so enables more subtle changes elicited by the supernatant to be seen. Another possibility is that some of the differences may be attributed to the subset of cells that are responsive to the initial stimuli provided. Since there is preferential expansion of memory cells with R848, the supernatant may exert a greater effect on this subset compared to the naïve fraction.

In conclusion, activation of WM B-cells within the *in vitro* system induces them to secrete factors into the culture media which can exert an effect on healthy cells. The secretion of factors by WM B-cells triggered by activation with R848 + F(ab')$_2$ anti-IgG/M, support the survival and proliferation of healthy differentiating cells and do not induce apoptosis.

7.4.2 The effect of WM supernatant on differentiating WM cells

The results from supernatant experiments with healthy differentiating cells suggest that the cell death observed in R848-stimulated WM cells may be intrinsic, since the secreted factors do not negatively impact these cells. Therefore, the effect of supernatant taken from WM cells and applied to a second WM differentiation was investigated.

A differentiation was performed with B-cells from two independent WM patients. Since WM B-cells die subsequent to stimulation with R848, they were activated with CD40L to assess if the survival signals would be overcome by factors secreted by the R848-stimulated WM cells. A similar selection of supernatants to the previous experiments were used (table 7.2), but the supernatants taken at day 13 were substituted for an additional day 6 sample, as they had virtually no effect on the healthy cells. As before, the phenotype, cell number and viability were assessed at day 6 (figure 7.10).

Table 7.2 Details of supernatants used for WM supernatant experiments.

Sample	Day harvested	Activating stimuli
Healthy	6	R848
WM 1	3	CD40L
WM 1	3	R848
WM 2	3	CD40L
WM 2	3	R848
WM 2	6	CD40L
WM 2	6	R848
WM 3	6	CD40L
WM 3	6	R848
WM 4	6	CD40L
WM 4	6	R848
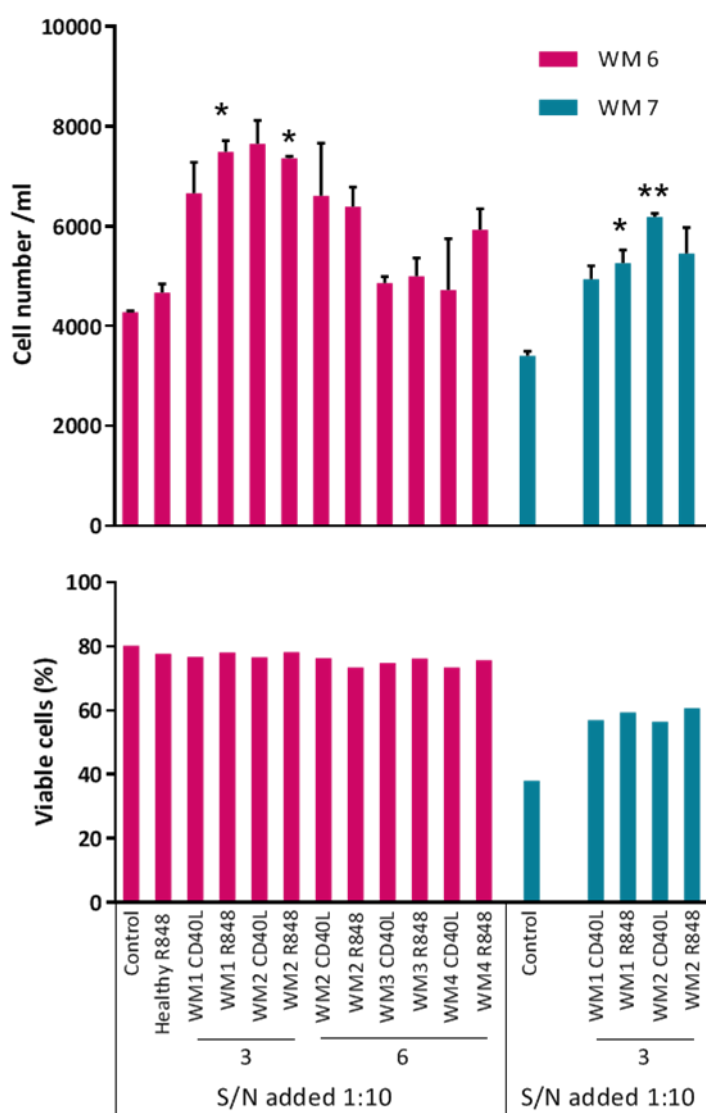
Figure 7.10 Addition of supernatant derived from an initial differentiation with WM B-cells to a second WM differentiating cells which have also been stimulated with CD40L + F(ab')$_2$ results in significantly increased cell numbers. Top – cell numbers determined by flow cytometry, data are in duplicate with error bars denoting S.D. Statistical analysis by Student's t-test with Welch's correction: *, $p < 0.05$; ** $p < 0.01$. Bottom - viability as measured by percentage 7-AAD negative cells.

In a similar manner to the healthy cells, supernatant derived from WM cells at day 3 that were initially stimulated with R848 increased the number of cells, but in this instance did not affect the viability. The day 3 supernatant from CD40L-stimulated WM cells also appears to increase the cell number, although this was not significant for WM6 due to higher variability in the cell numbers obtained. Supernatant taken from WM differentiations at day 6 did not have a significant effect on either the total cell number or the proportion of viable cells within the culture within the subsequent differentiations.

WM 6 – Stimulated with CD40L + F(ab')$_2$ anti-IgG/M

WM 7 – Stimulated with CD40L + F(ab')$_2$ anti-IgG/M
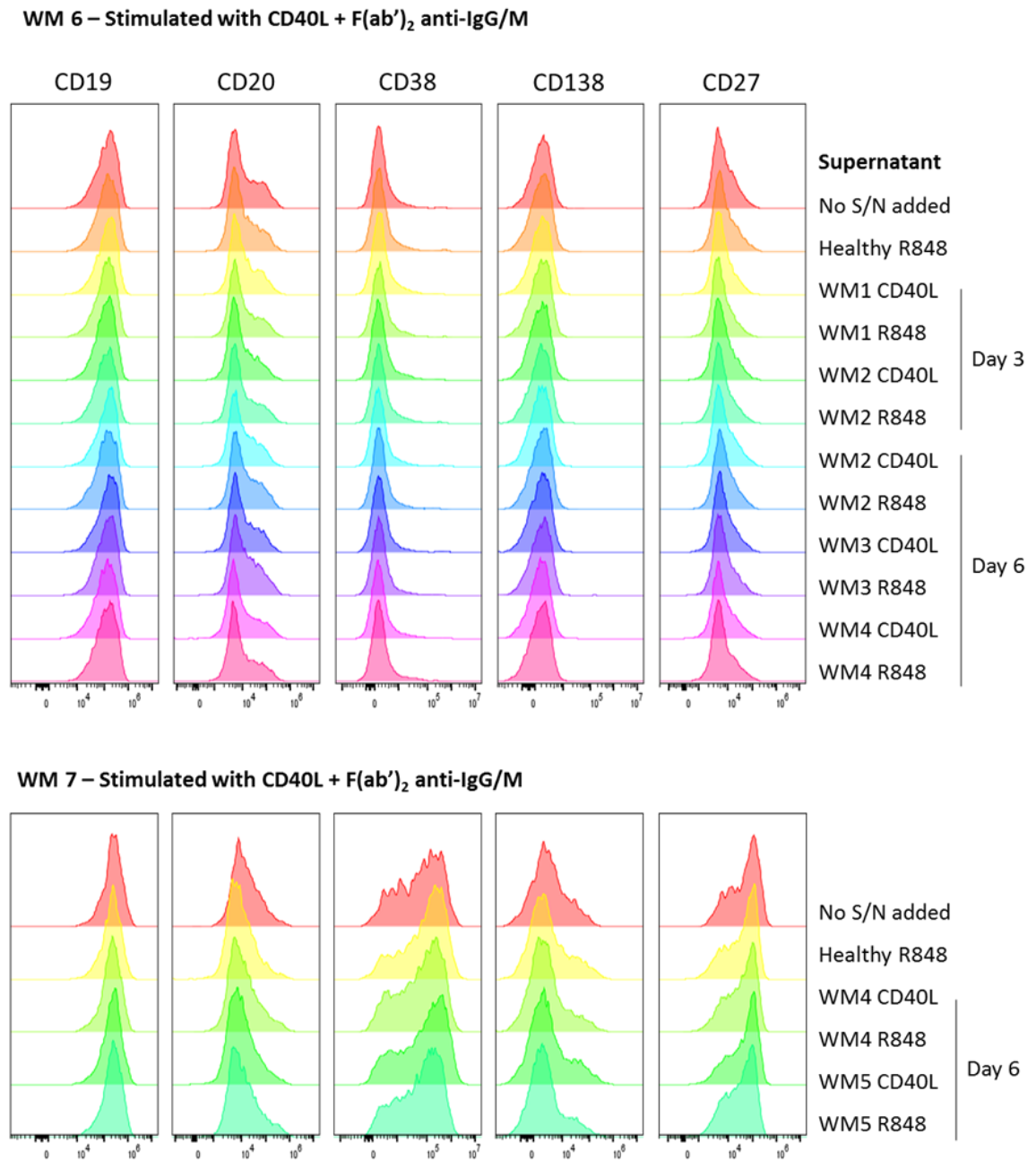
Figure 7.11 The phenotype of CD40L-stimulated WM cells is unaffected by the addition of supernatant from other WM differentiations. Histograms for the expression of each of the five cell surface markers on differentiating WM cells corresponding to the samples in figure 7.10 (isolation protocol B). Supernatant was added at a dilution of 1:10 at day 3 of the differentiation and the phenotype assayed by flow cytometry at day 6. Both WM samples were stimulated with CD40L + F(ab')$_2$ anti-IgG/M. Top – B-cells derived from patient WM 6, bottom – B-cells derived from WM 7. The identity of the supernatants used are displayed on the right.

Despite significant individual differences in the levels of differentiation observed between the two WM samples, the addition of supernatant has a negligible effect on the phenotype on either

one (figure 7.11). This data supports a conclusion that WM cells are capable of secreting one or more factors in response to stimulation with R848 and most likely also CD40L, which, through autocrine or paracrine signalling, results in proliferation of the population as a whole.

Interestingly, the addition of the WM supernatant demonstrated no effect on either the cell number or viability of SMZL cells (figure 7.12).
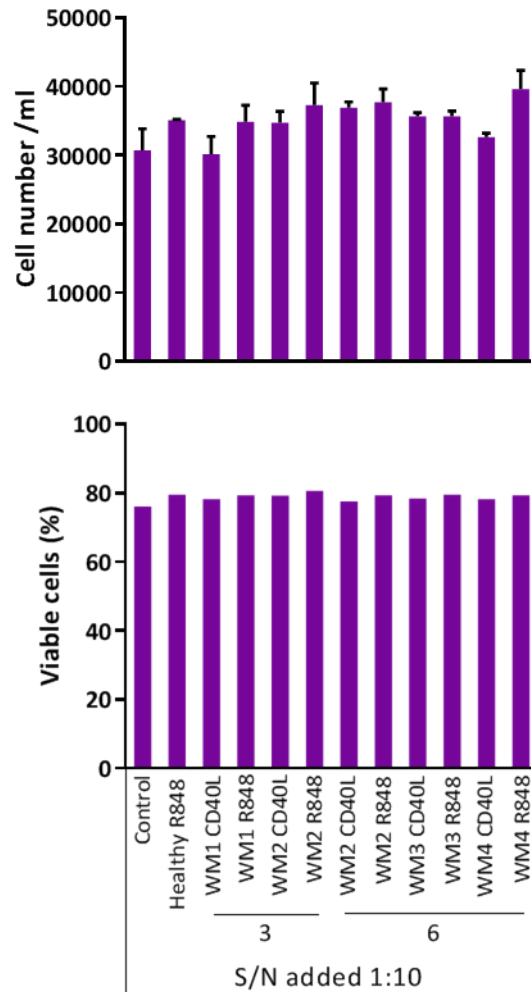
Figure 7.12 Addition of supernatant derived from an initial differentiation with WM B-cells to cells derived from a patient with SMZL which have been stimulated with CD40L + F(ab')$_2$ has no significant impact. Top – cell numbers determined by flow cytometry, data are in duplicate with error bars denoting S.D. Statistical analysis by Student's t-test with Welch's correction: *, $p < 0.05$; ** $p < 0.01$. Bottom - viability as measured by percentage 7-AAD negative cells.

In accordance with this, there was minimal impact on the phenotype of the SMZL cells, although the addition of some supernatants did result in CD20 retention (figure 7.13). This effect occurred most commonly following that addition of supernatant from R848-stimulated cells taken at both day 3 and day 6 of culture but can also be observed with the CD40L-stimulated supernatant. It

would therefore appear that this effect cannot be attributed to a particular type of stimulation or day the supernatant was collected.

SMZL - Stimulated with CD40L + F(ab')₂ anti-IgG/M
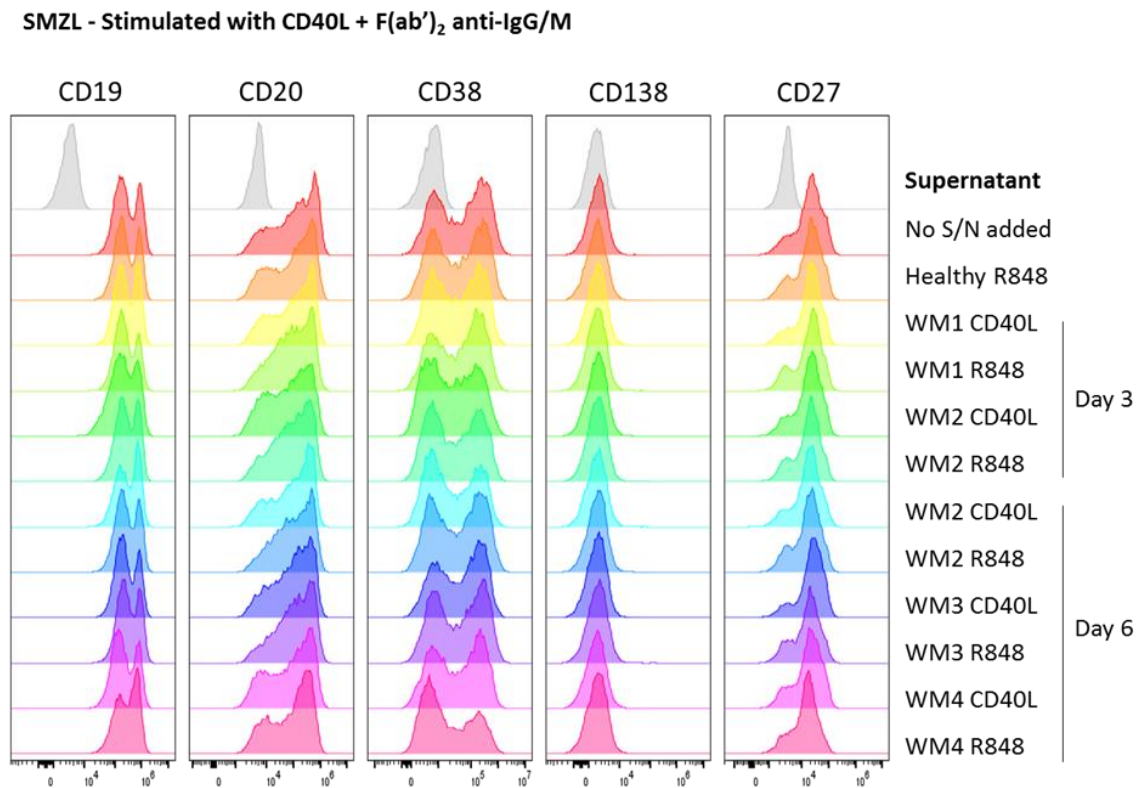
Figure 7.13 CD20 is retained in SMZL cells stimulated with CD40L following the addition of WM supernatant but the phenotype is otherwise unaffected. Histograms for the expression of each of the five cell surface markers on differentiating cells derived from the bone marrow of a patient with SMZL (isolation protocol B). The cells were activated with CD40L + F(ab')₂ anti-IgG/M., supernatant was added at a dilution of 1:10 at day 3 of the differentiation and the phenotype assayed by flow cytometry at day 6. The identity of the supernatants used are displayed on the right.

Surprisingly, the supernatant derived from R848-stimulated WM cells, which are undergoing high levels of apoptosis, did not result in a detrimental effect to either healthy cells or cells from other WM patients. On the contrary, the WM supernatant enhanced both the proliferation and viability of healthy cells and the proliferation of WM cells. The greatest effect was observed for the WM R848-stimulated supernatant, although the day 3 CD40L-stimulated supernatant also appeared to elicit a proliferative response, with a trend towards a significance. It is perhaps not unexpected that supernatant collected at day 3 of an *in vitro* differentiation would demonstrate a positive effect on other cells at this time point. It seems plausible that these cells would secrete factors into the local environment which enhance the proliferation of their peers to augment

the immune response. In the case of WM cells, it would similarly prove advantageous for the clonal population to enhance each other's survival.

The apoptotic response of WM cells to R848 stimulation now appears even more contrary, given that these cells are most likely concurrently in receipt of additional pro-survival and pro-proliferative signals from their neighbours. This indicates that either WM cells are reliant on supplementary signalling from the microenvironment of the bone marrow to enhance their survival or that they upregulate apoptotic genes in response to R848 to such a great extent that this overwhelms not only the constitutive NF-κB activation conferred by MYD88^{L265P} but also the autocrine and paracrine pro-survival signalling demonstrated here.

7.5   Evaluation of Fas and FasL expression in WM cells

Given that the cell death observed in WM cells does not appear to be as the result of a secreted factor, it could instead result from receptor-ligand interactions between the cells. The potency of the B-cell immune response requires exquisite control in order to prevent it from escalating disproportionately. One such mechanism that is essential for B-cell tolerance is activation-induced cell death (AICD) (Donjerković and Scott, 2000). The importance of regulatory mechanisms such as AICD for the prevention of autoimmunity is clear, with Fas mutations in humans and mice resulting in uncontrolled lymphocyte proliferation and severe autoimmune disorders (Krammer, 2000).

The interaction between CD40 on the B-cell surface and its ligand expressed on T-cells induces a potent activation signal, resulting in survival and proliferation (Lederman *et al.*, 1992; J Banchereau *et al.*, 1994). However, during T-dependent immune responses, Fas expression on activated B-cells is upregulated following CD40L stimulation from T-cells, priming them for sensitivity to FasL-mediated apoptosis (Schattner *et al.*, 1995; Nagata, 1997). However, concomitant BCR stimulation inhibits this process, enabling B-cells that have bound their cognate antigen to survive and undergo expansion and differentiation (Rothstein *et al.*, 1995). Once engagement of the BCR has ceased following the elimination of pathogens, resistance to FasL-mediated apoptosis diminishes and thus the response is controlled. The ability of WM cells to proliferate and differentiate subsequent to TD stimulation is in keeping with this, apoptotic signals are inhibited by simultaneous BCR and CD40 ligation, enabling the cell to avoid this fate and instead resulting in survival.

The response of WM cells to activation with R848 may therefore be due to activation-induced cell death. It is possible that the innate expression of Fas and/or FasL on WM cells is elevated in comparison to healthy cells and that stimulation of both the BCR and TLR7 are insufficient to

overcome the pro-apoptotic signals. An alternate explanation is that ligation of TLR7 in WM cells results in the upregulation of Fas or FasL to a greater extent than that which occurs in healthy cells and that this is the cause for the apoptotic response. The expression of Fas and FasL on WM and healthy cells at each time point of the differentiation were therefore evaluated to determine whether either of these hypotheses were correct. Histograms and corresponding MFI values for Fas and FasL expression are shown in figure 7.14 (details of antibodies used for this analysis are provided in methods section table 2.5.
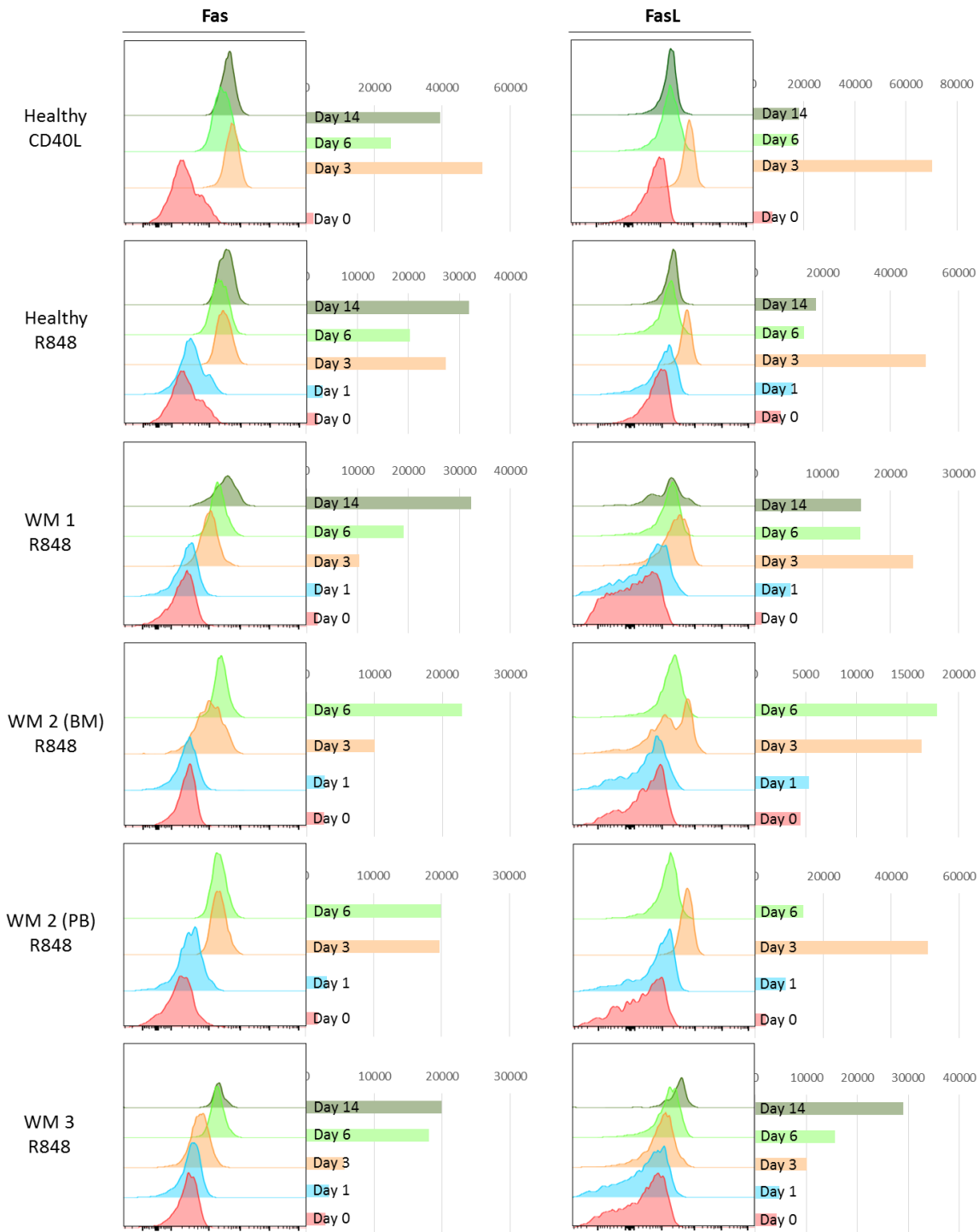
Figure 7.14 Fas and FasL are upregulated during differentiation. B-cells derived from the bone marrow or peripheral blood of WM patients or the peripheral blood of a healthy donor were stimulated as indicated and the expression of Fas and FasL were assessed by flow cytometry at the time points indicated. Histograms are displayed with the corresponding MFI values plotted to the right.

The pattern of expression of Fas and FasL is very similar in healthy cells between both types of stimulation. In accordance with the published literature, the expression of Fas remains

unchanged between day 0 and day 1, followed by a significant increase to day 3 as the B-cell population becomes activated. Subsequently, protein expression decreases to day 6 but once again rises to a similar level of expression as the cells at day 3. FasL expression follows a similar pattern, but expression falls to a greater extent between day 3 and day 6 and remains lower thereafter.

The Fas expression pattern in WM cells is slightly different, with a less pronounced increase at day 3, followed by an increase thereafter. Despite this, the MFI values for the later time points are comparable with the healthy controls. There are two patterns of FasL expression in the WM samples. WM1 and the peripheral blood sample from WM2 exhibit an expression pattern similar to that of the healthy sample, with the highest expression of FasL occurring at day 3 of the differentiation. In contrast, the matched bone marrow sample from patient WM2 and the sample from WM3 demonstrate increasing levels of FasL as the differentiation progressed. The bone marrow sample from WM2 possesses a bi-modal peak at day 3. This corresponds to a divergence in the phenotype observed for this sample, with a population of cells that are unable to differentiate in response to stimulation with R848 exhibiting lower FasL expression than the rest of the population.

The similarity between the overall levels of Fas and FasL expression between the healthy and WM samples and lack of a marked increase of either at early time points in the R848-stimulated WM cells suggests that activation-induced cell death via Fas or FasL is unlikely to be the cause of the profound apoptotic response elicited by this type of stimulation in WM cells.

7.6 Assessment of B-cell response to dual stimulation with CD40L and R848

WM B-cells *in vivo* encounter a variety of different stimuli within the bone marrow niche, simultaneously activating multiple signalling cascades. The potential for a combination of activating stimuli to overcome the effects of TLR7 stimulation was examined to provide further insight into the WM response.

7.6.1 Healthy cells

The effect of a combination of both CD40L and R848 stimulation was initially assessed in healthy B-cells to establish a control phenotype. B-cells from two donors were stimulated concurrently with either CD40L + F(ab)'$_2$ anti-IgG/M, 1µg/ml R848 + F(ab)'$_2$ anti-IgG/M or a combination of both CD40L and R848. B-cells from both donors proliferated more highly following stimulation

with CD40L when compared with those that received R848 stimulation (figure 7.15). Cells that received both CD40L and R848 stimulation proliferated to a similar extent to their counterparts that received CD40L + F(ab)'$_2$ anti-IgG/M stimulation, this being considerably more than the cells with R848. The difference in cell number between CD40L alone and CD40L + R848 for both donors at each time point was minimal. The response of donor 2 was the lowest observed of all the healthy differentiations that were stimulated with R848. Despite this, a combination of CD40L and R848 resulted in greater proliferation than was seen with CD40L alone.

Comparison of single and combined stimuli response in healthy cells
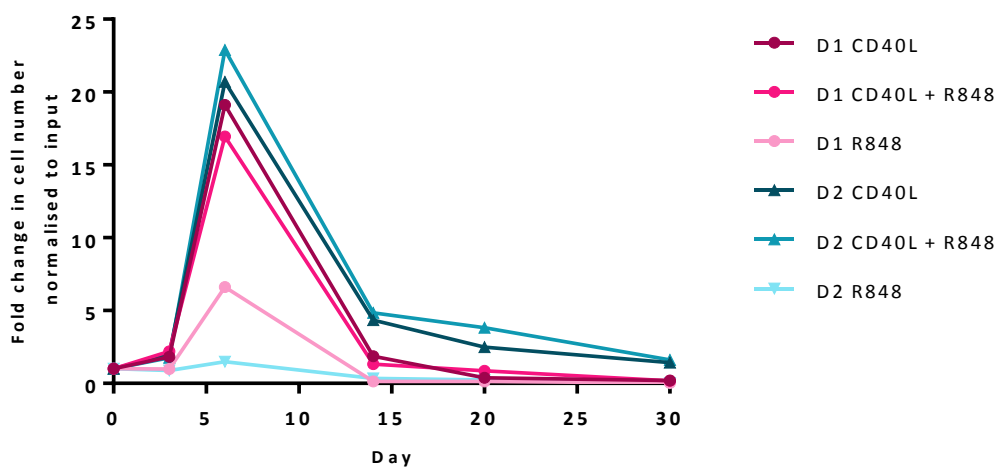
Figure 7.15 Dual stimulation with CD40L and R848 results in a cell number profile that is similar to CD40L stimulation alone. B-cells derived from the peripheral blood of two healthy donors were stimulated with CD40L, CD40L + 1μg/ml R848 or 1μg/ml R848 + F(ab')$_2$ anti-IgG/M. Cell number at each time point was determined by manual counts for days 3 and 6 and then by flow cytometry thereafter. The cell number at each point was normalised to the number of "input" cells for that specific patient obtained at day 0.

The phenotype of cells from both donors was highly comparable at each time point, despite the differences in the amplitude of the individual responses. A representative example from donor 1 is displayed in figure 7.16. At day 6, the difference in phenotype between the two basic conditions – CD40L alone versus R848 alone – are as expected, with a larger plasma cell population generated with R848 + F(ab)'$_2$ anti-IgG/M. The cells that were stimulated with a combination of CD40L + R848 + F(ab)'$_2$ anti-IgG/M possess a phenotype that is almost identical to those with CD40L alone, in line with the similarity in cell number. The differences in phenotype between the three conditions diminish by day 13 and remain consistent thereafter.

A combination of both CD40L and R848 stimulation does not appear to have an additive effect in the case of either individual, rather, the proliferation induced following activation with CD40L

+ F(ab)'$_2$ anti-IgG/M appears to elicit something close to maximal proliferative response. The strength of the CD40L stimulation appears to override the phenotypic response as well, with a combination of both stimuli yielding a phenotype that is very similar to that of CD40L + F(ab)'$_2$ anti-IgG/M alone, rather than an intermediate between that which is observed for the individual stimuli. As was previously shown with the two basic stimuli, the phenotypic differences that are observed at the early time points are lost as the differentiation proceeds and the phenotype of the plasma cells are indistinguishable from one another.
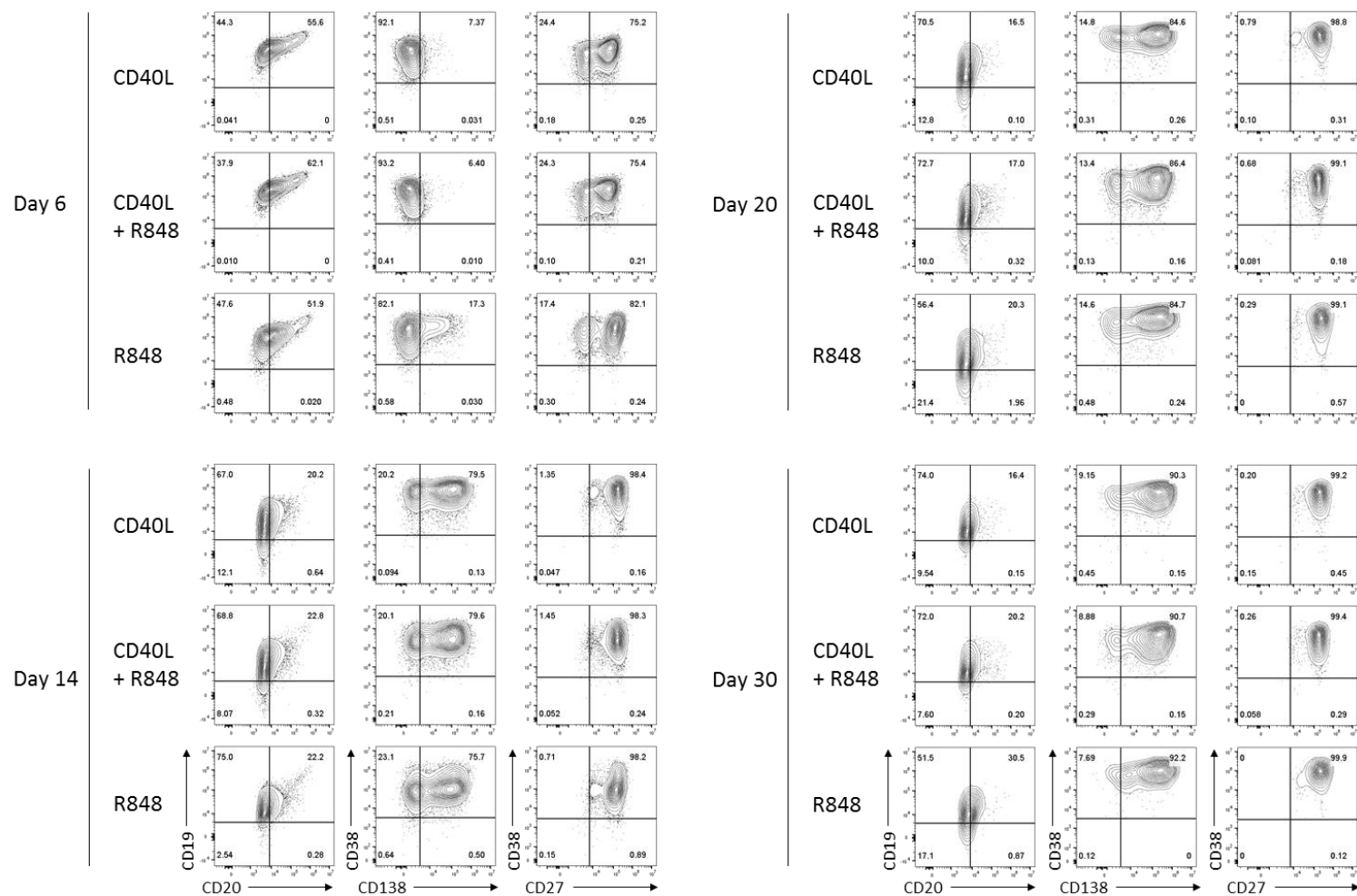
Figure 7.16 Representative phenotypes for single and combined CD40L and/or R848 B-cell stimulations for one donor. B-cells isolated from the peripheral blood of healthy donors (n = 2) were activated with CD40L, 1µg/ml R848 or both CD40L and 1µg/ml R848 + F(ab')$_2$ anti-IgG/M (isolation protocol B). The immunophenotype was assayed by flow cytometry at each time point. Percentages are displayed for each quadrant.

7.6.2   WM cells

The response of WM B-cells was then examined to investigate whether the failure to proliferate and differentiate following R848 stimulation could be ameliorated by co-stimulation with R848 and CD40L. As with the healthy cells, bone marrow-derived B-cells from a WM patient were stimulated with either CD40L, 1µg/ml R848 or a combination of CD40L + 1µg/ml R848, with F(ab)'$_2$ anti-IgG/M in each instance.

Between days 0 and 3, cell numbers were maintained within cultures which received CD40L stimuli but cells which were stimulated with R848 alone had considerably decreased in number (figure 7.17). The decline continued for the R848-stimulated cells until there were no cells left from day 13 onwards. In contrast, cells from both the CD40L-stimulated conditions proliferated between days 3 and 6, with WM cells stimulated with a combination of CD40L and R848 proliferating to a greater extent than those which received just CD40L. The numbers of cells from the dual-stimulated condition remained higher than those with CD40L alone until day 20 of the differentiation, after which both conditions had a very similar number of cells.
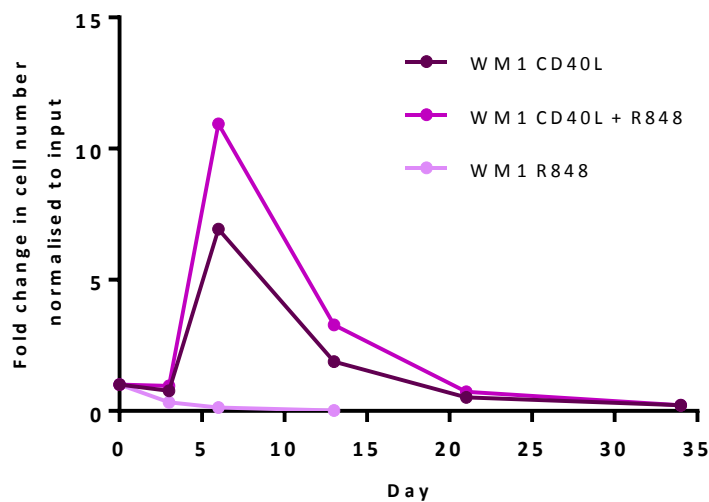
Figure 7.17 Dual stimulation of WM B-cells with CD40L and R848 has a synergistic effect on cell number. B-cells derived from the bone marrow of a WM patient were stimulated with either CD40L, a combination of CD40L + 1µg/ml R848 or 1µg/ml R848 + F(ab')$_2$ anti-IgG/M (isolation protocol B, with 10ml media wash at day 3). Cell number at each time point was determined by manual counts for days 3 and 6 and then by flow cytometry thereafter. The cell number at each point was normalised to the number of "input" cells for that specific patient obtained at day 0.

The phenotype of the cells in each condition are displayed in figure 7.18. At day 6, the phenotype of the dual-stimulated cells is virtually indistinguishable from those in receipt of CD40L alone. Whilst they have not progressed as far as the healthy cells by this time point, downregulation of CD20 is occurring in combination with CD38 upregulation, confirming that they are in the process of differentiating. In contrast, the phenotype of the WM cells receiving R848 stimulation only differs considerably. The cells in this condition are unable to respond correctly, maintaining a B-cell phenotype, with no evidence of differentiation. The cells stimulated with both CD40L and R848 continue to have almost exactly the same phenotype as the CD40L-only group throughout the rest of the differentiation, generating plasma cells by day 14 which are maintained thereafter. In contrast, the R848 stimulated cells fail completely to differentiate, with an inability to downregulate CD20 and failing to upregulate CD38 and CD138. Interestingly, this sample generated a population of $CD38^-$ $CD138^+$ cells in both the CD40L and CD40L + 1µg/ml R848 conditions.

Thus cells from this WM patient exhibited the same pattern of phenotypic response as the healthy cells, with the combinatorial stimuli resulting in a phenotype that closely resembles that of CD40L alone, rather than an intermediate phenotypic response. However, in contrast to the differentiations with healthy cells, addition of TLR7 agonist R848 resulted in a considerably greater fold change between days 3 and 6 compared to cells just stimulated with CD40L. Surprisingly, the combination of stimuli elicits an enhanced response, suggesting that perhaps WM cells *in vivo* would proliferate to a greater extent than the non-neoplastic clone when provided with the same stimulation.
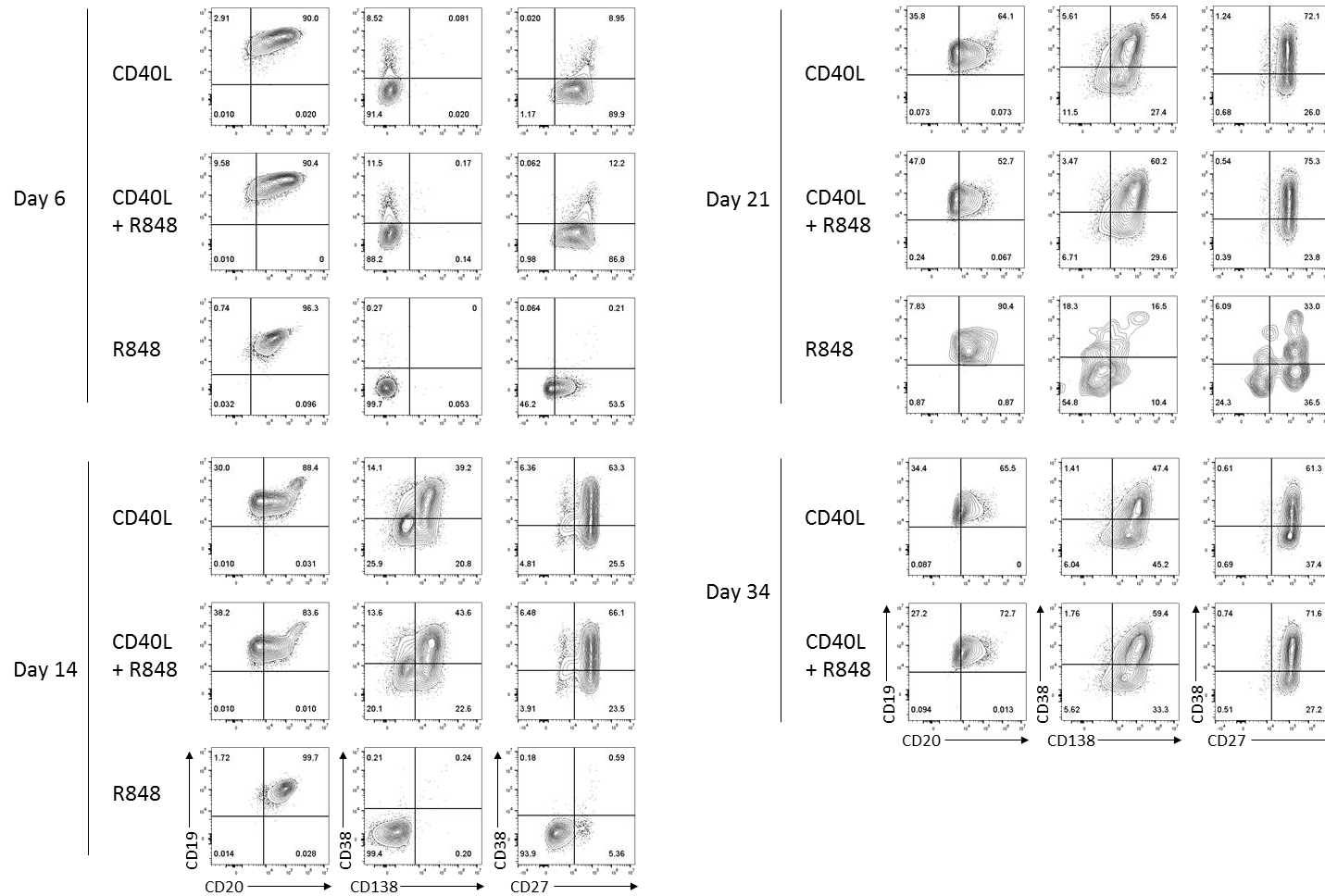
Figure 7.18 A comparison of the phenotype obtained following dual stimulation of WM cells to the two basic stimulations. B-cells were isolated from the bone marrow of a WM patient and activated with CD40L, 1µg/ml R848 or both CD40L and 1µg/ml R848 + F(ab')₂ anti-IgG/M (isolation protocol B, with 10ml media wash at day 3). The immunophenotype was assayed by flow cytometry at each time point. Percentages are displayed for each quadrant.

The response of B-cells isolated from a second WM patient was evaluated to determine if the results from the first WM sample could be replicated. For all conditions, cell numbers declined between day 0 and 3, but with a distinction between those that received CD40L or CD40L + R848 stimulation and those which did not (figure 7.19). This patient sample had been stored for an increased length of time in comparison to the first WM sample, which likely contributed to the decreased levels of viability and cell death observed here. Cell numbers in the R848 only condition continued to decline thereafter whereas there was an increase in numbers for both CD40L and CD40L + R848 between days 3 and 6. WM B-cells that received both CD40L and R848 stimuli proliferated to a greater extent than those with just CD40L. Cell numbers declined substantially between day 6 and 13 in these two conditions, but remained very similar at each subsequent time point.
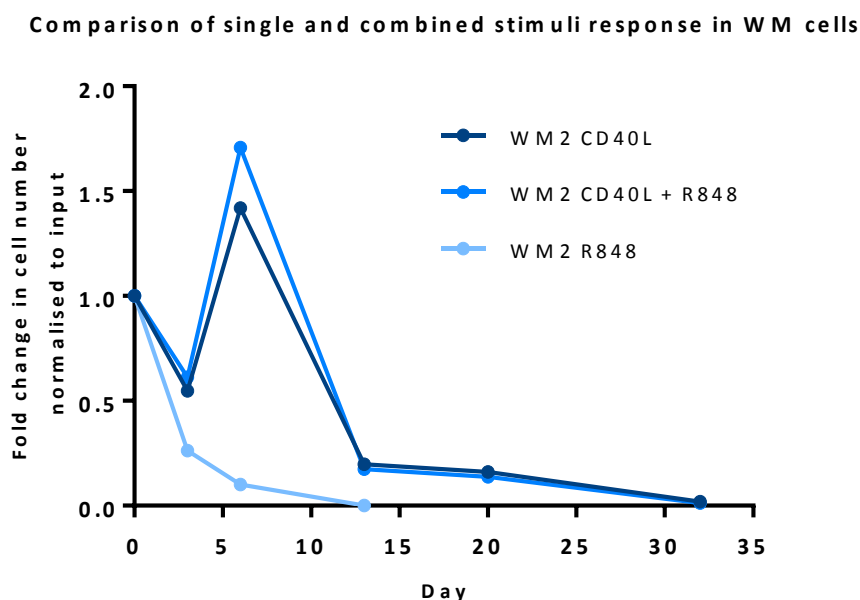
Figure 7.19 A combination of CD40L and R848 stimuli ameliorates the detrimental effect of R848 stimulation alone in WM B-cells. B-cells derived from the bone marrow of a WM patient were stimulated with either CD40L, a combination of CD40L + 1µg/ml R848 or 1µg/ml R848 + F(ab')$_2$ anti-IgG/M (isolation protocol B, with 10ml media wash at day 3). Cell number at each time point was determined by manual counts for days 3 and 6 and then by flow cytometry thereafter. The cell number at each point was normalised to the number of "input" cells for that specific patient obtained at day 0.

As with the previous WM sample, the phenotypes demonstrate a partition between cells that were stimulated with CD40L and those that were not (figure 7.20). Cells stimulated with R848 alone displayed a profound defect in their ability to differentiate, retaining a B-cell phenotype throughout. On the other hand, the phenotypes were very consistent between both conditions

that received CD40L stimulation, with no noticeable differences with the addition of R848. The cells from this patient showed a delay in the acquisition of CD38 at day 6 as with the first WM sample, but this was consistent between the two CD40L-stimulated conditions. Once again at day 13, the phenotypes remained very similar, with a delay in the downregulation of CD20 expression and a population of $CD38^-$ $CD138^+$ cells emerging in both instances. This consistency in phenotype was maintained to day 32 of the differentiation.

The similarity in phenotype between the CD40L and CD40L + R848 conditions is consistent between both the WM cells and their healthy counterparts. Whilst the healthy cells proceeded to differentiate more rapidly when provided with R848 + F(ab')$_2$ anti-IgG/M than the other two conditions, the WM cells were unable to differentiate properly in response to these stimuli. The combination of stimuli did not increase the fold-change response of the healthy cells, instead the response was comparable with the proliferation induced with the basic activation with CD40L + F(ab')$_2$ anti-IgG/M. For the WM samples, a combination of both stimuli at the very least ameliorates the apoptotic response normally induced by stimulation with R848. The presence of both signals appears to elicit a greater response from WM B-cells, with cells from both WM patients demonstrating an increase in fold-change between day 3 and day 6 of the differentiation, although this was somewhat more limited in the second patient sample.

The results would seem to suggest that WM cells are more reliant on additional pro-survival signals, in this instance provided by CD40 ligation, than their healthy counterparts, but when in receipt of these they are able to proliferate to a greater extent. This is perhaps not surprising given what is known about WM pathology. WM cells express high levels of both cytokine and adhesion receptors, enabling them to home to the bone marrow, aided by mutations in CXCR4 (Ngo *et al.*, 2008; Ghobrial *et al.*, 2011; Hunter *et al.*, 2013). Thus, they are situated within an environment rich in additional sources of support from stromal cells and secreted factors. Further stimulation of TLR7, in concert with the other signalling occurring *in vivo* may therefore contribute to enhanced levels of proliferation of the WM clone, helping it out-compete the healthy fraction.
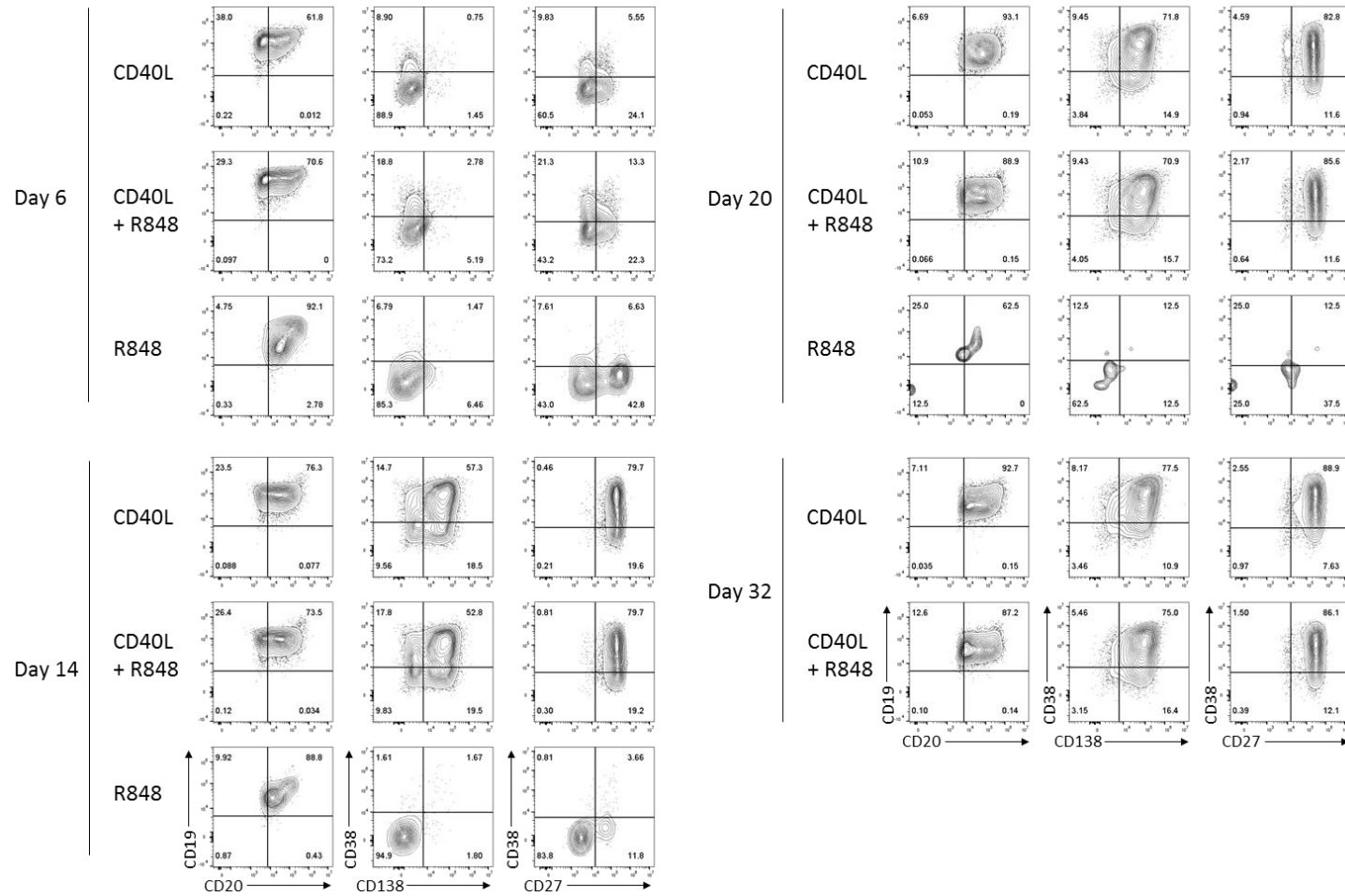
Figure 7.20 A comparison of the phenotype obtained following dual stimulation of WM cells to the two basic stimulations. B-cells were isolated from the bone marrow of a WM patient and activated with CD40L, 1µg/ml R848 or both CD40L and 1µg/ml R848 + F(ab')₂ anti-IgG/M (isolation protocol B, with 10ml media wash at day 3). The immunophenotype was assayed by flow cytometry at each time point. Percentages are displayed for each quadrant.

7.7   TLR expression in patient samples

Since a proportion of WM cells are completely unable to respond to R848 stimulation, it is possible that they have downregulated TLR expression. Hunter et al., have suggested that TLR7 is upregulated in MYD88^{L265P} CXCR4^{WHIM} patients but quantification of TLRs *in situ* has not been analysed (Hunter *et al.*, 2016). To provide insight into this, expression of endosomal TLRs in WM cell lines, samples of PB from healthy donors and a sample of BM from a WM patient were analysed by flow cytometry. The DLBCL cell line HBL-1 was found to express high levels of TLR9 in tests so was included as a positive control. For the primary samples, RBCs were lysed before cells were initially stained with antibodies to cell surface markers to enable the B-cell population to be identified and subsequently with the intracellular TLR antibodies.

The inclusion of a LAIR1 antibody facilitates identification of neoplastic WM cells since LAIR1 expression is commonly high in healthy individuals but conversely the WM clonal population can usually be distinguished by low to intermediate levels of this marker (Paiva *et al.*, 2015; Rawstron *et al.*, 2017). In addition, LAIR1 expression typically varies amongst other LPDs, with elevated expression in SMZL, whilst it is normally absent from GC DBLCL cells (Van Dongen *et al.*, 2012). The CD19$^+$ CD20$^+$ fraction was therefore subdivided based on LAIR1 expression (details of antibodies used for TLR analysis are provided in methods section table 2.6). The pattern of TLR expression is shown in figure 7.21.
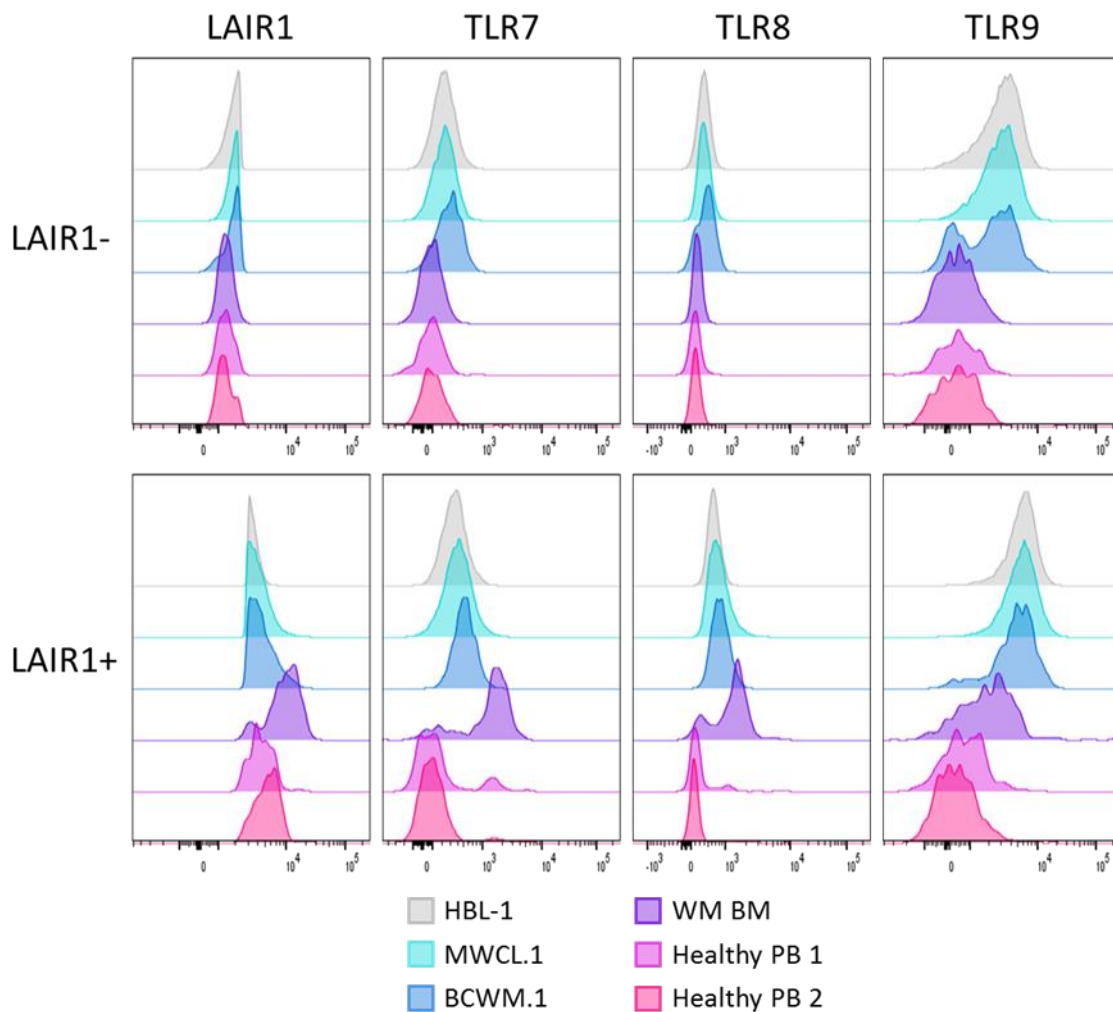
Figure 7.21 Endosomal TLR expression in cell lines and primary samples. Cells were stained for surface antigens and with a fixable viability dye before fixation, permeabilisation and staining with intracellular antibodies. For healthy and WM samples, B-cells were defined as CD19$^+$ CD20$^+$ and then gated on LAIR1 expression using FMO controls. Expression of TLR7-9 are shown for the LAIR1- fraction (top) and LAIR1+ fraction (bottom).

In general, TLR9 was the most highly expressed, with levels of TLR7 and 8 considerably lower, but still present in at least a proportion of cells in most samples. Interestingly, the TLR expression changes dramatically between the LAIR1$^+$ and LAIR1$^-$ fractions of the WM sample. Whilst expression of TLR7, 8 and 9 is low in the LAIR1$^-$ population, the expression of each increases substantially in the LAIR1$^+$ fraction. Strikingly, LAIR1$^+$ WM cells expressed the highest levels of TLR7 and 8 out of the 6 samples tested. This may suggest that the neoplastic fraction has downregulated TLR expression.

Both WM cell lines expressed particularly high levels of TLR9 and also express slightly elevated levels of TLR7 and 8 in comparison to the healthy samples and WM LAIR1$^-$ fraction. The majority

of the healthy cells were LAIR1^{+} as expected. Within this subgroup, both samples had a small proportion of cells that expressed high levels of both TLR7 and TLR8. Whilst not investigated here, it would be most interesting if this fraction corresponded to the subset of cells observed to respond particularly rapidly to R848 stimulation during differentiations.

The assessment of endosomal TLR expression within the B-cell population was extended with additional clinical samples from 8 patients with a selection of LPDs, summarised in table 7.3 below. The results from two staging marrows were also included as a surrogate for heathy controls as these did not display a neoplastic phenotype and provide the best comparison for the neoplastic bone marrow samples. Flow cytometry data for TLR expression is presented in figure 7.22.

Table 7.3 Clinical samples assessed for endosomal TLR expression.

Sample number	Diagnosis	Sample type
1	Staging marrow (normal)	BM
2	Staging marrow (normal)	BM
3	MZL	BM
4	Mantle cell	BM
5	CLL	PB
6	CLL	PB
7	CLL	BM
8	CLL	BM
9	CLL	BM
10	WM	BM

Expression of LAIR1 was highly variable, but in keeping with the published literature, with the staging samples generally positive for this marker, the MZL sample expressing even higher levels of LAIR1, whilst it is absent from the WM sample. The WM sample possessed a high level of clonality, with a correspondingly low expression of LAIR1 for virtually the entire B-cell population. Of all the samples tested, the LAIR1^{-} WM subset possessed the lowest MFI for TLR7 and TLR8 although TLR9 is expressed at an intermediate level in a large proportion of these cells. TLR expression in the other samples varied considerably, but levels were very similar between both the LAIR1 positive and negative fractions in all instances.

Whilst downregulation of TLR7 in the WM sample cannot be definitively determined due to lack of a non-neoplastic fraction within the sample to compare to, the average MFI for TLR7 the

LAIR1$^+$ population of two staging marrows is 352, whilst the WM sample is 279 suggesting that

TLR downregulation may be a possibility.
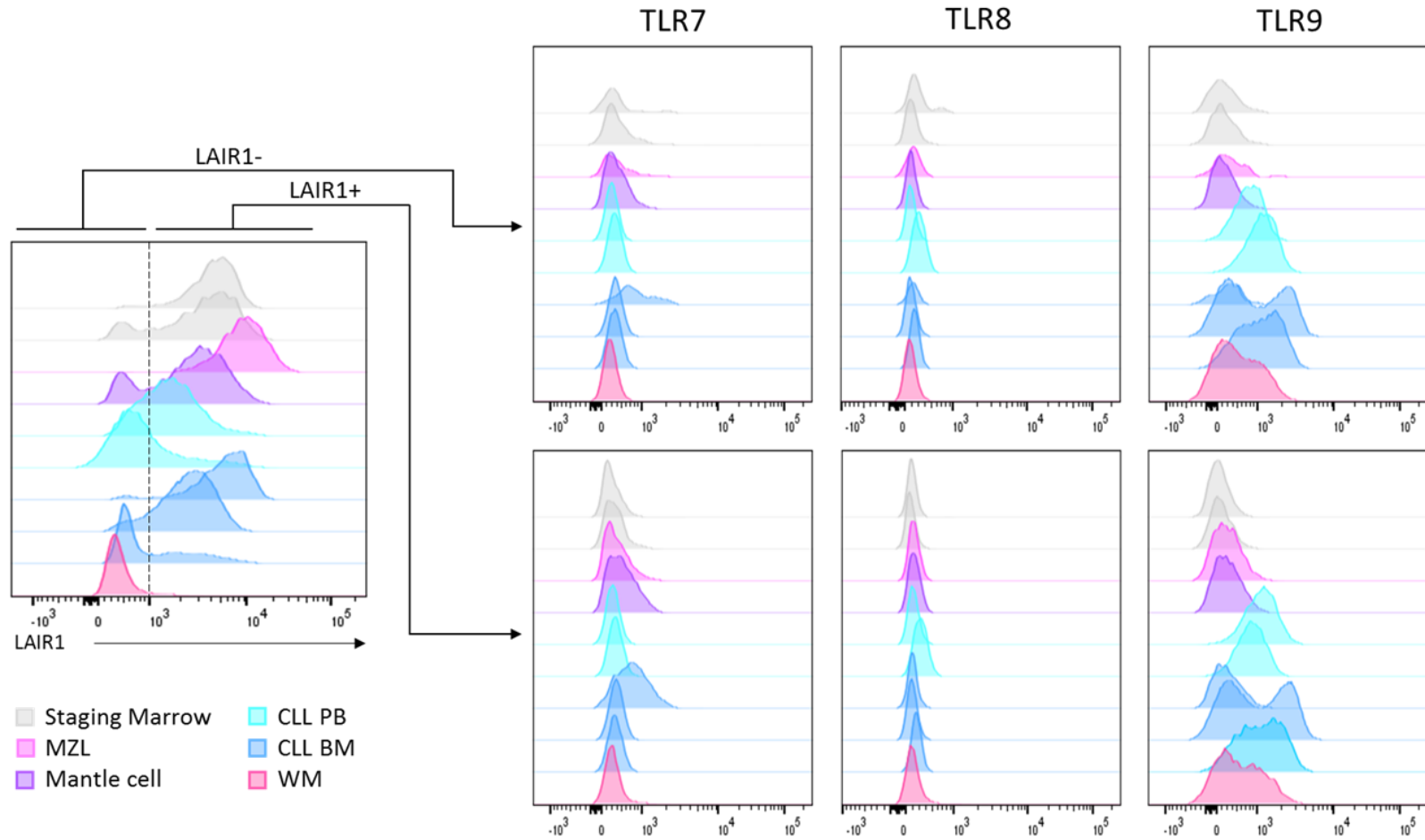
Figure 7.22 Endosomal TLR expression patterns in clinical samples. Cells were stained for surface antigens before fixation, permeabilisation and staining with intracellular antibodies. B-cells were defined as CD19+ CD20+ and then gated on LAIR1 expression as shown. Expression of TLR7-9 are shown for the LAIR1- fraction (top) and LAIR1+ fraction (bottom). Histograms represent individual samples, with samples grouped and coloured by type.

7.8 RNA-sequencing of differentiating cells from the *in vitro* system

RNA sequencing was performed on material harvested from differentiating cells at day 6 of culture within the *in vitro* system. The samples consisted of 3 healthy controls with matched samples for both CD40L and R848 stimulation and a total of 6 WM samples (table 7.4). Due to the paucity of WM samples and cell death that occurs within those cultured with R848, matched samples of WM cells of sufficient quality for sequencing were only obtained in two instances. Cells from four other patients were therefore used to increase the number of samples and enable an overview of WM cells in general.

Table 7.4 Samples used for RNA-sequencing.

Sample	CD40L	R848
WM4	x	
WM5	x	
WM6	x	x
WM7	x	x
WM11		x
WM15		x
Healthy1	x	x
Healthy2	x	x
Healthy3	x	x

The profound levels of apoptosis within the highly clonal WM samples 6 and 7 subsequent to R848 stimulation resulted in less material for sequencing and thus a reduced number of reads for both of these samples in comparison to the rest of the samples. The decreased number of read counts within these two samples resulted in larger values for gene dispersion during the analysis of the data, affecting subsequent modelling. Figure 7.23 is a heatmap generated during quality control assessment, illustrating the two outlying samples. Whilst a greater number of reads would improve the quality of the dataset as a whole, modification of the analysis pipeline to account for this flaw by shrinking the $\log_2$ fold change estimates enables meaningful conclusions to be determined.
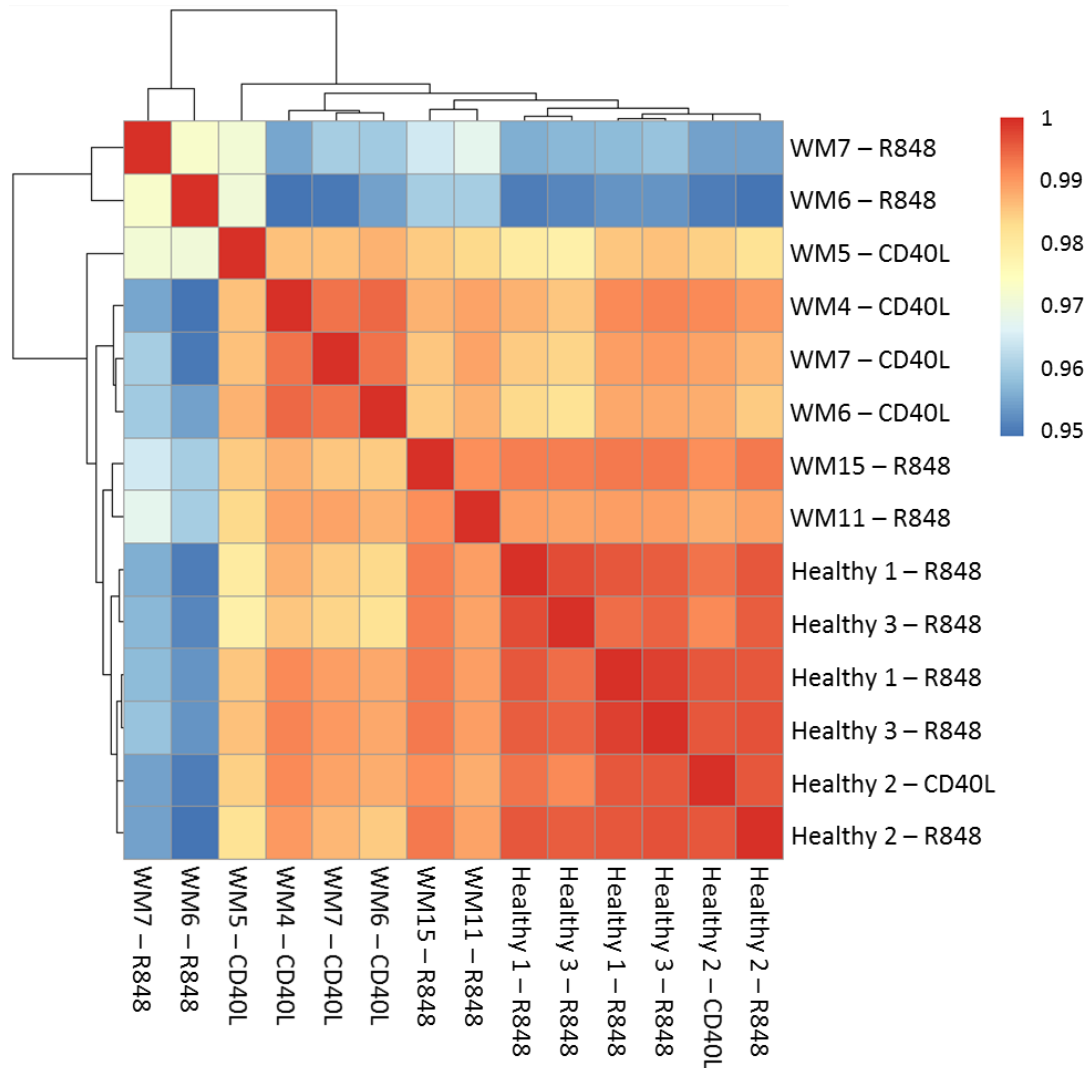
Figure 7.23 QC heatmap depicting outlying samples. Correlations were performed across all genes. The colour ranges from blue to red as the correlation trends towards 1.

7.8.1   Differentially expressed genes

The numbers of significantly up- or downregulated genes between healthy and WM samples and between the different activation stimuli, from a total of 50663, are displayed in figure 7.24.

The greatest difference in gene expression occurs between the WM and healthy samples, with WM samples demonstrating a considerably greater proportion of upregulated genes. A comparison of the two types of stimulation, encompassing both the WM and healthy samples reveals a more even split between the numbers of differentially expressed genes. The difference in gene expression between CD40L vs. R848 arises in the most part from the contribution of the WM samples, since the number of differentially expressed genes between the two conditions in

healthy samples is significantly lower. This is in accordance with the observed phenotype and proliferative responses of both healthy and neoplastic samples, with the former demonstrating highly similar responses to both activation conditions, whilst there exists a considerable disparity in the differentiation of the WM cohort in response to the two types of stimuli.

As might be anticipated from the characterisation of the differentiation responses, the number of differentially expressed genes between WM and healthy cells following CD40L stimulation is smaller than that for R848 stimulation. Surprisingly, the R848-stimulated WM samples demonstrate a greater number of upregulated genes than their healthy counterparts, despite failing to differentiate correctly.
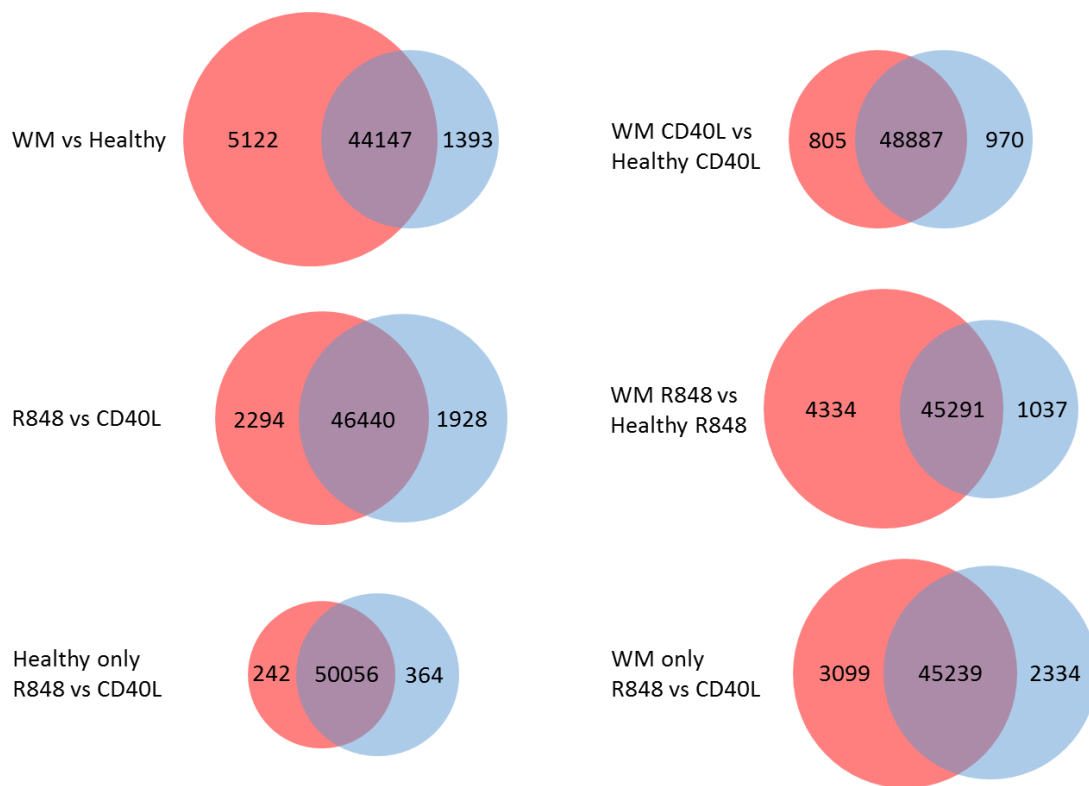
Figure 7.24 Comparison of the numbers of differentially expressed genes at day 6 of differentiation between WM and healthy individuals and between different stimuli. Venn diagrams depicting the significantly differentially expressed genes for each stated comparison. The numbers of upregulated genes are displayed in red, downregulated genes in blue and the non-significant genes in the centre. The threshold for significance was $p < 0.01$.

The difference in gene expression between the two WM samples with a heavy disease burden (WM6 and WM7) and their counterparts with low levels of clonality following R848 stimulation is highlighted in figure 7.25.
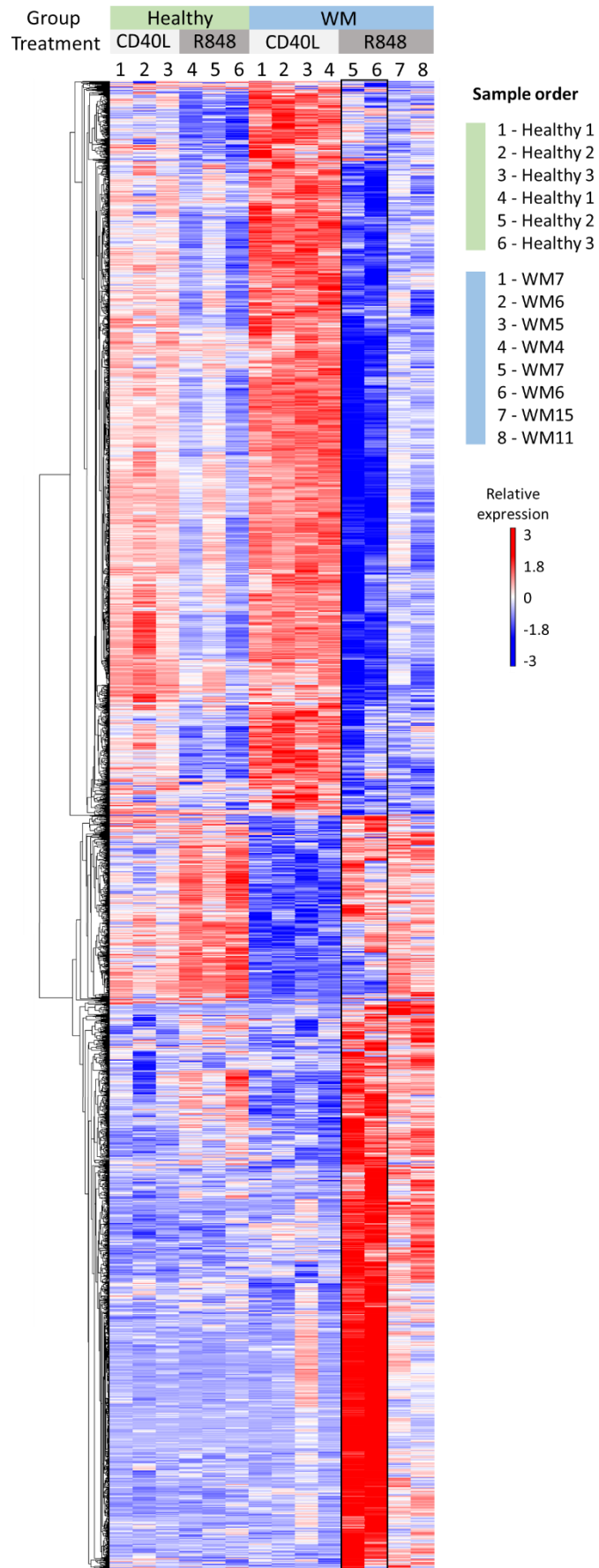
Figure 7.25 Heatmap of differentially expressed genes between R848 and CD40L stimulations.

Amongst the most significantly differentially expressed genes between samples derived from WM patients and those taken from healthy donors were those encoding the variable regions of immunoglobulin heavy and light chains, with a marked downregulation of many of these families in the WM samples. In particular, expression of the *IGHV3* family was almost completely absent in the WM samples. The lack of variability of immunoglobulin expression in the WM cells compared to the healthy controls reflects the skewing of the Ig repertoire due to the monoclonality of the population.

Components of the plasma cell differentiation pathway such as *PRDM1*, encoding BLIMP1, the master regulator of B-cell differentiation, and *IRF4* are equally highly expressed in the healthy cells from both conditions, indicating that both stimuli elicit a similar response. Interestingly however, one of the most significantly differentially expressed genes in healthy cells between the two conditions is *CD138*, with a 32-fold increase in those activated with R848 versus those activated with CD40L. This mirrors the increased alacrity of plasma cell generation by healthy cells stimulated with R848 and appears to be one of the few differences between the responses elicited by each stimuli.

In order to highlight specific pathways that would be affected by the altered expression levels between the different samples and conditions, comparisons of differentially expressed genes were performed between and within the healthy and WM groups. Subsequently, the significantly differentially expressed genes were input into the functional annotation tool DAVID. The pathways identified are listed in table 7.5.

Table 7.5 Pathways associated with differentially expressed genes between each sample group.

Up	Down
Healthy R848 vs. Healthy CD40L	
No significant pathways	ribosome
	cytokine-cytokine receptor interaction
	metabolism
	amino acid synthesis
	gluconeogenesis
	oxygen homeostasis
All WM vs. All Healthy	
MAPK signalling pathway	No significant pathways
NF-κB pathway	
cytokine-cytokine receptor interaction	
WM CD40L vs. Healthy CD40L	
cytokine-cytokine receptor interaction	JAK-STAT signalling pathway
TNF signalling pathway	endocytosis
TLR signalling pathway	NK cell mediated cytotoxicity
NF-κB pathway	FOXO signalling pathway
apoptosis	glycosaminoglycan biosynthesis
chemokine signalling pathway	
WM R848 vs. Healthy R848	
cell adhesion molecules	protein processing in ER
TNF signalling pathway	
TLR signalling pathway	
NF-κB pathway	
focal adhesion	
cytokine-cytokine receptor interaction	
PI3K-AKT signalling	
glutamatergic synapse	
neuroactive ligand-receptor interaction	
haematopoietic cell lineage	
RAP1 signalling pathway	
WM R848 vs. WM CD40L	
antigen processing and presentation	Ribosome
NK cell mediated cytotoxicity	spliceosome
ECM-receptor interaction	cell cycle
PI3K-AKT signalling pathway	DNA replication
endocytosis	ribosome biogenesis
choline metabolism in cancer	glycolysis
	RNA transport
	purine/pyrimidine metabolism
	leukocyte transendothelial migration
	regulation of actin cytoskeleton
	RNA degradation

7.8.1.1   Healthy CD40L vs. R848

A comparison of differentially expressed genes between the healthy cells activated with either CD40L or R848 reveals that there was no significant upregulation of any particular pathway, despite the differences in the initial activating stimuli. However, multiple components of various metabolic pathways exhibited decreased expression levels subsequent to TLR7 stimulation. The previously characterised effects of B-cell stimulation with R848 in comparison to CD40L activation in healthy cells are twofold, resulting in more rapid differentiation but overall generating fewer cells by day 6 than the CD40L stimulation. The cells successfully able to respond to activation with R848 have become plasmablasts at this time point, with a small proportion of plasma cells, whereas cells stimulated with CD40L do not acquire the plasma cell phenotype for another few days. Plasma cells are highly metabolically active due to their increased secretory burden and one might expect that cells derived from the R848 condition may begin to upregulate genes involved in this process at an earlier stage than their counterparts stimulated with CD40L. Thus, a decrease in genes involved with metabolism at this time point seems to reflect a state of lower activation within this population in general, consistent with a lower proportion of cells able to respond as effectively to this type stimuli.

7.8.1.2   WM vs. healthy

Components of three major pathways were upregulated amongst the WM samples compared to the healthy controls. As expected, the NF-κB pathway was highlighted by the functional annotation tool. Interestingly, whilst MYD88^{L265P} results in constitutive activation of the canonical NF-κB pathway, the transcription factor RelB, the central player involved in the non-canonical pathway was also significantly increased compared to healthy cells, suggesting an interplay between the two branches of the pathway.

Cytokine signalling plays a key role in WM pathogenesis, with mutations in CXCR4 being the most common after MYD88 and are central to the homing of WM cells to the bone marrow (Ngo *et al.*, 2008; Hunter *et al.*, 2013; Poulain *et al.*, 2016). It is therefore not surprising for components of these pathways to be upregulated. In particular, the chemokines CCR4, CCR7 and CCL5, CXCR4 itself and multiple members of the TNF family are all elevated in the WM samples. This is in accordance with the findings of Ngo and colleagues (Ngo *et al.*, 2008). Similarly, activation of MAPK is important for chemotaxis, adhesion and proliferation and this pathway is also upregulated in the WM samples.

Many of the genes upregulated in WM cells compared to heathy following CD40L stimulation correspond to the literature (Ghobrial *et al.*, 2011; Paiva *et al.*, 2015; Hunter *et al.*, 2016). Even in the absence of additional TLR stimulation, WM cells display upregulation of the TLR and NF-κB pathways, indicative of their constitutive activation in the neoplastic cells. In addition to this, a large group of both cytokines and chemokines are upregulated, highlighting the importance of the microenvironment to WM cells. Interestingly, genes associated with apoptosis were also upregulated in WM cells, but this was specific to the CD40L-stimulated group. Activation of B-cells results in the upregulation of pro-apoptotic genes to increase the susceptibility of these cells to activation-induced cell death in the absence of sufficient pro-survival factors in order to exert control over potentially damaging immune responses. The upregulation of this set of genes by CD40 ligation appears to be sufficiently countered in this instance by genes enhancing survival such as the constitutive activation of the NF-κB pathway. It may indicate that WM cells are more susceptible than healthy cells to cell death without additional support from stromal cells or other secreted factors within the bone marrow. Another factor that may oppose the cell death is the downregulation of members of the FOXO pathway. Activation of this pathway results in apoptosis, so its downregulation may counteract the increased expression of other pro-apoptotic genes. Genes associated with NK cell mediated cytotoxicity are also downregulated in the WM group, suggesting that WM cells may escape normal regulation, becoming less visible to immunosurveillance and thus creating an environment more conducive to their proliferation, unchecked by NK cells.

Despite the profound impairment to plasma cell differentiation in WM cells subsequent to TLR7 activation, only a limited number of genes were downregulated at this time point in comparison to healthy cells stimulated in the same manner. In contrast, a large number of genes in the WM cells demonstrated elevated expression. These included multiple genes involved in adhesion and cell-cell interaction. As with the comparison of cells stimulated with CD40L, WM cells stimulated with R848 demonstrate elevated expression levels of genes associated with TLR and NF-κB signalling. Once again, WM cells demonstrate upregulation of numerous components involved in cell-cell interaction, but to an even greater extent than following CD40L stimulation. This suggests that the WM cells may be attempting to initiate contact with other cells that would normally be found within the bone marrow or perhaps with each other. Of particular note is the absence of apoptosis associated genes, despite the virtual eradication of the WM population by this time point.

7.8.1.3   WM CD40L vs. R848

Once again, differential expression of genes involved with apoptosis are notable by their absence. In comparison to their CD40L-stimulated counterparts, the WM cells stimulated with R848 display a catastrophic breakdown of essential regulatory pathways. This reflects the cell death but does not enable the elucidation of the genes involved in the initiation of this response.

Interestingly, the PI3K-Akt signalling pathway is upregulated in R848-stimulated WM cells in comparison to both the CD40L-stimulated group and the healthy cohort stimulated with R848. Increased PI3K-Akt signalling in WM cell lines and primary cells was initially identified by Leleu and colleagues (Leleu *et al.*, 2007). Evidence of constitutive activation of this pathway in primary CD19$^+$ WM cells was further supported in a subsequent paper (Roccaro *et al.*, 2010). Activation of the PI3K-Akt signalling axis results in increased proliferation and survival and is involved the homing of WM cells to the bone marrow (Vivanco and Sawyers, 2002; Leleu *et al.*, 2007). Since the majority of the cell death in R848-stimulated WM cells occurs before day 6, it is interesting to speculate that the cells that have upregulated the PI3K-Akt pathway may be partially resistant to the apoptosis and that this is reflected in the differentially expressed genes between the two types of stimulation.

7.8.2   Evidence of B-cell activation in R848-stimulated WM samples and expression of TLR mRNA

One of the most important questions to address was whether WM cells are able to receive TLR7 signals and integrate them successfully in order to initiate B-cell activation, as a failure to do so could explain the profound apoptotic response. The results from the RNA sequencing indicate that TLR7 stimulation does indeed activate WM B-cells. Stimulation of WM cells with R848 upregulates multiple genes associated with B-cell activation that are similarly upregulated in R848-stimulated healthy cells including *FosB*, *JunD*, *IL2Rα* and *CD138* (figure 7.26). Other genes associated with activation that were upregulated in WM cells but not healthy cells were *CD83*, *CD22*, *CD69* and *IL7R*. This supports the data generated using WM supernatants, suggesting that WM cells could be sufficiently activated with R848 in order to trigger them to secrete one or more factors that can support B-cell proliferation and survival.

Genes associated with B-cell activation
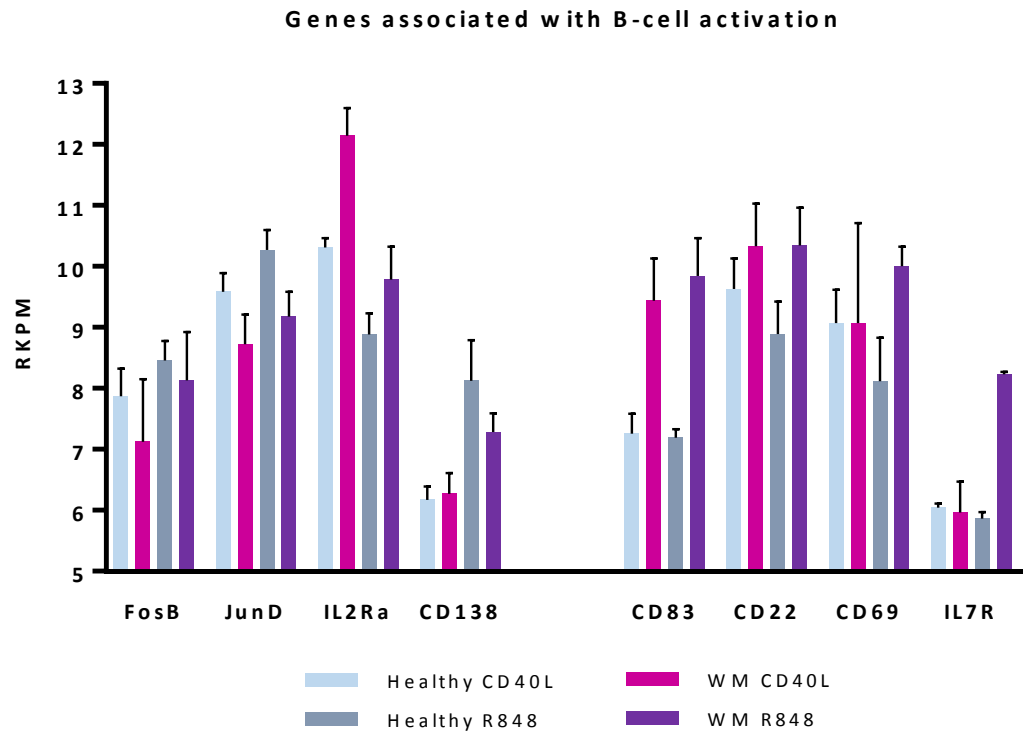
Figure 7.26 R848-stimulated WM cells demonstrate upregulation of multiple genes associated with B-cell activation. Activation associated genes that are similarly upregulated in both WM and healthy samples are on the left, whilst those more specific for WM samples are on the right hand side. Mean RKPM values are shown for each gene with error bars representing the range.

Evaluation of the expression of TLRs within the endosomes of WM cells by flow cytometry was inconclusive, but indicated that there might be variable expression between individuals. The sequencing data reveals that, in fact, *TLR7* mRNA is the most highly expressed of the endosomal TLRs in both healthy and WM samples.
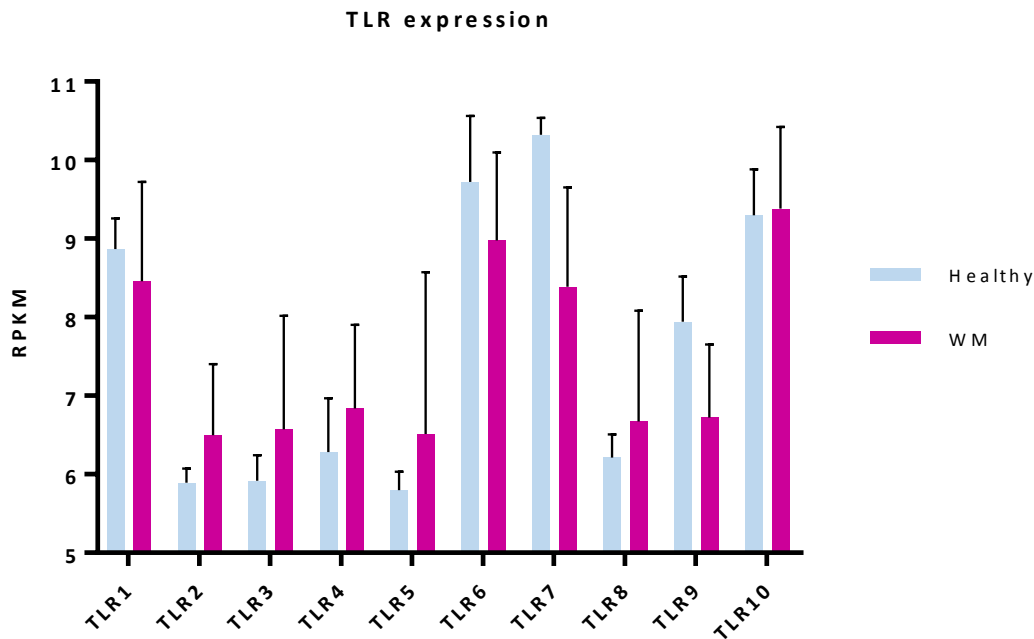
Figure 7.27 Expression of TLR genes in healthy and WM samples. Mean RKPM values are shown for each gene with error bars representing the range.

The expression of *TLR7* mRNA was fairly similar between healthy and WM cells, with WM cells expressing on average slightly lower levels. An exception to this was patient WM6, in which both samples possessed significantly lower expression of *TLR7*, significantly decreasing the average in figure 7.27. This is quite unexpected, as B-cells from this patient displayed some evidence of differentiation subsequent to R848 stimulation, whereas cells from patient WM7 appeared completely unable to respond to TLR stimulation, despite expressing similar levels of mRNA to healthy individuals. This implies that endosomal TLR expression is not necessarily correlated to mRNA expression levels and is controlled through post-translational mechanisms. The localisation of TLR7 to the endosome requires the shuttling protein UNC93B1 and it is also regulated by subsequent endosomal acidification and proteolytic cleavage, all of which are subject to additional control (Brinkmann *et al.*, 2007; Kim *et al.*, 2008; Ewald *et al.*, 2011). This is in accordance with the literature, whereby endosomal TLRs in particular are more tightly regulated due to their capacity to bind self-ligands and potentially initiate an autoimmune response (Barton *et al.*, 2006). The expression of the TLRs themselves therefore is likely quite variable, as the flow cytometry data suggested. Despite the potential variability of TLR expression between individuals, B-cells were activated in all instances, indicating that low levels of TLR7 are sufficient for B-cell activation. These results suggest that the TLR7 pathway within WM B-cells remains at least partly intact and that WM cells are receptive to additional activation signals via TLR7 ligation.

7.8.3 Expression of genes within the plasma cell differentiation pathway

Having established that WM cells remain capable of being activated by ligation of TLR7, the failure of these cells to successfully differentiate may be due to a perturbation of the genes associated with plasma cell differentiation. This, in turn, may provide evidence as to why WM cells are unable to survive following activation with R848.

WM cells demonstrated differential expression of multiple key genes within the plasma cell differentiation pathway compared with healthy cells. Differences in gene expression were apparent subsequent to both types of stimulation and these are highlighted in figure 7.28.
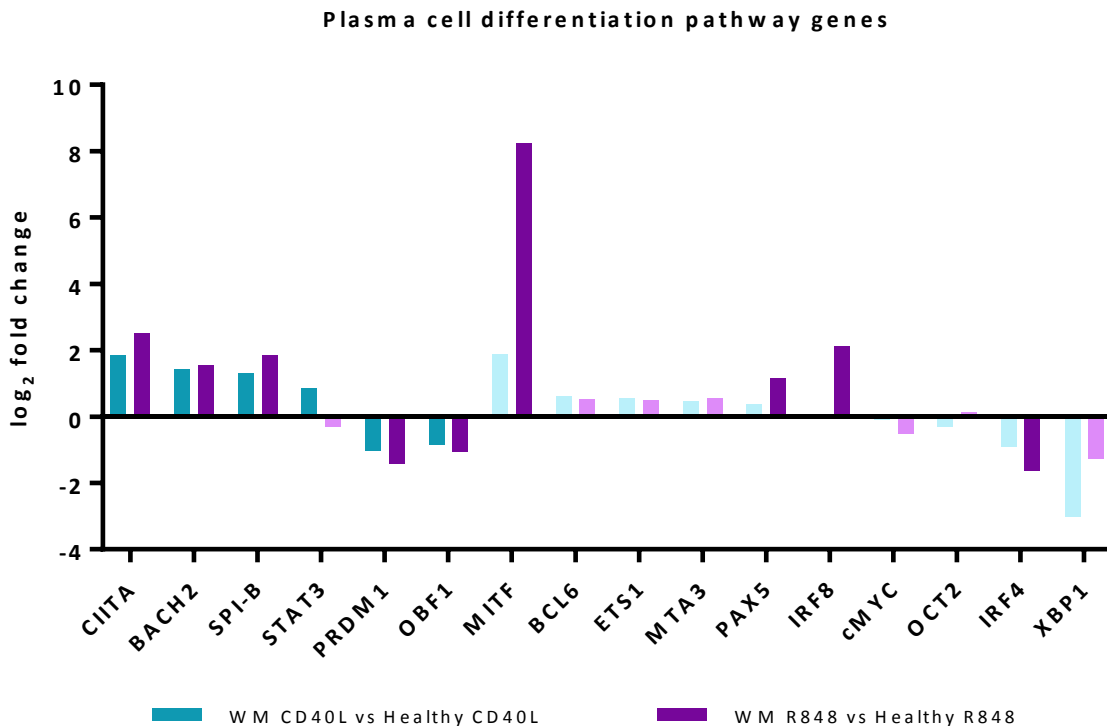
Figure 7.28 Differential expression of genes involved in plasma cell differentiation. A comparison between the fold change in expression in WM vs. healthy samples subsequent to either CD40L or R848 stimulation are depicted. The fold change was considered statistically significant if $p < 0.05$; bars for genes that did not fall below this threshold are shown in pale tones.

For WM cells stimulated with CD40L, fewer genes were significantly differentially expressed than for WM samples activated with R848. The magnitude of the fold change in expression was also lower for five of the six genes. WM cells exhibited decreased levels of *PRDM1* – encoding the master regulator of plasma cell differentiation BLIMP1 – and *POU2AF1* and conversely, increased levels of *BACH2, CIITA, STAT3* and *SPI-B*. The regulatory relationship between BACH2,

SPI-B and PRDM1, with an increase in the former and a decrease in the latter are suggestive of a slight suppression of plasma cell differentiation. The repression of *PRDM1* supports previous phenotypic analysis and may explain the delay in differentiation at this time point that is sometimes observed in WM cells in comparison to their healthy counterparts. Despite the slight delay in acquisition of PC phenotype in some instances, the effect of the differentially expressed genes is in general minimal, with the capacity of WM B-cells to generate plasma cells being retained (figure 7.29).
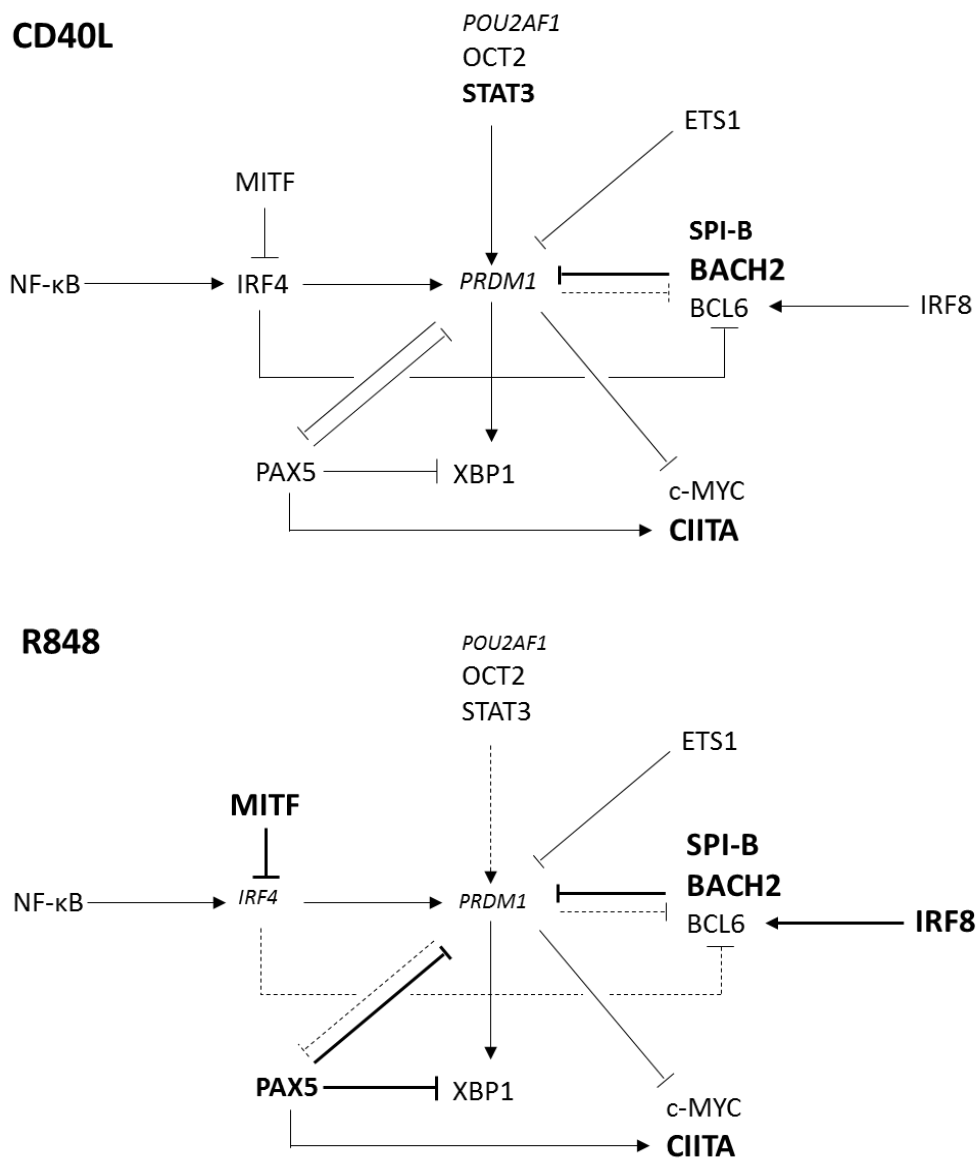
Figure 7.29 Differentially expressed genes within the plasma cell differentiation pathway between WM and Healthy cells stimulated with either CD40L or R848. The interaction between key genes involved in plasma cell differentiation is depicted for cells stimulated with CD40L + F(ab')$_2$ anti-IgG/M (top) or R848 + F(ab')$_2$ anti-IgG/M (bottom). Genes that are upregulated in WM samples compared to healthy are in a larger font and bold whereas those that are downregulated are shown in a smaller font and italicised.

A greater number of members of this pathway are perturbed in WM cells subsequent to R848 stimulation. *IRF8*, *BACH2*, *SPI-B* and *MITF* exhibit significantly increased expression, resulting in repression of both *IRF4* and *PRDM1*, indicative of an impediment to plasma cell differentiation. The elevated levels of *BACH2*, *SPI-B* and *IRF8* suggest that subsequent to activation, WM cells are able to become pre-plasmablasts or plasmablasts and are then unable to progress further (figure 7.29, bottom). Again, these data are in line with the results obtained from the *in vitro* experiments and provide an explanation for the decreased ability to generate plasma cells exhibited by the WM samples.

7.8.4   Apoptosis of WM cells subsequent to activation with R848

The most unanticipated result from the *in vitro* differentiation experiments was the profound cell death that occurred in WM cells following stimulation with R848 + F(ab')$_2$ anti-IgG/M. Given the ubiquity of the apoptosis within the WM cultures, one would anticipate either a substantial upregulation of pro-apoptotic genes or downregulation of pro-survival genes to be apparent, but this is not the case from the sequencing data. Within the WM cohort, the expression of Fas and FasL, key factors involved in activation-induced cell death are in accordance with the results presented earlier in this chapter, with *Fas* mRNA more highly expressed than *FasL*, but no different to the expression in healthy cells. There is no evidence of upregulation of caspases or members of the Bcl-2 family of proteins such as *BAD*, *BAX* and *BIM*.

The variation between WM and healthy cells instead appears to result from the underlying differences in biology and does not provide a clear explanation as to the reason behind the cell death. Whilst the difference in gene expression between the two types of stimulation in WM cells is clear, it does not directly implicate a specific pathway as the initiator of the cell death.

The cell death that is initiated in WM cells subsequent to stimulation with R848 occurs rapidly, with >50% of cells undergoing apoptosis between day 0 and day 3. This data provides a snapshot of the events occurring at day 6 of the differentiation and therefore reflects the end point of the life of the WM cells, where multiple essential pathways are profoundly affected. To provide greater insight into the genes and pathways involved in the initiation of this process, an earlier time point would need to be investigated.

7.8.5   Downregulation of CD38 expression in WM samples

The propensity of WM samples to generate a population of CD38$^-$ CD138$^+$ cells during the course of differentiation separates them from both healthy controls and differentiations with B-cells isolated from patients with other LPDs. Strikingly, the four WM samples that generated this

unusual population exhibited significantly lower expression of *CD38* mRNA, with an average expression of 7.63 compared to their healthy counterparts with an average expression of 11.49 (table 7.6).

Table 7.6 *CD38* expression at day 6 of the in vitro differentiation is predictive of the occurrence of the CD38⁻ CD138⁺ alternate plasmablast population at later time points. For matched samples, *CD38* RPKM values represent the average between the two values.

Patient	Sample type	% Neoplastic	CD38 RPKM	CD38⁻ CD138⁺	R848 differentiation?
WM7	BM	82	7.28	Yes	No
WM4	BM	69	7.39	Yes	No
WM6	BM	54	7.55	Yes	No
WM5	BM	31	8.3	Yes	No
WM11	BM	9.4	9.88	No	Some
WM15	PB	3.2 (in BM)	12.38	No	Yes
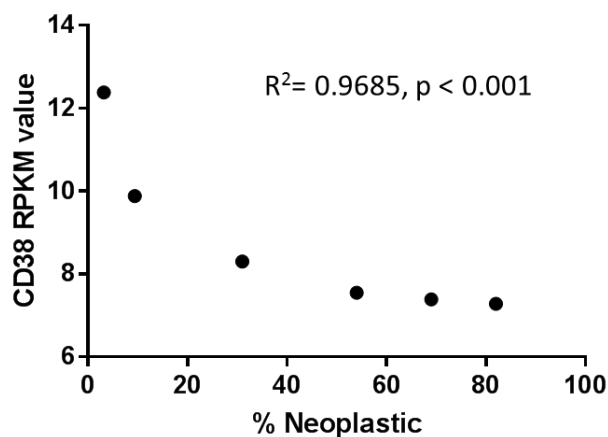
Figure 7.30 Expression of CD38 mRNA in WM cells is highly correlated with the percentage of neoplastic cells. Percentage neoplastic cells within samples of WM patient BM were determined by flow cytometry at HMDS Leeds. Statistical analysis of log transformed data by Pearson's correlation coefficient (n = 6, r = -0.9841, r^2 = 0.9685, p (two-tailed) = 0.0004).

Interestingly, *CD38* expression directly correlates with the proportion of neoplastic cells within the bone marrow (figure 7.30). There appears to be a threshold between approximately 10-30% neoplastic cells whereby the CD38⁻ fraction is sufficiently large in order to generate the CD38⁻ CD138⁺ plasmablast intermediate. B-cells derived from the peripheral blood of a patient with WM possessed *CD38* expression levels equivalent to the healthy controls (Table 7.6, WM15).

This sample did not generate a CD38$^-$ CD138$^+$ population and successfully differentiated into plasma cells following stimulation with 1μg/ml R848 + F(ab')$_2$ anti-IgG/M indicative of a markedly lower disease burden within the peripheral blood compared to samples derived from bone marrow aspirates.

CD38 is an ADP ribose hydrolase, cleaving NAD$^+$ and NADP$^+$ resulting in the generation of cyclic ADP ribose (cADPR), NAADP, and ADPR (Howard *et al.*, 1993). Multiple functions of CD38 have been identified, with the most well characterised being its involvement in calcium signalling, cell adhesion and signal transduction (Malavasi *et al.*, 2008). Whilst it has been found to play a role in B-cell signalling, the exact mechanism by which it does this remains unclear (Lund *et al.*, 1998; Moreno-García *et al.*, 2005).

A potential explanation for this unusual finding is that transcriptional regulation within the WM cells is perturbed and that the downregulation of CD38 is simply a symptom of this. Alternatively, the WM clone may be undergoing selection for CD38 negativity. This possibility, whilst intriguing, is currently hard to explain as there is no evidence to support a deleterious role for CD38 in lymphocytes. Any potential cause/effect relationship between the appearance of the CD38$^-$ fraction and the proportion of the neoplastic WM clone cannot be determined from this data but warrants further investigation.

7.8.6 Expression of MYD88 isoforms

Five representative transcripts of MYD88 have thus far been annotated according to the RefSeq database, with sequence alignment indicating that there are at least 13 splice variants. Description of the frequency and function of MYD88 isoforms is limited, particularly in the context of B-lymphocytes, with the exception of a short form of MYD88, termed MYD88$_S$ (NM_001172568.1), which was evaluated by Janssens and colleagues (Janssens *et al.*, 2002; Janssens *et al.*, 2003). They revealed that MYD88$_S$ acts as a dominant-negative regulator of MYD88 (NM_002468.4) as it is unable to bind to IRAK4, despite being able to dimerise with the regular form of MYD88, thus abrogating downstream signalling. The regulatory function of MYD88$_S$ is due to the absence of the intermediate domain as a result of exon 2 being skipped during the splicing process. Interestingly, one of the annotated isoforms (NM_001172567.1) is virtually identical to the regular form of MYD88, with the only difference in the final protein sequence being an 8 amino acid insertion within the TIR domain (figure 7.31). This insertion results from alternate splicing of exons 3 and 4, but leaves the rest of the sequence intact. The resultant protein can thus possess the leucine to proline mutation, but at position 273 (figure 7.32).
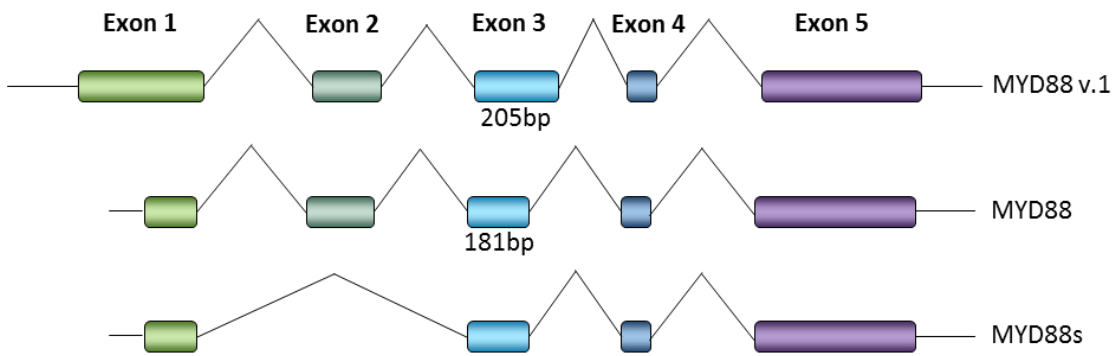
Figure 7.31 Alternate splicing of MYD88 generates multiple isoforms. Gene diagrams illustrating the variable splicing for three of the MYD88 isoforms, with each exon represented in a different colour. MYD88 variant 1 possesses a longer 5' UTR and exon 1 than the regular form of MYD88, but this does not alter the coding sequence. However, the alternate splicing of exons 3 and 4 results in the addition of an extra 8 amino acids. Complete skipping of exon 2 results in a short form of MYD88, MYD88s.
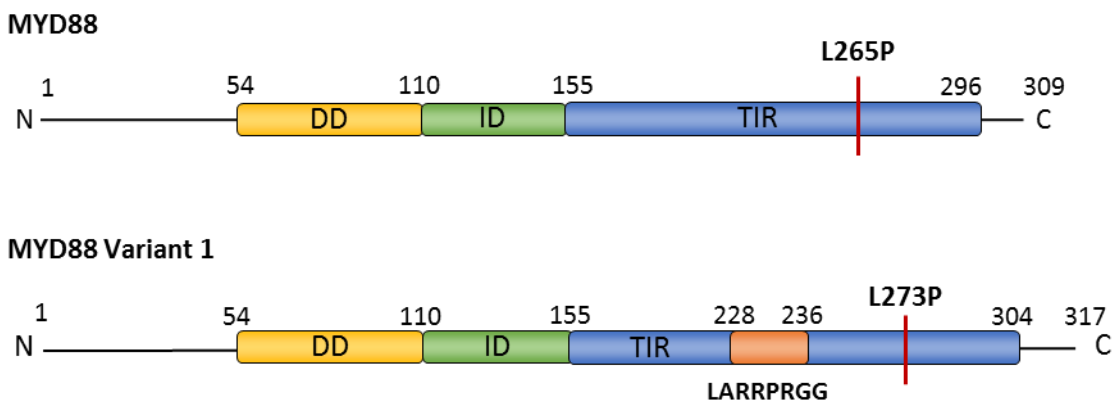
Figure 7.32 The domain structure of MYD88 and MYD88 variant 1. The location of the additional sequence within MYD88 v.1 is indicated in orange. Numbers indicate amino acid positions. DD – death domain, ID – intermediate domain, TIR – Toll-interleukin-1 receptor domain.

The potential for the expression of both MYD88 and MYD88 v.1 within several neoplastic B-cell and plasma cell lines and primary B-cells from a Schnitzler syndrome patient was initially investigated with a PCR that enables the two forms to be distinguished by their relative size (figure 7.33 top). However this preferentially amplified the regular isoform of MYD88 so MYD88 v.1-specific primers were subsequently used to confirm the result (figure 7.33 bottom).
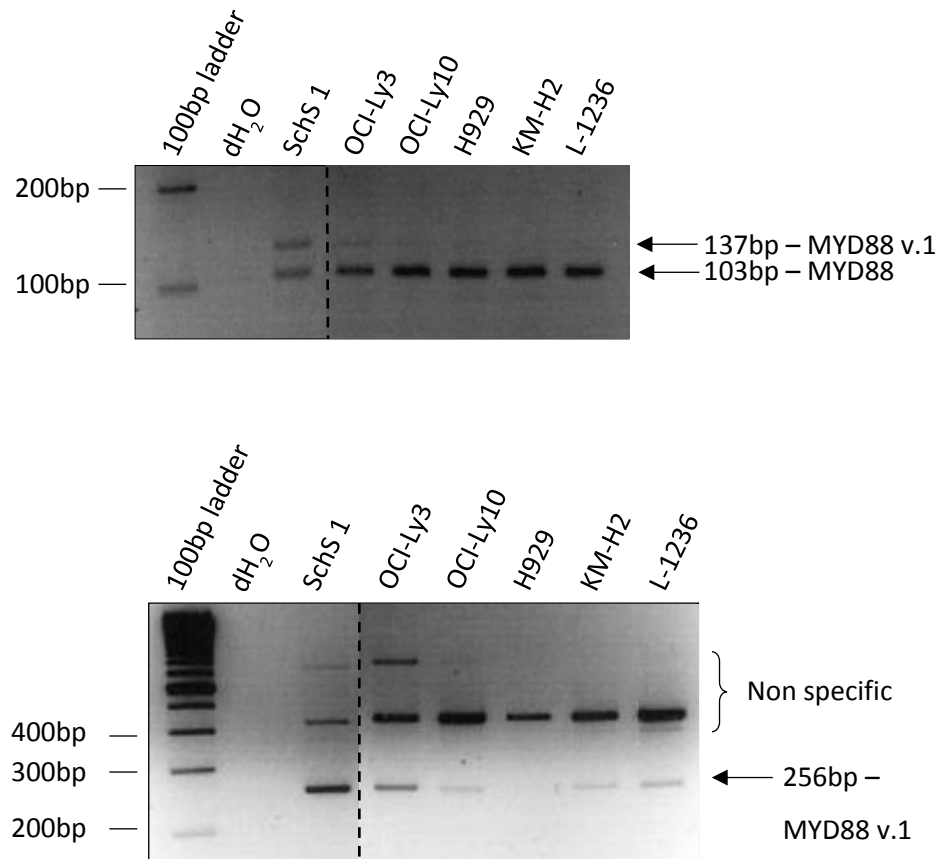
Figure 7.33 MYD88 v.1 is present in a variety of cell lines and a primary SchS sample. (Top) *MYD88* distiunguishing PCR. (Bottom) *MYD88* v.1-specific PCR. The size and identity of the bands are indicated on the right hand side. Samples were run on 3% agarose gels at 150V for 90min. The dashed line indicates where the images were cropped to remove samples that are not within the scope of this project. The larger bands from the lower gel were excised, sequenced and confirmed to be non-specific. *GAPDH* was used as a control for confirming equal amounts of input cDNA (not shown).

These data demonstrate that the variant 1 isoform is present within the L265P-mutated ABC DLBCL cell lines OCI-Ly3 and 10, the non MYD88-mutated Hodgkin lymphoma cell lines KM-H2 and L-1236, but it is not present in H929, a multiple myeloma cell line. The isoform is also present in SchS B-cells, which were previously confirmed to possess MYD88^{L265P}. The frequency of the co-occurrence of the variant 1 isoform with the regular form of *MYD88* prompted investigation as to its presence within the samples that were analysed by RNA sequencing. This data reveals that *MYD88* v.1 is present in 2/3 healthy individuals and 5/6 WM patients at approximately 1/5th the frequency of the regular form of *MYD88* (table 7.7). Its presence within the other two samples could not be confirmed due to poor sequencing coverage of this region.

Table 7.7 MYD88 v.1 is present in WM and healthy primary differentiating cells

Sample	% Neoplastic clone	MYD88 v.1	Comments
WM4	69	Yes	
WM5	31	Yes	
WM6	54	Yes	
WM7	82	Yes	
WM11	9.4	undetermined	Read depth too low
WM15	3.2	Yes	
Healthy1	-	Yes	
Healthy2	-	undetermined	Read depth too low
Healthy3	-	Yes	

The presence of *MYD88* v.1 in all samples that had suffcent sequence coverage suggests that this isoform has some functional significance and may act in a regulatory capacity. The high levels of clonality in WM4, 6 and 7 imply that *MYD88* v.1 is most likely mutated in these cases.

Modelling of the tertiary structure of the two isoforms demonstrates the effect of the additional amino acids to the conformation of the protein (figure 7.34).
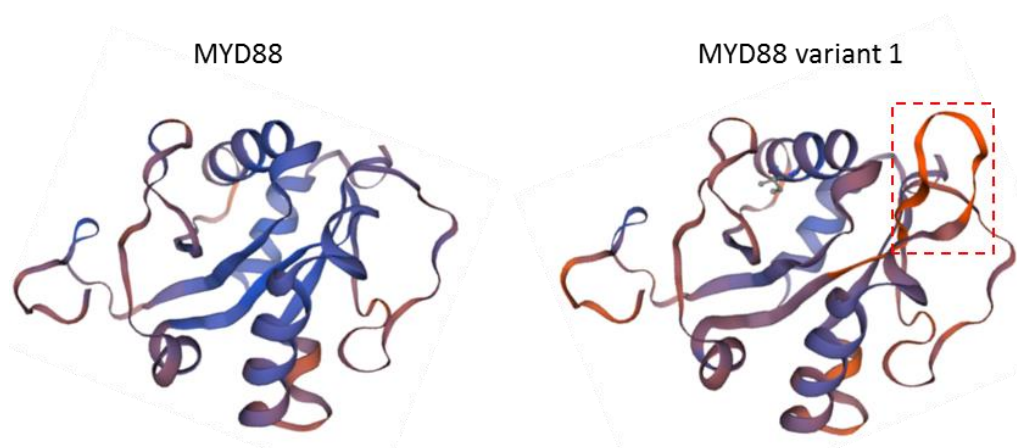
Figure 7.34 Ribbon diagram of the structure of MYD88 and MYD88 variant 1. The location of the additional sequence is highlighted.

The insertion of the additional sequence results in an extended loop between the βC and αC region of the protein which lies within the TIR domain. This conformational change has the potential to affect either the interaction of the protein with the intracellular TIR domain of TLRs or the subsequent formation of the Myddosome complex. However, preservation of the

intermediate domain suggests that variant 1 should be able to activate downstream signalling via IRAK1 and 4, if its oligomerisation is unaffected. Preliminary data tentatively suggests that L273P-mutated *MYD88* v.1 does indeed activate NF-κB, but not to the same extent as MYD88[L265P] (luciferase reporter assay performed by C. Evans). The potential for existence of a mutated version of MYD88 that retains functional capacity but without the gain-of-function normally conferred by the mutation is intriguing but more investigation is required to determine the functional capacity of the protein.

7.8.7 Summary of major findings from RNA-sequencing

There is evidence of upregulation of multiple key pathways that play a role in WM pathogenesis, including activation of NF-κB, TNF and TLR signalling and upregulation of a wide variety of chemokines and cell adhesion molecules in WM samples cultured with both types of stimulation (table 7.5). WM cells demonstrate their clonality via the loss of Ig repertoire in comparison to the healthy samples. WM cells are activated with R848, upregulating multiple genes associated with activation that are shared with the healthy contingent and exhibit high levels of *TLR7* gene expression, although this might not reflect the expression *in situ* (figures 7.28 and 7.29).

In contrast to the healthy cells, the WM cells show some evidence of constrained plasma cell differentiation that is more profound subsequent to R848 stimulation than CD40L stimulation. This is not replicated in healthy cells, where there is no significant difference in gene expression between the two types of stimulation (table 7.5).

The unusual population of CD38$^-$ CD138$^+$ cells that appears to be restricted to B-cells derived from WM patients is accompanied by a significant downregulation of *CD38*. The levels of *CD38* expression correlate with the total proportion of the neoplastic clone and may be linked with the extent of plasma cell differentiation (table 7.6, figure 7.30).

Whilst a multitude of pathways essential for cell survival are profoundly affected in the R848-activated WM cells, there is little evidence to suggest significant upregulation of either pro-apoptotic or downregulation of pro-survival genes. These results are tempered by the fact that sequencing data from cells at day 6 might be too late a time point to detect an initiating pathway. However, it does appear that the bone marrow microenvironment is of critical importance to WM cells and the susceptibility to apoptosis following TLR7 stimulation may be linked to an absence of additional survival signals. This interpretation would also concur with the ability of CD40L to rescue R848 stimulated WM cells.

7.9   Discussion

In previous chapters, the *in vitro* differentiations were performed with total B-cells. The closest analogue of WM cells in healthy individuals are memory B-cells, which comprise a smaller percentage of total B-cells than the naïve fraction, so it was possible that any similarities between healthy memory cells and WM cells were being masked by the naïve population. Therefore, the response of both the memory and naïve B-cell subsets to stimulation with the TLR7 agonist were characterised to assess whether the response of WM cells to this type of stimulation could be recapitulated. As expected and in accordance with the literature (Bernasconi *et al.*, 2003; Simchoni and Cunningham-Rundles, 2015), memory B-cells exhibited a significantly greater proliferative response to R848 stimulation than their naïve counterparts and generated not only a greater number of plasma cells, but these cells survived far better than the plasma cells generated by the naïve fraction (figures 7.1 and 7.2). This demonstrates that the impaired plasma cell differentiation and cell death exhibited by the WM cells is not as a consequence of a deficient memory B-cell response to TLR agonism, but rather it must be attributed to another factor.

Another potential cause of the aberrant response of WM cells to R848 stimulation is the presence of MYD88^{L265P}. However, the sensitivity of WM cells to R848-induced cell death could not be replicated in either WM or DLBCL cell lines possessing the MYD88^{L265P} mutation (figure 7.3). Similarly, addition of a synthetic TLR9 agonist, CpG ODN 2006, did not induce cell death (figure 7.4). This demonstrates that the apoptosis of WM cells following TLR7 stimulation is not a result of the MYD88^{L265P} *per se*.

Since the cell death in the WM population did not appear to be as a consequence of either an aberrant response of memory-like cells or be the attributed solely to the MYD88^{L265P} mutation itself, another avenue of investigation was pursued – that of autocrine or paracrine secretion as a potential trigger for apoptosis. An example of this phenomenon has been established in CLL cells following treatment with various TLR9 agonists. In this instance, B-cells isolated from the peripheral blood of patients with CLL were cultured with either class A or class B CpG ODNs (Liang *et al.*, 2010). Class B compounds potently induced apoptosis in these cells through autocrine production of IL-10 and subsequent STAT1 phosphorylation resulting in the activation of multiple pro-apoptotic genes.

In the light of the results published by Liang and colleagues, the effect of the addition of supernatant taken from differentiating WM cells at various time points to healthy cells was investigated. The most significant effect of the addition of WM supernatant occurred in healthy

cells that were activated with R848 + F(ab')$_2$ anti-IgG/M. Supernatant derived from WM cells that have been stimulated with R848 did not result in either a decrease in cell number or a reduction in viability in healthy differentiating cells, even though the WM cells are undergoing high levels of cell death in this condition (figures 7.6 and 7.8). Surprisingly, healthy cells with the addition of supernatant from R848-stimulated WM cells proliferated to a greater extent than the control cells and demonstrated increased viability. The proportion of viable cells within the cultures was increased by approximately 30% in each donor (figures 7.6 and 7.8). Whilst this contributes to the elevated total cell counts, the difference between the viability of the control group and that of the cells following the addition of the supernatant is not sufficient to explain this fully, therefore these cells must also be proliferating to a greater extent.

The increase in cell number and viability were accompanied by phenotypic changes, with these cells exhibiting a delay in the acquisition of markers signifying a more mature phenotype (figures 7.7 and 7.9). This indicates that stimulation with R848 induces WM B-cells to secrete one or more factors that delay differentiation, resulting in the healthy cells remaining in a more highly proliferative state for longer and which is reflected in the alteration to the observed phenotype. Whilst the delay to differentiation may account for some of the increase in the viability of these cells, it seems likely that the WM cells are also producing factors to support cell survival.

An important caveat to consider when assessing these results is the potential impact of R848 carryover between the WM and healthy cultures. Residual R848 has previously been shown to affect both the cell number and phenotype in a similar manner to that which was observed here. However, the supernatant taken from the differentiating WM cells was diluted 10-fold in the final volume added to the healthy cells, reducing the concentration from 1µg/ml to 0.1µg/ml. Assessment of the effect of prolonged stimulation with 0.1µg/ml R848 demonstrated that this concentration had a negligible impact on cell number and phenotype. Therefore, the effect of the secreted factors by the WM cells may be augmented by the residual R848 within the supernatant, but this likely does not account for the majority of the observed effect.

A considerably more limited effect was observed for healthy cells that received CD40L activation. In this instance, the addition of the WM supernatant did not significantly increase cell number or viability (figures 7.6 and 7.8). However, the day 3 supernatant from both types of stimulation may result in an increase to cell numbers as these trend towards significance. Subtle changes in the phenotype were observed subsequent to the addition of R848 supernatant (figures 7.7 and 7.9).

Potential candidate factors that the WM cells could be secreting are the cytokines BAFF and APRIL. BAFF - B-cell activating factor - is a member of the tumour necrosis factor (TNF) ligand family and plays a key role in B-cell development; it promotes differentiation, enhancing both

survival and proliferation (Mackay *et al.*, 2003). BAFF is able to bind to three TNF receptors found on B-cells, with a different affinity for each. In order of decreasing affinity, these are; BAFF receptor (BAFF-R), transmembrane activator and calcium modulator and cyclophilin ligand interactor (TACI) and B-cell maturation antigen (BCMA) (Thompson *et al.*, 2001). A related TNF ligand APRIL (a proliferation-inducing ligand) is also able to bind both TACI and BCMA, but not BAFF-R (Marsters *et al.*, 2000). Both BAFF and APRIL are upregulated by B-cells subsequent to activation (He *et al.*, 2004a; Kern *et al.*, 2004; Chu *et al.*, 2007). Addition of BAFF to CD40L-stimulated B-cells by Do et al., resulted in reduced apoptosis within the *in vitro* cultures and correspondingly increased the total cell counts, similar to that which was observed here (Do *et al.*, 2000).

In support of this hypothesis, WM cells have been shown to express high levels of BAFF-R and serum BAFF levels are significantly higher in WM than healthy controls (Elsawa *et al.*, 2006). It is perhaps not surprising that the secretome of activated WM B-cells and plasmablasts appear to foster an environment that is conducive to cell proliferation and survival as this support would be advantageous to the neoplastic clone. What is unexpected is the production of these factors by WM cells subsequent to R848 stimulation, when the cells are in terminal decline, enhancing the proliferation of healthy cells (figures 7.6 and 7.8). It is clearly not sufficient to rescue the WM cells from apoptosis. It may be, therefore, that in a different context, such as when the WM cells are *in vivo* and in receipt of supplementary signals from the bone marrow microenvironment, TLR7 stimulation elicits the production of additional secretory factors that, in turn, facilitate enhanced growth and survival of the WM clone.

The culture conditions used within the *in vitro* system, whilst efficient at generating plasma cells and facilitating their survival for long periods, represent a simplified version of the true bone marrow niche. *In vivo*, B-cells located within this niche would be subject to a myriad of signals from the stromal microenvironment (Tripodo *et al.*, 2011; Wang and Wagers, 2011; Smith and Calvi, 2013). Of particular note, mast cells are frequently observed in close proximity to WM cells in the bone marrow and have been shown to regulate WM proliferation through expression of CD40L, BAFF, PDGF and VEGF (Tournilhac *et al.*, 2006). The addition of CD40L at the initiation of the *in vitro* culture rescued the WM cells from decline and enabled their successful proliferation and differentiation (figures 7.17-7.19). Activation of WM cells with CD40L and R848 resulted in a synergistic effect on cell number at day 6, with a greater number of cells generated than would occur simply by combining the numbers from each individual stimulation together (figure 7.17). In contrast, the dual stimulation resulted in an increase to cell number in only one of the healthy donors and this was an additive rather than a synergistic response (figure 7.15).

Whilst the addition of only one extra stimuli does not recapitulate the complexity of the true bone marrow microenvironment, the ability for supplementary signalling to alter the fate of WM cells so drastically highlights the importance of a combination of signals to the maintenance of these cells. It is suggestive that when WM cells are localised within the multicellular environment of the bone marrow, along with the milieu of additional secreted elements, further activating stimuli may result in a proliferative response. The fact that the combination of activating stimuli has a synergistic effect on the WM cells may reflect their increased propensity to proliferate *in vivo* over the population of wild-type cells.

7.9.1 TLR expression in patient samples

A further possible factor in the aberrant response of WM cells is the level of expression of TLR7. Results of RNA sequencing on WM cells and data from Staudt and colleagues and Wang et al., suggest that functionally intact TLR7 are required, but TLR protein expression has not been quantified in any of these studies (Lim *et al.*, 2013; Wang *et al.*, 2014; Hunter *et al.*, 2016). Therefore, expression of the three endosomal TLRs – 7,8 and 9 – were assessed on primary B-cells isolated from healthy individuals and from patients with a variety of lymphoproliferative disorders. Unfortunately, data on WM samples was limited due to the scarcity of samples.

Interestingly, the WM cell lines expressed all three endosomal TLRs at high levels (figure 7.21). The high expression in these cell lines may contribute to differences between the results of experiments with cell lines compared to those with primary cells. In the primary samples assessed here, TLR expression was quite variable between individuals, but in general, TLR9 was the most highly expressed, with TLR7 and 8 expression considerably lower (figures 7.21 and 7.22). The absence of LAIR1 expression can be used to distinguish the WM clone from the non-neoplastic fraction, so this was used to identify the two populations, if present. The second WM sample consisted of a very high proportion of neoplastic cells, but the first sample could be clearly separated into LAIR1$^+$ and LAIR1$^-$ populations. For both samples, the LAIR1$^-$ cells possessed low levels of TLR7 expression, whereas the LAIR1$^+$ population in the first sample demonstrated significant TLR7 expression (figures 7.21 and 7.22). Whilst the expression of TLR7 and 8 in the healthy samples in general was low, interestingly, the WM LAIR1$^-$ populations possessed the lowest MFI value for both TLR7 and TLR8.

Surprisingly, the RNA sequencing data revealed that *TLR7* was the most highly expressed TLR in both healthy and WM samples (figure 7.27), although its expression was considerably lower in one of the six WM samples than the rest. The disparity between the gene expression and protein expression (figures 7.21 and 7.22) implies that post-translational regulation is occurring. It

remains possible that WM cells downregulate TLR7 protein expression but conclusions are currently very tentative. Nevertheless, this remains an interesting prospect and requires further investigation to determine if this is the case.

7.9.2   Fas/FasL expression during the course of *in vitro* differentiations

The results from the supernatant experiments suggested that stimulation with R848 may induce overexpression of pro-apoptotic genes that overcome the autocrine pro-survival signalling. Fas and FasL are essential for the regulation of the immune response via activation induced cell death. Therefore the expression of Fas and its ligand on the cell surface of WM cells were assessed. Whilst both were considerably upregulated from their basal expression, as expected, there was no significant differences between the WM samples and the healthy controls (figure 7.14). Whilst activation primes WM cells for AICD, it is unlikely to be the root cause for the profound apoptotic response of these cells following stimulation with R848. The RNA sequencing data concurs with these findings, confirming that the samples possessed greater expression of *Fas* than *FasL* at day 6 of the differentiation, but that there was no difference in gene expression between the healthy and WM samples.

7.9.3   RNA sequencing

RNA sequencing was performed on samples taken during *in vitro* differentiations in order to address several key questions. These included the ascertainment of whether WM B-cells were receptive to activation signals from TLR7 ligation, if there was any variability between the expression of genes involved in plasma cell differentiation compared to healthy cells, whether the apoptotic response of the WM cohort to R848 stimulation be attributed to the dysregulation of a particular pathway and how these results integrate with other data presented here and the current literature.

The clonal nature of the WM samples was confirmed by the highly skewed Ig repertoire. Kriangkum et al., reported that the most frequent family usage at 74% was *IGHV3 (Kriangkum et al., 2004b)*. However, in the data presented here, virtually all of the *IGHV3* genes were downregulated. This may be because the cohort of patients assessed by Kriangkum is much larger than that which was analysed here. Also, it is possible that the pool of WM B-cells is indeed skewed towards *IGHV3* but that these cells either do not or are unable to differentiate and therefore do not contribute to the population of plasmablasts at day 6.

The sequencing data highlights the essential contribution of the bone marrow environment to the pathogenesis of WM. The elevated expression of multiple genes involved in the localisation

of WM cells to the bone marrow demonstrates their propensity to home in on this niche and remain within it (table 7.5). In addition to this, the WM cells significantly upregulate genes that are key for cell-cell interaction and appear to secrete factors that support B-cell survival. This indicates that the WM cells may exert an influence on their environment in order to foster their own survival advantage.

WM cells stimulated with R848 upregulated multiple genes associated with B-cell activation that were similarly upregulated in the healthy cohort, confirming that they are able to integrate the signal into a response. However, there does appear to be a block in WM plasma cell differentiation, suggestive of an uncoupling of the differentiation signal somewhere downstream of TLR activation (figure 7.28). WM cells stimulated with R848 demonstrated elevated levels of *IRF8*, *BACH2* and *SPI-B*, which repress B-cell differentiation, with a corresponding decrease in *IRF4* and *PRDM1* (figures 7.28 and 7.29). The interplay between these genes suggests that the WM cells may reach a plasmablast or pre-plasmablast stage but are thereafter unable to proceed. This concurs with the phenotypic data, whereby the small proportion of WM cells that are able to respond following activation with R848 are able to begin to downregulate CD20 and upregulate CD38 but fail to generate plasma cells.

Accordingly, Zhou *et al*. observed an increase in *SPI-B* and decrease in *POU2AF1* in CD19$^+$ cells isolated from WM patients compared to their healthy counterparts (Zhou *et al.*, 2014). An impediment to plasma cell differentiation in WM cells may serve to maintain the neoplastic B-cell pool, with a proportion of these cells undergoing differentiation following the receipt of a sufficiently potent stimuli.

The phenotypic rescue by supplementary stimulation with CD40L in WM cultures that would have otherwise succumbed to apoptosis and failed to differentiate following activation with R848 suggests that WM B-cells may require additional activation signals, such as the ligation of CD40L to successfully progress past the plasmablast stage. *In vivo*, this signal is likely to be provided by mast cells which aggregate with WM cells within the bone marrow, promoting the proliferation of the neoplastic clone (Tournilhac *et al.*, 2006). Furthermore, mast cells have been shown to upregulate CD40L in response to soluble CD27, which is elevated in the sera of WM patients (Ho *et al.*, 2008).

Even with sufficient prerequisite signalling, WM cells may not differentiate in the conventional manner *in vivo*, with an intermediate CD38$^-$ CD138$^+$ population generated subsequent to both CD40L and dual CD40L + R848 stimulation during *in vitro* experiments, although this remains to be further substantiated.

Assessment of *CD38* expression in the WM cohort was most intriguing. WM cells displayed significantly decreased *CD38* expression in comparison to the healthy cells and the extent of the decrease was highly correlated with proportion of neoplastic cells (figure 7.30). From this data, it is currently impossible to determine whether this downregulation is significant to WM pathogenesis or whether it is simply a collateral effect from disruption to a related pathway. What is clear however, is that it substantially influences the phenotype of the differentiating cells, with WM samples below a certain threshold of *CD38* expression generating the enigmatic CD38⁻ CD138⁺ population that was not observed in any other sample type. Further investigation into CD38 expression is warranted as this may influence the viability of treatment with anti-CD38 antibodies in patients with a high disease burden.

The sequencing data enabled investigation into the presence of a second isoform of *MYD88* within the samples (figure 7.31). MYD88 variant 1 possesses an identical amino acid sequence to the regular form of MYD88, but with the addition of an 8 amino acid insertion that elongates a loop between the β-sheet C and α-helix C region of the protein (figure 7.32). Surprisingly, *MYD88* v.1 was detected in all samples which had sufficient read depth. The presence of this isoform within cell lines or primary B-cells has not previously been documented, but it may represent a mechanism by which MYD88 signalling is regulated. Further investigation as to its function in both a wild-type and L273P-mutated context is required to provide insight as to its role. Nevertheless, the ability to favour the production of a less pathogenic isoform over another whilst retaining overall protein function is an exciting prospect. Advances in the development of antisense oligonucleotides to influence splicing is a promising avenue for new therapeutics and could have potential in WM (Garcia-Blanco *et al.*, 2004; Havens and Hastings, 2016).

7.9.4   Apoptosis in WM cells

Work published by Wang *et al.* indicated a role for TNFAIP3 in the regulation of proliferation in murine B-cells that were retrovirally transduced with MYD88^L256P (Wang *et al.*, 2014). They reported that activated B-cells transduced with mutant MYD88 underwent proliferation in the absence of additional mitogens, but that this was self-limiting due to the induction of a negative feedback loop that was at least partly due to increased levels of TNFAIP3. They also suggest that, in order to overcome this innate regulation, additional dysregulation of genes involved in apoptosis, such as those from the BCL2 family or BCL2 itself are likely to be involved (Wang *et al.*, 2014). Indeed, WM cell lines that do not possess mutations in CXCR4 or BTK - which normally contribute to resistance to Ibrutinib - appear to acquire drug resistance by upregulating BCL2 (Cao *et al.*, 2015; Paulus *et al.*, 2017a). The BCL2 inhibitor Venetoclax has demonstrated efficacy in a small number of patients with relapsed/refractory WM, although examination of BCL2

expression alone is insufficient to predict response (Davids *et al.*, 2017). BCL2 is upregulated in the WM samples compared to the healthy samples at day 6 of differentiation, although only by a very modest $\log_2$ fold increase of 1.2. Further investigation is required to determine the contribution of BCL2 or other BCL2-family proteins to WM cell survival.

The expression of *TNFAIP3* in the WM samples was assessed in order to determine if a similar situation as postulated by Wang and colleagues was occurring in the primary cells, thus resulting in cell death subsequent to activation. In contrast to their findings, *TNFAIP3* was not upregulated in the WM cells, nor were there any significant differences in apoptosis associated genes. There are several explanations for this, the first of which being that it may simply reflect the differences between murine and human B-cells. However, it seems more likely that simply transducing B-cells with the MYD88^{L265P} mutation does not sufficiently recapitulate the complexity of this neoplasm. This is supported by the data from Knittel et al., demonstrating that MYD88^{L265P} is insufficient to cause a WM-like phenotype in mice (Knittel *et al.*, 2016). It is also possible that the gene expression data presented here is capturing a time point that is too late to identify an upregulation of *TNFAIP3* that may have occurred rapidly following B-cell activation. Assessment of *TNFAIP3* expression at an earlier time point in the differentiation would enable a more definitive conclusion to be made.

WM cells stimulated with R848 do not appear to upregulate a significant number of either pro-apoptotic genes or downregulate pro-survival genes, despite a profound breakdown in many essential pathways (table 7.5). Interestingly, a similar result was reported by Gaudette and colleagues following analysis of a gene expression database containing samples from WM, CLL, MM as well as healthy B-cells and plasma cells (Gaudette *et al.*, 2016). A comparison of WM cells to the other groups demonstrated that WM cells, similarly to healthy plasma cells, express low levels of both pro- and anti-apoptotic genes. In the light of the constitutively active NF-κB signalling responsible for the survival advantage of the neoplastic clone, they proposed a threshold model to explain the resistance to the induction of apoptosis in WM cells. They postulate that WM cells are resistant to apoptosis, not via the additional overexpression of anti-apoptotic genes, but rather by low expression of members of the pro-apoptotic Bcl2 family, creating a requirement for high levels of pro-apoptotic signalling to initiate cell death.

In accordance with this, the WM gene expression data indicates that these cells express Bcl2 family members such as *BAD*, *BAX*, *BIM* at similar levels to the healthy controls and that *BCL2* itself is not differentially expressed. Whilst the analysis by Gaudette *et al*. involves some data from cell lines that are not necessary representative of primary WM cells, the data generated from primary cells is consistent with the findings reported here.

Whilst the expression of both pro- and anti-apoptotic genes is low in WM cells, they appear to maintain their existence by a combination of constitutive activation of NF-κB, autocrine signalling and support from other cells within the bone marrow microenvironment. In this instance, the scales are firmly weighted towards the survival advantage of the neoplastic clone over the wild-type population. However, in the absence of additional signals, WM cells are more delicately balanced at a point between survival and apoptosis. It would appear therefore that stimulation with CD40L serves to tip the balance one way – towards proliferation, and that TLR7 stimulation tips the scales in the other direction, resulting in WM cell death.

Chapter 8 – Discussion

8.1 Feasibility of the *in vitro* system to model B-cell differentiation in Waldenström macroglobulinemia

The ability of the *in vitro* system to model WM B-cell differentiation was validated in comparison to healthy cells. The stimuli used initially were CD40L and F(ab')$_2$ anti-IgG/M, a combination which mimics T-cell dependent activation. The inclusion of F(ab')$_2$ anti-IgG/M was not required by either naïve or memory cells from healthy donors to generate plasma cells, although its omission resulted in a delay to differentiation (figure 3.6). In contrast, CD40L stimulation was essential for both cell survival and plasma cell generation (figures 3.8 and 3.9). The synergism between BCR and CD40L signalling is well established (Bishop *et al.*, 1995; Haxhinasto *et al.*, 2002; Haxhinasto and Bishop, 2004). However, when the BCR is ligated in the absence of a second signal, B-cells are primed to undergo activation-induced cell death to prevent autoimmunity and this appears to be recapitulated within the *in vitro* system (Lagresle *et al.*, 1996; Rathmell *et al.*, 1996).

Stimulation of B-cells isolated from the bone marrow of WM patients in a T-dependent manner generated plasma cells that were phenotypically identical to those from healthy individuals (figure 3.10). In contrast to healthy individuals however, approximately half of the WM samples generated a fraction of CD138$^+$ cells without prior upregulation of CD38, which will be discussed further (figure 3.12). The MYD88^{L265P} mutated fraction of WM cells continued to be present within the *in vitro* cultures to at least day 6, as confirmed by RNA sequencing and contributed to the observed phenotype.

Whilst WM cells generate plasma cells within the same time frame as healthy cells, they did not proliferate to the same extent as cells from healthy individuals (figure 3.11). It is worth noting that the viability of the isolated B-cells from samples of BM were affected by the length of time they were in storage. This resulted in a decrease in cell number between day 0 and day 3 of the differentiation that was not observed in the healthy controls, which were prepared within 24 hours of sample collection. Nevertheless, the magnitude of the proliferation between day 3 and day 6 in most WM samples was less than that observed for healthy cells. This may indicate that the WM cells require a further extracellular signalling component for optimal proliferation that is not being provided in the *in vitro* conditions used.

In comparison to healthy cells, a proportion of WM B-cells exhibited an impairment to CD20 downregulation following stimulation with CD40L + F(ab')$_2$ anti-IgG/M (figure 3.12). CXCR4 signalling is involved in the regulation of CD20 surface expression, with SDF-1 treatment increasing CD20 in CLL cells (Burger and Kipps, 2006; Pavlasova *et al.*, 2015; Pavlasova *et al.*, 2016). On the surface of mature B-cells, CD20 associates with the BCR in lipid rafts (Petrie and Deans, 2002; Polyak *et al.*, 2008). Chronic active BCR signalling is thought to play a role in WM (Ciric *et al.*, 2001; Argyropoulos *et al.*, 2016; Munshi *et al.*, 2017). However, the frequency of mutations within the BCR signalling cascade in WM appears to be limited to a small subset of patients, with an incidence of approximately 15% reported (Poulain *et al.*, 2013; Varettoni *et al.*, 2013). Nonetheless, preservation of the structure of surface IgM within the neoplastic clone and upregulation of basal levels of phosphorylation within the BCR signalling cascade indicates that a functional BCR is important for WM cells (Ciric *et al.*, 2001). Complete activation of B-cells subsequent to BCR ligation is dependent on an increase in cytoplasmic free calcium, initially from intracellular stores, but following their depletion there is an influx of extracellular calcium, facilitated by CD20 which acts as a store-operated cation channel (Li *et al.*, 2003). Intact BCR signalling is required for this process as CD20 is thought to co-opt components of the pathway to facilitate calcium influx (Walshe *et al.*, 2008). Retention of CD20 on the surface of WM cells may therefore serve to sustain their activation in concert with chronic active BCR signalling.

Analysis of the phenotype of isolated WM B-cells revealed that the expression of CD27 was lower than healthy controls. Initially, this appears to be at odds with the literature, as WM cells are thought to derive from a memory B-cell origin, which is classically identified by expression of CD27 (Agematsu *et al.*, 1997; Klein *et al.*, 1998; Tangye *et al.*, 1998; Agematsu *et al.*, 2000; Sahota *et al.*, 2002). However the incidence of CD27 negativity in WM cells has been established by multiple groups and is now generally accepted (Kriangkum *et al.*, 2004b; Babbage *et al.*, 2007; Sahota *et al.*, 2009; García-Sanz *et al.*, 2016). The absence of CD27 on WM cells may be due to shedding throughout disease advancement in a similar manner to multiple myeloma or derivation from a CD27$^-$ precursor, although a definitive conclusion has yet to be reached (Moreau *et al.*, 2006; Babbage *et al.*, 2007; Sahota *et al.*, 2009). Despite low initial expression of CD27, the upregulation of this marker appears unaffected in WM cells.

The *in vitro* system provides a unique opportunity to analyse WM cells in the process of differentiation. The robustness of this model has been confirmed by the uniformity of differentiation in healthy samples (figure 3.5) and conversely, samples from lymphoproliferative disorders determine that it does not confer the ability to differentiate on cells which would be unable to do so *in vivo* (figure 5.1). Validation of this model demonstrates that WM cells are successfully able to generate plasma cells following stimuli that mimic T-cell dependent

activation (figure 3.12). Cell lines lose the flexibility of WM primary cells to differentiate, a feature crucial for WM pathogenesis. The capacity of this model system to retain WM plasticity provides a valuable tool that complements current work with WM cell lines. Whilst a mouse model bearing a B-cell mutation orthologous to MYD88^{L265P} has been developed fairly recently, it does not recapitulate WM, confirming that the presence of this mutation alone is insufficient to accurately model this neoplasm (Knittel *et al.*, 2016).

8.2   CD38 expression in WM cells

A novel feature of differentiating WM cells was the generation of an unusual population of CD38$^-$ CD138$^+$ cells. This occurred in over 40% of differentiations with WM cells stimulated with CD40L (figure 3.12). In each instance, the population arose between day 6 and day 13. It was initially unclear as to whether this population represented an alternate plasmablast-like intermediate or a fully-fledged CD38$^-$ plasma cell population. The relationship between these cells to the other phenotypic fractions within the WM samples and to populations within healthy cultures by the SPADE algorithm suggests that these cells are more similar to fully differentiated plasma cells or at the very least plasmablasts on the cusp of becoming plasma cells, than traditional CD38$^+$ CD138$^-$ plasmablasts (figure 6.14). The expression of the other phenotypic markers assayed was unaffected in this unusual population of cells and they did not assist in predicting the appearance of the CD38$^-$ CD138$^+$ fraction. The best predictor of the CD38$^-$ CD138$^+$ population was CD38 expression at day 0 and day 6 of differentiation. Samples that generated CD38$^-$ CD138$^+$ cells demonstrated very low levels of expression of CD38 following B-cell isolation which did not increase to day 6, in contrast to the WM samples that did not produce this population, which expressed significantly higher levels of CD38 at this time point (figure 3.17).

The presence of this population was not detected in WM cells following stimulation with the TLR7 agonist R848 (figure 4.14). The samples with the highest proportion of neoplastic cells displayed an inability to differentiate, coupled with induction of a profound apoptotic response and thus these cells are eliminated (figure 4.12). This fraction may be particularly susceptible to apoptosis in the absence of the correct survival signals. In contrast, the proportion of CD38$^-$ CD138$^+$ cells in SchS samples increased in R848-stimulated cells following omission of F(ab')$_2$ anti-IgG/M (figure 5.15). CD38 and the BCR co-localise within lipid rafts and thus BCR stimulation may modulate CD38 surface expression (Lund *et al.*, 1996; Deaglio *et al.*, 2003; Malavasi *et al.*, 2008). The extent of ligation of the BCR may therefore influence the fate of these cells to become either traditional CD38$^+$ CD138$^+$ plasma cells or for them to adopt a CD38$^-$ CD138$^+$ phenotype.

CD38 was highly differentially expressed between WM and healthy individuals, with a significant downregulation of CD38 in WM cells. Fascinatingly, CD38 expression was very highly inversely correlated with the proportion of neoplastic B-cells within the bone marrow of these patients (figure 7.30). There appears to be a threshold of CD38 expression below which results in the generation of CD38$^-$ CD138$^+$ cells. Further investigation of this population is required in order to determine whether its presence is due to the influence of selective pressure or if it is a symptom of an underlying dysregulation to transcriptional regulation. The occurrence of this population in cells derived from Schnitzler syndrome patients could prove to be extremely helpful in determining the underlying cause of CD38 downregulation due to the different mutational burden in these cells.

The relative presence of CD38 on WM cells is likely to influence treatment decisions in the future. The CD38 monoclonal antibody Daratumumab is currently undergoing phase II trials in WM in combination with Ibrutinib (Trial number NCT03187262) but the results are as yet unpublished. Research into the efficacy of Daratumumab in WM has been carried out by Paulus and colleagues, however much of the analysis has been done in cell lines and this may not reflect the reality *in vivo* (Paulus *et al.*, 2016; Paulus *et al.*, 2017b; Paulus *et al.*, 2018). Expression of CD38 on the three most characterised WM cell lines is high but varies considerably, at 99.5%, 91.5% and 44.4% for RPCI-WM1, MWCL-1 and BCWM-1, respectively (Paulus *et al.*, 2015). The authors sought to confirm CD38 expression levels in primary cells and whilst they concluded that expression was similar to that of the cell lines, they only analysed two samples. Considerably more substantive prior reports on the phenotype of primary WM cells indicate that *in vivo* expression of CD38 is most likely lower than that suggested by Paulus et al. A large study conducted in 2001 analysing the bone marrow of over 100 patients identified CD38 expression in 37.8% in WM B-cells, with positivity defined as the presence of the marker in 50% of cells or above (Barrans *et al.*, 2001). Konoplev *et al.* subsequently reported CD38 expression in 48% of WM samples, with a cut-off of more than 20% defining antigen positivity (Konoplev *et al.*, 2005).

CD38 downregulation has been reported in patients with multiple myeloma following treatment with Daratumumab and there is evidence of a similar effect occurring in WM cell lines (Ise *et al.*, 2016; Nijhof *et al.*, 2016; Paulus *et al.*, 2016; Minarik *et al.*, 2017). The propensity of WM cells to downregulate CD38 to an increasingly greater extent as the proportion of neoplastic clone increases is of serious concern with regards to the efficacy of treatment with anti-CD38 antibodies. If anti-CD38 antibodies are approved for treatment of WM, inclusion of CD38 as standard in flow cytometry phenotyping panels may serve to identify patients that would respond best and also enable monitoring of CD38 expression during treatment to detect downregulation.

Intriguingly, analysis via viSNE and SPADE suggest that a precursor to the CD38⁻ CD138⁺ cells may exist in healthy individuals (figure 6.6). This population of cells exhibit a slightly delayed differentiation response in comparison to their peers. However, instead of failing to upregulate CD38, these cells differentiate into plasma cells that express an intermediate level of both CD38 and CD138. If a link between a potential precursor healthy population to the CD38⁻ CD138⁺ cells could be established it may provide insight to the molecular mechanisms behind its appearance in WM and SchS cells.

8.3 MYD88 isoforms

MYD88 has multiple isoforms but their expression and function within B-cells remains largely unexplored. An isoform of particular interest is in the context of WM is MYD88 variant 1, which shares the sequence of the regular form of MYD88, apart from the addition of 8 amino acids within the TIR domain due to alternate splicing of exons 3 and 4. MYD88 v.1 therefore can possess the same leucine to proline mutation as the regular form of MYD88, but it occurs after the inserted sequence, at position L273P instead. The additional sequence alters the conformation of the TIR domain, extending a loop between the third α-helix and β-sheet of the protein and as such potentially alters the kinetics of Myddosome formation. MYD88 v.1 was found to be present in both primary cells derived from healthy donors, WM and SchS patients as well as a variety of cell lines.

The presence of this isoform in such a high proportion of samples suggests that it may have a regulatory role. A precedent for this has been established for a different MYD88 isoform, MYD88$_S$ (Burns *et al.*, 2003; Janssens *et al.*, 2003). MYD88$_S$ lacks an intermediate domain due to exon 2 being skipped during splicing and regulates signalling in a dominant-negative manner by undergoing oligomerisation with the regular form of MYD88 but preventing subsequent activation of the IRAKs. Indeed, the therapeutic possibilities of skewing splicing to favour MYD88$_S$ over the regular form are under investigation (Vickers *et al.*, 2006; Janssen and Alper).

The possibility that MYD88 v.1 normally acts in a regulatory capacity raises the question as to what happens when it is mutated, as is likely the case in the highly clonal WM samples. Preliminary research suggests that L273P-mutated MYD88 v.1 retains its function as an adaptor for TLR signalling but is unable to constitutively activate NF-κB in an analogous manner to MYD88^{L265P}. Further investigation as to the function of this isoform in both healthy and WM cells is warranted in order to determine whether it does indeed regulate TLR signalling and what, if any, are the effects of the MYD88^{L273P} mutation. Characterisation of MYD88 isoforms in primary

cells may aid our understanding of the regulation of TLR signalling and manipulation of MYD88 splicing could present a new avenue for WM treatment in the future.

8.4   T-independent stimulation of healthy B-cells

There was remarkable uniformity in the phenotypes obtained from day 13 onwards for R848- and CD40L-stimulated healthy cells within the *in vitro* system, despite the contrasting modes of activation (figures 3.5 and 4.9). The similarity between the response of primary B-cells elicited by R848 stimulation to that of CD40L has been remarked upon previously within the published literature (Bishop *et al.*, 2001). The phenotypes of differentiating cells from multiple donors were visualised using viSNE and SPADE. These confirm that the phenotypes are very similar between the two types of stimulation but with the CD40L-stimulated cohort lagging slightly behind prior to day 13 (figure 6.13). It is notable from the RNA sequencing data of day 6 cells that there were no specific pathways upregulated in R848-stimulated healthy cells compared to their CD40L-stimulated counterparts (table 7.5). Whilst there were differences in the downregulated pathways, these were almost all associated with metabolism and not with B-cell activation or plasma cell differentiation, consistent with the observed phenotype.

Stimulation of total B-cells with TLR agonists preferentially expands the subset of memory B-cells due to their greater expression of TLRs, including TLR7, in comparison to naïve cells (Hornung *et al.*, 2002; Bernasconi *et al.*, 2003; Simchoni and Cunningham-Rundles, 2015). The heightened responsiveness of memory cells to TLR7 stimulation is reflected in the generation of a small CD38$^+$ CD138$^+$ plasma cell component as early as day 6 in the *in vitro* culture system (figure 7.2). Interestingly, samples of both peripheral blood and staging marrows from healthy individuals all shared a similar feature – that of a small proportion of cells expressing much greater levels of TLR7 and 8 than the rest of the population (figures 7.21 and 7.22). It seems likely that these are the subset of cells that are particularly sensitive to TLR stimulation and generate plasma cells by day 6 of culture.

The most significant difference between the two types of stimulation in healthy cells was the total expansion in cell number in the cultures as a whole. To establish the response of healthy cells, total B-cells were used, both to facilitate comparison to CD40L activation and to provide a greater number of cells for downstream analysis. The uniformity of response of memory and naïve B-cells alike to CD40L and IL-21 was reported by Simchoni & Cunningham-Rundles, in addition to their observations that agonists to TLR7 or 9 only induced a proliferative response in IgM$^+$ CD27$^+$ fraction (Simchoni and Cunningham-Rundles, 2015). The uneven response of the two subsets provides the most likely explanation for the observation of decreased numbers of

cells within the R848 cultures. Nevertheless, whilst the number of plasma cells generated per input cell was slightly lower for cells cultured with R848 + F(ab')$_2$ anti-IgG/M compared to cells activated with CD40L, their longevity appeared to be identical (figures 3.4 and 4.8).

In vivo, B-cells do not receive activation signals in isolation. Indeed, co-operation between BCR and TLR signalling enhances the ability of B-cells to respond to pathogens, such as BCR ligation facilitating the upregulation of TLR9 expression in naïve cells (Coutinho *et al.*, 1974; Leadbetter *et al.*, 2002; Bernasconi *et al.*, 2003). The synergism between the BCR and TLR7 became clear following omission of F(ab')$_2$ anti-IgG/M from the cultures, as this rendered a proportion of cells completely unresponsive to TLR ligation (figure 4.5). This implies that stimulation of the BCR can upregulate TLR7 in an analogous manner to that which was observed by Bernasconi and colleagues for TLR9 (Bernasconi *et al.*, 2003). Synergism between R848 and BCR signalling has been demonstrated in the Ramos B-cell line by Bishop and colleagues (Bishop *et al.*, 2001). Indeed, cooperation of TLR7 stimulation with a combination of CD40L and BCR signalling was also identified (Bishop *et al.*, 2001). Evidence of synergism between CD40L and TLR7 was observed in WM cells, with this combination of stimuli overcoming the negative effect of dual TLR7 and BCR activation and resulting in a greater number of cells than was generated by CD40L and BCR stimulation (figures 7.17 and 7.18). This effect did not appear to occur in cells from the healthy cohort, although this may be due to the CD40L stimulation eliciting a close to maximal proliferative effect within this population, preventing the detection of a synergistic response (figure 7.15).

Another aspect of TLR regulation became evident following dose response experiments. The presence of residual R848 within the culture media after day 3 resulted in a delay in the acquisition of a plasmablast phenotype (figure 4.2). A state of tolerance in myeloid cells defined as temporary hyporesponsiveness induced by repeated or chronic stimulation through the same or different TLRs (Broad *et al.*, 2006; Biswas and Lopez-Collazo, 2009). Prolonged TLR stimulation, for time periods of greater than 12 hours, results in tolerance and impairments to the NF-κB and MAPK signalling pathways in murine naïve splenic B-cells (Poovassery *et al.*, 2009). However, ligation of both TLR7 and the BCR simultaneously is able to both prevent B-cells from becoming refractory to TLR signal and also overcome a state of tolerance induced by prior TLR stimulation (Poovassery *et al.*, 2009). Residual R848 within the media therefore appears to induce tolerance within the B-cell population. This was resolved by adding an additional wash step to further dilute any remaining R848 but underscores the sensitivity of the cells to this type of stimulation.

In conclusion, both types of stimulation induce plasma cell differentiation, with no significant differences in the expression of essential regulatory genes involved in the differentiation

pathway. Despite some variation in the responsiveness of the B-cell population to each stimuli and limited temporal differences, B-cells from healthy individuals ultimately generate a population of phenotypically identical plasma cells with equivalent longevity in response to activation with either stimuli.

8.5   Response of WM cells to TLR7 and BCR stimulation

8.5.1   Cell death in WM cells activated with R848

Research undertaken by two different groups suggested that MYD88[L265P] cells still require TLR signals for proliferation and their continued survival (Lim *et al.*, 2013; Wang *et al.*, 2014). The effect of TLR7 stimulation on WM cells was therefore assessed in order to determine if this was indeed the case. In contrast to the expectation of enhanced survival, WM cells exhibited a profoundly deleterious response to R848 + F(ab')$_2$ anti-IgG/M stimulation, with a sharp decline in population from the initiation of culture and a failure to generate plasma cells.

To confirm that the WM response to TLR7 ligation was not as a consequence of the MYD88[L265P] mutation *per se*, the response of WM and ABC DLBCL cell lines bearing this mutation to the addition of TLR agonists was investigated. Stimulation of these cells with R848 or CpG had no negative impact on growth and survival which also remained unchanged when a combination of both TLR agonist and BCR ligation were used to replicate the conditions in the *in vitro* system (figures 7.3 and 7.4).

Memory B-cells in healthy individuals represent the closest analogue to WM cells, but they comprise a smaller proportion of total B-cells within the peripheral blood, at approximately 30%, than the naïve fraction (Sahota *et al.*, 2002; Sahota *et al.*, 2009; Perez-Andres *et al.*, 2010; García-Sanz *et al.*, 2016). It was therefore possible that the ratio of naïve to memory cells obtained in control samples was obscuring an equivalent response to that of the WM cells in the memory subset. The response of each fraction to TLR stimulation had not been previously characterised within the *in vitro* system so they were isolated and cultured concurrently.

As anticipated, TLR stimulation resulted in the preferential expansion of the memory B-cell subset (figure 7.1), in accordance with data published by other groups (Bernasconi *et al.*, 2003; Simchoni and Cunningham-Rundles, 2015). Despite the diminished proliferation from the naïve cells, they exhibited an equivalent phenotype from day 6 onwards to the memory cells (figure 7.2). Comparisons of the phenotype between differentiations with total B-cells stimulated with either CD40L or R848 + F(ab')$_2$ anti-IgG/M have been made throughout this report and these results confirm that the ratio of naïve to memory cells does not skew the phenotypic

observations. The aberrant response of WM cells does not result from their being more like memory B-cells and thus must be due to another factor.

It would be interesting to identify whether the negative response of WM cells was restricted to stimulation of TLR7. Substitution of R848 for the TLR9 agonist CpG ODN 2006 at a range of concentrations informed by the literature was trialled in healthy cells. However, cells from these individuals failed to proliferate and whilst there was evidence of differentiation, there were too few cells to enable analysis. TLR9 stimulation was discontinued as R848 proved to be considerably more efficacious at inducing B-cell proliferation and generating long-lived plasma cells. Various different groups initially claimed to generate plasma cells from primary human B-cells with CpG ODN 2006, but used CD38 expression as a surrogate plasma cell marker, rather than CD138 (Bernasconi *et al.*, 2002; Poeck *et al.*, 2004). Subsequently, optimised culture conditions have been proposed, with improved validation of plasma cells (He *et al.*, 2004b; Huggins *et al.*, 2006; Capolunghi *et al.*, 2008). Despite this, none of these groups appear to generate cells that were truly long-lived, with plasma cell characterisation occurring no later than day 11 (Huggins *et al.*, 2006). Optimisation of the culture conditions within the *in vitro* system for activation with CpG would enable the response of WM and healthy cells to this stimuli to be assessed.

A new publication from the Staudt lab offers another perspective on the mechanism of MYD88^{L265P}-mediated survival (Phelan *et al.*, 2018). The findings suggest that TLR9, rather than TLR7, may be required for a novel pro-survival signalling complex that assembles in the endolysosome, linking the BCR, TLR9 and MYD88, which has been termed the My-T-BCR complex. In this instance, signalling through TLR9 itself is not occurring, rather it acts like a scaffold, facilitating the formation of the supercomplex. BCR-dependent ABC DLBCL cell lines required the formation of this complex for their survival.

The authors extended the study to examine two WM cell lines and a small number of primary WM samples. Whilst RPCI-WM1 exhibited cytotoxicity in response to TLR9 shRNA, it had no effect on MWCL.1 and patient samples display little to no evidence of the formation of the My-T-BCR complex (Phelan *et al.*, 2018). An explanation for the importance of this mechanism in this cell line may derive from differences in TLR expression in comparison to primary samples. Whilst quantification of TLR7, 8 and 9 was not performed on RPCI-WM1 cells, BCWM.1 and MWCL.1 expressed substantially higher levels of TLR9 in comparison to WM or healthy samples and one would expect RPCI-WM1 to be similar.

This research does however provide insight into the findings published by Lim and Wang, suggesting that intact TLR signalling is required in MYD88-mutated cells (Lim *et al.*, 2013; Wang *et al.*, 2014). In the first study, depletion of proteins essential for endosomal TLR trafficking was

lethal for ABC DLBCL lines, as was the use of inhibitory oligonucleotides against TLR9 (Lim *et al.*, 2013). Reliance of ABC DLBCL cell lines on the My-T-BCR complex provides a mechanistic explanation for these results (Phelan *et al.*, 2018). Similarly, this complex may play a role in the findings by Wang et al, since both Unc93b1 mutations and TLR9 deficiency resulted in an inhibition of proliferation in MYD88-mutated murine B-cells (Wang *et al.*, 2014). It did not however, result in apoptosis of these cells and they remained able to proliferate, suggesting that these cells do not solely rely on the complex for survival. The transduction of MYD88^{L265P} into murine splenic B-cells most likely resulted in a population that more closely resembles ABC DLBCL rather than WM, akin to that generated by Knittel *et al*. (Knittel *et al.*, 2016). This explains the differences observed by these groups to that of the primary cells studied here.

The mutational burden in ABC DLBCL is very different to that of WM, with a hallmark of chronic active BCR signalling that is much less common in WM (Pasqualucci, 2013; Young *et al.*, 2015). In light of this evidence, it seems unlikely that the My-T-BCR complex is of critical importance in WM, although it may play a more substantial role in the rare cases of co-occurrence of MYD88 and BCR mutations.

Despite the considerable levels of apoptosis occurring within the WM population, there was no evidence of the upregulation of pro-apoptotic genes or conversely, downregulation of pro-survival genes (table 7.5). This may be due to the RNA sequencing representing a time point that is too far past the induction of these pathways. Whilst this appears to preclude the identification of any primary cascade that initiates WM cell death, it may also provide an alternate explanation as to the events that are occurring. Characterisation of BCL-2 family gene expression in WM cells in comparison to healthy B- or plasma cells and with other B-cell malignancies indicated that WM cells possess low levels of pro- and anti-apoptotic gene expression, similar to healthy plasma cells (Gaudette *et al.*, 2016). Thus the results of the RNA sequencing presented here may actually reflect innately low levels of both pro-survival and pro-apoptotic genes within the WM population. This appears to facilitate WM survival by increasing the threshold for WM apoptosis, due to low levels of apoptotic proteins (Gaudette *et al.*, 2016). WM cells may therefore rely less on intrinsic signalling, possessing a high threshold for apoptosis and are provided with additional support by the components of the bone marrow. The bone marrow microenvironment is vital to maintain plasma cells and forms an essential niche for WM cells that provides a myriad of survival signals which will be discussed subsequently in more detail (Ngo *et al.*, 2008; Elsawa *et al.*, 2011; Tangye, 2011; Jalali *et al.*, 2018).

8.5.2   Impaired PC differentiation

The apoptotic response of WM cells following R848 stimulation is rapid, thus appearing to preclude the generation of a plasma cell population simply because of the fact that the cells have been eliminated by the time point prior to that at which plasma cells would be generated. However, there may be a link between impaired differentiation and the lack of survival of these cells.

RNA sequencing has established that WM cells are able to be activated by a combination of TLR7 and BCR signalling, yet the majority of these cells are unable to generate a plasma cell population (figure 7.26). This implies that there is a failure of downstream signalling to integrate the activation signal with the plasma cell differentiation pathway (figure 8.1). In support of this, multiple essential regulators of plasma cell differentiation appear to be dysregulated in WM cells stimulated with the TLR7 agonist (figure 7.28). Central to differentiation is *PRDM1*, encoding BLIMP-1, termed the master regulator of plasma cell differentiation due to its essential nature for this process. RNA sequencing data confirmed that both *IRF4* and *PRDM1* were significantly downregulated in WM cells stimulated with R848, whilst suppressors of these transcription factors such as *SPI-B*, *BACH2* and *MITF* were significantly upregulated (figure 7.28). This provides a molecular explanation for the failure of R848-stimulated WM cells to generate plasma cells, despite retaining the capacity to do so following CD40L stimulation.
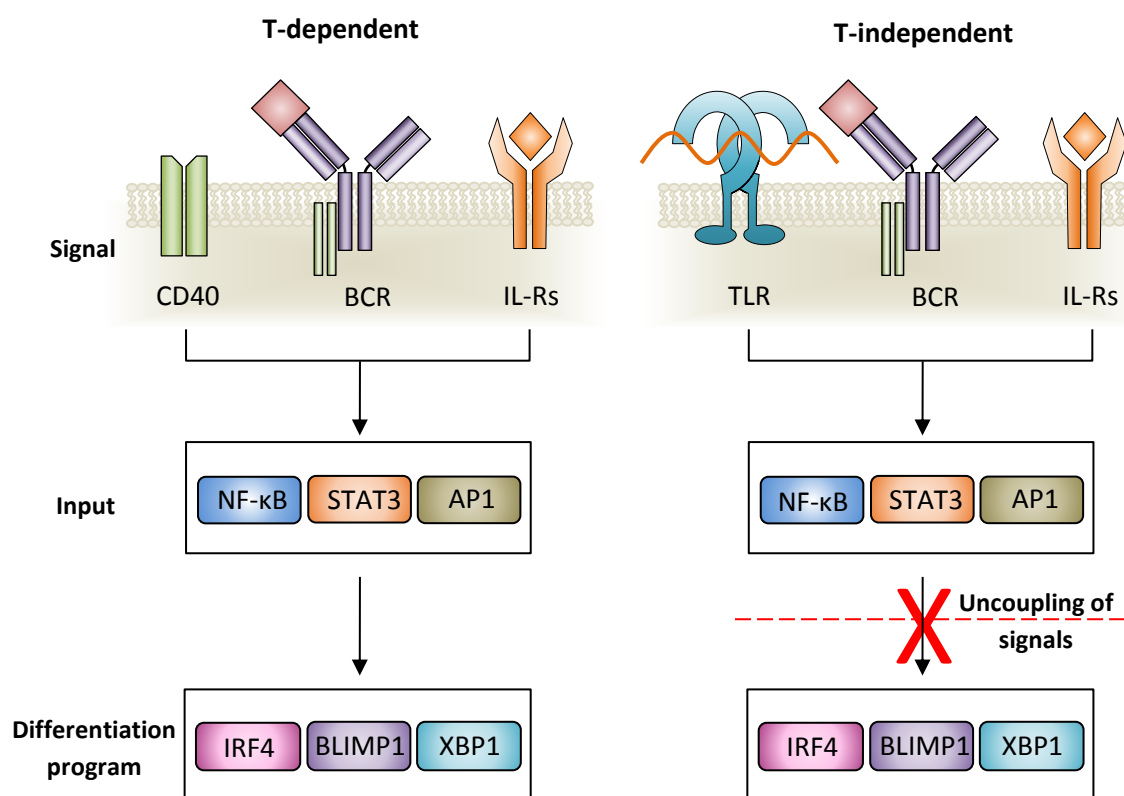
Figure 8.1 Failure to induce the plasma cell differentiation program subsequent to stimuli mimicking T-independent activation may be due to uncoupling of the signalling pathway. WM cells successfully initiate plasma cell differentiation subsequent to stimulation with CD40L and antigen to the BCR. In contrast, WM cells are receptive to an activation signal from a combination of TLR7 and BCR ligation but fail to integrate this fully with plasma cell differentiation.

B-cells unable to differentiate in response to binding of their cognate antigen either become anergic or undergo apoptosis to limit autoreactivity (Donjerković and Scott, 2000; Strasser and Bouillet, 2003; Yarkoni *et al.*, 2010). Activation induced cell death is an essential regulatory mechanism to control B-cell responses (Green and Scott, 1994; Rothstein, 1996). Upregulation of Fas and FasL following receptor ligation render B-cells susceptible to activation induced cell death, but simultaneous ligation of the BCR and CD40 serve to protect the cells from apoptosis (Rothstein *et al.*, 1995; Schattner *et al.*, 1995). The expression of these proteins was therefore assayed on both healthy and WM cells subsequent to activation with CD40L or R848 to determine whether if this was a likely cause of cell death. Whilst expression of both Fas and FasL rose substantially following activation, there was no significant difference between healthy and WM cells, supported by the RNA sequencing data (figure 7.14). Thus the mechanism behind the apoptosis observed in WM cells does not appear to be via activation-induced cell death.

It is possible that additional TLR7 stimulation, on top of the innate activation of the TLR pathway via MYD88[L265P] in WM cells is inducing tolerance, rendering them unable to progress further down the differentiation pathway once they have been activated. However, since the cells are also in receipt of a concomitant BCR signal, this should be sufficient to overcome any potential refractory state (Poovassery *et al.*, 2009). Addition of CD40L to TLR7 and BCR signalling rescued the cells from an apoptotic fate and enabled them to successfully undergo differentiation (figures 7.17-7.19). The synergism between these signalling cascades in WM but not in healthy cells suggests that the neoplastic clone may take advantage of multiple activation signals within the local environment.

There appears to be a link between the failure of WM cells to undergo plasma cell differentiation and the cell death that occurs within the population. RNA sequencing identifies a lack of expression of *PRDM1* following stimulation of TLR7 and the BCR as the likely central cause (figure 7.28). This suggests that there is an uncoupling of the differentiation pathway downstream of TLR7, however the point at which the signal fails to be propagated further has not been identified. Since constitutive activation of NF-κB is intrinsic to WM cells, it may be beneficial for these cells to remain at an earlier, highly proliferative stage of differentiation, refractory to differentiation with additional TLR stimulation.

8.6 SMZL and Schnitzler's syndrome B-cells

8.6.1 Response of SMZL cells

WM and SMZL share a similar clinical presentation, with patients presenting with IgM paraprotein, splenomegaly and cold agglutinin disease, making differential diagnoses challenging (Thieblemont *et al.*, 2002; Owen *et al.*, 2003). SMZL cells, akin to those from WM, retain the capacity to differentiate in a large proportion of cases (Van Huyen *et al.*, 2000; Dufresne *et al.*, 2010). Similarly, dysregulation of the NF-κB pathway is commonly affected in SMZL cells (Arcaini *et al.*, 2016). But, in contrast to WM, the prevalence of MYD88[L265P] mutation is only ~10% (Varettoni *et al.*, 2013).

SMZL B-cells displayed a range of differentiation capabilities in response to stimulation with CD40L + F(ab')$_2$ anti-IgG/M (figure 5.1), in contrast to WM, where the response of multiple samples generated a uniform phenotype (figure 3.12). WM cells demonstrated greater efficiency generating plasma cells, differentiating more swiftly and producing a greater proportion of plasma cells (figure 3.12). Interestingly, there was an overlap in the B-cell phenotype of WM and SMZL cells that became clear following visualisation by SPADE clustering. Whilst all the B-cells from healthy donors clustered into one of three groups – naïve, memory or

CD38$^+$ B-cells – a large proportion of cells from both SMZL and WM were clustered together in a separate "neoplastic" group that was not populated at all by the healthy samples (6.16). Subsequently, SMZL and WM samples generated distinct populations from one another as differentiation progressed, with no instances of CD38$^-$ CD138$^+$ cells in any of the SMZL samples and discrete plasma cell populations in those SMZL samples that were able to differentiate (figure 6.17).

WM cells are marked by their highly diverging responses to CD40L and R848 stimulation. The SMZL samples however, exhibited very similar responses in each condition, with some samples able to differentiate successfully in response to both stimuli whereas other were refractory to both types of stimulation (figure 5.4).

It would be interesting to profile cells from other B-cell neoplasms to provide further insight into the neoplastic phenotype. Application of SPADE clustering to diagnostic flow cytometry panels may facilitate differential diagnosis of these neoplasms due to the unbiased nature of the algorithm. Despite some similarities between WM and samples from other B-cell neoplasms, the divergent behaviour of WM cells in response to CD40L or R848 stimulation appears to be unique, as does the generation of the CD38$^-$ CD138$^+$ fraction.

8.6.2   Schnitzler syndrome

During the course of the project, an opportunity arose to assess the differentiation of B-cells from patients with Schnitzler syndrome. There is a link between the aetiology of SchS and WM, with cells from the haematopoietic lineage in SchS patients bearing the MYD88^{L265P} mutation and these individuals are predisposed to developing WM (Lim *et al.*, 2002; Lipsker, 2010; de Koning, 2014). There is also evidence of efficacy of Ibrutinib in these patients (Castillo *et al.*, 2016; Jani *et al.*, 2018). The SchS cells provided a rare prospect to compare the response of primary human B-cells in possession of MYD88^{L265P} - but without the additional mutational burden of a fully-fledged neoplasm - to both WM and healthy cells. The presence of the MYD88 mutation within the B-cell population of these patients was confirmed in both instances and persisted within the culture (figure 5.10), confirming that these cells are contributing to the observed phenotype as differentiation progresses.

B-cells from SchS individuals were unique amongst all of the primary samples in that they displayed hyperresponsiveness to TLR7 agonism, with levels of proliferation enhanced over and above that elicited by activation with CD40L (figures 5.7 and 5.11). The SchS cells responded in a manner that was initially expected of the WM samples and their divergence from the negative response of WM cells was surprising. Strikingly, one of the SchS samples generated CD38$^-$

CD138$^+$ cells, reinforcing the link between the L265P mutation and this unusual phenotype (figure 5.9). B-cells from SchS patients may be able provide further insight into this enigmatic population. RNA sequencing was not performed on the SchS samples but it would be most interesting to see the results of such an analysis in the context of the data presented here.

Analysis of SchS MYD88 PCR products revealed the existence of a novel mutation in two of these patients, MYD88^{L256P}, which was not found in any of the WM samples or cell lines tested (figure 5.17). Interestingly, this mutation shares similar features with MYD88^{L265P}; falling within the TIR domain, but appearing to preserve its integrity and being located on the MYD88 interaction axis (Bovijn *et al.*, 2013; Avbelj *et al.*, 2014). It is possible that the combination of both MYD88^{L256P} and MYD88^{L265P} confers further propensity for MYD88 to form Myddosomes and thus amplifies the TLR signal. Additional characterisation of this mutation in a larger cohort of SchS patients would enable its incidence to be determined and provide insight as to whether it has an effect on protein interaction dynamics.

A subset of SchS cells were able to respond very rapidly to TLR stimulation in a similar manner to that which occurred in healthy cells (figure 5.15). However, the majority of these cells were CD38$^-$ CD138$^+$, implying that the progenitors of this population are sensitive to TLR7 ligation. The identity of these cells in healthy individuals appear to be memory cells, thus this indicates that the progenitor of the CD38$^-$ CD138$^+$ population is of a memory cell origin. This ties in with the proposed memory cell precursor of WM and may explain the exclusivity of this unusual population to these two diseases (Kriangkum *et al.*, 2004b; Paiva *et al.*, 2015; García-Sanz *et al.*, 2016). The proportion of the CD38$^-$ CD138$^+$ cells further increased when F(ab')$_2$ anti-IgG/M was omitted from the culture (figure 5.15). This suggests that additional signals from the BCR may modulate this population. Regulation could occur through multiple means, BCR ligation may be suppressive of this subgroup, favour the expansion of the non CD38$^-$ precursors or instead push the CD38$^-$ cells towards upregulating CD38.

Figure 8.2 summarises the differentiation profiles for healthy, SMZL, SchS and WM B-cells subsequent to activation with either CD40L or R848.
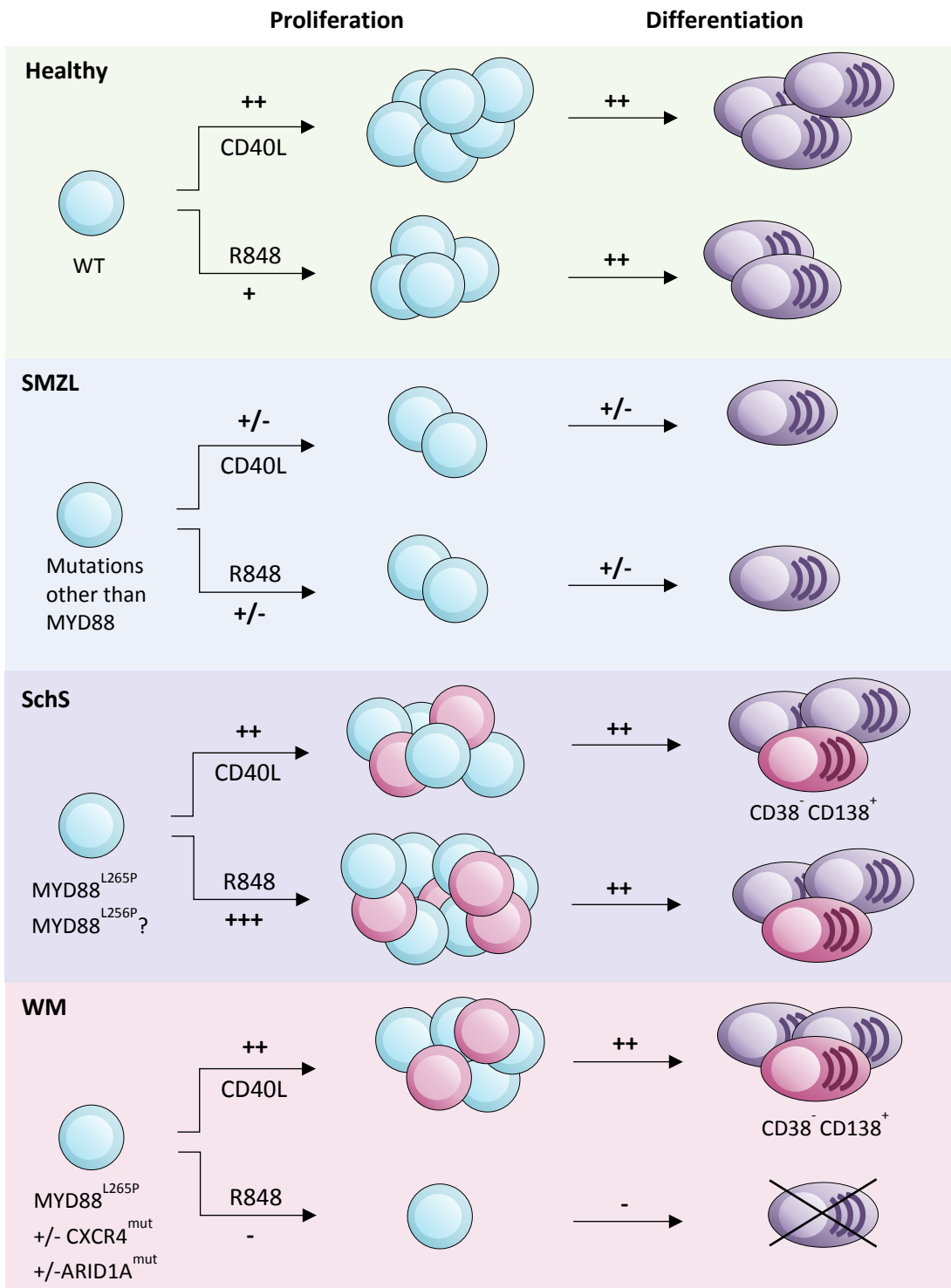
Figure 8.2 A summary of the differentiation responses of healthy and lymphoproliferative patient B-cells. Healthy B-cells proliferate and differentiate in response to both stimuli, with slightly lower levels of proliferation following activation with R848. SMZL samples respond variably but equally to both types of stimuli. SchS cells are hyperresponsive to R848 stimulation and generate CD38$^-$ CD138$^+$ cells in both instances. WM cells are able to proliferate and differentiate in response to CD40L stimulation, generating a CD38$^-$ CD138$^+$ population, but do not differentiate subsequent to activation with R848.

282

8.7 WM Bone marrow microenvironment

WM cells displayed a very strong bone marrow signature, with functional annotation software identifying the upregulation of numerous pathways involved in cell-cell interaction, cytokine production and migration. The bone marrow microenvironment clearly plays a central role in WM pathogenesis and this is reflected by the gene expression in cells from the *in vitro* system. Many of the key interactions that have been identified within the niche are summarised in figure 8.3.
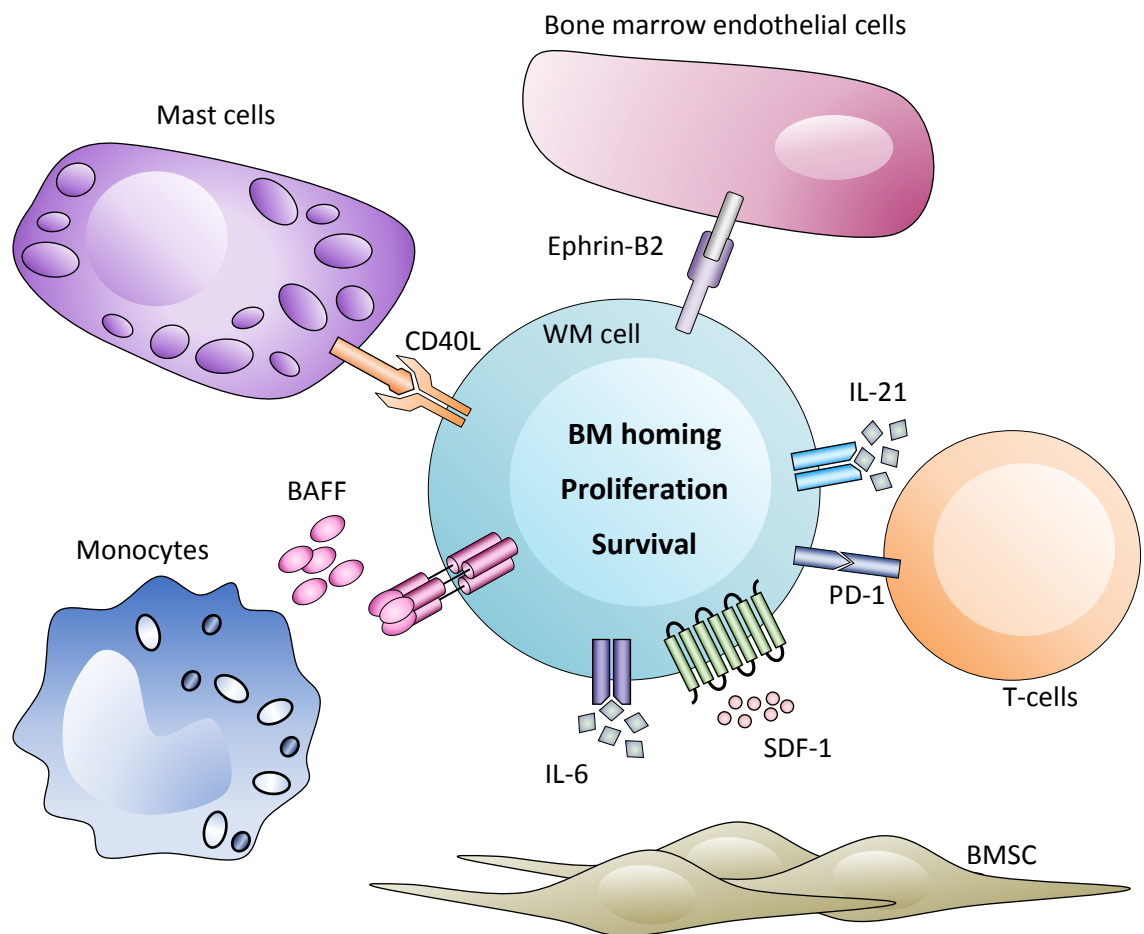
Figure 8.3 The bone marrow microenvironment and key factors influencing the survival of WM cells. WM cells interact with multiple components of the niche, which facilitate homing, survival and proliferation of the neoplastic clone. These include endothelial and stromal cells present within the local environment and accessory cells that are recruited by the WM clone such as mast cells, monocytes and T-cells.

8.7.1 Cellular interactions within the niche

Accumulation of excess mast cells within the BM is a characteristic feature of WM, with the presence of these cells often aiding differential diagnoses (Wilkins *et al.*, 2001; San Miguel *et al.*, 2003). The presence of mast cells has been demonstrated to promote the proliferation of the WM clone through CD40L-CD40 interaction (Tournilhac *et al.*, 2006). The upregulation of CD40L in mast cells of WM patients is thought to be mediated by soluble CD27 (sCD27) as elevated levels of sCD27 were identified in WM sera (Ho *et al.*, 2008). The addition of CD40L stimulation to the R848 + F(ab')$_2$ anti-IgG/M condition rescued the WM cells from undergoing apoptosis and enabled the cells to successfully generate plasma cells.

The classic source of CD40L signalling during an immune response is from T-cells. The expansion of a pool of monoclonal cytotoxic T-cells in 70% of WM patients was reported by Li and colleagues (Li *et al.*, 2010). The presence of these cells appear to be as a result of an immunomodulatory response towards the malignancy but are rendered anergic in proximity to the WM clone. It is thought that this may be due to the expression of immune checkpoint molecules on WM cells (Jalali *et al.*, 2018). Programmed death-1 (PD-1) receptor and its ligands, PD-L1 and PD-L2 are members of the B7-CD28 superfamily of immune checkpoint molecules (Ishida *et al.*, 1992; Freeman *et al.*, 2000). They negatively regulate the activation and proliferation of T-cells (Freeman *et al.*, 2000; Latchman *et al.*, 2001). Expression of PD-L1 and PD-L2 was found to be elevated in BM samples of patients with WM (Jalali *et al.*, 2018). These results suggest that the neoplastic cells may be able to subvert the antitumor T-cell response and instead turn the presence of these cells to their advantage, providing an additional source of cytokines such as IL-21.

8.7.2 WM cell homing

Another hallmark of WM is the infiltration of clonal B-cells into the bone marrow. The importance to WM pathology is evident in that the second most common mutation in WM is CXCR4 (Hunter *et al.*, 2014). The significance of CXCR4 signalling in WM was originally identified several years earlier whereby it was found to regulate homing and adhesion to endothelial cells and stromal cells (Ngo *et al.*, 2008). Multiple nonsense and frameshift mutations have been identified in CXCR4, all of which are located in the c-terminal tail, resulting in a truncation of the distal portion of the protein (Poulain *et al.*, 2016). Binding of SDF-1 to CXCR4 triggers phosphorylation of the receptor and its subsequent internalisation, facilitating desensitisation to prolonged signalling (Haribabu *et al.*, 1997; Signoret *et al.*, 1997; Signoret *et al.*, 1998). C-

terminal truncation attenuates the internalisation of the receptor and results in aberrant signalling. The most prevalent CXCR4 mutation S338X, was first described in WHIM syndrome (Hernandez *et al.*, 2003). Poulain *et al*. confirmed that CXCR4 expression was elevated on CXCR4-mutated WM cells, regardless of the type of mutation, facilitating homing to the bone marrow (Poulain *et al.*, 2016). In accordance with these findings, CXCR4 is significantly upregulated in the WM samples in comparison to the healthy controls.

Determination of the mutation status of CXCR4 has become particularly important in the light of the discovery that CXCR4 mutated cells are resistant to Ibrutinib (Hunter *et al.*, 2013; Roccaro *et al.*, 2014; Cao *et al.*, 2015; Treon *et al.*, 2015). Treatment with Ibrutinib results in the egress of WM cells from the bone marrow, which is particularly pronounced for MYD88^{L265P} CXCR4^{WT} patients and correlates with an improved clinical outcome (Treon *et al.*, 2015; de Rooij *et al.*, 2016). Deprivation of the support provided by the bone marrow niche thus appears to be an effective mechanism to induce WM cell death.

Once the WM cells are situated within the protective niche of the bone marrow microenvironment, it is advantageous for the cells to remain there. One such mechanism that is thought to facilitate retention of WM cells within the bone marrow locale is the interaction of ephrin-B2 on endothelial cells with the ephrin receptor on the neoplastic clone (Azab *et al.*, 2012). In agreement with these findings, cells from healthy individuals did not appear to express ephrin receptor B2, whereas it was significantly upregulated in the WM cohort (log$_2$ fold change = 3.93, p = 0.005).

Another component critical for homing and adhesion of WM cells is the PI3K-Akt signalling pathway (Leleu *et al.*, 2007). Constitutive activation of this pathway was first discovered by Leleu and colleagues (Leleu *et al.*, 2006; Leleu *et al.*, 2007). They observed that activation of Akt induced the proliferation of WM cells, whilst downregulation of Akt signalling resulted in inhibition of the ability of WM cells to home to the BM *in vivo*. Accordingly, the RNA sequencing results presented here demonstrate that PI3K-Akt signalling was significantly upregulated in WM cells compared to the healthy cohort. Regulation of signalling cascades such as the PI3K-Akt pathway can occur via miRNA (He and Hannon, 2004). WM cells have a specific miRNA signature which includes increased expression of multiple miRNAs, including miR-155 which regulates Akt (Roccaro *et al.*, 2009). It was found that miR-155 has multiple roles, regulating WM proliferation, adhesion and migration (Roccaro *et al.*, 2009). The sequencing data from samples taken during *in vitro* differentiation concurs with these findings. As with the PI3K-Akt pathway, *miR-155* is also significantly upregulated in the differentiating WM cells compared to healthy (data not shown).

PI3K-delta inhibitors showed promise in the killing of WM cell lines, and, in a similar manner to Ibrutinib, are thought to mobilise neoplastic cells from the bone marrow (Liu *et al.*, 2013; de Rooij *et al.*, 2016). A phase II trial of Idelalisib was instigated in patients with relapsed and/or refractory WM but was subsequently abandoned due to a high incidence of hepatotoxicity (Gustine *et al.*, 2017).

The myriad of upregulated genes in WM cells involved with cell-cell interaction, adhesion and homing are indicative of the importance of these factors in the survival of WM cells. Eviction of the neoplastic fraction from the protective environment represents a promising therapeutic strategy, inducing a state of susceptibility to cell death similar to anoikis.

8.7.3   Cytokines

The cytokine milieu within the bone marrow is essential for B-cell development and to maintain homeostasis (Carsetti, 2000; Cassese *et al.*, 2003; Vazquez *et al.*, 2015). Research has identified a marked difference in the BM cytokine environment in WM patients compared with healthy individuals (Elsawa and Ansell, 2009). A multitude of factors are therefore influencing WM pathogenesis.

Application of supernatant derived from WM cells during *in vitro* differentiation to activated healthy or WM B-cells resulted in an increase to cell survival and proliferation, with secretion of factors by WM cells appearing to peak at day 3 (figures 7.6 and 7.8). The effects were most pronounced for B-cells stimulated with R848 and F(ab')$_2$ anti-IgG/M (figures 7.7 and 7.9). Whilst there was less effect on CD40L stimulated cells, the levels of physiological stimulation are likely to be more subtle so the effect on the R848-stimulated cells is perhaps a closer reflection of what might happen *in vivo*. Whilst the identity of the factors eliciting this response were not determined, BAFF and APRIL appear to be likely candidates. Activation of human B-cells with CD40L induces production of BAFF (He *et al.*, 2004a; Kern *et al.*, 2004). Similarly, TLR simulation via LPS or CpG in murine B-cells resulted in upregulation of both BAFF and APRIL (Chu *et al.*, 2007). BAFF enhances the survival of both multiple myeloma and CLL and the observation of increased levels of BAFF in WM suggests that these cells may benefit from its presence in a similar manner (Novak *et al.*, 2002; Moreaux *et al.*, 2004; Elsawa *et al.*, 2006).

Whilst *BAFF* was not differentially expressed between WM and control cells, expression of *APRIL* was increased in WM cells at day 6. A possible mechanism to explain these observations is the sequential secretion of these factors by WM cells following activation, whereby BAFF is initially upregulated to enhance proliferation and survival of activated B-cells then APRIL takes over to sustain plasma cells. Monocytes are a potent source of BAFF (Nardelli *et al.*, 2001; Mueller *et*

al., 2007). The accumulation of monocytes within the bone marrow in close proximity to the WM clone represent a likely source of BAFF so the requirement for the WM cells themselves to be a source of autocrine BAFF within the niche is diminished.

The RNA sequencing data revealed that *BAFF-R* was highly upregulated in the WM samples, *TACI* was highly expressed in both healthy and WM cells, whilst *BCMA* was downregulated in WM cells. The lack of *BCMA* appears to contradict the findings of Elsawa and colleagues which suggest BCMA expression is elevated in WM cells, but closer inspection of their data reveals that only one of 5 primary samples demonstrated increased BCMA levels (Elsawa *et al.*, 2006). It is also possible that the expression of the three receptors alters during the course of differentiation. Elevated levels of BAFF-R in WM cells enables them to be receptive to external sources of BAFF.

CCL5 was the 8th most significantly differentially expressed protein coding gene between WM and healthy samples, with a 29-fold increase in WM. These results are replicated in the data from Elsawa *et al* (Elsawa *et al.*, 2011). They conducted a multiplex bead-based array analysis to quantify cytokines, chemokines and growth factors in WM sera, demonstrating that CCL5 the most elevated expression compared to healthy controls (Elsawa *et al.*, 2011). Despite this, they were unable to detect surface expression of CCR5 by flow cytometry or RT-PCR. In contrast to this, Ngo *et al.*, detected CCR5 in primary WM cells at the same level as healthy cells (Ngo *et al.*, 2008). CCR5 has previously been found to be expressed at low levels on mature B-cells (Lee *et al.*, 1999; Honczarenko *et al.*, 2002). The difference between the results in WM may be due to the identity of the isolated cells, with Ngo and colleagues using CD19+ cells, whilst the analysis by Elsawa was performed on CD19+CD138+ cells.

The expression of CCR5 in WM cells is likely to be low and this is corroborated by the RNA sequencing data. *CCR5* is expressed at relatively low levels in both the WM and healthy cells, however, it is increased in WM cells stimulated with R848. Interestingly, CCL5 enhanced B-cell proliferation and IgM secretion in murine B-cells activated with low doses of LPS, whilst ablation of endogenous CCL5 resulted in the opposite effect (Sullivan *et al.*, 2011). This indicates that autocrine CCL5 signalling is important in these cells so perhaps an analogous effect occurs to some extent in WM cells.

Further analysis by Elsawa revealed that CCL5 does not directly influence survival, proliferation or immunoglobulin secretion, in keeping with the lack of receptor surface expression (Elsawa *et al.*, 2011). Instead, they propose that CCL5 induces bone marrow stromal cells the secrete IL-6 (Elsawa and Ansell, 2009). IL-6 is added to the *in vitro* cultures at day 6 to promote plasma cell differentiation via activation of the STAT3 pathway, which induces upregulation of *PRDM1* (Reljic *et al.*, 2000; Jourdan *et al.*, 2009). The samples used for RNA sequencing were taken

before the addition of IL-6 and thus differences between the WM and healthy cells could be determined. The differential expression of *IL-6* between WM and control cells was highly statistically significant ($p < 1 \times 10^{-9}$). WM cells expressed elevated levels of IL-6, which is likely to be promoting IgM secretion in these cells. Interestingly, in the murine B-cell lymphoma cell line, CH12.LX, stimulation with R848 resulted in very high levels of IL-6 production in comparison to stimulation with CpG which did not induce secretion of this cytokine (Bishop *et al.*, 2001). Taken together, these data support a conclusion that high levels of CCL5 production by WM cells functions to recruit monocytes, which supplement the intrinsic production of IL-6 and contribute to an increase to IgM secretion that is so characteristic of WM. Expression of CCL5 may also serve to increase proliferation of the neoplastic clone via autocrine signalling.

Not only can WM cells exert influence over their neighbouring cells, they can also affect the architecture of the bone marrow niche itself through the production of cytokines (Terpos *et al.*, 2006). One such example is macrophage inflammatory protein-1 alpha (MIP-1α). Production of MIP-1α is virtually ubiquitous by both haematopoietic and stromal cells, however an increase in MIP-1α in lymphoid neoplasms was first discovered in multiple myeloma (Choi *et al.*, 2000). Abnormal bone remodelling is a classic feature of MM and whilst lytic bone disease does not occur in WM, alterations of the BM niche were identified in WM patients (Mundy *et al.*, 1974; Valentin-Opran *et al.*, 1982; Marcelli *et al.*, 1988). This effect was subsequently attributed to MIP-1α in WM (Terpos *et al.*, 2006). MIP-1α was significantly upregulated in the differentiating WM cells but was also highly variable within the group. Whilst data on the relapse/remission status of the patients is not available, it would be interesting to examine how closely these results reflect the disease activity as MIP-1α serum levels have been observed to correlate with active WM (Terpos *et al.*, 2006).

Further investigation of the WM secretome during the course of differentiation would provide valuable insight as to how the microenvironment is likely to be altered in the context of this neoplasm. Quantification of the cytokine milieu at different stages of disease progression would enable elucidation of temporal changes within the WM microenvironment. It would be most interesting to investigate how secretion is altered when the cells are activated by different stimuli and how other components of the BM niche such as stromal cells influence this. Use of the *in vitro* system would facilitate assessment of the secretome subsequent to drug treatment and may identify the most effective combinations of therapeutics.

8.8   NF-κB signalling in WM cells

The MYD88[L265P] mutation is responsible for activating the canonical NF-κB pathway (Ngo *et al.*, 2011; Treon *et al.*, 2012). This signalling is further supplemented by activation of the BCR and CXCR4 (Helbig *et al.*, 2003; Weil and Israël, 2004; Schulze-Luehrmann and Ghosh, 2006). Multiple components of the TLR, TNF and NF-κB pathways were significantly upregulated in WM cells, consistent with the constitutive signalling elicited by MYD88[L265P] (table 7.5). Interestingly, *RelB* was upregulated in the WM samples compared to the healthy controls, particularly in samples activated with R848, suggesting that non-canonical signalling is also occurring.

Stimulation of dendritic cells by TLR2, 4 and 9 resulted in the activation of RelB and that this was regulated by components of the canonical pathway (Shih *et al.*, 2012). However, signalling was not achieved by additional synthesis of protein, but by the pool of RelB already present. Upregulation of RelB mRNA is unlikely to be due to the ligation of TLR7 itself, however, RelA can induce RelB transcription and it will be undergoing nuclear translocation as a consequence of the constitutive signalling (Bren *et al.*, 2001).

Further induction of the non-canonical pathway in WM cells is likely to be achieved via ligation of BAFF-R. Whilst BAFF-R is able to induce canonical NF-κB signalling, ligation of the receptor preferentially induces the non-canonical pathway (Morrison *et al.*, 2005; Sun, 2011). Ligation of BAFF-R results in TRAF3 degradation, depleting the pool (Xu and Shu, 2002; Gardam *et al.*, 2008). TRAF3 suppresses NF-κB signalling by interacting with NIK, resulting in its degradation by the proteasome, thus removal of TRAF3 enables NIK to proceed (Liao *et al.*, 2004). In support of this mechanism, biallelic *TRAF3* inactivation has been identified in 5% of WM patients (Braggio *et al.*, 2009).

This involvement of non-canonical signalling in preventing apoptosis in non-Hodgkin lymphoma and CLL has been established (Gricks *et al.*, 2004; Lwin *et al.*, 2007; Mineva *et al.*, 2007). A similar protective mechanism may be occurring within WM cells exposed to R848, with those expressing the highest levels of RelB able to survive better in comparison to the rest of the population.

Activation of the canonical pathway within WM cells is enhanced by a variety of extrinsic signals provided by the bone marrow microenvironment. These include ligation of CXCR4 via secretion of SDF-1 from the stroma, CD40L signalling from mast cells and BCR ligation (Bleul *et al.*, 1996; Tournilhac *et al.*, 2006; Elgueta *et al.*, 2009). Cumulatively, the abundance of factors able to elicit NF-κB activation suggests that the WM neoplastic clone benefits from activation of both arms of the NF-κB signalling pathway (figure 8.4).
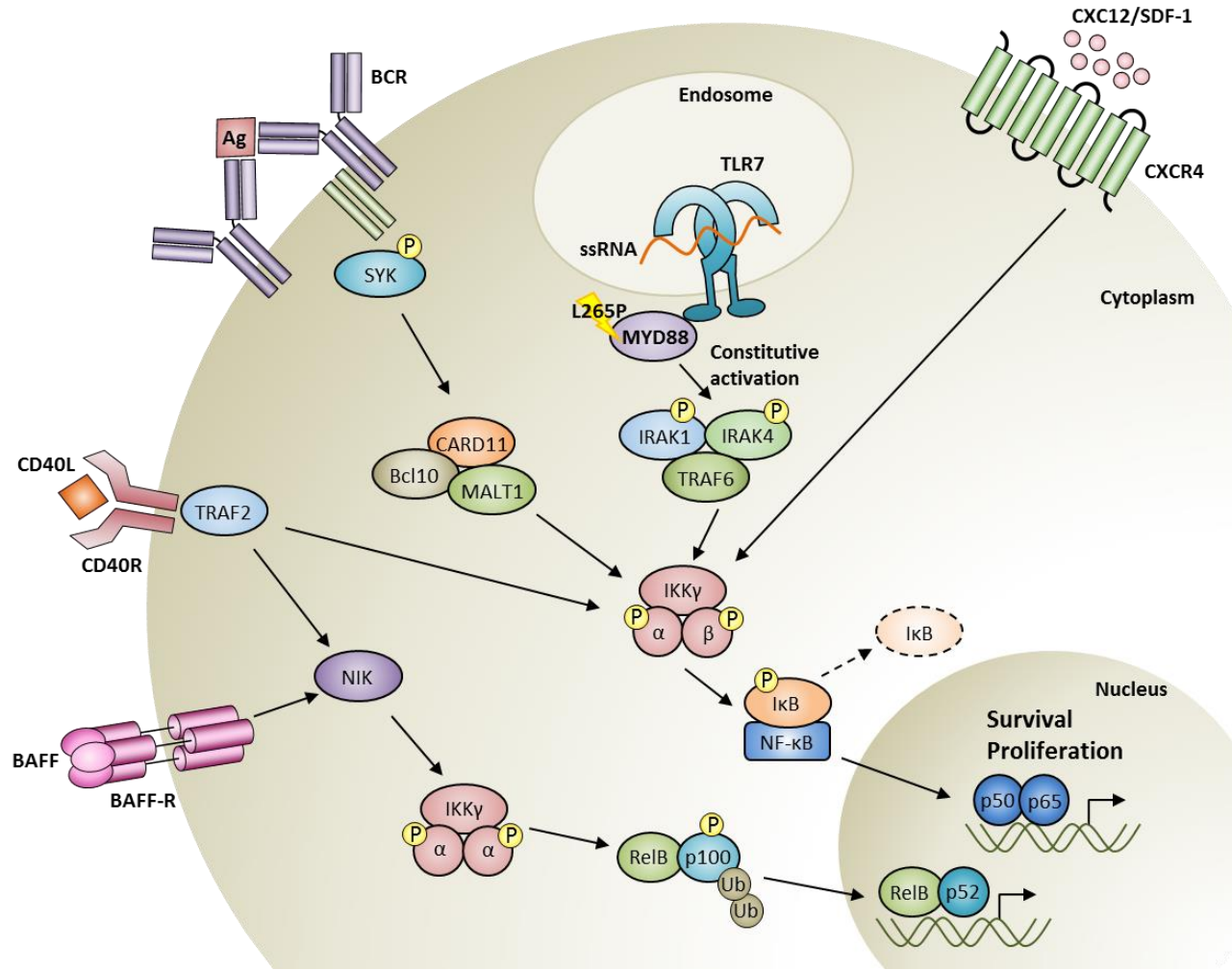
Figure 8.4 NF-κB signalling in WM cells is supplemented by multiple extrinsic signals. Constitutive activation of NF-κB by MYD88^{L265P} is augmented by additional signalling from the bone marrow environment. RNA sequencing indicates that co-operation between the canonical and non-canonical arms of the NF-κB pathway occurs within WM.

8.9   Concluding remarks

This work represents the first time the differentiation of primary human WM B-cells has been investigated in an *in vitro* setting, in response to both T-dependent and T-independent stimuli. WM cells successfully differentiate when provided with stimuli that mimics T-dependent B-cell activation and generate a novel population of CD38⁻ plasma cells that have not been previously described but is strongly linked to the presence of MYD88^L265P. Both this fraction and the conventional CD38⁺ CD138⁺ plasma cells generated by WM cells demonstrate an equivalent lifespan to those generated by healthy controls and represent a truly long-lived plasma cell population, persisting in culture in excess of 40 days.

As previously discussed, the downregulation of CD38 expression on the surface of a proportion of WM cells has ramifications for treatment decisions. Additional characterisation of CD38 expression within WM cells is warranted to determine if its absence is as a consequence of transcriptional dysregulation or driven by selection. The remarkable correlation between the loss of CD38 expression and the proportion of neoplastic clone within the bone marrow may prove to be a useful prognostic marker.

Strikingly, and in sharp contrast to their healthy counterparts, WM cells fail to generate plasma cells and undergo dramatic levels of apoptosis in response to TLR7 agonism with the synthetic ligand R848. WM cells express TLR7 and remain receptive to activation by TLR signalling, confirmed by RNA sequencing. However, it is not possible to pinpoint the initiating event that triggers apoptosis subsequent to R848 stimulation from the data generated from the day 6 cells. Of particular interest therefore is to examine gene expression at a much earlier time point following R848 stimulation in comparison to a baseline expression of unstimulated cells. This would provide insight as to whether TLR7 ligation directly initiates apoptosis or, as appears more likely, it is a result of WM cells being deprived of the additional pro-survival factors within the bone marrow niche.

It would be interesting to investigate whether the aberrant response of WM cells occurs following stimulation of any of the other TLRs. A natural candidate to extend the study would be TLR9, another endosomal TLR that is highly expressed on memory cells (Bernasconi *et al.*, 2003; Nishiya and DeFranco, 2004). TLR9 has been more extensively characterised than TLR7 and it may have a potential role in WM as a signalling scaffold as proposed by Staudt and colleagues (Phelan *et al.*, 2018).

Therapeutics inducing egress of neoplastic cells from the bone marrow have demonstrated efficacy in the treatment of WM via an anoikis-like mechanism (Treon *et al.*, 2015; Castillo *et al.*,

2016; de Rooij *et al.*, 2016; Treon *et al.*, 2017). It currently appears that removal of WM cells from the protective niche of the bone marrow microenvironment renders them susceptible to apoptosis due to a lack of additional pro-survival signals and this is responsible for the deleterious effect of R848 stimulation on WM cells. The apoptosis may not be induced by TLR7 ligation, rather, the combination of TLR7 and BCR ligation are insufficient to rescue the WM cells from death as is the case when CD40L stimulation is provided. This may be linked with the inability of WM cells to differentiate when provided with R848 stimulation. Failure to induce the plasma cell differentiation program in response to these signals may push the cells towards an apoptotic fate in a similar manner to B-cells that are unable to respond correctly *in vivo*.

The *in vitro* system represents a powerful tool for studying B-cell neoplasms. It is particularly useful for investigating WM as it enables analysis of the spectrum of B-cell differentiation which is impossible in cell lines. Understanding of the bone marrow microenvironment is increasingly being recognised as an essential component for treating WM. Currently, a mouse model that sufficiently recapitulates this neoplasm does not exist and thus the flexibility of the *in vitro* system will enable superior modelling of the BM niche with patient-derived primary cells.

References

Agematsu, K., Hokibara, S., Nagumo, H. & Komiyama, A. 2000. CD27: a memory B-cell marker. *Immunology Today,* 21**,** 204-206.

Agematsu, K., Kobata, T., Yang, F.-C., Nakazawa, T., Fukushima, K., Kitahara, M., Mori, T., Sugita, K., Morimoto, C. & Komiyama, A. 1995. CD27/CD70 interaction directly drives B cell IgG and IgM synthesis. *European Journal of Immunology,* 25**,** 2825-2829.

Agematsu, K., Nagumo, H., Yang, F.-C., Nakazawa, T., Fukushima, K., Ito, S., Sugita, K., Mori, T., Kobata, T., Morimoto, C. & Komiyama, A. 1997. B cell subpopulations separated by CD27 and crucial collaboration of CD27+ B cells and helper T cells in immunoglobulin production. *European Journal of Immunology,* 27**,** 2073-2079.

Ahmed, R. & Gray, D. 1996. Immunological Memory and Protective Immunity: Understanding Their Relation. *Science,* 272**,** 54-60.

Akira, S. & Takeda, K. 2004. Toll-like receptor signalling. *Nat Rev Immunol,* 4**,** 499-511.

Alessio, M., Roggero, S., Funaro, A., De Monte, L., Peruzzi, L., Geuna, M. & Malavasi, F. 1990. CD38 molecule: structural and biochemical analysis on human T lymphocytes, thymocytes, and plasma cells. *The Journal of Immunology,* 145**,** 878-884.

Alexopoulou, L., Holt, A. C., Medzhitov, R. & Flavell, R. A. 2001. Recognition of double-stranded RNA and activation of NF-kappaB by Toll-like receptor 3. *Nature,* 413**,** 732-8.

Algara, P., Mateo, M. S., Sanchez-Beato, M., Mollejo, M., Navas, I. C., Romero, L., Solé, F., Salido, M., Florensa, L., MartíNez, P., Campo, E. & Piris, M. A. 2002. Analysis of the IgV(H) somatic mutations in splenic marginal zone lymphoma defines a group of unmutated cases with frequent 7q deletion and adverse clinical course. *Blood,* 99**,** 1299-304.

Alizadeh, A. A., Eisen, M. B., Davis, R. E., Ma, C., Lossos, I. S., Rosenwald, A., Boldrick, J. C., Sabet, H., Tran, T. & Yu, X. 2000. Distinct types of diffuse large B-cell lymphoma identified by gene expression profiling. *Nature,* 403**,** 503-11.

Allen, C. D., Okada, T. & Cyster, J. G. 2007. Germinal-center organization and cellular dynamics. *Immunity,* 27**,** 190-202.

Amir, E.-a. D., Davis, K. L., Tadmor, M. D., Simonds, E. F., Levine, J. H., Bendall, S. C., Shenfeld, D. K., Krishnaswamy, S., Nolan, G. P. & Pe'er, D. 2013. viSNE enables visualization of high dimensional single-cell data and reveals phenotypic heterogeneity of leukemia. *Nature Biotechnology,* 31**,** 545-52.

Anderson, K. C., Bates, M. P., Slaughenhoupt, B. L., Pinkus, G. S., Schlossman, S. F. & Nadler, L. M. 1984. Expression of human B cell-associated antigens on leukemias and lymphomas: a model of human B cell differentiation. *Blood,* 63**,** 1424-1433.

Arcaini, L., Rossi, D. & Paulli, M. 2016. Splenic marginal zone lymphoma: from genetics to management. *Blood***,** 2072-81.

Argyropoulos, K. V., Vogel, R., Ziegler, C., Altan-Bonnet, G., Velardi, E., Calafiore, M., Dogan, A., Arcila, M., Patel, M., Knapp, K., Mallek, C., Hunter, Z. R., Treon, S. P., Van Den Brink, M. R. & Palomba, M. L. 2016. Clonal B cells in Waldenstrom's macroglobulinemia exhibit functional features of chronic active B-cell receptor signaling. *Leukemia,* 30**,** 1116-25.

Arpin, C., Dechanet, J., Van Kooten, C., Merville, P., Grouard, G., Briere, F., Banchereau, J. & Liu, Y. J. 1995. Generation of memory B cells and plasma cells in vitro. *Science,* 268**,** 720-2.

Arumugakani, G., Stephenson, S. J., Newton, D. J., Rawstron, A., Emery, P., Doody, G. M., Mcgonagle, D. & Tooze, R. M. 2017. Early Emergence of CD19-Negative Human Antibody-Secreting Cells at the Plasmablast to Plasma Cell Transition. *The Journal of Immunology,* 198**,** 4618.

Avbelj, M., Wolz, O. O., Fekonja, O., Bencina, M., Repic, M., Mavri, J., Kruger, J., Scharfe, C., Delmiro Garcia, M., Panter, G., Kohlbacher, O., Weber, A. N. & Jerala, R. 2014. Activation of lymphoma-associated MyD88 mutations via allostery-induced TIR-domain oligomerization. *Blood,* 124**,** 3896-904.

Azab, F., Azab, A. K., Maiso, P., Calimeri, T., Flores, L., Liu, Y., Quang, P., Roccaro, A. M., Sacco, A., Ngo, H. T., Zhang, Y., Morgan, B. L., Carrasco, R. D. & Ghobrial, I. M. 2012. Eph-

B2/Ephrin-B2 Interaction Plays a Major Role in the Adhesion and Proliferation of Waldenstrom's Macroglobulinemia. *Clinical Cancer Research,* 18**,** 91.

Babbage, G., Townsend, M., Zojer, N., Mockridge, I. C., Garand, R., Barlogie, B., Shaughnessy Jr, J., Stevenson, F. K. & Sahota, S. S. 2007. IgM-expressing Waldenstrom's macroglobulinemia tumor cells reveal a potential for isotype switch events in vivo. *Leukemia,* 21**,** 827.

Bagnara, D., Squillario, M., Kipling, D., Mora, T., Walczak, A. M., Da Silva, L., Weller, S., Dunn-Walters, D. K., Weill, J.-C. & Reynaud, C.-A. 2015. A Reassessment of IgM Memory Subsets in Humans. *The Journal of Immunology,* 195**,** 3716.

Banchereau, J. & Rousset, F. 1992. Human B lymphocytes: phenotype, proliferation, and differentiation. *Advances in immunology.* Elsevier.

Barrans, S. L., Child, J. A., O'connor, S. J. M., Jack, A. S., Morgan, G. J., Richards, S. J., Owen, R. G. & Parapia, L. A. 2001. Waldenström Macroglobulinemia: Development of Diagnostic Criteria and Identification of Prognostic Factors. *American Journal of Clinical Pathology,* 116**,** 420-428.

Barton, G. M., Kagan, J. C. & Medzhitov, R. 2006. Intracellular localization of Toll-like receptor 9 prevents recognition of self DNA but facilitates access to viral DNA. *Nature immunology,* 7**,** 49.

Bernasconi, N. L., Onai, N. & Lanzavecchia, A. 2003. A role for Toll-like receptors in acquired immunity: up-regulation of TLR9 by BCR triggering in naive B cells and constitutive expression in memory B cells. *Blood,* 101**,** 4500.

Bernasconi, N. L., Traggiai, E. & Lanzavecchia, A. 2002. Maintenance of serological memory by polyclonal activation of human memory B cells. *Science,* 298**,** 2199-202.

Bernfield, M., Kokenyesi, R., Kato, M., Hinkes, M. T., Spring, J., Gallo, R. L. & Lose, E. J. 1992. Biology of the Syndecans: A Family of Transmembrane Heparan Sulfate Proteoglycans. *Annual Review of Cell Biology,* 8**,** 365-393.

Bihui, H. Y., Cattoretti, G., Shen, Q., Zhang, J., Hawe, N., De Waard, R., Leung, C., Nouri-Shirazi, M., Orazi, A. & Chaganti, R. 1997. The BCL-6 proto-oncogene controls germinal-centre formation and Th2-type inflammation. *Nature genetics,* 16**,** 161.

Bishop, G. A., Ramirez, L. M., Baccam, M., Busch, L. K., Pederson, L. K. & Tomai, M. A. 2001. The immune response modifier resiquimod mimics CD40-induced B cell activation. *Cell Immunol,* 208.

Bishop, G. A., Warren, W. D. & Berton, M. T. 1995. Signaling via major histocompatibility complex class II molecules and antigen receptors enhances the B cell response to gp39/CD40 ligand. *European Journal of Immunology,* 25**,** 1230-1238.

Biswas, S. K. & Lopez-Collazo, E. 2009. Endotoxin tolerance: new mechanisms, molecules and clinical significance. *Trends in Immunology,* 30**,** 475-487.

Bleul, C. C., Fuhlbrigge, R. C., Casasnovas, J. M., Aiuti, A. & Springer, T. A. 1996. A highly efficacious lymphocyte chemoattractant, stromal cell-derived factor 1 (SDF-1). *The Journal of Experimental Medicine,* 184**,** 1101.

Bourke, E., Bosisio, D., Golay, J., Polentarutti, N. & Mantovani, A. 2003. The toll-like receptor repertoire of human B lymphocytes: inducible and selective expression of TLR9 and TLR10 in normal and transformed cells. *Blood,* 102**,** 956-963.

Bovijn, C., Desmet, A.-S., Uyttendaele, I., Van Acker, T., Tavernier, J. & Peelman, F. 2013. Identification of Binding Sites for Myeloid Differentiation Primary Response Gene 88 (MyD88) and Toll-like Receptor 4 in MyD88 Adapter-like (Mal). *Journal of Biological Chemistry,* 288**,** 12054-12066.

Braggio, E., Keats, J. J., Leleu, X., Van Wier, S., Jimenez-Zepeda, V. H., Valdez, R., Schop, R. F. J., Price-Troska, T., Henderson, K., Sacco, A., Azab, F., Greipp, P., Gertz, M., Hayman, S., Rajkumar, S. V., Carpten, J., Chesi, M., Barrett, M., Stewart, A. K., Dogan, A., Bergsagel, P. L., Ghobrial, I. M. & Fonseca, R. 2009. Identification of copy-number abnormalities and inactivating mutations in two negative regulators of NF-kB signaling pathways in Waldenström's Macroglobulinemia. *Cancer research,* 69**,** 3579-3588.

Braggio, E., Philipsborn, C., Novak, A., Hodge, L., Ansell, S. & Fonseca, R. 2012. Molecular pathogenesis of Waldenström's macroglobulinemia. *Haematologica,* 97**,** 1281.

Breitfeld, D., Ohl, L., Kremmer, E., Ellwart, J., Sallusto, F., Lipp, M. & Forster, R. 2000. Follicular B helper T cells express CXC chemokine receptor 5, localize to B cell follicles, and support immunoglobulin production. *J Exp Med,* 192**,** 1545-52.

Bren, G. D., Solan, N. J., Miyoshi, H., Pennington, K. N., Pobst, L. J. & Paya, C. V. 2001. Transcription of the RelB gene is regulated by NF-κB. *Oncogene,* 20**,** 7722.

Brinkmann, M. M., Spooner, E., Hoebe, K., Beutler, B., Ploegh, H. L. & Kim, Y.-M. 2007. The interaction between the ER membrane protein UNC93B and TLR3, 7, and 9 is crucial for TLR signaling. *The Journal of Cell Biology,* 177**,** 265.

Brint, E. K., Xu, D., Liu, H., Dunne, A., Mckenzie, A. N., O'neill, L. A. & Liew, F. Y. 2004. ST2 is an inhibitor of interleukin 1 receptor and Toll-like receptor 4 signaling and maintains endotoxin tolerance. *Nature immunology,* 5**,** 373.

Broad, A., Jones, D. E. & Kirby, J. A. 2006. Toll-like receptor (TLR) response tolerance: a key physiological "damage limitation" effect and an important potential opportunity for therapy. *Curr Med Chem,* 13**,** 2487-502.

Brynjolfsson, S. F., Mohaddes, M., Kärrholm, J. & Wick, M.-J. 2017. Long-lived plasma cells in human bone marrow can be either CD19$^+$ or CD19$^-$. *Blood Advances,* 1**,** 835.

Burger, J. A., Burger, M. & Kipps, T. J. 1999. Chronic Lymphocytic Leukemia B Cells Express Functional CXCR4 Chemokine Receptors That Mediate Spontaneous Migration Beneath Bone Marrow Stromal Cells. *Blood,* 94**,** 3658.

Burger, J. A. & Kipps, T. J. 2006. CXCR4: a key receptor in the crosstalk between tumor cells and their microenvironment. *Blood,* 107**,** 1761-1767.

Burns, K., Janssens, S., Brissoni, B., Olivos, N., Beyaert, R. & Tschopp, J. 2003. Inhibition of interleukin 1 receptor/Toll-like receptor signaling through the alternatively spliced, short form of MyD88 is due to its failure to recruit IRAK-4. *J Exp Med,* 197**,** 263-8.

Buske, C., Leblond, V., Dimopoulos, M., Kimby, E., Jäger, U., Dreyling, M. & Group, E. G. W. 2013. Waldenström's macroglobulinaemia: ESMO Clinical Practice Guidelines for diagnosis, treatment and follow-up. *Annals of oncology,* 24**,** vi155-vi159.

Calfon, M., Zeng, H., Urano, F., Till, J. H., Hubbard, S. R., Harding, H. P., Clark, S. G. & Ron, D. 2002. IRE1 couples endoplasmic reticulum load to secretory capacity by processing the XBP-1 mRNA. *Nature,* 415**,** 92.

Cao, Y., Hunter, Z. R., Liu, X., Xu, L., Yang, G., Chen, J., Patterson, C. J., Tsakmaklis, N., Kanan, S., Rodig, S., Castillo, J. J. & Treon, S. P. 2015. The WHIM-like CXCR4(S338X) somatic mutation activates AKT and ERK, and promotes resistance to ibrutinib and other agents used in the treatment of Waldenstrom's Macroglobulinemia. *Leukemia,* 29**,** 169-76.

Capolunghi, F., Cascioli, S., Giorda, E., Rosado, M. M., Plebani, A., Auriti, C., Seganti, G., Zuntini, R., Ferrari, S., Cagliuso, M., Quinti, I. & Carsetti, R. 2008. CpG Drives Human Transitional B Cells to Terminal Differentiation and Production of Natural Antibodies. *The Journal of Immunology,* 180**,** 800.

Carotta, S., Willis, S. N., Hasbold, J., Inouye, M., Pang, S. H. M., Emslie, D., Light, A., Chopin, M., Shi, W. & Wang, H. 2014. The transcription factors IRF8 and PU. 1 negatively regulate plasma cell differentiation. *Journal of Experimental Medicine,* 211**,** 2169-2181.

Carsetti, R. 2000. The development of B cells in the bone marrow is controlled by the balance between cell-autonomous mechanisms and signals from the microenvironment. *The Journal of experimental medicine,* 191**,** 5-8.

Carter, R. H. & Fearon, D. T. 1992. CD19: lowering the threshold for antigen receptor stimulation of B lymphocytes. *Science,* 256**,** 105-107.

Cascavilla, N., Bisceglia, M. & D'arena, G. 2010. Successful treatment of Schnitzler's syndrome with anakinra after failure of rituximab trial. *Int J Immunopathol Pharmacol,* 23**,** 633-6.

Cassese, G., Arce, S., Hauser, A. E., Lehnert, K., Moewes, B., Mostarac, M., Muehlinghaus, G., Szyska, M., Radbruch, A. & Manz, R. A. 2003. Plasma Cell Survival Is Mediated by Synergistic Effects of Cytokines and Adhesion-Dependent Signals. *The Journal of Immunology,* 171**,** 1684.

Castillo, J. J., Palomba, M. L., Advani, R. & Treon, S. P. 2016. Ibrutinib in Waldenstrom macroglobulinemia: latest evidence and clinical experience. *Ther Adv Hematol,* 7**,** 179-86.

Cheng, Z.-J., Zhao, J., Sun, Y., Hu, W., Wu, Y.-L., Cen, B., Wu, G.-X. & Pei, G. 2000. β-Arrestin Differentially Regulates the Chemokine Receptor CXCR4-mediated Signaling and Receptor Internalization, and This Implicates Multiple Interaction Sites between β-Arrestin and CXCR4. *Journal of Biological Chemistry,* 275**,** 2479-2485.

Chng, W. J., Schop, R. F., Price-Troska, T., Ghobrial, I., Kay, N., Jelinek, D. F., Gertz, M. A., Dispenzieri, A., Lacy, M., Kyle, R. A., Greipp, P. R., Tschumper, R. C., Fonseca, R. & Bergsagel, P. L. 2006. Gene-expression profiling of Waldenstrom macroglobulinemia reveals a phenotype more similar to chronic lymphocytic leukemia than multiple myeloma. *Blood,* 108**,** 2755-63.

Choi, S. J., Cruz, J. C., Craig, F., Chung, H., Devlin, R. D., Roodman, G. D. & Alsina, M. 2000. Macrophage inflammatory protein 1-alpha is a potential osteoclast stimulatory factor in multiple myeloma. *Blood,* 96**,** 671.

Chu, V. T., Enghard, P., Riemekasten, G. & Berek, C. 2007. In Vitro and In Vivo Activation Induces BAFF and APRIL Expression in B Cells. *The Journal of Immunology,* 179**,** 5947.

Chuang, T.-H. & Ulevitch, R. J. 2004. Triad3A, an E3 ubiquitin-protein ligase regulating Toll-like receptors. *Nature immunology,* 5**,** 495.

Cimmino, L., Martins, G. A., Liao, J., Magnusdottir, E., Grunig, G., Perez, R. K. & Calame, K. L. 2008. Blimp-1 attenuates Th1 differentiation by repression of ifng, tbx21, and bcl6 gene expression. *The Journal of Immunology,* 181**,** 2338-2347.

Ciric, B., Vankeulen, V., Rodriguez, M., Kyle, R. A., Gertz, M. A. & Pease, L. R. 2001. Clonal evolution in Waldenstrom macroglobulinemia highlights functional role of B-cell receptor. *Blood,* 97**,** 321-323.

Clipson, A., Wang, M., De Leval, L., Ashton-Key, M., Wotherspoon, A., Vassiliou, G., Bolli, N., Grove, C., Moody, S., Escudero-Ibarz, L., Gundem, G., Brugger, K., Xue, X., Mi, E., Bench, A., Scott, M., Liu, H., Follows, G., Robles, E. F., Martinez-Climent, J. A., Oscier, D., Watkins, A. J. & Du, M. Q. 2014. KLF2 mutation is the most frequent somatic change in splenic marginal zone lymphoma and identifies a subset with distinct genotype. *Leukemia,* 29**,** 1177.

Cobaleda, C., Jochum, W. & Busslinger, M. 2007. Conversion of mature B cells into T cells by dedifferentiation to uncommitted progenitors. *Nature,* 449**,** 473.

Cocco, M., Stephenson, S., Care, M. A., Newton, D., Barnes, N. A., Davison, A., Rawstron, A., Westhead, D. R., Doody, G. M. & Tooze, R. M. 2012. In vitro generation of long-lived human plasma cells. *J Immunol,* 189**,** 5773-85.

Coutinho, A., Gronowicz, E., Bullock, W. W. & Möller, G. 1974. Mechanism of thymus-independent immunocyte triggering. Mitogenic activation of B cells results in specific immune responses. *The Journal of experimental medicine,* 139**,** 74-92.

Dasari, P., Nicholson, I. C., Hodge, G., Dandie, G. W. & Zola, H. 2005. Expression of toll-like receptors on B lymphocytes. *Cellular Immunology,* 236**,** 140-145.

Davids, M. S., Roberts, A. W., Seymour, J. F., Pagel, J. M., Kahl, B. S., Wierda, W. G., Puvvada, S., Kipps, T. J., Anderson, M. A., Salem, A. H., Dunbar, M., Zhu, M., Peale, F., Ross, J. A., Gressick, L., Desai, M., Kim, S. Y., Verdugo, M., Humerickhouse, R. A., Gordon, G. B. & Gerecitano, J. F. 2017. Phase I First-in-Human Study of Venetoclax in Patients With Relapsed or Refractory Non-Hodgkin Lymphoma. *Journal of clinical oncology : official journal of the American Society of Clinical Oncology,* 35**,** 826-833.

De Koning, H. D. 2014. Schnitzler's syndrome: lessons from 281 cases. *Clinical and Translational Allergy,* 4**,** 41.

De Rooij, M. F. M., Kuil, A., Kraan, W., Kersten, M. J., Treon, S. P., Pals, S. T. & Spaargaren, M. 2016. Ibrutinib and idelalisib target B cell receptor- but not CXCL12/CXCR4-controlled integrin-mediated adhesion in Waldenström macroglobulinemia. *Haematologica,* 101**,** e111-e115.

De Weers, M., Tai, Y.-T., Van Der Veer, M. S., Bakker, J. M., Vink, T., Jacobs, D. C. H., Oomen, L. A., Peipp, M., Valerius, T., Slootstra, J. W., Mutis, T., Bleeker, W. K., Anderson, K. C., Lokhorst, H. M., Van De Winkel, J. G. J. & Parren, P. W. H. I. 2011. Daratumumab, a Novel Therapeutic Human CD38 Monoclonal Antibody, Induces Killing of Multiple Myeloma and Other Hematological Tumors. *The Journal of Immunology,* 186**,** 1840.

Deaglio, S., Capobianco, A., Bergui, L., Dürig, J., Morabito, F., Dührsen, U. & Malavasi, F. 2003. CD38 is a signaling molecule in B-cell chronic lymphocytic leukemia cells. *Blood,* 102**,** 2146.

Deans, J. P., Schieven, G. L., Shu, G. L., Valentine, M. A., Gilliland, L. A., Aruffo, A., Clark, E. A. & Ledbetter, J. A. 1993. Association of tyrosine and serine kinases with the B cell surface antigen CD20. Induction via CD20 of tyrosine phosphorylation and activation of phospholipase C-gamma 1 and PLC phospholipase C-gamma 2. *The Journal of Immunology,* 151**,** 4494-4504.

Dent, A. L., Shaffer, A. L., Yu, X., Allman, D. & Staudt, L. M. 1997. Control of inflammation, cytokine expression, and germinal center formation by BCL-6. *Science,* 276**,** 589-592.

Derksen, P. W., Keehnen, R. M., Evers, L. M., Van Oers, M. H., Spaargaren, M. & Pals, S. T. 2002. Cell surface proteoglycan syndecan-1 mediates hepatocyte growth factor binding and promotes Met signaling in multiple myeloma. *Blood,* 99**,** 1405-1410.

Development Core Team, R. 2008. *R: A Language and Environment for Statistical Computing*.

Dimopoulos, M. A., Anagnostopoulos, A., Kyrtsonis, M.-C., Zervas, K., Tsatalas, C., Kokkinis, G., Repoussis, P., Symeonidis, A., Delimpasi, S. & Katodritou, E. 2007. Primary treatment of Waldenstrom macroglobulinemia with dexamethasone, rituximab, and cyclophosphamide. *Journal of Clinical Oncology,* 25**,** 3344-3349.

Dimopoulos, M. A., Kastritis, E., Owen, R. G., Kyle, R. A., Landgren, O., Morra, E., Leleu, X., García-Sanz, R., Munshi, N. & Anderson, K. C. 2014. Treatment recommendations for patients with Waldenström macroglobulinemia (WM) and related disorders: IWWM-7 consensus. *Blood,* 124**,** 1404-1411.

Dimopoulos, M. A., Tedeschi, A., Trotman, J., García-Sanz, R., Macdonald, D., Leblond, V., Mahe, B., Herbaux, C., Tam, C., Orsucci, L., Palomba, M. L., Matous, J. V., Shustik, C., Kastritis, E., Treon, S. P., Li, J., Salman, Z., Graef, T. & Buske, C. 2018. Phase 3 Trial of Ibrutinib plus Rituximab in Waldenström's Macroglobulinemia. *New England Journal of Medicine,* 378**,** 2399-2410.

Ding, B. B., Bi, E., Chen, H., Yu, J. J. & Ye, B. H. 2013. IL-21 and CD40L Synergistically Promote Plasma Cell Differentiation through Upregulation of Blimp-1 in Human B Cells. *The Journal of Immunology,* 190**,** 1827.

Dispenzieri, A., Gertz, M. A., Therneau, T. M. & Kyle, R. A. 2001. Retrospective cohort study of 148 patients with polyclonal gammopathy. *Mayo Clinic Proceedings,* 76**,** 476-487.

Do, R. K., Hatada, E., Lee, H., Tourigny, M. R., Hilbert, D. & Chen-Kiang, S. 2000. Attenuation of apoptosis underlies B lymphocyte stimulator enhancement of humoral immune response. *Journal of Experimental Medicine,* 192**,** 953-964.

Dobin, A., Davis, C. A., Schlesinger, F., Drenkow, J., Zaleski, C., Jha, S., Batut, P., Chaisson, M. & Gingeras, T. R. 2013. STAR: ultrafast universal RNA-seq aligner. *Bioinformatics,* 29**,** 15-21.

Donjerković, D. & Scott, D. W. 2000. Activation-induced cell death in B lymphocytes. *Cell Research,* 10**,** 179.

Doody, G. M., Stephenson, S., Mcmanamy, C. & Tooze, R. M. 2007. PRDM1/BLIMP-1 modulates IFN-γ-dependent control of the MHC class I antigen-processing and peptide-loading pathway. *The Journal of Immunology,* 179**,** 7614-7623.

Dufresne, S. D., Felgar, R. E., Sargent, R. L., Surti, U., Gollin, S. M., Mcphail, E. D., Cook, J. R. & Swerdlow, S. H. 2010. Defining the borders of splenic marginal zone lymphoma: a multiparameter study. *Human pathology,* 41**,** 540-551.

Elgueta, R., Benson, M. J., De Vries, V. C., Wasiuk, A., Guo, Y. & Noelle, R. J. 2009. Molecular mechanism and function of CD40/CD40L engagement in the immune system. *Immunol Rev,* 229**,** 152-72.

Elsawa, S. F. & Ansell, S. M. 2009. Cytokines in the Microenvironment of Waldenström's Macroglobulinemia. *Clinical lymphoma & myeloma,* 9**,** 43-45.

Elsawa, S. F., Novak, A. J., Grote, D. M., Ziesmer, S. C., Witzig, T. E., Kyle, R. A., Dillon, S. R., Harder, B., Gross, J. A. & Ansell, S. M. 2006. B-lymphocyte stimulator (BLyS) stimulates immunoglobulin production and malignant B-cell growth in Waldenström macroglobulinemia. *Blood,* 107**,** 2882-2888.

Elsawa, S. F., Novak, A. J., Ziesmer, S. C., Almada, L. L., Hodge, L. S., Grote, D. M., Witzig, T. E., Fernandez-Zapico, M. E. & Ansell, S. M. 2011. Comprehensive analysis of tumor microenvironment cytokines in Waldenstrom macroglobulinemia identifies CCL5 as a novel modulator of IL-6 activity. *Blood,* 118**,** 5540.

Ewald, S. E., Engel, A., Lee, J., Wang, M., Bogyo, M. & Barton, G. M. 2011. Nucleic acid recognition by Toll-like receptors is coupled to stepwise processing by cathepsins and asparagine endopeptidase. *The Journal of Experimental Medicine,* 208**,** 643.

Fairfax, K. A., Kallies, A., Nutt, S. L. & Tarlinton, D. M. 2008. Plasma cell development: From B-cell subsets to long-term survival niches. *Seminars in Immunology,* 20**,** 49-58.

Fearon, D. T., Carroll, M. C. & Carroll, M. C. 2000. Regulation of B lymphocyte responses to foreign and self-antigens by the CD19/CD21 complex. *Annual review of immunology,* 18**,** 393-422.

Figgett, W. A., Fairfax, K., Vincent, F. B., Le Page, M. A., Katik, I., Deliyanti, D., Quah, P. S., Verma, P., Grumont, R., Gerondakis, S., Hertzog, P., O'reilly, L. A., Strasser, A. & Mackay, F. 2013. The TACI receptor regulates T-cell-independent marginal zone B cell responses through innate activation-induced cell death. *Immunity,* 39**,** 573-83.

Fitzsimmons, D., Hodsdon, W., Wheat, W., Maira, S.-M., Wasylyk, B. & Hagman, J. 1996. Pax-5 (BSAP) recruits Ets proto-oncogene family proteins to form functional ternary complexes on a B-cell-specific promoter. *Genes & development,* 10**,** 2198-2211.

Freeman, G. J., Long, A. J., Iwai, Y., Bourque, K., Chernova, T., Nishimura, H., Fitz, L. J., Malenkovich, N., Okazaki, T., Byrne, M. C., Horton, H. F., Fouser, L., Carter, L., Ling, V., Bowman, M. R., Carreno, B. M., Collins, M., Wood, C. R. & Honjo, T. 2000. Engagement of the Pd-1 Immunoinhibitory Receptor by a Novel B7 Family Member Leads to Negative Regulation of Lymphocyte Activation. *The Journal of Experimental Medicine,* 192**,** 1027.

Fukuda, T., Yoshida, T., Okada, S., Hatano, M., Miki, T., Ishibashi, K., Okabe, S., Koseki, H., Hirosawa, S. & Taniguchi, M. 1997. Disruption of the Bcl6 gene results in an impaired germinal center formation. *Journal of Experimental Medicine,* 186**,** 439-448.

Fulcher, D. & Basten, A. 1997. B-cell activation versus tolerance-the central role of immunoglobulin receptor engagement and T-cell help. *International reviews of immunology,* 15**,** 33-52.

Fuxa, M., Skok, J., Souabni, A., Salvagiotto, G., Roldan, E. & Busslinger, M. 2004. Pax5 induces V-to-DJ rearrangements and locus contraction of the immunoglobulin heavy-chain gene. *Genes & development,* 18**,** 411-422.

Galibert, L., Burdin, N., De Saint-Vis, B., Garrone, P., Van Kooten, C., Banchereau, J. & Rousset, F. 1996. CD40 and B cell antigen receptor dual triggering of resting B lymphocytes turns on a partial germinal center phenotype. *Journal of Experimental Medicine,* 183**,** 77-85.

Ganju, R. K., Brubaker, S. A., Meyer, J., Dutt, P., Yang, Y., Qin, S., Newman, W. & Groopman, J. E. 1998. The α-Chemokine, Stromal Cell-derived Factor-1α, Binds to the Transmembrane G-protein-coupled CXCR-4 Receptor and Activates Multiple Signal Transduction Pathways. *Journal of Biological Chemistry,* 273**,** 23169-23175.

Garcia-Blanco, M. A., Baraniak, A. P. & Lasda, E. L. 2004. Alternative splicing in disease and therapy. *Nature Biotechnology,* 22**,** 535.

García-Sanz, R., Jiménez, C., Puig, N., Paiva, B., Gutiérrez, N. C., Rodríguez-Otero, P., Almeida, J., San Miguel, J., Orfão, A., González, M. & Pérez-Andrés, M. 2016. Origin of Waldenstrom's macroglobulinaemia. *Best Practice & Research Clinical Haematology,* 29**,** 136-147.

Gardam, S., Sierro, F., Basten, A., Mackay, F. & Brink, R. 2008. TRAF2 and TRAF3 Signal Adapters Act Cooperatively to Control the Maturation and Survival Signals Delivered to B Cells by the BAFF Receptor. *Immunity,* 28**,** 391-401.

Garrett-Sinha, L. A., Su, G. H., Rao, S., Kabak, S., Hao, Z., Clark, M. R. & Simon, M. C. 1999. PU.1 and Spi-B Are Required for Normal B Cell Receptor–Mediated Signal Transduction. *Immunity,* 10**,** 399-408.

Gaudette, B. T., Dwivedi, B., Chitta, K. S., Poulain, S., Powell, D., Vertino, P., Leleu, X., Lonial, S., Chanan-Khan, A. A. & Kowalski, J. 2016. Low expression of pro-apoptotic Bcl-2 family proteins sets the apoptotic threshold in Waldenström macroglobulinemia. *Oncogene,* 35**,** 479.

Gay, N. J., Gangloff, M. & O'neill, L. A. 2011. What the Myddosome structure tells us about the initiation of innate immunity. *Trends Immunol,* 32**,** 104-9.

Gertz, M. A., Rue, M., Blood, E., Kaminer, L. S., Vesole, D. H. & Greipp, P. R. 2004. Multicenter phase 2 trial of rituximab for Waldenström macroglobulinemia (WM): an Eastern Cooperative Oncology Group Study (E3A98). *Leukemia & lymphoma,* 45**,** 2047-2055.

Ghobrial, I. M., Zhang, Y., Liu, Y., Ngo, H., Azab, F., Sacco, A., Azab, A., Maiso, P., Morgan, B., Quang, P., Issa, G. C., Leleu, X. & Roccaro, A. M. 2011. Targeting the bone marrow in Waldenstrom macroglobulinemia. *Clinical lymphoma, myeloma & leukemia,* 11 Suppl 1**,** S65-S69.

Glodek, A. M., Honczarenko, M., Le, Y., Campbell, J. J. & Silberstein, L. E. 2003. Sustained Activation of Cell Adhesion Is a Differentially Regulated Process in B Lymphopoiesis. *The Journal of Experimental Medicine,* 197**,** 461.

Green, D. R. & Scott, D. W. 1994. Activation-induced apoptosis in lymphocytes. *Current Opinion in Immunology,* 6**,** 476-487.

Gricks, C. S., Zahrieh, D., Zauls, A. J., Gorgun, G., Drandi, D., Mauerer, K., Neuberg, D. & Gribben, J. G. 2004. Differential regulation of gene expression following CD40 activation of leukemic compared to healthy B cells. *Blood,* 104**,** 4002.

Gustine, J. N., Meid, K., Dubeau, T., Yang, G., Xu, L., Hunter, Z. R. & Treon, S. P. 2017. Idelalisib in Waldenström macroglobulinemia: high incidence of hepatotoxicity AU - Castillo, Jorge J. *Leukemia & Lymphoma,* 58**,** 1002-1004.

Halliley, Jessica l., Tipton, Christopher m., Liesveld, J., Rosenberg, Alexander f., Darce, J., Gregoretti, Ivan v., Popova, L., Kaminiski, D., Fucile, Christopher f., Albizua, I., Kyu, S., Chiang, K.-Y., Bradley, Kyle t., Burack, R., Slifka, M., Hammarlund, E., Wu, H., Zhao, L., Walsh, Edward e., Falsey, Ann r., Randall, Troy d., Cheung, Wan c., Sanz, I. & Lee, F. E.-H. 2015. Long-Lived Plasma Cells Are Contained within the CD19−CD38hiCD138+ Subset in Human Bone Marrow. *Immunity,* 43**,** 132-145.

Hammer, R. D., Glick, A. D., Greer, J. P., Collins, R. D. & Cousar, J. B. 1996. Splenic Marginal Zone Lymphoma: A Distinct B-Cell Neoplasm. *The American Journal of Surgical Pathology,* 20**,** 613-626.

Hardiman, G., Rock, F. L., Balasubramanian, S., Kastelein, R. A. & Bazan, J. F. 1996. Molecular characterization and modular analysis of human MyD88. *Oncogene,* 13**,** 2467-75.

Harding, H. P., Novoa, I., Zhang, Y., Zeng, H., Wek, R., Schapira, M. & Ron, D. 2000. Regulated translation initiation controls stress-induced gene expression in mammalian cells. *Molecular cell,* 6**,** 1099-1108.

Hardy, M. P. & O'neill, L. A. 2004. The murine IRAK2 gene encodes four alternatively spliced isoforms, two of which are inhibitory. *Journal of Biological Chemistry,* 279**,** 27699-27708.

Haribabu, B., Richardson, R. M., Fisher, I., Sozzani, S., Peiper, S. C., Horuk, R., Ali, H. & Snyderman, R. 1997. Regulation of Human Chemokine Receptors CXCR4: Role of phosphorylation in desensitization and internalization. . *Journal of Biological Chemistry,* 272**,** 28726-28731.

Hasan, U., Chaffois, C., Gaillard, C., Saulnier, V., Merck, E., Tancredi, S., Guiet, C., Briere, F., Vlach, J., Lebecque, S., Trinchieri, G. & Bates, E. E. 2005. Human TLR10 is a functional receptor, expressed by B cells and plasmacytoid dendritic cells, which activates gene transcription through MyD88. *J Immunol,* 174**,** 2942-50.

Havens, M. A. & Hastings, M. L. 2016. Splice-switching antisense oligonucleotides as therapeutic drugs. *Nucleic acids research,* 44**,** 6549-6563.

Haxhinasto, S. A. & Bishop, G. A. 2004. Synergistic B Cell Activation by CD40 and the B Cell Antigen Receptor: Role of B lymphocyte antigen receptor-mediated kinase activation and tumor necrosis factor receptor-associated factor regulation *Journal of Biological Chemistry,* 279**,** 2575-2582.

Haxhinasto, S. A., Hostager, B. S. & Bishop, G. A. 2002. Cutting Edge: Molecular Mechanisms of Synergy Between CD40 and the B Cell Antigen Receptor: Role for TNF Receptor-Associated Factor 2 in Receptor Interaction. *The Journal of Immunology,* 169**,** 1145.

Hayashi, F., Smith, K. D., Ozinsky, A., Hawn, T. R., Yi, E. C., Goodlett, D. R., Eng, J. K., Akira, S., Underhill, D. M. & Aderem, A. 2001. The innate immune response to bacterial flagellin is mediated by Toll-like receptor 5. *Nature,* 410**,** 1099-103.

He, B., Chadburn, A., Jou, E., Schattner, E. J., Knowles, D. M. & Cerutti, A. 2004a. Lymphoma B Cells Evade Apoptosis through the TNF Family Members BAFF/BLyS and APRIL. *The Journal of Immunology,* 172**,** 3268.

He, B., Qiao, X. & Cerutti, A. 2004b. CpG DNA Induces IgG Class Switch DNA Recombination by Activating Human B Cells through an Innate Pathway That Requires TLR9 and Cooperates with IL-10. *The Journal of Immunology,* 173**,** 4479.

He, L. & Hannon, G. J. 2004. MicroRNAs: small RNAs with a big role in gene regulation. *Nature Reviews Genetics,* 5**,** 522.

Heil, F., Hemmi, H., Hochrein, H., Ampenberger, F., Kirschning, C., Akira, S., Lipford, G., Wagner, H. & Bauer, S. 2004. Species-Specific Recognition of Single-Stranded RNA via Toll-like Receptor 7 and 8. *Science,* 303**,** 1526.

Helbig, G., Christopherson , K. W., Bhat-Nakshatri, P., Kumar, S., Kishimoto, H., Miller, K. D., Broxmeyer, H. E. & Nakshatri, H. 2003. NF-κ B Promotes Breast Cancer Cell Migration and Metastasis by Inducing the Expression of the Chemokine Receptor CXCR4. *Journal of Biological Chemistry,* 278**,** 21631-21638.

Hemmi, H., Kaisho, T., Takeuchi, O., Sato, S., Sanjo, H., Hoshino, K., Horiuchi, T., Tomizawa, H., Takeda, K. & Akira, S. 2002. Small anti-viral compounds activate immune cells via the TLR7 MyD88-dependent signaling pathway. *Nat Immunol,* 3.

Hemmi, H., Takeuchi, O., Kawai, T., Kaisho, T., Sato, S., Sanjo, H., Matsumoto, M., Hoshino, K., Wagner, H., Takeda, K. & Akira, S. 2000. A Toll-like receptor recognizes bacterial DNA. *Nature,* 408**,** 740.

Hernandez, P. A., Gorlin, R. J., Lukens, J. N., Taniuchi, S., Bohinjec, J., Francois, F., Klotman, M. E. & Diaz, G. A. 2003. Mutations in the chemokine receptor gene CXCR4 are associated with WHIM syndrome, a combined immunodeficiency disease. *Nature Genetics,* 34**,** 70.

Hinton, G. E. & Roweis, S. T. Stochastic neighbor embedding. Advances in neural information processing systems, 2003. 857-864.

Ho, A. W., Hatjiharissi, E., Ciccarelli, B. T., Branagan, A. R., Hunter, Z. R., Leleu, X., Tournilhac, O., Xu, L., Connor, K., Manning, R. J., Santos, D. D., Chemaly, M., Patterson, C. J., Soumerai, J. D., Munshi, N. C., Mcearchern, J. A., Law, C.-L., Grewal, I. S. & Treon, S. P. 2008. CD27-CD70 interactions in the pathogenesis of Waldenström macroglobulinemia. *Blood,* 112**,** 4683.

Honczarenko, M., Douglas, R. S., Mathias, C., Lee, B., Ratajczak, M. Z. & Silberstein, L. E. 1999. SDF-1 Responsiveness Does Not Correlate With CXCR4 Expression Levels of Developing Human Bone Marrow B Cells. *Blood,* 94**,** 2990.

Honczarenko, M., Le, Y., Glodek, A. M., Majka, M., Campbell, J. J., Ratajczak, M. Z. & Silberstein, L. E. 2002. CCR5-binding chemokines modulate CXCL12 (SDF-1)–induced responses of progenitor B cells in human bone marrow through heterologous desensitization of the CXCR4 chemokine receptor. *Blood,* 100**,** 2321.

Horcher, M., Souabni, A. & Busslinger, M. 2001. Pax5/BSAP Maintains the Identity of B Cells in Late B Lymphopoiesis. *Immunity,* 14**,** 779-790.

Hornung, V., Rothenfusser, S., Britsch, S., Krug, A., Jahrsdörfer, B., Giese, T., Endres, S. & Hartmann, G. 2002. Quantitative Expression of Toll-Like Receptor 1–10 mRNA in Cellular

Subsets of Human Peripheral Blood Mononuclear Cells and Sensitivity to CpG Oligodeoxynucleotides. *The Journal of Immunology,* 168**,** 4531.

Hoshino, K., Takeuchi, O., Kawai, T., Sanjo, H., Ogawa, T., Takeda, Y., Takeda, K. & Akira, S. 1999. Cutting edge: Toll-like receptor 4 (TLR4)-deficient mice are hyporesponsive to lipopolysaccharide: evidence for TLR4 as the Lps gene product. *The Journal of Immunology,* 162**,** 3749-3752.

Howard, M., Grimaldi, J. C., Bazan, J. F., Lund, F. E., Santos-Argumedo, L., Parkhouse, R. M., Walseth, T. F. & Lee, H. C. 1993. Formation and hydrolysis of cyclic ADP-ribose catalyzed by lymphocyte antigen CD38. *Science,* 262**,** 1056.

Huggins, J., Pellegrin, T., Felgar, R. E., Wei, C., Brown, M., Zheng, B., Milner, E. C. B., Bernstein, S. H., Sanz, I. & Zand, M. S. 2006. CpG DNA activation and plasma cell differentiation of CD27<sup>-</sup> naive human B cells. *Blood*.

Hunter, Z., Liu, X., Xu, L., Yang, G., Tripsas, C. K., Manning, R., Patterson, C. & Treon, S. P. 2013. Somatic Activating Mutations In CXCR4 Are Common In Patients With Waldenstrom's Macroglobulinemia, and Their Expression In WM Cells Promotes Resistance To Ibrutinib. *Blood,* 122**,** 4424.

Hunter, Z. R., Xu, L., Yang, G., Tsakmaklis, N., Vos, J. M., Liu, X., Chen, J., Manning, R. J., Chen, J. G. & Brodsky, P. 2016. Transcriptome sequencing reveals a profile that corresponds to genomic variants in Waldenström macroglobulinemia. *Blood,* 128**,** 827-838.

Hunter, Z. R., Xu, L., Yang, G., Zhou, Y., Liu, X., Cao, Y., Manning, R. J., Tripsas, C., Patterson, C. J., Sheehy, P. & Treon, S. P. 2014. The genomic landscape of Waldenstrom macroglobulinemia is characterized by highly recurring MYD88 and WHIM-like CXCR4 mutations, and small somatic deletions associated with B-cell lymphomagenesis. *Blood,* 123**,** 1637-46.

Inoue, S., Leitner, W. W., Golding, B. & Scott, D. 2006. Inhibitory effects of B cells on antitumor immunity. *Cancer Res,* 66**,** 7741-7.

Ise, M., Matsubayashi, K., Tsujimura, H. & Kumagai, K. 2016. Loss of CD38 Expression in Relapsed Refractory Multiple Myeloma. *Clinical Lymphoma Myeloma and Leukemia,* 16**,** e59-e64.

Ishida, Y., Agata, Y., Shibahara, K. & Honjo, T. 1992. Induced expression of PD-1, a novel member of the immunoglobulin gene superfamily, upon programmed cell death. *The EMBO journal,* 11**,** 3887-3895.

J Banchereau, F Bazan, D Blanchard, F Briè, J P Galizzi, C Van Kooten, Y J Liu, F Rousset, A. & Saeland, S. 1994. The CD40 Antigen and its Ligand. *Annual Review of Immunology,* 12**,** 881-926.

Jalali, S., Price-Troska, T., Paludo, J., Villasboas, J., Kim, H.-J., Yang, Z.-Z., Novak, A. J. & Ansell, S. M. 2018. Soluble PD-1 ligands regulate T-cell function in Waldenstrom macroglobulinemia. *Blood advances,* 2**,** 1985-1997.

Jani, P., Vissing, M. B., Ahmed, S., Sluzevich, J. C., Aulakh, S., Alegria, V., Ailawadhi, M., Chanan-Khan, A. & Ailawadhi, S. 2018. Ibrutinib for the Management of Schnitzler Syndrome: A Novel Therapy for a Rare Condition. *Journal of Oncology Practice,* 14**,** 387-388.

Janssen, W. J. & Alper, S. Modulating MyD88 pre-mRNA Splicing to Treat Inflammatory Lung Diseases. *B80-A. Mechanisms and models of acute lung injury.*

Janssens, S. & Beyaert, R. 2002. A universal role for MyD88 in TLR/IL-1R-mediated signaling. *Trends Biochem Sci,* 27**,** 474-82.

Janssens, S., Burns, K., Tschopp, J. & Beyaert, R. 2002. Regulation of interleukin-1-and lipopolysaccharide-induced NF-κB activation by alternative splicing of MyD88. *Current Biology,* 12**,** 467-471.

Janssens, S., Burns, K., Vercammen, E., Tschopp, J. & Beyaert, R. 2003. MyD88S, a splice variant of MyD88, differentially modulates NF-kappaB- and AP-1-dependent gene expression. *FEBS Lett,* 548**,** 103-7.

Jefferies , C. A., Doyle , S., Brunner , C., Dunne, A., Brint, E., Wietek, C., Walch, E., Wirth, T. & O'neill, L. a. J. 2003. Bruton's Tyrosine Kinase Is a Toll/Interleukin-1 Receptor Domain-binding Protein That Participates in Nuclear Factor κB Activation by Toll-like Receptor 4. *Journal of Biological Chemistry,* 278**,** 26258-26264.

Jimenez, C., Sebastian, E., Chillon, M. C., Giraldo, P., Mariano Hernandez, J., Escalante, F., Gonzalez-Lopez, T. J., Aguilera, C., De Coca, A. G., Murillo, I., Alcoceba, M., Balanzategui, A., Sarasquete, M. E., Corral, R., Marin, L. A., Paiva, B., Ocio, E. M., Gutierrez, N. C., Gonzalez, M., San Miguel, J. F. & Garcia-Sanz, R. 2013. MYD88 L265P is a marker highly characteristic of, but not restricted to, Waldenstrom's macroglobulinemia. *Leukemia,* 27**,** 1722-8.

Jin, M. S. & Lee, J.-O. 2008. Structures of the Toll-like Receptor Family and Its Ligand Complexes. *Immunity,* 29**,** 182-191.

John, S. A., Clements, J. L., Russell, L. M. & Garrett-Sinha, L. A. 2008. Ets-1 regulates plasma cell differentiation by interfering with the activity of the transcription factor Blimp-1. *Journal of Biological Chemistry,* 283**,** 951-962.

Jourdan, M., Caraux, A., De Vos, J., Fiol, G., Larroque, M., Cognot, C., Bret, C., Duperray, C., Hose, D. & Klein, B. 2009. An in vitro model of differentiation of memory B cells into plasmablasts and plasma cells including detailed phenotypic and molecular characterization. *Blood,* 114**,** 5173.

Jung, J., Choe, J., Li, L. & Choi, Y. S. 2000. Regulation of CD27 expression in the course of germinal center B cell differentiation: the pivotal role of IL-10. *European journal of immunology,* 30**,** 2437-2443.

Kallies, A., Hasbold, J., Fairfax, K., Pridans, C., Emslie, D., Mckenzie, B. S., Lew, A. M., Corcoran, L. M., Hodgkin, P. D., Tarlinton, D. M. & Nutt, S. L. 2007. Initiation of Plasma-Cell Differentiation Is Independent of the Transcription Factor Blimp-1. *Immunity,* 26**,** 555-566.

Kastritis, E., Gavriatopoulou, M., Kyrtsonis, M.-C., Roussou, M., Hadjiharissi, E., Symeonidis, A., Repoussis, P., Michalis, E., Delimpasi, S. & Tsatalas, K. 2015. Dexamethasone, rituximab, and cyclophosphamide as primary treatment of Waldenström macroglobulinemia: final analysis of a phase 2 study. *Blood,* 126**,** 1392.

Kawai, T. & Akira, S. 2007. Signaling to NF-κB by Toll-like receptors. *Trends in Molecular Medicine,* 13**,** 460-469.

Kern, C., Cornuel, J.-F., Billard, C., Tang, R., Rouillard, D., Stenou, V., Defrance, T., Ajchenbaum-Cymbalista, F., Simonin, P.-Y., Feldblum, S. & Kolb, J.-P. 2004. Involvement of BAFF and APRIL in the resistance to apoptosis of B-CLL through an autocrine pathway. *Blood,* 103**,** 679.

Khotskaya, Y. B., Dai, Y., Ritchie, J. P., Macleod, V., Yang, Y., Zinn, K. & Sanderson, R. D. 2009. Syndecan-1 is required for robust growth, vascularization, and metastasis of myeloma tumors in vivo. *Journal of Biological Chemistry,* 284**,** 26085-26095.

Kim, Y.-M., Brinkmann, M. M., Paquet, M.-E. & Ploegh, H. L. 2008. UNC93B1 delivers nucleotide-sensing toll-like receptors to endolysosomes. *Nature,* 452**,** 234.

Klein, U., Casola, S., Cattoretti, G., Shen, Q., Lia, M., Mo, T., Ludwig, T., Rajewsky, K. & Dalla-Favera, R. 2006. Transcription factor IRF4 controls plasma cell differentiation and class-switch recombination. *Nature immunology,* 7**,** 773.

Klein, U., Rajewsky, K. & Küppers, R. 1998. Human Immunoglobulin (Ig)M+IgD+ Peripheral Blood B Cells Expressing the CD27 Cell Surface Antigen Carry Somatically Mutated Variable Region Genes: CD27 as a General Marker for Somatically Mutated (Memory) B Cells. *The Journal of Experimental Medicine,* 188**,** 1679.

Knittel, G., Liedgens, P., Korovkina, D., Seeger, J. M., Al-Baldawi, Y., Al-Maarri, M., Fritz, C., Vlantis, K., Bezhanova, S., Scheel, A. H., Wolz, O. O., Reimann, M., Moller, P., Lopez, C., Schlesner, M., Lohneis, P., Weber, A. N., Trumper, L., Staudt, L. M., Ortmann, M., Pasparakis, M., Siebert, R., Schmitt, C. A., Klatt, A. R., Wunderlich, F. T., Schafer, S. C., Persigehl, T., Montesinos-Rongen, M., Odenthal, M., Buttner, R., Frenzel, L. P., Kashkar, H. & Reinhardt, H. C. 2016. B-cell-specific conditional expression of Myd88p.L252P leads to the development of diffuse large B-cell lymphoma in mice. *Blood,* 127**,** 2732-41.

Kollewe, C., Mackensen, A.-C., Neumann, D., Knop, J., Cao, P., Li, S., Wesche, H. & Martin, M. U. 2004. Sequential Autophosphorylation Steps in the Interleukin-1 Receptor-associated

Kinase-1 Regulate its Availability as an Adapter in Interleukin-1 Signaling. *Journal of Biological Chemistry,* 279**,** 5227-5236.

Konoplev, S., Medeiros, L. J., Bueso-Ramos, C. E., Jorgensen, J. L. & Lin, P. 2005. Immunophenotypic profile of lymphoplasmacytic lymphoma/Waldenström macroglobulinemia. *American Journal of Clinical Pathology,* 124**,** 414-420.

Kost, C. B., Holden, J. T. & Mann, K. P. 2008. Marginal zone B-cell lymphoma: A retrospective immunophenotypic analysis. *Cytometry Part B: Clinical Cytometry,* 74B**,** 282-286.

Kotecha, N., Krutzik, P. O. & Irish, J. M. 2010. Web-Based Analysis and Publication of Flow Cytometry Experiments. *Current Protocols in Cytometry,* 53**,** 10.17.1-10.17.24.

Kozmik, Z., Wang, S., Dörfler, P., Adams, B. & Busslinger, M. 1992. The promoter of the CD19 gene is a target for the B-cell-specific transcription factor BSAP. *Molecular and cellular biology,* 12**,** 2662-2672.

Krammer, P. H. 2000. CD95's deadly mission in the immune system. *Nature,* 407**,** 789-95.

Kriangkum, J., Taylor, B., Treon, S., J Mant, M., Belch, A. & M Pilarski, L. 2004a. *Clonotypic IgM V/D/J sequence analysis in Waldenstrom macroglobulinemia suggests an unusual B-cell origin and an of polyclonal B cells in peripheral blood*.

Kriangkum, J., Taylor, B. J., Treon, S. P., Mant, M. J., Belch, A. R. & Pilarski, L. M. 2004b. Clonotypic IgM V/D/J sequence analysis in Waldenstrom macroglobulinemia suggests an unusual B-cell origin and an expansion of polyclonal B cells in peripheral blood. *Blood,* 104**,** 2134-42.

Krupa, A., Fudala, R., Florence, J. M., Tucker, T., Allen, T. C., Standiford, T. J., Luchowski, R., Fol, M., Rahman, M. & Gryczynski, Z. 2013. Bruton's tyrosine kinase mediates FcγRIIa/Toll-like receptor–4 receptor crosstalk in human neutrophils. *American journal of respiratory cell and molecular biology,* 48**,** 240-249.

Kukreja, P., Abdel-Mageed, A., Mondal, D., Liu, K. & C Agrawal, K. 2005. *Up-regulation of CXCR4 Expression in PC-3 Cells by Stromal-Derived Factor-1 (CXCL12) Increases Endothelial Adhesion and Transendothelial Migration: Role of MEK/ERK Signaling Pathway-Dependent NF- B Activation*.

Kuppers, R. 2005. Mechanisms of B-cell lymphoma pathogenesis. *Nat Rev Cancer,* 5**,** 251-262.

Kuraoka, M., Snowden, P. B., Nojima, T., Verkoczy, L., Haynes, B. F., Kitamura, D. & Kelsoe, G. 2017. BCR and Endosomal TLR Signals Synergize to Increase AID Expression and Establish Central B Cell Tolerance. *Cell Rep,* 18**,** 1627-1635.

Kyle, R. A., Therneau, T. M., Rajkumar, S. V., Remstein, E. D., Offord, J. R., Larson, D. R., Plevak, M. F. & Melton, L. J., 3rd 2003. Long-term follow-up of IgM monoclonal gammopathy of undetermined significance. *Blood,* 102**,** 3759-64.

Kyriakou, C., Boumendil, A., Finel, H., Vernant, J.-P., Cornelissen, J. J., Thieblemont, C., Chevallier, P., Hamladji, R.-M., Mufti, G. J., Mazza, P., Zachee, P., Niederwieser, D., Sureda, A., Montoto, S. & Dreger, P. 2014. Autologous Stem Cell Transplantation (ASCT) for the Treatment of Patients with Waldenstrom's Macroglobulinemia / Lymphoplasmacytic Lymphoma (WM/LPL). a Risk Factor Analysis By the European Society for Blood and Marrow Transplantation (EBMT) Lymphoma Working Party. *Blood,* 124**,** 678.

Lagresle, C., Mondière, P., Bella, C., Krammer, P. H. & Defrance, T. 1996. Concurrent engagement of CD40 and the antigen receptor protects naive and memory human B cells from APO-1/Fas-mediated apoptosis. *The Journal of Experimental Medicine,* 183**,** 1377.

Latchman, Y., Wood, C. R., Chernova, T., Chaudhary, D., Borde, M., Chernova, I., Iwai, Y., Long, A. J., Brown, J. A., Nunes, R., Greenfield, E. A., Bourque, K., Boussiotis, V. A., Carter, L. L., Carreno, B. M., Malenkovich, N., Nishimura, H., Okazaki, T., Honjo, T., Sharpe, A. H. & Freeman, G. J. 2001. PD-L2 is a second ligand for PD-1 and inhibits T cell activation. *Nature Immunology,* 2**,** 261.

Leadbetter, E. A., Rifkin, I. R., Hohlbaum, A. M., Beaudette, B. C., Shlomchik, M. J. & Marshak-Rothstein, A. 2002. Chromatin–IgG complexes activate B cells by dual engagement of IgM and Toll-like receptors. *Nature,* 416**,** 603.

Lederman, S., Yellin, M. J., Krichevsky, A., Belko, J., Lee, J. J. & Chess, L. 1992. Identification of a novel surface protein on activated CD4+ T cells that induces contact-dependent B cell differentiation (help). *The Journal of Experimental Medicine,* 175**,** 1091.

Lee, B., Sharron, M., Montaner, L. J., Weissman, D. & Doms, R. W. 1999. Quantification of CD4, CCR5, and CXCR4 levels on lymphocyte subsets, dendritic cells, and differentially conditioned monocyte-derived macrophages. *Proceedings of the National Academy of Sciences,* 96**,** 5215.

Lee, J., Chuang, T.-H., Redecke, V., She, L., Pitha, P. M., Carson, D. A., Raz, E. & Cottam, H. B. 2003. Molecular basis for the immunostimulatory activity of guanine nucleoside analogs: activation of Toll-like receptor 7. *Proceedings of the National Academy of Sciences of the United States of America,* 100**,** 6646-6651.

Lee, K., Tirasophon, W., Shen, X., Michalak, M., Prywes, R., Okada, T., Yoshida, H., Mori, K. & Kaufman, R. J. 2002. IRE1-mediated unconventional mRNA splicing and S2P-mediated ATF6 cleavage merge to regulate XBP1 in signaling the unfolded protein response. *Genes & development,* 16**,** 452-466.

Leleu, X., Jia, X., Runnels, J., Ngo, H. T., Moreau, A.-S., Farag, M., Spencer, J. A., Pitsillides, C. M., Hatjiharissi, E., Roccaro, A., Sullivan, G., Mcmillin, D. W., Moreno, D., Kiziltepe, T., Carrasco, R., Treon, S. P., Hideshima, T., Anderson, K. C., Lin, C. P. & Ghobrial, I. M. 2007. The Akt pathway regulates survival and homing in Waldenstrom macroglobulinemia. *Blood,* 110**,** 4417.

Leleu, X., Ngo, H., Runnels, J., Pitsillides, C., Spencer, J., Moreau, A.-S., Hatjiharisi, E., Jia, X., O'sullivan, G., Treon, S., Hideshima, T., Lin, C., Anderson, K. & Ghobrial, I. 2006. The PI3K/Akt Pathway Is an Important Regulator of Homing and Adhesion in Waldenstrom's Macroglobulinemia. *Blood,* 108**,** 2417.

Li, B. & Dewey, C. N. 2011. RSEM: accurate transcript quantification from RNA-Seq data with or without a reference genome. *BMC Bioinformatics,* 12**,** 323.

Li, C., Zienkiewicz, J. & Hawiger, J. 2005. Interactive Sites in the MyD88 Toll/Interleukin (IL) 1 Receptor Domain Responsible for Coupling to the IL1β Signaling Pathway. *Journal of Biological Chemistry,* 280**,** 26152-26159.

Li, H., Ayer, L. M., Lytton, J. & Deans, J. P. 2003. Store-operated Cation Entry Mediated by CD20 in Membrane Rafts. *Journal of Biological Chemistry,* 278**,** 42427-42434.

Li, J., Sze, D. M. Y., Brown, R. D., Cowley, M. J., Kaplan, W., Mo, S.-L., Yang, S., Aklilu, E., Kabani, K., Loh, Y. S., Yamagishi, T., Chen, Y., Ho, P. J. & Joshua, D. E. 2010. Clonal expansions of cytotoxic T cells exist in the blood of patients with Waldenström macroglobulinemia but exhibit anergic properties and are eliminated by nucleoside analogue therapy. *Blood,* 115**,** 3580.

Li, Q. & Verma, I. M. 2002. NF-κB regulation in the immune system. *Nat Rev Immunol,* 2.

Liang, X., Moseman, E. A., Farrar, M. A., Bachanova, V., Weisdorf, D. J., Blazar, B. R. & Chen, W. 2010. Toll-like receptor 9 signaling by CpG-B oligodeoxynucleotides induces an apoptotic pathway in human chronic lymphocytic leukemia B cells. *Blood,* 115**,** 5041-52.

Liao, G., Zhang, M., Harhaj, E. W. & Sun, S.-C. 2004. Regulation of the NF-κB-inducing Kinase by Tumor Necrosis Factor Receptor-associated Factor 3-induced Degradation. *Journal of Biological Chemistry,* 279**,** 26243-26250.

Lim, K.-H., Barton, G. M. & Staudt, L. M. 2013. Abstract 2332: Oncogenic MYD88 mutants require Toll-like receptors. *Cancer Research,* 73**,** 2332.

Lim, W., Shumak, K. H., Reis, M., Perez-Ordonez, B., Sauder, D., Fam, A. & Imrie, K. R. 2002. Malignant evolution of Schnitzler's syndrome--chronic urticaria and IgM monoclonal gammopathy: report of a new case and review of the literature. *Leuk Lymphoma,* 43**,** 181-6.

Lin, K.-I., Angelin-Duclos, C., Kuo, T. C. & Calame, K. 2002. Blimp-1-Dependent Repression of Pax-5 Is Required for Differentiation of B Cells to Immunoglobulin M-Secreting Plasma Cells. *Molecular and Cellular Biology,* 22**,** 4771.

Lin, S.-C., Lo, Y.-C. & Wu, H. 2010. Helical assembly in the MyD88–IRAK4–IRAK2 complex in TLR/IL-1R signalling. *Nature,* 465**,** 885.

Lin, Y., Wong, K.-K. & Calame, K. 1997. Repression of c-myc transcription by Blimp-1, an inducer of terminal B cell differentiation. *Science,* 276**,** 596.

Lipsker, D. 2010. The Schnitzler syndrome. *Orphanet Journal of Rare Diseases,* 5**,** 38-38.

Liu, X., Zhan, Z., Li, D., Xu, L., Ma, F., Zhang, P., Yao, H. & Cao, X. 2011. Intracellular MHC class II molecules promote TLR-triggered innate immune responses by maintaining activation of the kinase Btk. *Nature Immunology,* 12**,** 416.

Liu, X., Zhou, Y., Xu, L., Cao, Y., Manning, R., Patterson, C., Tripsas, C. K., Hunter, Z., Buhrlage, S., Gray, N. S. & Treon, S. P. 2013. PI3K/AKT Pathway Is Activated By MYD88 L265P and Use Of PI3K-Delta Inhibitors Induces Robust Tumor Cell Killing In Waldenstrom's Macroglobulinemia. *Blood,* 122**,** 4255.

Liu, Y.-J., Zhang, J., Lane, P. J. L., Chan, E. Y. T. & Maclennan, I. C. M. 1991. Sites of specific B cell activation in primary and secondary responses to T cell-dependent and T cell-independent antigens. *European Journal of Immunology,* 21**,** 2951-2962.

Lohr, Jens g., Stojanov, P., Carter, Scott l., Cruz-Gordillo, P., Lawrence, Michael s., Auclair, D., Sougnez, C., Knoechel, B., Gould, J., Saksena, G., Cibulskis, K., Mckenna, A., Chapman, Michael a., Straussman, R., Levy, J., Perkins, Louise m., Keats, Jonathan j., Schumacher, Steven e., Rosenberg, M., Anderson, Kenneth c., Richardson, P., Krishnan, A., Lonial, S., Kaufman, J., Siegel, David s., Vesole, David h., Roy, V., Rivera, Candido e., Rajkumar, S. V., Kumar, S., Fonseca, R., Ahmann, Greg j., Bergsagel, P. L., Stewart, A. K., Hofmeister, Craig c., Efebera, Yvonne a., Jagannath, S., Chari, A., Trudel, S., Reece, D., Wolf, J., Martin, T., Zimmerman, T., Rosenbaum, C., Jakubowiak, Andrzej j., Lebovic, D., Vij, R., Stockerl-Goldstein, K., Getz, G. & Golub, T. R. 2014. Widespread Genetic Heterogeneity in Multiple Myeloma: Implications for Targeted Therapy. *Cancer Cell,* 25**,** 91-101.

Loiarro, M., Sette, C., Gallo, G., Ciacci, A., Fanto, N., Mastroianni, D., Carminati, P. & Ruggiero, V. 2005. Peptide-mediated interference of TIR domain dimerization in MyD88 inhibits interleukin-1-dependent activation of NF-{kappa}B. *J Biol Chem,* 280**,** 15809-14.

Loiarro, M., Volpe, E., Ruggiero, V., Gallo, G., Furlan, R., Maiorino, C., Battistini, L. & Sette, C. 2013. Mutational analysis identifies residues crucial for homodimerization of myeloid differentiation factor 88 (MyD88) and for its function in immune cells. *J Biol Chem,* 288**,** 30210-22.

Lokhorst, H. M., Plesner, T., Laubach, J. P., Nahi, H., Gimsing, P., Hansson, M., Minnema, M. C., Lassen, U., Krejcik, J., Palumbo, A., Van De Donk, N. W. C. J., Ahmadi, T., Khan, I., Uhlar, C. M., Wang, J., Sasser, A. K., Losic, N., Lisby, S., Basse, L., Brun, N. & Richardson, P. G. 2015. Targeting CD38 with Daratumumab Monotherapy in Multiple Myeloma. *New England Journal of Medicine,* 373**,** 1207-1219.

Love, M. I., Huber, W. & Anders, S. 2014. Moderated estimation of fold change and dispersion for RNA-seq data with DESeq2. *Genome Biol,* 15**,** 550.

Lund, F. E., Cockayne, D. A., Randall, T. D., Solvason, N., Schuber, F. & Howard, M. C. 1998. CD38: a new paradigm in lymphocyte activation and signal transduction. *Immunological reviews,* 161**,** 79-93.

Lund, F. E., Yu, N., Kim, K. M., Reth, M. & Howard, M. C. 1996. Signaling through CD38 augments B cell antigen receptor (BCR) responses and is dependent on BCR expression. *The Journal of Immunology,* 157**,** 1455.

Lwin, T., Hazlehurst, L. A., Li, Z., Dessureault, S., Sotomayor, E., Moscinski, L. C., Dalton, W. S. & Tao, J. 2007. Bone marrow stromal cells prevent apoptosis of lymphoma cells by upregulation of anti-apoptotic proteins associated with activation of NF-κB (RelB/p52) in non-Hodgkin's lymphoma cells. *Leukemia,* 21**,** 1521.

Maaten, L. V. D. & Hinton, G. 2008. Visualizing data using t-SNE. *Journal of machine learning research,* 9**,** 2579-2605.

Mackay, F., Schneider, P., Rennert, P. & Browning, J. 2003. BAFF AND APRIL: a tutorial on B cell survival. *Annu Rev Immunol,* 21**,** 231-64.

Maclennan, I. C., Toellner, K. M., Cunningham, A. F., Serre, K., Sze, D. M., Zuniga, E., Cook, M. C. & Vinuesa, C. G. 2003. Extrafollicular antibody responses. *Immunol Rev,* 194**,** 8-18.

Malavasi, F., Deaglio, S., Funaro, A., Ferrero, E., Horenstein, A. L., Ortolan, E., Vaisitti, T. & Aydin, S. 2008. Evolution and Function of the ADP Ribosyl Cyclase/CD38 Gene Family in Physiology and Pathology. *Physiological Reviews,* 88**,** 841-886.

Mandelbaum, J., Bhagat, G., Tang, H., Mo, T., Brahmachary, M., Shen, Q., Chadburn, A., Rajewsky, K., Tarakhovsky, A., Pasqualucci, L. & Dalla-Favera, R. 2010. BLIMP1 Is a Tumor Suppressor Gene Frequently Disrupted in Activated B Cell-like Diffuse Large B Cell Lymphoma. *Cancer Cell,* 18**,** 568-579.

Månsson, A., Adner, M., Höckerfelt, U. & Cardell, L.-O. 2006. A distinct Toll-like receptor repertoire in human tonsillar B cells, directly activated by Pam3CSK4, R-837 and CpG-2006 stimulation. *Immunology,* 118**,** 539-548.

Marcelli, C., Chappard, D., Rossi, J.-F., Jaubert, J., Alexandre, C., Dessauw, P., Baldet, P. & Bataille, R. 1988. Histologic evidence of an abnormal bone remodeling in b-cell malignancies other than multiple myeloma. *Cancer,* 62**,** 1163-1170.

Marsters, S. A., Yan, M., Pitti, R. M., Haas, P. E., Dixit, V. M. & Ashkenazi, A. 2000. Interaction of the TNF homologues BLyS and APRIL with the TNF receptor homologues BCMA and TACI. *Curr Biol,* 10**,** 785-8.

Martinez-Lopez, A., Curiel-Olmo, S., Mollejo, M., Cereceda, L., Martinez, N., Montes-Moreno, S., Almaraz, C., Revert, J. B. & Piris, M. A. 2015. MYD88 (L265P) Somatic Mutation in Marginal Zone B-cell Lymphoma. *The American Journal of Surgical Pathology,* 39**,** 644-651.

Matas-Céspedes, A., Vidal-Crespo, A., Rodriguez, V., Villamor, N., Delgado, J., Giné, E., Roca-Ho, H., Menéndez, P., Campo, E., López-Guillermo, A., Colomer, D., Roué, G., Wiestner, A., Parren, P. W. H. I., Doshi, P., Van Bueren, J. L. & Pérez-Galán, P. 2017. The Human CD38 Monoclonal Antibody Daratumumab Shows Antitumor Activity and Hampers Leukemia–Microenvironment Interactions in Chronic Lymphocytic Leukemia. *Clinical Cancer Research,* 23**,** 1493.

Matutes, E., Oscier, D., Montalban, C., Berger, F., Callet-Bauchu, E., Dogan, A., Felman, P., Franco, V., Iannitto, E., Mollejo, M., Papadaki, T., Remstein, E. D., Salar, A., Solé, F., Stamatopoulos, K., Thieblemont, C., Traverse-Glehen, A., Wotherspoon, A., Coiffier, B. & Piris, M. A. 2007. Splenic marginal zone lymphoma proposals for a revision of diagnostic, staging and therapeutic criteria. *Leukemia,* 22**,** 487.

Maurer, D., Fischer, G. F., Fae, I., Majdic, O., Stuhlmeier, K., Von Jeney, N., Holter, W. & Knapp, W. 1992. IgM and IgG but not cytokine secretion is restricted to the CD27+ B lymphocyte subset. *The Journal of Immunology,* 148**,** 3700.

Mccarron, M. J., Park, P. W. & Fooksman, D. R. 2017. CD138 mediates selection of mature plasma cells by regulating their survival. *Blood,* 129**,** 2749-2759.

Mccartney-Francis, N., Jin, W. & Wahl, S. M. 2004. Aberrant Toll receptor expression and endotoxin hypersensitivity in mice lacking a functional TGF-β1 signaling pathway. *The Journal of Immunology,* 172**,** 3814-3821.

Medzhitov, R., Preston-Hurlburt, P., Kopp, E., Stadlen, A., Chen, C., Ghosh, S. & Janeway, C. A., Jr. 1998. MyD88 is an adaptor protein in the hToll/IL-1 receptor family signaling pathways. *Mol Cell,* 2**,** 253-8.

Mei, H. E., Wirries, I., Frölich, D., Brisslert, M., Giesecke, C., Grün, J. R., Alexander, T., Schmidt, S., Luda, K., Kühl, A. A., Engelmann, R., Dürr, M., Scheel, T., Bokarewa, M., Perka, C., Radbruch, A. & Dörner, T. 2015. A unique population of IgG-expressing plasma cells lacking CD19 is enriched in human bone marrow. *Blood,* 125**,** 1739.

Miggin, S. M. & O'neill, L. a. J. 2006. New insights into the regulation of TLR signaling. *Journal of Leukocyte Biology,* 80**,** 220-226.

Minarik, J., Novak, M., Flodr, P., Balcarkova, J., Mlynarcikova, M., Krhovska, P., Pika, T., Pikalova, Z., Bacovsky, J. & Scudla, V. 2017. CD38-negative relapse in multiple myeloma after daratumumab-based chemotherapy. *European Journal of Haematology,* 99**,** 186-189.

Mineva, N. D., Rothstein, T. L., Meyers, J. A., Lerner, A. & Sonenshein, G. E. 2007. CD40 Ligand-mediated Activation of the de Novo RelB NF-κB Synthesis Pathway in Transformed B

Cells Promotes Rescue from Apoptosis. *Journal of Biological Chemistry,* 282**,** 17475-17485.

Möhle, R., Failenschmid, C., Bautz, F. & Kanz, L. 2000. *Overexpression of the chemokine receptor CXCR4 in B cell chronic lymphocytic leukemia is associated with increased functional response to stromal cell-derived factor-1 (SDF-1).*

Molina, T. J., Lin, P., Swerdlow, S. H. & Cook, J. R. 2011. Marginal Zone Lymphomas With Plasmacytic Differentiation and Related Disorders. *American Journal of Clinical Pathology,* 136**,** 211-225.

Mollejo, M., Menárguez, J., Lloret, E., Sánchez, A., Campo, E., Algara, P., Cristóbal, E., Sánchez, E. & Piris, M. A. 1995. Splenic marginal zone lymphoma: a distinctive type of low-grade B-cell lymphoma. A clinicopathological study of 13 cases. *The American journal of surgical pathology,* 19**,** 1146-1157.

Mond, J. J., Lees, A. & Snapper, C. M. 1995. T cell-independent antigens type 2. *Annual review of immunology,* 13**,** 655-692.

Morbach, H., Eichhorn, E. M., Liese, J. G. & Girschick, H. J. 2010. Reference values for B cell subpopulations from infancy to adulthood. *Clinical and experimental immunology,* 162**,** 271-279.

Moreau, P., Robillard, N., Jégo, G., Pellat, C., Gouill, S. L., Thoumi, S., Avet-Loiseau, H., Harousseau, J.-L. & Bataille, R. 2006. Lack of CD27 in myeloma delineates different presentation and outcome. *British Journal of Haematology,* 132**,** 168-170.

Moreaux, J., Legouffe, E., Jourdan, E., Quittet, P., Rème, T., Lugagne, C., Moine, P., Rossi, J.-F., Klein, B. & Tarte, K. 2004. BAFF and APRIL protect myeloma cells from apoptosis induced by interleukin 6 deprivation and dexamethasone. *Blood,* 103**,** 3148.

Moreno-García, M. E., López-Bojórques, L. N., Zentella, A., Humphries, L. A., Rawlings, D. J. & Santos-Argumedo, L. 2005. CD38 signaling regulates B lymphocyte activation via a phospholipase C (PLC)-γ2-independent, protein kinase C, phosphatidylcholine-PLC, and phospholipase D-dependent signaling cascade. *The Journal of Immunology,* 174**,** 2687-2695.

Morrison, M. D., Reiley, W., Zhang, M. & Sun, S.-C. 2005. An Atypical Tumor Necrosis Factor (TNF) Receptor-associated Factor-binding Motif of B Cell-activating Factor Belonging to the TNF Family (BAFF) Receptor Mediates Induction of the Noncanonical NF-κB Signaling Pathway. *Journal of Biological Chemistry,* 280**,** 10018-10024.

Mosier, D., Mond, J. & Goldings, E. 1977. The ontogeny of thymic independent antibody responses in vitro in normal mice and mice with an X-linked B cell defect. *The Journal of Immunology,* 119**,** 1874-1878.

Motshwene, P. G., Moncrieffe, M. C., Grossmann, J. G., Kao, C., Ayaluru, M., Sandercock, A. M., Robinson, C. V., Latz, E. & Gay, N. J. 2009. An Oligomeric Signaling Platform Formed by the Toll-like Receptor Signal Transducers MyD88 and IRAK-4. *Journal of Biological Chemistry,* 284**,** 25404-25411.

Mueller, C. G., Boix, C., Kwan, W.-H., Daussy, C., Fournier, E., Fridman, W. H. & Molina, T. J. 2007. Critical role of monocytes to support normal B cell and diffuse large B cell lymphoma survival and proliferation. *Journal of Leukocyte Biology,* 82**,** 567-575.

Mundy, G. R., Raisz, L. G., Cooper, R. A., Schechter, G. P. & Salmon, S. E. 1974. Evidence for the Secretion of an Osteoclast Stimulating Factor in Myeloma. *New England Journal of Medicine,* 291**,** 1041-1046.

Munshi, M., Liu, X., Chen, J., Xu, L., Tsakmaklis, N., Demos, M., Kofides, A., Guerrera, M. L., Chan, G. & Hunter, Z. 2017. Mutated MYD88 Activates the BCR Component SYK and Provides a Rationale Therapeutic Target in Waldenstrom's Macroglobulinemia. Am Soc Hematology.

Muramatsu, M., Kinoshita, K., Fagarasan, S., Yamada, S., Shinkai, Y. & Honjo, T. 2000. Class Switch Recombination and Hypermutation Require Activation-Induced Cytidine Deaminase (AID), a Potential RNA Editing Enzyme. *Cell,* 102**,** 553-563.

Muzio, M., Bosisio, D., Polentarutti, N., D'amico, G., Stoppacciaro, A., Mancinelli, R., Van't Veer, C., Penton-Rol, G., Ruco, L. P., Allavena, P. & Mantovani, A. 2000. Differential Expression

and Regulation of Toll-Like Receptors (TLR) in Human Leukocytes: Selective Expression of TLR3 in Dendritic Cells. *The Journal of Immunology,* 164**,** 5998.

Nadler, L., Anderson, K., Marti, G., Bates, M., Park, E., Daley, J. & Schlossman, S. 1983. B4, a human B lymphocyte-associated antigen expressed on normal, mitogen-activated, and malignant B lymphocytes. *The Journal of Immunology,* 131**,** 244-250.

Nagata, S. 1997. Apoptosis by Death Factor. *Cell,* 88**,** 355-365.

Nagumo, H. & Agematsu, K. 1998. Synergistic augmentative effect of interleukin-10 and CD27/CD70 interactions on B-cell immunoglobulin synthesis. *Immunology,* 94**,** 388-394.

Nagumo, H., Agematsu, K., Shinozaki, K., Hokibara, S., Ito, S., Takamoto, M., Nikaido, T., Yasui, K., Uehara, Y., Yachie, A. & Komiyama, A. 1998. CD27/CD70 Interaction Augments IgE Secretion by Promoting the Differentiation of Memory B Cells into Plasma Cells. *The Journal of Immunology,* 161**,** 6496.

Nardelli, B., Belvedere, O., Roschke, V., Moore, P. A., Olsen, H. S., Migone, T. S., Sosnovtseva, S., Carrell, J. A., Feng, P., Giri, J. G. & Hilbert, D. M. 2001. Synthesis and release of B-lymphocyte stimulator from myeloid cells. *Blood,* 97**,** 198.

Ngo, H. T., Leleu, X., Lee, J., Jia, X., Melhem, M., Runnels, J., Moreau, A. S., Burwick, N., Azab, A. K., Roccaro, A., Azab, F., Sacco, A., Farag, M., Sackstein, R. & Ghobrial, I. M. 2008. SDF-1/CXCR4 and VLA-4 interaction regulates homing in Waldenstrom macroglobulinemia. *Blood,* 112**,** 150-8.

Ngo, V. N., Young, R. M., Schmitz, R., Jhavar, S., Xiao, W., Lim, K. H., Kohlhammer, H., Xu, W., Yang, Y., Zhao, H., Shaffer, A. L., Romesser, P., Wright, G., Powell, J., Rosenwald, A., Muller-Hermelink, H. K., Ott, G., Gascoyne, R. D., Connors, J. M., Rimsza, L. M., Campo, E., Jaffe, E. S., Delabie, J., Smeland, E. B., Fisher, R. I., Braziel, R. M., Tubbs, R. R., Cook, J. R., Weisenburger, D. D., Chan, W. C. & Staudt, L. M. 2011. Oncogenically active MYD88 mutations in human lymphoma. *Nature,* 470**,** 115-9.

Nijhof, I. S., Casneuf, T., Van Velzen, J., Van Kessel, B., Axel, A. E., Syed, K., Groen, R. W. J., Van Duin, M., Sonneveld, P., Minnema, M. C., Zweegman, S., Chiu, C., Bloem, A. C., Mutis, T., Lokhorst, H. M., Sasser, A. K. & Van De Donk, N. W. C. J. 2016. CD38 expression and complement inhibitors affect response and resistance to daratumumab therapy in myeloma. *Blood,* 128**,** 959.

Niscola, P., Scaramucci, L., Romani, C., Giovannini, M., Tendas, A., Brunetti, G., Cartoni, C., Palumbo, R., Vischini, G. & Siniscalchi, A. 2010. Pain management in multiple myeloma. *Expert review of anticancer therapy,* 10**,** 415-425.

Nishiya, T. & Defranco, A. L. 2004. Ligand-regulated Chimeric Receptor Approach Reveals Distinctive Subcellular Localization and Signaling Properties of the Toll-like Receptors. *Journal of Biological Chemistry,* 279**,** 19008-19017.

Norris, D. & Stone, J. 2008. WHO classification of tumours of haematopoietic and lymphoid tissues. *Geneva: WHO*.

Noubir, S., Hmama, Z. & Reiner, N. E. 2004. Dual Receptors and Distinct Pathways Mediate Interleukin-1 Receptor-associated Kinase Degradation in Response to Lipopolysaccharide: Involement of CD14/TLR4, CR3, and phosphatidylinositol 3-kinase. *Journal of Biological Chemistry,* 279**,** 25189-25195.

Novak, A. J., Bram, R. J., Kay, N. E. & Jelinek, D. F. 2002. Aberrant expression of B-lymphocyte stimulator by B chronic lymphocytic leukemia cells: a mechanism for survival. *Blood,* 100**,** 2973.

Nutt, S. L., Heavey, B., Rolink, A. G. & Busslinger, M. 1999. Commitment to the B-lymphoid lineage depends on the transcription factor Pax5. *Nature,* 401**,** 556.

Nutt, S. L., Morrison, A. M., Dörfler, P., Rolink, A. & Busslinger, M. 1998. Identification of BSAP (Pax-5) target genes in early B-cell development by loss-and gain-of-function experiments. *The EMBO Journal,* 17**,** 2319-2333.

Nutt, S. L., Urbanek, P., Rolink, A. & Busslinger, M. 1997. Essential functions of Pax5 (BSAP) in pro-B cell development: difference between fetal and adult B lymphopoiesis and reduced V-to-DJ recombination at the IgH locus. *Genes & development,* 11**,** 476-491.

O'connell, F. P., Pinkus, J. L. & Pinkus, G. S. 2004. CD138 (syndecan-1), a plasma cell marker: immunohistochemical profile in hematopoietic and nonhematopoietic neoplasms. *American journal of clinical pathology,* 121**,** 254-263.

Obukhanych, T. V. & Nussenzweig, M. C. 2006. T-independent type II immune responses generate memory B cells. *The Journal of experimental medicine,* 203**,** 305-310.

Ochiai, K., Maienschein-Cline, M., Simonetti, G., Chen, J., Rosenthal, R., Brink, R., Chong, A. S., Klein, U., Dinner, A. R. & Singh, H. 2013. Transcriptional regulation of germinal center B and plasma cell fates by dynamical control of IRF4. *Immunity,* 38**,** 918-929.

Ohnishi, H., Tochio, H., Kato, Z., Orii, K. E., Li, A., Kimura, T., Hiroaki, H., Kondo, N. & Shirakawa, M. 2009. Structural basis for the multiple interactions of the MyD88 TIR domain in TLR4 signaling. *Proc Natl Acad Sci U S A,* 106**,** 10260-5.

Ono, M., Bolland, S., Tempst, P. & Ravetch, J. V. 1996. Role of the inositol phosphatase SHIP in negative regulation of the immune system by the receptor FcγRIIB. *Nature,* 383**,** 263-266.

Otero, D. C., Omori, S. A. & Rickert, R. C. 2001. CD19-dependent Activation of Akt Kinase in B-lymphocytes. *Journal of Biological Chemistry,* 276**,** 1474-1478.

Owen, R. G., Pratt, G., Auer, R. L., Flatley, R., Kyriakou, C., Lunn, M. P., Matthey, F., Mccarthy, H., Mcnicholl, F. P., Rassam, S. M., Wagner, S. D., Streetly, M. & D'sa, S. 2014. Guidelines on the diagnosis and management of Waldenström macroglobulinaemia. *British Journal of Haematology,* 165**,** 316-333.

Owen, R. G., Treon, S. P., Al-Katib, A., Fonseca, R., Greipp, P. R., Mcmaster, M. L., Morra, E., Pangalis, G. A., San Miguel, J. F., Branagan, A. R. & Dimopoulos, M. A. 2003. Clinicopathological definition of Waldenstrom's macroglobulinemia: consensus panel recommendations from the Second International Workshop on Waldenstrom's Macroglobulinemia. *Semin Oncol,* 30**,** 110-5.

Paiva, B., Corchete, L. A., Vidriales, M. B., Garcia-Sanz, R., Perez, J. J., Aires-Mejia, I., Sanchez, M. L., Barcena, P., Alignani, D., Jimenez, C., Sarasquete, M. E., Mateos, M. V., Ocio, E. M., Puig, N., Escalante, F., Hernandez, J., Cuello, R., Garcia De Coca, A., Sierra, M., Montes, M. C., Gonzalez-Lopez, T. J., Galende, J., Barez, A., Alonso, J., Pardal, E., Orfao, A., Gutierrez, N. C. & San Miguel, J. F. 2015. The cellular origin and malignant transformation of Waldenstrom macroglobulinemia. *Blood,* 125**,** 2370-80.

Paiva, B., Montes, M. C., Garcia-Sanz, R., Ocio, E. M., Alonso, J., De Las Heras, N., Escalante, F., Cuello, R., De Coca, A. G., Galende, J., Hernandez, J., Sierra, M., Martin, A., Pardal, E., Barez, A., Alonso, J., Suarez, L., Gonzalez-Lopez, T. J., Perez, J. J., Orfao, A., Vidriales, M. B. & San Miguel, J. F. 2014. Multiparameter flow cytometry for the identification of the Waldenstrom/'s clone in IgM-MGUS and Waldenstrom/'s Macroglobulinemia: new criteria for differential diagnosis and risk stratification. *Leukemia,* 28**,** 166-173.

Paiva, B., Montes, M. C., García-Sanz, R., Ocio, E. M., Alonso, J., De Las Heras, N., Escalante, F., Cuello, R., De Coca, A. G., Galende, J., Hernández, J., Sierra, M., Martin, A., Pardal, E., Bárez, A., Alonso, J., Suarez, L., González-López, T. J., Perez, J. J., Orfao, A., Vidríales, M. B. & San Miguel, J. F. 2013. Multiparameter flow cytometry for the identification of the Waldenström's clone in IgM-MGUS and Waldenström's Macroglobulinemia: new criteria for differential diagnosis and risk stratification. *Leukemia,* 28**,** 166.

Palmesino, E., Moepps, B., Gierschik, P. & Thelen, M. 2006. Differences in CXCR4-mediated signaling in B cells. *Immunobiology,* 211**,** 377-389.

Park, B., Brinkmann, M. M., Spooner, E., Lee, C. C., Kim, Y.-M. & Ploegh, H. L. 2008. Proteolytic cleavage in an endolysosomal compartment is required for activation of Toll-like receptor 9. *Nature Immunology,* 9**,** 1407.

Park, H. H., Lo, Y.-C., Lin, S.-C., Wang, L., Yang, J. K. & Wu, H. 2007. The Death Domain Superfamily in Intracellular Signaling of Apoptosis and Inflammation. *Annual Review of Immunology,* 25**,** 561-586.

Parry, M., Rose-Zerilli, M. J., Ljungström, V., Gibson, J., Wang, J., Walewska, R., Parker, H., Parker, A., Davis, Z., Gardiner, A., Mciver-Brown, N., Kalpadakis, C., Xochelli, A., Anagnostopoulos, A., Fazi, C., De Castro, D. G., Dearden, C., Pratt, G., Rosenquist, R.,

Ashton-Key, M., Forconi, F., Collins, A., Ghia, P., Matutes, E., Pangalis, G., Stamatopoulos, K., Oscier, D. & Strefford, J. C. 2015. Genetics and Prognostication in Splenic Marginal Zone Lymphoma: Revelations from Deep Sequencing. *Clinical cancer research : an official journal of the American Association for Cancer Research,* 21**,** 4174-4183.

Pasqualucci, L. 2013. The genetic basis of diffuse large B-cell lymphoma. *Current opinion in hematology,* 20**,** 336-344.

Pasqualucci, L., Compagno, M., Houldsworth, J., Monti, S., Grunn, A., Nandula, S. V., Aster, J. C., Murty, V. V., Shipp, M. A. & Dalla-Favera, R. 2006. Inactivation of the PRDM1/BLIMP1 gene in diffuse large B cell lymphoma. *The Journal of Experimental Medicine,* 203**,** 311.

Paulus, A., Akhtar, S., Bashir, Y., Paulus, S. M., Yousaf, H., Roy, V., Ailawadhi, S., Ansell, S., Witzig, T. E. & Chanan-Khan, A. A. 2016. Drug Resistance Alters CD38 Expression and in Vitro Response to Daratumumab in Waldenstrom Macroglobulinemia Cells. *Blood,* 128**,** 3018.

Paulus, A., Akhtar, S., Yousaf, H., Manna, A., Paulus, S. M., Bashir, Y., Caulfield, T. R., Kuranz-Blake, M., Chitta, K., Wang, X., Asmann, Y., Hudec, R., Springer, W., Ailawadhi, S. & Chanan-Khan, A. 2017a. Waldenstrom macroglobulinemia cells devoid of BTKC481S or CXCR4WHIM-like mutations acquire resistance to ibrutinib through upregulation of Bcl-2 and AKT resulting in vulnerability towards venetoclax or MK2206 treatment. *Blood Cancer Journal,* 7**,** e565.

Paulus, A., Chitta, K. S., Wallace, P. K., Advani, P. P., Akhtar, S., Kuranz-Blake, M., Ailawadhi, S. & Chanan-Khan, A. A. 2015. Immunophenotyping of Waldenströms macroglobulinemia cell lines reveals distinct patterns of surface antigen expression: potential biological and therapeutic implications. *PloS one,* 10**,** e0122338-e0122338.

Paulus, A., Manna, A., Akhtar, S., Paulus, S. M., Sharma, M., Coignet, M. V., Jiang, L., Roy, V., Witzig, T. E., Ansell, S. M., Allan, J., Furman, R., Aulakh, S., Manochakian, R., Ailawadhi, S., Chanan-Khan, A. A. & Sher, T. 2018. Targeting CD38 with daratumumab is lethal to Waldenström macroglobulinaemia cells. *British Journal of Haematology,* 183**,** 196-211.

Paulus, A., Manna, A., Akhtar, S., Sher, T., Roy, V., Coleman, M., Novak, A. J., Ansell, S. M., Malavasi, F., Ailawadhi, S. & Chanan-Khan, A. A. 2017b. Targeting CD38 with Daratumumab Suppresses B-Cell Receptor Signaling and Enhances the Activity of Ibrutinib in Waldenstrom Macroglobulinemia Cells. *Blood,* 130**,** 1529.

Pavlasova, G., Borsky, M., Seda, V., Cerna, K., Osickova, J., Doubek, M., Mayer, J., Calogero, R., Trbusek, M., Pospisilova, S., Davids, M. S., Kipps, T. J., Brown, J. R. & Mraz, M. 2016. Ibrutinib inhibits CD20 upregulation on CLL B cells mediated by the CXCR4/SDF-1 axis. *Blood,* 128**,** 1609.

Pavlasova, G., Seda, V., Borsky, M., Cerna, K., Osickova, J., Mayer, J., Pospisilova, S., Davids, M. S., Brown, J. R. & Mraz, M. 2015. Microenvironmental Interactions up-Regulate CD20 Expression in CLL B Cells through the CXCR4/SDF-1 Axis: Implications for CD20-Targeting Antibodies and the Use of BCR-Inhibitors in Combination. *Blood,* 126**,** 4124.

Perez-Andres, M., Paiva, B., Nieto, W. G., Caraux, A., Schmitz, A., Almeida, J., Vogt Jr., R. F., Marti, G. E., Rawstron, A. C., Van Zelm, M. C., Van Dongen, J. J. M., Johnsen, H. E., Klein, B. & Orfao, A. 2010. Human peripheral blood B-cell compartments: A crossroad in B-cell traffic. *Cytometry Part B: Clinical Cytometry,* 78B**,** S47-S60.

Petrie, R. J. & Deans, J. P. 2002. Colocalization of the B Cell Receptor and CD20 Followed by Activation-Dependent Dissociation in Distinct Lipid Rafts. *The Journal of Immunology,* 169**,** 2886.

Phelan, J. D., Young, R. M., Webster, D. E., Roulland, S., Wright, G. W., Kasbekar, M., Shaffer, A. L., Ceribelli, M., Wang, J. Q., Schmitz, R., Nakagawa, M., Bachy, E., Huang, D. W., Ji, Y., Chen, L., Yang, Y., Zhao, H., Yu, X., Xu, W., Palisoc, M. M., Valadez, R. R., Davies-Hill, T., Wilson, W. H., Chan, W. C., Jaffe, E. S., Gascoyne, R. D., Campo, E., Rosenwald, A., Ott, G., Delabie, J., Rimsza, L. M., Rodriguez, F. J., Estephan, F., Holdhoff, M., Kruhlak, M. J., Hewitt, S. M., Thomas, C. J., Pittaluga, S., Oellerich, T. & Staudt, L. M. 2018. A multiprotein supercomplex controlling oncogenic signalling in lymphoma. *Nature.*

Piva, R., Deaglio, S., Famà, R., Buonincontri, R., Scarfò, I., Bruscaggin, A., Mereu, E., Serra, S., Spina, V., Brusa, D., Garaffo, G., Monti, S., Dal Bo, M., Marasca, R., Arcaini, L., Neri, A., Gattei, V., Paulli, M., Tiacci, E., Bertoni, F., Pileri, S. A., Foà, R., Inghirami, G., Gaidano, G. & Rossi, D. 2014. The Krüppel-like factor 2 transcription factor gene is recurrently mutated in splenic marginal zone lymphoma. *Leukemia,* 29**,** 503.

Poeck, H., Wagner, M., Battiany, J., Rothenfusser, S., Wellisch, D., Hornung, V., Jahrsdorfer, B., Giese, T., Endres, S. & Hartmann, G. 2004. Plasmacytoid dendritic cells, antigen, and CpG-C license human B cells for plasma cell differentiation and immunoglobulin production in the absence of T-cell help. *Blood,* 103**,** 3058.

Poltorak, A., Smirnova, I., He, X., Liu, M.-Y., Van Huffel, C., Birdwell, D., Alejos, E., Silva, M., Du, X., Thompson, P., Chan, E. K. L., Ledesma, J., Roe, B., Clifton, S., Vogel, S. N. & Beutler, B. 1998. Genetic and Physical Mapping of theLpsLocus: Identification of the Toll-4 Receptor as a Candidate Gene in the Critical Region. *Blood Cells, Molecules, and Diseases,* 24**,** 340-355.

Polyak, M. J., Li, H., Shariat, N. & Deans, J. P. 2008. CD20 Homo-oligomers Physically Associate with the B Cell Antigen Receptor: Dissociation upon receptor engagement and recruitment of phosphoproteins and calmodulin-binding proteins. *Journal of Biological Chemistry,* 283**,** 18545-18552.

Pone, E. J., Zan, H., Zhang, J., Al-Qahtani, A., Xu, Z. & Casali, P. 2010. Toll-like receptors and B-cell receptors synergize to induce immunoglobulin class-switch DNA recombination: relevance to microbial antibody responses. *Critical reviews in immunology,* 30**,** 1-29.

Pone, E. J., Zhang, J., Mai, T., White, C. A., Li, G., Sakakura, J. K., Patel, P. J., Al-Qahtani, A., Zan, H., Xu, Z. & Casali, P. 2012. BCR-signalling synergizes with TLR-signalling for induction of AID and immunoglobulin class-switching through the non-canonical NF-kappaB pathway. *Nat Commun,* 3**,** 767.

Poovassery, J. S., Vanden Bush, T. J. & Bishop, G. A. 2009. Antigen Receptor Signals Rescue B Cells from TLR Tolerance. *The Journal of Immunology,* 183**,** 2974.

Poulain, S., Roumier, C., Galiègue-Zouitina, S., Daudignon, A., Herbaux, C., Aiijou, R., Lainelle, A., Broucqsault, N., Bertrand, E. & Manier, S. 2013. Genome wide SNP array identified multiple mechanisms of genetic changes in Waldenstrom macroglobulinemia. *American journal of hematology,* 88**,** 948-954.

Poulain, S., Roumier, C., Venet-Caillault, A., Figeac, M., Herbaux, C., Marot, G., Doye, E., Bertrand, E., Geffroy, S. & Lepretre, F. 2016. Genomic landscape of CXCR4 mutations in Waldenström macroglobulinemia. *Clinical Cancer Research,* 22**,** 1480-1488.

Pridans, C., Holmes, M. L., Polli, M., Wettenhall, J. M., Dakic, A., Corcoran, L. M., Smyth, G. K. & Nutt, S. L. 2008. Identification of Pax5 Target Genes in Early B Cell Differentiation. *The Journal of Immunology,* 180**,** 1719.

Puga, I., Cols, M., Barra, C. M., He, B., Cassis, L., Gentile, M., Comerma, L., Chorny, A., Shan, M., Xu, W., Magri, G., Knowles, D. M., Tam, W., Chiu, A., Bussel, J. B., Serrano, S., Lorente, J. A., Bellosillo, B., Lloreta, J., Juanpere, N., Alameda, F., Baro, T., De Heredia, C. D., Toran, N., Catala, A., Torrebadell, M., Fortuny, C., Cusi, V., Carreras, C., Diaz, G. A., Blander, J. M., Farber, C.-M., Silvestri, G., Cunningham-Rundles, C., Calvillo, M., Dufour, C., Notarangelo, L. D., Lougaris, V., Plebani, A., Casanova, J.-L., Ganal, S. C., Diefenbach, A., Arostegui, J. I., Juan, M., Yague, J., Mahlaoui, N., Donadieu, J., Chen, K. & Cerutti, A. 2012. B cell-helper neutrophils stimulate the diversification and production of immunoglobulin in the marginal zone of the spleen. *Nat Immunol,* 13**,** 170-180.

Qian, Y., Commane, M., Ninomiya-Tsuji, J., Matsumoto, K. & Li, X. 2001. IRAK-mediated Translocation of TRAF6 and TAB2 in the Interleukin-1-induced Activation of NFκB. *Journal of Biological Chemistry,* 276**,** 41661-41667.

Qiu, P., Simonds, E. F., Bendall, S. C., Gibbs, K. D., Jr., Bruggner, R. V., Linderman, M. D., Sachs, K., Nolan, G. P. & Plevritis, S. K. 2011. Extracting a cellular hierarchy from high-dimensional cytometry data with SPADE. *Nature biotechnology,* 29**,** 886-891.

Randall, T. D., Heath, A. W., Santos-Argumedo, L., Howard, M. C., Weissman, I. L. & Lund, F. E. 1998. Arrest of B Lymphocyte Terminal Differentiation by CD40 Signaling: Mechanism for Lack of Antibody-Secreting Cells in Germinal Centers. *Immunity,* 8**,** 733-742.

Rao, N., Nguyen, S., Ngo, K. & Fung-Leung, W.-P. 2005. A novel splice variant of interleukin-1 receptor (IL-1R)-associated kinase 1 plays a negative regulatory role in Toll/IL-1R-induced inflammatory signaling. *Molecular and cellular biology,* 25**,** 6521-6532.

Rathmell, J. C., Townsend, S. E., Xu, J. C., Flavell, R. A. & Goodnow, C. C. 1996. Expansion or Elimination of B Cells In Vivo: Dual Roles for CD40- and Fas (CD95)-Ligands Modulated by the B Cell Antigen Receptor. *Cell,* 87**,** 319-329.

Rawlings, D. J., Schwartz, M. A., Jackson, S. W. & Meyer-Bahlburg, A. 2012. Integration of B cell responses through Toll-like receptors and antigen receptors. *Nature reviews. Immunology,* 12**,** 282-294.

Rawstron, A. C., Ssemaganda, A., De Tute, R., Doughty, C., Newton, D., Vardi, A., Evans, P. A., Stamatopoulos, K., Owen, R. G. & Lightfoot, T. 2017. Monoclonal B-cell lymphocytosis in a hospital-based UK population and a rural Ugandan population: a cross-sectional study. *The Lancet Haematology,* 4**,** e334-e340.

Ray, D., Bosselut, R., Ghysdael, J., Mattei, M. G., Tavitian, A. & Moreau-Gachelin, F. 1992. Characterization of Spi-B, a transcription factor related to the putative oncoprotein Spi-1/PU.1. *Molecular and Cellular Biology,* 12**,** 4297.

Reid, G. S. D., She, K., Terrett, L., Food, M. R., Trudeau, J. D. & Schultz, K. R. 2005. CpG stimulation of precursor B-lineage acute lymphoblastic leukemia induces a distinct change in costimulatory molecule expression and shifts allogeneic T cells toward a Th1 response. *Blood,* 105**,** 3641.

Reijmers, R. M., Groen, R. W., Rozemuller, H., Kuil, A., De Haan-Kramer, A., Csikós, T., Martens, A. C., Spaargaren, M. & Pals, S. T. 2010. Targeting EXT1 reveals a crucial role for heparan sulfate in the growth of multiple myeloma. *Blood,* 115**,** 601-604.

Reimold, A. M., Iwakoshi, N. N., Manis, J., Vallabhajosyula, P., Szomolanyi-Tsuda, E., Gravallese, E. M., Friend, D., Grusby, M. J., Alt, F. & Glimcher, L. H. 2001. Plasma cell differentiation requires the transcription factor XBP-1. *Nature,* 412**,** 300.

Reimold, A. M., Ponath, P. D., Li, Y.-S., Hardy, R. R., David, C. S., Strominger, J. L. & Glimcher, L. H. 1996. Transcription factor B cell lineage-specific activator protein regulates the gene for human X-box binding protein 1. *Journal of Experimental Medicine,* 183**,** 393-401.

Reljic, R., Wagner, S. D., Peakman, L. J. & Fearon, D. T. 2000. Suppression of Signal Transducer and Activator of Transcription 3–Dependent B Lymphocyte Terminal Differentiation by Bcl-6. *The Journal of Experimental Medicine,* 192**,** 1841.

Ribera-Cortada, I., Martinez, D., Amador, V., Royo, C., Navarro, A., Beà, S., Gine, E., De Leval, L., Serrano, S., Wotherspoon, A., Colomer, D., Martinez, A. & Campo, E. 2015. Plasma cell and terminal B-cell differentiation in mantle cell lymphoma mainly occur in the SOX11-negative subtype. *Modern Pathology,* 28**,** 1435.

Ridley, R. C., Xiao, H., Hata, H., Woodliff, J., Epstein, J. & Sanderson, R. D. 1993. Expression of syndecan regulates human myeloma plasma cell adhesion to type I collagen. *Blood,* 81**,** 767.

Roccaro, A. M., Sacco, A., Chen, C., Runnels, J., Leleu, X., Azab, F., Azab, A. K., Jia, X., Ngo, H. T., Melhem, M. R., Burwick, N., Varticovski, L., Novina, C. D., Rollins, B. J., Anderson, K. C. & Ghobrial, I. M. 2009. microRNA expression in the biology, prognosis, and therapy of Waldenström macroglobulinemia. *Blood,* 113**,** 4391.

Roccaro, A. M., Sacco, A., Husu, E. N., Pitsillides, C., Vesole, S., Azab, A. K., Azab, F., Melhem, M., Ngo, H. T., Quang, P., Maiso, P., Runnels, J., Liang, M.-C., Wong, K.-K., Lin, C. & Ghobrial, I. M. 2010. Dual targeting of the PI3K/Akt/mTOR pathway as an antitumor strategy in Waldenstrom macroglobulinemia. *Blood,* 115**,** 559.

Roccaro, A. M., Sacco, A., Jimenez, C., Maiso, P., Moschetta, M., Mishima, Y., Aljawai, Y., Sahin, I., Kuhne, M., Cardarelli, P., Cohen, L., San Miguel, J. F., Garcia-Sanz, R. & Ghobrial, I. M. 2014. C1013G/CXCR4 acts as a driver mutation of tumor progression and modulator of drug resistance in lymphoplasmacytic lymphoma. *Blood,* 123**,** 4120.

Rossi, D., Deaglio, S., Dominguez-Sola, D., Rasi, S., Vaisitti, T., Agostinelli, C., Spina, V., Bruscaggin, A., Monti, S., Cerri, M., Cresta, S., Fangazio, M., Arcaini, L., Lucioni, M., Marasca, R., Thieblemont, C., Capello, D., Facchetti, F., Kwee, I., Pileri, S. A., Foà, R., Bertoni, F., Dalla-Favera, R., Pasqualucci, L. & Gaidano, G. 2011. Alteration of BIRC3 and multiple other NF-κB pathway genes in splenic marginal zone lymphoma. *Blood,* 118**,** 4930-4934.

Rothstein, T. L. 1996. Signals and susceptibility to programmed death in B cells. *Current Opinion in Immunology,* 8**,** 362-371.

Rothstein, T. L., Wang, J. K., Panka, D. J., Foote, L. C., Wang, Z., Stanger, B., Cui, H., Ju, S. T. & Marshak-Rothstein, A. 1995. Protection against Fas-dependent Th1-mediated apoptosis by antigen receptor engagement in B cells. *Nature,* 374**,** 163-5.

Rui, L., Vinuesa, C. G., Blasioli, J. & Goodnow, C. C. 2003. Resistance to CpG DNA–induced autoimmunity through tolerogenic B cell antigen receptor ERK signaling. *Nature Immunology,* 4**,** 594.

Rummel, M. J., Al-Batran, S. E., Kim, S.-Z., Welslau, M., Hecker, R., Kofahl-Krause, D., Josten, K.-M., Dürk, H., Rost, A. & Neise, M. 2005. Bendamustine plus rituximab is effective and has a favorable toxicity profile in the treatment of mantle cell and low-grade non-Hodgkin's lymphoma. *J Clin Oncol,* 23**,** 3383-3389.

Rummel, M. J., Niederle, N., Maschmeyer, G., Banat, G. A., Von Grünhagen, U., Losem, C., Kofahl-Krause, D., Heil, G., Welslau, M. & Balser, C. 2013. Bendamustine plus rituximab versus CHOP plus rituximab as first-line treatment for patients with indolent and mantle-cell lymphomas: an open-label, multicentre, randomised, phase 3 non-inferiority trial. *The Lancet,* 381**,** 1203-1210.

Sahota, S. S., Babbage, G. & Weston-Bell, N. J. 2009. CD27 in defining memory B-cell origins in Waldenstrom's macroglobulinemia. *Clin Lymphoma Myeloma,* 9**,** 33-5.

Sahota, S. S., Forconi, F., Ottensmeier, C. H., Provan, D., Oscier, D. G., Hamblin, T. J. & Stevenson, F. K. 2002. Typical Waldenstrom macroglobulinemia is derived from a B-cell arrested after cessation of somatic mutation but prior to isotype switch events. *Blood,* 100**,** 1505.

San Miguel, J., Vidriales, M., Ocio, E., Mateo, G., Sanchez-Guijo, F., Sanchez, M., Escribano, L., Barez, A., Moro, M. & Hernandez, J. Immunophenotypic analysis of Waldenstrom's macroglobulinemia. Seminars in oncology, 2003. Elsevier, 187-195.

Sato, S., Miller, A. S., Howard, M. C. & Tedder, T. F. 1997. Regulation of B lymphocyte development and activation by the CD19/CD21/CD81/Leu 13 complex requires the cytoplasmic domain of CD19. *The Journal of Immunology,* 159**,** 3278-3287.

Schaerli, P., Willimann, K., Lang, A. B., Lipp, M., Loetscher, P. & Moser, B. 2000. CXC chemokine receptor 5 expression defines follicular homing T cells with B cell helper function. *J Exp Med,* 192**,** 1553-62.

Schattner, E. J., Elkon, K. B., Yoo, D. H., Tumang, J., Krammer, P. H., Crow, M. K. & Friedman, S. M. 1995. CD40 ligation induces Apo-1/Fas expression on human B lymphocytes and facilitates apoptosis through the Apo-1/Fas pathway. *J Exp Med,* 182**,** 1557-65.

Schebesta, A., Mcmanus, S., Salvagiotto, G., Delogu, A., Busslinger, G. A. & Busslinger, M. 2007. Transcription Factor Pax5 Activates the Chromatin of Key Genes Involved in B Cell Signaling, Adhesion, Migration, and Immune Function. *Immunity,* 27**,** 49-63.

Schebesta, M., Pfeffer, P. L. & Busslinger, M. 2002. Control of pre-BCR signaling by Pax5-dependent activation of the BLNK gene. *Immunity,* 17**,** 473-485.

Schulze-Luehrmann, J. & Ghosh, S. 2006. Antigen-Receptor Signaling to Nuclear Factor κB. *Immunity,* 25**,** 701-715.

Schwede, T., Kopp, J., Guex, N. & Peitsch, M. C. 2003. SWISS-MODEL: An automated protein homology-modeling server. *Nucleic acids research,* 31**,** 3381-3385.

Sciammas, R., Shaffer, A., Schatz, J. H., Zhao, H., Staudt, L. M. & Singh, H. 2006. Graded expression of interferon regulatory factor-4 coordinates isotype switching with plasma cell differentiation. *Immunity,* 25**,** 225-236.

Shaffer, A., Yu, X., He, Y., Boldrick, J., Chan, E. P. & Staudt, L. M. 2000. BCL-6 represses genes that function in lymphocyte differentiation, inflammation, and cell cycle control. *Immunity,* 13**,** 199-212.

Shaffer, A. L., Lin, K.-I., Kuo, T. C., Yu, X., Hurt, E. M., Rosenwald, A., Giltnane, J. M., Yang, L., Zhao, H., Calame, K. & Staudt, L. M. 2002. Blimp-1 Orchestrates Plasma Cell Differentiation by Extinguishing the Mature B Cell Gene Expression Program. *Immunity,* 17**,** 51-62.

Shapiro-Shelef, M., Lin, K.-I., Mcheyzer-Williams, L. J., Liao, J., Mcheyzer-Williams, M. G. & Calame, K. 2003. Blimp-1 Is Required for the Formation of Immunoglobulin Secreting Plasma Cells and Pre-Plasma Memory B Cells. *Immunity,* 19**,** 607-620.

Shih, V. F. S., Davis-Turak, J., Macal, M., Huang, J. Q., Ponomarenko, J., Kearns, J. D., Yu, T., Fagerlund, R., Asagiri, M., Zuniga, E. I. & Hoffmann, A. 2012. Control of RelB during dendritic cell activation integrates canonical and noncanonical NF-κB pathways. *Nature Immunology,* 13**,** 1162.

Signoret, N., Oldridge, J., Pelchen-Matthews, A., Klasse, P. J., Tran, T., Brass, L. F., Rosenkilde, M. M., Schwartz, T. W., Holmes, W., Dallas, W., Luther, M. A., Wells, T. N. C., Hoxie, J. A. & Marsh, M. 1997. Phorbol Esters and SDF-1 Induce Rapid Endocytosis and Down Modulation of the Chemokine Receptor CXCR4. *The Journal of Cell Biology,* 139**,** 651.

Signoret, N., Rosenkilde, M. M., Klasse, P. J., Schwartz, T. W., Malim, M. H., Hoxie, J. A. & Marsh, M. 1998. Differential regulation of CXCR4 and CCR5 endocytosis. *Journal of Cell Science,* 111**,** 2819.

Simchoni, N. & Cunningham-Rundles, C. 2015. TLR7- and TLR9-responsive human B cells share phenotypic and genetic characteristics. *Journal of immunology (Baltimore, Md. : 1950),* 194**,** 3035-3044.

Sivori, S., Carlomagno, S., Moretta, L. & Moretta, A. 2006. Comparison of different CpG oligodeoxynucleotide classes for their capability to stimulate human NK cells. *European Journal of Immunology,* 36**,** 961-967.

Slifka, M. K., Antia, R., Whitmire, J. K. & Ahmed, R. 1998. Humoral immunity due to long-lived plasma cells. *Immunity,* 8**,** 363-72.

Smith, J. N. P. & Calvi, L. M. 2013. Concise Review: Current Concepts in Bone Marrow Microenvironmental Regulation of Hematopoietic Stem and Progenitor Cells. *STEM CELLS,* 31**,** 1044-1050.

Soneson, C., Love, M. I. & Robinson, M. D. 2015. Differential analyses for RNA-seq: transcript-level estimates improve gene-level inferences. *F1000Res,* 4**,** 1521.

Souchet, L., Levy, V., Ouzegdouh, M., Tamburini, J., Delmer, A., Dupuis, J., Le Gouill, S., Pégourié-Bandelier, B., Tournilhac, O. & Boubaya, M. 2016. Efficacy and long-term toxicity of the rituximab-fludarabine-cyclophosphamide combination therapy in Waldenstrom's macroglobulinemia. *American journal of hematology,* 91**,** 782-786.

Stamatopoulos, K., Belessi, C., Papadaki, T., Kalagiakou, E., Stavroyianni, N., Douka, V., Afendaki, S., Saloum, R., Parasi, A., Anagnostou, D., Laoutaris, N., Fassas, A. & Anagnostopoulos, A. 2004. Immunoglobulin heavy- and light-chain repertoire in splenic marginal zone lymphoma. *Molecular medicine (Cambridge, Mass.),* 10**,** 89-95.

Stashenko, P., Nadler, L., Hardy, R. & Schlossman, S. F. 1980. Characterization of a human B lymphocyte-specific antigen. *The Journal of Immunology,* 125**,** 1678-1685.

Stashenko, P., Nadler, L. M., Hardy, R. & Schlossman, S. F. 1981. Expression of cell surface markers after human B lymphocyte activation. *Proceedings of the National Academy of Sciences,* 78**,** 3848-3852.

Strasser, A. & Bouillet, P. 2003. The control of apoptosis in lymphocyte selection. *Immunological Reviews,* 193**,** 82-92.

Su, G. H., Chen, H. M., Muthusamy, N., Garrett-Sinha, L. A., Baunoch, D., Tenen, D. G. & Simon, M. C. 1997. Defective B cell receptor-mediated responses in mice lacking the Ets protein, Spi-B. *The EMBO Journal,* 16**,** 7118-7129.

Su, G. H., Ip, H. S., Cobb, B. S., Lu, M.-M., Chen, H.-M. & Simon, M. C. 1996. The Ets protein Spi-B is expressed exclusively in B cells and T cells during development. *Journal of Experimental Medicine,* 184**,** 203-214.

Sullivan, N. L., Eickhoff, C. S., Zhang, X., Giddings, O. K., Lane, T. E. & Hoft, D. F. 2011. Importance of the CCR5–CCL5 Axis for Mucosal Trypanosoma cruzi Protection and B Cell Activation. *The Journal of Immunology,* 187**,** 1358.

Sultzer, B. M. 1968. Genetic Control of Leucocyte Responses to Endotoxin. *Nature,* 219**,** 1253-1254.

Sun, S.-C. 2011. Non-canonical NF-κB signaling pathway. *Cell research,* 21**,** 71-85.

Swerdlow, S. H., Campo, E., Pileri, S. A., Harris, N. L., Stein, H., Siebert, R., Advani, R., Ghielmini, M., Salles, G. A., Zelenetz, A. D. & Jaffe, E. S. 2016. The 2016 revision of the World Health Organization classification of lymphoid neoplasms. *Blood,* 127**,** 2375.

Takeda, K. & Akira, S. 2005. Toll-like receptors in innate immunity. *International Immunology,* 17**,** 1-14.

Takeuchi, O., Hoshino, K., Kawai, T., Sanjo, H., Takada, H., Ogawa, T., Takeda, K. & Akira, S. 1999. Differential roles of TLR2 and TLR4 in recognition of gram-negative and gram-positive bacterial cell wall components. *Immunity,* 11**,** 443-51.

Takeuchi, O., Kawai, T., Muhlradt, P. F., Morr, M., Radolf, J. D., Zychlinsky, A., Takeda, K. & Akira, S. 2001. Discrimination of bacterial lipoproteins by Toll-like receptor 6. *Int Immunol,* 13**,** 933-40.

Takeuchi, O., Sato, S., Horiuchi, T., Hoshino, K., Takeda, K., Dong, Z., Modlin, R. L. & Akira, S. 2002. Cutting edge: role of Toll-like receptor 1 in mediating immune response to microbial lipoproteins. *J Immunol,* 169**,** 10-4.

Tangye, S. G. 2011. Staying alive: regulation of plasma cell survival. *Trends in Immunology,* 32**,** 595-602.

Tangye, S. G., Avery, D. T., Deenick, E. K. & Hodgkin, P. D. 2003. Intrinsic Differences in the Proliferation of Naive and Memory Human B Cells as a Mechanism for Enhanced Secondary Immune Responses. *The Journal of Immunology,* 170**,** 686.

Tangye, S. G., Liu, Y.-J., Aversa, G., Phillips, J. H. & De Vries, J. E. 1998. Identification of Functional Human Splenic Memory B Cells by Expression of CD148 and CD27. *The Journal of Experimental Medicine,* 188**,** 1691.

Taubenheim, N., Tarlinton, D. M., Crawford, S., Corcoran, L. M., Hodgkin, P. D. & Nutt, S. L. 2012. High rate of antibody secretion is not integral to plasma cell differentiation as revealed by XBP-1 deficiency. *The Journal of Immunology,* 189**,** 3328-3338.

Tedder, T., Boyd, A., Freedman, A., Nadler, L. & Schlossman, S. 1985. The B cell surface molecule B1 is functionally linked with B cell activation and differentiation. *The Journal of Immunology,* 135**,** 973-979.

Tedder, T. F. & Engel, P. 1994. CD20: a regulator of cell-cycle progression of B lymphocytes. *Immunology today,* 15**,** 450-454.

Tedeschi, A., Benevolo, G., Varettoni, M., Battista, M. L., Zinzani, P. L., Visco, C., Meneghini, V., Pioltelli, P., Sacchi, S. & Ricci, F. 2012. Fludarabine plus cyclophosphamide and rituximab in Waldenstrom macroglobulinemia: an effective but myelosuppressive regimen to be offered to patients with advanced disease. *Cancer,* 118**,** 434-443.

Tedeschi, A., Picardi, P., Ferrero, S., Benevolo, G., Margiotta Casaluci, G., Varettoni, M., Baratè, C., Motta, M., Gini, G. & Goldaniga, M. C. 2015. Bendamustine and rituximab combination is safe and effective as salvage regimen in Waldenström macroglobulinemia. *Leukemia & lymphoma,* 56**,** 2637-2642.

Terpos, E., Anagnostopoulos, A., Kastritis, E., Bamias, A., Tsionos, K. & Dimopoulos, M.-A. 2006. *Abnormal bone remodelling and increased levels of macrophage inflammatory protein-1 alpha (MIP-1α) in Waldenström macroglobulinaemia*.

Terpos, E., Berenson, J., Raje, N. & Roodman, G. D. 2014. Management of bone disease in multiple myeloma. *Expert review of hematology,* 7**,** 113-125.

Thieblemont, C., Felman, P., Berger, F., Dumontet, C., Arnaud, P., Hequet, O., Arcache, J., Callet-Bauchu, E., Salles, G. & Coiffier, B. 2002. Treatment of Splenic Marginal Zone B-Cell Lymphoma: An Analysis of 81 Patients. *Clinical Lymphoma,* 3**,** 41-47.

Thompson, J. S., Bixler, S. A., Qian, F., Vora, K., Scott, M. L., Cachero, T. G., Hession, C., Schneider, P., Sizing, I. D., Mullen, C., Strauch, K., Zafari, M., Benjamin, C. D., Tschopp, J., Browning,

J. L. & Ambrose, C. 2001. BAFF-R, a Newly Identified TNF Receptor That Specifically Interacts with BAFF. *Science,* 293**,** 2108.

Tierens, A., Delabie, J., Malecka, A., Wang, J., Gruszka-Westwood, A., Catovsky, D. & Matutes, E. 2003. Splenic marginal zone lymphoma with villous lymphocytes shows on-going immunoglobulin gene mutations. *The American journal of pathology,* 162**,** 681-689.

Todd, D. J., Lee, A.-H. & Glimcher, L. H. 2008. The endoplasmic reticulum stress response in immunity and autoimmunity. *Nature reviews immunology,* 8**,** 663.

Todd, D. J., Mcheyzer-Williams, L. J., Kowal, C., Lee, A.-H., Volpe, B. T., Diamond, B., Mcheyzer-Williams, M. G. & Glimcher, L. H. 2009. XBP1 governs late events in plasma cell differentiation and is not required for antigen-specific memory B cell development. *The Journal of Experimental Medicine,* 206**,** 2151.

Toma, A., Le Garff-Tavernier, M., Brissard, M., Bonnemye, P., Musset, L., Azar, N., Leblond, V. & Merle-Beral, H. 2007. Immunophenotypic Analysis of Waldenstrom's Macroglobulinemia: A Study of 63 Cases. *Blood,* 110**,** 4399.

Tooze, R. M., Stephenson, S. & Doody, G. M. 2006. Repression of IFN-γ induction of class II transactivator: a role for PRDM1/Blimp-1 in regulation of cytokine signaling. *The Journal of Immunology,* 177**,** 4584-4593.

Tournilhac, O., Santos, D. D., Xu, L., Kutok, J., Tai, Y. T., Le Gouill, S., Catley, L., Hunter, Z., Branagan, A. R., Boyce, J. A., Munshi, N., Anderson, K. C. & Treon, S. P. 2006. Mast cells in Waldenstrom's macroglobulinemia support lymphoplasmacytic cell growth through CD154/CD40 signaling. *Ann Oncol,* 17**,** 1275-82.

Traverse-Glehen, A., Baseggio, L., Salles, G., Felman, P. & Berger, F. 2011. Splenic marginal zone B-cell lymphoma: a distinct clinicopathological and molecular entity. Recent advances in ontogeny and classification. *Current Opinion in Oncology,* 23**,** 441-448.

Treon, S., Emmanouilides, C., Kimby, E., Kelliher, A., Preffer, F., Branagan, A., Anderson, K. & Frankel, S. 2005. Extended rituximab therapy in Waldenström's macroglobulinemia. *Annals of Oncology,* 16**,** 132-138.

Treon, S. P., Agus, D. B., Link, B., Rodrigues, G., Molina, A., Lacy, M. Q., Fisher, D. C., Emmanouilides, C., Richards, A. I. & Clark, B. 2001. CD20-directed antibody-mediated immunotherapy induces responses and facilitates hematologic recovery in patients with Waldenstrom's macroglobulinemia. *Journal of immunotherapy,* 24**,** 272-279.

Treon, S. P., Branagan, A., Hunter, Z., Santos, D., Tournhilac, O. & Anderson, K. 2004. Paradoxical increases in serum IgM and viscosity levels following rituximab in Waldenstrom's macroglobulinemia. *Annals of Oncology,* 15**,** 1481-1483.

Treon, S. P., Gertz, M. A., Dimopoulos, M., Anagnostopoulos, A., Blade, J., Branagan, A. R., Garcia-Sanz, R., Johnson, S., Kimby, E. & Leblond, V. 2006. Update on treatment recommendations from the Third International Workshop on Waldenström's macroglobulinemia. *Blood,* 107**,** 3442-3446.

Treon, S. P., Gustine, J., Meid, K., Dubeau, T., Severns, P., Patterson, C., Xu, L., Yang, G., Liu, X., Demos, M., Kofides, A., Chen, J., Munshi, M., Tsakmaklis, N., Chan, G., Yee, A. J., Raje, N., Donnell, E., Hunter, Z. & Castillo, J. J. 2017. Ibrutinib Is Highly Active As First Line Therapy in Symptomatic Waldenstrom's Macroglobulinemia. *Blood,* 130**,** 2767.

Treon, S. P., Hanzis, C., Tripsas, C., Ioakimidis, L., Patterson, C. J., Manning, R. J. & Sheehy, P. 2011. Bendamustine therapy in patients with relapsed or refractory Waldenström's macroglobulinemia. *Clinical Lymphoma Myeloma and Leukemia,* 11**,** 133-135.

Treon, S. P., Tripsas, C. K., Meid, K., Warren, D., Varma, G., Green, R., Argyropoulos, K. V., Yang, G., Cao, Y., Xu, L., Patterson, C. J., Rodig, S., Zehnder, J. L., Aster, J. C., Harris, N. L., Kanan, S., Ghobrial, I., Castillo, J. J., Laubach, J. P., Hunter, Z. R., Salman, Z., Li, J., Cheng, M., Clow, F., Graef, T., Palomba, M. L. & Advani, R. H. 2015. Ibrutinib in previously treated Waldenstrom's macroglobulinemia. *N Engl J Med,* 372**,** 1430-40.

Treon, S. P., Xu, L., Yang, G., Zhou, Y., Liu, X., Cao, Y., Sheehy, P., Manning, R. J., Patterson, C. J., Tripsas, C., Arcaini, L., Pinkus, G. S., Rodig, S. J., Sohani, A. R., Harris, N. L., Laramie, J. M., Skifter, D. A., Lincoln, S. E. & Hunter, Z. R. 2012. MYD88 L265P somatic mutation in Waldenstrom's macroglobulinemia. *N Engl J Med,* 367**,** 826-33.

Tripodo, C., Sangaletti, S., Piccaluga, P. P., Prakash, S., Franco, G., Borrello, I., Orazi, A., Colombo, M. P. & Pileri, S. A. 2011. The bone marrow stroma in hematological neoplasms—a guilty bystander. *Nature Reviews Clinical Oncology,* 8**,** 456.

Tuveson, D. A., Carter, R. H., Soltoff, S. P. & Fearon, D. T. 1993. CD19 of B cells as a surrogate kinase insert region to bind phosphatidylinositol 3-kinase. *Science,* 260**,** 986.

Upadhyay, M., Priya, G. K., Ramesh, P., Madhavi, M. B., Rath, S., Bal, V., George, A. & Vaidya, T. 2014. CD40 Signaling Drives B Lymphocytes Into an Intermediate Memory-Like State, Poised Between Naïve and Plasma Cells. *Journal of Cellular Physiology,* 229**,** 1387-1396.

Usmani, S. Z., Weiss, B. M., Plesner, T., Bahlis, N. J., Belch, A., Lonial, S., Lokhorst, H. M., Voorhees, P. M., Richardson, P. G., Chari, A., Sasser, A. K., Axel, A., Feng, H., Uhlar, C. M., Wang, J., Khan, I., Ahmadi, T. & Nahi, H. 2016. Clinical efficacy of daratumumab monotherapy in patients with heavily pretreated relapsed or refractory multiple myeloma. *Blood,* 128**,** 37.

Usui, T., Wakatsuki, Y., Matsunaga, Y., Kaneko, S., Koseki, H., Kita, T. & Kosek, H. 1997. Overexpression of B cell-specific activator protein (BSAP/Pax-5) in a late B cell is sufficient to suppress differentiation to an Ig high producer cell with plasma cell phenotype. *The Journal of Immunology,* 158**,** 3197.

Valentin-Opran, A., Charhon, S. A., Meunier, P. J., Edouard, C. M. & Arlot, M. E. 1982. Quantitative histology of myeloma-induced bone changes. *British Journal of Haematology,* 52**,** 601-610.

Van Der Maaten, L. 2014. Accelerating t-SNE using tree-based algorithms. *The Journal of Machine Learning Research,* 15**,** 3221-3245.

Van Dongen, J., Lhermitte, L., Böttcher, S., Almeida, J., Van Der Velden, V., Flores-Montero, J., Rawstron, A., Asnafi, V., Lecrevisse, Q. & Lucio, P. 2012. EuroFlow antibody panels for standardized n-dimensional flow cytometric immunophenotyping of normal, reactive and malignant leukocytes. *Leukemia,* 26**,** 1908.

Van Huyen, J.-P. D., Molina, T., Delmer, A., Audouin, J., Le Tourneau, A., Zittoun, R., Bernadou, A. & Diebold, J. 2000. Splenic Marginal Zone Lymphoma With or Without Plasmacytic Differentiation. *The American Journal of Surgical Pathology,* 24**,** 1581-1592.

Varettoni, M., Arcaini, L., Zibellini, S., Boveri, E., Rattotti, S., Riboni, R., Corso, A., Orlandi, E., Bonfichi, M., Gotti, M., Pascutto, C., Mangiacavalli, S., Croci, G., Fiaccadori, V., Morello, L., Guerrera, M. L., Paulli, M. & Cazzola, M. 2013. Prevalence and clinical significance of the MYD88 (L265P) somatic mutation in Waldenstrom's macroglobulinemia and related lymphoid neoplasms. *Blood,* 121**,** 2522-8.

Vazquez, M. I., Catalan-Dibene, J. & Zlotnik, A. 2015. B cells responses and cytokine production are regulated by their immune microenvironment. *Cytokine,* 74**,** 318-326.

Vickers, T. A., Zhang, H., Graham, M. J., Lemonidis, K. M., Zhao, C. & Dean, N. M. 2006. Modification of MyD88 mRNA splicing and inhibition of IL-1β signaling in cell culture and in mice with a 2'-O-methoxyethyl-modified oligonucleotide. *The Journal of Immunology,* 176**,** 3652-3661.

Victora, G. D. & Nussenzweig, M. C. 2012. Germinal centers. *Annu Rev Immunol,* 30**,** 429-57.

Viglianti, G. A., Lau, C. M., Hanley, T. M., Miko, B. A., Shlomchik, M. J. & Marshak-Rothstein, A. 2003. Activation of Autoreactive B Cells by CpG dsDNA. *Immunity,* 19**,** 837-847.

Vinuesa, C. G. & Chang, P.-P. 2013. Innate B cell helpers reveal novel types of antibody responses. *Nat Immunol,* 14**,** 119-126.

Vinuesa, C. G., Sanz, I. & Cook, M. C. 2009. Dysregulation of germinal centres in autoimmune disease. *Nat Rev Immunol,* 9**,** 845-857.

Vivanco, I. & Sawyers, C. L. 2002. The phosphatidylinositol 3-Kinase–AKT pathway in human cancer. *Nature Reviews Cancer,* 2**,** 489.

Vollmer, J., Weeratna, R., Payette, P., Jurk, M., Schetter, C., Laucht, M., Wader, T., Tluk, S., Liu, M., Davis, H. L. & Krieg, A. M. 2003. Characterization of three CpG oligodeoxynucleotide classes with distinct immunostimulatory activities. *European Journal of Immunology,* 34**,** 251-262.

Vollmer, S., Strickson, S., Zhang, T., Gray, N., Lee, K., Rao, V. & Cohen, P. 2017. The mechanism of activation of IRAK1 and IRAK4 by interleukin-1 and Toll-Like receptor agonists. *Biochemical Journal*.

Vos, Q., Lees, A., Wu, Z. Q., Snapper, C. M. & Mond, J. J. 2000. B-cell activation by T-cell-independent type 2 antigens as an integral part of the humoral immune response to pathogenic microorganisms. *Immunological reviews,* 176**,** 154-170.

Waldenstrom, J. 1961. Studies on conditions associated with disturbed gamma globulin formation (gammopathies). *Harvey Lect,* 56**,** 211.

Waldenström, J. 1944. Incipient myelomatosis or "essential" hyperglobulinemia with fibrinogenopenia—a new syndrome? *Acta Medica Scandinavica,* 117**,** 216-247.

Walshe, C. A., Beers, S. A., French, R. R., Chan, C. H. T., Johnson, P. W., Packham, G. K., Glennie, M. J. & Cragg, M. S. 2008. Induction of Cytosolic Calcium Flux by CD20 Is Dependent upon B Cell Antigen Receptor Signaling. *Journal of Biological Chemistry,* 283**,** 16971-16984.

Wang, J. Q., Beutler, B., Goodnow, C. C. & Horikawa, K. 2016. Inhibiting TLR9 and other UNC93B1-dependent TLRs paradoxically increases accumulation of MYD88L265P plasmablasts in vivo. *Blood,* 128**,** 1604-1608.

Wang, J. Q., Jeelall, Y. S., Beutler, B., Horikawa, K. & Goodnow, C. C. 2014. Consequences of the recurrent MYD88(L265P) somatic mutation for B cell tolerance. *J Exp Med,* 211**,** 413-26.

Wang, L. D. & Wagers, A. J. 2011. Dynamic niches in the origination and differentiation of haematopoietic stem cells. *Nature Reviews Molecular Cell Biology,* 12**,** 643.

Watters, T. M., Kenny, E. F. & O'neill, L. A. 2007. Structure, function and regulation of the Toll/IL-1 receptor adaptor proteins. *Immunol Cell Biol,* 85**,** 411-9.

Weil, R. & Israël, A. 2004. T-cell-receptor- and B-cell-receptor-mediated activation of NF-κB in lymphocytes. *Current Opinion in Immunology,* 16**,** 374-381.

Wilkins, B. S., Buchan, S. L., Webster, J. & Jones, D. B. 2001. Tryptase-positive mast cells accompany lymphocytic as well as lymphoplasmacytic lymphoma infiltrates in bone marrow trephine biopsies. *Histopathology,* 39**,** 150-155.

Wilson, W. H., Young, R. M., Schmitz, R., Yang, Y., Pittaluga, S., Wright, G., Lih, C. J., Williams, P. M., Shaffer, A. L., Gerecitano, J., De Vos, S., Goy, A., Kenkre, V. P., Barr, P. M., Blum, K. A., Shustov, A., Advani, R., Fowler, N. H., Vose, J. M., Elstrom, R. L., Habermann, T. M., Barrientos, J. C., Mcgreivy, J., Fardis, M., Chang, B. Y., Clow, F., Munneke, B., Moussa, D., Beaupre, D. M. & Staudt, L. M. 2015. Targeting B cell receptor signaling with ibrutinib in diffuse large B cell lymphoma. *Nat Med,* 21**,** 922-6.

Wu, C. D., Medeiros, L. J. & Jackson, C. L. 1996. Splenic Marginal Zone Cell Lymphoma: An Immunophenotypic and Molecular Study of Five Cases. *American Journal of Clinical Pathology,* 105**,** 277-285.

Xu, L., Hunter, Z. R., Yang, G., Zhou, Y., Cao, Y., Liu, X., Morra, E., Trojani, A., Greco, A., Arcaini, L., Varettoni, M., Brown, J. R., Tai, Y. T., Anderson, K. C., Munshi, N. C., Patterson, C. J., Manning, R. J., Tripsas, C. K., Lindeman, N. I. & Treon, S. P. 2013. MYD88 L265P in Waldenstrom macroglobulinemia, immunoglobulin M monoclonal gammopathy, and other B-cell lymphoproliferative disorders using conventional and quantitative allele-specific polymerase chain reaction. *Blood,* 121**,** 2051-8.

Xu, L. G. & Shu, H. B. 2002. *TNFR-associated factor-3 is associated with BAFF-R and negatively regulates BAFF-R-mediated NF-kappa B activation and IL-10 production*.

Yamamoto, H., Kishimoto, T. & Minamoto, S. 1998. NF-κB activation in CD27 signaling: involvement of TNF receptor-associated factors in its signaling and identification of functional region of CD27. *The Journal of Immunology,* 161**,** 4753-4759.

Yan, Q., Huang, Y., Watkins, A. J., Kocialkowski, S., Zeng, N., Hamoudi, R. A., Isaacson, P. G., De Leval, L., Wotherspoon, A. & Du, M.-Q. 2012. BCR and TLR signaling pathways are recurrently targeted by genetic changes in splenic marginal zone lymphomas. *Haematologica,* 97**,** 595-598.

Yang, G., Zhou, Y., Liu, X., Xu, L., Cao, Y., Manning, R. J., Patterson, C. J., Buhrlage, S. J., Gray, N., Tai, Y.-T., Anderson, K. C., Hunter, Z. R. & Treon, S. P. 2013. A mutation in MYD88 (L265P)

supports the survival of lymphoplasmacytic cells by activation of Bruton tyrosine kinase in Waldenström macroglobulinemia. *Blood,* 122**,** 1222-1232.

Yang, Y., Yaccoby, S., Liu, W., Langford, J. K., Pumphrey, C. Y., Theus, A., Epstein, J. & Sanderson, R. D. 2002. Soluble syndecan-1 promotes growth of myeloma tumors in vivo. *Blood,* 100**,** 610-617.

Yarkoni, Y., Getahun, A. & Cambier, J. C. 2010. Molecular underpinning of B-cell anergy. *Immunological reviews,* 237**,** 249-263.

Yoshida, H., Matsui, T., Yamamoto, A., Okada, T. & Mori, K. 2001. XBP1 mRNA is induced by ATF6 and spliced by IRE1 in response to ER stress to produce a highly active transcription factor. *Cell,* 107**,** 881-891.

Yoshida, H., Okada, T., Haze, K., Yanagi, H., Yura, T., Negishi, M. & Mori, K. 2000. ATF6 activated by proteolysis binds in the presence of NF-Y (CBF) directly to the cis-acting element responsible for the mammalian unfolded protein response. *Molecular and cellular biology,* 20**,** 6755-6767.

Young, K. H., Chan, W. C., Fu, K., Iqbal, J., Sanger, W. G., Ratashak, A., Greiner, T. C. & Weisenburger, D. D. 2006. Mantle Cell Lymphoma With Plasma Cell Differentiation. *The American Journal of Surgical Pathology,* 30**,** 954-961.

Young, R. M., Shaffer, A. L., 3rd, Phelan, J. D. & Staudt, L. M. 2015. B-cell receptor signaling in diffuse large B-cell lymphoma. *Seminars in hematology,* 52**,** 77-85.

Zarember, K. A. & Godowski, P. J. 2002. Tissue Expression of Human Toll-Like Receptors and Differential Regulation of Toll-Like Receptor mRNAs in Leukocytes in Response to Microbes, Their Products, and Cytokines. *The Journal of Immunology,* 168**,** 554.

Zhang, D., Zhang, G., Hayden, M. S., Greenblatt, M. B., Bussey, C., Flavell, R. A. & Ghosh, S. 2004. A Toll-like Receptor That Prevents Infection by Uropathogenic Bacteria. *Science,* 303**,** 1522.

Zhou, Y., Liu, X., Xu, L., Hunter, Z. R., Cao, Y., Yang, G., Carrasco, R. & Treon, S. P. 2014. Transcriptional repression of plasma cell differentiation is orchestrated by aberrant over-expression of the ETS factor SPIB in Waldenström macroglobulinaemia. *British Journal of Haematology,* 166**,** 677-689.

Zhu, A., Ibrahim, J. G. & Love, M. I. 2018. Heavy-tailed prior distributions for sequence count data: removing the noise and preserving large differences. *bioRxiv***,** 303255.

Zibellini, S., Capello, D., Forconi, F., Marcatili, P., Rossi, D., Rattotti, S., Franceschetti, S., Sozzi, E., Cencini, E., Marasca, R., Baldini, L., Tucci, A., Bertoni, F., Passamonti, F., Orlandi, E., Varettoni, M., Merli, M., Rizzi, S., Gattei, V., Tramontano, A., Paulli, M., Gaidano, G. & Arcaini, L. 2010. Stereotyped patterns of B-cell receptor in splenic marginal zone lymphoma. *Haematologica,* 95**,** 1792-1796.

Zocchi, E., Daga, A., Usai, C., Franco, L., Guida, L., Bruzzone, S., Costa, A., Marchetti, C. & De Flora, A. 1998. Expression of CD38 Increases Intracellular Calcium Concentration and Reduces Doubling Time in HeLa and 3T3 Cells. *Journal of Biological Chemistry,* 273**,** 8017-8024.